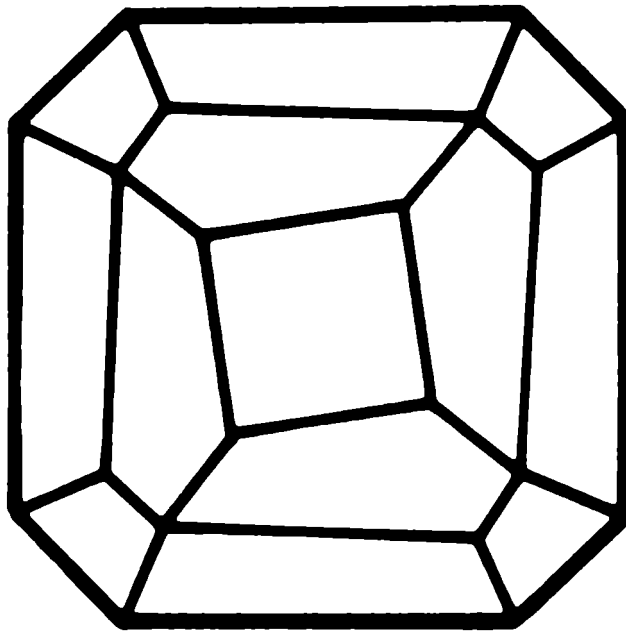


Mitteilungen der Österreichischen Mineralogischen Gesellschaft



Band 149

2004

Herausgegeben von der Österreichischen Mineralogischen Gesellschaft
für das Vereinsjahr 2003
Eigenverlag

Mitteilungen der Österreichischen Mineralogischen Gesellschaft

Band 149



2004

Vereinsjahr 2003

Gefördert aus Mitteln des Bundesministeriums für Bildung, Wissenschaft und Kultur in Wien.

Impressum:

Eigentümer, Herausgeber und Verleger: Österreichische Mineralogische Gesellschaft
p.A. Mineralogisch-Petrographische Abteilung, Naturhistorisches Museum Wien
Burgring 7, A-1014 Wien
Homepage: <http://www.univie.ac.at/Mineralogie/Oemg.htm>
ISSN 1609-0144

Redaktion:

Friedrich Koller, Institut für Geologische Wissenschaften, Universität Wien
Geozentrum, Althanstraße 14, A-1090 Wien
Anton Beran, Institut für Mineralogie & Kristallographie, Universität Wien
Geozentrum, Althanstraße 14, A-1090 Wien
Richard Tessadri, Institut für Mineralogie & Petrographie, Universität Innsbruck
Innrain 52, A-6020 Innsbruck
Guest Editor: R. Oberhänsli, Universität Potsdam

Gestaltung und Layout:
R. Tessadri (Innsbruck)

Für den Inhalt sind die Autoren selbst verantwortlich.

Druck: Anton Riegelnik, Piaristengasse 19, A-1080 Wien

Printed in Austria

INHALT

6th EMU School “Spectroscopic Methods in Mineralogy”

August 30th - September 8th, Vienna, Austria – Abstracts

ECMS 2004, 5th European Conference on Mineralogy and Spectroscopy

September 4th - September 8th, Vienna, Austria – Abstracts

- Andreozzi G. B., Bernardini G. P., Borgheresi M., Caneschi A., Cipriani C.,
Di Benedetto F., Gatteschi D. & Romanelli M.: Short-range order of Fe(II) in
sphalerite by magnetic susceptibility and ⁵⁷Fe Mössbauer spectroscopy S. 13
- Bellatreccia F., Della Ventura G., Libowitzky E., Beran A. & Ottolini L.: A calibration
curve for the OH content of vesuvianite: a polarized single-crystal FTIR study S. 14
- Borgheresi M., Bernardini G. P., Caneschi A., Cipriani C., Di Benedetto F., Pardi L. A.
& Romanelli M.: EPR, HF²EPR spectroscopy and SQUID study of natural bornite:
preliminary results S. 15
- Bornefeld M., Gasharova B., Garbev K., Mangold S., Beuchle G. & Stemmermann P.:
Spectroscopic examinations of the structure and alkali sorption of highly polymerized
C-S-H phases S. 16
- Borovikova E., Kovalchuk R., Kurazhkovskaya V. S. & Rusakov V. S.: Vesuvianite:
IR and Mössbauer spectroscopy data S. 17
- Buçşa M., Oprean I. & Ristoiu D.: Pheromones analysis by vibrational spectroscopy S. 18
- Carbone C., Di Benedetto F., Marescotti P., Martinelli A., Lima N., Pardi L.,
Romanelli M., Sangregorio C. & Sorace L.: EPR study and magnetic investigation of
synthetic hematite α -Fe₂O₃ S. 19
- Carbone C., Di Benedetto F., Marescotti P., Martinelli A., Sangregorio C., Lucchetti G.,
Sorace L., Cipriani C. & Romanelli M.: Spectroscopic characterization of Fe-oxides
and -oxyhydroxides assemblages related to ARD processes (Libiola Mines, Italy) S. 20
- Cibin G., Marcelli A., Mottana A. & Brigatti M. F.: Interlayer cation characterization
in phyllosilicates: a XANES investigation S. 21
- Dagounaki K., Zorba T., Anastasiou M., Chatzistavrou X. & Paraskevopoulos K. M.:
Comparative spectroscopic study of carbonate rocks from Western Macedonia in Greece S. 22
- Della Ventura G., Iezzi G., Bellatreccia F., Cámara F. & Oberti R.: The $P2_1/m \leftrightarrow C2/m$
phase-transition of synthetic amphiboles in the system Na₂O-Li₂O-MgO-SiO₂-H₂O:
an HT-FTIR study S. 23
- Di Benedetto F., Montegrossi G., Pardi L. A., Bercu V., Romanelli M., Minissale A. &
Paladini M.: Spectroscopic characterisation of travertines by EPR techniques:
a multifrequency study S. 24
- Dondi M., Cruciani G., Matteucci F. & Raimondo M.: UV-Visible-NIR spectroscopy
and XRPD of rutile pigments doped with chromophores (Cr, Mn, Ni, V) and counterions
(Mo, Nb, Sb, W) S. 25

Drakoulis A., Kantiranis N., Filippidis A., Stergiou A., Zorba T., Paraskevopoulos K. M. & Squires C.: The estimation of volcanic glass content in natural materials using PXRD and FTIR techniques	S. 26
Emiliani C., Bernardini G. P., Trosti-Ferroni R., Vaughn D. J., Wincott P. L. & Walton J.: XPS studies of binary Cu-Sn alloys aged in climatic chamber	S. 27
Evstigneeva T., Di Benedetto F., Kulikova I. & Rusakov V.: Crystal chemistry of the stannite-group compounds (EPMA, EPR, SQUID, Mössbauer Spectroscopy)	S. 28
Farges F., Galois L., Balan E., Fuchs Y. & Linares J.: Structure and color of the Jack Creek dumortierite (Montana, USA) using spectroscopic approaches	S. 29
Ferreira J. A. & Figueiredo M. O.: Electronic state of sulfur in tetrahedrite-tennantite series: a Micro-XANES study	S. 30
Figueiredo M. O. & Susini J.: Crystal chemical bases for a data bank on sulphur K-edge XANES spectra in sulphide and sulphosalt minerals	S. 31
Figueiredo M. O., Pereira da Silva T., Silva L. C., Mirão J. & Mendes M. H.: An X-ray absorption spectroscopy study at sulfur K-edge haüyne from Sant Antão (Cap Verde)	S. 32
Filip J. & Novák M.: OH defects in spodumene: a comparative study of spodumene of various genetic types	S. 33
Gaft M., Nagli L. & Waychunas G.: Nature of bentonite BaTiSi ₃ O ₉ luminescence	S. 34
Galuskin E. V., Galuskina I. O., Janeczek J. & Wzalik R.: Single-crystal Raman spectroscopy of vesuvianite group minerals in the OH region	S. 35
Gasharova B., Mathis Y.-L., Garbev K., Guilhaumou N., Moss D. A. & Bornefeld M.: The infrared micro-spectroscopy facility at the synchrotron ANKA: mineralogical applications	S. 36
Gasharova B., Garbev K., Stumm A. & Mathis Y.-L.: Infrared and Raman spectroscopy study on gyrolite-group minerals	S. 37
Gâz S. A., Gropeanu R., Roiban D. & Grosu I.: Synthesis, stereochemistry and reactivity of some 2-methyl-2-(3'-nitrophenyl)-4-hydroxymethyl-1,3-dioxolanes	S. 38
Gorea M. & Kristaly F.: Chemical and mineralogical characterization of some raw ceramic materials and their transformations during the thermal treatment	S. 39
Hammer V. M. F., Brandstätter F. & Ponahlo J.: Prehnite – a new lapidary material	S. 40
Iezzi G., Liu Z., Della Ventura G. & Hemley R.: Synchrotron infrared spectroscopy of synthetic <i>P2₁/m</i> amphiboles at high pressure	S. 41
Kaindl R., Tropper P. & Bertoldi C.: CO ₂ and H ₂ O in cordierite from thin-sections: a Raman-spectroscopic approach	S. 42
Karampelas S. & Fritsch E.: Infrared absorption as a useful tool to separate natural from synthetic amethysts	S. 43
Khisina N. R., Wirth R., Andrut M. & Churakov S.: On a mode of Fe ⁺ , OH ⁻ occurrence in olivine (Mössbauer, IR, EELS combined with TEM)	S. 44
Khomenko V. & Langer K.: Molecules of carbon oxides in cordierite channels: a spectroscopic study	S. 45
Kleppe A. K., Jephcoat A. P. & Smyth J. R.: New Raman spectroscopic observations of hydrated transition zone spinel/spineloid phases	S. 46
Kolb C., Abart R., Lottermoser W., Kaindl R. & Lammer H.: Importance of weathered meteorites for Mars: data on VNIR reflectance-spectroscopy, Raman-spectroscopy and Mössbauer-spectroscopy	S. 47

Kolesov B. & Geiger C.: A Raman spectroscopic study of Fe-Mg olivines	S. 48
Kolesov B. & Geiger C.: Molecule-mineral inner surface interactions in nanoporous silicates: a Raman spectroscopic investigation	S. 49
Kolitsch U., Bernhardt H.-J. & Blaß G.: $\text{Fe}_3(\text{PO}_4)_2(\text{OH})_3 \cdot 5\text{H}_2\text{O}$, a new monoclinic ferric iron phosphate mineral from Germany: crystal structure, single-crystal Raman spectra and close relation to wavellite	S. 50
Korinevskaja G. & Bykov V.: Raman spectra of titanosilicate melts	S. 51
Kostov-Kyтин V., Mihailova B., Ferdov S. & Petrov O.: Temperature-induced structural transformations of layered titanosilicate JDF-L1	S. 52
Kotova Y. N. & Lutoev V. P.: Results of an ESR-study of quartz from the archaean metamorphic complexes on the Kola superdeep borehole section	S. 53
Kovács L.: Hydroxyl ions in synthetic crystals: do they differ from those in minerals ?	S. 54
Kovács L., Gospodinov M. & Capelletti R.: FTIR spectroscopy of OH ⁻ ions in $\text{Pb}_5(\text{GeO}_4)(\text{VO}_4)_2$ apatite	S. 55
Kovalev O., Gies H. & Fechtelkord M.: NMR and diffraction of acetone intercalated in the layer silicate RUB-18	S. 56
Kukuy A. L., Matveeva O. P. & Sokolova N. G.: The revelation of typomorphic properties of metamorphic carbonate rocks	S. 57
Ladenberger A.: Application of microanalysis (SEM-EDS) in the study of heavy minerals from recent stream alluvia in the Tatra Mts.	S. 58
Lebedeva S. M., Bykov V. N. & Mironov A. B.: Infrared and Mössbauer spectroscopy of natural glasses	S. 59
Lengyel K., Péter Á., Polgár K., Kovács L. & Corradi G.: Optical spectroscopic studies in LiNbO_3 : Mg crystals below and above the photorefractive threshold	S. 60
Lorenzi G., Baldi G., Di Benedetto F., Faso V., Lattanzi P. F., Pardi L. A. & Romanelli M.: Crystal chemistry of gahnite-based pigments: a DRS, EPR and HF ² EPR study	S. 61
Lysiuk A. Y.: Spectroscopy of fulgurite glasses	S. 62
Magdaš D. A., Cozar O., Ardelan I., Leopold N. & David L.: IR and Raman studies of some molybdenum-lead-phosphate glasses	S. 63
Matovic V. & Rosic A.: Chemical investigations of incrustated stone on historical monuments	S. 64
Matteucci F., Dondi M., Cruciani G., Baldi G. & Barzanti A.: Investigation of colouring mechanism of REE-perovskites through combining structural and UV-VIS-NIR spectroscopy data	S. 65
McCammon C. A., O'Neill H. S. C., Berry A. J., Jayasuriya K. D. & Campbell S. J.: Short-range structure of iron in anorthite-diopside glass	S. 66
Mihajlović T., Libowitzky E. & Effenberger H.: Synthesis, crystal structure, Infrared and Raman spectra of $\text{Sr}_5(\text{As}_2\text{O}_7)_2(\text{AsO}_3\text{OH})$	S. 67
Mills S. J., Frost R. L., Grey I. E., Mumme W. G. & Weier M. L.: Crystallography, Raman and IR spectroscopy of perhamite – an interesting silico-phosphate	S. 68
Mineeva R. M., Speransky A. V., Titkov S. V. & Zudin N. G.: Ordering of paramagnetic defects in natural diamonds with microtwins	S. 69
Mirão J. & Figueiredo M. O.: X-ray absorption at 3d-metal $L_{2,3}$ and O K-edges in columbites	S. 70
Mookherjee M. & Stixrude L.: Equation of state and transition pressure for brucite dehydration: theoretical approach	S. 71

Moroz N. K.: NMR studies of molecular diffusion and proton transfer in hydrated minerals	S. 72
Moroz T., Shcherbakova E. & Kostrovsky V.: Vibrational spectra of kladnoite, natural analogue of phthalimide $C_6H_4(CO_2)NH$	S. 73
Morozov M., Azimov P., Musso M., Dolivo-Dobrovolsky D. V., Asenbaum A. & Amthauer G.: Raman microspectroscopy: the key role in the reconstruction of PT-paths of HP-metamorphism	S. 74
Morozov M., Nusso M., Asenbaum A. & Amthauer G.: Raman spectroscopy of rocks in thin sections: analytical constraints	S. 75
Nasdala L.: Raman barometry of mineral inclusions in diamond crystals	S. 76
Pawlowski J., Fehr K. T. & Hochleitner R.: Infrared spectroscopy of natural and synthetic tobermorites	S. 77
Piccinini M., Bellatreccia F. & Della Ventura G.: A polarized single-crystal study of synthetic water-poor beryl	S. 78
Pichler H., Haase A., Stadlober B., Maresch H. & Satzinger V.: Phase-controlled pentacene thin films and their characteristics in organic transistors	S. 79
Platonov A. N., Langer K. & Matsyuk S. S.: Influence of Ca-Mg substitution on the Cr^{3+} crystal field parameters in natural garnet solid solutions	S. 80
Posch T., Hodouš I., Kerschbaum F., Richter H. & Mutschke H.: Asteromineralogy of circumstellar oxide dust	S. 81
Quartieri S., Dalconi M. C., Oberti R., Boscherini F., Iezzi G. & Boiocchi M.: Site preference and partitioning of scandium in silicate garnets	S. 82
Redhammer G. J., Tippelt G., Lottermoser W., Amthauer G. & Roth G.: ^{57}Fe Mössbauer spectroscopic investigations on the brownmillerrite solid solution series $Ca_2(Fe_{2-x}Al_x)O_5$	S. 83
Redhammer G. J., Tippelt G., Lottermoser W., Amthauer G. & Roth G.: Magnetic ordering in the quasi-1d compound $Cu_2Fe_2Ge_4O_{13}$ as monitored by ^{57}Fe Mössbauer spectroscopy and SQUID magnetometry	S. 84
Richter H., Kerschbaum F., Mutschke H. & Posch T.: Absorption efficiencies of stardust minerals	S. 85
Rinaudo C., Gastaldi D. & Belluso E.: Application of Raman spectroscopy to the identification of asbestos minerals	S. 86
Roiban D. G., Gropeanu R., Gâz S. A. & Grosu I.: Spectroscopic methods used for structure investigations of some new dioxane derivatives	S. 87
Shchapova J. V., Votyakov S. L. & Ivanovskii A. L.: <i>Ab Initio</i> simulation of the electronic structure of zircon ($ZrSiO_4$) and quartz (SiO_2)	S. 88
Shchapova J. V., Votyakov S. L., Porotnikov A. V., Yuryeva E. I. & Ivanovskii A. L.: $MgAl_2O_4$ - $MgCr_2O_4$ - $FeAl_2O_4$ -natural spinels from the Urals ultramafites: Mössbauer study, quantum-chemical simulation of the local atomic and electronic structure	S. 89
Shcherbakova E., Nikandrova N. & Zvonareva G.: Mössbauer spectroscopy of Fe-containing sulfates	S. 90
Shiryaev A. & Zedgenizov D.: Optical studies of fluids in fibrous diamonds	S. 91
Soltay L. G. & Henderson G. S.: Comparing the structure of lithium containing germanate and silicate glasses	S. 92
Starzec K. & Pop D.: Mineralogy and chemistry of some glauconites from Polish Flysch Carpathians determined by infrared spectroscopy, SEM-EDS analyses and X-ray diffraction	S. 93

Taran M. N., Koch-Müller M. & Langer K.: Electronic absorption spectroscopy of natural (Fe ²⁺ , Fe ³⁺)-bearing spinels of magnesio-spinel-hercynite and gahnite-hercynite solid solutions at different temperatures and high pressures	S. 94
Tătar S.-D., Constantina C., Pop D. & Kiefer W.: Raman spectroscopy on gem-quality microcrystalline and amorphous silica varieties from Romania	S. 95
Titorenkova R. & Mihailova B.: Local structural state of zircon from metagranites – a Raman spectroscopic study	S. 96
Toderaş F., Farcău C. A. & Aştilean S.: Optical and spectroscopic properties of self-assembled nanoparticles	S. 97
Tomašić N., Gajović A. & Bermanec V.: Gradual recrystallisation of metamict fergusonite: X-ray diffraction and Raman spectroscopy study	S. 98
Văju C., Miron M. & Andreica D.: A muon spin rotation investigation of the magnetic structure of CeRh ₂ Si ₂	S. 99
Van Alboom A., De Grave E. & Wohlfahrt-Mehrens M.: Temperature dependence of the Fe ²⁺ Mössbauer parameters in triphylite (LiFePO ₄)	S. 100
Vantelon D., Bac S., Cauchon G., Dubuisson J.-M., Idir M., Flank A.-M., Janousch M., Lagarde P. & Wetter R.: LUCIA, a microfocus soft XAS beamline	S. 101
Vaskovic N. & Eric S.: White mica from the Brnjica granitoids (Eastern Serbia)	S. 102
Vedeanu N., Cozar O. & Ardelean I.: Spectroscopic investigations on some vanadium-calcium-phosphate glasses	S. 103
Viktorov M. A., Marfunin A. S. & Shelementiev Y. B.: Spectroscopy application for modelling of transformational mechanisms of lattice defects in diamonds during annealing and irradiation	S. 104
Votyakov S. L., Shchapova J. V., Porotnikov A. V. & Galahova O. L.: ESR and luminescent study, <i>Ab Initio</i> modelling of atomic and electronic structure of natural carbonate minerals (Ca, Mg)CO ₃ : Mn ²⁺	S. 105
Watterich A., Beregi E., Aleshkevych P., Borowiec M. T., Zayarnyuk T. & Szymczak H.: Spectroscopic characterisation of YAl ₃ (BO ₃) ₄ : Gd ³⁺ crystals	S. 106
Weikusat C., Nasdala L. & Häger T.: Spectroscopic study of Canada Balsam used as filler substance in emerald	S. 107
Woodland A. B.: Application of Mössbauer spectroscopy in mantle petrology	S. 108
Zaharia L. & Suciuc-Krausz E.: Spectroscopic investigation of some minerals from cave No.4 – Runcului Hill (Metaliferi Mts., Romania)	S. 109
Zhdanova A. N.: X-ray diffraction and IR-spectroscopy of bottom sediments in Lake Hovsgol for paleoclimatic reconstructions	S. 110
Zviagina B. B.: Interpretation of IR spectra of mixed-layer illite-smectites and illite-tobelite-smectites in the region of OH-stretching vibrations	S. 111

Explanatory Notes to the Map: Metamorphic Structure of the Alps

Oberhänsli R. (Ed.) & Goffé B.: Introduction	S. 115
Goffé B., Schwartz S., Lardeaux J. M. & Bousquet R.: Western and Ligurian Alps	S. 125
Bousquet R., Engi M., Gosso G., Oberhänsli R., Berger A., Spalla M. I., Zucali M. & Goffé B.: Transition from the Western to the Central Alps	S. 145

- Engi M., Bousquet R. & Berger A.: Central Alps S.
- Schuster R., Koller F., Hoek V., Hoinkes G. & Bousquet R.: Metamorphic evolution of the Eastern Alps S.
- Handy M. R. & Oberhänsli R.: Age map of the metamorphic structure of the Alps – tectonic interpretations and outstanding problems S.
- Metamorphic Structures of the Alps (color map) S.

Originalarbeiten

- Augustin-Gyurits K. & Pertlik F.: Erich Schroll, ein Wegbereiter für die geochemische Forschung in Österreich. Zum 80. Geburtstag (Mit einem Schriftenverzeichnis) S.
- R. Krickl: Geometrische Studien zu den pentagonalen und dekadagonalen dreidimensionalen Punktgruppen S.

MinPet 2003

15. - 21. September 2003, Neukirchen am Großvenediger, Salzburg – Abstracts – Nachtra
 Friedrich A., Knorr K., Lieb A., Rath St., Höpfe H. A., Winkler B., Schnick W. & Hanfland M.: Bulk moduli and phase transitions of carbonditridosilicates and oxonitridosilicates at high pressures up to 36 GPa S.

Diplomarbeiten und Dissertationen von österreichischen Universitäten (Auszüge)

- Amare K.: Shock petrography and geochemical studies of rocks from the Woodleigh (Australia), Chesapeake Bay (USA), El gygytyn (Russia) impact structures and variation in chemical composition in Australasian tektites from different localities of Vietnam S.
- Bertle R. J.: Zur Geologie des Piz Mundin-Gebietes (Engadiner Fenster, Österreich-Schweiz): Stratigraphie, Geochronologie, Strukturen S.
- Bidner T.: Natürliche Gesteine als Sensormaterialien zur Erfassung von Umwelteinflüssen auf Baudenkmäler S.
- Constantin A.: Hydrogeologische, sedimentpetrographische und hydrogeochemische Untersuchungen im Raum von Sterzing/Italien S.
- Humer F. D.: Kontamination oder natürliche Lösungserscheinungen: Untersuchungen an Wässern und Sedimenten im Nordosten der Landseer Bucht, Burgenland S.
- Katongo C.: Petrography and geochemistry of metasedimentary, impactoclastic and granitoid rocks from diverse geological settings S.
- Kneringer E. K.: Der Rehove-Ophiolit im südlichen Albanien S.
- Mayr N.: Zur Petrologie und ausgewählten technologischen Eigenschaften der Inschriftentafeln des römischen Tempelbezirkes auf dem Pfaffenberg bei Carnuntum S.
- Pimraksa K.: Fabrication of bricks using fly ash from Mae Moh power plant (Thailand) S.
- Schroll H.: Hydrogeologische, sedimentpetrographische und hydrogeochemische Untersuchungen im oberen Vinschgau, Bereich Suldental-Prad/Italien S.

Tomberger A.: Hydrogeologische, sedimentpetrographische und hydrogeochemische
Untersuchungen im oberen Vinschgau, Bereich Suldental-Laas/Italien S. 296

Vereinsnachrichten
Tätigkeitsbericht über das Vereinsjahr 2003 S. 299

Autorenhinweise S. 306

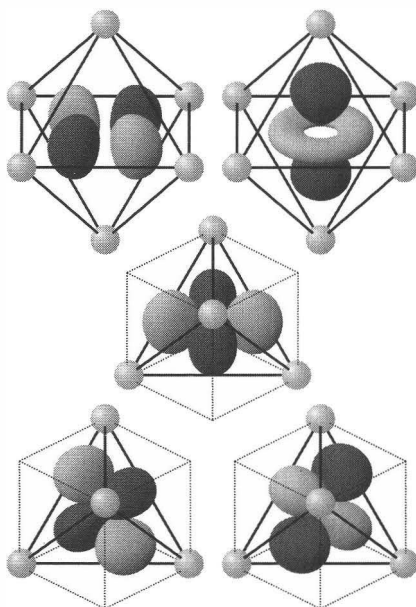
6th EMU School
“Spectroscopic Methods in Mineralogy”
August 30th - September 8th, 2004

&

ECMS 2004
5th European Conference on Mineralogy and Spectroscopy
September 4th - September 8th, 2004

Vienna, Austria

Abstracts



SHORT-RANGE ORDER OF Fe(II) IN SPHALERITE BY MAGNETIC SUSCEPTIBILITY AND ⁵⁷Fe MÖSSBAUER SPECTROSCOPY

Andreozzi, G.B.¹, Bernardini, G.P.², Borgheresi, M.², Caneschi, A.³, Cipriani, C.⁴, Di Benedetto, F.⁴, Gatteschi, D.³ & Romanelli, M.³

¹Dipartimento di Scienze della Terra, Università di Roma "La Sapienza", P.le A. Moro 5, 00185 Roma (Italy)

²Dipartimento di Scienze della Terra, Università di Firenze, via G. La Pira 4, I50121, Firenze (Italy)

³Dipartimento di Chimica, Università di Firenze, via della Lastruccia 3, I50019 Sesto Fiorentino (Italy)

⁴Museo di Storia Naturale, Università di Firenze, via G. La Pira 4, I50121, Firenze (Italy)

e-mail: miria.borgheresi@geo.unifi.it

Several physical properties of sphalerite, which propose cubic ZnS as "tunable" material with non-linear magnetic and magneto-optic properties, are associated to the most common substitutions of Zn by paramagnetic cations (Fe and Mn) thus defining the class of the Diluted Magnetic Semiconductors (DMS). The replacement of Fe and Mn for Zn in sphalerite, where no structural constraints are present, is assumed to occur with a statistical metal distribution. However, the possible presence of short-range ordering phenomena cannot be ruled out, thus affecting the fine electronic properties of this material, which may significantly change as a function of the short-range distribution.

An extensive study of natural and synthetic Fe-bearing sphalerites (Fe-content ranging between 0.005 and 0.250 afu) has been carried out through the combined characterisation of the temperature dependence of the magnetic susceptibility (investigated from 300 to 2 K) and of the room-temperature ⁵⁷Fe Mössbauer spectroscopic features.

Magnetic susceptibility measurements evidence, in the low temperature range, the presence of clustered Fe(II) even in the most diluted samples, whereas in the high temperature range magnetic data account for the molar contribution in the standard Curie-Weiss model.

All the Mössbauer spectra (may be) are described in terms of variable proportions of three components, namely one singlet and two doublets absorptions, centered at the same isomer shift, relative to isolated Fe(II) ions and different Fe(II) clusters, respectively.

The comparison of all the experimental results points out a self-affinity of Fe(II) ions in sphalerite favoured by the superexchange interaction, which stabilises the formation of clusters even in the relatively diluted samples.

**A CALIBRATION CURVE FOR THE OH CONTENT OF VESUVIANITE:
A POLARIZED SINGLE-CRYSTAL FTIR STUDY**

Bellatreccia, F.¹, Della Ventura, G.¹, Libowitzky, E.², Beran, A.² & Ottolini, L.³

¹ Dipartimento Scienze Geologiche, Università di Roma Tre, Largo S. Leonardo Murialdo 1, I-00146 Roma

² Institut für Mineralogie und Kristallographie, Geozentrum, Althanstr. 14, A-1090 Wien, Austria

³ CNR-Istituto di Geoscienze e Georisorse, Sezione di Pavia, via Ferrata 1, I-27100 Pavia, Italy
e-mail: bellatre@uniroma3.it

A well-characterized suite of vesuvianite samples from the volcanic ejecta of Latium (Italy) was studied by SREF (single-crystal X-ray refinement), EMPA, SIMS (Secondary-Ion Mass Spectrometry) and single-crystal, polarized radiation, FTIR spectroscopy in the OH-stretching region. Light elements in particular were analyzed by SIMS using an ion microprobe (Cameca IMS 4f) at CNR-Istituto di Geoscienze e Georisorse (Pavia). A ¹⁶O⁻ primary ion beam accelerated at 12.5 kV, with a beam intensity of 3 nA and a beam diameter ≤ 5 μm was employed. The SiO₂ (wt%) content (from EMPA) was selected as an internal reference for H, Li, Be and B (OTTOLINI et al., 2002; OTTOLINI & OBERTI, 2000). Most samples are B- (up to 3.67 wt%) and F-rich (up to 2.38 wt%). All IR spectra consist of a rather well-defined triplet of broad bands at higher frequency (3700-3300 cm⁻¹), and a very broad, composite absorption below 3300 cm⁻¹. These spectra are characteristic of B-rich and F-rich vesuvianites (GROAT et al., 1995). Measurements with E//c or E.Lc show that all bands are strongly polarized with maximum absorption for E//c, and agree with previous band assignment to the two O(11)-H(1) and O(10)-H(2) groups in the structure (GROAT et al., 1995). Pleochroic measurements with changing direction of the E vector of the incident radiation shows that the orientation of the O(11)-H(1) dipole is OH^{^c} ~ 35°, in excellent agreement with the neutron data of LAGER et al. (1999). A calibration curve, based on SIMS data on the same crystals used for FTIR analysis is presented. The integrated molar absorption coefficient for vesuvianite is ε_i = 97.000 ± 2000 l mol⁻¹ cm⁻². This value is in good agreement with the calibration curve for minerals established by LIBOWITZKY & ROSSMAN (1997). Preliminary data show that a quantitative determination of water in vesuvianites is also possible using powder IR spectroscopy, provided the sample is prepared in a well-standardized way.

References

- GROAT, L.A., HAWTHORNE, F.C., ROSSMAN, G.R. & ERCIT, T.S. (1995): *Can. Mineral.*, **33**: 609-626.
LAGER, G.A., XIE, Q., ROSS, F.K., ROSSMAN, G.R., ARMBRUSTER, T., ROTELLA, F.J. & SCHULTZ, A.J. (1999): *Can. Mineral.*, **37**: 763-768.
LIBOWITZKY, E. & ROSSMAN, G.R. (1997): *Am. Mineral.*, **82**: 1111-1115.
OTTOLINI, L., CAMARA, F., HAWTHORNE, F.C. & STIRLING, J. (2002): *Am. Mineral.*, **87**: 1477-1485.
OTTOLINI, L. & OBERTI, R. (2000): *Analyt. Chem.*, **72**: 3731-3738.

**EPR, HF²EPR SPECTROSCOPY AND SQUID STUDY OF NATURAL BORNITE:
PRELIMINARY RESULTS**

Borgheresi, M.¹, Bernardini, G.P.¹, Caneschi, A.², Cipriani, C.³, Di Benedetto, F.^{3,*},
Pardi, L.A.⁴ & Romanelli, M.²

¹ Dipartimento di Scienze della Terra, Università di Firenze, via G. La Pira 4, I50121, Firenze (Italy)

² Dipartimento di Chimica, Università di Firenze, via della Lastruccia 3, I50019, Sesto Fiorentino (Italy)

³ Museo di Storia Naturale, Università di Firenze, , via G. La Pira 4, I50121, Firenze (Italy)

⁴ Istituto per i Processi Chimico Fisici-CNR, via G. Moruzzi 1, I56124, Pisa (Italy)

*e-mail: dibenefr@geo.unifi.it

Bornite (Cu₅FeS₄) is a copper ore mineral of considerable economic relevance, playing an important role in the solar cells, as a composite superconductor, or as a DMS. In order to study its magnetic structure, the metal ions valence distribution and their interactions, X-band and high frequency EPR and magnetisation measurements were performed on a natural bornite sample of the Natural History Museum of Florence University.

The obtained magnetic data show a magnetic phase transition from a paramagnetic to an antiferromagnetic state with a Néel temperature $T_N \sim 75$ K and other discontinuities in the full investigated range (0 - 300 K). The evidence of a further magnetic phase transition was also observable near 30 K.

The experimental Curie constant value found in the high temperature regime is lower than the theoretical value for spin-only Fe(III) ions and suggests a high Fe(II) content. This observation suggest the hypothesis of bornite as a mixed valence system, with electron hopping taking place both between Fe(II) \leftrightarrow Fe(III) and Cu(I) \leftrightarrow Cu(II), the latter being required by charge neutrality. The observed EPR spectra, however, are different both from the typical Cu(II) and Fe(III) spectra. The 300 K and 5 K data show the same very intense peak centred at $g \sim 2.02$, the linewidth of which increases by decreasing temperature. This behaviour is characteristic of a concentrated system, where the exchange interaction prevents the determination of the single ion features. This is in line with a transient redox mechanism between adjacent ions.

Due to the peculiar electronic structure of this semiconductor, paramagnetic resonance experiments have been performed also on powders aged under pressure (1350 atm). The pressed sample, studied at X-band, shows a superposition of two lines, the former at $g \sim 2.02$ and a second, very narrow, at $g \sim 2.00$, thus pointing to an evident pressure influence. In the EPR measurements, performed at 95 and 190 GHz, the narrow line is always observed, whereas the broader X-band EPR line is not detectable.

SPECTROSCOPIC EXAMINATIONS OF THE STRUCTURE AND ALKALI SORPTION OF HIGHLY POLYMERIZED C-S-H PHASES

Bornefeld, M.¹, Gasharova, B.¹, Garbev, K.², Mangold, S.¹, Beuchle, G.² & Stemmermann, P.²

¹ Forschungszentrum Karlsruhe, Institut für Synchrotronstrahlung (ISS), P.O. Box 3640, D-76021 Karlsruhe, Germany

² Forschungszentrum Karlsruhe, Institut für Technische Chemie, Wasser- und Geotechnologie (ITC-WGT), P.O. Box 3640, D-76021 Karlsruhe, Germany
e-mail: marc.bornefeld@iss.fzk.de

Cement is an inorganic hydraulic binder widely used in civil engineering, etc. By the reaction of cement with water Calcium-Silicate-Hydrate (C-S-H) gel is the principal hydration product (TAYLOR, 1964). For example, building materials based on Portland cement could contain up to 70 wt% C-S-H gel. Therefore, the structure of the C-S-H gel is responsible for the mechanical properties of the hardened cement paste.

The composition of the C-S-H gels within the CaO-SiO₂-H₂O system varies over a large molar CaO/SiO₂ (C/S) range: from about 0.5 in older and partly carbonated hardened cement pastes up to 2.2 in fresh ones. Even lower C/S are probable due to weathering of hardened cement pastes and deteriorative reactions like alkali-silica-reaction (ASR). The latter leads to the formation of highly polymerized, alkali bearing C-S-H gels. The formation processes and the structure of these gels are widely unknown.

The existing models for the structure of C-S-H gel, mainly based on the structures of the crystalline C-S-H phases tobermorite and jennite, are suitable only for C-S-H gels with C/S ratios between 2/3 and 3/2. Despite the widespread occurrence of highly polymerized C-S-H gels there is still no proposal for a structural model for C-S-H gels with a C/S ratio < 2/3.

Due to the lack of long range order, spectroscopic methods such as FT-IR, XAFS and NMR are of great relevancy for structural investigations of the C-S-H gels. First results from these spectroscopic methods will be discussed and gain an insight in the structure and formation processes of alkali bearing highly polymerized C-S-H gels.

IR spectra of several C-S-H gels with C/S ratios varying between 0.2-1.5 and different alkali concentrations have been recorded at the IR-Beamline at ANKA (Angströmquelle Karlsruhe). The IR spectra of our samples clearly demonstrate systematical high frequency shifts of the Si-O-Si stretching vibrations with decreasing C/S ratio, thus indicating an increasing of the polymerization of the silicate structure (YU et al., 1999). In the OH stretching region a systematical shift of the broad absorption band provides useful information about changes of the H₂O environment upon varying C/S ratios. Additionally to the IR data, XAFS measurements at the Ca absorption edge provide detailed informations about the local environment around the Ca atom. ²⁹Si NMR data provide informations about the degree of polymerization of the SiO₄-tetrahedra in the gel structure.

References

- TAYLOR, H.F.W. (1964): *The Chemistry of Cements*. Academic Press, London, New York. 168 p.
YU, P., KIRKPATRICK, R.J., POE, B., MCMILLAN, P.F. & CONG, X. (1999): *J. Am. Ceram. Soc.*, **82**: 742-748.

VESUVIANITE: IR AND MÖSSBAUER SPECTROSCOPY DATA

Borovikova, E.¹, Kovalchuk, R.², Kurazhkovskaya, V.S.¹ & Rusakov, V.S.²

¹ MSU, Geological faculty, Department of Crystallography, A-403, Leninskie Gory, 119992, Moscow, Russia

² MSU, Physical faculty, Department General Physics, Leninskie Gory, 119992, Moscow, Russia
e-mail: alena@geol.msu.ru

Vesuvianite is chemically and structurally one of the most complicated rock-forming minerals. Vesuvianite can crystallize in three space groups: $P4/nnc$ (high vesuvianites), $P4/n$ and $P4nc$ (low vesuvianites) in dependence on string ordering in structural channels. The circumstance that the space group of vesuvianite depends on ordering of only 4 atoms in the unit cell makes it difficult to distinguish these “rod” polytypes by diffraction methods. Spectroscopic methods are more sensible to local structure and therefore we used IR and Mössbauer spectroscopy to investigate these samples.

We recorded the infrared spectra of high and low vesuvianite samples in the region of Si-O and B-O fundamental vibrations and also in the OH stretching region. It was revealed that by means of factor group analysis it is possible to predict the number of infrared active internal modes of SiO_4 ions and hydroxyl in different positions and to explain the differences of the spectra due to symmetry and composition of these varieties. Thus, IR spectra gave us the possibility to immediately differentiate between high and low vesuvianites. In addition, also the IR spectra of partly ordered vesuvianite samples were described: they have the characteristic features of both varieties in the OH stretching region.

It is considered that high vesuvianite forms at high temperature (> 400 °C) and low vesuvianite is characteristic for rocks formed at low temperatures (< 300 °C). But we have found in our collection some samples which do not obey this rule. The fact that temperature is not the only factor leading to one or another space group is of great importance from a petrological point of view.

We assigned the absorption bands in low vesuvianites spectra to MgAlOH , AlAlOH , AlTiOH , $\text{AlFe}^{3+}\text{OH}$. These cations are ordered in the inequivalent Y(3a) and Y(3b) octahedra of the low vesuvianite structure. IR spectra of boron-bearing samples have shown that boron occurs only in triangular positions of the low vesuvianite structure and in both, triangular and tetrahedral positions of the high vesuvianite structure. A diffuse character of the IR spectra and the presence of a band at 1110 cm^{-1} are prominent features of wiluite.

A Mössbauer spectroscopy study has been carried out with the purpose to determine the valence and structural conditions of iron atoms and also to investigate isomorphic substitutions in the vesuvianite structure. It was shown that Fe^{2+} and Fe^{3+} ions occupy both octahedral and 5-coordinated sites with a slight preference for the latter. Concerning the relative content of Fe^{2+} and Fe^{3+} ions, Mössbauer data allowed to establish two main schemes of isovalent substitutions in the investigated collection of vesuvianite samples: $\text{Mg}^{2+} \Leftrightarrow \text{Fe}^{2+}$ and $\text{Fe}^{3+} \Leftrightarrow \text{Al}^{3+}$. It is shown that along with isovalent schemes, two schemes of heterovalent substitutions occur: $\text{B}^{3+} + \text{Mg}^{2+} \Leftrightarrow 2\text{H}^+ + (\text{Fe}^{3+}, \text{Al}^{3+})$ and $\text{Ti}^{4+} + \text{O}^{2-} \Leftrightarrow (\text{Al}^{3+}, \text{Fe}^{3+}) + \text{OH}^-$. The case of replacement including Fe^{3+} ions is preferable for the first mechanism of heterovalent substitution, and the second scheme involves predominantly Al ions.

PHEROMONES ANALYSIS BY VIBRATIONAL SPECTROSCOPY

Bucşa, M.¹, Oprean, I.^{1,2} & Ristoiu, D.³

¹ Babeş-Bolyai University, Faculty of Chemistry and Chemical Engineering (Arany Janos Str., 11, 400028, Cluj-Napoca, Romania)

² "Raluca Ripan" Institute of Chemistry (Fantanele Str., 30, 400327, Cluj-Napoca, Romania)

³ Babeş-Bolyai University, Faculty of Physics (Kogalniceanu Str., 1, 400084, Cluj-Napoca, Romania)
e-mail: bmonica@chem.ubbcluj.ro

The application of Infrared and Raman spectroscopies with a view to determine the structure of some pheromone components is presented. The pheromones are used in horticulture, to prevent the sickness of the forest, and in agriculture for pest control (SIMIONESCU & MIHALACHE, 2000). The studied pheromones have unsaturated long linear or branched chains (8-23 carbon atoms), functionalized with various groups like carbonyl, ester, hydroxyl. The IR and Raman spectra give information about the qualitative aspects of the pheromonal cocktail. We used both above mentioned vibrational spectroscopies since these methods are non destructive and complementary techniques (ILIESCU et al., 2002; COLTHUP et al., 1964). These spectroscopic methods allowed us to study the structure of these natural compounds and made also possible the identification of its E (965 cm⁻¹) and Z isomers (Fig. 1).

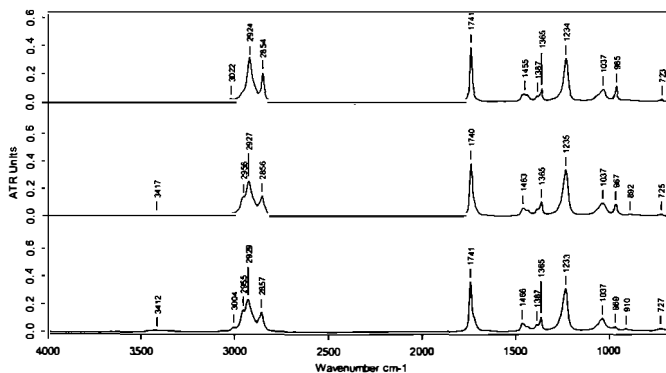


Fig. 1. Similarities and differences between E and Z isomers at E – 10,12OAc, E – 8,12OAc, Z – 7,12OAc

References

- COLTHUP, N.B., DALY, L.H. & WIBERLY, S.E. (1964): Introduction to Infrared and Raman Spectroscopy. Academic Press, New York. 199 p.
- ILIESCU, T., CINTA PANZARU, S., MANIU, D., GRECU, R. & ASTILEAN, S. (2002): Aplicații ale spectroscopiei vibraționale. Casa de Știință, Cluj-Napoca. 17 p.
- SIMIONESCU, A. & MIHALACHE, G. (2000): Protecția pădurilor. Ed. Mușatină, Suceava. 305 p.

**EPR STUDY AND MAGNETIC INVESTIGATION OF SYNTHETIC HEMATITE,
 α -Fe₂O₃**

Carbone, C.¹, Di Benedetto, F.², Marescotti, P.¹, Martinelli, A.³, Lima, N.⁴,
Pardi, L.⁵, Romanelli, M.⁴, Sangregorio, C.⁴ & Sorace, L.⁴

¹ DIP.TE.RIS., Università di Genova, C.so Europa, 26 – 16132 Genova

² Museo di Storia Naturale, Università di Firenze, Via G. la Pira, 4 – 50121 Firenze

³ INFN-LAMIA, C.so Perrone, 24 - 16152 Genova

⁴ UdR INSTM-Dip. Chimica, Università di Firenze, Via della Lastruccia, 3 – 50019 Firenze

⁵ I.P.C.F.-C.N.R. Area della Ricerca, via G. Moruzzi, 1 – 56124 Pisa

e-mail: carbone@dipteris.unige.it

Hematite (α -Fe₂O₃) belongs to the iron oxides group and is widely distributed in nature. The hematite structure can be described as corundum type, and consists of an arrangement of Fe³⁺ ions in octahedral coordination with oxygens in hexagonal close-packing.

Hematite is an antiferromagnetic mineral with Néel temperature $T_N = 960$ K and presents a first-order magnetic transition at $T_M = 265$ K, called Morin transition. Below this temperature the spins are aligned along the *c*-axis and hematite is antiferromagnetic; above T_M the spins lie in the basal plane of the crystal and show a weak ferromagnetism due to a slight spin canting out of the basal plane (DUNLOP & ÖZDEMİR, 1997). Despite its complex magnetic behaviour has been widely investigated, some questions, such as the origin of memory effect when it is thermally cycled through T_M , are still matter of debate (DE BOER et al., 2001).

In this contribution we present a thorough magnetic study on a fine powdered sample of synthetic hematite using a superconducting quantum interference device (SQUID) magnetometer and electron paramagnetic resonance (EPR) at different frequencies (from 9.25 GHz up to 285 GHz). The structural characterisation of this sample was performed through powder XRD and TEM.

The use of multifrequency EPR to characterise nanostructured metal oxide based material is a novel approach that can provide new and unique insights of the properties of these minerals. The Morin Transition was observed by EPR, as well as its strong dependence on the applied field, which was confirmed by magnetisation measurements.

References

DE BOER, C.B., MULLENDER, T.A.T. & DEKKERS, M.J. (2001): *Geophys. J. Int.*, **146**: 201-216.

DUNLOP, D.J. & ÖZDEMİR, Ö. (1997): *Rock magnetism: fundamentals and frontiers*. Cambridge University Press. 537 p.

**SPECTROSCOPIC CHARACTERIZATION OF Fe-OXIDES AND -
OXYHYDROXIDES ASSEMBLAGES RELATED TO ARD PROCESSES (LIBIOLA
MINE, ITALY)**

Carbone, C.¹, Di Benedetto, F.², Marescotti, P.¹, Martinelli, A.³, Sangregorio, C.⁴,
Lucchetti, G.¹, Sorace, L.⁴, Cipriani, C.² & Romanelli, M.⁴

¹ DIP.TE.RIS., Università di Genova, C.so Europa, 26 – 16132 Genova

² Museo di Storia Naturale, Università di Firenze, Via G. la Pira, 4 – 50121 Firenze

³ INFN-LAMIA, C.so Perrone, 24 – 16152 Genova

⁴ UdR INSTN-Dip. Chimica, Università di Firenze, Via della Lastruccia, 3 – 50019 Firenze
e-mail: carbone@dipteris.unige.it

The Libiola Fe-, Cu-sulfide mine (Eastern Liguria, Italy) represents one of the most important Italian exploited sulfide-ores. The ore deposit was mined from 1864 to 1962 either through open pits and underground excavations, in an area comprising 18 galleries, 7 open pits, and over 30 vertical shafts. Mine wastes were deposited in five major piles and in several minor waste-rock and tailings dumps, placed throughout the mining area.

In the Libiola Mine area numerous evidences of active ARD processes are present, occurring where the water-sulfides interactions are strongly favoured by the mining activities. The major mineral phases, resulting from these processes are the Fe-oxides and -oxyhydroxides occurring within ochreous to reddish crusts or within ochreous unconsolidated muds (MARESCOTTI & CARBONE, 2003).

An accurate characterization of the nanocrystalline Fe-oxides and -oxyhydroxides has been undertaken using X-ray powder diffraction (through the Rietveld quantitative interpretation), several spectroscopic techniques (Diffuse Reflectance Spectroscopy, IR, μ -Raman, EPR) and magnetic measurements (performed using a SQUID magnetometer).

The experimental evidences of XRPD, DRS and IR point to the presence of hematite and goethite as the main constituents of the crusts, with rare minor associations of quartz. The complex banded pattern of the samples has been related to different stages of the evolution of the precipitate. Thus, most of the macroscopic features of the assemblages arise from the intergrowth of these two main components. Moreover, both the IR and μ -Raman investigations revealed the presence of some accessory phases, namely lepidocrocite and schwertmannite, which represent “relics” of the pristine deposition of the precipitates and of the early stages of their evolution.

EPR spectra present features which can not be simply related to bulk hematite and goethite and to their relative proportions. In fact the reduced size of the grains substantially modifies the magnetic behavior of both minerals as indeed shown by magnetic measurements, which show for all the investigated samples, the characteristic behavior of superparamagnetic assemblies of particles.

References

MARESCOTTI, P. & CARBONE, C. (2003): *GEAM*, **109**: 45-53.

**INTERLAYER CATION CHARACTERIZATION IN PHYLLOSILICATES:
A XANES INVESTIGATION**

Cibin, G.^{1,2}, Marcelli, A.¹, Mottana, A.^{2,1} & Brigatti, M.F.³

¹ I.N.F.N., Laboratori Nazionali di Frascati, v. E. Fermi 40, I-00044 Frascati, Italy

² Dipartimento di Scienze Geologiche, Università Roma Tre,
Largo S. Leonardo Murialdo 1, I-00146 Roma, Italy

³ Dipartimento di Scienze della Terra, Università degli Studi di Modena e Reggio Emilia,
Via S. Eufemia 19, I-41100 Modena, Italy
e-mail: cibin@lnf.infn.it

Micas are the most common group of phyllosilicates, minerals that are among the least studied by XAS although being interesting for their two-dimensional structure properties. Micas are structural systems made up of infinite, parallel sheets two-dimensionally extending along the *a* and *b* axes and stacked on *c**. The three-dimensional mica structure consists of a composite M module made up of an octahedral sheet sandwiched between two facing tetrahedral T sheets, plus a pseudo-hexagonal planar network of cations, again extending along the *a* and *b* axes, which form the interlayer A. This latter layer is bound to the facing T sheets of two opposite TMT layers by weak ionic forces. Potassium, present in micas only as interlayer cation, is surrounded by two facing distorted hexagonal networks of O atoms belonging to two opposite tetrahedral sheets, with Al, Si and Fe atoms being the tetrahedral centres. In this study we tried to identify and reconstruct, using XANES spectroscopy, the local distortions of the tetrahedral sheets induced by the presence of Fe in both the tetrahedral and octahedral sites, by means of a systematic comparison of powder and single-crystal polarized XANES spectra taken at the potassium *K* edge. Previous XANES investigations performed at the Al, Mg, and Fe *K* edges have already demonstrated correlation between the total Fe content in the octahedral sheet and the overall structural modifications occurring in trioctahedral micas (TOMBOLINI et al., 2002a, b). In this work, using the MXAN code to fit the XANES spectra, we discuss the correlation existing between distortions at the interlayer cation sites and the experimental features at the potassium *K* edge in micas having different Fe concentrations. In these layered structures, the fitting method shows that multiple scattering calculations succeed in measuring the distortions induced by Fe; moreover, the quality of the data greatly depends upon sample orientation with respect to the incident beam direction, so that in-plane and out-of-plane orientations can also be determined. A general reconstruction of the structural environment of the interlayer cations in micas will be presented and discussed.

References

- TOMBOLINI, F., BRIGATTI, M.F., MARCELLI, A., CIBIN, G., MOTTANA, A. & GIULI, G. (2002a): Eur. J. Mineral., **14**: 1075-1085.
TOMBOLINI, F., MARCELLI, A., MOTTANA, A., CIBIN, G., BRIGATTI, M.F. & GIULI, G. (2002b): Int. J. Mod. Phys. B, **16**: 1673-1679.

**COMPARATIVE SPECTROSCOPIC STUDY OF CARBONATE ROCKS
FROM WESTERN MACEDONIA IN GREECE**

Dagounaki, K.¹, Zorba, T.², Anastasiou, M.², Chatzistavrou, X.²
& Paraskevopoulos, K.M.²

¹Department of Mineralogy-Petrology-Economic Geology, School of Geology, Aristotle University of Thessaloniki, 54124 Thessaloniki, Greece

²Physics Department, Aristotle University of Thessaloniki, 54124 Thessaloniki, Greece
e-mail: dagounaki@geo.auth.gr

Naturally occurring carbonate rocks are extremely important natural resources finding widespread applications (TULYAGANOV et al., 2002; MA et al., 2000), thus being placed among the most important raw materials and their study is the subject of the work of many researchers (DEER et al., 1992). Samples were collected from the broader Kozani area (north-western Macedonia, Greece), which geotectonically belongs to the Pelagonian zone. The Pelagonian zone consists of a crystalline pre-Carboniferous basement, which includes a series of metamorphic rocks intruded by large masses of Upper Carboniferous granites. The samples in powder form, with major components in different proportions of calcite CaCO₃, the most stable phase of calcium carbonate, and dolomite CaMg(CO₃)₂ were studied, aiming in the determination of the calcite/dolomite ratio. Other minerals (quartz, feldspars, micas, etc.) were participating in minor quantities in their mineralogical composition. The samples were also analyzed by XRD and other methods. The particle size was the same for all studied samples. For the quantitative characterization, a FTIR based method is used (ZORBA 2003, 2004). FTIR spectroscopy is an established experimental technique for qualitative mineral identification (McMILLAN & HOFMEISTER, 1988; WHITE, 1974) and is also being developed for quantitative mineralogy. FTIR relies on the detection of vibrational modes and mineral identification is possible because minerals have characteristic absorption bands in the mid infrared. In the present study the qualitative determination is based on the frequency shifts in the vibrational frequencies of functional groups due to chemical composition and the quantitative analysis of mineral sample is extracted from the FTIR spectrum through the use of appropriate peak analysis software employed for the calculation of the constituents' ratio. Comparison of the results with those received from XRD leads to the examination of the accuracy of the method used.

References

- DEER, W.A., HOWIE, R.A. & ZUSSMAN, J. (1992): An Introduction to the Rock-Forming minerals, 2nd edition. Longman, London, 696 p.
- MA, X., KANEKO, T., TASHIMO, T., YOSHIDA, T. & KATO, K. (2000): Chem. Eng. Sci., **55**: 4643.
- McMILLAN, P.F. & HOFMEISTER, A.M. (1998): In: HAWTHORNE, F.C. (ed.) Reviews in Mineralogy, 18, Spectroscopic Methods in Min. and Geology. Min. Soc. Amer., Washington D.C., 99.
- TULYAGANOV, D.U., RIBEIRO, M.J. & LABRINCHA, J.A. (2002): Ceramics Intern., **28**: 515.
- WHITE, W.B. (1974): In: FARMER, V.C. (ed.) The infrared spectra of minerals. Min. Soc., London, 227.
- ZORBA, T., ANASTASIOU, M., DAGOUNAKI, K., CHATZISTAVROU, X. & PARASKEVOPOULOS, K.M. (2003): Proceedings of the XIX Hellenic Conference on Materials, in press.
- ZORBA, T., ANASTASIOU, M., DAGOUNAKI, K., CHATZISTAVROU, X. & PARASKEVOPOULOS, K.M. (2004): submitted.

THE $P2_1/m \leftrightarrow C2/m$ PHASE-TRANSITION OF SYNTHETIC AMPHIBOLES IN THE SYSTEM $\text{Na}_2\text{O-Li}_2\text{O-MgO-SiO}_2\text{-H}_2\text{O}$: AN HT-FTIR STUDY

Della Ventura, G.¹, Iezzi, G.², Bellatreccia, F.¹, Cámara, F.³ & Oberti, R.³

¹ Dipartimento Scienze Geologiche, Università di Roma Tre, Largo S. Leonardo Murialdo 1, I-00146 Roma

² Dipartimento Scienze della Terra, Università di Chieti, I-66013 Chieti Scalo, Italy

³ CNR-Istituto di Geoscienze e Georisorse, Via Ferrata 1, I-27100 Pavia, Italy

e-mail: dellaven@uniroma3.it

In the last few years a series of experimental studies has renewed the interest in the $\text{Na}(\text{NaMg})\text{Mg}_5\text{Si}_8\text{O}_{22}(\text{OH})_2$ amphibole end-member, studied long ago by GIBBS et al. (1962) and MARESCH & LANGER (1976). $\text{Na}(\text{NaMg})\text{Mg}_5\text{Si}_8\text{O}_{22}(\text{OH})_2$ has the $P2_1/m$ space group at room temperature (IEZZI et al., 2004), and undergoes a displacive $P2_1/m \leftrightarrow C2/m$ phase-transition at 257 °C (CÁMARA et al., 2003). The room- T OH-stretching IR spectrum of $\text{Na}(\text{NaMg})\text{Mg}_5\text{Si}_8\text{O}_{22}(\text{OH})_2$ is characterised by two distinct groups of bands, which can be assigned to the two non-equivalent O-H dipoles in the $P2_1/m$ structure; this implies that the IR OH-spectrum of these amphiboles is a powerful tool for a fast detection of $P2_1/m$ symmetry. We present here a powder high- T FTIR study of amphiboles synthesised in the $\text{Na}_2\text{O-Li}_2\text{O-MgO-SiO}_2\text{-H}_2\text{O}$ system. Spectra were collected in the T range 25-380 °C on KBr disks, using a Linkam THS600 heating stage mounted on a NicPlan microscope at the University of Roma Tre. At 800 °C and 0.4 GPa, the $^{\text{B}}\text{Na} \Rightarrow ^{\text{B}}\text{Li}$ exchange is complete along the $\text{Na}(\text{NaMg})\text{Mg}_5\text{Si}_8\text{O}_{22}(\text{OH})_2 - \text{Na}(\text{LiMg})\text{Mg}_5\text{Si}_8\text{O}_{22}(\text{OH})_2$ join. Both XRD and FTIR spectroscopy show that all solid-solution terms have $P2_1/m$ symmetry at room- T . In particular, the IR spectra consist of two main bands around 3740 and 3715 cm^{-1} , the exact position of which being a function of $^{\text{B}}\text{Li}$ (NNN effect), and two minor bands at 3690 and 3667 cm^{-1} . At the transition temperature, the two main bands merge into one single absorption around 3720 cm^{-1} . No significant change is observed beyond this T . The behaviour of the IR OH-stretching bands is in agreement with the second-order character of the $P2_1/m \leftrightarrow C2/m$ phase-transition, which was obtained by single-crystal XRD studies of $\text{Na}(\text{NaMg})\text{Mg}_5\text{Si}_8\text{O}_{22}(\text{OH})_2$. The IR spectra show that the T_C of the phase-transition is linearly dependent on the amphibole composition: for $^{\text{B}}\text{Li} = 0$ apfu it is close to 250 °C (in agreement with CÁMARA et al., 2003), whereas for $^{\text{B}}\text{Li} = 1.0$ apfu it is close to 340 °C; this latter value is coherent with preliminary powder-XRD synchrotron data on the same sample. Therefore, in this system where the composition of the A and C-group sites is virtually constant, the $P2_1/m \leftrightarrow C2/m$ phase-transition is determined by the aggregate mean ionic radius at the B-group sites.

References

- GIBBS, G.V., MILLER, J.L. & SHELL, H.R. (1962): Am. Mineral., **47**: 75-82.
 MARESCH, W.V & LANGER, K. (1976): Contrib. Mineral. Petrol., **56**: 27-34.
 IEZZI, G., DELLA VENTURA, G., CÁMARA, F., OBERTI, R. & HOLTZ, F. (2004): Am. Mineral., **89**: 640-646.
 CÁMARA, F., OBERTI, R., IEZZI, G. & DELLA VENTURA, G. (2003): Phys. Chem. Minerals, **30**: 570-581.

**SPECTROSCOPIC CHARACTERISATION OF TRAVERTINES BY EPR
TECHNIQUES: A MULTIFREQUENCY STUDY**

Di Benedetto, F.¹, Montegrossi, G.^{2,*}, Pardi, L.A.³, Bercu, V.³, Romanelli, M.⁴, Minissale, A.²
& Paladini, M.⁵

¹ Museo di Storia Naturale, Università di Firenze, via G. La Pira 4, I50121, Firenze (Italy)

² Istituto di Geoscienze e Georisorse - CNR, via G. La Pira 4, I50121, Firenze (Italy)

³ Istituto per i Processi Chimico- Fisici - CNR, via G. Moruzzi 1, I56124 Pisa (Italy)

⁴ Dipartimento di Chimica, Università di Firenze, via della Lastruccia 3, I50019 Sesto Fiorentino (Italy)

⁵ Dipartimento di Scienze della Terra, Università di Firenze, via G. La Pira 4, I50121, Firenze (Italy)

*e-mail: giordano@geo.unifi.it

The EPR characterisation of paramagnetic metal cations, *e.g.* Mn(II), Fe(III), in calcite-based materials has attracted many studies, because of the very informative experimental spectra and the peculiar crystal field of the Ca site in this mineral. Recently, EPR spectroscopy has been also applied to the travertine characterisation, appearing a promising tool for the understanding of the physico-chemical condition of its genesis.

Mn(II), occurring as an ubiquitous trace substituent of Ca, may be considered as an ideal tool for the systematic investigation of travertines of different localities and origins, because the EPR spectrum depends on the local ionic crystal field. Several parameters (zero-field and hyperfine structure, linewidth, isorientation) appear to be promising criteria to distinguish and classify different travertines. A significant variability of the EPR spectral parameters, in fact, can justify their use as minero-chemical and geochemical markers. Nevertheless, a very accurate knowledge of the dependence of the spectrum on all the Hamiltonian interactions is required. A multifrequency approach, therefore, has been undertaken, in order to refine and clarify the informations contained in the very complex X-band spectrum.

The study has been carried out on a sample, coming from Papigno (Terni, central Italy), a very recent deposit (60 ka), inactive nowadays. At present, a meteoene travertine is being deposited near the village of Marmore and the isotopic $\delta^{13}\text{C}$ composition of the two deposits is very similar (from -1.9 to 1.0 ‰ PDB at Papigno and from -0.8 to 0.5 ‰ PDB at Marmore). Room temperature 9.5, 95, 190 and 285 GHz EPR spectra were recorded at very low scan speed. While the 9.5 spectrum consists of the well-known sextet, characterised by a splitting of each major peak in positive and negative portions and by the forbidden lines, the high frequency spectra are simplified, being constituted only by the six $m_S -1/2 \Rightarrow +1/2$ allowed transitions. The multifrequency approach evidences a reduction of the linewidth passing from X band to 95 GHz and the presence of a field independent splitting of the transitions. The latter must be due to either fine or hyperfine structure or both. An interpretation of the multifrequency spectra in terms of the fine structure including third order perturbation terms is presented.

UV-VISIBLE-NIR SPECTROSCOPY AND XRPD OF RUTILE PIGMENTS DOPED WITH CHROMOPHORES (Cr, Mn, Ni, V) AND COUNTERIONS (Mo, Nb, Sb, W)

Dondi, M.¹, Cruciani, G.², Matteucci, F.¹ & Raimondo, M.¹

¹ CNR-ISTEC, Institute of Science and Technology for Ceramics, via Granarolo 64, 48018 Faenza (Italy)

² Earth Sciences Department, University of Ferrara, Corso Ercole I d'Este 32 44100 Ferrara (Italy)
e-mail: dondi@istec.cnr.it

The high refractive indices and melting point of TiO₂ make it a valuable pigment for ceramic applications, where anatase is progressively converted to rutile on heating. The capacity of the rutile structure to host a number of the first row transition elements allows to get a rather wide colour palette: orange (Cr), brown (Mn), yellow (Ni) and gray (V). Together with the chromophore, a high field strength ion (so-called *counterion*) is added in the industrial practice to achieve the desired colour and improve the technological properties of pigments.

The colouring mechanisms have been not thoroughly investigated, being generally attributed to crystal field transitions, with some role played by a Ti-O charge transfer (EPPLER, 1987; ISHIDA et al., 1990; SORLÍ et al., 2004).

The aim of this work is to understand better these mechanisms on typical industrial co-doped rutile pigments having the stoichiometry Ti_{1-2x}A_xB_xO₂, where A = Cr, Mn, Ni, V (chromophore ion) and B = Mo, Nb, Sb, W (counterion), with x=0.03. Samples were prepared by conventional ceramic process (firing from 700 to 1100 °C). A combination of UV-visible-NIR spectroscopy (diffuse reflectance, Perkin Elmer λ35, 200-1100 nm, integrating sphere, BaSO₄ as reference, standard illuminant D₆₅ and observer 10°) and X-ray powder diffraction (Philips PW 1820/00, monochromated-CuK_{α1,2} radiation, 15-130°2θ, 0.02°2θ/10s) with Rietveld refinement (GSAS-EXPGUI) was used for pigment characterization.

The colour of rutile pigments is determined by both charge transfer (CT) and crystal field (CF) effects: a Ti⁴⁺-O²⁻ CT band shifts from the UV to the visible region with the anatase-to-rutile transformation, contributing to get an intense coloration. A progressive incorporation of chromophore into the rutile lattice produces CF d-d transitions, partially overlapped with the CT band, and complex spectra very difficult to be quantitatively interpreted. Moreover, there are clues that the valence of some transition elements changes during the synthesis: the cell volume is correlated with the weighed cationic radius assuming the following valence, coherent with optical spectroscopic data: Cr³⁺, Mn³⁺, Ni²⁺/Ni³⁺, V⁴⁺, Mo⁵⁺, Nb⁵⁺, Sb⁵⁺/Sb³⁺, W⁵⁺. The cell dimensions *a* and *c* are mainly affected by the ionic radii of chromophores and counterions, respectively, according to the sequences: V<Cr<Mn<Ni and Mo~W<Nb<Sb.

References

- EPPLER, R.A. (1987): J. Am. Ceram. Soc., **70**: C64-C66.
ISHIDA, S., HAYASHI, M. & FUJIMURA, Y. (1990): J. Am. Ceram. Soc., **73**: 3351-3355.
SORLÍ, S., TENA, M.A., BADENES, J.A., CALBO, J., LLUSAR, M. & MONRÓS, G. (2004): J. Eur. Ceram. Soc., **24**: 2425-2432.

THE ESTIMATION OF VOLCANIC GLASS CONTENT IN NATURAL MATERIALS USING PXRD AND FTIR TECHNIQUES

Drakoulis, A.¹, Kantiranis, N.², Filippidis, A.¹, Stergiou, A.³, Zorba, T.³, Paraskevopoulos, K.M.³ & Squires, C.¹

¹Department of Geology, Aristotle University of Thessaloniki, 54124 Thessaloniki, Greece

²Faculty of Sciences, Aristotle University of Thessaloniki, 54124 Thessaloniki, Greece

³Department of Physics., Aristotle University of Thessaloniki, 54124 Thessaloniki, Greece
e-mail: alexdr@geo.auth.gr

One of the basic constituents of the industrial rocks is the volcanic glass. Therefore, the calculation of its percentage in a sample is important in Economic Geology. Volcanic glass is usually observed in PXRD as a broad background hump starting at approximately $10^\circ 2\theta$. Five standard sample mixtures were used with the following weight percent ratios of amorphous and crystalline phases: 100-0 %, 75-25 %, 50-50 %, 25-75 % and 0-100 %, respectively. The 100 % volcanic glass used as standard material, is obsidian from the island of Santorini (KANTIRANIS et al., 1999). Crystalline materials chosen for the preparation of the sample mixtures were quartz, calcite, muscovite, montmorillonite and heulandite. The five constituents of the crystalline phases in the samples were present in equal quantities. The conditions for the preparation and analysis of the samples were identical.

PXRD analysis was performed on randomly oriented samples, which were scanned over the interval $3-63^\circ 2\theta$, using a Philips PW1710 diffractometer, Ni-filtered CuK_α radiation and PCAPD v.3.6 (1994) software. The PXRD patterns were studied by two methods. For the first method, the area of the broad background hump of each sample was compared with the corresponding area of the broad background hump of the 100 % volcanic glass. For the second method, which calculates the crystallinity of the sample, each individual peak of the PXRD patterns of the samples was analyzed using exponential shape functions (pseudo-Voigt function), including those for amorphous material (STERGIOU, 1995). The results of the two methods were used providing that the variance of values of volcanic glass were ± 3 %.

FTIR measurements were performed using the KBr pellet technique. The transmission spectra were recorded using a Bruker IFS113v spectrometer under vacuum in the MIR region, with a resolution of 2 cm^{-1} . The presence and characteristics of each band is due to vibrations related to sites with corresponding symmetry. Any structural change taking place influences characteristic bands and this gives direct information on the crystallinity. The development of these bands through the increase of volcanic glass participation is used for the quantitative analysis of the studied samples.

The results indicate that the two techniques could constitute a reliable procedure for the accurate estimation of the amount of volcanic glass contained in a natural rock sample.

References

- KANTIRANIS, N., TSIRAMBIDES, A., FILIPPIDIS, A. & CHRISTARAS, B. (1999): *Mat. Struct.*, **32**: 546-551.
PC-APD (1994): Automated powder diffraction Software, v3.6, Philips Analytical X-ray B.V.
STERGIOU, A. (1995): "CRYST" Program for crystallinity determination by XRD profile fitting., Dep. of Physics, Aristotle Univ. Thessaloniki.

XPS STUDIES OF BINARY Cu-Sn ALLOYS AGED IN CLIMATIC CHAMBER

Emiliani, C.¹, Bernardini, G.P.¹, Trosti-Ferroni, R.¹, Vaughan, D.J.², Wincott, P.L.²
& Walton, J.³

¹ Dept. Of Earth Sciences, University of Florence, via La Pira 4, I-50121, Florence, Italy

² Dept. Of Earth Sciences, University of Manchester, Oxford Road, M13 9PL

³ Corrosion and Protection Centre, UMIST, Sackville Street, P.O. Box 88, Manchester, M60 1QD
e-mail: emiliani@geo.unifi.it

During the last few decades great interest has arisen concerning conservation problems of metal artefacts exposed in an open environment due to the formation of alteration products. Alteration patinas have greatly increased as a result of the increase in pollutants produced by human activity. In recent years, non-destructive surface analytical probes, such as PIXE, LIPS, and XPS have been applied to this problem. X-ray Photoemission Spectroscopy (XPS) is not always suitable for natural patinas which are often quite thick, but it can be applied to studies of patina onset obtained by ageing materials in a climatic chamber. The characteristics of this technique, in fact, make it especially suitable for studies of the initial alteration mechanisms for a large range of materials. During the initial alteration step, the corrosion products formed are usually extremely thin so that XPS may be used to detect the presence and determine the chemistry of alteration products, produced at this stage.

XPS has previously been used to detect initial corrosion products formed on metals and alloy surfaces (in particular copper, bronzes and brasses) exposed to pollutant gases such as SO₂, NO_x and Cl₂. These include phases such as Cu₂O, CuO, CuCl, which correspond to the minerals cuprite, tenorite, nantokite. Here, a new XPS imaging instrument has been used to detect the formation of copper carbonates, sulphates and chlorides and tin sulphides on the surfaces of binary Cu-Sn alloys aged in a climatic chamber with SO₂ as a pollutant. Parallel XPS imaging has been used to acquire a wide energy spectrum at each pixel, which coupled with PCA analysis has been employed to obtain enhanced image contrast between elemental and chemical speciation at the alloy surface.

**CRYSTAL CHEMISTRY OF THE STANNITE-GROUP COMPOUNDS
(EPMA, EPR, SQUID, MÖSSBAUER SPECTROSCOPY)**

Evstigneeva, T.¹, Di Benedetto, F.², Kulikova, I.³ & Rusakov, V.⁴

¹ IREM RAS, Staromonetny, 35, Zh-17 109017, Moscow, Russia

² Dept. Sci. Earth, University of Florence, via La Pira, 4, I-50121, Florence, Italy

³ IMGRE, Veresayeva str., 15, 121357, Moscow, Russia

⁴ Phys. Dept., Vorobjevy Gory, GSP-2, 119992, Moscow, Russia

e-mail: evst@igem.ru; dibenofr@steno.geo.unifi.it; rusakov@moss.phys.msu.ru

In order to check the model of complex isomorphous replacement “Cu → Fe” (EVSTIGNEEVA et al., 2003), and to determine the metal valence states, EPMA, EPR, SQUID, and Mössbauer spectroscopy were performed on 10 synthetic analogues of the kuramite - stannite series, $\text{Cu}_{3-x}\text{Fe}_x\text{SnS}_4$ ($0 < x < 1$). The Cu valence and the character of chemical bond were studied with EPMA on the base of self-absorption of the measured copper X-ray emission. According to the first results the contribution of Cu 3d electrons to the chemical bond increases if the Fe content increases from 0 to 0.5 afu. It is caused by the Cu-Fe interaction due to the short Cu-Fe distance between Cu_{Tet} and Fe_{Oct} . The general dependency of experimental magnetic susceptibility on the temperature corresponds to the theoretical high-temperature limit of the Curie constants calculated on the base of the proposed model of isomorphism (EVSTIGNEEVA et al., 2003). The magnetic susceptibility line is bent at $[\text{Fe}] \sim 0.5$ afu, and consists of two positive linear trends. The Curie constant values are located below the theoretical line at $[\text{Fe}] < 0.5$ afu, while above 0.5 Fe afu they plot slightly above this line. The first trend should be explained by the intermediate spin state of Fe^{3+} , the best fit agrees with $S = 3/2$. The second trend, parallel to the theoretical one, but shifted to higher emu/mol values, corresponds to the $\text{Fe}^{3+}/\text{Fe}^{2+}$ exchange model considering that a small spin-orbit interaction increases the Fe^{2+} contribution in comparison with stannite, 3.15 in spite of 3 emu/mol., as was shown by BERNARDINI et al. (2000). These results can prove the Fe spin transition between 0.5 – 0.6 Fe afu. The Fe spin state and antiferromagnetic interactions like those established for natural and synthetic stannites (BERNARDINI et al., 2000) are discussed. The data obtained are in good agreement with results of Mössbauer spectroscopy, but the schemes of isomorphism in stannite family compounds proposed earlier need to be precised.

References

- BERNARDINI, G.P., BORRINI, D., CANESCHI, A., DI BENEDETTO, F., GATTESCHI, D., RISTON, S. & ROMANELLI, M. (2000): *Phys. Chem. Minerals*, **27**: 453-461.
EVSTIGNEEVA, T.L., RUSAKOV, V.S., KABALOV, Y.K. (2003): *New Data on Minerals*, **32**: 1325-1331.

STRUCTURE AND COLOR OF THE JACK CREEK DUMORTIERITE (MONTANA, USA) USING SPECTROSCOPIC APPROACHES

Farges, F.^{1,2}, Galois, L.³, Balan, E.^{3,4}, Fuchs, Y.¹ & Linares, J.⁵

¹ Lab. Géomatériaux, Univ. Marne la Vallée, CNRS FRE 2455, 77454 Marne la Vallée cedex 02, France

² Department of Geological Sciences, Stanford University, USA

³ LMCP, UMR CNRS 7590 and IPGP. Université Paris VII, 4 place Jussieu, 75252, Paris cedex05, France

⁴ LMCP, UMR CNRS 7590, and IRD. Université Paris VII, 4 place Jussieu, 75252, Paris cedex05, France

⁵ LMOV, CNRS UMR 8634, UVSQ, Ave. des Etats Unis, 78000, Versailles, France

e-mail: fuchs@univ-mlv.fr

A blue dumortierite sample from the Jack Creek hydrothermal system (Boulder Basin, Montana, USA) (FOIT et al., 1989) was studied using Fourier-transform infrared spectroscopy (FTIR), electron paramagnetic resonance (EPR) spectroscopy, near UV-visible-near Infrared spectroscopy, X-ray absorption near edge spectroscopy (XANES) and Mössbauer spectroscopy.

FTIR spectroscopy shows for the OH groups the existence of various environments, which are related to substitutions and/or vacancies in the M1 octahedral site. Mössbauer spectroscopy consistently reveals the presence of Fe²⁺ and Fe³⁺ in octahedral sites, Fe³⁺ being dominantly represented. The strong and sharp signal observed at 0.113 T in the EPR spectra of pink dumortierite samples with low Fe content (Lincoln Hill and Louvincourt) (FUCHS et al., 2004) and related to a site with a pure axial distortion, [i. e., a site symmetry with a n-fold ($n \geq 3$) rotation axis, corresponding to the A11 site in dumortierite] is not present in the Jack Creek sample. In contrast, the signals observed at 0.16 T correspond to more distorted sites (ABRAGAM & BLEANEY, 1970). This rhombic signal can be related to Fe³⁺ ions located in tetrahedral or in distorted octahedral sites (A12, A13 or A14).

EPR and XANES also indicate that a fraction of the Fe atoms are not isolated but concentrated in magnetic domains. Optical spectroscopy indicates an important contribution of intervalence charge transfer transitions (IVCT), the most important between Fe²⁺ and Fe³⁺ and a smaller contribution between Fe²⁺ and Ti⁴⁺. These transitions are responsible for the blue color of the Jack Creek Dumortierite sample.

Based on the XANES study of the Jack Creek (Montana) sample Ti seems to be mainly restricted to the M1 site (95%). Ab initio XANES (using FEFF) calculations at the Fe K-edge suggest that Fe is located mainly in the A12, A13 and A14 sites (having the highest energy and shorter average Al-O distances). Thermodynamically, Fe would preferentially partition toward the A11 site. But, a temperature dependence of different site distortion could explain this apparent discrepancy as for Fe in olivine.

References

- ABRAGAM, A. & BLEANEY, B (1970): Electron paramagnetic resonance of transition ions. Clarendon Press, Oxford. 911p.
- FOIT, JR., F.F., FUCHS, Y. & MYERS, P.E. (1989): *Am. Mineral.*, **74**: 1317-1324.
- FUCHS, Y., BALAN, E., FARGES, F., LINARÈS, J. & HORN A. (2004): *Lithos*, **73**: 39.

**ELECTRONIC STATE OF SULFUR IN TETRAHEDRITE-TENNANTITE SERIES:
A MICRO-XANES STUDY**

Ferreira, J.A.¹ & Figueiredo, M.O.²

¹ Geosciences Lab., INETInovação, Rua da Amieira, 4466-956 S. Mamede de Infesta, Portugal

² Cryst. Mineralogy Centre, IICT, Al. D. Afonso Henriques, 41-4º, 1000-123 Lisboa, Portugal
e-mail: jorge.ferreira@ineti.pt

Tetrahedrites (*s.l.*) are an important group of economically valuable sulphosalt minerals with ideal simplified formula (WU & PETERSEN, 1977), $(M^{1+})_{10} (M^{2+})_2 (M^{3+})_4 [S_{13}]$, where M^{1+} ions are mainly Cu with some Ag, divalent ions being Cu, Zn, Fe, Hg, Cd, Pb, and trivalent ions Sb, As, Bi. The cubic crystal structure of tetrahedrite (*s.l.*) contains two formula units per unit cell. The atomic array derives from the arrangement in sphalerite - the prototype of so-called "tetrahedral structures" where each one of the constituting ions (Zn^{2+} and S^{2-}) is surrounded by a tetrahedron of species with opposite sign, by leaving unoccupied (vacant) four out of sixteen cubic closest-packing anion positions, and further replacing this tetrahedral cluster of vacancies by one sole S-atom. This replacement process provides pyramidal and triangular coordinations to some of the metal ions, and gives rise to a peculiar coordination and binding situation for one out of thirteen sulphur atoms in the formula unit. The S-atom replacing a tetrahedral cluster of packing vacancies becomes octahedrally coordinated by six close Cu/Ag and additionally by four Sb/As (themselves in pyramidal coordination by S^{2-}) with the lone electron pair probably oriented towards that peculiar central S-atom.

X-ray absorption experiments at the sulphur *K*-edge were performed using the instrumental set-up of beam line ID-21 (SUSINI et al., 2000) at the ESRF* with the purpose of disclosing the influence of the environment (geometry and nature of metal ions coordinating sulphur) and of eventual bonding effects upon details of S 1s XANES spectra.

Samples of minerals belonging to the tetrahedrites-tennantite series with varied chemical composition and geologic provenance (Neves-Corvo mine in Portugal and Atacocha mine in Perú), plus synthetics with established composition within the systems Cu-As-Sb-S were studied.

The general trend of S *K*-edge XANES spectra from tetrahedrites, compared to prototype minerals (e.g. chalcopyrite), is similar but the white line does not occur with similar intensity and some post-edge features display different relative intensity, being sometimes split.

Theoretical calculations and XANES spectra modelling with FEFF8.10 code (ANKUNDINOV et al., 2000) were performed with the purpose of interpreting the observed details, either for the model minerals or the tetrahedrite-tennantite series, both minerals and synthetics.

*Financing from EU is acknowledged. Thanks are due to Drs. Jean Susini and Barbara Fayard (ESRF beam line scientists) for their support.

References

- ANKUDINOV, A., RAVEL, B. & REHR, J. (2000): Manual of FEFF8.10 Program. The FEFF Project. Dept. Phys., Univ. Washington, Seattle. 62 p.
SUSINI, J. et al. (2000): X-Ray Microscopy. Proc IV Int. Conf., Am. Inst. Phys., N. Y., **507**: 19-26.
WU, I. & PETERSEN, U. (1977): Econ. Geol., **77**: 993-1016.

CRYSTAL CHEMICAL BASES FOR A DATA BANK ON SULPHUR *K*-EDGE XANES SPECTRA IN SULPHIDE AND SULPHOSALT MINERALS

Figueiredo, M.O.¹ & Susini, J.²

¹ Cryst. Miner. Centre, ICT, Al. D. Afonso Henriques, 41-4°, 1000-123 Lisboa, Portugal

² European Synchrotron Radiation Facility (ESRF), BP 220, 38043 Grenoble, France
e-mail: crysmin@clix.pt

The general trend of the X-ray absorption spectrum close to an edge – either *K* for low atomic number elements or *L* for heavier ones – is known to respond to the electronic state of the absorber, allowing for deducing the formal valence of this element mainly through the energy shift observed for the discontinuity.

The atomic vicinity of the absorbing species within the host condensed-phase (that is, the chemical binding) also affects the energy region close to an edge. Beyond depending on the nature of coordinating species, the particular features of pre- and post-edge regions in XANES spectra also reflect the joint influence of geometry and symmetry of the coordination polyhedron – features that are well established in solids with known crystal structure.

Minerals are then suitable model compounds for interpreting XANES data, both through the direct comparison of collected spectra and via theoretical modeling using any of the available calculation codes – e.g. FEFF (ANKUNDINOV et al., 1998), WINXAS (RESSLER et al., 1999). A crystal chemical approach to the mineral crystal structures therefore becomes most useful for disclosing true cause-effect relations.

Sulphur-containing minerals are essentially sulphates with SO_4^{2-} tetrahedra as anionic groups linked to a diversity of cations and not seldom to water molecules, sulphides (isolated S^{2-} anions), disulphides (S_2^{2-} dimers) and sulphosalts where various situations may coexist, including a high coordination number for peculiar S-atoms – e.g. in tetrahedrites (FIGUEIREDO & FERREIRA, 2002). Coordination environments of S^{2-} by metal ions in sulphides range from tetrahedral in sphalerite-type to octahedral in galena-type sulphides, being less regular in sulphosalts (FIGUEIREDO et al., 1988). Both cubic crystal structure types, $\text{Zn}^{\text{I}}[\text{S}^{\text{I}}]$ and $\text{Pb}^{\text{0}}[\text{S}^{\text{0}}]$, as well as the cubic disulphides typified by pyrite $\text{Fe}^{\text{0}}[\text{S}_2^{\text{I}}]$, display wide morphotropic domains. Accordingly, it is possible to find suitable examples for modeling different bonding situations.

If the electronic state of the metal(s) is also studied, the success of theoretically modeling the S *K*-edge XANES spectra is highly enhanced. The building up of a data bank could then be envisaged, under the requisite of strictly quoting the provenance of mineral samples and their physical characteristics. The aim of this work is just to settle the crystal chemical bases for such a data bank, starting with a small illustrative group of sulphide and sulphosalt minerals.

References

- ANKUNDINOV, A.L., RAVEL, B., REHR, J.J. & CONRADSON, S.D (1998): Phys. Rev. B, **58**: 7565-7576.
FIGUEIREDO, M.O., BRIANSÓ, J.L., BASTO, M.J. & ALVAREZ, A. (1988): Acta Geol. Hisp., **23**: 33-38.
FIGUEIREDO, M.O. & FERREIRA, J.A. (2002): 9th Int. Symp. Exp. Miner. Petrol. & Geochem. EMPG-IX, Zürich. Poster MPC-25.
RESSLER, T., WONG, J. & ROOS, J. (1999): J. Synchr. Rad., **6**: 656-658.

**AN X-RAY ABSORPTION SPECTROSCOPY STUDY AT SULFUR K-EDGE OF
HAÜYNE FROM SAINT ANTÃO ISLAND (CAPE VERDE)**

Figueiredo, M.O.¹, Pereira da Silva, T.¹, Silva, L.C.², Mirão, J.³ & Mendes, M.H.²

¹Cryst. Miner. Centre, ICT, Al. D. Afonso Henriques, 41-4^oesq., 1000-123 Lisboa

²Geology Centre, ICT, Al. D. Afonso Henriques 41-4^odto, 1000-123 Lisboa

³Geophysics Centre, Univ. of Évora, Aptd. 92, 7001-019 Évora, Portugal
e-mail: crysmin@clix.pt

Haüyne is an aluminosilicate first described by Brunn-Neergard in 1807 (quoting Dana, 6th ed., p. 431). The crystal structure was determined by MACHATSCHKI (1934) and received the SB symbol S6₉. Since then various isotypical minerals were identified, namely sodalite, nosean and lazurite – the latter being sulphur-enriched and used as a natural and valuable blue pigment named ultramarine. The cubic framework of Al and Si tetrahedra forms large cages identical to those found in zeolites, where a large anion (mainly sulphate, but also chlorine) is hosted, surrounded by alkali cations (mainly Na with minor K and Ca).

Despite being known for almost two centuries, haüyne is still nowadays a subject of intense structural and chemical study (TAUSON et al., 1998) and its occurrence in mantle rocks has been reported for the first time only a few years ago (WULFF-PEDERSEN et al., 2000).

Recently, haüyne was identified in tephritic and phonolitic rocks from Santo Antão Island, Cape Verde Arquipelago, and a peculiar microstructure was remarked (SILVA & MENDES, in preparation). A chemical study with synchrotron radiation X-ray fluorescence (SRXRF) was subsequently undertaken using the photon microprobe of the LURE* (line D-15A at DCI), aiming at understanding the chemical variations that could be associated to fluctuations in the bluish colour. A systematic presence of Sr and Mo as trace elements was noticed by SRXRF analysis in all haüyne samples from Santo Antão.

In parallel, an X-ray absorption study at the sulphur K-edge was undertaken at the ESRF* using beam line ID-21 in order to ascertain the speciation state of that element in relation to colouring. XANES spectra clearly denoted the presence of oxidised sulphur in the form of sulphate through the characteristic sharp white line at 2482 eV. *Ab-initio* simulations based on the multiple scattering approximation implemented in the FEFF code (ANKUNDINOV et al., 1998) were carried out to model S K-edge XANES spectra. Observed post-edge features and other details are discussed taking into account SRXRF data and theoretical spectra modelling.

*Financing from EU to perform SR studies is acknowledged. Thanks are due to Prof. P. Chevallier from the LURE and to Drs. J. Susini and Barbara Fayard from the ESRF for their support in the experiments.

References

- ANKUNDINOV, A.L., RAVEL, B., REHR, J.J. & CONRADSON, S.D. (1998): Phys. Rev. B, **58**: 7565-7576.
MACHATSCHKI, F. (1934): Strukturbericht, **3**: 166.
TAUSON, V.L., AKIMOV, V.V., SAPOZHNIKOV, A.N. & KUZNETSOV, K.E. (1998): Geochem. Internat., **38**: 717-733.
WULFF-PEDERSEN, E., NEUMANN, E.-R., BURKE, E.A.J., VANNUCCI, R., BOTTAZZI, P., OTTOLINI, L., GJØNNES, J. & HANSEN, V. (2000): Am. Mineral., **85**: 1397-1405.

**OH DEFECTS IN SPODUMENE:
A COMPARATIVE STUDY OF SPODUMENE OF VARIOUS GENETIC TYPES**

Filip, J. & Novák, M.

Institute of Geological Sciences, Masaryk University in Brno, Kotlářská 2, 611 37, Brno, Czech Republic
e-mail: filip@sci.muni.cz

Lithium-bearing pyroxene, spodumene (ideally $\text{LiAlSi}_2\text{O}_6$), is a nominally anhydrous mineral (NAM). As recent research shows, many of NAMs (including pyroxenes) contain various concentrations of incorporated OH defects (ROSSMAN, 1996). Polarised FTIR absorption spectra of spodumene single-crystals were measured to compare the water contents in spodumenes of four genetic types (magmatic, hydrothermal, secondary – after petalite, and metamorphic) with other pyroxenes. Well developed spodumene crystals of hydrothermal origin (kunzite and hiddenite) were studied to understand the OH bonding system in spodumene. Sections parallel to (100), (010) and (110) were measured. On the basis of these measurements and due to the excellent cleavage of spodumene crystals, only polished cleavage plates parallel to (110) were used in cases of spodumenes of other genetic types. OH defect concentrations were calculated using the Lambert-Beer's law (for details see LIBOWITZKY & ROSSMAN, 1997).

FTIR spectra of all samples are characterized by pleochroic absorption bands in the 3400 to 3500 cm^{-1} spectral region (predominantly two bands at around 3409 and 3423 cm^{-1}). From the pleochroic behaviour of these spectra it seems that the OH dipole direction is oriented approximately parallel to n_γ in the spodumene structure, as observed for other pyroxenes (BERAN & LIBOWITZKY, 2003). Small variations of water content in spodumenes of various genetic types were detected: magmatic spodumenes contain <0.1 to 3.3 wt. ppm H_2O , hydrothermal spodumenes 0.1 to 0.2 wt. ppm H_2O , spodumene after petalite contains up to 0.6 wt. ppm H_2O and metamorphic spodumene contains up to 2.0 wt. ppm H_2O . Heterogenous distribution of OH defects within one single crystal was observed.

Water content calculations from sections or cleavage plates parallel to (110) produce slightly overestimated values (< +10 % rel.). Therefore, and because of high background from fluid inclusions and interference fringes, the calculated concentrations of OH defects have relatively large errors. In comparison with other pyroxenes (usually 1200 to 20 wt. ppm H_2O , depending on geological environment; SKOGBY et al., 1990), all spodumenes contain significantly lower contents of OH in the structure.

This work has been supported by a Marie Curie Fellowship of the European Commission under contract number HPMT-CT-2000-00138. We thank U. Kolitsch, A. Wiczorek and A. Wagner for technical assistance and A. Beran and E. Libowitzky for constructive criticism that significantly improved the manuscript. Samples for this study were kindly provided by Moravian Museum in Brno, Czech Republic, and by E. Libowitzky.

References

- BERAN, A. & LIBOWITZKY, E. (2003): *Phase Trans.*, **76**: 1-15.
LIBOWITZKY, E. & ROSSMAN, G.R. (1997): *Am. Mineral.*, **82**: 1111-1115.
ROSSMAN, G.R. (1996): *Phys. Chem. Minerals*, **23**: 299-304.
SKOGBY, H., BELL, D.R. & ROSSMAN, G.R. (1990): *Am. Mineral.*, **75**: 764-774.

NATURE OF BENITOITE $\text{BaTiSi}_3\text{O}_9$ LUMINESCENCE

Gaft, M.¹, Nagli, L.² & Waychunas, G.³

¹ International Technologies Lasers (ITL), Rishon-Lezion, Hachoma 12, Israel

² Tel-Aviv University, School of Physics and Astronomy, Tel-Aviv, Israel

³ Geochemistry Dept., Earth Sciences Division, MS 70-108B E.O. Lawrence Berkeley National Laboratory, One Cyclotron Road, Berkeley, CA 94720
e-mail: michael_g@itlasers.com

Three broad bands and one narrow line have been detected in laser-induced luminescence spectra of benitoite. At 300 K the first band has $\lambda_{\text{max}} = 420$ nm, $\Delta = 80$ nm and $\tau = 2.6$ μs . The excitation spectrum consists of a narrow band peaking at 290 nm with a shoulder at 245 nm. At lower temperatures luminescence intensity and band shape remain practically the same, but τ becomes substantially longer, up to 1.1 ms at 40 K. It is proved that this blue band is connected with intrinsic isolated TiO_6 octahedra. The metastable level $^3\text{T}_{1u}$ is the emitting level at low temperatures with long τ . At higher temperatures an energy level with higher radiation probability must be involved in the emission process, and this level is situated at 0.06 eV higher than the lowest level. These two levels may be connected with $^3\text{T}_{1u}$ level splitting or with closely spaced $^3\text{T}_{1u}$ and $^3\text{T}_{2u}$ levels. Decay time shortening and thermal quenching are connected with non-radiative decay within the TiO_6 luminescence center, while energy migration does not take place at least up to room temperature.

At 300 K the second band has $\lambda_{\text{max}} = 660$ nm, $\Delta = 135$ nm and $\tau = 1.1$ μs . The excitation spectrum consists of an asymmetric band peaking at 350 nm. At lower temperatures the luminescence intensity is 10 times stronger and the emission band becomes narrower with longer τ (100 nm and 25 μs at 40 K, respectively). Such behavior may be connected with an intrinsic Ti^{3+} luminescence center. Excitation peaking at 355 nm is connected with the $^2\text{T}_2$ - ^2E transition, while the splitting of the ^2E state is a reason of the two shoulders present in the excitation spectrum. At lower temperature the opposite transition generates an intensive luminescence band peaking at 660 nm with $\tau = 20$ μs . Thermal quenching and drastically reduced decay time with increasing temperature result from a non-radiative transition from excited to ground state.

At 300 K the third band has $\lambda_{\text{max}} = 725$ nm, $\Delta = 125$ nm and $\tau = 100$ μs . It is accompanied by a narrow line at 682 nm with similar τ . At lower temperatures the broad band is much weaker, while the narrow line becomes substantially stronger with longer τ , reaching 1.1 ms at 40 K. Such behavior is suitable for a d^3 luminescence center, possibly Mn^{4+} or Cr^{3+} .

SINGLE-CRYSTAL RAMAN SPECTROSCOPY OF VESUVIANITE GROUP MINERALS IN THE OH REGION

Galuskin, E.V.¹, Galuskina, I.O.¹, Janeczek, J.¹ & Wzałik, R.²

¹ Faculty of Earth Sciences, University of Silesia, Bedzinska 60, 41-200 Sosnowiec, Poland

² Institute of Physics, University of Silesia, Bankowa 12, 00-000 Katowice, Poland
e-mail: galuskin@us.edu.pl, irina@wnoz.us.edu.pl

Minerals of the vesuvianite group with formulae $X(1-3)_{18}X'(4)Y(1)Y(2,3)_{12}T(1,2)_5[Z(1,2)O_4]_{10}[Z(3)_2O_7]_4W_9O_{1-2}$ ($Z = 2$) are presented by “rod” polytypes: $P4/nmc$, $P4/n$, $P4nc$ (ARMBRUSTER & GNOS, 2000). Symmetry of vesuvianite is defined by string ordering of 4 cations at 8 channel positions (Y' , X'). Character and the number of IR and Raman bands poorly depend on the symmetry of the polytype and in general will be assigned by local site arrangement. Principle of the local site arrangement analysis was before used by GROAT et al. (1995) for interpretation of vesuvianite IR spectra in OH region. The cation composition of $Y(3)$ sites, presence of B, Al at $T(1)$, $OH \rightarrow F$ substitution at $O(11)$ and hydrogarnet defects at $Z(1,2)$ have principal influence on position and character of OH-bands of the Raman spectra in the region $3300-3700\text{ cm}^{-1}$ (Fig. 1, Table 1). The bands of OH groups taking part in formation of strong H-bonds ($<3300\text{ cm}^{-1}$) will be defined by cation composition at $Y'(1)$, presence of B at $T(2)$ and $OH \rightarrow F$, Cl substitution at $O(10)H(2)$ (Fig. 1, Table 1).

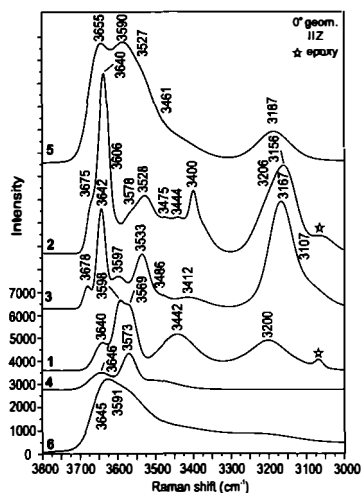


Fig. 1. Raman spectra of vesuvianite

Table 1. Symmetry and site occupation of investigated vesuvianite group minerals

	Y(1)	Y(3)	W [O(10)+O(11)]	T	Z
1. $P4/nmc$	1Fe	6.1Al + 1.2Mg + 0.4Ti + 0.3Fe	4.5OH + 3.1F + 0.4Cl	0	18
2. $P4/n$	0.6Fe + 0.4Mg	7.2Al + 0.8Mg	9OH	0	18
3. $P4/n$	1Fe	5Al + 2Mg + 1Fe	~9OH	0	18
4. $P4/nmc$	0.6Fe + 0.4Mg	4.3Mg + 3Al + 0.6Fe + 0.1Ti	0.3F + 0.nOH	4.2B	17.6Si + ?
5. $P4nc$	1Fe (+Mg?)	3.7Al + 3.1Mg + 1.2Fe	~5OH + 0.5F + 0.3Cl	1.4B + 0.5Al	17.5Si + 2OH
6. $P4/nmc$	0.5Fe + 0.5Mg	7.8Al + 0.2Fe	~6.3OH + 0.4F + 0.1Cl	0.6B	16.25Si + 7OH

1 – vesuvianite-F, Polar Yakutia, Russia (GALUSKIN et al., 2003a); 2 – vesuvianite-Al-OH, Kazakhstan; 3 – vesuvianite-OH, Ural, Russia; 4 – wiluite, Wiluy, Yakutia, Russia; 5 – vesuvianite-B, Wiluy, Yakutia, Russia; 6 – Si-deficient vesuvianite (“hydrovesuvianite”), Wiluy, Yakutia, Russia (GALUSKIN et al., 2003b).

References

ARMBRUSTER, T. & GNOS, E. (2000): Schweiz. Mineral. Petrogr. Mitt., **80**: 109-116.
 GALUSKIN, E.V., ARMBRUSTER, T., MALSY, A., GALUSKINA, I.O. & SITARZ, M. (2003a): Can. Mineral., **41**: 843-856.
 GALUSKIN, E.V., GALUSKINA, I.O., SITARZ, M. & STADNICKA, K. (2003b): Can. Mineral., **41**: 833-842.
 GROAT, L.A., HAWTHORNE, F.C., ROSSMAN, G.R. & ERCIT, T.S. (1995): Can. Mineral., **33**: 609-626.

THE INFRARED MICRO-SPECTROSCOPY FACILITY AT THE SYNCHROTRON ANKA: MINERALOGICAL APPLICATIONS

Gasharova, B.¹, Mathis, Y.-L.¹, Garbev, K.², Guilhaumou N.³, Moss D.A.¹ & Bornefeld, M.¹

¹ Institute for Synchrotron Radiation, Forschungszentrum Karlsruhe, P.O. Box 3640, 76021 Karlsruhe, Germany

² ITC-WGT / Techn. Mineralogy, Forschungszentrum Karlsruhe, P.O. Box 3640, 76021 Karlsruhe, Germany

³ MNHN, Earth Science Dept., 61 rue Buffon, 75231 Paris cedex 05, France
e-mail: biliana.gasharova@anka.fzk.de

ANKA is a new synchrotron at the Forschungszentrum Karlsruhe. It has been in user operation since March 2003 and it is running routinely at 2.5 GeV beam energy and 200 mA current.

At the infrared (IR) beamline, we have been developing mineralogical applications based on Fourier transform IR micro-spectroscopy. Our aim is to address the need for more sophisticated investigations by using the advantages of the synchrotron radiation compared to laboratory sources such as higher flux in the far IR and higher spatial resolution because of the higher brilliance in the complete IR spectral range. The infrared beamline ANKA-IR uses a bending magnet edge as a source and covers a spectral range from 4 to 10000 cm⁻¹ (0.5 meV - 1.24 eV; 2.5 mm - 1 µm). Its end is coupled with two experimental stations centered around two Bruker IFS66v/s spectrometers. One of them is equipped with an infrared microscope (Bruker IRscopeII) covering the far-, mid- and near-IR ranges. Set-ups for studies at low/high temperatures as well as at high pressure are under construction.

Our research directions include the study of new and not fully understood mineral crystal structures, transitions from semi-amorphous to crystalline state, mechanisms of incorporation of toxic ions into crystal structures, etc.

In many mineralogical applications there is a need for spatially resolved studies at the microscale. IR and Raman microscopy combines the rich crystallochemical specificity for samples even in amorphous state associated with vibrational spectroscopy. Compared to the spatial resolution achieved by Raman micro-spectroscopy the spatial resolution, which can be achieved by infrared micro-spectroscopy, is diffraction limited and of the order of a few tens of micrometers. Using a conventional infrared thermal source, the resolution cannot be made as low as the diffraction limit would. This is because of the lack of energy at the sample position when measuring samples smaller than 20 µm. High brilliance is desirable for any measurement with a limited "throughput" By using synchrotron-based IR micro-spectroscopy we can investigate samples down to the diffraction limit.

In this presentation two different examples of synchrotron based infrared studies combined with Raman spectroscopy with application to cement mineralogy, e.g. mechanisms of incorporation of Zn and the reaction of the crystal structure of synthetic Ca-gyrolite upon heating, and characterization of hydrocarbon bearing small sized fluid inclusions in minerals, that demonstrate the power of this technique will be given.

INFRARED AND RAMAN SPECTROSCOPIC STUDY ON GYROLITE-GROUP MINERALS

Gasharova, B.¹, Garbev, K.², Stumm, A.² & Mathis, Y.-L.¹

¹ ISS / ANKA, Forschungszentrum Karlsruhe, P.O. Box 3640, 76021 Karlsruhe, Germany

² ITC-WGT / Techn. Mineralogy, Forschungszentrum Karlsruhe, P.O. Box 3640, 76021 Karlsruhe, Germany
e-mail: biliana.gasharova@anka.fzk.de

Gyrolite, $\text{Ca}_{16}[\text{Si}_8\text{O}_{20}]_3(\text{OH})_8 \cdot 14\text{H}_2\text{O}$, is a member of the large family of the calcium-silicate-hydrate (C-S-H) phases, which are of great importance in cement chemistry. It occurs in hydrothermally-treated cement systems with low CaO/SiO₂-ratios.

The mechanisms of incorporation of Zn and the reaction of the crystal structure of synthetic Ca-gyrolite upon heating in air at temperatures greater than 400 °C were investigated.

After our X-ray analysis Zn substitutes Ca in the so-called X octahedral layer consisting of isolated octahedra. The maximum substitution corresponds to $\text{Zn}/(\text{Zn}+\text{Ca}) = 1/6$. In this case the X layer is fully occupied by Zn: $\text{Zn}_3\text{Ca}_4[\text{Si}_8\text{O}_{20}]_3\text{O}_2(\text{OH})_6 \cdot 14\text{H}_2\text{O}$. Results from infrared spectroscopic investigations of a series of Zn substituted gyrolites between $\text{Zn}/(\text{Zn}+\text{Ca}) = 0$ up to 1/6 will be presented. Incorporation of Zn causes a disorder in the positions of the OH groups pointing towards the X octahedral layer as shown by the disappearing of a well defined OH stretching band at 3615 cm⁻¹ characteristic for the pure Ca-gyrolite and the broadening of the main OH stretching band at 3638 cm⁻¹. The two crystallographically different positions of H₂O molecules (coordinating Ca and free water molecules) are reflected in the two bending bands at about 1633 and 1670 cm⁻¹. Increasing Zn content changes the crystallographical environment of the water molecules shown by the “smearing” of the bending bands. In the case of a fully occupied X octahedral layer by Zn, the former free water molecules coordinate Zn octahedra. Correspondingly to that the higher frequency bending peak disappears. The intensity of the asymmetrical Q³ Ca_X – O – Si₂ bond stretching at about 1134 cm⁻¹ decreases relatively to the intensity of the 1148 cm⁻¹ peak with increasing Zn doping.

Synthetic Ca-gyrolite (consisting of single silicate sheets) transforms to a truscottite-like phase (single + double silicate sheets) upon heating at 400-600 °C in air as evidenced by XRD, IR and Raman spectroscopy. The trigger for the gyrolite – truscottite phase transition is the loss of the water molecules at 400 °C. There exists a correlation in the IR spectra between the decrease in the intensity of the main H₂O bending band at 1633 cm⁻¹, the disappearance of the shoulders at 1595 and 1666 cm⁻¹, and the appearance of two additional OH stretching bands at about 3697 and 3740 cm⁻¹ after heating at 400 °C. We suppose that the new OH groups giving rise to the higher frequency bands at 3697 cm⁻¹, appearing also in the Raman spectra are coordinated only by one Ca atom in the interstices of the truscottite-like structure. The FIR spectra of gyrolite heated at 400 and 500 °C support the idea that the main changes in the Ca structure occur during the gyrolite – truscottite phase transition at 400 °C. These are related to the transformation of two of the water molecules coordinating Ca_X cations into OH groups thus provoking the breakdown of the Ca X-sheet. At the same time, two S₂ silicate sheets condense forming new 180° Si-O-Si bonds and giving rise to new symmetrical and asymmetrical Si-O-Si (Q⁴) stretching bands at about 806 and 1253 cm⁻¹ (IR) and 1182 cm⁻¹ (Raman).

SYNTHESIS, STEREOCHEMISTRY AND REACTIVITY OF SOME 2-METHYL-2-(3'-NITROPHENYL)-4-HYDROXYMETHYL-1,3-DIOXOLANES

Gâz, S.A., Gropeanu, R., Roiban, D. & Grosu, I.

Babeş-Bolyai University, Organic Chemistry Department (Arany Janos Str., 11, 400028, Cluj-Napoca, Romania)
e-mail: agaz@chem.ubbcluj.ro

The efficient synthesis (SOLOMONS & GRAHAM, 1996) of new dioxolane compounds used in treatment of contaminated water with heavy metals like mercury, cadmium or lead was performed. Two stereoisomers were identified using ^1H and ^{13}C NMR (MAGER et al., 1996; SILVERSTEIN, 1997) and X-ray diffraction techniques.

The ^1H -NMR spectra showed major differences in aliphatic area (McCLELLAND et al., 1993), differences which lead to the separation of two pure stereoisomers. Only the *anti* stereoisomer was used in the further steps of the synthesis due to the π stacking interactions (STEED & ATWOOD, 2000) observed, which influenced the final conformation of the structure.

The ORTEP plot of the *anti* stereoisomer crystals (Fig. 1) highlighted π stacking interactions that confirm in this way the NMR data (STENBERG & KILIK, 1974).

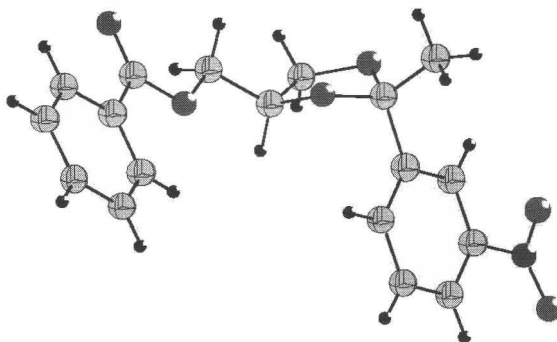


Fig. 1. ORTEP plot for *anti* 2-methyl-2-(3'-nitrophenyl)-4-hydroxymethyl-1,3-dioxolane

References

- GRAHAM SOLOMONS T.W. (1996): Fundamentals of Organic Chemistry. John Wiley & Sons, 724 p.
MAGER, S., GROSU, I., PLE, G. & DARABANTU, M. (1996): Aplicatii ale RMN in analiza structurala organica. University Press, Cluj-Napoca.
McCLELLAND, A.R., WATADA, B. & LEW C.S.Q. (1993): J. Chem. Perkin Trans. 2, **10**: 1723-1728.
SILVERSTEIN R.M. (1997): Spectrometric Identification of Organic Compounds. Wiley Text Books.
STEED, W.J. & ATWOOD, J.L. (2000): Supramolecular Chemistry. John Wiley & Sons, New York, 443 p.
STENBERG, V.I. & KILIK, D.A. (1974): J. Org. Chem., **39**: 215-219.

CHEMICAL AND MINERALOGICAL CHARACTERIZATION OF SOME RAW CERAMIC MATERIALS AND THEIR TRANSFORMATIONS DURING THE THERMAL TREATMENT

Gorea, M. & Kristaly, F.

Babeş-Bolyai University, Department of Mineralogy (Kogălniceanu Str., 1, 400084, Cluj Napoca, Romania)
e-mail: mgorea@bioge.ubbcluj.ro

Various types of kaoline, feldspar and sand as representative raw materials for electrical ceramics were investigated in order to determine their effect on ceramic properties and microstructure.

The mineralogical composition and structural particular features of the samples of raw materials were tested by X-ray diffraction (XRD), Differential Thermal Analysis (DTA), and Infrared Spectroscopy (IR). The chemical composition of four kaoline samples, a sample of feldspar and one of sand was also determined.

IR spectra present the characteristic bands of raw and thermally treated kaoline; the variations of the intensities in the $3690\text{-}3620\text{ cm}^{-1}$ region are related to the crystallization degree (from well- or poorly-crystalline kaolinite). The mullite formation as ceramic phase is strongly influenced by the type or crystallization degree of the clay minerals.

A mixture of these raw materials following the recipe and the specific technology of an usual electroceramic composition was prepared. The thermal treatment of the ceramic mixture and respectively of the raw material was carried out at $1300\text{ }^{\circ}\text{C}$ for 1 hour.

The firing transformations in the mixture and the final microstructure of the ceramics were studied by optical and electron microscopy. The chemical composition of the crystalline and amorphous phases determined by EDX indicated the presence of a certain degree of heterogeneity in the ceramic body's microstructure.

It is concluded that the final microstructure and properties of ceramic products are influenced by chemical and mineralogical composition of the raw materials. Impurities (such as Fe and Ti oxides) have a great influence on the electrical properties. The mineral components, especially those of the kaoline, play an important role during wet preparing of ceramic masses (the presence of smectites increases the plasticity but also the fired shrinkage) and crystalline phase formation during thermal treatment (poorly- or well-crystallized mullite and cristobalite).

PREHNITE – A NEW LAPIDARY MATERIAL

Hammer, V.M.F., Brandstätter, F. & Ponahlo, J.

NHMW, Museum of Natural History, Vienna, Burgring 7, A-1010 Vienna
e-mail: vera.hammer@nhm-wien.ac.at; franz.brandstaetter@nhm-wien.ac.at; ponahlo.lum@aon.at

For more than three years pale green jewellery enters the mineral and gem markets under the erroneous name of garnet with tourmaline inclusions. XRD analyses have identified the material as prehnite. The spectacular green and brown bacillary inclusions were detected by EDS as epidote and amphibole. The prehnite locality is Diakon, Niore du Sahel, Diakon Arrondissement, Kayes Region, Mali, Africa and it was disposed in Hong Kong.

The orthorhombic rock-forming mineral prehnite was named after the Dutch colonel *Hendrik von Prehn* (*1733 – †1785), who discovered this mineral near the Cape of Good Hope as the first type mineral of the African continent. The ideal formula of this combined sheet and chain silicate is $\text{Ca}_2(\text{Al,Fe})[\text{AlSi}_3\text{O}_{10}](\text{OH})_2$. The EDS analysis gave SiO_2 48.0 wt%, Al_2O_3 26.3 wt%, CaO 23.2 wt%, FeO 1.41 wt%.

Prehnite from Mali has pale grey green colour. Other localities as the Australian ones produce prehnite with a more yellow tint. Good quality prehnite can be semitransparent to translucent in some cases. The physical properties of the semiprecious prehnite from Mali are concordant with the properties from single crystal prehnite given in literature from other localities. The average refractive index $n = 1.627$, dependent of epidote and amphibole inclusions. Prehnite from Mali has a specific gravity of 2.86-2.98 g/cm^3 and a hardness of about 6-6.5.

Distinct single crystals of prehnite are relatively rare but known from alpine fissures like the famous "Prehnitinsel" in the Austrian Habachtal. More commonly, prehnite occurs as secondary mineral filling in volcanic cavities, like the amygdales of more than 10 cm at Hall's Creek in Western Australia.

As the prehnite of the new find of the Kayes Region in Mali is characterised by numerous inclusions of epidote, dispersed amphibole needles, small idiomorphic garnet and magnetite, the development of this prehnite could be given as low grade metamorphic.

Prehnite is also used as a simulant for jade. It can be distinguished from jadeitites by means of CL-microphotography and CL-microspectrography. Similar textures, which can quickly be made visible by CL, have never been found in all jadeitites investigated so far. Careful measurements of CL spectra might also help. In spite of the close proximity of maxima of CL bands of both species, prehnites can be energized at far lower energies than jadeitites. Both methods are non-destructive.

**SYNCHROTRON INFRARED SPECTROSCOPY
OF SYNTHETIC $P2_1/m$ AMPHIBOLES AT HIGH PRESSURE**

Iezzi, G.¹, Liu, Z.², Della Ventura, G.³ & Hemley, R.²

¹ Dip. Scienze della Terra, Università di Chieti, Chieti Scalo

² Geophysical Laboratory, Carnegie Institution of Washington, 5251 Broad Branch Rd., N.W.
Washington DC 20015, USA

³ Dip. Scienze Geologiche, Università di Roma Tre, Largo S. Leonardo Murialdo 1, I-00146 Roma
e-mail: g.iezzi@unich.it

The Na(NaMg)Mg₅Si₈O₂₂(OH)₂ amphibole represents a key double-chain silicate to model the $P2_1/m - C2/m$ phase-transition in A-site filled amphiboles (IEZZI et al., 2004). It has $P2_1/m$ symmetry at room- T , and reverses to the usual $C2/m$ space-group of monoclinic amphiboles at ~ 257 °C (CAMARA et al., 2003). Della Ventura et al. (this volume) found that the aggregate B-site dimension has a strong influence on the transition temperature (T_c) based on high temperature infrared (HTIR) studies of the OH stretching vibrations. We report here an IR study of the same samples studied by Della Ventura et al. (this volume) at high pressure up to 30 GPa using synchrotron radiation.

The experiments were carried out at U2A beamline on the VUV ring of the National Synchrotron Light Source, Brookhaven National Laboratory. The fine amphibole powder was loaded into a symmetric diamond anvil cell (DAC) together with some ruby chips as pressure gauge. High-pressure IR absorption spectra of the synthetic amphiboles were collected using a Bruker IFS 66v/S vacuum Fourier transform interferometer, Bruker IRscope II microscope equipped with a HgCdTe type-A detector.

The spectrum of the Na end-member shows three bands: (A) at 3740 cm⁻¹, (B) at 3715 cm⁻¹ and (C) at 3667 cm⁻¹, respectively (IEZZI et al., 2004). The higher-frequency bands are assigned to two non equivalent H atoms interacting with ^ANa; this pattern is typical of an amphibole with a P -lattice. The ^BLi-bearing amphiboles show in addition a fourth, minor band at 3690 cm⁻¹. The bulk intensity of the A and B bands is > 95%, suggesting that the analysed amphiboles have virtually full A-sites. With increasing P , we observe two main modifications of the spectra: 1) all bands linearly shift toward higher frequency. At 20.8 GPa, the peak centroid of the main (A) band is > 3800 cm⁻¹ 2) the A and B bands merge into a single, broad absorption, and the P value at which the A-B doublet disappear is a function of the B-site occupancy. For the ^BNa end-member the A and B bands merge at around 18 GPa; for sample 406, with nominal B-site composition (Na_{0.2}Li_{0.8}Mg₁), the A and B bands merge around 13 GPa. These results show that the Na(NaMg)Mg₅Si₈O₂₂(OH)₂ amphibole undergoes a $P2_1/m - C2/m$ phase transition at high P , and that the transition pressure, P_c , is a function of the aggregate dimension of the B-site, in a fashion similar to that observed by Della Ventura et al. (this volume) for increasing T . However, while for decreasing $\langle \text{B}_T \rangle$ (increasing ^BLi in solid-solution) Della Ventura et al. observe an increase in the T_c , the results presented here show that the reverse is true for P_c , in a fashion similar to what occurs in clinopyroxenes.

References

- CAMARA, F., OBERTI, R., IEZZI, G. & DELLA VENTURA, G. (2003): Phys. Chem. Minerals, **30**: 570-581.
IEZZI, G., DELLA VENTURA, G., CAMARA, F., OBERTI, R. & HOLTZ, F. (2004): Am. Mineral., **89**: 640-646.

**CO₂ AND H₂O IN CORDIERITE FROM THIN-SECTIONS:
A RAMAN-SPECTROSCOPIC APPROACH**

Kaindl, R.¹, Tropper, P.² & Bertoldi, C.³

¹ Institute of Earth Science (Universitätsplatz 2, A-8010 Graz, Austria)

² Institute of Mineralogy and Petrography (Innrain 52, A-6020 Innsbruck, Austria)

³ Faculty of Geography, Geology and Mineralogy (Hellbrunnerstr. 54, A-5020 Salzburg, Austria)
e-mail: reinhard.kaindl@uni-graz.at; tropper@uibk.ac.at; christian.bertoldi@sbg.ac.at

Cordierite is a common metamorphic mineral in aluminous, medium- to high-grade crustal rocks. In equilibrium with other Fe-Mg-silicates, cordierite changes its Fe-Mg-ratio comprehensible with temperature and may therefore be used as geothermometer in e.g. granulite-facies rocks (DEIBL et al., 2003a). However, molecular CO₂ and H₂O can be incorporated in the channels and cavities of cordierite, greatly influencing its stability field and distorting the geothermometric calculations. CO₂ and H₂O in natural Mg- and Fe-rich cordierite single crystals were previously studied and quantified by combined Raman and IR-spectroscopy (e.g. KOLESOV & GEIGER, 2000). In this study, we tried to estimate the CO₂ and H₂O content of natural Mg-rich cordierite in a thin section from a granulite-facies metapelite (Grt + Sp + Crd + Sill + Bt + Fsp + Qtz) from the Sauwald (Southern Bohemian Massif). The *P-T* conditions of this rock were determined to be 750 – 800 °C and 4 – 6 GPa (DEIBL et al., 2003b). Spectra were obtained by a JOBIN-YVON™ LabRAM-HR800 Raman spectrometer, a He-Ne 633nm laser and an OLYMPUS™ 100x objective (n.a. 0.9). The laser spot on the surface had a diameter of approx. 1µm. All spectra were recorded at parallel orientation of the incident laser beam and the scattered light. Nine natural and synthetic cordierite single-crystals of known CO₂- and H₂O-concentration (colorimetric titration; BERTOLDI et al., 2004) were measured for calibration purposes. The x-axes of the single crystals were oriented parallel to the polarization of the incident laser beam and the x-parallel CO₂-molecule in the structure. Fitting of relative intensity ratios of the CO₂ stretching mode at 1383 cm⁻¹ and two cordierite lattice vibration modes at 973 and 1185 cm⁻¹ against CO₂-concentration resulted in a linear calibration curve. This curve can be used to calculate the CO₂-content with a precision around 0.1wt%. It was applied to a natural cordierite of 600 µm diameter in an uncovered thin-section from the Sauwald. The x-axis of the grain laid approximately in the thin-section plane and was oriented parallel to the polarization of the incident laser beam. Fifteen spots across the grain were measured, showing a complex variation in CO₂-content from core to rim. A non-linear relation between H₂O intensity ratios and concentration indicate complex orientation and bonding of the H₂O-molecule in cordierite and prevented quantification. Polarized micro Raman spectroscopy of cordierite in thin sections provides information about CO₂-content down to 0.1wt% at a spatial resolution of about 2 µm³. Further research is necessary for the Raman-spectroscopic determination of the H₂O-content.

References

- BERTOLDI, C., PROYER, A., GARBE-SCHÖNBERG, D., BEHRENS, H. & DACHS, E. (2004): Lithos, *subm.*
DEIBL, I., TROPPEL, P., MIRWALD, P. & FINGER, F. (2003a): J. Czech Geol. Soc., **48**: 40-41.
DEIBL, I., TROPPEL, P., KAINDL, R. & MIRWALD, P. (2003b): Mitt. Österr. Mineral. Ges., **148**: 117-118.
KOLESOV, B.A. & GEIGER, C.A. (2000): Am. Mineral., **85**: 1265-1274.

**INFRARED ABSORPTION AS A USEFUL TOOL TO SEPARATE
NATURAL FROM SYNTHETIC AMETHYSTS**

Karamelas, S.¹ & Fritsch, E.²

¹Department of Geology, Laboratory of Mineralogy - Petrology - Economic Geology, Aristotle University of Thessaloniki, 54124 Thessaloniki, Greece.

²Institut des Matériaux Jean Rouxel (IMN), Laboratoire de Physique Cristalline - Equipe Matériaux Absorbants et Photoluminescents, 2 rue de la Houssinière, BP32229, F-44322 NANTES, Cedex 3, France.
e-mail: steka@physics.auth.gr

The study presents results of investigations made for a representative series of samples that consisted of natural and synthetic amethysts. The investigations have been conducted in a parallel and vertical direction to the optical axis (*c*) of the stones. Infrared absorption has been used for testing and developing analytical methods useful for detection of differences between these two categories of stones. We were able to reject several criteria of selection proposed by authors of previous publications - SMAALI (1998), ZECCHINI et al. (1999) - who claimed that the absorption peak at 3595 cm⁻¹ should only appear in the case of natural amethysts. Furthermore, we were able to contradict their claim that the absorption peak at 3543 cm⁻¹ is only observed for synthetic amethysts. The deconvolution of the spectra allows the determination of the band widths. This value (important or feeble) will be criteria of differentiation between the natural and the synthetic amethysts. Moreover, for the synthetic "prismatic" amethysts, only the absorption bands at 3543, 3585, 3614 cm⁻¹ have been revealed, whereas the bands at 3589 cm⁻¹ and 3595 cm⁻¹, as observed by NOTARI et al. (2001), were not detectable in the case of using the same stones. In addition, the investigations of peaks at 3575 cm⁻¹ in amethyst of Bolivia (Altiplano) and at 3630 cm⁻¹ in some amethysts from Madagascar, Mexico (Vera Cruz) and Russia (Ural), allows us to suggest that there are specific properties originating in these countries' amethysts. It should be taken under account, which further measurements taken for a larger number of amethyst samples are needed in order to prove this claim. Finally we were able to say that with the orientation only the intensity of the peaks changes, but none of them disappeared. By inference, the significant infrared absorption of amethysts can be measured in any direction.

References

- FRITSCH, E. & KOIVULA, J.I. (1987): *Jewelers Circular Keystone*, **154**: 322-324.
NOTARI, F., BOILLAT, P.Y. & GROBON, C. (2001): *Rev. Gemmologie*, **141/142**: 75-80.
SMAALI, M. (1998): *Mém. thèse doctorat, Univ. Franche-Comté, Besançon, France*, 134 p.
ZECCHINI, P. & SMAALI, M. (1999): *Rev. Gemmologie*, **138/139**: 74-80.

ON A MODE OF Fe^{3+} , OH^- OCCURRENCE IN OLIVINE (MÖSSBAUER, IR, EELS COMBINED WITH TEM)

Khisina, N.R.¹, Wirth, R.², Andrut, M.³ & Churakov, S.²

¹ Institute of Geochemistry and Analytical Chemistry of RAS, Moscow

² GeoForschungszentrum, Potsdam

³ Technical University, Berlin

e-mail: khisina@geokhi.ru

Traces of Fe^{3+} or OH^- detected by spectroscopic methods in olivine samples can either be incorporated in the olivine lattice (intrinsic mode) or form their own phases included in the olivine host (extrinsic mode). We used the combination of TEM, Mössbauer spectroscopy, IR, EELS and *ab initio* methods to elucidate the intrinsic and extrinsic mode of Fe^{3+} and OH^- occurrence in olivine samples from mantle xenoliths in kimberlites.

We found that *intrinsic* H^+ is incorporated in the olivine structure via formation of M1 vacancies. *Intrinsic* H^+ can occur in olivine as (i) OH^- -bearing point defects homogeneously distributed in the olivine matrix (isolated point defects) and (ii) OH^- -bearing point defects arranged into planar defects parallel to either (100) or (001) and (101). *Extrinsic* OH^- occurs as nano-inclusions of OH^- -bearing phases such as hydrous olivine, 10Å-Phase, serpentine and talc precipitated at planar defects and dislocations. The planar defects are distributed in the olivine matrix either randomly or regularly; in the latter case they produce the *2a*, *3a*, *3c* and *3d*₁₀₁ superperiodicity with respect to the olivine structure by formation of hydrous olivine structures. *Ab initio* methods were used to predict the H^+ location and hydrogen bonds parameters for the *2a*-hydrous olivine structure.

From IR and TEM data we conclude that protonation of olivine occurred during crystallization in the mantle and is not a result of a later metasomatic hydration.

The *intrinsic* Fe^{3+} ions are incorporated in the olivine structure via formation of M1 vacancies which form planar defects parallel to (001) of olivine under low-temperature oxidation. Periodic arrangement of such kind of planar defects results in the laihunite (or, the same, ferriolivine) formation. Low-temperature oxidation of olivine which contains OH^- -bearing nano-inclusions results in transformation of precursor hydrous olivine phases to a mixture of nanometer-sized FeOOH , $\text{Fe}(\text{OH})_3$ and SiO_2 due to interaction between Fe^{3+} and OH^- defects (*extrinsic* Fe^{3+} and OH^-).

**MOLECULES OF CARBON OXIDES IN CORDIERITE CHANNELS:
A SPECTROSCOPIC STUDY**

Khomenko, V.¹ & Langer, K.²

¹ Institute of Geochemistry, Mineralogy and Ore Formation, Ukrainian Academy of Science,
pr. Palladina 34, 03142 Kyiv, Ukraine

² Institut für Angewandte Geowissenschaften, Technische Universität Berlin,
Ernst-Reuter-Platz 1, D-10623 Berlin, Germany
e-mail: vladkhom@hotmail.com

The spectroscopic micro-FTIR technique has been used to examine a series of natural cordierite samples of different geological environments and chemical composition. Polarized single-crystal spectra were measured in the range 3000-2000 cm⁻¹ on oriented polished platelets (100), (010) and (001). The behaviour of CO₂ and CO molecules, as well as other minor volatile components trapped in the structural channels of the cordierites, was studied in the temperature range 80-700 K. An experiment on degassing was performed by heating a cordierite sample at a temperature of 1250 K during 10 hours. Location and orientation of ¹²CO₂, ¹³CO₂ and CO molecules in structural channels, as well as the character of CO₂ libration were determined. Polarization-dependent complex sets of valence vibrations were identified for CO₂ molecules. Most intense bands were measured in *a*-polarization at 2348 and 2283 cm⁻¹, the latter was assigned to ¹³CO₂. δ¹³C values were calculated for different samples from the *A*₂₂₈₃/*A*₂₃₄₈ band intensities ratio and compared with published data. A weak CO band at 2135 cm⁻¹ is detected in samples of CO₂-enriched cordierites from granulites. The main *a*-polarized ¹²CO₂ band at 2348 cm⁻¹ becomes narrower and exhibits fine structure at LN₂ temperature: an additional band at 2330 cm⁻¹ and a shoulder at 2352 cm⁻¹ appear in the spectra. The molecular axes of the CO₂ and CO molecules are parallel to the *a*-axis of cordierite crystals. Only trace amounts of CO₂ oriented parallel to the *c*-axis were found in some samples. This confirms recent results of KOLESOV & GEIGER (2000). The complex spectral shape of CO₂ band envelopes in *a*- and *b*-polarizations is very likely due to a rotational motion of the carbon oxides molecules. Repeating spectral measurements after heating confirm the weak mobility of CO₂ and CO molecules in the channel sites at temperatures below 700 K and the full degassing of cordierite after heating at 1250 K. Differences in the carbon oxides spectra observed in cordierites from genetically different environments, including variations in CO/CO₂ ratio and in the δ¹³C of captured carbon dioxide molecules, are discussed.

References

KOLESOV, B.A. & GEIGER, C.A. (2000): Am. Mineral., **85**: 1265-1274.

NEW RAMAN SPECTROSCOPIC OBSERVATIONS OF HYDRATED TRANSITION ZONE SPINEL/SPINELLOID PHASES

Kleppe, A.K.¹, Jephcoat, A.P.^{1,2} & Smyth, J.R.³

¹ University of Oxford, Department of Earth Sciences, Parks Road, Oxford, OX1 3PR, UK

² Diamond Light Source, Rutherford Appleton Laboratory, Chilton, Didcot, OX11 0QX, UK

³ University of Colorado, Department of Geological Sciences, Boulder, CO80309, USA

e-mail: annettek@earth.ox.ac.uk

Wadsleyite [β -(Mg,Fe)₂SiO₄, spinelloid III] and ringwoodite [γ -(Mg,Fe)₂SiO₄, spinel], the nominally anhydrous high pressure polymorphs of olivine are thought to be the most abundant minerals in the Earth's mantle transition zone between 410 and 660 km depth. They can incorporate respectively up to 3.3 and 2.5 wt% H₂O in form of OH into their crystal structure. While the Fe-content of wadsleyite and ringwoodite with an assumed natural amount of ~11% Fe influences transition zone properties (e.g., elasticity) globally the OH content may be more important within and adjacent to cool subducting slabs. Wadsleyite II (spinelloid IV) is a hydrous, Fe-bearing silicate phase that might occur between the stability regions of wadsleyite and ringwoodite.

We present Raman spectra from ~50 to 4000 cm⁻¹ of high-quality single-crystals of hydrous Mg-endmember and hydrous Fe-bearing wadsleyite, wadsleyite II, and ringwoodite. The transition zone phases were synthesized in a multi-anvil apparatus at the Bayerische Geoinstitut, Germany and high-pressure Raman spectra were obtained up to 60 GPa using a diamond-anvil cell and solid helium as pressure-transmitting medium.

The Raman spectra of wadsleyite and wadsleyite II are similar as would be expected from their closely related structures. In the OH stretching region the spectrum of wadsleyite II appears more complex than the spectrum of wadsleyite consisting of at least 6 modes. The most interesting observation of the high-pressure study of wadsleyite II is the appearance of Raman bands (not detectable/resolvable at 1 bar) in the region 450-650 cm⁻¹ above ~35 GPa. For ringwoodite, the Raman spectrum of Fo₁₀₀ composition shows all five characteristic spinel modes whereas the hydrous Fo₈₉ composition exhibits additional modes in the range 709-939 and 100-250 cm⁻¹. In both phases the SiO₄ stretching modes shift continuously up to 60 GPa; additional bands emerge in the region 550-580 cm⁻¹ near 40 GPa in the Fo₈₉ sample. Comparisons of Raman spectra of hydrated transition zone phases with varying iron content reveal that pure protonation has only a minor effect on the lattice dynamics while coupled iron and proton substitution leads to additional levels of transformation complexity reflected in reversible, pressure-induced modifications in the Raman spectra of hydrous Fo₈₉ ringwoodite and wadsleyite II. The present observations could provide additional insight into the existence of new protonated, iron-bearing, unquenchable phases in cool, wet regions near subducted material.

**IMPORTANCE OF WEATHERED METEORITES FOR MARS: DATA ON VNIR
REFLECTANCE-SPECTROSCOPY, RAMAN-SPECTROSCOPY AND
MÖSSBAUER-SPECTROSCOPY**

Kolb, C.^{1,2}, Abart, R.^{2,3}, Lotternoser, W.⁴, Kaindl, R.² & Lammer, H.¹

¹ Space Research Institute, Austrian Academy of Sciences, Schmiedlstrasse 6, A-8042 Graz, Austria

² Institute for Mineralogy and Petrology, University of Graz, Universitätsplatz 2, A-8010 Graz, Austria

³ Mineralogical-Petrographic Institute, University of Basel, Bernoullistrasse 30, CH-4056 Basel, Switzerland

⁴ Institute for Mineralogy, Hellbrunnerstrasse 34/III, University of Salzburg, A-5020 Salzburg, Austria
e-mail: christoph.kolb@oeaw.ac.at

With respect to global tectonics the present day Mars is considered as a single plated planet. Due to the lack of consumptive plate tectonics, the Martian sedimentary record represents a long-term archive of exogenic processes. The compositions and mixing relationships of three principal components, which may be inherent in Martian soil, were derived from APXS-Pathfinder and XRFS-Viking chemical data (KOLB et al., 2003). The principal soil components were chosen to represent Pathfinder Soil Free Rock, physical weathering products of Pathfinder andesites and meteoritic material with CI-chondrite composition. Correlation trends of the available chemical data in the ternary composition space of the principal components corroborate the existence of a Global Dust Unit and provide constraints on its composition. Evidence from spectroscopic data, returned by numerous Mars missions, has to be found to strengthen the argument of substantial meteoritic contribution to the Martian soil. VNIR reflectance spectroscopy has been used from the beginning of spectroscopic Mars research, because of the strong ferric absorption edge of Martian soil materials and easy achievement of space-flight proven hardware and telescopic observation. Mössbauer-spectroscopy is used for in-situ soil science in the frame of the Mars Exploration Rover mission (SQUYRES et al., 2003). Future mars missions will involve Raman-spectroscopy due to its capability in phase identification among intimate phase mixtures (ELLERY et al., 2003). We investigated meteoritic finds by means of VNIR reflectance-spectroscopy, Raman-spectroscopy and Mössbauer-spectroscopy. Current focus is given on meteoritic finds from Omani desert. Future investigations will consider chondritic finds from Antarctica, too.

References

- ELLERY, A., KOLB, C., LAMMER, H., PARNELL, J., EDWARDS, H.G.M., RICHTER, L., PATEL, M.R., ROMSTEDT, J., DICKENSHEETS, D., STEELE, A. & COCKELL, C.S. (2003): *Int. J. Astrobiol.*, **1**: 365-380.
- KOLB, C., ABART, R., WAPPIS, E., PENZ, T., JESSBERGER, E.K. & LAMMER, H. (2003): In: JULL, A.J.T. (ed.) *Meteoritics & Planetary Science* 38, 7, Supplement, Meteoritical Society, Tucson, A15.
- SQUYRES, S.W., ARVIDSON, R.E., BAUMGARTNER, E.T., BELL, J.F., III, CHRISTENSEN, P.R., GOREVAN, S., HERKENHOFF, K.E., KLINGELHÖFER, G., MADSEN, M.B., MORRIS, R.V., RIEDER, R. & ROMERO, R.A. (2003): *J. Geophys. Res.*, **108**: 8062.

A RAMAN SPECTROSCOPIC STUDY OF Fe-Mg OLIVINES

Kolesov, B.¹ & Geiger, C.²¹ Institute of Inorganic Chemistry, Lavrentiev prosp. 3, 630090 Novosibirsk, Russia² Institut für Geowissenschaften der Universität Kiel, Olshausenstr. 40, 24098 Kiel, Germany
e-mail: kolesov@che.nsk.su

End-member synthetic fayalite and forsterite and a natural solid-solution composition crystal of composition $(\text{Mg}_{1.80}, \text{Fe}_{0.20})\text{SiO}_4$ as well as polycrystalline forsterite and fayalite isotopically enriched in ^{26}Mg and ^{57}Fe , respectively, were synthesized and their Raman spectra were measured. The observed isotopic shift of vibrational modes permits the assignment of spectra, especially in low-frequency region, to be improved. The low wavenumber Raman modes in olivine are best described as lattice modes consisting to a large degree of mixed vibrations of M(2) cation translations and external vibrations of the SiO_4 tetrahedra. The polarized single-crystal spectra of forsterite and $\text{Fo}_{90}\text{Fa}_{10}$ were recorded at a number of temperatures from room temperature to about 1200 °C. From these data, the microscopic Grüneisen parameters for three different A_g modes for both compositions were calculated, and also the structural state of the solid solution crystal was investigated. The difference in the measured mode wavenumbers between the heating and cooling is due to hysteresis effect. The spectra of the $\text{Fo}_{90}\text{Fa}_{10}$ crystal, unlike the spectra of forsterite, show a discontinuity in the wavenumber behavior for the mode at $\sim 220 \text{ cm}^{-1}$ at 700-1000 °C upon heating and cooling (Fig. 1). Both these observations are discussed taking into account the various crystalline effects, i.e. annealing of the point defects, structural transformation, rigid rotation of the SiO_4 tetrahedra, changing of the oxygen-oxygen interaction. The discontinuity in the wavenumber behavior of the mixed Mg/T(SiO_4) mode (Fig. 1) may be related to variations in the Fe-Mg intracrystalline partitioning behavior in the $\text{Fo}_{90}\text{Fa}_{10}$ crystal, i.e. to some decrease in the concentration of Fe^{2+} at M(2).

The mode wavenumber and intensity behavior of internal SiO_4 vibrations as a function of temperature are discussed in terms of crystal field and dynamic splitting and also ν_1 and ν_3 coupling. Crystal field splitting increases very slightly with temperature, whereas dynamical field splitting is temperature dependent. The degree of ν_1 - ν_3 coupling decreases with increasing temperature.

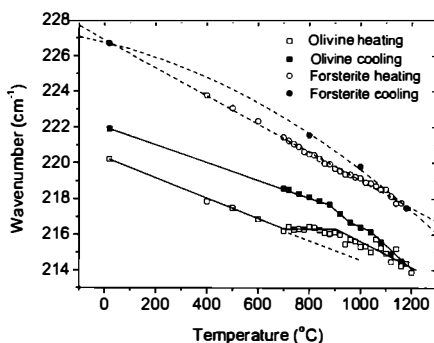


Fig. 1. Temperature dependence of the wavenumber of the A_g mode at 220 cm^{-1} in Fo_{100} and $\text{Fo}_{90}\text{Fa}_{10}$.

MOLECULE-MINERAL INNER SURFACE INTERACTIONS IN NANOPOROUS SILICATES: A RAMAN SPECTROSCOPIC INVESTIGATION

Kolesov, B.¹ & Geiger, C.²

¹ Institute of Inorganic Chemistry, Lavrentiev prosp. 3, 630090 Novosibirsk, Russia

² Institut für Geowissenschaften der Universität Kiel, Olshausenstr. 40, 24098 Kiel, Germany
e-mail: kolesov@che.nsk.su

We have undertaken single-crystal Raman measurements of zeolites (bikitaite, natrolite), SiO₂-clathrates (melanophlogite) and other silicate structure types with small nanopores (beryl, cordierite, hemimorphite) at different temperatures. The goal is to investigate the nature of inner surface molecule-crystal interactions and the role of hydrogen bonding in minerals. The angular dependencies of the OH-mode scattering intensities in single-crystal measurements, made at low and ambient temperatures, permit the direction of the molecular bonds and the main molecular polarizabilities for different O-H bonds to be obtained.

In bikitaite, H₂O molecules occur in infinite [010] channel ways and build a hydrogen-bonded H₂O chain termed 'one-dimensional ice'. The molecules are ordered, whereby one H atom per molecule is unbonded and the other is hydrogen-bonded to a neighboring H₂O molecule. They show little interaction with the framework. The hydrogen-bonded O-H stretching bands in the Raman spectra show little line broadening, which is not typical for many hydrogen-bonded systems. With increasing temperature, the hydrogen bonding weakens continuously until the chain 'breaks' and isolated H₂O molecules are present.

The Raman spectrum of melanophlogite shows the presence of quasi-free N₂, CO₂ and CH₄, but no H₂O molecules. Most of the CH₄ is partitioned into the smaller nearly spherical [5¹²] cage, while CO₂ and N₂ appear to prefer the larger more oblate [5¹²6²] cage. The difference in wavenumber for their stretching modes between room temperature and 4 K is minimal. The molecules are orientationally disordered in the cavities and they have only weak dispersion interactions with the SiO₂-crystal framework. However the incorporation of molecules is necessary to allow the SiO₂ framework to condense.

Cordierite and beryl contain quasi-free CO₂ molecules, as well as H₂O in small cavities. The CO₂ molecules are orientated parallel to the crystallographic *x*-axis. The H₂O molecules have their H-H vector parallel to the *z*-axis in alkali-free crystals and are dynamically disordered about the *z*-axis. They show little hydrogen bonding with their frameworks.

It is noteworthy that the polar H₂O molecule can be found in these two 'zeolite-like phases', but not in melanophlogite. Melanophlogite is hydrophobic, while nearly all other nanoporous silicates are hydrophilic. The incorporation of the polar H₂O molecule may be related to the nature of the electronic charge distribution within the crystal framework.

**Fe₃(PO₄)₂(OH)₃·5H₂O, A NEW MONOCLINIC FERRIC IRON PHOSPHATE
MINERAL FROM GERMANY: CRYSTAL STRUCTURE, SINGLE-CRYSTAL
RAMAN SPECTRA AND CLOSE RELATION TO WAVELLITE**

Kolitsch, U.¹, Bernhardt, H.-J.² & Bläß, G.³

¹ Institut für Mineralogie und Kristallographie, Universität Wien, Geozentrum, Althanstr. 14,
A-1090 Vienna, Austria

² Ruhr-Universität Bochum, Zentrale Elektronen-Mikrosonde, N-Südstr., D-44801 Bochum, Germany

³ Merzbachstr. 6, D-52249 Eschweiler, Germany

e-mail: uwe.kolitsch@univie.ac.at

A new monoclinic ferric iron phosphate mineral has been found at the abandoned Grube Mark near Essershausen, Taunus, Hesse, Germany (BLAß, 2002). The mineral forms pale brown-yellow, translucent to transparent, acicular crystals (rarely up to 1.5 mm in length) which are always intergrown to form bundles of subparallel crystals. These are associated with beraunite (reddish "oxiberaunite" variety) and cacoxenite.

All acicular crystals studied were twinned by non-merohedry. The crystal structure has been determined using single-crystal intensity data (MoK α X-radiation, CCD area detector, 293 K) collected from a twin. The model was refined in space group $P2_1/n$ ($a = 9.777(3)$, $b = 7.358(2)$, $c = 17.830(5)$ Å, $\beta = 92.19(4)^\circ$, $V = 1281.7(6)$ Å³, $Z = 4$) to $R1 = 13.3$ % and $wR2_{all} = 35.3$ % from 2045 'observed' reflections with $F_o > 4 \sigma(F_o)$. The relatively high residuals are due to the twinning and weak intensity data. The chemical formula obtained from the refinement is Fe₃(PO₄)₂(OH)₃·5H₂O, which was confirmed by quantitative electron microprobe analyses. Single-crystal laser-Raman spectra (Renishaw M1000 MicroRaman Imaging System) show, in the region > 1500 cm⁻¹, several bands (s = strong; sh = shoulder) due to OH stretching vibrations (at ~ 3567 , $3412(s)$, $\sim 3197(s)$, ~ 3060 to $\sim 3052(sh)$ cm⁻¹) and H-O-H bending vibrations of water molecules (~ 1625 cm⁻¹).

Chemically, the new mineral is the Fe³⁺-analogue of wavellite (Al₃(PO₄)₂(OH,F)₃·5H₂O, orthorhombic, space group $Pcmm$; ARAKI & ZOLTAL, 1968). Structurally, however, it is not isotypic with wavellite, but crystallises in a monoclinically distorted variant ($P2_1/n$; subgroup of $Pcmm$) of the wavellite structure type. Details of the structure and its hydrogen bonding scheme will be discussed.

The title compound has the same chemical formula as the amorphous species santabarbarite (PRATESI et al., 2003) which forms, however, exclusively on in-situ oxidative alteration of vivianite, Fe²⁺₃(PO₄)₂·8H₂O.

Mr. Michael Legner is thanked for providing the studied samples. Financial support by the Austrian Science Foundation (FWF) (Grant P15220-N06) is gratefully acknowledged.

References

ARAKI, T. & ZOLTAL, T. (1968): Z. Kristallogr., **127**: 21-33.

BLAß, G. (2002): Mineralien-Welt, **13**: 18-43.

PRATESI, G., CIPRIANI, C., GIULI, G. & BIRCH, W.D. (2003): Eur. J. Mineral., **15**: 185-192.

RAMAN SPECTRA OF TITANOSILICATE MELTS

Korinevskaja, G. & Bykov, V.

Institute of Mineralogy, Miass, 456317, Russia
e-mail: kor@ilmeny.ac.ru

Titanium is a minor element in most rock-forming silicate melts. Nevertheless, this element is petrologically significant (MYSEN et al., 1980). Titanium is in six-fold coordination by oxygen in the majority of natural silicates, and titanium can replace silicon in four-fold coordination in alkaline minerals. A structural feature of titanosilicate glasses is that titanium can be both in six-fold coordination, and in four-fold coordination. Structure of melts of systems: 33%Na₂O·67%SiO₂-x%TiO₂, 40%Na₂O·60%SiO₂-x%TiO₂, 50%Na₂O·50%SiO₂-x%TiO₂ (x=1, 5, 10, 20 %) have been investigated by Raman high-temperature spectroscopy. The pulse laser was used for excitation of spectra and a synchronized system of account of photons was used for the registration. It is necessary to discriminate a thermal background from the heating furnace and melt.

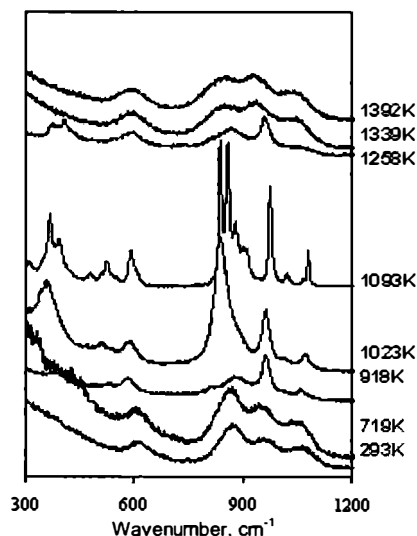


Fig. 1. Raman spectra of the compound with 50%Na₂O-45%SiO₂-5%TiO₂ at different temperatures

As an example, Raman spectra of the compound with 50%Na₂O-45%SiO₂-5%TiO₂ are shown in Fig. 1 at temperatures of 293-1389 K. Bands in the range of 1050-1075 cm⁻¹, 940-970 cm⁻¹, 860-880 cm⁻¹ and 570-625 cm⁻¹ are observed in the spectra of titanosilicate glasses and melts. Bands at 1050-1075 cm⁻¹ and 940-970 cm⁻¹ are attributed to the highly localized symmetric Si-nonbridging O stretching vibrations of Q³ and Q² species, respectively (MYSEN & NEUVILLE, 1995). The low frequency bands are associated with stretching vibrations of Si-O-Si linkages. The band at 860-880 cm⁻¹ is assigned to vibrations of TiO₄ units (FURUKAWA & WHITE, 1979). Raman spectra of crystalline phases which are formed at heat treatment of glasses at temperatures of 800-1000 K were obtained too. Systematics of the band behavior in Raman spectra depending on composition (SiO₂ and TiO₂ content) and temperature are established.

References

- FURUKAWA, T. & WHITE, W.B. (1979): Phys. Chem. Glasses, **20**: 69-80.
 MYSEN, B.O. & NEUVILLE, D. (1995): Geochim. Cosmochim. Acta, **59**: 325-342.
 MYSEN, B.O., RYERSON, F.J. & VIRGO, D. (1980): Am. Mineral., **65**: 1150-1165.

TEMPERATURE-INDUCED STRUCTURAL TRANSFORMATIONS OF LAYERED TITANOSILICATE JDF-L1

Kostov-Kytin, V., Mihailova, B., Ferdov, S. & Petrov, O.

Central Laboratory of Mineralogy and Crystallography, Bulgarian Academy of Sciences, Acad. G. Bonchev
Street 107, 1113 Sofia, Bulgaria
e-mail: stanislav_ferdov@hotmail.com

The efforts to produce new materials with industrially useful properties in the past years resulted in the synthesis of a number of microporous titanosilicates with potential applications in catalysis, ion exchange, separation processes. Some of these materials do not have mineral analogues and their comprehensive characterization may contribute significantly to understand their nature and properties as well as to optimize the preparation of titanosilicates having desired structural topology.

Layered titanosilicate JDF-L1 is synthesized in a $\text{Na}_2\text{O-TiO}_2\text{-SiO}_2\text{-H}_2\text{O}$ system, applying a rapid procedure without using organic additives in the synthesis mixture. The thermal evolution of the JDF-L1 structure is studied by thermogravimetric-differential thermal analysis, powder X-ray diffraction and Raman spectroscopy. It is shown that on heating JDF-L1 undergoes a sequence of structural rearrangements causing formation of non-crystalline alkali titanate-titanosilicate phases, defect-rich microcrystalline silica and crystalline titanosilicate narsarsukite, the latter becoming the dominant phase at high temperatures. Upon thermal treatment JDF-L1 undergoes reconstructive phase transitions involving order-disorder-order processes and resulting in formation of narsarsukite as a final dominant phase. According to XRD and Raman spectroscopic data, the thermal evolution of the JDF-L1 structure consists of three main stages:

- (i) below 550 °C - a gradual decrease in the interlayer spacing caused by H_2O removal, accompanied by topological changes in the Si-O entities and layer undulation;
- (ii) near 580 °C - total collapse of the JDF-L1 structure, providing material for formation of X-ray amorphous Ti-rich phases, microcrystalline silica of opal CT-type, and nucleation of narsarsukite;
- (iii) above 600 °C - atomic rearrangements in the matrix of non-crystalline alkali titanate-titanosilicate phases and opaline silica resulting in enhanced crystallization of narsarsukite.

**RESULTS OF AN ESR-STUDY OF QUARTZ
FROM THE ARCHAEOAN METAMORPHIC COMPLEXES
IN THE KOLA SUPERDEEP BOREHOLE SECTION**

Kotova, Y.N. & Lutoev, V.P.

Pervomaiskaya st, 54, Institute of Geology, Syktyvkar, Russia
e-mail: ENKotova@geo.komisc.ru; VLutoev@geo.komisc.ru

The researches were made within IGCP Project 408 (UNESCO). The main tasks of the Project are to compare properties of rocks in the section of the Kola Superdeep Borehole SG-3 (0-12262 m) and their homologues as well as geological correlation of the rocks in the SG-3 section with Precambrian formations of the Pechenga structure frame.

Present results are mainly based on a spectroscopic study of the extensive collection of samples of quartz (ca. 150) from the core SG-3 material and supposed rocks-homologues of the borehole area. ESR (electron spin resonance) was a main method for the study of quartz from the rocks. This method allows a selective registration of different atomic defects in the mineral structure. We used a multistage procedure of radiation-thermal influence on the mineral in order to reveal the highest possible diversity of atomic defects in quartz and facilitate their concentration evaluation. This procedure includes annealing at temperatures of 320, 530, and 1000 °C, and γ -irradiation of the samples by doses of 0.5 and 30 Mrad. ESR spectra of the powder samples of quartz were recorded at room temperature and boiling-point of liquid nitrogen with the commercial radiospectrometer SE/X 2547 (RadioPAN, Poland). The investigations were made on vacancy defects (E_1 -centres) and defects associated with isomorphous incorporation of Al-, Ge-, Ti-ions into the lattice of rock-forming quartz.

The dependence of impurity-related Al-, Ge-, Ti-centres, and proper structural defects in the quartz along the SG-3 section on the bedding depth and petrogenesis of the Precambrian host rocks were estimated. Concentration shifts (vacancy defects) and redistribution of defects according to the structural positions (lithium and proton species of Ti-centres, Al-centres in regular and irregular positions) are evident.

The investigations carried out show that the impurities and structural defects in the rock-forming quartz can serve as a genetic mark for metamorphic rocks of the Precambrian formation complexes and as one of the criteria for typification and correlation of deep strata of the early Precambrian, exposed by the SG-3 section.

The research was made within the financial support of the Russian Foundation for Basic Research, (grant RFBR #02-05-64747) and the integral project of the Earth Science Department of the Russian Academy of Sciences.

HYDROXYL IONS IN SYNTHETIC CRYSTALS: DO THEY DIFFER FROM THOSE IN MINERALS?

Kovács, L.

Research Institute for Solid State Physics and Optics, Hungarian Academy of Sciences, Konkoly-Thege M. út
29-33, H-1121 Budapest, Hungary
e-mail: lkovacs@szfki.hu

Synthetic crystals are produced for practical applications where the presence of hydroxyl ions in the material may be either desirable or undesirable. In any case a small amount of OH⁻ ions in *as-grown* anhydrous crystals (alkali halides, fluoroperovskites, oxides etc.) can easily be detected by the high resolution FTIR absorption technique, if the crystals are grown at high temperatures (600 – 1600 °C) from melt or solution in air atmosphere. Unlike to many cases of minerals, the relatively large single crystal samples do not require special microsampling methods or FTIR microscopes. The information obtained from the vibrational frequency of the OH⁻ ions, and from the pleochroism of the absorption bands are in general very similar and can be used to determine the structural site of the hydroxyl defect in the crystal lattice.

Two review papers have recently been published on OH⁻ defects in minerals and synthetic oxide crystals by BERAN & LIBOWITZKY (2003) and WÖHLECKE & KOVÁCS (2001), respectively, which present the main similarities and differences between the two classes of materials. In the present work, the anharmonicity of the stretching mode characteristic for all O-H vibrations, the weak coupling to phonon bands in some complex oxides derived from the temperature dependence of the OH⁻ bands, and the effect of a structural phase transitions on the O-H vibrational frequency in LaGaO₃ crystals will be surveyed. The role of hydroxyl ions in the thermal fixing of holographic gratings in photorefractive materials is also shown, and how the composition of some niobates and tantalates can be characterized by the shape of the OH⁻ bands.

This work has been partially supported by the Hungarian Scientific Research Fund (OTKA No. T047265).

References

- BERAN, A. & LIBOWITZKY, E. (2003): *Phase Transitions*, **76**: 1-15.
WÖHLECKE, M. & KOVÁCS, L. (2001): *Crit. Rev. Sol. St. Mat. Sci.*, **26**: 1-86.

FTIR SPECTROSCOPY OF OH⁻ IONS IN Pb₅(GeO₄)(VO₄)₂ APATITE

Kovács, L.¹, Gospodinov, M.² & Capelletti, R.³

¹ Research Institute for Solid State Physics and Optics, Hungarian Academy of Sciences, Konkoly-Thege M. út 29-33, H-1121 Budapest, Hungary

² Institute of Solid State Physics, Bulgarian Academy of Sciences, 72 Tzarigradsko Chaussee, 1784 Sofia, Bulgaria

³ INFN-CNR and Department of Physics, University of Parma, Parco Area delle Scienze 7/A, 43100 Parma, Italy
e-mail: lkovacs@szfki.hu

Lead germanate vanadate – Pb₅(GeO₄)(VO₄)₂ (PGV) – is a promising acousto-optical material, which can be grown from melt by the Czochralski method (YANO et al., 1971). PGV crystallizes in a hexagonal structure characterized by the space group P6₃/m (IVANOV & ZAVODNIK, 1989). It belongs to the general A₄B₆(XO₄)₆Y₂ apatite structure, where lead occupies both A and B positions, germanium and vanadium are randomly located in tetrahedral sites, X, and the anionic position, Y, remains empty. In hydroxyapatites Y denotes the OH group. In oxide crystals grown in air atmosphere, however, hydroxyl ions are usually present as impurities occupying oxygen sites (WÖHLECKE & KOVÁCS, 2001). The aim of this paper is to study the vibrational properties of hydroxyl ions possibly incorporated in synthetic Pb₅(GeO₄)(VO₄)₂ single crystals, using the Fourier Transform InfraRed (FTIR) absorption technique.

The presence of hydroxyl ions in *as-grown* Pb₅(GeO₄)(VO₄)₂ crystals has been confirmed by detecting an absorption band related to the stretching vibration of OH⁻ ions at $\nu = 3558 \text{ cm}^{-1}$ wavenumber at 300 K, $\Delta\nu \approx 20 \text{ cm}^{-1}$. These values are in relatively good agreement with those reported for Ca₁₀(PO₄)₆(OH)₂ hydroxylapatites, $\nu \approx 3572 \text{ cm}^{-1}$, $\Delta\nu \approx 10 \text{ cm}^{-1}$ (CANT et al., 1971). The OD⁻ isotopic replica at 2625 cm⁻¹ wavenumber has appeared in the crystal after a high temperature treatment at 1073 K in D₂O vapour atmosphere. The anharmonicity of the stretching mode calculated from the frequencies of the OH⁻/OD⁻ ions is $x_e \approx 0.024$, in excellent agreement with those found for hydroxyl ions in other oxides (WÖHLECKE & KOVÁCS, 2001). The stretching mode frequency has shifted to higher energies, while the halfwidth of the slightly asymmetric band has shown an anomalous increase for decreasing temperatures ($\nu = 3561.5 \text{ cm}^{-1}$, $\Delta\nu = 24 \text{ cm}^{-1}$ at 9 K). Anomalous behaviour has also been observed for the halfwidth of the absorption band using polarized light. At 300 K for light propagating along the *c* axis (ordinary polarization) $\Delta\nu$ is about 20 cm⁻¹, while for extraordinary polarization $\Delta\nu = 13 \text{ cm}^{-1}$. The band intensity, however, shows only a slight change for *o* and *eo* polarization directions. The anomalous temperature and polarization behaviour of the OH⁻ absorption band and the possible lattice sites of the hydroxyl ions in synthetic Pb₅(GeO₄)(VO₄)₂ apatite single crystals will be discussed.

This work has been partially supported by the Hungarian Scientific Research Fund (OTKA No. T047265), the CNR-HAS and BAS-HAS cooperation programs.

References

- CANT, N.W., BETT, J.A.S., WILSON, G.R. & HALL, W.K. (1971): Spectrochim. Acta A, **27**: 425-439.
 IVANOV, S.A. & ZAVODNIK, V.E. (1989): Soviet Phys. – Cryst., **34**: 824-828.
 WÖHLECKE, M. & KOVÁCS, L. (2001): Crit. Rev. Sol. St. Mat. Sci., **26**: 1-86.
 YANO, T., NABETA, Y. & WATANABE, A. (1971): Appl. Phys. Lett., **18**: 570-571.

NMR AND DIFFRACTION STUDY OF ACETONE INTERCALATED IN THE LAYER SILICATE RUB-18

Kovalev, O., Gies, H. & Fechtelkord, M.

Ruhr-Universität-Bochum, Institut für GMG, Universitätstr. 150, 44780 Bochum
e-mail: oleg.kovalev@ruhr-uni-bochum.de

Interaction of organic molecules with inorganic surfaces is of interest because of a variety of technical applications and because of the environmental impact (OGAWA & KURODA, 1995). In order to study these processes intercalates are used as model system. In particular the analysis of the hydrogen bond network established between guest-molecules and the host-compound are of interest. As simplest molecule for the study of the interaction, acetone has been used (BOROVKOV et al., 1982).

The synthesis of Acetone-Rub-18 was carried out starting from H-Rub-18, a derivative of the Na-form (BOROWSKI et al., 2002), by treatment with acetone or D6-acetone at room temperature. The level of intercalation is about 95%. The sample was stored at room temperature in D₂O atmosphere to avoid D-H exchange. DTA, TGA investigations (measured with a BÄHR STH 503, T=293-463 K, heat rate 3 K/min) show two weak signals at 318 and 382 K which are explained as processes involving the intercalated acetone molecule. In the ¹H MAS NMR spectra (spectrometer: Bruker ASX-400, spinning rate - 12 kHz, dwell time - 4 μs, D1 10 s) there are two signals at 2.0 ppm (methyl group) and 6.0 ppm (silanol group). The high temperature (temperature range 298-430 K) ¹H MAS NMR spectra show the splitting of the two main signals into 5 and 6 signals with greater amplitude than at room temperature, respectively. The chemical shift values of the two signals in a ²⁹Si MAS NMR spectroscopy experiment (spinning rate-3.5 kHz, dwell time- 25 μs, D1- 60 s) are typical for Q³ (Si(-OSi)₃(-OH)) and Q⁴ (Si(-OSi)₄)-connected silicate tetrahedra, respectively. Powder neutron diffraction data were used to investigate the crystal structure of the composite. The data were collected on the high-resolution powder diffractometer HRPT (PSI Villigen, Swiss) at λ=1.886 Å from 5-163° 2θ with step width 0.1°. The symmetry of the structure of D6-Acetone-Rub-18 was determined as P4₁2₁2. Unit cell parameters were refined with least square methods: a₀=7.479(7), c₀=37.334(9) Å. The location of intercalated guest molecules was determined using Fourier syntheses maps. The geometric parameters of the silicate layers shifted only slightly upon the intercalation. The acetone molecules are located in the “semi cages” between silicate layers and stabilize the structure (Fig. 1).

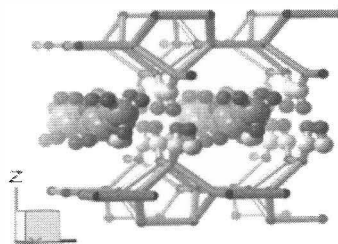


Fig. 1. Fragment of the crystal structure of H-Rub-18 intercalated with D6-Acetone

References

- BOROVKOV, V.Y. et al. (1982): J. Catal., **75**: 219-224.
BOROWSKI, M. et al. (2002): Z. Kristallogr., **217**: 233-241.
OGAWA, M. & KURODA, K. (1995): Chem. Rev., **220**: 399-438.

THE REVELATION OF TYPOMORPHIC PROPERTIES OF METAMORPHIC CARBONATE ROCKS.

Kukuy, A.L., Matveeva, O.P. & Sokolova, N.G.

Saint Petersburg Mining Inst., 21 liniya VO, 2, 199026, SPb, Russia
e-mail: sonja@spbtlg.ru

To determine the belonging of marble to a certain deposit, these laboratory methods of testing can be used: spectrophotometry, luminescence analyses and X-ray diffraction. Marble specimens from Karelia (Tivdia, Juven, Ruskeala), Middle Ural (Polevskoe, Ufaley), Greece and Italy (Carrara Mountains) were investigated using these methods. The age and formation condition of these rocks differ considerably and thus influenced the composition and structural features of the composing minerals. This is confirmed by the chemical analysis (Table 1).

Table 1. Chemical composition of marbles in ppm

Sample	Mg	Fe	Mn	Pb	Ce	Σ REE
Polevskoe	6488	111	44,1	0,8	0,5	5,9
Carrara Mount.	9958	287	102,8	1,1	1,5	6,4
Juven	1900	321	47,1	1,4	2,9	10,5

X-ray analysis revealed a significant difference in phase composition. Marbles from Juven (white-grey, coarse-grained) and Greece (white, fine-grained) proved to be the most similar to pure calcite. They contained only a little amount of quartz. Ural marbles (grey and white) contained a considerable dolomite and quartz mixture, and pink Tivdia marble consisted almost completely of dolomite with small amount of quartz. Lattice parameters of the investigated carbonates varied within the range $a_0 = 4.804-4.981$, $c_0 = 15.996-17.028$ Å; $c/a = 3.33-3.44$. Photoluminescence (PL) of marbles was investigated in visible and ultraviolet range. The intensive blue-violet luminescence is typical for white coarse-grained marbles. It is related to cerium impurities and is typical for Iceland spar. Other sorts of marble have different colors and variable luminescence in sample volumes. To obtain more extensive spectroscopic data, some samples were dissolved in hydrochloric acid. The optical absorption and the PL of their solution were investigated. We also investigated carbonates, used in the construction of Saint Isaac's Cathedral (architect Rinaldi, 18 c., Saint Petersburg) and Queen's pavilion in Peterhof (19 c.). The results are shown in Table 2.

Table 2. Spectral characteristics of marbles

Sample	Color	PL, λ_{max}^{em} , nm	Solutions	
			absorp., λ_{max}^{ab} , nm	PL, λ_{max}^{em} , nm
Polevskoe	white	530	360	430
Carrara Mount.	white	340, 400 - 450	250, 330	340, 540
Juven	white - grey	430	250, 300, 360	420
Ruskeala	grey	520 - 550		
Tivdia	pink + white	520, 540	260, 335	540
Ufaley	grey	-		
ruins 18 c.	white	340, 400 - 450		

Thus, this investigation has shown that using these methods enables to determine characteristic features of marbles of a certain type and to determine its origin. The results can be used for the characterisation of the marble and during the construction and restoration works.

APPLICATION OF MICROANALYSIS (SEM-EDS) IN THE STUDY OF HEAVY MINERALS FROM RECENT STREAM ALLUVIA IN THE TATRA MTS.

Ladenberger, A.

Institute of Geological Sciences, Jagiellonian University, Oleandry 2a, 30-063 Kraków, Poland
e-mail: berg@geos.ing.uj.edu.pl

Heavy minerals from the recent alluvia in the upper parts of valleys in the Tatra Mts. were studied. Samples of alluvia were collected from six streams in the Tatra Mts. and examined using a scanning electron microscope fitted with an energy dispersive spectrometer (JEOL 5410 and NORAN Voyager 3100). Polished thin sections of heavy mineral fractions were prepared and studied in an optical microscope in transmitting and reflected light and examined in a scanning electron microscope fitted with a dispersive energy spectrometer (SEM-EDS).

Heavy minerals assemblages from recent alluvia in the Western Tatra Mts. are composed of garnets, opaque minerals (magnetite, ilmenite), amphiboles, zircon, tourmaline, and rutile. Xenotime and monazite occur in relatively high amount. Staurolite, apatite, and sillimanite are present as minor components. In the Western Tatras a relatively high content of sulphides was noted. Garnet grains are characterised by high content of almandine end-member (Alm 45-75 %); spessartite is also present in significant amount (Sps 5-55 %). Amphiboles are represented mostly by magnesio-hornblende. All sulphide grains (pyrite, Fe-Cu sulphides) are strongly oxidised. Heavy minerals assemblages from the High Tatra Mts. consist of apatite, epidote, ilmenite, magnetite, zircon, monazite, rutile, hematite, chlorite, allanite, titanite, prehnite, pumpellyite, sillimanite, pyrite, barite. Amphibole, prehnite, xenotime, allanite, barite and pyrite are scarce. Apatite grains exhibit variations in chemical composition (Mn and Cl content). Most Fe-Ti oxides exhibit complex intergrowths of very thin lamellae and lenses of Ti-ilmenite and rutile enclosed in Ti-hematite host.

Heavy mineral assemblages generally reflect the composition of accessory minerals (both primary and formed during hydrothermal alterations) present in source rocks. High abundance of crushed and irregular grains can be related to glacial transport and subsequent extraction of grains from moraines. Presence of grains with porous margins indicates intense leaching related probably to the activity of humic acids in alluvia. Scarcity of sulphide veins in the Western Tatras suggests that a relatively high content of oxidised sulphide grains in heavy mineral assemblages is related to their removal from old mine tailings present in upper parts of valleys.

Results of heavy minerals from alluvia in the Tatra Mts. can be important in the discussion on the origin of young clastic deposits in the Podhale and Orava basins (KIEBAŁA et al., 2001).

References

KIEBAŁA, A., KUSIAK, M., MICHALIK, M. & PASZKOWSKI, M. (2001): Polskie Tow. Mineral. - Prace Specj., **19**: 79-81.

INFRARED AND MÖSSBAUER SPECTROSCOPY OF NATURAL GLASSES

Lebedeva, S.M., Bykov, V.N. & Mironov, A.B.

Russian Academy of Science Ural Branch, Institute of Mineralogy, Miass, Chelyabinsk region, Russia
e-mail: lebedeva@ilmeny.ac.ru

Natural glasses have been investigated by methods of IR- and Mössbauer spectroscopy. The ^{57}Fe Mössbauer spectra were obtained at room temperature using spectrometer MC-2201. The spectra of the studied glasses represent an asymmetrical doublet, the high-velocity peak is slightly wider and less intense in comparison with low-speed peak. The mathematical simulation of spectra was done by the program UNIVEM. At modeling of spectra the equaling of half-widths and intensities of low- and high-velocity lines of each doublet was supposed.

It is shown, that ferrous iron dominates in modern basalt glasses. The Fe^{2+} ions occupy octahedral positions in glasses, which are characterized by a different degree of distortion of the polyhedron. The Fe^{3+} ions also occupy octahedral positions. The redox ratio of iron in basalts from the East-Pacific Rise is slightly higher than the redox ratio of iron in oceanic basalts from the Mid-Atlantic Ridge. The redox ratio of iron in basalts from the Bouvet triple junction varies from 10 to 28 %. The redox ratio of Fe ions in ancient glasses considerably exceeds that of Fe ions in modern basalt glasses. It is related with secondary changes due to postmagmatic hydration.

In investigated tektites and impact glasses ferric iron is in tetrahedral positions. Its content amounts to 2-7 % of the total content of iron in glasses. The Fe^{2+} ions are in octahedral coordination and occupy structurally nonequivalent positions. This is related to the formation of tektites and impacts as a result of fast cooling from high temperatures.

The IR-spectra of investigated tektites and basalt glasses show three major absorption bands: the high-frequency region above 1000 cm^{-1} contains a strong, broad asymmetric band with a maximum near 1100 cm^{-1} ; a peak is centred at 800 cm^{-1} and a strong band appears in the low-frequency region at 470 cm^{-1} . The band at 1100 cm^{-1} is assigned to Si-O stretching vibrations associated with tetrahedral SiO_4 groups. The band in the region $400\text{-}500\text{ cm}^{-1}$ is assigned to the bending mode Si-O-Si(Al) (TAYLOR, 1990; POE et al., 1992). The band with maximum at 800 cm^{-1} is connected to vibrations of AlO_4 tetrahedra. In some samples bands in the region $580\text{-}640\text{ cm}^{-1}$ are observed. These bands are related to vibrations of AlO_5 and AlO_6 groups (McMILLAN et al., 1992). In some samples also a shoulder is present in the $900\text{-}1000\text{ cm}^{-1}$ region which is due to stretching vibrations of non-bridging Si-O bonds.

This work was supported by the Russian Foundation for Basic Research (Grant 04-05-96070).

References

- McMILLAN, P.F., WOLF, G.H. & POE, B.T. (1992): *Chem. Geol.*, **96**: 351-366.
POE, B.T., McMILLAN, P.F., ANGELL, C.A. & SATO, R.K. (1992): *Chem. Geol.*, **96**: 333-349.
TAYLOR, W.R. (1990): *Proc. Indian Acad. Sci., Earth Planet. Sci.*, **99**: 99-117.

OPTICAL SPECTROSCOPIC STUDIES IN LiNbO₃: Mg CRYSTALS BELOW AND ABOVE THE PHOTOREFRACTIVE THRESHOLD

Lengyel, K., Péter, Á., Polgár, K., Kovács, L. & Corradi, G.

Research Institute for Solid State Physics and Optics, Hungarian Academy of Sciences,
Konkoly Thege M. str. 29-33, H-1121, Budapest, Hungary
e-mail: klengyel@szfki.hu

LiNbO₃ is a well known non-linear optical material, but in many cases its application is limited by the photorefractive effect. The optical damage resistance can be improved by doping the melt with MgO above a threshold concentration. The threshold was found at about 5 mol % MgO for the congruent composition (BRYAN et al., 1984), but it strongly depends on the stoichiometry of the crystal. Several seemingly contradictory defect structure models have been developed to interpret this phenomenon (DONNERBERG et al., 1991; IYI et al., 1995; LIU et al., 1996).

Optical absorption methods are very simple and sensitive tools for the determination of the threshold concentration. The UV absorption edge and the IR spectrum of the OH⁻ ion vibration have systematically been measured in LiNbO₃ samples for wide composition and Mg concentration ranges. The Mg content (0-9 mol %) of the crystals with congruent, stoichiometric and an intermediate composition has been determined by atomic absorption spectroscopy. At the threshold the vibrational frequency of the hydroxyl ions moves abruptly to higher energies, while the shift of the UV-edge changes its direction. Above the threshold value, however, there is a linear dependence for the UV-edge and for the halfwidth of the A₁ Raman peak at 631 cm⁻¹ and an approx. square root dependence for the OH⁻ frequency as a function of Mg concentration. The halfwidths of the A₁ Raman peaks at 251 and 275 cm⁻¹ are also influenced by the sample composition. Our results confirm the model of LIU et al. (1996), in which the number of antisite Nb_{Li} decreases and that of Mg_{Li}V_{Li}(NbO₃)₂ defects increases with increasing Mg content up to the threshold, and for Mg concentrations exceeding the threshold, complexes containing Mg on both Li and Nb sites are formed.

References

- BRYAN, D.A., GERSON, R. & TOMASCHKE, H.E. (1984): *Appl. Phys. Lett.*, **44**: 847-849.
DONNERBERG, H., TOMLINSON, S.M., CATLOW, C.R.A. & SCHIRMER, O.F. (1991): *Phys. Rev. B*, **44**: 4877-4883.
IYI, N., KITAMURA, K., YAJIMA, Y., KIMURA, S., FURUKAWA, Y. & SATO, M.J. (1995): *J. Sol. State Chem.*, **118**: 148-152.
LIU, J., ZHANG, W. & ZHANG, G. (1996): *Phys. Stat. Sol. (a)*, **156**: 285.

**CRYSTAL CHEMISTRY OF GAHNITE-BASED PIGMENTS:
A DRS, EPR AND HF²EPR STUDY**

Lorenzi, G.¹, Baldi, G.¹, Di Benedetto, F.², Faso, V.¹, Lattanzi, P.F.³, Pardi, L.A.⁴ & Romanelli, M.⁵

¹Laboratorio di Ricerca Avanzata, Colorobbia Group, via Pietramarina 123, I50053, Sovigliana Vinci (Italy)

²Museo di Storia Naturale, Università di Firenze, via G. La Pira 4, I50121, Firenze (Italy)

³Dipartimento di Scienze della Terra, Università di Cagliari Via Trentino, 51 - I09127 - Cagliari (Italy)

⁴Istituto per i Processi Chimico- Fisici -CNR, via G. Moruzzi 1, I56124 Pisa (Italy)

⁵Dipartimento di Chimica, Università di Firenze, via della Lastruccia 3, I50019 Sesto Fiorentino (Italy)
e-mail: dibenefr@geo.unifi.it

The exact knowledge of the phase composition and of the crystal chemistry of the inorganic pigments, in relation to their colouring properties, represents a fundamental step to improve the quality of the final product and to lower the production costs. Spinel-based pigments are widely studied because of their stability even in drastic thermal and redox industrial treatments. The insertion of metal ion chromophores into this structure allow, not only to improve and control the relative synthesis, but also to exploit their use in ceramic applications as fast firing and in high temperature glazes.

Two synthetic Cr- and Ni- bearing gahnite ($ZnAl_2O_4$) based pigments, pink and blue, respectively, representing potential candidates in the manufacturing of coloured bulk glass-ceramics, have been investigated by different spectroscopic techniques: DRS, EPR and HF²EPR. The two pigments were synthesised from industrial raw materials (Al_2O_3 , ZnO and $Cr_2O_3/NiCO_3$) by firing at elevated temperatures with a short thermal cycle. The final products were investigated by X-ray powder diffraction (XRPD), thus revealing gahnite as major/unique phase. Rietveld refinements, performed on high-quality powder patterns, suggest the doping chromophore (Cr/Ni) to be quantitatively incorporated in the spinel structure. Nevertheless, the data do not allow to ascertain the crystal chemistry of the synthesised gahnite, and its relation to the observed colour.

Diffuse reflectance spectra were collected on both pigments, to identify the transitions in the UV and VIS range, whereas EPR and HF²EPR spectroscopies were applied only on the Cr-bearing material, because Ni^{2+} is undetectable in room temperature experiments. The obtained results point to an octahedral coordination for both Cr^{3+} and Ni^{2+} in gahnite; a small fraction of tetrahedral Ni was determined in the blue pigment. Both ions have been found to be isolated, the spectral evidence of pairs and/or clusters being absent. In both materials, the bulk colours arise from single ion crystal field transitions of the doping chromophore, Cr and Ni, respectively. The crystal field surrounding the chromophore has been fully interpreted. Moreover, the systematic characterisation of the products of several syntheses allowed to establish the efficiency of the doping process and dependence of the crystal chemistry on the synthesis condition, thus giving relevant information on the stability of the pigment colour.

SPECTROSCOPY OF FULGURITE GLASSES

Lysiuk, A. Y.

Pervomaiskaja 54, 167982 Syktyvkar, Russia
e-mail: rmin@geo.komisc.ru.

Fulgurites are glassy tubular bodies, which formed after the melting of rocks by the stroke of a lightning. They are relatively rare and not sufficiently enough studied geological objects. In our investigations we use several methods such as X-ray analysis, Mössbauer spectroscopy, infra-red spectroscopy, and electronic microscopy. We studied fulgurite from the area of Nigoziro in Karelia, Russia, which formed on carbon-containing aleurolits. The main component of fulgurite is alumosilicate glass; its chemical composition roughly corresponds with the composition of carbon-bearing aleurolits.

With the help of X-ray analysis we found that fulgurite glasses have quartzo-felsphatic composition. We also exposed the heterogeneity of the glasses which consist in combined presence of an amorphous glassy matrix and of crystalline formations differing in composition: orthoclase, hematite, chlorite, pyrite.

The state of iron in fulgurite was studied with the help of Mössbauer spectroscopy. In the spectrum four double-peaks of iron can be distinguished. One double-peak of trivalent iron in tetrahedral position ($\delta = 0.32$) which contains 4.1 % of all iron, and three double-peaks of divalent iron in octahedral positions. The latter differ by the extent of distortion of the octahedra ($\delta = 1.1; 1.13; 1.05$). Accordingly, the content of iron at these positions amounts to 33.9, 30.4, and 31.6 from total iron.

The infra-red spectra of fulgurites consists of absorption bands which are typical for silicate glasses and which are related to the silicon-oxygen vibrations of the glassy fulgurite matrix. We also found several narrow bands of crystalline quartz giving evidence for the presence of crystalline quartz.

Using micro-probe analysis we determined that the main mass of the glassy fulgurite substance consists of a Si-Al-Fe melt. In main parts of the melt areas of almost pure glasses are distinguished. The simultaneous appearance of fragments such as residual quartz tells that the temperature of the melt in that zone was near the temperature of quartz melting, this is about 1700 °C.

We also often found inclusions of hematite Fe_2O_3 . Its grains have straight borders. The appearance of these inclusions allows us to estimate the temperature of the fusion which did not reach the temperature of hematite melting. Besides, in the glass we found inclusions of hematite with tracks of partial melting.

Appearance of a great amount of skeleton formations with the composition such as FeO (wüstite) gives evidence for a high cooling speed. Such structures form because of dissociation in the cooling stage.

**IR AND RAMAN STUDIES OF SOME
MOLYBDENUM-LEAD-PHOSPHATE GLASSES**

Magdaş, D.A., Cozar, O., Ardelean I., Leopold, N. & David, L.

Babeş-Bolyai University, Faculty of Physics (Kogălniceanu Str., 1, 400084 Cluj-Napoca, Romania)
e-mail: amagdas@phys.ubbcluj.ro

The structure of $x\text{MoO}_3 \cdot (1-x)[2\text{P}_2\text{O}_5 \cdot \text{PbO}]$ glass system with $0 \leq x \leq 0.5$ was investigated by IR and Raman spectroscopies.

FT-IR spectra of the $x\text{MoO}_3 \cdot (1-x)[2\text{P}_2\text{O}_5 \cdot \text{PbO}]$ glasses exhibit the characteristic bands for the $2\text{P}_2\text{O}_5 \cdot \text{PbO}$ glass matrix and of MoO_3 oxide. At low concentration of MoO_3 the bands characteristic for phosphate oxide dominate. The strong bands around $900\text{-}950\text{ cm}^{-1}$ were assigned to the P-O-H bending and to the harmonics of P-O-P bending vibrations, whereas the 1047 cm^{-1} band is due to the stretching vibration of the PO_4^{3-} group (DAYANAND et al., 1996). The strong band around 1240 cm^{-1} is attributed to the P=O stretching vibration. The weak band around 1150 cm^{-1} is assigned to the P-O^(*c*) ionic stretching vibration, whereas the 500 cm^{-1} band is due to the harmonics of the P-O bending vibration. With the increase of the molybdenum oxide content the shape of the bands is changed, and a new band around 780 cm^{-1} occurs for high concentrations of MoO_3 . Other characteristic bands of MoO_3 are not present because these are overlapped by the characteristic bands for the P_2O_5 .

The characteristic bands of the $2\text{P}_2\text{O}_5 \cdot \text{PbO}$ matrix are also obtained from Raman spectra. Thus, the band at 696 cm^{-1} is attributed to the P-O stretching vibration (ILIESCU et al., 1994). The P-O stretching vibration arises at 1068 cm^{-1} , whereas the O-P-O stretching vibration appears at 1174 cm^{-1} (SCAGLIOTTI et al., 1987). The P=O stretching vibration is present at 1220 cm^{-1} .

It can be seen from the spectra that the IR and Raman bands are influenced by the presence of MoO_3 oxide in the glass matrix. This fact suggests that from low concentrations of MoO_3 , structural changes occur in the $2\text{P}_2\text{O}_5 \cdot \text{PbO}$ glass matrix due to molybdenum ions that play the role of network modifiers.

References:

- DAYANAND, C., BHIKSHAMAIHAH, G., JAYA TYAGARAJU, V., SALAGRAM, M. & KRISHNA MURTHY, A.S.R. (1996): *J. Mater. Sci.*, **31**: 1945-1967.
ILIESCU, T., ARDELEAN, I., SIMON, V. & LAZAR, D. (1994): *Studia Univ. Babeş-Bolyai, Physica*, **XXXIX**
SCAGLIOTTI, M., VILLA, M. & CHIODELLI, G. (1987) : *J. Non-Cryst. Solids*, **93**: 350-360.

CHEMICAL INVESTIGATIONS OF INCRUSTED STONE ON HISTORICAL MONUMENTS

Matovic, V & Rosic, A.

Faculty of Mining and Geology, Djusina 7, 11000 Belgrade, Serbia Montenegro
e-mail: vesnamat@beotel.yu

The corrosion damages on natural stones of historical buildings have accelerated during the last decades. The cause of the accelerated corrosion is connected to the nature of building materials, partly with construction style, but the most important factors are environmental conditions. After some years the built stone becomes discolored or covered by aggressive incrustations/crusts and finally the stone may be totally destroyed. The knowledge of causes and mechanism of decay is necessary for the conservation of historical monuments. Especially, it is very important for the choice of appropriate ways of cleaning of incrustated stones. These problems were subject of the investigations carried out on the monument "Unknown soldier" on the Mt. Avala near Belgrade.

The monument built from 1934 to 1938 is made of blocks of gabbro (Jablanica quarries). In this monumental mausoleum, 3971.95 m³ of stone blocks were built (ZIVANOVIC, 1962). The blocks are of different size and mortar connected with some joints filled by molten lead. At that time building contractors put sheets of lead alloy between the blocks. Today, we found relicts of these sheets and lead in empty joints. After 65 years of their exposing to atmospheric influence the stone blocks show different forms of physical-chemical and biological degradations.

A visual observation of stone blocks pointed out immediately on the very different state of the gabbro decay between the outer part (exposed to rain water) and the protected, inner one. On the outer parts of facade the most important damage types of stone are: blistering, peeling, granular disintegration and scaling. All of these pathological forms are induced by aggressive incrustations from joints (MATOVIC & ROSIC, 2004).

The two different types of incrustations were identified on stone surfaces (white and black). Using X-ray diffraction (XRD) it was possible to identify their mineral compositions responsible for the genesis of stone decay. The following associations of minerals were identified in samples of incrustations:

white sample: hydrocerussite $Pb_3(CO_3)_2(OH)_2$, X $NaPb_2(CO_3)_2OH$, plumbonacrite $Pb_{10}(CO_3)_6(OH)_6O$, calcite - $CaCO_3$;
black sample: anglesite - $PbSO_4$.

The forms of decay and obtained data show that the main causes of gabbro decay are atmospheric water, moisture, frost, hard dissolved salts, dissolution of mortar and lead in joints, thermal changes of stone etc.

References

- MAROVIC, V. & ROSIC, A. (2004): Conf. Environmental problems of cities, Belgrade, 65-66.
ZIVANOVIC, G. (1962): Vesnik, br. 13-14. Vojni muzej - Beograd, 1968: 247-275.

INVESTIGATION OF COLOURING MECHANISM OF REE-PEROVSKITES
THROUGH COMBINING STRUCTURAL AND
UV-VIS-NIR SPECTROSCOPY DATA

Matteucci, F.¹, Dondi, M.¹, Cruciani, G.², Baldi, G.³ & Barzanti, A.³

¹ ISTECC – CNR, Via Granarolo 64, 48018 Faenza, Italy

² Earth Science Department, University of Ferrara, Corso Ercole I d'Este 32, 44100 Ferrara, Italy

³ Colorobbia Italia SpA, Via Pietramarina 123, 50023 Sovigliana Vinci, Italy
e-mail: matteucci@istec.cnr.it

The research of red ceramic pigments is a current topic in traditional ceramics since most industrial products give hues far away from the pure red. New red pigments have been developed based on the perovskite $A^{III}B^{III}O_3$ structure, with $A=Y$ or REE and $B=Al_{1-x}Cr_x$, where $0.03 < x < 0.12$ (BALDI & DOLEN, 1999). Though extensively characterised from the technological viewpoint, perovskite pigments still present unsolved questions concerning the mechanisms involved in their coloration. This study was carried out through combining high resolution XRPD, performed using synchrotron radiation at the ESRF, with UV-Vis-NIR spectroscopy, performed using diffuse reflectance measurements.

Rietveld refinements of XRPD data confirmed the substitution of Cr for Al in the 6-coordinated B site and a decrease of B-O distance when the A site is filled with bigger REEs; hence an inverse correlation exists between the A-O and B-O distances.

UV-Vis-NIR spectra showed the existence of rare earth multiplets in the red region and the occurrence of peaks due to Cr^{3+} transitions ${}^4A_2-{}^2E$, but the final colour of pigments is due to a broad band absorbing the blue and green visible region never observed in the literature (WEBER & VARITIMOS, 1974). Besides, a shift of the broad band in the visible region was observed and related with the type of REE inside the site A. The origin of this broad absorption band is still unknown, but on the basis of the up to date results it can be hypothesized the following origins:

coalescence of the two Cr^{3+} peaks due to ${}^4A_2g({}^4F) \rightarrow {}^4T_2g({}^4F)$ and ${}^4A_2g({}^4F) \rightarrow {}^4T_1g({}^4F)$ transitions, but the shift of the absorption band does not follow the trend predicted by the crystal field theory;

charge transfer between Cr-O, but from literature data (POOLE & ITZEL, 1963) the absorption band for Cr^{4+} and Cr^{6+} is predicted at higher energies than those observed.

In conclusion, the red colour of (Y or REEs) $(Al_xCr_{1-x})O_3$ perovskites is due to multiple mechanisms, involving crystal field $d-d$ and $f-f$ spin allowed and spin forbidden transitions and particularly an absorption band, whose origin is still debated.

References

BALDI, G. & DOLEN, N. (1999): *Mat. Eng.*, **10**: 151-164.

POOLE, C.P. & ITZEL, J.F. (1963): *J. Chem. Phys.*, **39**: 3445-3455.

WEBER, M.J. & VARITIMOS, T.E. (1974): *J. Appl. Phys.*, **45**: 810-815.

SHORT-RANGE STRUCTURE OF IRON IN ANORTHITE-DIOPSIDE GLASS

McCammon, C.A.^{1,2}, O'Neill, H.S.C.², Berry, A.J.², Jayasuriya, K.D.^{3,4} & Campbell, S.J.³

¹ Bayerisches Geoinstitut, Universität Bayreuth, D-95440 Bayreuth, Germany

² Research School of Earth Sciences, Australian National University, Canberra ACT 0200, Australia

³ School of Physical, Environmental and Mathematical Sciences, University of New South Wales, Australian Defence Force Academy, Canberra ACT 2600, Australia

⁴ now at: Department of Physics, University of Kelaniya, Kelaniya, Sri Lanka

e-mail: catherine.mccammon@uni-bayreuth.de

Iron is the dominant transition element in natural glasses and melts; hence an understanding of its structural behaviour is of primary importance to knowledge of physical properties such as density and viscosity, chemical properties such as redox behaviour, and dynamic processes such as magma generation and volcanism. Mössbauer spectroscopy provides a measure of the short-range structure of iron in glass, as well as a quantitative determination of $\text{Fe}^{3+}/\Sigma\text{Fe}$, which can provide information on the T- $f\text{O}_2$ history of natural magmas. However Mössbauer spectra reflect site-to-site distortions of iron coordination polyhedra which complicate spectral analysis. Various approaches have been suggested, and while $\text{Fe}^{3+}/\Sigma\text{Fe}$ is relatively independent of the fitting method, the hyperfine parameters that relate to the short-range structure of iron are generally not. We therefore undertook a study of a well characterised suite of glasses in order to develop a fitting approach that could be applied over a wide range of iron compositions (both Fe^{2+} and Fe^{3+}), with the goal of characterising the effect of oxygen fugacity and glass composition on the short-range structure of iron in these glasses.

The glasses comprised two series: (1) 1 wt% $^{57}\text{Fe}_2\text{O}_3$ added to $\text{An}_{42}\text{Di}_{58}$ (nominally corresponding to the eutectic composition) and equilibrated at 1409°C over a range of oxygen fugacities from $f\text{O}_2 \sim 10^5$ bars ($\text{Fe}^{3+}/\Sigma\text{Fe}=1$) to 10^{-13} bars ($\text{Fe}^{3+}/\Sigma\text{Fe}=0$); (2) increasing amounts of Fe_2O_3 (2, 4, 7, 10, 20 or 30 wt%) added to the same $\text{An}_{42}\text{Di}_{58}$ starting composition and equilibrated at 1409 °C and three different oxygen fugacities (10^0 , 10^{-4} and 10^{-7} bars). The glasses were studied using XANES (BERRY et al., 2003) where Fe^{3+} concentrations were calibrated based on Mössbauer analysis using a multiple Lorentzian doublet approach (JAYASURIYA et al., 2004). The derived $\text{Fe}^{3+}/\text{Fe}^{2+}$ values are proportional to $\log f\text{O}_2$ with a slope of 0.245 ± 0.004 , in excellent agreement with the theoretical value of 0.25 predicted by thermodynamics (JAYASURIYA ET AL., 2004). The present study evaluates the degree to which structural information can be extracted from the Mössbauer data, and shows that an extended Voigt-based fitting analysis with two-dimensional distributions of isomer shift and quadrupole splitting reveals significant trends in the dataset, including the presence of four- and five-fold coordinated Fe^{2+} . Variations in the structural state of iron as a function of oxygen fugacity and total iron concentration provide insight into the physical and chemical properties of the corresponding silicate melts.

References

- BERRY, A.J., JAYASURIYA, K.D., O'NEILL, H.S.C., CAMPBELL, S.J. & FORAN, G.J. (2003): *Am. Mineral.*, **88**: 967-977.
 JAYASURIYA, K.D., O'NEILL, H.S.C., BERRY, A.J. & CAMPBELL, S.J. (2004): *Am. Mineral.*, in press.

**SYNTHESIS, CRYSTAL STRUCTURE, INFRARED AND RAMAN SPECTRA OF
 $\text{Sr}_5(\text{As}_2\text{O}_7)_2(\text{AsO}_3\text{OH})$**

Mihajlović, T., Libowitzky, E. & Effenberger, H.

Institut für Mineralogie und Kristallographie, Universität Wien, Geozentrum, Althanstrasse 14, A-1090 Wien,
Austria
e-mail: tamara.mihajlovic@univie.ac.at

The new compound $\text{Sr}_5(\text{As}_2\text{O}_7)_2(\text{AsO}_3\text{OH})$ was synthesized under hydrothermal conditions. It represents a previously unknown structure type and it is the first substance known to contain both $(\text{As}_2\text{O}_7)^{4-}$ and $(\text{AsO}_3\text{OH})^{2-}$ groups.

The crystal structure of $\text{Sr}_5(\text{As}_2\text{O}_7)_2(\text{AsO}_3\text{OH})$ was determined by single-crystal X-ray diffraction (293 K, $\text{MoK}\alpha$, $2\theta_{\text{max}} = 60^\circ$): space group $P2_1/n$ ($a = 7.146(1)$, $b = 7.142(1)$, $c = 32.750(1)$ Å, $\beta = 93.67(3)^\circ$, $V = 1668.0(5)$ Å³, $Z = 4$). It is built from five crystallographically unique SrO_{6-8} polyhedra and two $(\text{As}_2\text{O}_7)^{4-}$ groups besides a protonated $(\text{AsO}_3\text{OH})^{2-}$ group. $(\text{As}_2\text{O}_7)^{4-}$ groups involve four crystallographically non-equivalent $(\text{AsO}_4)^{3-}$ tetrahedra. The position of the hydrogen atom was located experimentally. To obtain further information on the anion groups and especially on the very short hydrogen bond length of 2.494(4) Å, where the donor and acceptor atoms are not equal due to (average) space-group symmetry, infrared and Raman spectra were acquired.

The IR spectral region between 3500 and 1000 cm^{-1} shows a peculiar increase in "background absorption", which is a typical feature of compounds with very short hydrogen bonds. It represents an extremely broad (FWHM ~ 1000 cm^{-1}) and low-energetic band that is assigned to the OH stretching mode of the $(\text{AsO}_3\text{OH})^{2-}$ group. It is quite characteristic that this band can be observed only in one of the polarized spectra, whereas it is absent in the other polarization directions and almost invisible in powder spectra. The former is caused by the preferred orientation of the OH vectors in the structure. Because of the broad band shape, As—O tetrahedral stretching vibrations and lattice modes are superimposed in the low-energy region of the spectrum (stretching modes < 1100 cm^{-1} ; bending + lattice modes < 450 cm^{-1}). The large FWHM aggravates a precise determination of the band center, which is estimated to be roughly at $\sim 1600 \pm 200$ cm^{-1} . According to the d — ν correlation for hydrogen bonds (NOVAK, 1974; LIBOWITZKY, 1999) this wavenumber is in excellent agreement with the refined O_h —H \cdots O bond length. The sharp and truncated band at ~ 1250 – 1300 cm^{-1} in the IR powder spectrum is assigned to the bending mode of the OH group and it corresponds with typical bending frequencies of strongly H bonded hydroxyl groups (NOVAK, 1974; BERAN & LIBOWITZKY, 1999).

Financial support of the Austrian Science Foundation (FWF) (Grant P15875-N03) is gratefully acknowledged.

References

- BERAN, A. & LIBOWITZKY, E. (1999): In: WRIGHT, K. & CATLOW, R. (eds.) Microscopic properties and processes in minerals. Kluwer Academic Publishers, Dordrecht, 493-508.
LIBOWITZKY, E. (1999): Mh. Chem., **130**: 1047-1059.
NOVAK, A. (1974): Struct. Bond., **18**: 177-216.

CRYSTALLOGRAPHY, RAMAN AND IR SPECTROSCOPY OF PERHAMITE – AN INTERESTING SILICO-PHOSPHATE

Mills, S.J.^{1,2,3}, Frost R.L.⁴, Grey, I.E.³, Mumme, W.G.³ & Weier, M.L.⁴

¹Department of Earth Sciences, The University of Melbourne, Parkville 3010, Victoria, Australia

²Geosciences, Museum Victoria, GPO Box 666E, Melbourne 3001, Victoria, Australia

³CSIRO Minerals, Box 312, Clayton South 3169, Victoria, Australia.

⁴Inorganic Materials Research Program, School of Physical and Chemical Sciences, Queensland University of Technology, GPO Box 2434, Brisbane 4001, Queensland, Australia.

e-mail: smills@museum.vic.gov.au; *corresponding address

Perhamite, $\text{Ca}_3\text{Al}_7(\text{SiO}_4)_2(\text{PO}_4)_4(\text{OH})_6 \cdot 16.5\text{H}_2\text{O}$, is an interesting silico-phosphate found in pegmatitic veins and rock phosphate deposits in the United States, Germany and Australia (MILLS, 2003). Its combination of mixed anion, hydroxyl and water units make it ideal for an integrated Raman and IR study. The crystal structure has also recently been revised giving new insight into the framework of this mineral. Perhamite morphology consists of very thin intergrown platelets that can form a variety of habits such as stalagmite-like aggregates and rosettes generally less than 40 μm across.

The structure of perhamite is related to that of the crandallite-group minerals and the chain silicate vlasovite. A disordered region of vlasovite-like $(\text{Si,Al})_4\text{O}_{11}$ ribbons together with water molecules is sandwiched between blocks of ordered crandallite-type structure.

Raman spectroscopy of perhamite has revealed intense bands in the regions 1110–1130 and 966–996 cm^{-1} . In these regions the SiO_4 and PO_4 symmetric stretching modes can be found. Other bands observed in the range 1005–1096 cm^{-1} are attributed to the ν_3 antisymmetric bending modes of PO_4 . Bands in the low-wavenumber region are assigned to the ν_4 and ν_2 out-of-plane bending modes of the SiO_4 and PO_4 units.

Infrared spectroscopy in the hydroxyl-stretching region (Fig. 1) shows a number of overlapping bands which are observed in the range 3581–3078 cm^{-1} . These wavenumbers enable an estimation to be made of the hydrogen bond distances and correspond to 3.176(0), 2.880(5), 2.779(6), 2.749(3), 2.668(1) and 2.599(7) Å. An arbitrary cut-off point of 2.74 Å (based upon the wavenumber 3300 cm^{-1}) was used to distinguish the weak hydrogen bonding from the strong hydrogen bonds.

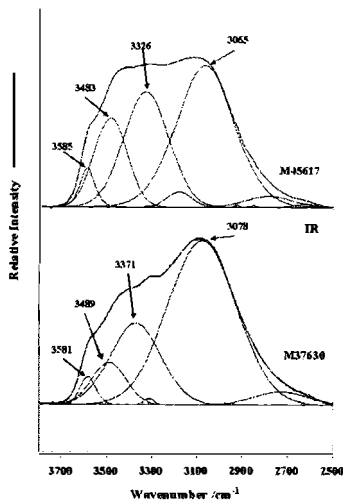


Fig. 1. Infrared spectra of perhamite samples M37630 and M45617 in the hydroxyl stretching region

References

MILLS, S.J. (2003): Aust. J. Mineral., **9**: 41-43.

ORDERING OF PARAMAGNETIC DEFECTS IN NATURAL DIAMONDS WITH MICROTWINS.

Mineeva, R.M.¹, Speransky, A.V.¹, Titkov, S.V.¹ & Zudin, N.G.²

¹ Institute of Geology of Ore Deposits, Petrography, Mineralogy and Geochemistry of RAS, Staromonetny 35, 119017, Moscow, Russia

² Rony Carob Ltd, Zelenograd 338B/40, 103305, Moscow, Russia
e-mail: mineeva@igem.ru

Up to now all paramagnetic centers observed in diamond crystals were found to align with a single coordinate system determined by crystallographic axes. In this respect, natural plastically deformed diamonds with brown and pink colours were not different from diamonds, which had not suffered any postgrowth transformation. However, the present EPR

study of violet diamonds with planar deformation lamellae observed with an optical microscope has shown that the behaviour of such crystals was very unusual.

A large number of additional lines was discovered in an EPR spectrum of violet diamond recorded at standard diagnostic orientation with $H \parallel L_4$ (Fig. 1). There was no doubt that these lines belong to a center including two nonequivalent nitrogen atoms, as well known *N1* and *W7* centers and recently discovered by us *M2* and *M3* centers. Analysis of the angular dependence of the spectra shows that hyperfine parameters for both nitrogen atoms are similar to

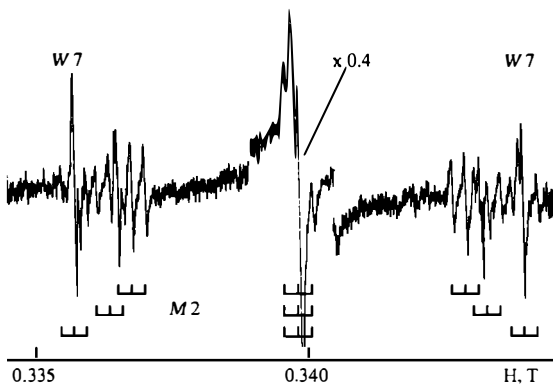


Fig. 1. X-band EPR spectrum for violet diamond containing *W7* and unusually oriented *M2* centers, recorded at room temperature with magnetic field along [001]

those for *M2*. However, the main axes of these tensors do not coincide with the crystal axes, but correspond to {111} orientations of lamellae, which are twinned after a spinel law. Visual analysis displays that the amount of twinned lamellae in violet diamonds is not more than 1%, but all observed *M2* centers are located in them. Regarding the *W7* center, the most characteristic for plastically deformed diamonds, its content is roughly the same in the whole main part of the crystal and in the twinned lamellae.

Therefore, our investigation reveals that plastic deformation in natural violet diamonds could occur by a mechanical microtwinning. EPR gives the possibility to see this process from the inside through the analysis of paramagnetic defect transformations showing the change in the crystal structure at the level of individual atoms.

This work was supported by the Russian Foundation for Basic Research (Grant 02-05-64696).

X-RAY ABSORPTION SPECTROSCOPY AT 3d-METAL $L_{2,3}$ AND O K-EDGES IN COLUMBITES

Mirão, J.¹ & Figueiredo, M.O.²

¹ Geophysics Center, University of Évora, Apdo. 92, 7001-019 Évora, Portugal

² Cryst. Miner. C., ICT, Al. Afonso Henriques, 41-4º, 1000-123 Lisboa & CENIMAT, UNL, Caparica, Portugal
e-mail: jmirao@uevora.pt

Columbites are economically important Nb and Ta ores typical of pegmatites. Structurally identical synthetic compounds are intensively studied due to magnetic and electronic properties that make them technologically important materials. The crystal structure of these oxide minerals is a derivative from α -PbO₂ structure, based on a hexagonal closest packing of oxygen anions with cations half-filling the octahedral interstices in a chain-pattern. Cation octahedra share edges along each zigzag chain and vertices with adjacent chains in neighbouring layers. A triple unit cell comes out from the ordering of two consecutive layer levels of pentavalent cations interleaved by one layer of transition metals (Fe,Mn). Oxygen anions display a triangular coordination by coplanar cations from which at least one is pentavalent. Cation disordering induces the mixing of three possible configurations – three (Nb,Ta), two (Nb,Ta) plus one (Fe,Mn), one (Nb,Ta) plus two (Fe,Mn) – , a quite common feature in natural compounds that is apparently precluded in synthetics.

Ordering may be attained by heating mineral fragments in air and rapidly cooling from about 1000 °C (ERCIT et al., 1995), but some discussion still prevails on the oxidation of 3d transition metals upon heating (ZAWISLAK et al., 1997). To ascertain the valence state of Fe and Mn, soft X-ray absorption at metal $L_{2,3}$ and O 1s edges was performed at BESSY* using beam line D11.1A-PM3 (SX700 monochromator with an energy resolution better than 0.2 eV). Studied columbites (from Zambezia mineralurgical province in Mozambique) cover a wide range of compositions checked by electron microprobe. The ordering state of as-collected and heated samples was monitored by X-ray diffraction.

To model O 1s XANES spectra, *ab-initio* simulations were carried out based on the multiple scattering approximation implemented in the FEFF code (ANKUNDINOV et al., 1998). Comparison of experimental and calculated spectra with data collected from simple oxide minerals (FIGUEIREDO & MIRÃO, 2002) allows for identifying features of O 1s XAS spectra explained by hybridisation of oxygen 2p with metal 3d states disturbed by chemical bonding.

Conversely, intensity variations of particular features in metal $L_{2,3}$ spectra indicates oxidation by heat treatment progressing from the surface inwards the mineral fragments.

*Financing from EU is acknowledged. Thanks are due to Drs. R. Mittthank and T. Kachel for their support.

References

- ANKUNDINOV, A.L., RAVEL, B., REHR, J.J. & CONRADSON, S.D. (1998): Phys. Rev. B, **58**: 7565-7576.
ERCIT, T.S., WISE, P. & ČERNÝ, P. (1995): Am. Mineral., **80**: 613-619.
FIGUEIREDO, M.O. & MIRÃO, J. (2002): Eur. J. Mineral., **14**: 1061-1067.
ZAWISLAK, L., ANTONIETTI, V., CUNHA, J. & SANTOS, C.A. (1997): Sol. State Comm., **101**: 767-770

**EQUATION OF STATE AND TRANSITION PRESSURE FOR BRUCITE
DEHYDRATION: THEORETICAL APPROACH**

Mookherjee, M. & Stixrude, L.

Department of Geological Sciences, University of Michigan, Ann Arbor, MI 48109, USA
e-mail: mainak@umich.edu

Brucite, $\text{Mg}(\text{OH})_2$ is a simple crystalline hydroxide, and is an end-member for hydrous minerals that hosts H_2O in the crust and mantle of the Earth. Owing to its structural simplicity, it serves as useful prototype for layered hydrous minerals.

In order to explore the high pressure behaviour of brucite, *ab initio* total energy calculations based on local density approximation (LDA) and generalized gradient approximation (GGA) of density functional theory have been performed. Using neutron diffraction it has been observed that at high pressures, hydrogen atoms are disordered over the three 6i Wyckoff sites with one-third occupancies where as at ambient pressures they are oriented parallel to *c*-axis (2d Wyckoff site). In order to explore such order-disorder behaviour, we constructed a $3 \times 3 \times 1$ super-cell with hydrogen occupying only one of the three 6i sites, and arranged the H atoms such that displacement of each hydrogen atoms from 2d to 6i position forms an enclosed ring. *Ab initio* structural relaxations confirm the mechanical stability, and energetic favorability, as compared with the 2d structure, of this arrangement. We determine the theoretical equation of state for brucite with K_0 of 53 GPa and its pressure derivative, K_0' of 6.2, using LDA, and a K_0 value of 34 GPa and K_0' of 5.8 with GGA (both corrected for zero pressure and thermal pressures at $T = 300$ K). We also simulate the transition pressure for the dehydration of brucite at $T = 0$ K, comparing the enthalpies of $\text{Mg}(\text{OH})_2$ and sum of enthalpies of MgO and H_2O (ice-VIII). We are exploring possibilities of formation of symmetric hydrogen bonding at higher pressures. We are also exploring the elastic constants (c_{ij}) for brucite and their pressure dependence.

NMR STUDIES OF MOLECULAR DIFFUSION AND PROTON TRANSFER IN HYDRATED MINERALS

Moroz, N.K.

Institute of Inorganic Chemistry, Russian Academy of Sciences, Siberian Branch
Avenue Lavretiev 3, 630090 Novosibirsk, Russian Federation
e-mail: moroz@che.nsk.su

The physical-chemical properties of hydrated minerals in which the H₂O molecules are located in structural cavities, channels or between layers, essentially depend on the librational and translational motions of the water molecules (WINKLER, 1996; PAUKOV et al., 2002). Along with infrared-, dielectric-spectroscopy, and incoherent neutron scattering, the most often used technique to determine the low-frequency dynamics of molecular H₂O in minerals is ¹H-NMR spectroscopy (STEBBINS, 1988). Recently, we proposed a new wide-line ¹H NMR approach based on the consideration of the anisotropy of the fluctuations of the intramolecular proton-proton interaction, arising during the process of the H₂O molecular diffusion. With this approach, a number of intriguing results, such as the pressure-enhanced H₂O self-diffusion in natural zeolites (MOROZ et al., 2001), have been obtained. The ensuing development of the approach discussed enabled us to suggest a way to measure the rates of the proton-transfer reactions in water subsystems of hydrated microporous minerals (AFANASSYEV et al., 2000; AFANASSYEV & MOROZ, 2003). It has been shown that the intermolecular proton transfer is due to the interaction of water molecules with the protonic defects, presented by the acid (Brønsted) sites. As a rule, these reactions are exhibited at temperatures corresponding to the intense H₂O self-diffusion. These circumstances allow one to use water molecules as a NMR molecular probe for visualization of the active acid sites and consequently for characterization of the catalytic activity of minerals even if the site concentration is small enough that obstacle its detection with available spectroscopic techniques (MOROZ et al., 2003).

This work was supported by Russian Academy of Sciences (Program #26, Hydrogen Energetic).

References

- AFANASSYEV, I.S. & MOROZ, N.K. (2003): *Solid State Ionics*, **160**: 125-129.
AFANASSYEV, I.S., MOROZ, N.K. & BELITSKY, I.A. (2000): *J. Phys. Chem. B*, **104**: 6804-6808.
MOROZ, N.K., AFANASSYEV, I.S., PAUKSHTIS, E.A. & VALUEVA, G.P. (2003): *Phys. Chem. Minerals*, **30**: 243-247.
MOROZ, N.K., KHOLOPOV, E.V., BELITSKY, I.A. & FURSENKO, B.A. (2001): *Micropor. Mesopor. Mater.*, **42**: 113-119.
PAUKOV, I.E., MOROZ, N.K., KOVALEVSKAYA, YA. & BELITSKY, I.A. (2002): *Phys. Chem. Minerals*, **29**: 300-306.
STEBBINS, J.F. (1988): In: HAWTHORNE, F.C. (ed.) *Spectroscopic Methods in Mineralogy and Geology. Rev. Mineral.*, **18**, Miner. Soc. Amer., Washington D.C., 405-429.
WINKLER, B. (1996): *Phys. Chem. Minerals*, **23**: 310-318.

VIBRATIONAL SPECTRA OF KLDNOITE, NATURAL ANALOGUE OF PHTHALIMIDE C₆H₄(CO)₂NH

Moroz, T.¹, Shcherbakova, E.² & Kostrovsky, V.³

¹ United Institute of Geology, Geophysics & Mineralogy SB RAS (Novosibirsk, 630090, Russia)

² Institute of Mineralogy, Ural Branch of Russian Acad. Sci. (Miass, 456317, Russia)

³ Institute of Solid State Chemistry and Mechanochemistry SB RAS (Novosibirsk, 630090, Russia)
e-mail: moroz@uiggm.nsc.ru

Aromatic compounds occur very rarely as minerals. Kladnoite, the only mineral containing nitrogen as NH-group, was discovered on the burnt coal dumps of Kladno, Czech Republic in 1937 and more later it was found in the Chelyabinsk coal basin, Russia (ROST, 1937; CHESNOKOV & SHCHERBAKOVA, 1991). X-ray diffraction patterns of Czech and Russian kladnoite are similar and correspond to synthetic phthalimide (CHESNOKOV & SHCHERBAKOVA, 1991; ZACEK et al., 2000). A detailed assignment of most of the observed frequencies in vibrational infrared (IR) and Raman spectra of phthalimide (PIMH) polycrystalline and single crystal samples has been previously reported (HASE, 1978). For monoclinic phthalimide crystals symmetry (space group $P2_1/n$ = C_{2h}^5 , $Z = 4$), all vibrational A_g and B_g (A_u , B_u) fundamentals are Raman (IR) active (MOROZ, 1998). Main PIMH modes are observed in the Fourier transformed (FT) IR (Fig. 1a) and FT-Raman (1064 nm excitation, Fig. 1b) spectra of kladnoite from Russia. As against a Raman spectrum of synthetic PIMH (HASE, 1978; AROCA & CLAVIJO, 1988), attempts to record Raman spectra using 514.5 nm excitation were unsuccessful due to strong fluorescence with maximum at 568.6 nm shown by the samples with this laser line. An analysis of NIR FT-Raman, FT-IR spectra and fluorescence of both Russian and Czech kladnoites is presented.

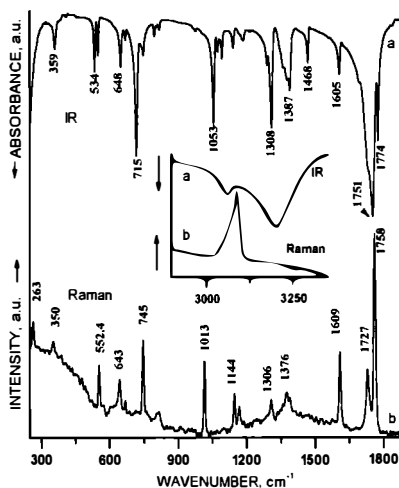


Fig. 1. FT-IR (a) and NIR FT-Raman (b) spectra of Russian kladnoite

References

AROCA, R. & CLAVIJO, R.E. (1988): Spectrochim. Acta A, 44: 171-174.
 CHESNOKOV, B.V. & SCHCHERBAKOVA, E.P. (1991): Mineralogy of burning dumps of the Chelyabinsk coal basin (the South Ural). Nauka, Moscow. 152 p, in Russian.
 HASE, Y (1978): J. Mol. Struct., 48: 33-42.
 MOROZ, T.N. (1998): Space-group symmetry and selection rules for infrared and Raman spectra. Preprint No. 98-71, Novosibirsk, 1-22.
 ROST, R. (1937): Bull. Intern. Acad. Sci. Bohem., 11: 1-7.
 ZACEK, V., DVORAK, Z., MRAZ, J., ONDRUS, P. & DOBES, P. (2000): Bull. Mineral. Petrol. Odd. Nar. Muz. (Praha), 8: 267-268.

RAMAN MICROSCPECTROSCOPY: THE KEY ROLE IN THE RECONSTRUCTION OF PT-PATHS OF HP-METAMORPHISM

Morozov, M.¹, Azimov, P.², Musso, M.³, Dolivo-Dobrovolsky, D.V.², Asenbaum, A.³
& Amthauer, G.³

¹ St. Petersburg Mining Institute (Technical University), 21st line. 2, 199106 St. Petersburg, Russia

² Institute of Precambrian Geology and Geochronology, Makarov emb., 2, St. Petersburg, 199034, Russia

³ University of Salzburg, Hellbrunnerstr. 34, A-5020, Salzburg, Austria

e-mail: michael@mvm.usr.spmi.spb.ru

Raman microspectroscopy was applied to determine Al₂SiO₅ polymorphs situated in high-ALMg sapphirine-bearing metamorphic rocks from shear zones in the Central-Kola terrain (Kola Peninsula, Russia). Rocks consist predominantly of cordierite, biotite, orthopyroxene, sapphirine, spinel and sillimanite. The rocks also contain very small acicular crystals and ultra fine-grained orthopyroxene-Al₂SiO₅ intergrowths that replace cordierite and biotite. These aggregates mark a late rock alteration. Previous investigators considered the aluminosilicate as sillimanite (fibrolite). Hence, the rock alteration was interpreted as retrograde branch of the granulitic metamorphism.

Previously reported Raman spectra of Al₂SiO₅ polymorphs allow a clear identification of the mineral observed. Polarized Raman spectra were taken at room temperature from polished thin sections using the microscope-based DILOR XY Raman spectrometer equipped with 514.5 nm Ar⁺ ion laser, backscattering geometry, lateral resolution ≤12 μm, spectral resolution 1 cm⁻¹. To control the anisotropy of crystals, the spectra were registered for two crystal orientations for each measured point (the polarization plane of incident light was oriented parallel and perpendicular to the crystal elongation [001] or to the cleavage {010}). Most of the Raman band positions and intensities from the studied acicular aggregates are in full conformity with the Raman spectrum of kyanite. In some measured points up to 15 additional bands in the spectrum of acicular aggregates have been revealed. Most of them exactly correspond to the Raman spectrum of cordierite. One can conclude, Raman microprobe undoubtedly reveals the presence of kyanite both in its intergrowths with orthopyroxene and (for most long needle-shaped grains) in the surrounding rock matrix represented by early cordierite.

The kyanite-orthopyroxene paragenesis is an extremely rare one world-wide and the Central-Kola terrain is the second proved granulitic locality of it. Reaction textures and thermodynamic considerations suggest that this assemblage was prograde and formed at a new HP metamorphic event (ca. 700 °C and 8-9 kbar) which followed another HP-HT metamorphism (peak at ca. 920 °C and 9.5 kbar). Both these HP events overprinted metamorphic rocks locally within long-lived shear zones.

This work was supported by RFBR (grant № 01-05-65174), Russian Ministry of Industry and Science (grant for the support of scientific schools SS-615.2003.5), Austrian Exchange Service (ÖAD), Russian Ministry of Education (grants № PD02-1.5-361 and E02-2.0-58), Administration of St.-Petersburg (Russia) (grant № PD03-1.5-55), CRDF (grants № Y1-G-15-01 and Y1-G-15-04) and Russian Science Support Foundation.

RAMAN SPECTROSCOPY OF ROCKS IN THIN SECTIONS: ANALYTICAL CONSTRAINTS

Morozov, M.¹, Musso, M.², Asenbaum, A.² & Amthauer, G.²

¹ St. Petersburg Mining Institute (Technical University), 21st line. 2, 199106 St. Petersburg, Russia

² University of Salzburg, Hellbrunnerstr. 34, A-5020, Salzburg, Austria
e-mail: michael@mvm.usr.spmi.spb.ru

Raman spectroscopy is a well-known technique used for the fingerprinting of mineral substances. The Raman technique can be well adapted for studies of thin sections of rocks and minerals. If the Raman spectroscopic determination of minerals in thin sections is made as a routine procedure, both sample properties and individual characteristics of studied crystals constrain the resulting information. The main constraints are discussed below.

1. Constraints caused by properties of minerals and mineral aggregates.

1a. Some characteristic Raman bands of minerals reveal strong depolarization ratios. In this case the effectiveness of the Raman fingerprinting strongly depends on the spatial orientation of crystallographic axes in a grain of the studied mineral. In case of textured samples (in many metamorphic, some magmatic rocks and also vein aggregates) the Raman fingerprinting will depend on the orientation of the rock by which the thin section was produced. The effect of crystal orientation cannot be fully eliminated. It can be reduced by measuring of depolarized scattered light.

1b. The topology of the Raman spectrum can differ according to the retardation of the crystal. Birefringence causes the rotation of polarization plane of the scattered light. It is especially important for structural studies (order/disorder phenomena, phase transformations). If crystals are zoned with the variable retardation in different zones, false conclusions about the breaking of symmetry selection rules can be made. To avoid such artefacts the observation in depolarized light can be used. By the polarized exciting light the measurement with the crystal in position of optical extinction can be used.

1c. Luminescence from the studied mineral and from the surrounding matrix causes the common constraints by Raman fingerprinting. This phenomenon is well-known and will be not considered here.

2. Constraints caused by the nature of sample. Rock thin sections are mounted on glass plates using special types of organic glue (Canadian balsam etc.). The excitation area when using conventional non-confocal microscope-based Raman systems can be large enough to partially include the glue layer. It can result in strong background luminescence, heating and evaporation of glue, which makes Raman observation impossible.

The outlined analytical problems demonstrate that a careful mineralogical examination of a thin section must be made before the Raman investigation can be carried out. The microscope attached to the Raman spectrometer must be equipped with a transmitted light illumination system, rotating stage and a set of polarizers for visible light. Confocal microscope geometry is desirable. A depolarizer (i.e., $\lambda/4$ plate) for the scattered laser light is required.

This work was supported by Russian Ministry of Education grants # PD02-1.5-361 and # E02-2.0-58, Administration of St. Petersburg (Russia) grant # PD03-1.5-55 and the BRHE Program (incl. grant Y1-G-15-01).

RAMAN BAROMETRY OF MINERAL INCLUSIONS IN DIAMOND CRYSTALS

Nasdala, L.

Institut für Geowissenschaften - Mineralogie, Johannes Gutenberg-Universität, D-55099 Mainz, Germany
 e-mail: nasdala@uni-mainz.de

Inclusions of high-pressure minerals trapped inside diamond crystals may provide valuable information about the conditions under which their diamond host was formed. A “minimum value” for the pressure in the source region is determined through the estimation of fossilised pressures of inclusions. Note that the observed pressure will always be lower than the formation pressure, especially if pressure has been released partially through the formation of fractures in the diamond host (Fig. 1). Such remnant pressures can be determined *in situ* from shifts of vibrational modes. The application of this technique to an inclusion, however, requires the availability of a precise pressure-calibration of band shifts, which are for instance determined in diamond anvil experiments, for the respective phase. The remnant pressure on included minerals for which such pressure-calibration has not been done can nevertheless be estimated. Raman maps of the diamond LO=TO mode reveal not only the strain distribution in the host diamond (NASDALA et al., 2003) but can also be used to locate the diamond micro-area with the strongest compression and, with that, the highest preserved pressure.

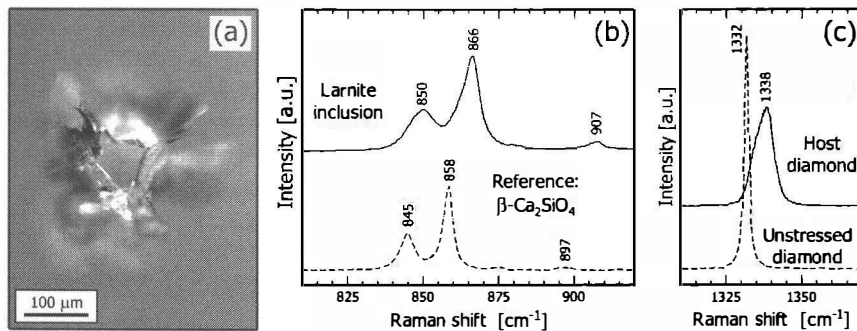


Fig. 1. The Raman spectrum of a larnite inclusion (a) inside a large diamond crystal from the Kankan district, Guinea, is shifted with respect to that of unpressurised $\beta\text{-Ca}_2\text{SiO}_4$ (b) due to significant remnant pressure acting on the inclusion. The fossilised pressure can be determined from the frequency of the LO=TO mode of the neighbouring diamond host. An up-shift of $\sim 6 \text{ cm}^{-1}$ (c) corresponds to $\sim 2.7 \text{ GPa}$ (e.g., HANFLAND et al., 1985)

References

- HANFLAND, M., SYASSEN, K., FAHY, S., LOUIE, S.G. & COHEN, M.L. (1985): Phys. Rev. B, **31**: 6896-6899.
 NASDALA, L., BRENNER, F.E., GLINNEBANN, J., HOFMEISTER, W., GASPARIK, T., HARRIS, J.W., STACHEL, T. & REESE, I. (2003): Eur. J. Mineral., **15**: 931-935.

INFRARED SPECTROSCOPY OF NATURAL AND SYNTHETIC TOBERMORITES

Pawlowski, J.¹, Fehr, K.T.¹ & Hochleitner, R.²

¹ Sektion Mineralogie, Petrologie und Geochemie, LMU München, Theresienstr. 41, 80333 München, Germany

² Mineralogische Staatssammlung München, Theresienstr. 41, 80333 München, Germany

e-mail: pawlowski@min.uni-muenchen.de

IR-spectra of natural and synthetic tobermorites show many similarities, but there are some obvious differences between natural and synthetic phases and also between the single phases (MERLINO et al., 1999; HOCHLEITNER, 2000). An important influence on the form of the spectra has the ratio calcium/silicon of each sample, but also the quality of the crystals. The ratio is mainly responsible for the position of each band and the quality is responsible for the sharpness of the bands (Fig. 1).

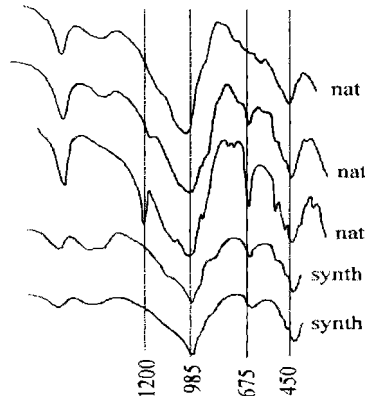


Fig. 1. IR-spectra of natural and synthetic tobermorite.
1200 = Si-O-stretching vibrations of Q^3 -places,
985 = Si-O-stretching vibrations of Q^2 -places,
675 = Si-O-Si bending vibrations,
450 = internal deformation of SiO_4 -tetrahedron

References

- HOCHLEITNER, R. (2000): In: RAMMELMAIR, D., MEDERER, J., OBERTHÜR, T., HEIMANN, R.B. & PENTINGHAUS, H. (eds.) Applied Mineralogy in Research, Economy, Technology, Ecology and Culture. A.A. Balkema, Rotterdam, 799-801.
- MERLINO, S., BONACCORSI, E. & ARMBRUSTER, N. (1999): Am. Mineral., **84**: 1613-1621.

**A POLARIZED SINGLE-CRYSTAL STUDY OF SYNTHETIC
WATER-POOR BERYL**

Piccinini, M.^{1,2}, Bellatreccia, F.¹ & Della Ventura, G.¹

¹Dipartimento Scienze Geologiche, Università di Roma Tre, Largo S. Leonardo Murialdo 1, I-00146 Roma

²INFN-LNF, Via Enrico Fermi 40, I00044 Frascati (Italy)

e-mail: massimo.piccinini@lnf.infn.it

Beryl typically contains extraframework alkali-ions, H₂O and/or CO₂ molecules in the structural channel. The water molecules occur in two different orientations: type I, having their two-fold axis perpendicular to the *c* axis of beryl, and type II, typically adjacent to alkali ions, having their two-fold symmetry axis parallel to [100] (e.g., WOOD & NASSAU, 1968). The OH-stretching IR spectra of beryl have been extensively studied (see KOLESOV & GEIGER, 2000 and references therein). However there is no general consensus on the assignment of the observed bands to structural configurations. Much confusion probably arises from the fact that most beryls contain simultaneously both types of water, and there is no knowledge on the effect of a possible interaction between them. We present here a single-crystal, polarized-light FTIR study (done on a NicPlan microscope, equipped with a MCT detector and a gold-wire polarizer) on oriented polished sections of a flux-grown emerald. Contrary to the synthesis conditions, the emerald was found to contain low amounts of type II water exclusively, possibly associated with trace alkali ions in the channels (detected by EMPA). On the (100) section, the *E*⊥*c* spectrum shows a unique sharp and intense band at 3643 cm⁻¹, while the *E*//*c* spectrum consists of two low-intensity bands at 3643 and 3587 cm⁻¹, respectively. Based on this pleochroic behavior, the 3643 cm⁻¹ band is assigned to the ν₃ antisymmetric stretching of type II water. The second, minor band at 3587 cm⁻¹ has maximum absorbance for *E*//*c*; it is assigned to the ν₁ symmetric stretching of type II water, as also suggested by the intensity ratio I₃₆₄₃ / I₃₅₈₇ close to 1:20. The polarization of the observed bands definitely indicates that type II water has its molecular axis //*c* with its H...H vector ⊥*c*. The integrated molar absorbance for beryl, never calibrated so far, has been determined from the curve of LIBOWITZKY & ROSSMAN (1997) to be ε_I at 3643 cm⁻¹ = 27126 l mol⁻¹ cm⁻². This value allows to calculate a water content of 30 ppm for our synthetic, nominally anhydrous, beryl.

References

- KOLESOV, B.A. & GEIGER, C.A. (2000): *Phys. Chem. Minerals*, **27**: 557-564.
LIBOWITZKY, E. & ROSSMAN, G.R. (1997): *Am. Mineral.* **82**: 1111-1115.
WOOD, D.L & NASSAU, K. (1967): *Am. Mineral.*, **53**: 777-800.

**PHASE-CONTROLLED PENTACENE THIN FILMS AND THEIR
CHARACTERISTICS IN ORGANIC TRANSISTORS**

Pichler, H., Haase, A., Stadlober, B., Maresch, H. & Satzinger, V

Institute of Nanostructured Materials and Photonics, Joanneum Research,
Franz-Pichler-Straße 30, 8160 Weiz, Austria
e-mail: heinz.pichler@joanneum.at

Pentacene is an organic molecule consisting of five fused aromatic rings and there are at least four known crystalline phases in pentacene thin films. By variation of different parameters such as substrate temperature and by choosing the right substrate the portion of each phase can be controlled in a defined manner.

One of the two main phases, the so called thin film phase, is of high importance in thin-film transistors, because of its high mobility, which is similar to those in amorphous silicon TFTs. The second main phase is the bulk phase and there are strong indications that the intrinsic mobility is much lower compared to the thin film phase (BOUCHOMS et al., 1999; GUNDLACH et al., 1999).

In the present work we grow and analyse polycrystalline pentacene films on different substrate materials. These films were treated either by immersion in an organic liquid or by temperature treatment to cause phase conversion between the thin film- and the bulk phase of pentacene. The films were analysed with optical microscopy, Atomic Force Microscopy and by X-ray diffraction. Based on these techniques we could observe the change of the morphology of the polycrystalline films with respect to their ratio between the phases. The characteristics of pentacene based thin film transistors were measured in dependence on the different phases.

References

- BOUCHOMS, I.P.M., SCHOONVELD, W.A., VRIJMOETH, J. & KLAPWIJK, T.M. (1999): *Synth. Mat.*, **104**: 175-178.
GUNDLACH, D.J., JACKSON, T.N., SCHLOM, D.G. & NELSON, S.F. (1999): *Appl. Phys. Letters*, **74**: 3302-3304.

INFLUENCE OF Ca-Mg SUBSTITUTION ON THE Cr³⁺ CRYSTAL FIELD PARAMETERS IN NATURAL GARNET SOLID SOLUTIONS

Platonov, A.N.¹, Langer, K.² & Matsyuk, S.S.¹

¹ Institute of Geochemistry, Mineralogy and Ore Formation, National Academy of Science of Ukraine, Prospect Palladina 34, 03680 Kiev, Ukraine

² Institute of Applied Geosciences I, Technical University of Berlin, D-10623 Berlin, Germany
e-mail: platonov@i.com.ua

Electronic absorption spectra of a series (19 samples) of natural Mg,Ca-garnets with constant amount of octahedral Cr³⁺, $^{[8]}(\text{Mg}_{1-x}\text{Ca}_x)_3^{[6]}(\text{Al}_{0.67}\text{Cr}_{0.33})_2^{[4]}\text{Si}_3\text{O}_{12}$, from deep-seated xenoliths in kimberlite pipes of Siberia and South Africa were measured and evaluated. It was established that increasing of x_{Ca} from 0.02 to 0.745 results in decreasing of: (i) $10Dq_{\text{Cr}^{3+}}$ from 17800 cm⁻¹ to 16580 cm⁻¹, (ii) β parameter, reflecting the ionicity of the Cr-O bond, from 0.714 to 0.682, and (iii) FWHM values of ν_1 and ν_2 absorption bands of Cr³⁺. The above dependences are represented by two distinct linear trends (a) ($x_{\text{Ca}} < x_{\text{Cr}}$) ($10Dq = 17845 - 2469.5 \cdot x_{\text{Ca}}$, $r = 0.992$) and (b) ($x_{\text{Ca}} > x_{\text{Cr}}$) ($10Dq = 17583.3 - 1361.1 \cdot x_{\text{Ca}}$, $r = 0.995$) with the boundary between these trends that corresponds to the composition $x_{\text{Ca}} = x_{\text{Cr}}$.

The observed character of variation of the Cr³⁺ crystal field parameters along the garnet solid solution studied reflects, most probably, different stages of the Ca and Cr³⁺ ordering in the shared X- and Y-sites of the structure, respectively. Such ordering is caused by the mechanism of the optimization of Ca and Cr³⁺ local environment (BOSENICK et al., 2000). The presence of large Cr³⁺-centered octahedra in the pyrope host structure is energetically favourable when Ca replaces Mg if Ca and Cr³⁺ are placed in adjacent (shared) X and Y sites, respectively (UNGARETTI et al., 1995).

In garnets with ratio $x_{\text{Ca}} < x_{\text{Cr}}$, two types of Cr³⁺-centers occur: (i) Cr³⁺-ions in a pure pyrope matrix, that is octahedral Cr³⁺ surrounded by six next-next-neighbour Mg atoms (Mg₆-Cr³⁺); (ii) Cr³⁺-ions in "mixed" X-cation surrounding, that is (Mg_{6-x}Ca_x)-Cr³⁺, where $\lim(x) \rightarrow 6$.

In garnets with $x_{\text{Ca}} > x_{\text{Cr}}$ ratio only Ca₆-Cr³⁺ centers ("uvarovite like" clusters) exist.

In both cases the mentioned change of Cr³⁺ crystal field parameters is caused by an increase of the Ca amount and as result of increasing Cr-O distances and their covalency. However, in the first case (trend (a)) Ca atoms replace Mg in local environment of Cr³⁺ and in the second one (trend (b)) – in the Cr-free parts of the garnet structure.

References

- BOSENICK, A., DOVE, M.T. & GEIGER, C.A. (2000): *Phys. Chem. Minerals*, **27**: 398-418.
UNGARETTI, L., LEONA, M., MERLI, M. & OBERTI, R. (1995): *Eur. J. Mineral.*, **7**: 1299-1312.

ASTEROMINERALOGY OF CIRCUMSTELLAR OXIDE DUST

Posch, T.¹, Hodouš, I.¹, Kerschbaum, F.¹, Richter, H.¹ & Mutschke, H.²

¹ Institut für Astronomie, Türkenschanzstraße 17, A-1180 Wien, Austria

² Astrophysikalisches Institut, Schillergäßchen 2-3, D-07745 Jena, Germany
e-mail: posch@astro.univie.ac.at

Within asteromineralogy – the research field dealing with the mineralogical composition of solids in space – substantial progress has been achieved during the past few years by *spectroscopic* and *microanalytic* methods (see, e.g., HENNING, 2003). In the infrared spectra of circumstellar shells and other dust-forming environments, several emission and absorption bands produced by sub-micron-sized dust particles could be identified.

While substantial efforts have been taken to detect the signatures of silicates (such as olivine), carbon and carbon compounds (such as diamond and silicon carbide) in the infrared spectra of astronomical objects, *oxides* have been more or less neglected as potential components of cosmic dust. No systematic investigation of these solids, combining astronomical and mineralogical information, has been carried out. The present contribution tries to fill this gap.

As first shown by POSCH et al. (1999), spinels can be detected in the IR spectra of circumstellar shells of red giant stars. It is noteworthy that terrestrial spinels, unless exposed to temperatures in the order of 1000 K, have different IR properties than their cosmic counterparts. By annealing experiments and subsequent FTIR spectroscopy, FABIAN et al. (2001) have been able to reproduce the emission features of the latter. We will deliver further evidence for this feature carrier identification.

Furthermore, Mg-Fe-oxides with stoichiometries close to that of wüstite are shown to be the carriers of a strong, comparatively broad emission feature located at 19.4-19.6 μm , which is observed in the spectra of red giant stars as well (POSCH et al., 2002, 2004). This mineral species is also characterized by a temperature-dependence of its IR spectra, especially at low temperatures (~ 100 K), at which the widths of the main band decreases. We show that there are both cold and warm cosmic environments in which magnesiowüstites are able to form and survive. Other potential components of circumstellar dust are titanium oxides (POSCH et al., 2003), but for their formation, no spectroscopic evidence is available as yet.

References

- FABIAN, D., POSCH, T., MUTSCHKE, H., KERSCHBAUM, F. & DORSCHNER, J. (2001): *Astron. Astrophys.*, **373**: 1125-1138.
- HENNING, T. (2003): *Asteromineralogy*. Springer, Berlin. 281 p.
- POSCH, T., KERSCHBAUM, F., FABIAN, D., MUTSCHKE, H., DORSCHNER, J., TAMANAI, A. & HENNING, T. (2003): *Astrophys. J. Suppl.*, **149**: 437-445.
- POSCH, T., KERSCHBAUM, F., MUTSCHKE, H., DORSCHNER, J. & JÄGER, C. (2002): *Astron. Astrophys.*, **393**: L7-10.
- POSCH, T., KERSCHBAUM, F., MUTSCHKE, H., FABIAN, D., DORSCHNER, J. & HRON, J. (1999): *Astron. Astrophys.*, **352**: 609-618.
- POSCH, T., MUTSCHKE, H. & ANDERSEN, A. (2004): *Astrophys. J.*, submitted.

**SITE PREFERENCE AND PARTITIONING
OF SCANDIUM IN SILICATE GARNETS**

Quartieri, S.¹, Dalconi, M.C.², Oberti, R.³, Boscherini, F.⁴, Iezzi, G.⁵ & Boiocchi, M.⁶

¹Dip. di Scienze della Terra, Salita Sperone 31, 98166 Messina S. Agata, Italy

²Dip. di Scienze della Terra, C.so Ercole I° d'Este, 44100 Ferrara, Italy

³CNR, Istituto di Geoscienze e Georisorse, via Ferrata 1, 27100 Pavia, Italy

⁴INFM and Dip. di Fisica, Viale Berti Pichat 6/2, 40127 Bologna, Italy.

⁵Dip. di Scienze della Terra, via dei Vestini 30, 66013 Chieti Scalo, Italy

⁶Centro Grandi Strumenti, Pavia, Italy

e-mail: simonaq@unimo.it

Incorporation and site preference of Sc (~ 5 %) in four synthetic garnets (Py, Py₆₀Gr₄₀, Py₂₀Gr₈₀, and Gr) along the join pyrope-grossular were investigated by a multi-disciplinary experimental–theoretical approach, which combines EMPA, SC and powder XRD, and Sc K-edge XAFS. The XAFS experiments were performed at ID26 (ESRF). The XANES spectra clearly show significant differences in the spectral features of grossular and pyrope, suggesting different local environments for Sc. This finding is supported by the results of the multi-shell fit of the EXAFS signals: Sc is incorporated into the dodecahedral X site in the pyrope-type structure, but in the octahedral Y site in the grossular-type structure. Moreover, a different site-partitioning behaviour is observed for Sc in the solid-solution terms. The first shells contributions of the Py₆₀Gr₄₀ EXAFS signal could be obtained by a weighted combination of Sc in tetrahedral (T) and X site, while the first shells fit of Py₂₀Gr₈₀ EXAFS signal could be fitted by a weighted combination of single scattering paths calculated for Sc in both Y and T site. In this last case, however, a minor partitioning of Sc also in X site cannot be ruled out. These results are fully compatible with those of the structure refinement of the end-members, which showed (i) higher site-scattering (ss) and ADP values at the X site and lower ss at T in Py; (ii) higher ss and longer mean bond lengths at Y (and T) in Gr. The site partitioning and preference of Sc in garnets is thus dramatically determined by the matrix.

**^{57}Fe MÖSSBAUER SPECTROSCOPIC INVESTIGATIONS ON THE
BROWNMILLERITE SOLID SOLUTION SERIES $\text{Ca}_2(\text{Fe}_{2-x}\text{Al}_x)\text{O}_5$**

Redhammer, G.J.^{1,2}, Tippelt, G.¹, Lottermoser, W.¹, Amthauer, G.¹ & Roth, G.²

¹ Division of Mineralogy and Material Science, Department of Geography, Geology and Mineralogy,
Hellbrunnerstr. 34, A-5020 Salzburg, Austria

² Institute of Crystallography, University of Technology Aachen (RWTH), Jägerstr. 17/19, D-52056 Aachen
e-mail: guenther.redhammer@aon.at

Brownmillerite $\text{Ca}_2\text{FeAlO}_5$ is one of the four main components of portland cement clinkers. For $\text{Ca}_2(\text{Fe}_{2-x}\text{Al}_x)\text{O}_5$, there is a complete solid solution between $\text{Ca}_2\text{Fe}_2\text{O}_5$ (mineral name srebredolskite) and $\text{Ca}_2\text{Al}_2\text{O}_5$ up to $x = 1.36$ at ambient conditions (REDHAMMER et al., 2004 and references therein). Using ceramic sintering and slow cooling of the melt, 32 different samples between $x = 0.00$ and 1.36 have been synthesized. Besides the investigation by powder and single crystal X-ray diffraction, most of the samples were investigated by ^{57}Fe Mössbauer spectra at room and elevated temperatures also.

At room temperature pure $\text{Ca}_2\text{Fe}_2\text{O}_5$ exhibits two magnetically ordered subspectra, which can be assigned to ferric iron on both the octahedral (O) and the tetrahedral (T) sites. The ratio O : T corresponds to the ideal 1 : 1 ratio. Both sites show unusual large quadrupole splittings of -1.471(5) mm/s for the tetrahedral and +1.514 mm/s the octahedral site respectively. The internal magnetic field at the probe nucleus is 42.8(1) and 50.4(1) Tesla, values typical for ferric iron. The main component V_{zz} of the electric field gradient at the octahedral site spans up an angle of 85° with the direction of the internal magnetic field, whereas it is oriented at 90° to V_{zz} at the tetrahedral site. In situ heating experiments have shown that the Néel - temperature in pure $\text{Ca}_2\text{Fe}_2\text{O}_5$ is 450°C . Exchanging ferric iron by aluminum causes an increasing complexity of the spectra. Besides one spectrum for ferric iron on (O), two subspectra for tetrahedrally coordinated ferric iron can be resolved, which only differ in the size of the internal magnetic field. Additionally, the incorporation of aluminum causes the spectra to become successively more relaxed and data evaluation becomes highly difficult. Increasing aluminum content causes the Néel temperature to decrease. For samples with $x = 1.10$ only paramagnetic two line spectra are revealed at room temperature. The Al/Fe distribution has been determined both, from the Mössbauer data and the single crystal intensity data. For low aluminum contents, they show a distinct preference of aluminum for the tetrahedral site. Above a $2/3$ filling of the tetrahedral site with aluminum, additional Al is equally distributed over both sites. Within the complete solid solution series, the quadrupole splitting for both the (O) and the (T) sites slightly increases linearly, suggesting somewhat more distorted crystallographic sites in the high aluminum containing samples.

References

REDHAMMER, G.J., TIPPELT, G., ROTH, G. & AMTHAUER, G. (2004): Am. Mineral., **89**: 405-420.

MAGNETIC ORDERING IN THE QUASI-1D COMPOUND $\text{Cu}_2\text{Fe}_2\text{Ge}_4\text{O}_{13}$ AS MONITORED BY ^{57}Fe MÖSSBAUER SPECTROSCOPY AND SQUID MAGNETOMETRY

Redhammer, G.J.^{1,2}, Tippelt, G.¹, Lottermoser, W.¹, Amthauer, G.¹ & Roth, G.²

¹ Division of Mineralogy and Material Science, Department of Geography, Geology and Mineralogy, Hellbrunnerstr. 34, A-5020 Salzburg, Austria

² Institute of Crystallography, University of Technology Aachen (RWTH), Jägerstr. 17/19, D-52056 Aachen
e-mail: guenther.redhammer@aon.at

The germanate compound $\text{Cu}_2\text{Fe}_2\text{Ge}_4\text{O}_{13}$ has been synthesized by solid state ceramic sintering techniques between 1173 K and 1423 K. The structure is isotypic with $\text{Cu}_2\text{Sc}_2\text{Ge}_4\text{O}_{13}$, described recently by REDHAMMER & ROTH (2004). The title compound is monoclinic, space group $P2_1/m$, $Z = 4$, $a = 12.134(2)$ Å, $b = 8.5153(9)$ Å, $c = 4.8795(8)$ Å, $\beta = 96.10(2)^\circ$. The structure consists of crankshaft-like chains of edge-sharing FeO_6 octahedra running parallel to the crystallographic b -axis. These chains are linked laterally by $[\text{Cu}_2\text{O}_6]^{6-}$ dimers forming a sheet of metal-oxygen-polyhedra within the a - b plane. These sheets are separated along the c -axis by $[\text{Ge}_4\text{O}_{13}]^{10-}$ clusters. Cooling to 15 K does not alter the crystallographic symmetry of $\text{Cu}_2\text{Fe}_2\text{Ge}_4\text{O}_{13}$. SQUID magnetometric measurements at an external field above 0.1 T show two events in $\chi(T)$, one at around 100 K, and one at 40 K. The first one is characterized by a broad maximum in the temperature dependence of the magnetic susceptibility χ , the second one by a change in slope. At low external magnetic fields (0.01 T), the second event is also visible as a clearly resolved peak. The question arises, which magnetic ordering phenomena can be assigned to these two events. In situ low-temperature ^{57}Fe Mössbauer spectroscopy has been used to get a deeper insight into these ordering processes. At room temperature, the spectrum consists of a single quadrupole doublet with a large quadrupole splitting. This doublet can be assigned to the strongly distorted CuO_6 octahedron. Cooling down to liquid nitrogen temperature does not alter the general appearances of the spectrum, i.e. no magnetic ordering can be detected. However, a distinct increase of the width of the resonance absorption lines is observable between 140 K and 100 K. Thus the 100 K maximum in $\chi(T)$ is assigned to low dimensional magnetic ordering within the Cu-dimers. At 40 K full magnetic 3-dimensional ordering takes place expressed by the appearance of a magnetically split ^{57}Fe Mössbauer spectrum.

References

REDHAMMER, G.J. & ROTH, G. (2004): J. Solid State Chem., in press.

ABSORPTION EFFICIENCIES OF STARDUST MINERALS

Richter, H.¹, Kerschbaum, F.¹, Mutschke, H.² & Posch, T.¹

¹ Institut für Astronomie, Türkenschanzstraße 17, A-1180 Wien, Austria

² Astrophysikalisches Institut, Schillergäßchen 2-3, D-07745 Jena, Germany
e-mail: richter@astro.univie.ac.at

Oxide and silicate minerals are not only important components of the Earth's mantle, but they form also as small solid particles ("dust grains") in the extended atmospheres of pulsating red giant stars at temperatures below 1500 K. Astronomical infrared spectroscopy, combined with measurements of "cosmic dust analogues" in the laboratory, has enabled significant progress in the identification of IR emission bands detected at wavelengths between 8 and 70 μm in the spectra of circumstellar shells. We present results of this combined laboratory and astronomical spectroscopy approach to the task of establishing a circumstellar dust mineralogy (see DORSCHNER in HENNING, 2003).

The present contribution is focused on the absorption efficiencies of astronomically relevant oxides like the TiO_2 modifications anatase (RICHTER et al., 2004) and rutile (POSCH et al., 2003) and MgAl_2O_4 (spinel) (FABIAN et al., 2001). Reflectance and transmittance measurements of these materials result in new refractive indices (n) and absorption indices (k) in the NIR (0.5 – 2.5 μm) & MIR (2.5 – 25 μm) range. The n and k values are not sufficient for the calculation of model spectra of dust enshrouded astronomical objects. Therefore, we derived absorption efficiencies (Q_{abs}) for different particle shapes (e.g. spheres) from the n and k values of different materials according to the numerical schemes compiled by BOHREN & HUFFMAN (1983). These Q_{abs} values are different from those derived from measurements of powder samples which contain grains of unknown shape and orientation. Only Q_{abs} can be compared with the spectra of circumstellar dust shells. We show the influence of grain shapes on Q_{abs} and compare spinel's and other minerals' Q_{abs} -profiles with astronomical emission bands.

On the basis of the absorption efficiencies it is also possible to calculate the temperature of the dust grains in circumstellar shells. For selected minerals, we demonstrate also the influence of the magnitude of k in the NIR on stardust radiative equilibrium temperature (RICHTER et al., 2004).

References

- BOHREN, C.F. & HUFFMAN, D.R. (1983): *Absorption and Scattering of Light by Small Particles*. John Wiley, Ney York. 530 p.
- FABIAN, D., POSCH, T., MUTSCHKE, H., KERSCHBAUM, F. & DORSCHNER, J. (2001): *Astron. Astrophys.*, **373**: 1125-1138.
- HENNING, T. (2003): *Astromineralogy*. Springer, Berlin. 281 p.
- POSCH, T., KERSCHBAUM, F., FABIAN, D., MUTSCHKE, H., DORSCHNER, J., TAMANAI, A. & HENNING, T. (2003): *Astrophys. J. Suppl.*, **149**: 437-445.
- RICHTER, H. et al. (2004): in preparation.

**APPLICATION OF RAMAN SPECTROSCOPY TO THE IDENTIFICATION OF
ASBESTOS MINERALS**

Rinaudo, C.¹, Gastaldi, D.² & Belluso, E.²

¹ Dipartimento di Scienze dell'Ambiente e della Vita - Università del Piemonte Orientale "Amedeo Avogadro"-
Piazza Ambrosoli 5-15100 Alessandria- Italy

² Dipartimento di Scienze Mineralogiche e Petrologiche- Università di Torino- Via Valperga Caluso 35- 10125
Torino- Italy
e-mail: caterina.rinaudo@unipmn.it

The techniques normally employed in the identification of asbestos phases often require lengthy sample preparation, implying a greater risk for the creation of artefacts. Raman spectroscopy, instead, is useful in determining the mineralogical phases present in fibrous minerals because it does not require sample preparation and because it allows the Raman spectrum of a mineral to be obtained by placing the specimen directly in the path of the incident beam. If an optical microscope is coupled with the spectrometer, the Raman spectrum of a small, optically selected portion of the sample can also be obtained. The potential applications of this technique are especially promising in the case of specimens composed of different mineralogical phases, as is often the case with asbestos; moreover, the technique can also be applied to different materials, such as those used in the building industry, to determine whether they contain asbestos or not. This study demonstrates that unequivocal identification of the mineral phase can be attained by analyzing the position in the Raman spectrum of the bands related to the $[\text{SiO}_4]^{4-}$ vibrational modes. A practical application of Raman spectroscopy to a synthetic cement is also presented.

SPECTROSCOPIC METHODS USED FOR STRUCTURE INVESTIGATION OF SOME NEW DIOXANE DERIVATIVES

Roiban, D.G., Gropeanu, R., Gâz, S.A. & Grosu, I.

Babeş-Bolyai University, Organic Chemistry Department (Arany Janos Str., 11, 400028, Cluj-Napoca, Romania)
e-mail: gdroiban@chem.ubbcluj.ro

New 2-aryl-5-hydroxy-1,3 dioxane derivatives were obtained by the acetalization reaction of glycerol with several aldehydes (MURZA & SAFAROV, 1987; GARDINER et al., 2002). The compounds were investigated by X-ray diffraction techniques and high-field ^1H and ^{13}C NMR spectroscopy. The assignment of the signals is based on bidimensional NMR spectra. The complex NMR spectra suggest anancomeric structures.

We succeeded to isolate adequate crystals for some of these compounds which could be analyzed using X-ray diffraction techniques. The DIAMOND diagrams (Fig. 1) revealed the chair conformation of the 1,3-dioxane rings, the equatorial or axial preference of the aromatic substituents and important intramolecular and intermolecular aromatic π stacking interactions (GROSU et al., 2003; BALOG et al., 2004).

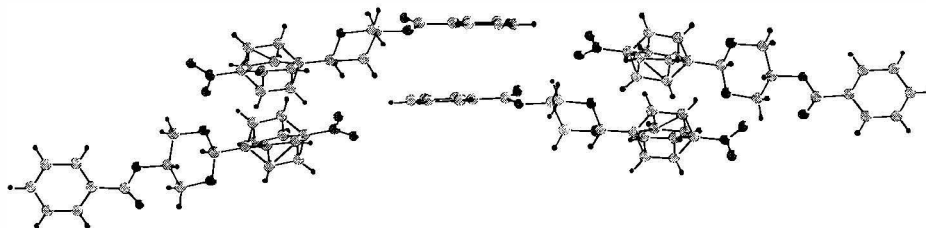


Fig. 1. DIAMOND diagram for *trans*-5-benzoiloxo-2(*p*-NO₂-phenyl)-1,3-dioxane

References

- BALOG, M., GROSU, I., PLÉ, G., RAMONDENC, Y., CONDAMINE, E. & VARGA, R. (2004): *J. Org. Chem.*, **69**: 1337.
GARDINER, J.M., MATHER, P. & PRITCHARD, R. (2002): *Tetrahedron Lett.*, **43**: 2091-2094.
GROSU, I., BOGDAN, E., PLE, G., TOUPET, L., RAMONDENC, Y., CONDAMINE, E., PEULON-AGASSE, V. & BALOG, M. (2003): *Eur. J. Org. Chem.*, **16**: 3153-3161.
MURZA, M. & SAFAROV, M. (1987): *Izvestiya Vysshikh Uchebnykh Zavedenii, Khimiya i Khimicheskaya Tekhnologiya*, **30**: 118-119.

**AB INITIO SIMULATION OF THE ELECTRONIC STRUCTURE
OF ZIRCON (ZrSiO₄) AND QUARTZ (SiO₂)**

Shchapova, J.V.¹, Votyakov, S.L.¹ & Ivanovskii, A.L.²

¹ Institute of Geology and Geochemistry UrB of RAS, Pochtovii Per. 7, 620151, Ekaterinburg, Russia

² Institute of Solid-State Chemistry UrB of RAS, Pervomaiskaya Str., 91, 620219, Ekaterinburg, Russia
e-mail: shchapova@igg.uran.ru

Zircon, ZrSiO₄, is the widespread natural mineral that usually concentrates uranium and thorium. It is characterized by an extremely high resistance to chemical and physical degradation. Recently zircon has been proposed as the prospective material for the immobilization of plutonium. For the industrial applications as waste forms, it is important to develop the microscopic model of the radiation damage of zircon including the atomic and electronic structure of metamict (amorphous) and heterogeneous (ZrSiO₄+SiO₂+ZrO₂) areas of the mineral.

Ab initio quantum-chemical cluster calculations of ZrSiO₄ electronic structure were carried out using the MO LCAO discrete-variation X_α-method. Zircon was simulated by the clusters [Si₅Zr₆O₄₄]⁴⁴⁻ and [Zr₅Si₆O₄₄]⁴⁴⁻ containing the central tetrahedron SiO₄ and the central dodecahedron ZrO₈, respectively. The comparative analysis of the electronic structure of SiO₄ tetrahedra in zircon and those in alpha-quartz has been performed on the base of the cluster models [Si₅Zr₆O₄₄]⁴⁴⁻ (for zircon) and [Si₅O₁₆]¹²⁻ (for quartz). When constructing the clusters, the following structural features of the minerals have been taken into account: (1) the isolated SiO₄ tetrahedra in ZrSiO₄ and polymerized ones in SiO₂; (2) the three-fold coordination of oxygen atoms (^{III}O) in ZrSiO₄ and two-fold coordination of oxygen atoms (^{II}O) in SiO₂; (3) the [001] edge-connected chains of Zr and Si polyhedra in zircon; (4) the nonequivalence of the connection of ZrO₈ dodecahedra in [100] and [001] directions of zircon.

For the energy spectrum of both minerals, electronic configurations, effective charges of atoms, total and deformation electron density maps have been calculated. It was shown that the energetic and spatial electron density distributions for ^{III}O and ^{II}O atoms differed noticeably. In particular, the ^{III}O_{2s}, 2p spectrum is characterized by a smaller width that may be explained as the result of increasing ionicity and decreasing of the oxygen orbitals hybridization in zircon as compared with quartz. It was supposed that the higher chemical stability of zircon was due to the peculiarities of the electronic structure of ^{III}O atoms. Using the spatial integrating of the electron density in the clusters the effective charges of atoms have been calculated. Their values were the following: Q_{Si} = 2.51 e, Q_{Zr} = 2.78-2.87 e, Q_O = -1.28 e in zircon, Q_{Si} = 2.57 e, Q_O = -1.24 e in quartz. The larger Q_{Si}-value in quartz as compared with zircon indicates the more covalent character of the Si-O bonding in the latter mineral. This is a result of increasing covalent mixing of Si3s, 3p and O2p states in isolated SiO₄ tetrahedra of zircon. It was established that the Zr-O bonding features differed in [100] and [001] directions of zircon. It was shown that the theoretical results were in the good agreement with the experimental data of optical spectroscopy and XPS.

The work was supported by RFBR, No. 04-05-96016-r, 04-05-64346.

**MgAl₂O₄-MgCr₂O₄-FeAl₂O₄-NATURAL SPINELS FROM THE URALS
ULTRAMAFITES: MÖSSBAUER STUDY, QUANTUM-CHEMICAL SIMULATION
OF THE LOCAL ATOMIC AND ELECTRONIC STRUCTURE**

Shchapova, J.V.¹, Votyakov, S.L.¹, Porotnikov, A.V.¹, Yuryeva, E.I.² & Ivanovskii, A.L.²

¹ Institute of Geology and Geochemistry UrB of RAS, Pochtovii Per. 7, 620151, Ekaterinburg, Russia

² Institute of Solid-State Chemistry UrB of RAS, Pervomaiskaya Str., 91, 620219, Ekaterinburg, Russia
e-mail: votyakov@igg.uran.ru

Crystal chemistry of MgAl₂O₄-MgCr₂O₄-FeAl₂O₄ natural spinels from the Urals ultramafites has been investigated by means of Mössbauer spectroscopy and microprobe analysis. The Urals ultramafites are represented by the main massifs of the alpine-type and dunite-clinopyroxenite-gabbro complexes. They characterize the redox state evolution of ultramafites from their formation up to the early serpentinization process. The oxidation state of the iron atoms in the minerals has been estimated and the site distributions of Fe³⁺ and Fe²⁺ ions has been analyzed. The Mössbauer parameter variations in 150 samples of the spinels have been discussed. The *ab initio* quantum-chemical cluster calculations of the short-range order structure relaxation and the electronic state spectrum for normal and partially inverse spinel solid solutions MgAl₂O₄-MgCr₂O₄-FeAl₂O₄ was carried out. The relaxed atomic positions were found by the cluster total-energy minimization within the GAMESS program; the electronic structure of relaxed clusters were analyzed by DVM program by discrete-variation X_α-method. Spinel was simulated by the cluster [^{VI}Me_{cent}^{IV}(Mg,Al)₆^{VI}(Mg,Al)₆O₃₈] containing the central octahedron ^{VI}Me_{cent}O₆ (Me_{cent} = Al, Mg, Fe, Cr) surrounded by six tetrahedra (^{IV}MgO₄ or ^{IV}AlO₄) and six octahedra (^{VI}MgO₆ or ^{VI}AlO₆). To find the total energy minimum, the coordinates of six oxygen atoms nearest to the central cation were varied. The equilibrium distances ^{VI}Me_{cent}-O were found to be 1.93 Å for Me_{cent} = Al, 2.03 Å for Mg, 2.00 Å for Fe, and 1.97 Å for Cr, that were in satisfactory agreement with structure refinement data for natural spinels. The central octahedron was shown to be trigonally distorted. The deviations from the cubic symmetry of the nearest oxygen surrounding were obtained to increase at the substitutions Al→Cr→Fe→Mg. The local values of the oxygen parameter *u* were calculated and compared with the experimental averaged values of *u*. The electronic structure and effective atomic charges were calculated both for “idealized” clusters and those with relaxed structure. The influence of relaxation effects on the changing of the spatial distribution of electronic density and integral atomic charges was considered. In particular, effective cation charges increase as the interatomic distances decrease; the ionicity of bonding between cations and the surrounding oxygen atoms increases. The theoretical results were used for evaluation of the spectroscopic parameters of the spinel solid solutions, such as electric field gradient at the iron core (or the quadrupole splitting of Mössbauer spectra) and the transition energies of the optical absorption spectra. Comparable analysis of the data obtained on the base of “idealized” and relaxed models showed that the octahedra distortions should be taken into account when interpreting spectroscopic parameters of natural spinels.

The work was supported by RFBR, No. 04-05-64346; the study was executed within the framework of the program №10 of the basic research of the Russian Academy of Science «Experimental Investigations of Physical and Chemical Problems of the Geological Processes».

MÖSSBAUER SPECTROSCOPY OF Fe-CONTAINING SULFATES

Shcherbakova, E., Nikandrova, N. & Zvonareva, G.

Institute of Mineralogy, Ural Branch of Russian Acad. Sci., Miass, 456317, Russia
e-mail: founds@ilmeny.ac.ru

Mössbauer spectroscopy has been applied to study Fe-containing sulfates of melanterite $M^{2+}[\text{SO}_4]\cdot 7\text{H}_2\text{O}$ ($M^{2+} = \text{Fe}^{2+}$, Mn, Co, Zn, Cu), halotrichite $\text{AR}_2[\text{SO}_4]_4\cdot 22\text{H}_2\text{O}$ ($A = \text{Fe}^{2+}$, Mg, Zn, Mn, Co; $R = \text{Al}$, Fe^{3+}) and copiapite $\text{AFe}^{3+}_4[\text{SO}_4]_6(\text{OH})_2\cdot 20\text{H}_2\text{O}$ ($A = \text{Fe}^{2+}$, Mg, Zn, Cu, Al, Fe^{3+}) groups from the various localities of the Ural, Russia.

Mössbauer spectra of melanterites may be considered as superposition of two doublets corresponding to Fe^{2+} . In the spectra of melanterites having compositions most close to ideal $\text{Fe}[\text{SO}_4]\cdot 7\text{H}_2\text{O}$, the doublets are characterized by nearly equal isomer shift (δ) and various quadrupole splitting (Δ); squares of both doublets are practically equal that means uniform (1:1) distribution of Fe^{2+} between both sites. Replacement of Fe^{2+} by Cu or/and Zn leads to such effects that ratios of doublet squares are changed from 1:1 to 1:2 and more, indicating irregularity of Fe^{2+} distribution between the structural sites; the values of quadrupole splitting are increased for a site with a smaller part of Fe^{2+} and decreased for a site with a high part of Fe^{2+} . The results are in excellent agreement with modern data according to those two types of Fe^{2+} octahedra, M1 and M2, existing in the structure of melanterite. Cu replacing Fe^{2+} is concentrated mainly in the M2 site (PETERSON, 2003).

As distinct from melanterites, sulfates of halotrichite and copiapite groups may contain both Fe^{2+} and Fe^{3+} . For this reason, a spectrum is complicated and interpretation is getting more difficult. Mössbauer spectra of halotrichites may be characterized by three doublets at minimum, two of those with the greater values of δ and Δ correspond to Fe^{2+} , the parameters of the doublets being close to that observed for melanterite, giving evidence for the common features in the structures of these minerals (HAWTHORNE et al., 2000). The third doublet, with lower values of δ and Δ is related to Fe^{3+} . The spectra of Fe^{2+} -free copiapites from the burnt dumps of coal mines close to ideal alumino- and magnesiocopiapite are characterized by two doublets referring to Fe^{3+} . The ratio of doublet squares is 1:1. The spectra of most occurring copiapites containing both Fe^{2+} and Fe^{3+} are supposed as superposition of three doublets, two of those as in a previous case correspond to Fe^{3+} and the third doublet is classified as Fe^{2+} .

For halotrichites and copiapites, the contents of Fe total, Fe^{2+} and Fe^{3+} have been defined by methods of wet chemistry. In addition, the contents of Fe^{2+} and Fe^{3+} have been calculated on the base of $\text{Fe}^{2+}/\text{Fe}^{3+}$ doublet squares and total content of Fe. Differences vary from 0.01 - 0.43 % for Fe^{2+} and from 0.08 - 0.50 % for Fe^{3+} . To calculate the formulae of these sulfates, Mössbauer data give the most satisfactory results.

References

- HAWTHORNE, F.C., KRIVOVICHEV, S.V. & BURNS, P.C. (2000): In: ALPERS, C.N., JAMBOR, J.L. & NORDSTROM, D.K. (eds.) *Rev. Mineral. Geochem.*, 40, Sulfate Minerals. Miner. Soc. Amer., Washington, D.C., 1-112.
PETERSON, R.C. (2003): *Can. Mineral.*, 41: 937-939.

OPTICAL STUDIES OF FLUIDS IN FIBROUS DIAMONDS

Shiryaev, A.^{1,2} & Zedgenizov, D.³

¹ Institute of crystallography RAS, Leninsky Pr. 59, 119333, Moscow, Russia

² BGI, Universitatstr. 30, D-95448, Bayreuth, Germany

³ Institute of Mineralogy and Petrology, Novosibirsk, Russia
e-mail: andrej.shiryaev@uni-bayreuth.de

Fibrous diamonds can provide unique information about fluids from upper mantle and contribute to our understanding of diamond growth conditions. In the course of this study we applied several complementary local techniques for a comprehensive study of microinclusion chemistry and phase composition as well as distribution of carbon and nitrogen isotopes within samples cross section. This approach permitted to monitor the evolution and changes of fluids and isotopes during different growth steps. In this presentation we will discuss results of microscopic IR measurements performed on these samples. Similarly to previous investigations of fibrous diamonds (e.g., CHARETTE, 1966; CHRENKO et al., 1967; GALIMOV et al., 1979) we observe numerous infra-red (IR) absorption bands due to microinclusions. It is interesting to note that the mineral species in fibrous diamonds from different world deposits (Africa, Canada, Yakutia, Brasil) are broadly similar: Phosphates (e.g., apatite), carbonates (probably ankerite), and silicates are among the most common minerals. Shift of quartz and CO₂ absorption bands indicates that the inclusions are under confining pressure in the range 1.5-2.5 GPa. A common feature for IR spectra of many fibrous diamonds is the absorption ascribed to silicate melt phase (around 1000 and 1100 cm⁻¹).

In some stones point-by-point spectroscopic investigations (Fig. 1) clearly indicate some compositional evolution of growth medium, which is often supported by chemical and isotopic analysis. It is notable that in some cases the evolution could be observed even within single growth zone as revealed by CL.

A remarkable feature of fibrous diamonds is that microinclusions also contain different water solutions and CO₂. In many spectra several lines in the region of OH valence vibrations are observed, indicating that minerals in inclusions contain OH groups. Possibly some of the observed lines are related to OH-groups in talc and/or serpentine. IR measurements at different temperatures will be reported. This work will give more reliable information about chemical and phase composition of microinclusions.

This work was partially supported by AvH (A. Shiryaev).

References

- CHARETTE, J.J. (1966): *Ind. Diam. Rev.*, **305**: 144-148.
CHRENKO, R.M., MCDONALD, R.S. & DARROW, K.A. (1967): *Nature*, **214**: 474-476.
GALIMOV, E.M., KLYUEV, Y.A. & IVANOVSKAYA, I.N. (1979): *Doklady Acad. Sci.*, **249**: 958-962.

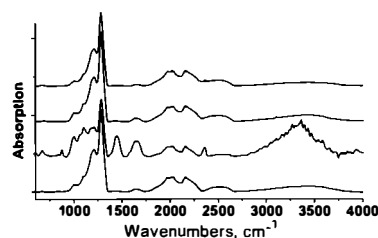


Fig. 1. IR spectra of fibrous diamonds

**COMPARING THE STRUCTURE OF LITHIUM CONTAINING
GERMANATE AND SILICATE GLASSES**

Soltay, L.G. & Henderson, G.S.

Department of Geology, University of Toronto, 22 Russell Street, M5S 3B1, Toronto, Ontario, Canada
e-mail: leonie.soltay@utoronto.ca

The addition of alkali cations to silicate melts and glasses results in the depolymerisation of the silicate network, and formation of non-bridging oxygens (NBOs). The size of the alkali cation has recently been observed to influence the distribution of Q species (Q^3 , Q^2) that exist within silicate glasses. In particular, lithium-containing glasses have higher Q^2/Q^3 ratios than equivalent Na or K containing glasses. However, this Q species dependence on alkali size appears to be different for germanate melts and glasses. We are currently investigating the Q species distribution between lithium containing silicates and germanate glasses. Silicate and germanate glasses containing from 5 to 30 mol% Li_2O have been prepared and examined using Si *K*-edge XANES/EXAFS, Si *L*-edge XANES, Raman spectroscopy, ^{29}Si NMR and 7Li NMR. Our studies have revealed that lithium-containing germanate glasses appear to have a lower Q^2/Q^3 ratio than the equivalent Na- and K-containing compositions. Furthermore, with the addition of lithium, the Q^2/Q^3 ratio increases for silicate glasses, but decreases for germanate glasses. The lithium containing germanate glasses also appear to have greater amounts of Q^2 relative to Q^3 species, than comparable lithium-containing silicate glasses.

MINERALOGY AND CHEMISTRY OF SOME GLAUCONITES FROM POLISH FLYSCH CARPATHIANS DETERMINED BY INFRARED SPECTROSCOPY, SEM-EDS ANALYSES AND X-RAY DIFFRACTION

Starzec, K.¹ & Pop, D.²

¹ Institute of Geological Sciences, Jagiellonian University, Oleandry 2a St., 30-063 Krakow, Poland

² Babeş-Bolyai University, 1 Kogălniceanu St., 400084 Cluj-Napoca, Romania
e-mail: star@geos.ing.uj.edu.pl

Four samples of glauconites from flysch deposits of the Polish Outer Carpathians were studied for characterization of their most significant mineralogical and chemical features. Samples were collected from two cross-sections (near Ropica and Folsz) which are situated in the marginal, northern part of the Magura Nappe (Siary subunit). Glauconite host-rocks are sandstones of the Magura Beds, Lower Oligocene in age.

The glauconitic grains were separated using the following methods: glauconite-bearing rocks were disaggregated, submitted to magnetic separation, acetic acid treatment, purification by ultrasonic cleaning, and finally handpicking. The main properties (morphology, mineralogy and chemistry) of the green grains were studied by applying: optical microscopy, scanning electron microscopy (SEM-EDS), X-ray diffraction and IR spectroscopy.

The polycrystalline glauconitic grains occur mainly in the 50 µm – 500 µm size range. They are dark-green in colour and exhibit considerable variety in morphology. Most frequent morphological types are (according to TRIPLEHORN, 1966): spheroidal-ovoidal with smooth surface; tabular-discoidal; irregular shapes are also observed. XRD analyses of the oriented powder samples display the characteristic (001), (003), (112), (112) peaks of glauconitic minerals (ODIN & MATTER, 1981). The chemical data of the grains such as high K₂O content (average 7 to 8 wt%) and Fe₂O₃ content (up to 19 wt%) confirm their glauconitic nature. The mineralogical and the chemical evidences indicate that glauconitic grains of each sample reflect the evolved (or even highly evolved) stage of glauconitization.

The IR spectra were interpreted from a qualitative point of view, based on the data published by WIEWIÓRA & ŁACKA (1980). All the bands characteristic for the glauconitic minerals can be observed. The major Si–O_{basal} (990-1025 cm⁻¹) bands are shifted towards lower wavenumbers which indicates a low amount of expanding layers in the glauconitic minerals. Also the two distinct Si–O bands in the region between 990-1100 cm⁻¹ are clearly divided. In the region between 450-465 cm⁻¹ the bands of the samples containing more aluminium are shifted towards higher wavenumbers as compared with high-iron samples; all the samples have bands at around 3500 cm⁻¹ which indicate that they represent Fe-glauconites.

The IR spectra confirm the chemical and mineralogical data that the studied material represents the last stages of glauconitic evolution. In general, the differences between samples are not significant and they represent similar types from the point of view of maturity, morphology and crystal chemistry.

References

- ODIN, G.S. & MATTER, A. (1981): *Sedimentology*, **28**: 611-641.
TRIPLEHORN, D.M. (1966): *Sedimentology*, **6**: 247-266.
WIEWIÓRA, A. & ŁACKA, B. (1980): *Arhiwum Mineral.*, **35**: 57-86.

**ELECTRONIC ABSORPTION SPECTROSCOPY OF NATURAL
(Fe²⁺, Fe³⁺)-BEARING SPINELS OF MAGNESIO-SPINEL-HERCYNITE AND
GAHNITE-HERCYNITE SOLID SOLUTIONS AT DIFFERENT TEMPERATURES
AND HIGH PRESSURES**

Taran, M.N.¹, Koch-Müller, M.² & Langer, K.³

¹ Institute of Geochemistry, Mineralogy and Ore Formation, National Academy of Science of Ukraine, Palladin Ave., 34, 03680 Kyiv-142, Ukraine

² GeoForschungsZentrum, Sektion 4.1, Telegrafenberg, 14473 Potsdam, Germany

³ Institute of Applied Geosciences, Technical University of Berlin, D-10623 Berlin, Germany
e-mail: taran@mineral.freenet.kiev.ua

Natural Fe²⁺, Fe³⁺-bearing spinel solid solutions from the magnesiospinel-hercynite and gahnite-hercynite series were analyzed and studied by electronic absorption spectroscopy in the spectral range 30000-3500 cm⁻¹ in the temperature and pressure ranges 77 ≤ T_K ≤ 600 and 10⁻⁴ ≤ P_{GPa} ≤ 11.0. Two crystals were light-violet in color (type I) and six green or bluish-green (type II). The spectra of both types of spinel are dominated by an UV-absorption edge near 28000 to 24000 cm⁻¹, depending on the iron contents, and a very intense band system in the NIR centered around 5000 cm⁻¹, which is caused by spin-allowed *dd*-transition of tetrahedral Fe²⁺, derived from ⁵E → ⁵T₂. The strong band is split into four sub-bands, which can only be observed in very thin platelets. Between the UV-edge and the high-energy wing of the NIR-band there occur a number of very weak bands in type I spinels while the green type II spinels show some of these with significantly enhanced intensity. The intensity of the very weak bands is nearly independent on temperature. Such bands are attributed to spin-forbidden electronic transitions of ^{IV}Fe²⁺. Temperature and pressure dependence of the intensity enhanced bands of spinels type II indicate that they are caused by ^{IV}Fe²⁺ and ^{VI}Fe³⁺. By temperature and pressure behaviors they are attributed to spin-forbidden transitions ⁶A_{1g} → ⁴A_{1g}, ⁴E_g → ⁴T_{2g} and → ⁴T_{1g} of ^{VI}Fe³⁺, the two latter being strongly intensified by exchange-coupling interaction with adjacent ^{IV}Fe²⁺. The pressure dependence of ^{IV}Fe²⁺ *dd*-band system in the NIR caused by spin-allowed ⁵E → ⁵T₂ transition noticeably differs from that of octahedral Fe²⁺, an effect which is attributed to a dynamic Jahn-Teller effect of ^{IV}Fe²⁺ in the spinel structure. In difference to ^{VI}Fe²⁺ in many oxygen-based minerals, the splitting of the spin-allowed bands derived from ⁵E → ⁵T₂ transition of ^{IV}Fe²⁺ in spinels does not decrease with pressure. On the contrary, it markedly increases showing that values of vibronic coupling coefficients of ^{IV}Fe²⁺ are rising. Also, the values of tetrahedral moduli of Fe²⁺ in spinel, evaluated from high-pressure spectra and X-ray diffraction structural refinements, are significantly different that again may be caused by a dynamic Jahn-Teller effect of ^{IV}Fe²⁺ in the spinel structure.

**RAMAN SPECTROSCOPY ON GEM-QUALITY MICROCRYSTALLINE
AND AMORPHOUS SILICA VARIETIES FROM ROMANIA**

Tătar, S.-D.¹, Constantina, C.², Pop, D.² & Kiefer, W.¹

¹ Institut für Physikalische Chemie, Am Hubland, 97074, Würzburg, Germany

² Babeş-Bolyai University, 1 Kogălniceanu St., 400084 Cluj-Napoca, Romania
e-mail: dantatar@yahoo.com

Raman spectroscopy is used as a powerful tool for mineral phase identification in geological samples, and for characterizing the crystal chemistry of heterogeneous materials. A special case is represented by mineral polymorphs, such as the SiO₂ phases. On the basis of optical microscopy, microcrystalline silica (low- or α -quartz) has been usually reported as “chalcedony”, “jasper”, “chert”, or “flint”. Previous micro-Raman investigations (KINGMA & HEMLEY, 1994) have evidenced the presence of a new tetrahedrally coordinated silica polymorph, *i.e.* moganite in virtually every studied microcrystalline silica sample.

In order to test the ubiquity of moganite in such geological materials, and for checking if a relationship between the colour/textural variations *vs.* the presence of specific polymorphs could be established, micro-Raman measurements were performed on gem-quality microcrystalline and amorphous silica varieties from several Romanian occurrences. The best studied occurrence was Gurasada (Apuseni Mts.), due to the remarkable diversity of SiO₂ varieties found in Paleocene („banatic“) pyroclastic agglomerates and tuffs: chalcedony (including agate), jasper, opal, silicified wood. Most of the samples show macroscopic and/or microscopic variations in colour (grey-red-blue-white), transparency or texture (from massive to banded). Other studied occurrences from the Apuseni Mts. were Rachiş and Techereu (both of “ophiolitic” pyroclastic origin), but also famous sites from Baia Mare area (Trestia and Oraşu Nou - related to the Neogene volcanism) were included for comparison.

The measurements were performed on a Dilor Labram system equipped with an Olympus LMPlan Fl 50 microscope objective, an 1800 lines/mm grating and an external laser with an emission wavelength of 514 nm, and additionally 632 nm. In the recording of the micro-Raman spectra a power of 100 mW on the sample has been employed. The focal length of the spectrometer is 300 mm and the slit used for all measurements was 100 μ m. Thus, the spectral resolution was about 4 cm^{-1} .

The Raman spectra show the presence of low-quartz in all the microcrystalline silica varieties (chalcedony, agate, jasper), but also in some areas of the studied opals. The shoulder of the 465 cm^{-1} quartz band which is noticeable at values around 500 cm^{-1} is interpreted as an evidence of an intergrowth with moganite (KINGMA & HEMLEY, 1994), thus present in small amounts in most of the studied samples (including opal). The pattern of the coloured areas could not be correlated to the presence of a specific silica polymorph; however, in some cases certain non-silica phases (such as calcite, or organic carbon sp²-containing phases) may be responsible for the observed colour and/or transparency variations.

References

KINGMA, K.J. & HEMLEY, R. (1994): *Am. Mineral.*, **79**: 269-273.

**LOCAL STRUCTURAL STATE OF ZIRCON FROM METAGRANITES –
A RAMAN SPECTROSCOPIC STUDY**

Titorenkova, R. & Mihailova, B.

Central Laboratory of Mineralogy and Crystallography, Bulgarian Academy of Sciences, Acad. G. Bonchev
Street 107, 1113 Sofia, Bulgaria
e-mail: rositorenkova@dir.bg

Zircon from amphibolite facies metagranites (Ograzhden Mountain, Serbo-Macedonian massif, Bulgaria) exhibits complex internal structures visible in cathodoluminescence (CL) and backscattered electrons (BSE) microscope images. Different processes, such as metamictization, annealing, diffusion and recrystallization, cause alteration of the protolith, magmatic zonation and form secondary internal features. The determination of the process governing the formation of a particular internal area is of a great importance for geochronological reconstructions. We have applied Raman spectroscopy, CL and electron microprobe to analyze the correlation between the local structural peculiarities and the radioactive element content of natural inhomogeneous zircon. The Raman spectroscopic data reveal different degree of structural disorder that can be estimated by the following spectral features: a) the position and the width of the peak near 1008 cm^{-1} , generated by the $\nu_3(\text{SiO}_4)$, which is sensitive to point defects and distribution in the Si-O bond lengths; b) the relative intensity of the same peak, indicating disruption of the translation symmetry in the zircon lattice; c) additional Raman signals between 150 and 650 cm^{-1} indicating a formation of ZrO_2 phases as a consequence of the zircon structure damage on nanometric scale; d) existence of a halo between 1000 - 1200 cm^{-1} , due to diffuse light scattering from dislocations and related defects resulting from the accumulations of point defects such as vacancies and broken Si-O-Zr linkages; e) additional well-pronounced peaks in the range 1100 - 1250 cm^{-1} that do not depend on the excitation light wavelength, pointing to occurrence of chain-like clusters of linked SiO_4 tetrahedra. Zircon separated from equigranular metagranites exhibits three types of spatial regions: poorly damaged zircon, for which the structural alteration consists mainly in short-range disorder of SiO_4 ; moderately damaged zircon, characterized by faults in the long range order and presence of polymerised SiO_4 tetrahedra; heavily damaged zircon, exhibiting a high degree of long- and medium-range disorder and formation of zirconia polymorphs. The studied zircon samples separated from porphyritic metagranites exhibit incipient recrystallization with presence of nuclei that enlarge upon laser-induced heating. The spectroscopic data show that the width of the peaks at 357 and 439 cm^{-1} , originating from SiO_4 rotation and bending mode, respectively, can be used for estimating the degree of metamictization of zircon.

OPTICAL AND SPECTROSCOPIC PROPERTIES OF SELF-ASSEMBLED NANOPARTICLES

Toderaş, F., Farcău, C.A. & Aştilean, S.

Babeş-Bolyai University, Faculty of Physics (Kogălniceanu Str., 1, 400084, Cluj-Napoca, Romania)
e-mail: ftoderaş@phys.ubbcluj.ro; c_farcău@yahoo.com

In recent years, there has been an increasing interest in the synthesis of nanostructures (LIU et al., 2003) due to their various potential applications such as optoelectronic (SHIPWAY et al., 2000), microelectronic (LYNCH et al., 1997), and bio-moleculars (GRABAR et al., 1995). Fabrication of nanostructures by self-assembled methods has attracted much attention due to their simplicity and flexibility (WANG et al., 1998). A method for control of surface morphology (KEATING et al., 1998; FREEMAN et al., 1995; XIA et al., 2000) is through assembly of small, spherical, uniformly sized particles at an interface, imparting a repeating feature size that is dependent upon the particles used. In the present work gold colloids were prepared and self-assembled onto glass substrates by using an organic coupling agent as 3-aminopropyltrimethoxysilane (APTMS). Moreover, polystyrene beads were also assembled in a regular hexagonal lattice on hydrophilic glass slides surfaces. The substrates were characterized by transmission electron microscopy (TEM) and optical absorption spectroscopy (Fig. 1). The optical absorption spectra show a well defined surface plasmon resonance peak at 520 nm for the self-assembled gold monolayers and at 632 nm for the gold coated polystyrene nanospheres. The as prepared substrates are under current investigation for applications in the field of surface plasmon resonance (SPR), optical biosensing as well as in surface-enhanced Raman spectroscopy (SERS) studies.

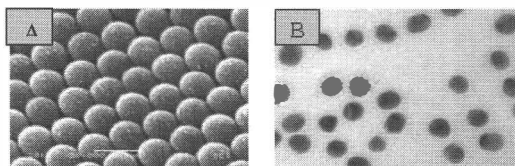


*Fig. 1. TEM images of self-assembled nanoparticles:
(A) polystyrene nanospheres
(B) gold colloids*

References

- FREEMAN, R.G., GRABAR, K.C., ALISON, K.J., BRIGHT, R.M., DAVIS, J.A., GUTHRIE, A.P., HOMMER, M.B., JACKSON, M.A., SMITH, P.C., WALTER, D.G. & NATAN, M.J. (1995): *Science*, **267**: 1629-1632.
- GRABAR, K.C., FREEMAN, R.G., HOMMER, M.B. & NATAN, M.J. (1995): *Anal. Chem.*, **67**: 7359-7364.
- KEATING, C.D., MUSICK, M.D., KEEFE, M.H. & NATAN, M.J. (1999): *J. Chem. Educ.*, **76**: 949-956.
- LIU, F.K., CHANG, Y.C., KO, F.H., CHU, T.C. & DAI, B.T. (2003): *Microelectr. Engineering*, **67-68**: 702-709.
- LYNCH, J.E., PEHRSSON, P.E., LEONARD, D.N. & CALVERT, J.M. (1997): *J. Electrochem. Soc.*, **144**: 1698-1704.
- SHIPWAY, A.N., KATZ, E. & WILLNER, I. (2000): *Chem. Phys. Chem.*, **1**: 18-52.
- WANG, J., ZHU, T., SONG, J. & LIU, Z. (1998): *Thin Solid Film*, **327**: 591-594.
- XIA, Y., GATES, B., YIN, Y. & LU, Y. (2000): *Adv. Mater.*, **12**: 693-713.

GRADUAL RECRYSTALLISATION OF METAMICT FERGUSONITE: X-RAY DIFFRACTION AND RAMAN SPECTROSCOPY STUDY

Tomašić, N.¹, Gajović, A.² & Bernanec, V.¹

¹ University of Zagreb, Institute of Mineralogy and Petrography, Horvatovac bb, HR-10000 Zagreb, Croatia

² Ruđer Bošković Institute, POB 180, 10002 Zagreb, Croatia

e-mail: ntomasic@jagor.srce.hr

Fergusonite mineral samples, mainly represented as YNbO_4 , are frequently metamict. Heating experiments induce crystal structure recovery, but also cause phase transition processes, since fergusonite is a polymorphic substance (WOLTEN & CHASE, 1967).

X-ray powder diffraction and Raman spectroscopy were employed to monitor the sequences of fergusonite recrystallisation. The corresponding Raman spectra were also used to reveal possible presence of original structure remnants in the metamict mineral. Two metamict mineral samples previously identified as fergusonite were heated in air at 400, 500, 650, 800, 1000 and 1300 °C for 24 hours in each case.

The mineral sample from Bakkane-Steane, Norway, was completely amorphous to X-rays and started to recrystallise at 400 °C with scheelite type structure (space group $I4_1/a$) being stable up to 1000 °C. At 1000 °C monoclinic (space group $I2$) β -fergusonite dominated, with the tetragonal phase still present. At 1300 °C the transformation from tetragonal to monoclinic fergusonite was completed. Raman spectra confirmed the gradual fergusonite recrystallisation by sharpening and intensifying of vibrational bands. The number of bands increased with the lowering of the symmetry. For the metamict mineral the vibrational bands at 779, 685, 697, 310, 208 and 108 cm^{-1} were present indicating the residue of the original crystal structure. At lower heating temperatures the bands were broad, but at higher temperatures reappeared more sharpened, resolved and intensified. The second mineral sample, originating from Ytterby, Sweden, was almost completely metamict, with only a few low-intensity diffraction lines superimposed on the characteristic amorphous diffraction peak. At 400 °C pyrochlore phase started to recrystallise, being continuously present through the whole temperature range. At 1000 °C the monoclinic β -fergusonite appeared with recrystallisation completed at 1300 °C. Raman bands were similar to those of fergusonite from Bakkane-Steane, although some of them had different intensities and were slightly shifted. Vibration bands were not present in the spectrum of the unheated metamict mineral.

The vibrational spectra of the complex oxide structures are difficult to calculate, but a relation to the analogous synthetic compounds (YASHIMA et al., 1997) could be established. McCONNELL et al. (1976) indicate that LO and TO Nb-O stretching modes of niobium oxides appear in the range 1010-620 cm^{-1} . Therefore, the observed lattice vibrations reveal partial preservation of Nb-O polyhedra stacking in metamict fergusonite from Bakkane-Steane.

References

- McCONNELL, A.A., ANDERSON, J.S. & RAO, C.N.R. (1976): Spectrochim. Acta A, **32**: 1067-1076.
WOLTEN, G.M. & CHASE, A.B. (1967): Am. Mineral., **52**: 1536-1541.
YASHIMA, M., LEE, J.H., KAKIHANA, M. & YOSHIMURA, M. (1997): J. Phys. Chem. Solids, **58**: 1593-1597.

A MUON SPIN ROTATION INVESTIGATION OF THE MAGNETIC STRUCTURE OF CeRh₂Si₂

Văju, C., Miron, M. & Andreica, D.

Babeş Bolyai University, Faculty of Physics (Kogălniceanu Str., 1, 400084, Cluj Napoca, Romania)
e-mail: cvaju@yahoo.com; im_miron@yahoo.com

The muon spin rotation (μ SR) technique makes use of a short-lived subatomic particle called muon, a spin-1/2 particle. Spin polarized muon beams can be prepared and subsequently implanted in various types of matter. The muons precess around the local magnetic field and then disintegrate preferentially in the direction pointed by their spins. Therefore muons can be used to investigate a variety of static and dynamic magnetic effects and hence to deduce properties concerning magnetism, superconductivity and molecular dynamics. The use of muons in condensed matter physics has shed new light on subjects as diverse as passivation in semiconductors, frustrated spin systems, vortex lattice melting, phase separation and phase coexistence in magnetic materials.

In general, μ SR gives information that is complementary to that provided by other well-recognized techniques such as neutron scattering, ESR and NMR. The μ SR technique has a unique time window for the study of magnetic fluctuations in materials that is complementary to other experimental techniques like those mentioned above.

We have used the muon spin rotation (μ SR) method to investigate the magnetic properties of CeRh₂Si₂. CeRh₂Si₂ crystallizes in a body-centred tetragonal structure of ThCr₂Si₂ type (space group *I4/mmm*). It is an antiferromagnet with two magnetic transitions, at 36 K (T_{N1}) and 25 K (T_{N2}). The magnetic structure of CeRh₂Si₂ below T_{N2} is still ambiguous. From neutron diffraction experiments done by GRIER et al. (1984) and KAWARAZAKI et al. (1995), the magnetic structure is a modulated structure described by two k vectors, $k1$ and $k2$, which reflect either a multidomain structure or a multi-q structure. KAWARAZAKI et al. (2000), from another neutron diffraction experiment reported a $4-k$ structure. We have performed μ SR experiments to confirm/deny the proposed magnetic structures. Below T_{N2} we observed a slowly depolarized oscillating component superposed over two Kubo Lorentz depolarisation functions. This indicates that there are several magnetically inequivalent muon-stopping sites. The $4-k$ structure predicts two magnetic inequivalent sites, one with zero field and one with finite magnetic field which should be detected in a μ SR experiment as a flat component and an oscillating one respectively. By performing computer simulations we have tried to associate the depolarisation functions with imperfections of the magnetic ($4-k$) structure: tilted magnetic moments, missing magnetic ions, but this explains only partially the depolarisation rates observed in the μ SR experiments.

References

- GRIER B.H., LAWRENCE, J.M., MURGAI, V. & PARKS, R.D. (1984): Phys. Rev. B, **29**: 2664-2672.
KAWARAZAKI, S., KOBASHI, Y., FERNANDEZ-BACA, J.A., MURAYAMA, S., ONUKI, Y. & MIYAKO, Y. (1995): Physica B, **206-207**: 298-232.
KAWARAZAKI, S., SATO, M., MIYAKO, Y., CHIGUSA N., WATANABE, K., METOKI, N., KOIKE, Y. & NISHI, M. (2000): Phys. Rev. B, **61**: 4167-4173.

TEMPERATURE DEPENDENCE OF THE Fe^{2+} MÖSSBAUER PARAMETERS IN TRIPHYLITE (LiFePO_4)

Van Alboom, A.¹, De Grave, E.² & Wohlfahrt-Mehrens, M.³

¹ Department of Industrial Sciences BME-CTL, Highschool Ghent,
Schoonmeersstraat 52, B-9000, Gent, Belgium

² Department of Subatomic and Radiation Physics, University of Ghent,
Proeftuinstraat 86, B-9000, Gent, Belgium

³ Center for Solar Energy and Hydrogen Research, Baden-Württemberg Division 3,
Helmholtzstraße 8, D89081, Ulm, Germany
e-mail: toon.vanalboom@hogent.be

Triphylite (LiFePO_4) has an olivine type structure (Pnma) and has received much attention because of its application as possible electrode active material for lithium rechargeable batteries.

In this work, the temperature dependence of the Mössbauer parameters of Fe^{2+} in synthetic triphylite (ARNOLD et al., 2003) is determined between 4 K and room temperature. From the Mössbauer measurements a sharp magnetic ordering transition is observed at 53 K, which is in line with the Néel temperature as is determined by neutron diffraction (ROUSSE, 2003). The Mössbauer spectra in the paramagnetic region are well fitted by one Fe^{2+} quadrupole doublet with small linewidth. The spectra in the magnetic region are typical for Fe^{2+} , showing the maximum of eight absorption lines. They are analysed using the diagonalization of the full nuclear-interaction Hamiltonian and could be successfully fitted with a model independent distribution of hyperfine fields.

The hyperfine field is always collinear to the local principal axis of the electric field gradient tensor. The asymmetry parameter is about 0.79 and the quadrupole coupling constant is 2.79 mm/s, which is perfect in line with the quadrupole splitting $\Delta E_Q = 3.06$ mm/s at 80 K in the paramagnetic region.

The temperature dependence of the quadrupole splitting is interpreted within the ^5D orbital energy level scheme of Fe^{2+} by a crystal field calculation (VAN ALBOOM et al., 1993) based on the point symmetry of the Fe^{2+} site in triphylite (ANDERSON et al., 2000).

When triphylite is used as electrode material in lithium rechargeable batteries, there is a conversion of triphylite in its delithiated form FePO_4 (heterosite) and vice versa during the charge/discharge process. The characteristic Mössbauer temperature is an important parameter in order to determine accurate ratios of both compounds during the process (ANDERSON et al., 2000). From the temperature dependence of the isomer shift its value is determined to 390 K for Fe^{2+} in triphylite. The intrinsic isomershift is 1.45 mm/s.

References

- ANDERSON, A.S., KALSKA, B., HÄGGSTRÖM, L. & THOMAS, J.O. (2000): *Sol. St. Ion.*, **130**: 41-52.
ARNOLD, G., GANCHE, J., HEMMER, R., STROBELE, S., VOGLER, C. & WOHLFAHRT-MEHRENS, A. (2003): *J. Power Sources*, **119**: 247-251.
ROUSSE, G. (2003): *Chem. Mater.*, **15**: 4082-4090.
VAN ALBOOM, A., DE GRAVE, E. & VANDENBERGHE, R.E. (1993): *Phys. Chem. Minerals*, **20**: 263-275.

LUCIA, A MICROFOCUS SOFT XAS BEAMLINE

Vantelon, D.¹, Bac, S.², Cauchon, G.², Dubuisson, J.-M.¹, Idir, M.¹, Flank, A.-M.², Janousch, M.³, Lagarde, P.² & Wetter, R.³

¹SOLEIL, L'Orne des Merisiers, Saint Aubin, BP 48, F-91192 GIF S/Yvette Cedex

²LURE, Bât. 209D, Centre Universitaire, BP 34, F-91898 Orsay Cedex

³Paul Scherrer Institut, SLS, Villigen-PSI, CH 5232

e-mail: delphine.vantelon@psi.ch

The microfocus X-ray beamline LUCIA (Line for Ultimate Characterization by Imagery and Absorption) is devoted to microspectroscopy in the 1-8 keV energy range. The energy domain covers the K edges of low Z elements (from sodium to iron), the L edges from nickel to gadolinium, and the M edges of lanthanides and actinides. Thus, at the same time, it gives an unique access to the major elements constituting minerals (low Z elements) and it is also of importance in geosciences as well as in environmental sciences for which the energy range covers metals and other heavy pollutants. The goal of the beamline is to achieve a spot size on the sample of the order of $1 \times 1 \mu\text{m}^2$, while allowing energy scans on the entire range. Structural investigations of spatially complex systems will be therefore considered with various applications, including archeometry, Earth and extraterrestrial sciences or environmental science. This latest topic contains typical examples for which such *in situ* spatial investigations are particularly powerful. Indeed, it is now well known that toxicity and bioavailability of many compounds depends not only on their nature and bulk concentration but much more on their spatial distribution and chemical speciation.

Born from a collaboration between LURE, SOLEIL and PSI, this beamline installed on the Swiss Light Source is now in its commissioning phase. An Apple II insertion device has been installed (SCHMIDT et al., 2003) during the summer 2003. This undulator (54mm period length) provides X-rays in an energy range which corresponds to the best performances in term of brilliance of both machines, SLS and SOLEIL. This device emits linear light with variable polarization direction as well as circular polarized light. The period length was set such that no 'energy gap' appears between the harmonics in the 1-8 keV energy range. The horizontal photon source size is demagnified by a fixed spherical mirror. Two plane mirrors reject the higher harmonics contributions. The final focusing is accomplished through a Kirkpatrick-Baez (KB) mirror system aligned automatically (IDIR et al., 2003). A fixed exit double-crystal monochromator is equipped with five different types of crystals to cover the full energy domain. A motorized (xyz) stage allows the precise positioning and mapping of the sample. XAS measurements can be done by measuring the transmitted beam, the total electron yield or the fluorescence yield. For micro-XRF cartography, a single-element silicon drift detector is used.

Proposals can be submitted to the SLS Users Office. The next program committee is in September for beamtime allocation starting in December.

References

IDIR, M. et al. (2003): AIP conference proceedings: Eight International Conference on Synchrotron Radiation Instrumentation, San Francisco.

SCHMIDT, T. et al. (2003): PSI Scientific Report Volume VII.

WHITE MICA FROM THE BRNJICA GRANITOIDS (EASTERN SERBIA)

Vaskovic, N. & Eric, S.

Faculty of Mining and Geology, Djusina 7, 11000 Belgrade, Yugoslavia

e-mail: nadavask@eunet.yu.

Granitoids of East Serbia, associated with the Carpathian-Balkan arc, form a NNW-SSE elongated zone of about 200 km in length. It starts from the river Danube to the north and extends up to the southern slopes of Mt. Stara Planina, at the Yugoslavian-Bulgarian border. These granitoids were studied by numerous researchers from the end of 19th century till 1970, but many features related to mineralogy (i.e. mineral chemistry) are still unsolved. The magmatic activity in the above mentioned area was very intensive during Carboniferous and Permian time (259 to 342 Ma). In this paper we present new mineralogical data and chemistry of white mica and an attempt is made to investigate its origin in the Brnjica Granitoids (BG), located in the Danube Gorge. The BG (272-259 Ma - Rb/Sr) occurs in the Kucaj terrane (KARAMATA & KRSTIĆ, 1996), the oldest rocks of which are the Proterozoic metamorphic rocks, followed by the late Proterozoic to early Cambrian "Green Complex". During the Variscan magmatism the BG intruded the above rock formations as a late- to post-kinematic intrusion, causing extensive thermal metamorphic phenomena. The BG is a composite pluton consisting of (\pm Hb)-Bi tonalite (TON), (\pm Ms)-Bi granodiorite (GRD), two-mica granite (TMG), and leucogranite (LG). Fe-biotite is the main ferromagnesian constituent in all rock-types except LG. Mg-hornblende is present, in small quantities, only in TON. Plagioclase is of oligoclase-andesine composition. Late and/or subsolidus muscovite is present in small quantities in GRD, although some grains have features of primary muscovite, and also as the main phase in TMG and LG. White mica (1-10 vol%) occurs as primary idiomorphic or secondary flakes commonly 0.15 to 0.6 mm long, rarely up to 1.25 mm, emplaced between feldspar or intergrown with biotite in TMG, GRD and LG. The interlayering of muscovite and biotite is used as textural evidence for its primary origin. Sometimes it makes fine-grained elongated segregations. According to their chemical composition some grains in GDR are TiO₂-rich (1.96-3.27 wt%). Ti concentrations are relatively high for this mineral (~ 0.06-0.12 apfu), while Mn does not exceed 0.02 of an atom in octahedral site. The interlayer site is mainly filled with K (1.7 apfu on average) with lower amounts of Na (0.1 atoms), resulting in relatively low paragonite component (~6 % on average). The examined white micas have phengitic composition in GDR slightly approaching the muscovite end-member from TMG to LG. The phengitic component expressed as the percentage of the $(\text{Fe}^{2+} + \text{Mg} + \text{Ti} + \text{Mn}) / (\text{Fe}^{2+} + \text{Mg} + \text{Ti} + \text{Mn} + \text{Al})$ ratio, ranges from 4 to 18 %. The chemistry of muscovite is characterized by variable levels of substitution of octahedral Al by Mg, Fe and Ti. X_{Mg} ranges from 0.32 to 0.62. The mean composition of muscovite suggests that biotites with high Al content coexist with muscovite close to the ideal composition (VASKOVIC et al., 2004).

References

- KARAMATA, S. & KRSTIC, B. (1996): In: KNEZEVIC-DJORDJEVIC, V & KRSTIC, B. (eds.) Terranes of Serbia. Beograd, 25-40.
- VASKOVIC, N., KORONEOS, A., CHRISTOFIDES, G., SRECKOVIC-BATOCANIN, D. & MILOVANOVIC, D. (2004): 10th Intern. Congress GSG, Thessaloniki, 646-647.

SPECTROSCOPIC INVESTIGATIONS ON SOME VANADIUM-CALCIUM-PHOSPHATE GLASSES

Vedeanu, N., Cozar, O. & Ardelean, I.

Babeş-Bolyai University, Faculty of Physics (Kogălniceanu Str., 1, 400084 Cluj-Napoca, Romania)
e-mail: nvedeanu@phys.ubbcluj.ro

IR and EPR investigations on $xV_2O_5 \cdot (1-x)[P_2O_5 \cdot CaF_2]$ glasses with $0.005 \leq x \leq 0.4$ are reported. Both methods give information about the structural effect of the V_2O_5 oxide component on the glass matrix.

IR spectra contain the absorption bands characteristic for both P_2O_5 and V_2O_5 oxides. The IR spectra for $0.005 \leq x \leq 0.1$ show the characteristic bands of phosphate glasses because of the small content of V_2O_5 oxide. These bands are: O-P-O and O=P-O bending vibrations at 518 cm^{-1} and P-O-P stretching vibrations at 760 cm^{-1} . Between $920\text{-}1280 \text{ cm}^{-1}$ a very large band with three distinct peaks dominates the spectra. These peaks are due to the P-O-P stretching vibration, ionic groups $P-O^{(-)}$ stretching vibration and P=O stretching vibration respectively (DAYANAND et al., 1996). At high concentration of V_2O_5 ($x \geq 0.1$) the bands specific for P_2O_5 become weaker and at $x = 0.4$ the spectrum shows clearly all the typical bands belonging to V_2O_5 oxide. Thus at 595 cm^{-1} is present the V-O-V bending vibration, at 980 cm^{-1} the V-O stretching vibration and at 1080 cm^{-1} the V=O stretching vibration appears (BRATU et al., 1999). It can be concluded that with the increase of V_2O_5 content in the studied glasses the peaks attributed to P_2O_5 are partially covered by those attributed to V_2O_5 oxide; in consequence, the V_2O_5 oxide plays the role of a network modifier at low concentrations and network former at high concentrations.

The shape of the EPR spectra is also changed with the increase of the vanadium content, this consisting in a progressive disappearance of the hyperfine structure characteristic to the V^{4+} ions. This fact may be explained by the superposition of two EPR signals, one with a well-resolved hyperfine structure typical for isolated V^{4+} ions in a C_{4v} symmetry and the other one consisting in a broad line without hyperfine structure characteristic for clustered V^{4+} ions (RAMESH KUMAR et al., 2003). These EPR data are in agreement with those obtained from IR spectra and show that at low concentration V^{4+} ions destroy the phosphate matrix structure imposing their own coordination polyhedra in an isolated scattered manner. At high concentration ($x > 0.1$) the broad line typical for clustered ions shows that the magnetic interactions prevail between paramagnetic centers.

References

- BRATU, I., ARDELEAN, I., BARBU, A., MANIU, D. & BORSA, C. (1999): *J. Mol. Struct.*, **482**: 675-678.
DAYANAND, C., BHIKSHAMIAH, G., JAYA TYAGARAJU, V., SALAGRAM, M. & KRISHNA MURTHY, A.S.R. (1996): *Mater. Sci.*, **31**:1945-1967.
RAMESH KUMAR, V., CHAKRADHAR, R.P.S., MURALI, A., GOPAL, N.O. & LAKSHMANA RAO, J. (2003): *Int. J. Mod. Phys.*, **17**: 3033-3047.

**SPECTROSCOPY APPLICATION FOR MODELLING OF TRANSFORMATIONAL
MECHANISMS OF LATTICE DEFECTS IN DIAMONDS DURING
ANNEALING AND IRRADIATION**

Viktorov, M.A., Marfunin, A.S. & Shelementiev, Y.B.

Moscow State University, Geological Faculty, Department of Mineralogy, 119992, Moscow, Russia
e-mail: viktorov@pisem.net

There is still some concern about mechanisms of defect transformations and structure of some lattice defects in diamonds. This work is performed for better understanding of processes which take place in diamond lattice during irradiation and annealing.

Samples of natural and synthetic diamonds were investigated by means of VIS-IR-range absorption spectroscopy (at room temperature), spectral (at liquid nitrogen temperature) and colour cathodoluminescence and laser induced photoluminescence. Among the studied samples there are several octahedral natural diamond crystals, synthetic diamond crystals, flat plates cut from natural and synthetic diamonds, and also treated black diamonds and natural black diamonds. Several samples (natural octahedral diamond crystals) have undergone annealing at temperatures of 1700-1800 °C under high pressure (6 GPa) and some samples (octahedral natural diamond crystals, natural and synthetic diamond flat plates) were irradiated by different types of radiation such as protons, gamma, and electron. Irradiated samples then were annealed at different temperatures in the range of 800-900 °C. At every stage spectroscopic data were acquired.

The colour of the irradiated samples has changed to green for natural diamonds and to greenish-yellow for synthetic diamonds. In the absorption spectra of the irradiated samples the line at 503 nm appeared (H3-center). Images of the colour cathodoluminescence of the irradiated natural diamond samples revealed no changing of colour and distribution of luminescence (remain blue), but the intensity seems to be weaker. Images of the colour cathodoluminescence of the irradiated synthetic diamond samples revealed changing of the intensity of luminescence, i.e. a weakening of red cathodoluminescence.

Interpretation of acquired data allows to model the structure of some lattice defects in diamond and also provides a useful information on mechanisms of the transformation and stability of lattice defects in diamonds and causes of diamond colour.

ESR AND LUMINESCENT STUDY, *AB INITIO* MODELLING OF ATOMIC AND ELECTRONIC STRUCTURE OF NATURAL CARBONATE MINERALS (Ca,Mg)CO₃:Mn²⁺

Votyakov, S.L., Shchapova, J.V., Porotnikov, A.V. & Galahova, O.L.

Institute of Geology and Geochemistry UrB of RAS, Pochtovii Per. 7, 620151, Ekaterinburg, Russia
e-mail: votyakov@igg.uran.ru

The scheme of calcite and dolomite classification based on the data of ESR, thermo- and X-ray luminescence (in the temperature range 77-400 K) of the typical impurity Mn²⁺-ions replacing Ca²⁺ (Mg²⁺)-ions in carbonates is under consideration. The scheme is based on the statistical analysis of more than 1000 carbonate samples of different Mn²⁺ content, genesis and age (from Riphean up to the modern sediments). Numerical ESR and luminescence databases have been created. It has been shown that under the temperature changes analytical spectroscopic Mn²⁺ line widths, their intensities and their dynamics varied essentially in the samples and depended on the minerals content, their structure defectness and genesis. Suggested scheme of carbonates classification has been used for the analysis of stromatolite-containing limestones, dolomites and interstromatolitic layers from all main South Urals Riphean formations series and some Riphean carbonates from other Russian and world regions. The experimental spectroscopic data have been analyzed using the results of theoretical modelling for calcite and dolomite. The atomic and electronic structures of the minerals were simulated by *ab initio* quantum-chemical cluster methods in terms of GAMESS and X_α-DVM codes on the base of the multiprocessing computer system MVS-1000 of the Institute of Mathematics and Mechanics UrB of RAS (Ekaterinburg). For investigation of pure calcite we used 53-atomic [Ca_{cent}Ca₆C₆O₄₂]⁴⁶⁻ and 64-atomic [C_{cent}C₁₂Ca₆O₄₅]²⁶⁻ clusters containing the central octahedron Ca_{cent}O₆ and the central CO₃-group, respectively. For investigation of dolomite we used 71-atomic [Ca_{cent}Ca₄Mg₆C₆O₅₄]⁶²⁻, [Mg_{cent}Mg₄Ca₆C₆O₅₄]⁶²⁻ and 49-atomic [C_{cent}C₆Mg₃Ca₆O₃₆]³²⁻ clusters corresponding to its structure. The isomorphic substitutions of Ca (Mg) by Mn, Sr, Fe, Mg, Ca-ions have been analyzed as well. The relaxed structure of the clusters with the impurities was determined by the total-energy minimization using the GAMESS software. Using the spatial integrating of the electron density in the clusters the effective charges of atoms have been calculated. Taking into account the peculiarities of spatial distribution of the total and deformation electronic density in the clusters the high covalency within the CO₃-groups has been revealed. The variations of the spectroscopic properties of the Mn impurity ion in calcites and dolomites of the different geneses have been explained due to the variations of settlement values of Mn effective charge, the ionicity degree and Mn-O length in MnO₆ octahedrons.

The study was executed within the framework of the programs №2 of the basic researches of Presidium of the Russian Academy of Science «Origin and Evolution of Biosphere».

SPECTROSCOPIC CHARACTERISATION OF $YAl_3(BO_3)_4 : Gd^{3+}$ CRYSTALS

Watterich, A.¹, Beregi, E.¹, Aleshkevych, P.², Borowiec, M.T.², Zayarnyuk, T.² & H. Szymczak²

¹ Research Institute for Solid State Physics and Optics, Konkoly-Thege M. út 29-33, 1121 Budapest, Hungary

² Institute of Physics, Polish Academy of Sciences, Al. Lotników 32/46, 02-668 Warsaw, Poland
e-mail: watter@szfki.hu

Yttrium aluminium borate is a non-linear optical material with excellent chemical and physical properties. It is a possible self-frequency-doubling UV-VIS laser material when doped with rare earth ions. The aim of this work is to characterise the Gd^{3+} in $YAl_3(BO_3)_4$ single crystals with EPR and optical spectroscopy. $YAl_3(BO_3)_4$ belongs to the double borates having a trigonal structure with space group R32. There are two different boron sites (with C_3 and C_2 point symmetry, respectively), three differently oriented but energetically equivalent Al sites (C_2 symmetry) and only one Y site with D_{3h} symmetry.

0.01 Gd/ $YAl_3(BO_3)_4$ molecule was added to the starting material and the crystal samples were grown from $K_2Mo_3O_{10}$ - B_2O_3 flux by High Temperature Top Seeded Solution Method.

The angular variation of EPR spectra of Gd^{3+} was measured in two different planes: around the c axes the spectra are isotropic, however, rotating from c to a crystallographic axis, strong anisotropy is observed. The D_{3h} symmetry of the EPR spectra for Gd^{3+} ions unequivocally means that the dopant ion substitutes for Y. The angular variation data are fit and the spin Hamiltonian parameters are determined.

The optical absorption of Gd^{3+} has three groups of bands in the UV range attributable to $^8S_{7/2} \rightarrow ^6D$, 6I and 6P transitions, respectively. Relatively strong luminescence is observed at 314.4 nm due to $^6P \rightarrow ^8S_{7/2}$ transition, when excited at the above absorption bands.

This research was partly supported by the National Science Research Fund (OTKA, Hungary, T-37669 and T-34176).

SPECTROSCOPIC STUDY OF CANADA BALSAM USED AS FILLER SUBSTANCE IN EMERALD

Weikusat, C., Nasdala, L. & Häger, T.

Abteilung Edelsteinforschung, Institut für Geowissenschaften,
 Johannes Gutenberg-Universität, D-55099 Mainz, Germany
 e-mail: nasdala@uni-mainz.de

It is a common practice to fill fractures or voids in cut emerald gemstones to enhance their clarity (KIEFERT et al., 1999; NASDALA et al., 2001). A variety of filler substances is used, ranging from volatile and, therefore, easily removable oils (e.g., oil of cedar wood) to glass and durable hydrocarbons (e.g., epoxy resins). After being applied to the stone, fillers undergo an aging process in the course of which they may even decompose. Because solidified fillers or decomposition products may lower a stone's value appreciably, these substances need to be identified prior to the sale. We have studied a suite of cut emerald stones treated with Canada balsam, and commercial Canada balsams. Even though all Raman spectra show somehow similar patterns of bands in the spectral regions of C-C (below 1700 cm^{-1}) and C-H vibrational modes (at around 2900 cm^{-1}), we found notable differences among them (Fig. 1). It is obvious to assume that Canada balsam is not well defined in terms of its composition. Unambiguous identification of Canada balsam in cut stones is even more difficult because of (1) strong Cr^{3+} -related luminescence of emerald, (2) often a strong broad-band luminescence of the balsam, and (3) changed Raman spectra of balsams that have been applied several years ago already.

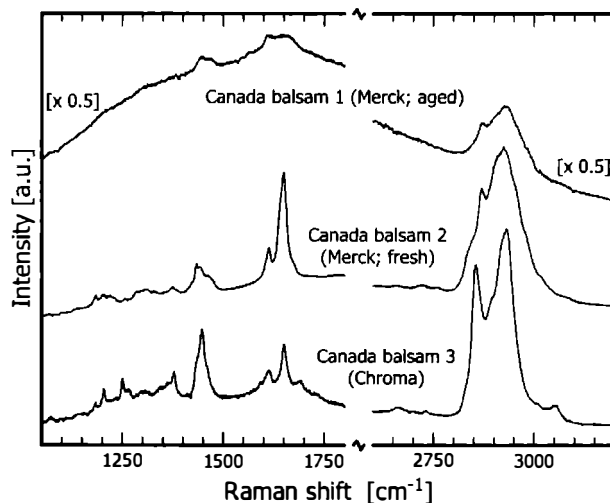


Fig. 1 Three Raman spectra of Canada balsam (stacked). There are already significant differences among spectra of the commercial chemicals (compare 2 and 3). Variations among Raman spectra become even more significant as a result of aging (see the broadening and intensity loss of Raman bands especially in the region below 1700 cm^{-1}). Aging of Canada balsam is often accompanied by a dramatic increase of the background luminescence (compare 1 and 2)

References

- KIEFERT, L., HÄNNI, H.A., CHALAIN, J.-P. & WEBER, W. (1999): *J. Gemmol.*, **26**: 501-520.
 NASDALA, L., BANERJEE, A., HÄGER, T. & HOFMEISTER, W. (2001): *Microsc. Anal., Eur. ed.*, **70**: 7-9.

APPLICATIONS OF MÖSSBAUER SPECTROSCOPY IN MANTLE PETROLOGY

Woodland, A.B.

Institut für Mineralogie, Universität Frankfurt, Senckenberganlage 30, D-60054 Frankfurt, Germany
e-mail: woodland@em.uni-frankfurt.de

Since the Earth's mantle is composed predominantly of minerals that are Fe-bearing solid solutions, Mössbauer spectroscopy (MS) is an essential tool for helping to understand many geochemical and petrological processes that occur at depth. The oxygen fugacity (fO_2) plays an important role in many processes since it influences mineral stability, the volatile species, as well as the rheological and transport properties of minerals. The fO_2 can be estimated through chemical equilibria involving the Fe^{3+} and Fe^{2+} -bearing components in mantle minerals, such as spinel and garnet (WOOD et al., 1990). Thus, a primary task for MS is the accurate determination of the Fe^{3+} -contents in such minerals. Extended Voigt-based fitting (LAGAREC & RANCOURT, 1997) yields a better overall fit for spinel compared to a pure Lorentzian line shape model. For garnet, unequal recoil free fractions for Fe^{3+} and Fe^{2+} need to be accounted for (e.g. WOODLAND & ROSS, 1994). Regional variations and depth profiles in mantle fO_2 can be derived from such data (e.g. WOOD et al., 1990; WOODLAND & KOCH, 2003).

Spectroscopic measurement of $Fe^{3+}/\Sigma Fe$ in coexisting pyroxenes allows a test of redox equilibrium within the mantle assemblage by comparing cpx-based (LUTH & CANIL, 1993) and spinel-based oxybarometers. Fe^{3+} -partitioning between phases can also be assessed, along with the estimation of whole rock Fe_2O_3 contents in mantle samples. This yields a better understanding of the behaviour of Fe^{3+} at high pressures and temperatures.

Many crystal chemical aspects of mantle phases can also be investigated by MS. For example, ordering of Mg and Fe^{2+} on the M1 and M2 sites in pyroxene can be determined (WOODLAND et al., 1997). In mixed valence phases such as garnet, spinel and the spinelloid polymorphs, MS allows investigation of magnetic properties and site occupancies of Fe^{2+} and Fe^{3+} , and provides information complementary to magnetic susceptibility and XRD measurements.

References

- LAGAREC, K. & RANCOURT, D.G. (1997): Nucl. Instr. Meth. Phys. Res. B, **129**: 266-280.
LUTH, R.W. & CANIL, D. (1993): Contrib. Mineral. Petrol., **113**: 236-248.
WOOD, B.J., BRYNDZIA, L.T. & JOHNSON, K.E. (1990): Science, **248**: 337-345.
WOODLAND, A.B. & KOCH, M. (2003): Earth Planet. Sci. Letters, **214**: 295-310.
WOODLAND, A.B. & ROSS II, C.R. (1994): Phys. Chem. Minerals, **21**: 117-132.
WOODLAND, A.B., McCAMMON, C. & ANGEL, R.J. (1997): Am. Mineral., **82**: 923-930.

**SPECTROSCOPIC INVESTIGATION OF SOME MINERALS FROM
CAVE NO.4 – RUNCULUI HILL (METALIFERI MTS, ROMANIA)**

Zaharia, L. & Suciu-Krausz, E.

Babeş-Bolyai University, Department of Mineralogy (Kogălniceanu Str., 1, 400084 Cluj-Napoca, Romania)
e-mail: lumiok@yahoo.com

Trestia-Băita is a metallogenic region located in the central part of the Metaliferi Mountains (South Eastern Apuseni Mts), characterised by a complex geological setting: Tithonic reefal limestone blocks disposed over an Early Jurassic ophiolitic basement (volcanoclastic basalts). Both limestone and ophiolites are part of the Căpâlnaş – Techereu Nappe (BALINTONI, 1997), affected by the Neogene volcanic activity. The hydrothermal activity associated to the Neogene volcanism resulted in the formation of several sulphide veins, emplaced both within limestone and basalt.

Cave no. 4 from Runcului Hill (D = 127.4 m, H = 10 m) is the largest cave in the respective karst area and consists of several rooms linked by small pits and narrow passages. One of the cave passages connects with a 13 m long and 2 m high mine gallery, with collapsed entrance, which ends in a hydrothermal vein.

The geological complexity of the area complicates the range of cave mineralogy. Fourteen minerals were identified by means of X-ray diffraction. Along with common minerals in limestone caves (calcite, aragonite and gypsum), an interesting range of other minerals were reported, few of them being exotic for cave environment.

IR and Raman spectroscopy have been used to analyse the most interesting minerals: sulphates such as serpierite $\text{Ca}(\text{Cu},\text{Zn})_4(\text{OH})_6(\text{SO}_4)_2 \cdot 3\text{H}_2\text{O}$ and barite BaSO_4 , and carbonates such as smithsonite ZnCO_3 and cerussite PbCO_3 (the last one occurring together with galena PbS).

One Raman spectrum was recorded from serpierite in the range up to 3700 cm^{-1} . The other three minerals were analysed by means of IR spectroscopy, the spectra being obtained in the range of $400\text{-}4000\text{ cm}^{-1}$. For each spectrum the wavenumbers, characters and intensities of the bands are reported. The bands were assigned to vibrational modes of different structural groups.

Due to the fact that spectroscopic methods provide information about local structure (as site, symmetry, coordination number, local chemical and crystallographic environment) (PUTNIS, 1992), the aim of this paper is to present an interpretation of IR and Raman spectra recorded for the above-mentioned minerals, in order to give a better crystal chemical characterisation in each case.

References

- BALINTONI, I. (1997): Geologia terenurilor metamorfice din Romania. Ed. Carpatica, Cluj-Napoca. 174 p.
PUTNIS, A. (1992): Introduction to Mineral Sciences. Cambridge Univ. Press. 479 p.

X-RAY DIFFRACTION AND IR-SPECTROSCOPY OF BOTTOM SEDIMENTS IN LAKE HOVSGOL FOR PALEOCLIMATIC RECONSTRUCTIONS

Zhdanova, A.N.

United Institute of Geology, Geophysics and Mineralogy, SB RAS, Kopyug pr., 3, 630090, Novosibirsk, Russia
e-mail: zhdanova@uiggm.nsc.ru

Lake Hovsgol, on the territory of Mongolia, lies in a region critical for understanding global climate change in central Asia during the late Cenozoic. Biogenic silica is known to serve as a useful climate proxy. Biogenic silica tends to increase in the sediments as a result of elevated diatom productivity in the lake, which is responding to warmer water temperatures, but it does not provide any information about paleoclimatic changes in catchment basin. Clay minerals, in particular, would therefore be more likely to preserve the conditions of hydrolysis that generated them in the weathering profile. We focus on determining whether patterns in the mineralogical composition of the sediments can also be used as a supporting tool for paleoclimatic interpretation.

The series of short cores (up to 1.15 m depth) have been obtained from different parts of this lake during 2001-2002 as a part of the Russian Academy of Sciences' expeditions. The cores show two distinct sedimentary divisions. The upper part of core is dominated by fine-grained silts and the lower part is generally sandier with numerous intervals of graded bedding. The mineral composition of the original samples and their fine granulometric fractions were analysed by X-ray powder diffraction and IR spectroscopy. For X-ray the oriented mounts were prepared by transferring the suspension of bulk sample in distilled water onto a glass slide and drying at room temperature. Then they were solvating for about 24 hours with ethylene-glycol vapor in an evacuated exicator. The measurements were conducted on a DRON-4 automated powder diffractometer system with CuK α radiation, graphite monochromator. Scans were performed from 2° to 35° 2 θ with speed of 0.05° 2 θ /s. A new method was proposed for modeling X-ray diffraction profiles in order to identify correctly clay minerals and evaluate the amount of each clay mineral. The method is based on the calculation of the interference function of the one-dimensional disordered crystals with finite thickness and using a specially developed optimization procedure. Quantitative estimations of the composition of minerals such as quartz, plagioclase, carbonate and biogenic silica were made by IR. Samples were prepared using the KBr pellet method. The measurements were conducted on a Specord-75 IR spectrometer.

A consistent clay mineral assemblage containing illite, illite-smectite, chlorite, chlorite-smectite, muscovite and kaolinite, characterizes much of the studied sediments. Dominating illite and smectite layers in illite-smectite indicate chemical weathering condition under a warm and humid climate in an interglacial period. Prevalence of muscovite and illite layers in illite-smectite shows the influence of physical weathering in the glacial period. The clay-mineral-based fluctuations are correlated well with the abundance of biogenic silica and provide an independent tool for gaining insight into the paleoclimate of interior continental site.

The work was supported by RFBR, project 02-05-64504.

**INTERPRETATION OF IR SPECTRA OF MIXED-LAYER ILLITE-SMECTITES
AND ILLITE-TOBELITE-SMECTITES IN THE REGION OF
OH-STRETCHING VIBRATIONS**

Zviagina, B.B.

Geological Institute RAS, Pyzhevsky per., 7, 119017 Moscow, Russia
e-mail: zviagina@ginras.ru

Illite-smectite (I-S) and illite-tobelite-smectite (I-T-S) samples of various compositions were studied by infrared (IR) spectroscopy. A special sample preparation technique was used to eliminate the contribution of molecular water. The OH-stretching regions of the spectra were decomposed and curve-fitted, and the individual OH stretching bands were assigned to all the possible types of OH-bonded cation pairs that involve Al, Mg and Fe. The integrated optical densities of the OH bands were assumed to be proportional to the contents of the specific types of OH-linked cation pairs with the absorption coefficients being the same for all individual OH bands. Good agreement between the samples' octahedral cation compositions calculated from the IR data and those given by chemical analysis was obtained for a representative collection of samples in terms of a unique set of individual OH band positions that vary within narrow wavenumber intervals. This has allowed minimizing the ambiguity in spectra decomposition imposed by the poor resolution of smectite spectra and confirmed the validity of the resulting band identification.

For I-S and I-T-S with relatively low proportions of expandable layers (up to 25%) and high total amount of fixed interlayer K and NH₄, the OH stretching bands attributions found by BESSON & DRITS (1997) for dioctahedral micas was found relevant. For samples having higher proportions of expandable layers, the bands associated with specific OH bonded cation pairs may tend to be shifted to greater wavenumbers with respect to the corresponding bands in micas. In addition to OH bands that refer to the smectite structure, AlOHAl and AlOHFe bands of the pyrophyllite structural fragments were identified.

Unambiguous interpretation of the OH stretching vibrations was found to be possible only for I-S and I-T-S samples with known chemical compositions, so that IR data cannot be used for quantitative determination of octahedral cation composition of mixtures of dioctahedral 2:1 phyllosilicates. In the case of monomineral samples with known chemical compositions, IR data can provide information on the short-range order/disorder in the distribution of octahedral cations along cation-OH-cation directions. This information can be employed, in combination with the data of other spectroscopic and diffraction techniques, in the analysis of two dimensional octahedral cation distribution.

References

BESSON, G. & DRITS, V.A. (1997): *Clays Clay Minerals*, **45**: 168-169.

Explanatory Notes to the Map

**METAMORPHIC STRUCTURE
OF THE ALPS**

(Roland Oberhänsli, Editor)



**EXPLANATORY NOTES TO THE MAP:
METAMORPHIC STRUCTURE OF THE ALPS
INTRODUCTION**

by

Roland Oberhänsli¹ & Bruno Goffé²

¹Institut für Geowissenschaften

Universität Potsdam, Karl-Liebknecht-Str. 25, 14476 Potsdam-Golm, Germany

²Laboratoire de Géologie

UMR 8538, CNRS, Ecole Normale Supérieure, 24 rue Lhomond, 75005 Paris, France

Abstract

Two new maps describing the Mesozoic-Cenozoic, Alpine metamorphic structure (1:1'000'000) and metamorphic ages (1:2'000'000) are presented. A short discussion of the map units used is provided to introduce some key papers summing up new ideas, lines of thought, the data used and the problems encountered.

General remarks

These maps and notes are based on studies of Austrian, French, Italian and Swiss earth scientists who worked in the Alps for the last 30 years, trying to understand the Mesozoic and Cenozoic evolution of the orogen. We investigated the Cretaceous and Tertiary closing of the Tethyan realm, subduction related processes, and the exhumation of the Alps. Most data have been published in specialized journals, others are the result of recent investigations of our working groups.

Concise compilations of recent geophysical data have been published from ECORS-CROP (ROURE et al., 1990; DAL PIAZ et al., 2003) and NRP20 (BLUNDELL et al., 1992; PFIFFNER et al., 1997) for the Western and the Central Alps. Results from the Eastern Alps are about to be published (TransAlp, 2002). A new compilation is given by SCHMID et al. (2004b). These studies resulted in a better knowledge of the present deep structure documenting subducted remains of passive margins and a distinct variation along strike in the deep structure of the Alpine orogen. These results added substantially to the pioneering ideas of geologists during the last century (ARGAND, 1911, 1916, 1924, 1934; AMPFERER, 1906; BERTRAND, 1884; FRANCHI et al., 1908; HEIM, 1919-22; LUGEON, 1902; LUGEON & ARGAND, 1905; STEINMANN, 1905; TERMIER, 1904) who conceived and developed the nappe theory from the cover to the basement nappes throughout the Alps (historical review in DAL PIAZ, 2001).

ELLENBERGER (1958), TRÜMPY (1960) and TOLLMANN (1963) gave further advances in stratigraphy, regional tectonics and paleogeographic reconstructions. DAL PIAZ (1928) gave one of the earliest modern works on Alpine eclogites and glaucophane-bearing rocks. ERNST (1971), DAL PIAZ (1971) and DAL PIAZ et al. (1972) innovated the interpretation of HP metamorphism in the Alps. Further compilation were presented by SPALLA et al., (1996) and GODARD (2001).

As the map of the distribution of metamorphic rocks of the Alps compiled by the late Martin Frey and co-workers did not account for tectonic setting and geodynamic evolution, our initial objective was to show differences in the geodynamic evolution of various parts of the Alpine orogen. To do so, we should have included kinematic information based on structural and paleomagnetic data, as well as the age and distribution of flysch sequences, much of which has been published over the last thirty years. The regional distribution of such data, however, is quite uneven and would have hampered the readability of the map, hence we decided to concentrate on the type and grade of the metamorphism. To the extent that metamorphism is related to geodynamic processes, our new maps show which units underwent which process, approximately at what time and to what depth. We made the choice to refer to conditions where pressure and temperature peak were reached simultaneously or where a temperature peak was reached at lower pressures after a significant temperature increase during the decompression path (hatched areas). These choices at the first glance clearly show what type of process is linked the main metamorphic structure: subduction process as for the Western Alps or collision process for Central Alps, and complex metamorphic structures as in the Eastern Alps being due to a complex geodynamic and metamorphic history involving the succession of the two types of process. The new maps show where subduction-, collision-, exhumation-related types of metamorphism are found in the Alps. The FREY et al. (1999) map was an obvious and excellent starting point for this task.

In addition we are working on an interactive CD version of the maps, presenting information on the data used for this compilation. Our working philosophy is explained in the chapter Extended Legend and in the regional compilations that follow.

Since the aim of these maps is to address the Mesozoic-Cenozoic evolution of the Alps, all pre-Alpine metamorphic features have been omitted. Highlighting domains overprinted by Alpine "peak" metamorphic reactions typical for certain geotectonic settings results in a picture much easier to read than previous maps of the metamorphic evolution of the Alps published by NIGGLI & NIGGLI (1965), NIGGLI & ZWART (1973), ZWART et al. (1973, 1978) and FREY et al. (1974, 1999), which all strive to emphasize polymetamorphic and/or plurifacial complexities. Our new map shows Alpine metamorphic peak conditions irrespective of when these were attained. The age information is given in a separate map shown as inset (1:2'000'000). We also added new data, notably compiled from high-pressure metamorphic metapelites. Thus the wide distribution of subduction related metasediments of the Valais ocean domain have brought forth new geodynamic aspects and paleogeographic reconstructions.

Fig. 1 shows local names used in the text but partly omitted on the metamorphic map and the position of the main Jurassic paleogeographic elements within the Mid- to Late Tertiary structure of the present Alps; it also indicates major metamorphosed fault zones. Although our metamorphic map tries to show a general picture of the Alpine thermo-mechanical evolution, this

could not be done without reference to local names. To maintain clarity on the metamorphic map and as thesaurus for the "non-Alpine" reader we used a modified version of the tectonic map by SCHMID et al. (2004a). The map of SCHMID et al. (2004a) is based on the structural model of Italy (BIGI, et al., 1989, 1990a, 1990b, 1992).

The metamorphic map clearly shows a relatively simple picture for the Western Alps with an internal high-pressure dominated part thrust over an external greenschist to low grade domain, although both metamorphic domains are structurally very complex (GOFFÉ et al., 2004 this volume; BOUSQUET et al., 2004, this volume). Such a metamorphic pattern is generally produced by subduction followed by exhumation along a cool decompression path. In contrast, the Central Alps document conditions typical for subduction (and partial accretion) followed by an intensely evolved collision process resulting to an heating event during the decompression path of the early subducted units (hatched units in the map) (ENGI et al., 2004, this volume). Subduction-related relics and (collisional/decompressional) heating phenomena in different tectonic edifices characterize the Eastern Alps (Schuster et al., 2004, this volume). This complex picture is due to a dual Cretaceous and Tertiary metamorphic evolution related to a complex tectonic history. For the Tuscan and Corsica parts of the map the reader is invited to see the synthetic work of JOLIVET et al. (1998) that was used as reference to draw this part of the map.

Legend of the metamorphic structure map

The following divisions were used as legend on the map

- LGM Low grade metamorphism**
DIA: Diagenesis / sub-anchizone (T < 200°C; P < 0.3 GPa)
zeolite / illite – kaolinite
SGS: Sub-greenschist facies (T 200–300°C; P < 0.5 GPa)
laumontite – prehnite – pumpellyite / kaolinite – chlorite – illite – interlayered illite – smectite
- GS Greenschist facies**
LGS: Lower greenschist facies (T 300–450°C; P < 0.7 GPa)
albite – chlorite – epidote ± actinolite / albite – chlorite – phengite / pyrophyllite – chlorite – illite – phengite – paragonite ± chloritoid
UGS: Upper greenschist facies (T 420–500°C; P < 0.8 GPa)
actinolite / biotite – chlorite – kyanite ± chloritoid
HPGS: High-pressure greenschist facies (T 300–450°C; 0.6 < P < 1.0 GPa)
albite – lawsonite – chlorite ± crossite / phengite – chlorite ± chloritoid ± kyanite
- GAT Greenschist- amphibolite transitional facies** (T 450–600°C; 0.8 < P < 1.2 GPa)
albite – epidote – amphibole / biotite – garnet – chloritoid / phengite – chloritoid – kyanite
- AM Amphibolite facies** (T 500–650°C; 0.5 < P < 1.3 GPa)
plagioclase – hornblende – garnet / biotite – garnet – staurolite – phengite ± kyanite

BS	Blueschist facies	
	BS: Blueschist facies	(T 250–400°C; 0.8 < P < 1.5 GPa)
	<i>glaucophane – lawsonite – jadeite – quartz / Fe-Mg-carpholite – phengite ± pyrophyllite ± chloritoid</i>	
	UBS: Upper blueschist facies	(T 380–550°C; 1.0 < P < 1.5 GPa)
	<i>glaucophane – epidote – garnet / chloritoid – glaucophane – phengite ± garnet</i>	
BET	Blueschist to eclogite transitional facies	(380–550°C; 1.3 < P < 1.8GPa)
	<i>blue amphibole – zoisite – garnet ± clinopyroxene / garnet – Mg-rich chloritoid – phengite</i>	
ECL	Eclogite facies	(T 450–750°C; 1.3 < P < 2.5 GPa)
	<i>garnet – omphacite – zoisite – quartz ± amphibole ± phengite / garnet – Mg-rich chloritoid – kyanite – phengite / garnet – lawsonite</i>	
UHP	Ultrahigh-pressure facies	(T 600–800 °C; 2.5 < P < 4.0 GPa)
	<i>garnet – omphacite – coesite – zoisite / Mg-rich chloritoid – talc – phengite – kyanite – pyrope – coesite</i>	
VT	Variegated HT facies	(T 600–800°C; 0.7 < P < 2.5 GPa)
	<i>Tectonic mélange with relics of ECL, AM, and local granulite facies, interpreted as tectonic accretion channel (TAC); in the Southern Steep Belt evidence of partial melting is widespread</i>	

These divisions are based on metamorphic assemblages identified in mafic and in pelitic compositions. Temperature and pressure limits for different facies are far from being precisely defined but represent a compromise for different rock compositions. Sketches of P-T grids give the P-T paths used to define the P-T grid shown in the map..

Large parts of the Austroalpine unit consist exclusively of pre-Alpine metamorphic rocks overprinted during the Eo-Alpine event at various grade. In these rocks the prograde assemblages defined above can not be recognised, but the following criteria have been used to cover the area:

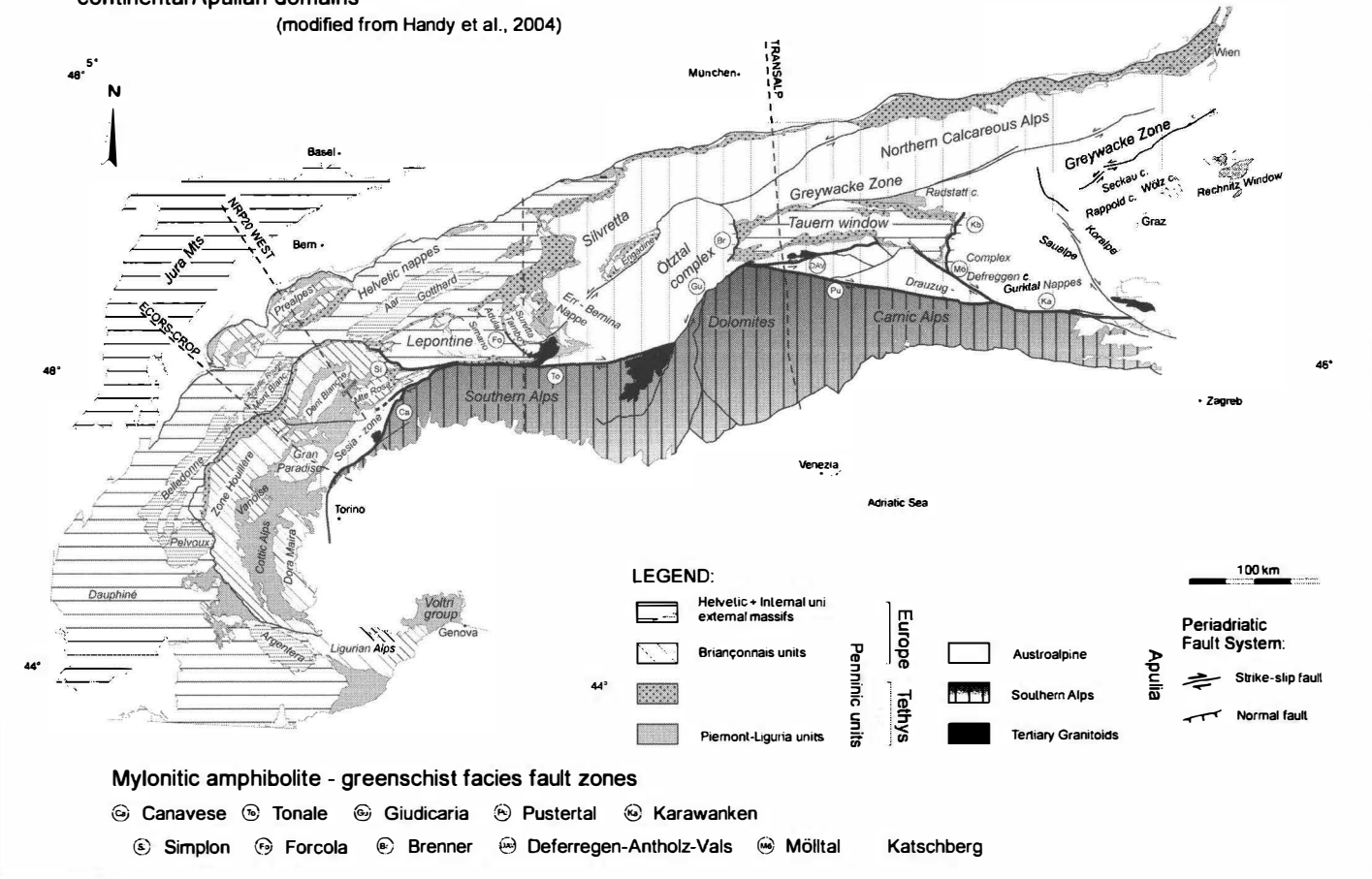
LGM	(low grad metamorphism)	
	diagenesis / sub anchizone	illite cristallinity and coalification data
	sub greenschist facies	illite cristallinity and coalification data
LGS	~ 300 °C	total reset of Rb-Sr isotopic system in biotite
UGS	~ 400 °C	total reset of K-Ar isotopic system in muscovite
GAT	~ 500 °C	garnet-in, assemblage Ms + Ca-amphibole
AM	~ 600 °C	staurolite-in

As far as sub-anchi facies (DIA), sub-greenschist facies (SGS), lower greenschist facies (LGS), upper greenschist facies (UGS) and high-pressure greenschist facies (HPGS) are concerned, these facies terms as well as the corresponding P and T conditions can be considered as standard. The transitional greenschist amphibolite facies (GAT) accounts for the fact that different bulk rock compositions either produce greenschist or amphibolite facies mineral assemblages within this pressure and temperature realm.

No Eo-Alpine blueschist facies rocks are reported from the Austroalpine units.

Fig. 1: Simplified tectonic map of the Alps
 indicating regional names and showing:
 continental European, oceanic Tethyan and
 continental Apulian domains

(modified from Handy et al., 2004)



Instead the collision-related pressure-dominated rocks between greenschist facies and eclogite facies re-equilibrated in the GAT field. For some areas clear amphibolite facies (AM) conditions are evident in the field. Blueschist facies rocks can be divided into normal blueschist facies (BS) rocks and garnet-bearing blueschists that experienced somewhat higher temperatures and are classified as upper blueschist facies (UBS) rocks. For the transition from blueschist to eclogite facies, where all intermediate stages can be found in various tectonic units, we chose to lump the different rock types in a blueschist to eclogite transitional facies (BET). The eclogite facies is subdivided into eclogite facies (ECL) and ultrahigh-pressure facies (UHP), based on the quartz – coesite phase transition. In the southern part of the Central Alps rocks occur that apparently underwent different metamorphic conditions within coherent tectonic units. As these outcrops are too small to be mapped, the composite zone has been interpreted as remnant of a tectonic accretion channel (see below). In order to avoid a tectonic term in the legend, we summarize all rocks exhibiting amphibolite, eclogite or granulite facies metamorphism, as well as migmatization (in the Southern Steep Belt) under the term variegated high temperature facies (VT). The colour code applied to the metamorphic facies domains indicates subduction-related metamorphic conditions by blue, pink and violet tints. Yellow, green to red colours indicate conditions related to continental collision. Red to orange tints suggest high temperature conditions, which appear to be related to exhumation (e.g. TAC, see ENGI et al., 2004.).

Legend of the Alpine tectono-metamorphic age map

The choices made for the presentation of metamorphic ages is discussed by HANDY & OBERHÄNSLI (2004, this volume).

High-retentivity isotopic systems such as Sm-Nd, Hf-Lu of HP assemblages and U-Pb SHRIMP data of zircon were used to assess ages of high-pressure metamorphism. Rb-Sr, Ar-Ar and K-Ar biotite and white mica cooling ages were used to separate areas dominated by cooling ages from areas where mixed ages are observed. For some areas biotite cooling ages were contoured to show the cooling pattern of the thermal overprint.

Green and yellow-orange colours indicate, respectively, the Cretaceous and Tertiary metamorphic cycle. Dotted areas show tectonic units that experienced high-pressure metamorphism.

Conclusions

These maps include information based on recent data from high-pressure metasediments that yields new aspects of the geodynamic evolution of the Alps. The fact that subduction-related high-pressure metamorphism can be identified all along the Valais ocean domain calls for adapted paleogeographic reconstructions.

The compilation of this new map resulted in two aspects. In our opinion, the Mesozoic and Tertiary evolution of the Alps has been depicted in a way permitting an easier approach to a geodynamic understanding of this orogen.

Acknowledgements

I would like to thank Christine Miller, Martin Engi, Mark Handy and Ralf Schuster for their constructive comments and help with the English.

References

- AMPFERER, O. (1906): Über das Bewegungsbild von Faltengebirgen. - *Jb. Geol. Reichsanst. Wien*, 77, 539-622.
- ARGAND, E. (1911): Les nappes de recouvrement des Alpes Pennines et leurs prolongements structuraux. - *Mat. Carte géol. Suisse n. s.*, 31.
- ARGAND, E. (1916): Sur l'arc des Alpes Occidentales. - *Ecolae geol. Helv.*, 14, 145-189.
- ARGAND, E. (1924): Des Alpes et de l'Afrique. - *Bull. Soc. Vaud. Sci. Nat.*, 55, 233-236.
- ARGAND, A. (1934): La zone pennique. - *Guide géol. Suisse*, Wepf & Co., Basel, 149-189.
- BERTRAND, M., (1884): Rapports de structure des Alpes de Glaris et du bassin houiller du Nord. - *Bull. Soc. Géol. France*, 3, 12, 18-330.
- BIGI, G., CASTELLARIN, A., CATALANO, R., COLI, M., COSENTINO, D., DAL PIAZ, G. V., LENTINI, F., PAROTTO, M., PATACCA, E., PRATURLON, A., SALVINI, F., SARTORI, R., SCANDONE, P. & VAI, G. B. (1989): Synthetic structural-kinematic map of Italy. - *C.N.R., Progetto Finalizzato Geodinamica*, SELCA Firenze.
- BIGI, G., CASTELLARIN, A., COLI, M., DAL PIAZ, G. V., SARTORI, R., SCANDONE, P. & VAI, G. B. (1990a): Structural Model of Italy, sheet 1. - *C.N.R., Progetto Finalizzato Geodinamica*, SELCA Firenze.
- BIGI, G., CASTELLARIN, A., COLI, M., DAL PIAZ, G. V. & VAI, G. B. (1990b): Structural Model of Italy, sheet 2. - *C.N.R., Progetto Finalizzato Geodinamica*, SELCA Firenze.
- BIGI, G., COLI, M., COSENTINO, D., DAL PIAZ, G. V., PAROTTO, M., SARTORI, R. & SCANDONE, P. (1992): Structural Model of Italy, sheet 3. - *C.N.R., Progetto Finalizzato Geodinamica*, SELCA Firenze.
- BLUNDELL, D., FREEMAN, R. & MUELLER, S. (EDS) (1992): A continent revealed: The European Geotraverse. - Cambridge University Press, 1992, pp. 180-198.
- BOUSQUET, R., ENGI, M., GOSSO, G. & SPALLA, I. (2004): Metamorphic structure of the Alps: Transition from the Central Alps to the Western Alps. IN: Explanatory notes to the Map of Metamorphic Structures of the Alps. OBERHÄNSLI, R. (ED). - *Mitt. Öster. Min. Ges.*, 149, 145-156.
- DAL PIAZ, G. B. (1928): Geologia della catena Herbetet-Grivola-Grand Nomenon. - *Mem. Ist. Geol. Univ. Padova*, 7, 83 pp.
- DAL PIAZ, G. V. (1971): Alcune considerazioni sulla genesi delle ofiolti piemontesi e dei giacimenti ad esse associati. - *Boll. Ass. Miner. Subalpina*, 8, 365-388.
- DAL PIAZ, G. V. (2001): History of tectonic interpretations of the Alps. - *J. Geodynamics*, 32, 99-114.
- DAL PIAZ, G. V., BISTACCHI, A. & MASSIRONI, M. (2003): Geological outline of the Alps. - *Episodes*, 26/3, 175-180.
- DAL PIAZ, G. V., HUNZIKER, J. C. & MARTINOTTI, G. (1972): La zona Sesia-Lanzo e l'evoluzione tettonico-metamorfica delle Alpi nordoccidentali interne. - *Mem. Soc. Geol. It.*, 11, 433-466.
- ELLENBERGER, F. (1958): Etude géologique du pays de la Vanoise. - *Mém. explicative Carte géol. France*, 561 pp.
- ENGI, M., BOUSQUET, R. & BERGER, A. (2004): Metamorphic Structure of the Alps: Central Alps, IN: Explanatory notes to the Map of Metamorphic Structures of the Alps. OBERHÄNSLI, R. (ED). - *Mitt. Öster. Min. Ges.*, 149, 157-173.
- ERNST, W. G. (1971): Metamorphic zonation on presumably subducted lithospheric plates from Japan, California and the Alps. - *Contrib. Mineral. Petrol.*, 34, 43-59.

- FRANCHI, S., MATTIROLO, E., NOVARESE, V., STELLA, A. & ZACCAGNA, D. (1908): Carta geologica delle Alpi occidentali al 1:400.000. Dai rilievi al 1:25.000 eseguiti nel 1888-1906 per la nuova Carta Geologica d'Italia al 100.000. - Regio Ufficio Geologico, Roma.
- FREY, M., HUNZIKER, J. C., FRANK, W., BOCQUET, J., DAL PIAZ, G. V., JAEGER, E. & NIGGLI, E. (1974): Alpine metamorphism of the Alps: a Review. - Schweiz. Mineral. Petrol. Mitt., 54, 247 - 290.
- FREY, M., DESMONS, J. & NEUBAUER, F. (1999): Metamorphic map of the Alps. 1:500'000 - Schweiz. Mineral. Petrogr. Mitt., 79. 1.
- GODARD G. (2001): Histoire des éclogites et de leurs interprétations géodynamiques. - Travaux Comité Franc. Hist. Géol., 15, 51-76.
- GOFFÉ, B., SCHWARTZ, S., LARDEAUX, J. M. & BOUSQUET, R. (2004): Metamorphic Structure of the Alps: Western and Ligurian Alps, IN: Explanatory notes to the Map of Metamorphic Structures of the Alps. OBERHÄNSLI, R. (ED). - Mitt. Öster. Min. Ges., 149, 125-144.
- HANDY, M. & OBERHÄNSLI, R. (2004): Metamorphic Structure of the Alps: Tectonometamorphic Age Map, IN: Explanatory notes to the Map of Metamorphic Structures of the Alps. OBERHÄNSLI, R. (ED). - Mitt. Öster. Min. Ges., 149, yyy
- HANDY, M. R., BABIST, J., ROSENBERG, C. L., WAGNER, R. & M. KONRAD (2004): Decoupling from the brittle-viscous transition downwards and its relation to strain partitioning in the continental crust - Insight from the Periadriatic Fault System (European Alps). IN: BRUN, J. P., COBBOLD, P. R. & GAPAIS, D. (EDS): Deformation mechanisms, Rheology and tectonics. - Geol. Soc., London, Spec. Pub. (in press).
- HEIM, A. (1919-22): Geologie der Schweiz. - Tauchnitzverlag Leipzig, Vol I , 704 p, Vol II/1, 476 p, Vol II/2, 541 p.
- HUNZIKER, J. C., DESMONS, J. & HURFORD, A. J. (1992): Thirty-two years of geochronological work in the Central and Western Alps: a review on seven maps. - Mém. Géol., Lausanne, 13, 59 p.
- JOLIVET, L., FACCENNA C., GOFFÉ, B., MATTEI, M., ROSSETTI, F., BRUNET, C., STORTI, F., FUNICIELLO, R., CADET, J. P. & PARA. T. (1998): Midcrustal shear zones in post-orogenic extension: the Northern Tyrrhenian Sea case. - J.G.R., 103, 12123-12160.
- LUGEON, M. (1902): Les grandes nappes de recouvrement des Alpes du Chablais et de la Suisse. - Bull. Soc. géol. France, sér. 4, 1 (1901), 723-825.
- LUGEON, M. & ARGAND, E. (1905): Sur les grandes nappes de recouvrement de la zone Piémont. - Comptes rendus acad. Sci. Paris, CXL, 1491.
- NIGGLI, E. & NIGGLI, C. (1965): Karten der Verbreitung einiger Mineralien der alpidischen Metamorphose in den Schweizer Alpen (Stilpnomelan, Alkali-Amphibol, Chloritoid, Staurolith, Disthen, Sillimanit). - Eclogae geol. Helv., 58, 335-368.
- NIGGLI, E. & ZWART, H. J (1973): Metamorphic map of the Alps, scale 1:1'000'000. Explanatory text. Sub-commission of Cartography of the Metamorphic Belts of the World. Sheet 17 of the metamorphic map of Europe. - Leiden / UNESCO, Paris.
- PFIFNER, O. A., LEHNER, P., HEITZMANN, P., MUELLER, ST., & STECK, A. (EDS) (1997): Results of NRP 20: Deep Structure of the Swiss Alps. - Birkhäuser Verlag, Basel, Boston, Berlin, 305-325.
- ROURE, F., HEITZMANN, P. & POLINO, R. (EDS.). (1990): Deep Structure of the Alps. - Soc. geol. de France, Paris, 156; Mem. Soc. geol. suisse, Zürich, 1; Vol. spec. Soc. Geol. It., Roma, 1, 350 p.
- SCHMID, S. M., FÜGENSCHUH, B., KISSLING, E. & SCHUSTER, R. (2004a): Tectonic map and overall architecture of the Alpine orogen. - Eclogae geol. Helv, 97/1, 93-117.
- SCHMID, S. M., FÜGENSCHUH, B., KISSLING, E. & SCHUSTER, R. (2004b): TRANSMED Transects IV, V and VI: Three lithospheric transects across the Alps and their forelands. - In: Cavazza, W., ROURE, F., SPAKMAN, W., STAMPFLI, G. M. & ZIEGLER, P. A. (eds.) - The TRANSMED Atlas: The Mediterranean Region from the Crust to Mantle. Springer Verlag, in press.

- SCHUSTER, R., KOLLER, F., HOECK, V., HOINKES, G. & BOUSQUET, R. (2004): Metamorphic Structure of the Alps: Eastern Alps. IN: Explanatory notes to the Map of Metamorphic Structures of the Alps. OBERHÄNSLI, R. (ED). - Mitt. Öster. Min. Ges., 149, 175-199.
- SPALLA, M. I., LARDEAUX, J. M., DAL PIAZ, G. V., GOSSO, G. & MESSIGA, B. (1996): Tectonic significance of Alpine eclogites. - J. Geodynamics 21, 257-285.
- STEINMANN, G. (1905): Geologische Beobachtungen in den Aalpen II. Die Schardtsch Überfaltungstheorie und die geologische Bedeutung der Tiefseeabsätze und der ophiolithischen Massengesteine. - Ber. Naturf. Ges. Freiburg i. Br., 16, 18-67.
- TERMIER, P. (1904): Les nappes des Alpes orientales et la synthèse des Alpes. - Bull. Soc. géol. France, sér. 4, vol. 3 (1903), 843-928.
- TOLLMANN, A. (1959): Ostalpensynthese. - Deuticke, Wien, 256p.
- TRANSALP WORKING GROUP (2002): First deep seismic reflection images of the Eastern Alps reveal giant crustal wedges and transcrustal ramps. - Geophys. Res. Lett., 29, 10.1029/2002GL014911.
- TRÜMPY, R. (1960): Paleotectonic evolution of the Central and the Western Alps. - Bull. geol. Soc. Amer., 71, 843-908.
- TRÜMPY, R. (1973): Timing of the Orogenic Events in the Central Alps. In: "Gravity and Tectonics" (De Jong, K. & Scholten, R.). - Wiley, New York, 229-251.
- ZWART, H. J. (1973): Metamorphic map of Europe, scale 1:2'500'000. - Subcommittee of Cartography of the Metamorphic Belts of the World. Leiden / UNESCO, Paris.
- ZWART, H. J., SOBOLEV, V. S. & NIGGLI, E. (1978): Metamorphic map of Europe, scale 1:2'500'000. Explanatory text. Subcommittee of Cartography of the Metamorphic Belts of the World. - Leiden / UNESCO, Paris, 244 pp.

manuscript received: June 2004

manuscript accepted: July 2004

**EXPLANATORY NOTES TO THE MAP:
METAMORPHIC STRUCTURE OF THE ALPS
WESTERN AND LIGURIAN ALPS**

by

Bruno Goffé¹, Stephane Schwartz², Jean Marc Lardeaux³ & Romain Bousquet⁴

¹Laboratoire de Géologie

UMR 8538, CNRS, Ecole Normale Supérieure, 24 rue Lhomond, 75005 Paris, France

²Université Joseph Fourier Maison des Géosciences
Lirigm BP 53, 38041 Grenoble, CEDEX 9, France

³Géosciences Azur- Faculté des Sciences
Parc Valrose 06108 Nice cédex 02, France

⁴GeoSciences Department
University of Basel, Bernoullistr. 30, CH-4056 Basel, Switzerland

1 - Generalities and choice for the representation

In the Western and Southwestern part of the Alps from Val d'Aoste in the North to Genova in the South, the Alpine Type Metamorphism, characterized by a high-pressure low-temperature regime (HP-LT), is particularly well expressed.

In this area, the retromorphic conditions influencing the rocks during their exhumation paths have never exceeded the temperatures attained at peak pressure. As a result, during decompression of the metamorphic rocks the PT-t trajectories always remained cooling paths. Therefore, our choice was to represent the metamorphic peak conditions, while the retromorphic evolutions are only indicated together with ages in the inset map and not on the main map. However, these retromorphic imprints exist and can be locally intense.

2 - The main metamorphic zones

In the area of the Western Alps the HP-LT conditions range from the very low-grade greenschist facies to the Ultra High Pressure (UHP) conditions crossing 8 of the 14 metamorphic facies encountered in the whole map.

Generally the contacts between the metamorphic units correspond to tectonic contacts (thrusts, normal faults, strike-slip faults). However, on the map, the boundaries between the metamorphic units frequently appear as crossing the tectonic contacts mainly when they correspond to the limits of paleogeographic domains.

Detailed examination of these contacts shows that this feature is the result of the late tectonic evolution bringing into contact units of equal metamorphic grade but different ages. Two main examples of this feature can be found in the blueschist and in the eclogite facies zones that overlap both oceanic (Schistes Lustrés nappe) and continental (Briançonnais and internal basements) domains: the high pressure metamorphic conditions prevailing in the Briançonnais domain and in the internal basements are Late Tertiary in age (Oligocene) while in the oceanic domain these conditions are Early Tertiary in age (early Eocene) (DUCHENE et al, 1987; AGARD et al. 2002).

Despite the simplistic choice of the metamorphic criteria, only oriented on the metamorphic peak conditions and thus related to early orogenic processes (subduction), the metamorphic imprint at the map scale is consistent with the geometry of the Western alpine arc, i.e. the PT metamorphic conditions increase from the external to the internal part of the arc with an inward movement of the subducting slab. However, more complex situations resulting from the initial structure of the European or Apulian margins or resulting of the late tectonic of the belt can be depicted. Two main examples of this situation are particularly interesting to be mentioned (see also the general cross section of the Western Alps shown in Figure 1):

- 1) The repetition of the metamorphic sequence (greenschist-blueschist-eclogite facies) observed in the Northwestern part of the Alps from the external to internal basements through the Valaisan, the Briançonnais and the Ligurian domains. This can be related to the prolongation of the southern realm of the Valaisan oceanic domain;
- 2) The decrease of the metamorphic grade in the deepest part of the belt, i.e. the easternmost side of the Dora Maira internal basement, with a reappearance of HT blueschists facies conditions in the Pinerolo unit below the overlying eclogitic units. This metamorphic structure can be interpreted as the result of the late tectonic evolution of the orogenic wedge.

The nature of some boundaries of the metamorphic facies is still not totally determined. Some boundaries run along isograds as for the appearance of the very low-grade metamorphism in the external part of the belt or as for the external limit of the HP greenschist facies in the Briançonnais domain, North-West of Briançon. Some could be undefined tectonic contacts as for the Blueschist - Upper Blueschist facies limits in the Schistes Lustrés nappe in the Cottian Alps, East and South-East of Briançon.

The HP-LT metamorphic conditions occur in all rocktypes encountered in the belt including continental basements, oceanic crust and an exceptional variety of metasediments. Generally, the PT conditions recorded by the different rocktypes are consistent. Only in two specific areas of the Schistes Lustrés domain, West of the Gran Paradiso and West of the Monviso, the metamorphic imprint of mafic blocks or slices contrasts with the surrounding pelitic lithologies. This is represented, on the map, by coloured dots superposed on the main metamorphic facies. These features suggest the possible existence of a melange of high grade metamorphic blocks in a matrix of lower metamorphic degree.

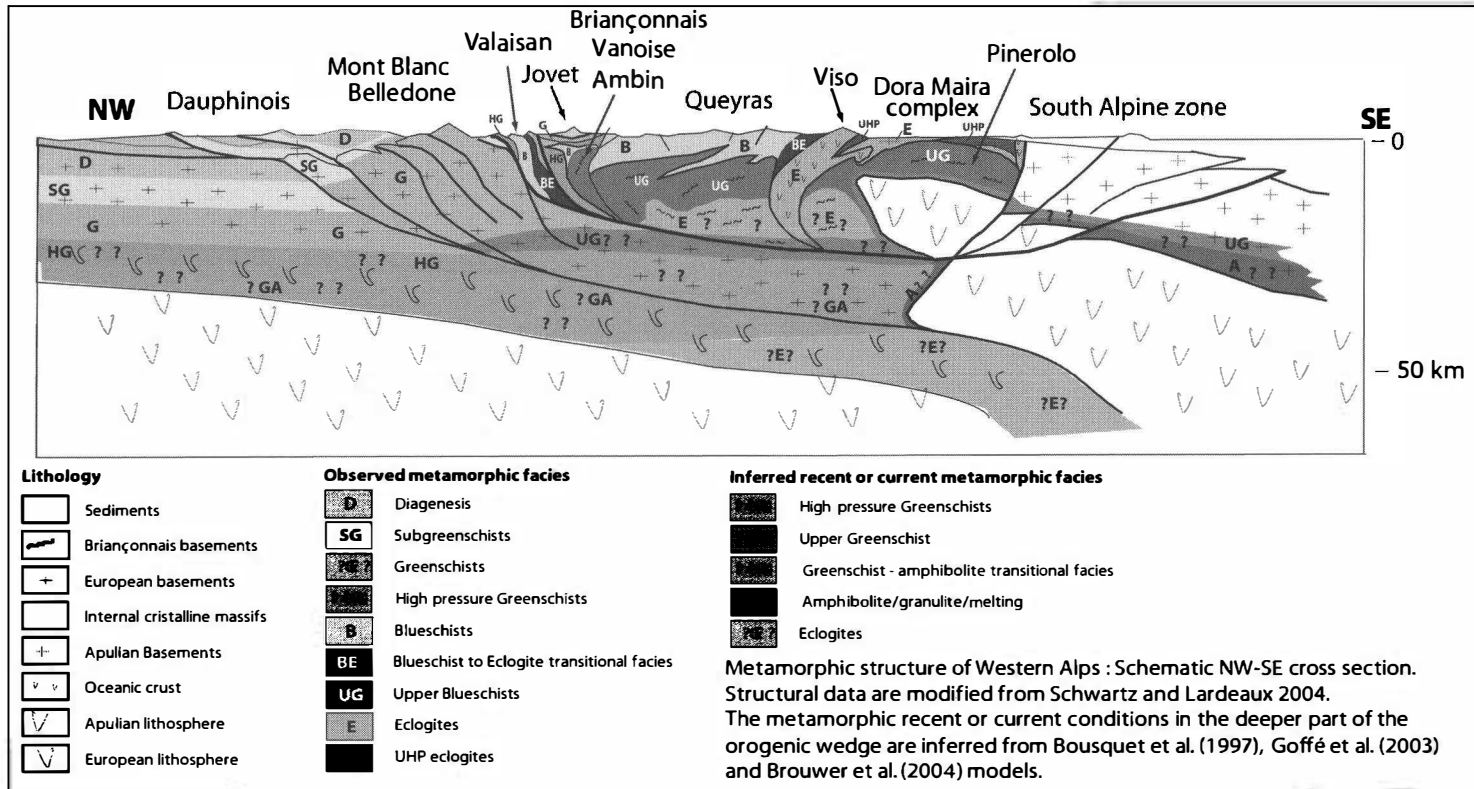


Figure 1

Schematic projected NW-SE cross section of the Western Alps showing the metamorphic structure. The upper part of the cross section is drawn using surface metamorphic data as drawn in the map. The deeper part of the cross section is hypothetically inferred from numerical modelling and data coming from Central Alps, considering this area as a possible further evolution for Western Alps. A moderated thermal imprint is also considered as a possible current deep metamorphic structure resulting from a slab breakoff event as modelled by BROUWER et al. (2004). This metamorphic thermal imprint around the mantel indenter could thus be compared to those observed around the peridotitic bodies of Beni Bousera and Ronda in the Rif and Betic Chain.

3 - The metamorphic facies in the Western Alps

The metamorphic facies used here are mainly based on B. EVANS (1990) metamorphic grid defined for metabasites. In the case of the Western and South-Western Alps, these facies definitions actually cover a large variety of other index minerals depending of the nature of the protoliths, particularly, the metasediments. In the following, the specific index minerals found in the belt are listed and discussed for each metamorphic facies in function of the lithology. In each facies the minerals regarded as defining the metamorphic index mineral assemblages are printed in bold, while additional index minerals, locally present, are added in italic. Localities where a specific mineralogy can be found are indicated in brackets.

For organic matter, only the appearance of graphite is considered to enhance the absence of diamond in the HP conditions. In the other case the organic matter is considered as disordered carbonaceous matter.

- **Sub greenschist facies (200–300°C; P < 4kbar)**
Mafic system: albite – chlorite – pumpellyite (Chenaillet)
Volcanoclastic metasediments: **laumontite – prehnite** (Champsaur)
Pelitic system: **kaolinite – chlorite – illite - interlayered illite-smectite**,
Rectorite (Nappe de Digne)
Metabauxites (Prealpes, Devreunse): **diaspore – kaolinite – berthierite**
- **Lower greenschist facies (300–400°C; P < 4kbar)**
Mafic system and Volcanoclastic metasediments: **albite – chlorite – epidote – actinolite**
Na rich metapelites: **albite – chlorite – phengite**
Al rich metapelites: **pyrophyllite – chlorite – illite-phengite – paragonite - cookeite**
(Ultra-Dauphinois unit, La Grave and la Mure area) – chloritoid (Northern part of Ultra-Dauphinois North of the Maurienne valley) – paragonite
- **Upper greenschist facies (300–400°C; 4 < P < 8kbar)**
Mafic system and Volcanoclastic metasediments: **albite – lawsonite – chlorite – paragonite – phengites – riebeckite-crossite – pumpellyite – stilpnomelane**
Pelitic system: **phengite – chlorite – chloritoid (Northern Vanoise, Ligurian Alps)**
- **Blueschist facies (300–400°C; 8 < P < 15kbar)**
Mafic system: **glaucophane – lawsonite – jadeite-quartz – pumpellyite**
Marble and calcschists: **aragonite - glaucophane**
Evaporites (Maurienne Valley near Bramans): **jadeite + quartz – anhydrite – selate – sulfur**
Pelitic system: **ferro- magnesiocarpholite –phengite – chloritoid – pyrophyllite – lawsonite – aragonite – cookeite – paragonite**
Na rich metapelites: jadeite + quartz – glaucophane – chlorite – paragonite
Al rich metapelites and metabauxites: **ferro- magnesiocarpholite – pyrophyllite – diaspore – chloritoid – lawsonite – aragonite – cookeite – paragonite – sudoite**
(Antoroto metabauxite, Liguria) – gahnite – euclase (Western Vanoise)

- **Upper Blueschist facies (400–500°C; 10 < P < 15kbar)**
Mafic system: glaucophane – epidote - garnet or omphacite (+ jadeite)-sphene
Granitic System: phengite – jadeite- epidote (Southern Vanoise, Ambin, Acceglio)
Pelitic system: chloritoid – glaucophane – phengite – graphite (Southern Vanoise, Ambin massif)
- **Blueschist to eclogite transitional facies (400–480°C; 15 < P < 20kbar)**
Mafic system: glaucophane – epidote (+ garnet) – omphacite (+ jadeite)-sphene
Pelitic system: Mg rich chloritoid – phengite – magnesiocarpholite – garnet – graphite
- **Eclogite facies (500–600°C; 13 < P < 25kbar)**
Mafic system: garnet – omphacite – quartz – zoisite – phengite- rutile
Granitic system: garnet-jadeite-phengite- zoisite-rutile (Sesia-Lanzo zone)
Pelitic system: chloritoid – kyanite – phengite – garnet – glaucophane – paragonite-graphite (Sesia-Lanzo zone)
- **Ultra high-pressure facies (600–800°C; 25 < P < 40kbar)**
Mafic system: garnet – omphacite – zoisite – coesite – kyanite – Mg-chloritoid – talc (Monviso)
Pelitic system: Magnesiochloritoid – kyanite – phengite – pyrope – talc – coesite – Magnesiostauroilite – ellenbergerite– bearthite – magnesiodumortierite – graphite (Dora Maira massif)

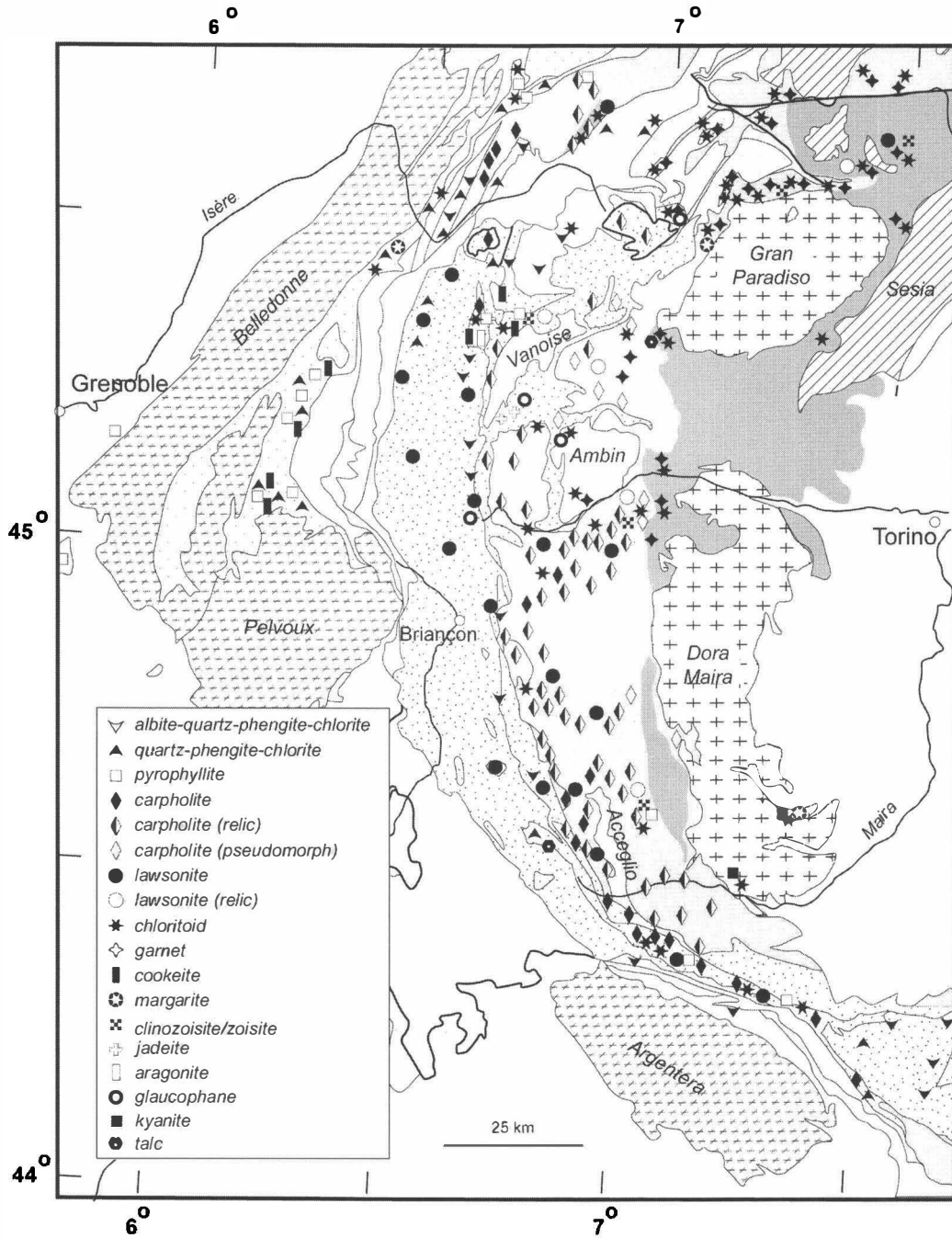
4 - Diversity of Alpine high-pressure mineralogy: an overview

The diversity of the Alpine metamorphic high-pressure assemblages reflects the contrasted bulk-rock chemistries of the metamorphosed protoliths. Hereafter, we present a review of the metamorphic assemblages recognized in different chemical systems.

a) Metasediments

Compared to the earlier published metamorphic maps FREY et al. (1999), and beside the different choice of the metamorphic representation, the main new data of this present map is the large and continuous expression of the high-pressure and low temperature metamorphic conditions in the metasediments as shown in Figure 2 and 3.

This new data mainly results from the consideration of the ferro- and magnesiocarpholite occurrences in the metapelites. The magnesiocarpholite first discovered in the metabauxites of Western Vanoise (GOFFÉ et al., 1973, GOFFÉ & SALIOT 1977) is now known in all the high-pressure metasedimentary lithologies having initially a low Na content (i.e. bauxite, aluminous pelites, common pelites, sandstones, conglomerates). They occur abundantly in the Briançonnais domain in Western and Southern Vanoise, Cottian and Ligurian Alps, both in the Paleozoic series (Stephanian and Permian schists and metaconglomerates) and in the Mesozoic cover (Triassic series, Dogger metabauxites, Eocene flysch).



- ▽ albite-quartz-phengite-chlorite
- ▲ quartz-phengite-chlorite
- pyrophyllite
- ◆ carpholite
- ◇ carpholite (relic)
- ◇ carpholite (pseudomorph)
- lawsonite
- lawsonite (relic)
- ★ chloritoid
- ◇ garnet
- cookeite
- ⊗ margarite
- ⊗ clinzoisite/zoisite
- ⊕ jadeite
- aragonite
- glaucophane
- kyanite
- talc

- | | |
|---|---|
| <ul style="list-style-type: none"> ⊞ a: External Crystalline Basements □ b: Briançonnais Basements + c: Internal Crystalline Basements ▨ d: Austroalpin Units | <ul style="list-style-type: none"> ■ e: High grade metamorphic metasediments (mainly eclogitic) □ Oceanic metasediments of the Valaisan and Ligurian domain □ Continental metasediment of Briançonnais zone ⊞ Continental metasediments of Dauphinois and Helvetic domain |
|---|---|

Figure 2

Occurrences of metamorphic index mineral observed in Alpine metasediments of the Greenschist and Blueschist metamorphic zones of Western Alps used to draw the metamorphic map.

White: Sediments or very low grade metasediments.

They occurs also widely in blueschists facies metapelites of the Tethys oceanic domain in the Valaisan realm (Versoyen and Brêches de Tarentaise units) and in the Ligurian zone from the more external klippe of Mont Jovet (AGARD, 2001, pers. com.) to the more internal one in the Sestri-Voltaggio-Cravasco unit. Its stability domain in blueschists metamorphic facies and its progressive replacement during the prograde and retrograde metamorphic evolution by chloritoid, chlorite, phengite and generally numerous minerals of the KMAH reduced system can be used to describe and to quantify continuously the metamorphic evolution (GOFFÉ, 1982; CHOPIN 1983; GOFFÉ & CHOPIN 1986; VIDAL et al., 1992; GOFFÉ et al., 1997; JOLIVET et al. 1998; VIDAL & PARRA 2000; PARRA et al., 2002; AGARD et al., 2001; among others). In the Western Alps, ferro- and magnesiocarpholite ranges from 80% of the Fe end member to 85% of the Mg one. In the Briançonnais domain, Fe-Mg-carpholites are commonly associated to pyrophyllite and record pressures between 8 to 12 kbar for temperatures ranging from 330°C to 400°C. In the Schistes Lustrés domain, the Fe-Mg-carpholites are never associated to pyrophyllite and shown equilibrium with phengites through the reaction: Chlorite + muscovite + quartz \leftrightarrow phengite + Fe-Mg-carpholite. The reported maximum pressures for this reaction are around 15-18 kbar for temperatures reaching 480°C (GOFFÉ et al., 1997; AGARD et al. 2001). These conditions are those of the upper blueschists facies reported on the map in the inner part of the Schistes Lustrés domain and the Valaisan, at the external limit of the eclogite domain.

Lawsonite occurrences are also very common in metapelites and calcschists of the Schistes Lustrés units (CARON & SALIOT, 1969; SICARD et al., 1986) and in meta-sandstones of the Briançonnais domain. Lawsonite is often associated to Fe-Mg-carpholite in continental and oceanic metasediments. Its distribution is wider than that of Fe-Mg-carpholite with occurrences in upper greenschist and eclogite facies units, where Fe-Mg carpholite is not stable and was never found. This widest distribution is in accordance with a largest stability field toward both low pressure and high temperature conditions.

Cookeite (lithium chlorite) is also an important metamorphic index mineral in the Briançonnais (Barrhorn, Vanoise, Cottian and Ligurian Alps) and Dauphinois (la Grave, La Mure) domains of the Western Alps. It occurs widely in metapelites, metaconglomerates and metabauxites in association with quartz or diaspore in a large variety of low to high-pressure metamorphic assemblages (GOFFÉ, 1977, 1980, 1984; SARTORI, 1988; JULLIEN & GOFFÉ, 1996). Cookeite records medium temperature conditions (300 to 450°C) of the greenschist to blueschist facies (VIDAL & GOFFÉ, 1991). Cookeite shows a pressure dependence of its polytypism with an increase of structural ordering with pressures from 100 to 1500 Mpa (JULLIEN et al., 1996).

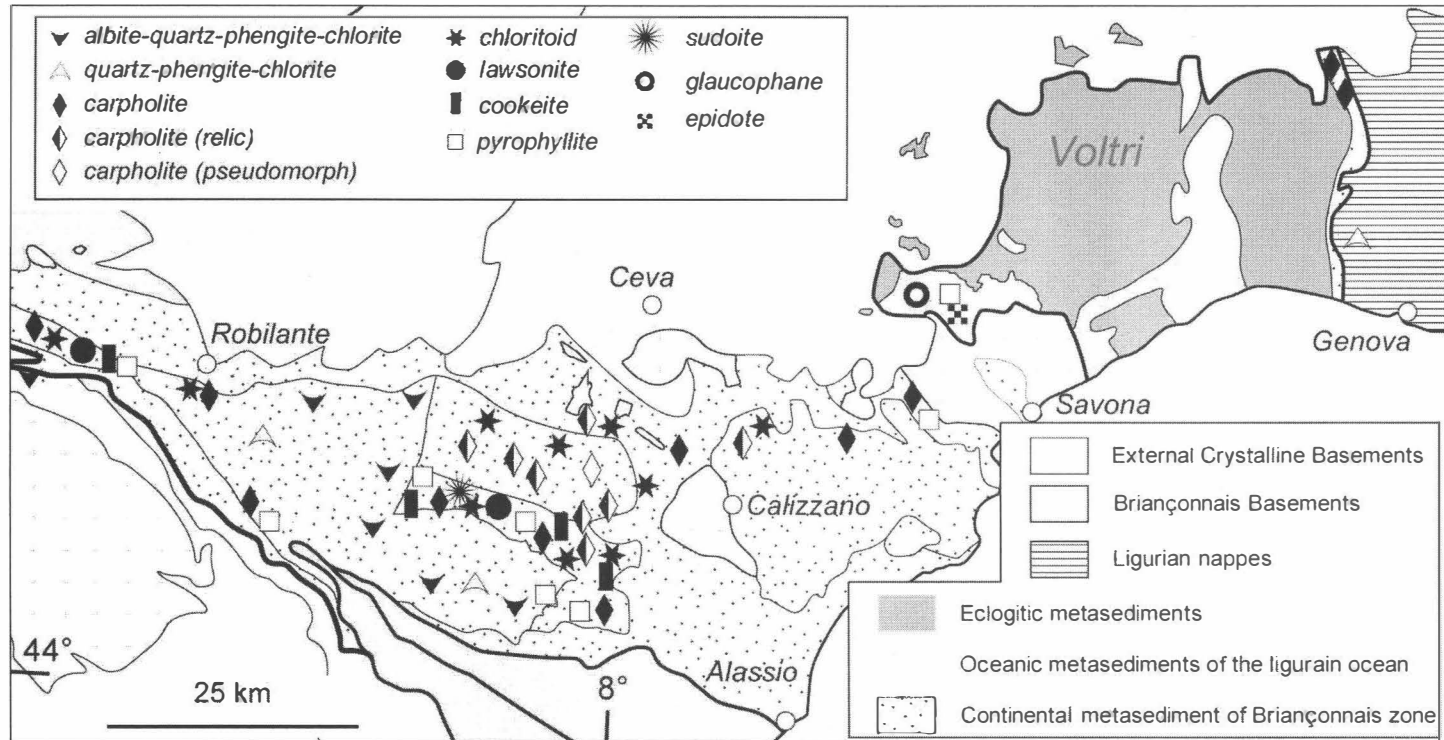


Figure 3

Occurrences of metamorphic index mineral observed in Alpine metasediments of the Greenschist and Blueschist metamorphic zones of Ligurian Alps used to draw the metamorphic map. The structural frame is from the general map.

Very high metamorphic conditions lead the metapelitic system to react continuously to give appearance to kyanite which is associated to a specific mineralogy showing a linear increase of Mg content with the metamorphic grade. This results in pure Mg-endmembers of FMASH system minerals in the coesite stability field such as: magnesiochloritoid, magnesiostauroilite, pyrope, talc, clinocllore in association with unique very high pressure minerals like ellenbergerite, magnesiudumortierite or bearthite (CHOPIN and CHOPIN et al., 1981-1995, SIMON et al., 1997).

Under quartz-eclogite facies conditions, metapelites have been described and analysed in details since their discovery in the Sesia-Lanzo zone (DAL PIAZ et al, 1972; COMPAGNONI et al., 1977; LARDEAUX et al., 1982; VUICHARD & BALLÈVRE, 1988), where the association of quartz, phengite, jadeite, chloritoid, garnet and glaucophane characterizes the so-called "eclogitic micaschists". Similar well preserved eclogitic metapelites occur in other Austro-Alpine units of the Western Alps for example the Monte Emilius massif (DAL PIAZ et al., 1983).

The organic carbonaceous matter of the metasediments is also an interesting way to follow the metamorphic evolution. The organic carbonaceous matter is particularly abundant in the Western Alps either as coal in the Briançonnais domain or as diffuse marine organic matter in the Schistes Lustrés series. With increasing metamorphic grade the organic matter evolves continuously from disoriented structures (turbostratic) in the sub-greenschist facies to perfectly organized graphite in UHP facies in the Dora Maira massif through carbons having peculiar onion like shaped structures in the blueschist facies (BEYSSAC et al., 2002). This evolution can be linked to the temperature evolution without evidences of a pressure effect (BEYSSAC et al., 2002). Graphite appears in high temperature and high-pressure blueschist facies. Diamond was never found, neither characteristic carbonaceous structures resulting of its retro-morphosis (BEYSSAC & CHOPIN, 2003). Anomalous well preserved organic matter (C_n gas, liquid hydrocarbons, low evolved solid carbonaceous matter) are reported in the blueschist facies of the Western Vanoise (GOFFÉ, 1982, GOFFÉ & VILLEY, 1984).

b) Mafic rocks

Mafic rocks from the Western Alps represent ophiolite suites mainly formed during the opening of the Piemont-Ligurian oceanic basin during Jurassic times (LOMBARDO et al., 1978; POGNANTE, 1980; LOMBARDO & POGNANTE, 1982). However, a limited number of mafic rocks derive from metamorphosed continental crust as for example meta-amphibolites and meta-granulites from the Sesia-Lanzo zone (LARDEAUX & SPALLA, 1991).

Mineralogical and geochemical studies have demonstrated that the Western Alps ophiolites derive from partial melting of rather homogeneous peridotites which generated melts similar to normal – MORB. Consequently Alpine metabasalts represent differentiated (Fe-Ti rich) tholeiitic liquids. On the other hand, metagabbros display a wide spectrum of compositions ranging from Cr-Mg rich gabbros to Fe-Ti gabbros. Therefore, the so-called mafic metamorphic rocks in the Western Alps derive from the various protoliths following a tholeiitic differentiation trend:

Mg (\pm Cr) rich gabbros: olivine-bearing cumulates,
Intermediate gabbros: gabbro-norites,
Fe-Ti rich gabbros: ilmenite and magnetite-bearing gabbros,
Fe-Ti rich basalts

Moreover, some of these lithologies have been subjected to ocean-floor hydrothermal activity leading to the development of rodingitic alterations. When affected by high-pressure Alpine metamorphism, these rocks correspond to metarodingites with peculiar mineralogical associations (BEARTH, 1967; DAL PIAZ, 1967).

In our metamorphic map, we select Fe-Ti rich metabasalts and metagabbros for the definition of the metamorphic facies because, in comparison with other gabbro compositions, the ophiolitic Fe-Ti rocks show better developed high- pressure and low-temperature metamorphic assemblages. Metagabbros, in many cases, show incomplete metamorphic recrystallization allowing to study reaction mechanisms at the boundaries between the magmatic mineral relics.

At quartz-bearing eclogite-facies conditions, the following mineralogical associations have been recognized (LOMBARDO et al, 1978; DAL PIAZ & ERNST, 1978; LARDEAUX et al., 1986, 1987; POGNANTE & KIENAST, 1987).

Mg (\pm Cr) rich metagabbros: omphacite (\pm smaragdite), pale blue/colourless glaucophane, zoisite, \pm chlorite, \pm Mg-chloritoid, \pm talc, \pm kyanite, \pm scarce garnet, \pm fuchsite

Intermediate metagabbros: omphacite, garnet, zoisite, glaucophane, \pm jadeite, \pm talc, \pm paragonite

Fe-Ti rich metagabbros and metabasalts: omphacite (\pm jadeite), garnet, zoisite, rutile, glaucophane, \pm paragonite, \pm phengite, \pm clinozoisite, \pm Fe-talc

Metarodingites: diopside and / or «omphacitic clinopyroxene», grandite and / or grossular rich garnet, epidote, chlorite, \pm idocrase, \pm amphibole, \pm Ti-clinohumite

Under blueschist-facies conditions, the following associations have been described:

Mg (\pm Cr) rich metagabbros: Amphibole, chlorite, clinozoisite, \pm white micas

Intermediate metagabbros: Na-amphibole, chlorite, \pm clinozoisite, \pm sphene, \pm lawsonite

Fe-Ti rich metagabbros and metabasalts: Acmite-rich clinopyroxene, «omphacitic» clinopyroxene, glaucophane, epidote (or lawsonite), sphene, \pm garnet, \pm white micas

In Fe-Ti metagabbros, at P-T blueschist facies conditions, the chemical evolution of the clinopyroxenes is controlled by the existence of non-omphacitic unmixing domains for temperatures lower than 350°C (CARPENTER, 1980). Fe-Ti metagabbros show different chemical evolution of their initial magmatic clinopyroxene (augitic-cpx). Indeed, under low-temperature blueschist facies conditions (i.e. lawsonite-glaucophane conditions), the increase of the P-T conditions during Alpine metamorphism is recorded by an increase of the Fe-content in clinopyroxene from the core to the rim of the initial magmatic clinopyroxene, with apparition of acmite-rich clinopyroxene on the crystal rims (POGNANTE & KIENAST, 1987). Whereas under high-temperature blueschist (i.e. zoisite-glaucophane conditions), the increase of the P-T conditions during Alpine metamorphism is characterized by an increase of the Na component in clinopyroxene leading to the crystallisation of omphacite (SCHWARTZ, 2001).

Spectacular metamorphic transformations can be observed in mafic rocks of continental origin. In eclogitized amphibolites and granulites, high-temperature calcic amphiboles are progressively replaced by calco-sodic (barroisite) and sodic amphiboles (glaucophane), sometimes in association with phengites. Associations of zoisite, garnet and omphacite are developed at the expense of plagioclase or at the plagioclase/amphibole, plagioclase/ilmenite or plagioclase/pyroxene boundaries, while coronas of rutile are frequently developed around ilmenite grains.

c) Meta-granitoids

In the Western Alps the following protoliths have been recognized for the meta-granitoids:

- Biotite-bearing granites and granodiorites,
- Two-micas granites,
- Fe-rich syenites,
- Trondhjemites, plagiogranites and quartz-keratophyres in ophiolites.

It should be underlined that eclogitized metagranites from the Sesia-Lanzo zone have been regarded as the first indication for the subduction of the continental crust (DAL PIAZ et al., 1972; COMPAGNONI & MAFFEO, 1976; COMPAGNONI et al., 1977; LARDEAUX et al., 1982; OBERHÄNSLI et al., 1982).

Under quartz-eclogite facies conditions, in mica-rich granites and granodiorites, the igneous mineralogy is replaced by an high-pressure metamorphic association composed of: jadeite, phengite, garnet, zoisite, rutile and quartz. K-feldspar is generally recrystallised but remains stable sometimes with intergrowths of white micas and quartz. An association of jadeite and zoisite replaces plagioclase, while, close to the biotites/plagioclases boundaries, Ca-rich garnet develops as thin coronas. Biotites are replaced by coronitic garnets and an association of phengite, quartz and rutile. Magmatic muscovites are replaced by celadonites-rich white micas, while quartz recrystallised (sometimes in coesite) and zircons, apatite and tourmalines remain as residual phases.

In Fe-rich syenites (LARDEAUX et al., 1983), the metamorphic high-pressure mineralogy is composed by ferro-omphacites, garnets and epidotes.

In leucocratic rocks from Alpine ophiolites (i.e. trondhjemites, quartz-keratophyres or plagiogranites), the Alpine eclogite facies metamorphism leads the development of: jadeite, quartz, phengite, ± garnet, ± epidote and rutile (LOMBARDO et al., 1978; POGNANTE et al., 1982).

Meta-granitoids reworked under blueschist facies conditions have been described in Vanoise, Ambin and Acceglio massifs (GAY, 1973; SALIOT, 1978; GANNE et al., 2003; ROLLAND et al., 2000; SCHWARTZ et al., 2000). In the Acceglio massif the metamorphic conditions reach the transition between high-temperature blueschist and eclogite facies conditions. The observed metamorphic assemblages consist of an association of quartz, jadeite, phengite, lawsonite or epidote, ± almandine-rich garnet. Secondary magmatic minerals like zircons, apatite and tourmaline are frequently well preserved.

5 - Conclusions

The metamorphic structure of the western part of the Alpine belt shows probably the best preserved example of the "Alpine-type" metamorphism with a continuous evolution of high pressure conditions from very low temperature conditions to the highest ones. These conditions can be observed in all lithologies with a near theoretical coherence between them.

As shown in the synthetic cross section through the Western Alps (Fig.1), these high-pressure and low-temperature conditions can be considered as relicts of the early (pre Oligocene) evolution of the belt related to the subduction processes. Three main geodynamic consequences can be emphasised after our metamorphic analysis:

Even in a mature collisional belt like the Western Alps, the memory of subduction processes should be well preserved in a fossil accretionary wedge like the western internal Alps.

Both oceanic and continental crustal slices should be involved in the subduction zone during plate convergence. In Western Alps, numerous examples of subducted continental crust have been exhumed and are now preserved in Austro-Alpine (i.e. Sesia-Lanzo, Mt. Emilius klippe, etc.) and Penninic units (i.e. Internal Crystalline Massifs, Dora-Maira, Gran-Paradiso, Monte Rosa, etc.).

The huge mass of weathered sediments issued from the erosion of the Hercynian belt and reworked during the Thethys opening along its passive margins, led to a peculiar metamorphic belt constituted by a large metasedimentary orogenic wedge characterized by prevalent high pressure-low temperature conditions (GOFFÉ et al. 2003). This could be considered as the definition of the so-called Alpine type metamorphism *sensus stricto* characterized by a high-pressure – low-temperature regime of 10°C/km or less. These metamorphic conditions contrast with those prevailing early in the Eastern Alps and lately in Central Alps where the pressure-temperature ratio is highest even at high pressure (see the map) and where mainly continental crust is involved in the orogenic process.

Now, the present-day ongoing continental collision process involves the European crust and the thermal regime is changing. Alpine metamorphism evolves from the early high-pressure and low-temperature conditions to present-day high-temperature and medium-pressure metamorphic conditions. These conditions, clearly expressed in the Central Alps, can be already observed in the external part of the Western Alps around the external crystalline massifs and probably prevail at depth in the orogenic root (Fig. 1).

Cited and selected relevant bibliographic references

- AGARD, P., JOLIVET, L. & GOFFÉ, B. (2001): Tectonic evolution of the Schistes lustrés complex: implications for the exhumation of HP and UHP rocks in the Western Alps. - *Bull. Soc. Geol. France*, 172, 617-636.
- AGARD, P., VIDAL, O. & GOFFÉ, B. (2001): Interlayer and Si content of phengite in HP-LT carpholite-bearing metapelites. - *J. metamorphic Geol.*, 19, 477-493.
- AGARD, P., MONIÉ, P., JOLIVET, L. & GOFFÉ, B. (2002): In situ laser probe $^{40}\text{Ar}/^{39}\text{Ar}$ constraints on the exhumation of the Schistes Lustrés unit: geodynamic implications for the evolution of the Western Alps. - *J. metamorphic Geol.*, 20, 599-618.

- APRAHAMIAN, J. (1988); Cartographie du métamorphisme faible à très faible dans les Alpes Françaises externes par l'utilisation de la cristallinité de l'illite. - *Geodinamica acta*, 2, 1, 25-32.
- AVIGAD, D. (1992): Exhumation of coesite-bearing rocks in the Dora-Maira massif (western Alps, Italy). - *Geology* 20, 947-950.
- AVIGAD, D. N., CHOPIN, C. & LE BAYON, R. (2003): Thrusting and extension in the southern Dora-Maira Ultra-high-Pressure massif (Western Alps): View from below the Coesite-bearing Unit. - *J. Geol.*, 111, 57-70.
- BADOUX, H. & DE WEISSE, G. (1959) : Les bauxites siliceuses de Drévenouse. - *Bull. soc. Vaud. Sci. Nat.*, 67, 169-177.
- BARLIER, J., RAGOT, J. P. & TOURAY J. C. (1974) L'évolution des Terres Noires Subalpines méridionales d'après l'analyse minéralogique des argiles et de la réflectométrie des particules carbonées. *Bull B.R.G.M.*, serie 2, II/6, 533-548.
- BEARTH, P. (1967): Die Ophiolithe der Zone von Zermatt-Saas Fee. *Beitr. Geol. Karte CH*, NF 132, 130p.
- BEYSSAC, O., GOFFÉ, B., CHOPIN, C. & ROUZAUD, J. N. (2002): Raman spectrum of carbonaceous material in metasediments: a new geothermometer. - *J. metamorphic Geol.*, 20, 859-871.
- BEYSSAC, O., ROUZAUD, J. N., GOFFÉ, B., BRUNET, F. & CHOPIN, C. (2002): Graphitization in a high-pressure, low-temperature metamorphic gradient: a Raman microspectroscopy and HRTEM study. - *Contrib. Mineral. Petrol.*, 143, 19-31.
- BEYSSAC, O. & CHOPIN, C. (2003): Comment on "Diamond, former coesite and supersilicic garnet in metasedimentary rocks from the Greek Rhodope: a new ultrahigh-pressure metamorphic province established" by E. D. Mposkos and D.K. Kostopoulos - [*Earth Planet. Sci. Lett.* 192 (2001) 497-506] *Earth. Planet. Sci. Lett.*, 214, 3-4, 669-674.
- BIINO, G. & COMPAGNONI, R. (1992): Very-High Pressure Metamorphism of the Brossasco Coronite Metagranite, Southern Dora-Maira-Massif, Western Alps. - *Schweiz. Mineral. Petrogr. Mitt.*, 72, 3, 347-363.
- BOCQUET, J. (1971): Cartes de répartition de quelques minéraux du métamorphisme alpin dans les Alpes franco-italiennes. - *Eclogae geol. Helv.*, 64, 71-103.
- BOCQUET, J. (1974): Etudes minéralogiques et pétrographiques sur les métasédiments d'âge alpin dans les Alpes françaises. - Thèse de doctorat, Grenoble, 476 p.
- BORGHI, A., CADOPPI, P., PORRO, A. & SACCHI, R. (1985): Metamorphism in the northern part of the Dora Maira Massif (Cottian Alps). - *Boll. Mus. Reg. Sci. Nat; Torino*, 3, 369-380.
- BORGHI, A., COMPAGNONI, R. & SANDRONE, R. (1996): Composite PT paths in the internal massifs of the Western Alps: petrological constraints to their thermomechanical evolution. - *Eclogae geol. Helv.* 89, 345-367.
- BOUFFETTE, J., LARDEAUX, J. M. & CARON, J. M. (1993): Le passage des granulites aux éclogites dans les métapélites de l'unité de la Punta Muret (Massif Dora-Maira, Alpes occidentales). - *C. R. Acad. Sci. Paris* 317/2, 1617-1624.
- BOUSQUET, R., GOFFÉ, B., HENRY, P., LE PICHON, X. & CHOPIN, C. (1997): Kinematic, thermal and petrological model of the Central Alps: Lepontine metamorphism in the Upper Crust and eclogitisation of the lower crust. - *Tectonophysics*, 273, 105-127.
- BROUWER, F. M., VISSERS, R. L. M. & LAMB, W. M. (2002): Metamorphic history of eclogitic metagabbro blocks from a tectonic melange in the Voltri Massif, Ligurian Alps, Italy. - *Ophioliti*, 27, 1, 1-16.
- BROUWER, F. M., VAN DE ZEDDE, D. M. A., WORTEL, M. J. R. & VISSERS, R. L. M. (2004): Late-orogenic heating during exhumation: Alpine PT trajectories and thermomechanical models. - *Earth. Planet. Sci. Lett.*, 220, 1-2, 185-199.

- BRUNET, F. & CHOPIN, C. (1995): Bearhite, $\text{Ca}_2\text{Al}(\text{PO}_4)_2\text{OH}$: synthesis, stability and thermodynamic properties. - *Contrib. Mineral. Petrol.*, 121, 258-266.
- CABELLA, R., CORTESOGNO, L., DALLAGIOVANNA, G., GAGGERO, L. & LUCCHETTI, G. (1991): Metamorfismo alpino a giadeite + quarzo in crosta continentale nel Brianzonese ligure. - *Atti Tic. Sci. Terra, Pavia*, 34, 43-54.
- CABELLA, R., CORTESOGNO, G., GAGGERO, L. & LUCCHETTI, G. (1994): Clinopyroxene through the blueschists facies metamorphisms of the Ligurian Alps: compositional variability and miscibility gaps. - *Atti Tic. Sci. Terra, Pavia (serie speciale)*, 1, 55-63.
- CABY, R., KIENAST, J. R. & SALIOT, P. (1978): Structure, Métamorphisme et modèle d'évolution tectonique des Alpes Occidentales. - *Rev. Géographie Phys. & Géol. dynamique*, 20, 307-322.
- CABY, R. (1996): Low-angle extrusion of high-pressure rocks and the balance between outward and inward displacements of Middle Penninic units in the western Alps. - *Eclogae geol. Helv.*, 89, 1, 229-267.
- CANNIC, S., LARDEAUX, J. M., MUGNIER, J. L. & HERNANDEZ, J. (1996): Tectono-metamorphic evolution of the Roignais-Versoyen Unit (Valaisan domain, France). - *Eclogae geol. Helv.*, 89, 1, 321-343.
- CARON, J. M. (1974): Rapports entre diverses 'generations' de lawsonite et les déformations dans les Schistes lustrés des Alpes cottiennes septentrionales (France et Italie). - *Bull. Soc. Geol. de France*, 16, 255-268.
- CARON, J. M. (1977): Lithostratigraphie et tectonique des schistes lustrés dans les Alpes cottiennes septentrionales et en Corse orientale. - *Sci. Géol., Strasbourg, mémoire* 48, 326p.
- CARON, J. M. & SALIOT, P. (1969): Nouveaux gisements de lawsonite et de jadeite dans les alpes franco-Italienne; *C. R. Acad. Sc. Paris*, 268, 3153-3156.
- CARON, J. M. & PÉQUIGNOT, G. (1986): The transition between blueschists and lawsonite-bearing eclogites based on observations from Corsican metabasalts. - *Lithos*, 19, 205-218.
- CARPENTER, M. A. (1980): Mechanism of exsolution in pyroxenes. - *Contrib. Mineral. Petrol.*, 71, 289-300.
- CHOPIN, C. (1981): Talc-phengite: a widespread assemblage in high-grade pelitic blueschists of the Western Alps. - *J. Petrol.* 22, 628-650.
- CHOPIN, C. (1983): Magnesiochloritoid, a key-mineral for the petrogenesis of high-grade pelitic blueschists. - *Bull. Minéral.*, 106, 715-717.
- CHOPIN, C. (1984): Coesite and pure pyrope in high-grade blueschists of the western Alps: a first record and some consequences. - *Contrib. Mineral. Petrol.*, 86, 107-118.
- CHOPIN, C. (1985): Les relations de phases à haute pression dans les roches pélitiques. Approche expérimentale et naturaliste. Conséquences géodynamiques pour les Alpes occidentales. - *Doctorat d'Etat, Université Paris 6, Mémoires des Sciences de la Terre n° 85-11*, 80 p. + annexes.
- CHOPIN, C. (1986): Phase relationships of ellenbergerite, a new high-pressure Mg-Al-Ti-silicate in pyrope-coesite-quartzite from the Western Alps. IN: *Blueschists and eclogites*, E. H. BROWN & B. W. EVANS (EDS). - *Geol. Soc. Amer. Mem.* 164, 31-42.
- CHOPIN, C. (1987): Very-high-pressure metamorphism in the western Alps: implications for the subduction of continental crust. IN: *Tectonic settings of regional metamorphism*, E. R. OXBURGH, B. W. D. YARDLEY, P. C. ENGLAND (EDS). - *Phil. Trans. Royal Soc. London A*-321, 183-197.
- CHOPIN, C. & SCHREYER, W. (1983): Magnesiochloritoid and Magnesiochloritoid: two index minerals of pelitic blueschists and their preliminary phase relations in the model system $\text{MgO-Al}_2\text{O}_3\text{-SiO}_2\text{-H}_2\text{O}$. - *Am. J. Sci.*, 283-A, 72-96.
- CHOPIN, C. & MONIÉ, P. (1984): A unique magnesiochloritoid-bearing, high-pressure assemblage from the Monte Rosa, Western Alps: petrologic and $^{40}\text{Ar}/^{39}\text{Ar}$ radiometric study. - *Contrib. Mineral. Petrol.*, 87, 388-398.
- CHOPIN, C., HENRY, C. & MICHARD, A. (1991): Geology and Petrology of the coesite-bearing, Dora Maira Massif, Western Alps. - *Eur. J. Mineral.*, 3, 263-289.

- CHOPIN, C., BRUNET, F., GEBERT, W., MEDENBACH, O. & TILLMANN, E. (1993): Bearthite, $\text{Ca}_2\text{Al}[\text{PO}_4]_2(\text{OH})$, a new mineral from high-pressure terranes of the western Alps. - *Schweiz. Mineral. Petrogr. Mitt.*, 73, 1-9.
- CHOPIN, C., FERRARIS, G., IVALDI, G., SCHERTL, H-P., SCHREYER, W., COMPAGNONI, R., DAVIDSON, C. & DAVIS, M. (1995): Magnesiodumortierite, a new mineral from very-high-pressure rocks (western Alps). II. Crystal chemistry and petrological significance. - *Eur. J. Mineral.*, 7, 525-535.
- CHOPIN, C. & SCHERTL, H. P. (1999): The UHP unit in the Dora Maira Massif, Western Alps. - *Int. Geo. Rev.*, 41, 765-780.
- CHOPIN, C., GOFFÉ, B., UNGARETTI, L. & OBERTI, R. (2003): Magnesio-stauroilite and zinc-stauroilite, a petrologic and crystal-chemical set-up. - *Eur. J. Mineral.*, 15, 167-176.
- COMPAGNONI, R. (1977): The Sesia-Lanzo zone: high pressure- low temperature metamorphism of the Austro-alpine continental margin. - *Rend. Soc. It. Min. Petrol.*, 33, 335-374.
- COMPAGNONI, R. (2003): HP metamorphic belt of the western Alps. - *EPISODES* 26, 3, 200-204.
- COMPAGNONI, R. & MAFFEO, B. (1973): Jadeite-Bearing Metagranites I. s. and Related Rocks in the Mount Mucrone Area (Sesia-Lanzo Zone, Western Italian Alps). - *Schweiz. Mineral. Petrogr. Mitt.*, 53, 3, 355-378.
- COMPAGNONI, R., HIRAJIMA T. & CHOPIN C. (1995): Ultrahigh-pressure metamorphism in the western Alps. Chapter 7 IN: Ultra-high-pressure metamorphism. COLEMAN, R. G. & WANG, X. (EDS). - Cambridge University Press, 206-243.
- DAL PIAZ, G. V. (1974): Le métamorphisme de haute-pression et basse-température dans l'évolution structurale du bassin ophiolitique alpino-apenninique. - *Schweiz. Mineral. Petr. Mitt.*, 54, 399-424.
- DAL PIAZ, G. V. & GRASSO, F. (1967): Le rodingiti I.s. nelle gallerie 'Petit Monde' della autostrada Quincinetto-Aosta; Rodingite in the 'Petit Monde' of the Quincinetto-Aosta tunnel. - *Boll. Soc. Geol. It.*, 86, 3, 395-401.
- DAL PIAZ, G. V. & ERNST, W. G. (1978): Areal geology and petrology of eclogites and associated metabasites of the Piemonte ophiolite nappe, Breuil-St. Jacques area, Italian Western Alps. - *Tectonophysics*, 51, 1-2, 99-126.
- DAL PIAZ, G. V. & LOMBARDO, B. (1986): Early Alpine eclogite metamorphism in the Penninic Monte Rosa-Gran Paradiso basement nappes of the western Alps. - *Geol. Soc. Am. Mem.*, 164, 249-265.
- DAL PIAZ, G. V., HUNZIKER, J. C. & MARTINOTTI, G. (1972): La zona Sesia-Lanzo e l'evoluzione tettonico-metamorfica delle Alpi nord-occidentali interne. - *Mem. Soc. Geol. It.* 11, 433-460.
- DESMONS, J., APRAHAMIAN, J., COMPAGNONI, R., CORTESOGNO, L. & FREY, M. (1999): Alpine metamorphism of the Western Alps: I. Middle to high T/P metamorphism. - *Schweiz. Mineral. Petrogr. Mitt.*, 79, 1, 89-110.
- DESMONS, J., COMPAGNONI, R., CORTESOGNO, L., FREY, M., GAGGERO, L., DALLAGIOVANNA, G., SENO, S. & RADELLI, L. (1999): Alpine metamorphism of the Western Alps: II. High-P/T and related pre-greenschist metamorphism. - *Schweiz. Mineral. Petrogr. Mitt.*, 79, 1, 111-134.
- DEVILLE, M., FUDRAL, S., LAGABRIELLE, Y., MARTHALER, M. & SARTORI, M. (1992): From oceanic closure to continental collision: A synthesis of the 'Schistes Lustrés' metamorphic complex of the Western Alps. - *Bull. Geol. Soc. Amer.*, 104, 127-139.
- DUCHENE, S., BLICHERT-TOFT, J., LUIS, B., TELOUK, P., LARDEAUX, J. M. & ALBAREDE, F. (1997): The Lu-Hf dating of alpine eclogites. - *Nature*, 387, 586-589.
- ELLENBERGER, F. (1958): Etude géologique du pays de Vanoise. - *Mém. expl. Carte géol. Fr.*, 1-562.
- ERNST, W. G. (1973): Interpretative synthesis of the metamorphism in the Alps. - *Bull. Geol. Soc. Amer.*, 84, 2053-2078.
- EVANS, B. W. (1990): Phase relations of epidote-blueschists. - *Lithos*, 25, 3-23.

- FREY, M., HUNZIKER, J. C., FRANK, W., BOCQUET, J., DAL PIAZ, G. V., JAGER, E. & NIGGLI, E. (1974): Alpine metamorphism of the Alps a review. - Schweiz. Mineral. Petrogr. Mitt., 54, 247-291.
- FREY, M., DESMONS, J. & NEUBAUER, F. (1999) The new metamorphic map of the Alps; 1:500000; 1:1000000, Schweiz. Mineral. Petrogr. Mitt., 79, 1, 230.
- GANNE, J., BUSSY, F. & VIDAL, O. (2003): Multi-stage garnet in the internal Briançonnais basement (Ambin massif, Savoie): New petrological constraints on the blueschist-facies metamorphism in the Western Alps and tectonic implications. - J. Petrol., 44, 7, 1281-1308.
- GAY, M. (1973): Le massif d'Ambin et son cadre de schistes lustres (Alpes franco-italiennes); evolution structurale. - Archives des Sciences. 25, 2, 165-214.
- GEBAUER, D. (1995): Geochronology of central and western Alps - new methods, new data, new interpretations. - 2nd workshop Alpine Geology, Basel, 32-34.
- GÉLY, J. P. (1989): Stratigraphie, tectonique et métamorphisme comparés de part et d'autre du Front pennique en Tarentaise (Alpes de Savoie, France). - Thèse de doctorat, Chambéry, 343 p.
- GELY, J. P. & BASSIAS, Y. (1990): Le front pennique: implications structurales d'un métamorphisme transporté (Savoie, France). - C. R. Acad. Sci. Paris, T. 310, Série II, 37-43.
- GILLET, P. & GOFFÉ, B. (1988): On the significance of aragonite occurrence in the Western Alps. - Contrib. Mineral. Petrol., 99, 70-81.
- GOFFÉ, B. (1975): Etude structurale et pétrographique du versant occidental du massif paléozoïque de Chasseforêt (Vanoise méridionale). - Thèse 3ème cycle, Orsay.
- GOFFÉ, B. (1977): Présence de cookéite dans les bauxites métamorphiques du dogger de Vanoise. - Bull. Soc. Fr. Miner. Crist., 100, 254-257.
- GOFFÉ, B. (1977): Succession de subfaciès métamorphiques en Vanoise méridionale (Savoie). - Contrib. Mineral. Petrol., 62, 23-41.
- GOFFÉ, B. (1980): Magnésiocarpholite, cookéite et euclase dans les niveaux continentaux métamorphiques de la zone briançonnaise. Données minéralogiques et nouvelles occurrences. - Bull. Mineral., 103, 297-302.
- GOFFÉ, B. (1982): Définition du faciès à Fe-Mg-carpholite-chloritoïde, un marqueur du métamorphisme de HP-BT dans les métasédiments alumineux. - Thèse Doct. Sci. Paris, 2 vol., 212p.
- GOFFÉ, B. (1984): Le faciès à carpholite-chloritoïde dans la couverture briançonnaise des Alpes Ligures: un témoin de l'histoire tectono-métamorphique régionale. - Mém. Soc. Géol. It., 28, 461-479.
- GOFFÉ, B., GOFFÉ-URBANO, G. & SALIOT P. (1973): Sur la présence d'une variété magnésienne de ferro-carpholite en Vanoise (Alpes françaises). Sa signification probable dans le métamorphisme alpin. - C.R. Acad. Sci., série D, 277, 1965-1968.
- GOFFÉ, B. & SALIOT, P. (1977) Les associations minéralogiques des roches hyperalumineuses du dogger de Vanoise. Leur signification dans le métamorphisme régional. - Bull. Soc. Fr. Miner. Crist., 100, 302-309.
- GOFFÉ, B. & VELDE, B. (1984): Contrasted metamorphic evolutions in the thrust cover units of Briançonnais zone (French Alps): a model for the conservation of HP-LT metamorphic mineral assemblages. - Earth. Plan. Sci. Lett., 68, 351-360.
- GOFFÉ, B. & VILLEY, M. (1984): Texture d'un matériel carboné impliqué dans un métamorphisme haute pression-basse température (Alpes françaises). Les hautes pressions influencent-elles la carbonification? - Bull. Mineral., 107, 81-91.
- GOFFÉ, B. & CHOPIN, C. (1986): High-pressure metamorphism in the Western Alps: zoneography of metapelites, chronology and consequences. - Schweiz. Mineral. Petrogr. Mitt., 66, 41-52.
- GOFFÉ, B., MURPHY, W. M. & LAGACHE, M. (1987): Experimental transport of Si, Al and Mg in hydrothermal solutions: an application to vein mineralization during high-temperature, low pressure metamorphism in French Alps. - Contrib. Mineral. Petrol., 97, 438-450.

- GOFFÉ, B. & BOUSQUET, R. (1997) Ferrocapholite, chloritoïde et lawsonite dans les métapélites des unités du Versoyen et du Petit St Bernard (zone valaisanne, Alpes occidentales). - *Schweiz. Mineral. Petrogr. Mitt.*, 77, 137-147.
- GOFFÉ, B., BOUSQUET, R., HENRY, P. & LE PICHON X. (2003): Effect of the chemical composition of the crust on the metamorphic evolution of orogenic wedges. - *J. metamorphic Geol.*, 21, 123-141.
- HENRY, C. (1990): L'Unité à coesite du massif de Dora maira dans son cadre pétrologique et structural (Alpes occidentales, Italie). - Ph D. Thesis, Université paris VI, 453p
- HENRY, C., BURKHARD, M. & GOFFÉ, B. (1996): Evolution of symetamorphic veins and their wallrocks through a Western Alps transect: no evidence for large-scale fluid flow! Stable isotope, major-, trace and rare-earth- elements systematics. - *Chemical Geology*, 127, 81-109.
- HIRAJIMA, T. & COMPAGNONI, R. (1993) Petrology of a jadeite quartz coesite almandine phengite fels with retrograde ferro-nyboite from the Dora-Maira massif, western Alps. - *Eur. J. Mineral.* 5, 5, 943-955.
- HUNZIKER, J. C., DESMONS, J. & HURFORD, A. J. (1992): Thirty-two years of geochronological work in the Central and Western Alps: a review on seven maps. - *Mém. Géol. Lausanne*, 13, 1-59.
- JABOYEDOFF, M. & THELIN, P. (1996): New data on low grade metamorphism in the Briançonnais domain of the Préalpes, Western Switzerland. - *Eur. J. Mineral.*, 8, 577.
- JULLIEN, M. & GOFFÉ, B. (1993): Occurrences de cookeite et de pyrophyllite dans les schistes du Dauphinois (Isère, France). Conséquences sur la répartition du métamorphisme dans les zones externes alpines. - *Schweiz. Mineral. Petrogr. Mitt.*, 73, 357-363.
- JULLIEN, M., BARONNET, A. & GOFFÉ, B. (1996): Ordering of the stacking sequence in cookeite ordering with increasing pressure: An HRTEM study. - *Amer. Mineral.*, 81, 67-78.
- KIENAST, J. R. & MESSIGA, B. (1987): Cr-rich Mg-chloritoid, a first record in high-pressure metagabbros from Monviso (Cottian Alps), Italy. - *Min. Mag.*, 51, Part 5, 681-687, illus. incl. 4 tables, 16 refs.
- KIENAST, J. R., LOMBARDO, B., BIINO, G. & PINARDON, J. L. (1991): Petrology of very-high-pressure eclogitic rocks from the Brossasco-Isasca Complex, Dora-Maira Massif, Italian Western Alps. - *J. metamorphic Geol.*, 9, 19-34.
- LARDEAUX, J. M., GOSSO, G., KIENAST, J. R., & LOMBARDO, B. (1982): Relations entre le métamorphisme et la déformation dans la zone Sesia-Lanzo (Alpes occidentales) et le problème de l'éclogitisation de la croûte continentale. - *Bull. Soc. géol. Fr.*, 7, 24, 793-800.
- LARDEAUX, J. M., LOMBARDO, B., GOSSO, G. & KIENAST, J. R. (1983): Découverte de paragenèses à ferro-omphacites dans les orthogneiss de la zone Sésia-Lanzo septentrionale (Alpes Italiennes). - *C.R. Acad. Sc. Paris*, t. 296, sér. II, 453-456.
- LARDEAUX, J. M., CARON, J. M., NISIO, P., PEQUIGNOT, G. & BOUDEULLE, M. (1986): Microstructural criteria for reliable thermometry in low-temperature eclogites. - *Lithos*, 19, 187-203.
- LARDEAUX, J. M., NISIO, P. & BOUDEULLE, M. (1987): Deformational and metamorphic history at the Lago Superiore area of the Monviso ophiolitic complex (Italian Western Alps): a record of subduction-collision cycle? - *Ophioliti*, 12, 3, 479-502.
- LARDEAUX, J. M. & SPALLA, M. I. (1991): From granulites to eclogites in the Sesia Zone (Italian Western Alps); a record of the opening and closure of the Piedmont ocean. IN: COMPAGNONI, R. & PICCARDO, G. B. (EDS), High-pressure metamorphism in the Western Alps. - *J. metamorphic Geol.*, 9, 1, 35-59.
- LEIKINE, M., KIENAST, J. R., ELTCHANINOFF-LANCELOT, C. & TRIBOULET, S. (1983): Le métamorphisme polyphasé des unités dauphinoises entre Belledonne et Mont Blanc (Alpes occidentales). Relation avec les épisodes de déformation. - *Bull. Soc. géol. France*, t XXV, 575-587.
- LOMBARDO, B., NERVO, R., COMPAGNONI, R., MESSIGA, B., KIENAST, J. R., MEVEL, C., FIORA, L., PICCARDO, G. B. & LANZA, R. (1978): Osservazioni preliminari sulle ofioliti metamorfiche del

- Monviso (Alpi Occidentali); Preliminary observations of the Monviso ophiolite complex; Western Alps. - *Rend. Soc. Ital. Miner. Petrol.*, 34, 2, 253-302.
- LOMBARDO, B. & POGNANTE, U. (1982): Tectonic implications in the evolution of the Western Alps ophiolite metagabbros IN: BORTOLOTTI, V. (ED), *Ophiolites and actualism.* - *Ofoliti*, 7, 2-3, 371-394.
- LOMBARDO, B. (1995) Studies on metamorphic rocks and minerals of the Western Alps; a volume in memory of Ugo Pognante (1954-1992) - *Bollettino Museo Regionale di Scienze Naturali*, 13, 2, Suppl., 362p.
- LUCCHETTI, G., CABELLA, R. & CORTESOGNO, L. (1990): Pumpellyites and coexisting minerals in different low-grade metamorphic facies of Liguria, Italy. - *J. metamorphic Geol.*, 8, 5, 539-550.
- MESSIGA, B. (1984): Il metamorfismo alpino nelle Alpi Liguri; alcuni aspetti petrologici; Alpine metamorphism in the Ligurian Alps; some petrologic aspects. IN: *Atti del convegno sul tema Geologia delle Alpi Liguri.* VANOSSI, M. (ED). - *Mem. Soc. Geol. Ital.*, 28, 151-179.
- MESSIGA, B. (1987): Alpine metamorphic evolution of Ligurian Alps (Northwest Italy) - chemography and petrological constraints inferred from metamorphic climax assemblages. - *Contrib. Mineral. Petrol.*, 95, 3, 269-277.
- MESSIGA, B., PICCARDO, G. B. & VANOSSI, M. (1978): Dati preliminari sulla distribuzione del metamorfismo alpino nei terreni pre-mesozoici liguri; Preliminary data on the distribution of alpine metamorphism in the territory of pre-Mesozoic Liguria. - *Rend. Soc. Ital. Min. Petr.*, 34, 2, 351-368.
- MESSIGA, B., OXILIA, M., PICCARDO, G. B. & VANOSSI, M. (1982): Fasi metamorfiche e deformazioni alpine nel Brianzonese e nel Pre-Piemontese - Piemontese esterno delle Alpi liguri: un possibile modello evolutivo. - *Rend. Soc. Ital. Miner. Petr.*, 38, 1, 261-280.
- MESSIGA, B., TRIBUZIO, R. & SCAMBELLURI, M. (1992): Mafic eclogites from the valosio crystalline massif (Ligurian Alps, Italy). - *Schweiz. Mineral. Petrogr. Mitt.*, 72, 3, 365-377.
- MESSIGA, B., SCAMBELLURI, M. & PICCARDO, G. B. (1995) Chloritoid-bearing assemblages in mafic systems and eclogite-facies hydration of alpine Mg-Al metagabbros (Erro-Tobbio unit, Ligurian Western Alps). - *Eur. J. Miner.*, 7, 5, 1149-1167.
- MESSIGA, B., KIENAST, J. R., REBAY, G., RICCARDI, M. P. & TRIBUZIO, R. (1999): Cr-rich magnesiochloritoid eclogites from the Monviso ophiolites (Western Alps, Italy). - *J. metamorphic Geol.*, 17, 3, 287-299.
- MICHARD, A., HENRY, C. & CHOPIN, C. (1995): Structures in ultrahigh-pressure rocks, a case study from the Alps. IN: Chapter 4: Ultra-high-pressure metamorphism, R.G. COLEMAN & X. WANG (EDS). - Cambridge University Press, 132-158.
- MONIÉ, P. & PHILIPOT, P. (1989): Mise en évidence de l'âge éocène moyen du métamorphisme de haute pression dans la nappe ophiolitique du Monviso (Alpes occidentales) par la méthode ^{40}Ar - ^{39}Ar . - *C.R. Acad. Sci. Paris*, 309/2, 245-251.
- MONIÉ, P. & CHOPIN, C. (1991): $^{40}\text{Ar}/^{39}\text{Ar}$ dating in coesite-bearing and associated units of the Dora-Maira massif, Western Alps. - *Eur. J. Mineral.* 3, 239-262.
- NISIO, P. & LARDEAUX, J. M. (1987): Retromorphic Fe-rich talc in low-temperature eclogites: example from Monviso (Italian Western Alps). - *Bull. Minéral.*, 110, 427-437.
- OBERHÄNSLI, R., J. C. HUNZIKER, G. MARTINOTTI & STERN, W. F. (1982): Monte Muchrone: Eine eoalpin eklogitsierter permischer Granit. - *Schweiz. Mineral. Petrogr. Mitt.* 62.
- OBERHÄNSLI, R., HUNZIKER, J. C., MARTINOTTI, G. & STERN, W. B. (1985): Geochemistry geochronology and petrology of Monte Muchrone: an example of Eo-Alpine eclogitization of Permian granitoids in the Sesia-Lanzo zone, Western Alps, Italy. - *Chemical Geology*, 52, 165-184.
- OBERHÄNSLI, R., GOFFÉ, B. & BOUSQUET, R. (1995): Record of a HP-LT metamorphic evolution in the Valais zone; Geodynamic implications. IN: *Studies on metamorphic rocks and minerals of the Western Alps*,

- B. LOMBARDO (ED.). - Boll. Museo Reg. Sci. Nat., 13/2, 221-240.
- PHILIPPOT, P. & SCAMBELLURI, M. (1995): The composition and behaviour of fluids in high-pressure rocks from the Alps: a review. IN: Studies on metamorphic rocks and minerals of the western alps, LOMBARDO, B. (ED). – Suppl. Boll. museo regionale di scienze naturali, 13, 75-102.
- PIANTONE, P. (1980) Magmatisme et Métamorphisme des roches intrusives calco-alkalines du Carbonifère briannonnais entre Arc et Durance : minéralogie, pétrographie, géochimie. -Thèse 3eme cycle, Univ. Sci. Médic. Grenoble, 215p.
- POGNANTE, U. (1980): Preliminary data on the Piemonte ophiolite nappe in the lower Val Susa-Val Chisone area, Italian western Alps. - *Ofoliti*, 5, 2-3, 221-240.
- POGNANTE, U. (1984): Eclogitic versus blueschist metamorphism in the internal Western Alps along the Susa Valley traverse. - *Sciences Geologiques (Bulletin)*, 37, 1, 29-36.
- POGNANTE, U. (1989): Lawsonite, blueschist and eclogite formation in the southern Sesia zone (western Alps, Italy). - *Eur. J. Mineral.*, 1, 89-104.
- POGNANTE, U. (1991): Petrological constraints on the eclogite- and blueschist-facies metamorphism and P-T-t paths in the Western Alps. - *J. metamorphic Geol.*, 9, 5-17.
- POGNANTE, U., LOMBARDO, B. & VENTURELLI, G. (1982): Petrology and geochemistry of Fe-Ti gabbros and plagiogranites from the Western Alps ophiolites. - *Schweiz. Mineral. Petrogr. Mitt.*, 62, 3, 457-472.
- POGNANTE, U. & KIENAST, J. R. (1987): Blueschist and eclogite transformations in Fe-Ti gabbros; a case from the Western Alps ophiolites. - *J. Petrol.*, 28, 2, 271-292.
- POGNANTE, U., TALARICO, F., RASTELLI, N. & FERRATI, N. (1987): High pressure metamorphism in the nappes of the Valle dell'Orco traverse (Western Alps collisional belt). - *J. metamorphic Geol.*, 5, 3, 397-414.
- POGNANTE, U., TALARICO, F. & BENNA, P. (1988): Incomplete blueschist re-crystallization in high-grade metamorphics from the Sesia-Lanzo Unit (Vasario-Sparone Subunit, Western Alps); a case history of metastability. - *Lithos*, 21, 2, 129-142.
- POGNANTE, U. & SANDRONE, R. (1989): Eclogites in the northern Dora-Maira Nappe (Western Alps, Italy). - *Mineralogy and Petrology*, 40, 1, 57-71.
- POINSSOT, C., GOFFÉ, B. & TOULHOAT, P. (1997): Geochemistry of the Triassic-Jurassic Alpine continental deposits: origin and geodynamic implications. - *Soc Géol. Fr.*, 168, 3, 287-300.
- ROLLAND, Y., LARDEAUX, J. M., GUILLOT, S. & NICOLLET, C. (2000): A comparison of syn-convergent extension, vertical pinching, and metamorphic units at the western margin of Grand Paradis, French-Italian Alps. - *Geodinamica Acta*, 13, 2-3, 133-148.
- SALOT, P. (1978): Le métamorphisme dans les Alpes françaises. - Thèse d'Etat, Univ. Paris, 1-183.
- SALOT, P. (1979): La jadéite dans les Alpes françaises. - *Bull. Minéral.*, 102, 391-401.
- SALOT, P., DAL PIAZ, G. V. & FREY, M. (1980): Métamorphisme de haute-pression dans les Alpes franco-italo-suissees. - *Géologie Alpine* 56:203-215
- SALOT, P. & VELDE, B. (1982): Phengite composition and post-nappe high-pressure metamorphism in the Pennine zone of the French Alps. - *Earth. Planet. Sci. Lett.*, 57, 133-138.
- SANDRONE, R., SACCHI, R., CORDOLA, M., FONTAN, D. & VILLA, I. M. (1988): Metadiorites in the Dora-Maira polymetamorphic basement (Cottian Alps). - *Rend. Soc. It. Mineral. Petrol.* 43, 593-608.
- SARTORI, M. (1988): L'unité du Barrhorn (zone pennique, Valais, Suisse). Un lien entre les Préalpes médianes rigides et leur socle paléozoïque. - Thèse de doctorat, Université de Lausanne, 157 p.
- SCHERTL, H. P., SCHREYER, W. & CHOPIN, C. (1991): The pyrope-coesite rocks and their country rocks at Parigi, Dora Maira Massif, western Alps: detailed Petrography, Mineral Chemistry and PT-Path. *Contrib. Mineral. Petrol.*, 108, 1-21.

- SCHÜRCH, M. L. (1987): Les ophiolites de la zone du versoyen : témoin d'un bassin à évolution métamorphique complexe. - Thèse de doctorat, Genève, 157 p.
- SCHÜRCH, M.-L., BERTRAND, J., CHESSEX, R. & LOUBAT, H. (1986): Présence de l'omphacite dans la zone du Versoyen (Alpes franco-italiennes): implications structurales. - Abstr. 4e réunion groupe tect. Suisse Genève déc. 1986.
- SCHWARTZ, S. (2001) : La zone piémontaise des Alpes occidentale: un paléo-complexe de subduction; arguments métamorphiques, géochronologiques et structuraux. - Doc. BRGM, vol. 302, 313 pp.
- SCHWARTZ, S., LARDEAUX, J. M. & TRICART P. (2000): La zone d'Acceglio (Alpes cottiennes): un nouvel exemple de croûte continentale éclogitisée dans les Alpes occidentales. - C. R. Acad. Sci. Fr, 312, 859-866.
- SCHWARTZ, S., LARDEAUX, J. M., GUILLOT, S. & TRICART, P. (2000): Diversité du métamorphisme éclogitique dans le massif ophiolitique du Monviso (Alpes occidentales, Italie). - Geodinamica Acta, 13, 169-188.
- SICARD, E, CARON, J. M., POTDEVIN, J. L. & DECHOMETS, R. (1986): Mass-transfer and synmetamorphic deformation in a fold .2. Lawsonite pseudomorphs and characterization of interstitial fluids. Bull. Mineral, 109, 4, 411-422.
- SIMON, G., CHOPIN, C. & SCHENK, V. (1997): Near-end-member magnesiochloritoid in prograde-zoned pyrope, Dora-Maira massif, Western Alps. - Lithos, in press
- SPALLA, M. I, DE MARIA, L., GOSSO, G., MILETTO, M. & POGNANTE, U. (1983): Deformazione e metamorfismo della Zona Sesia-Lanzo meridionale al contatto con la falda piemontese e con il Massiccio di Lanzo, Alpi Occidentali. Gosso, G., Atti del convegno sul Terna; "Geologia strutturale e stratigrafia" Mem. Soc. Geol. It., 26, 2, 499-514.
- SPALLA, M. I., LARDEAUX, J. M., DALPIAZ, G. V., GOSSO, G. & MESSIGA, B. (1996): Tectonic significance of Alpine eclogites. - Journal of Geodynamics., 21, 3, 257-285.
- STEEN, D. & BERTRAND, J. (1977) Sur la présence de ferrocapholite associée aux schistes à glaucophane de haute Ubaye (Basses Alpes, France). - Schweiz. Mineral. Petrogr. Mitt., 57, 157-168.
- VANOSSI, M. (1981): Les unités géologiques des Alpes maritimes entre l'Ellero et la mer Ligure; un aperçu schématique. - Mem. Sci. Geol. It., 34, 101-142.
- VANOSSI, M. (1990): Alpi Liguri. Parte generale. Guide Geol. Region. - Soc. Geol. It. 2, 13-55.
- VANOSSI, M., CORTESOGNO, C., GALBIATI, B., MASSIGA, B., PICCARDO, G., VANNUCI, R., (1984): Geologia delle alpi Liguri : Dati, problemi, ipotesi. - Mem. Soc. Geol. It., 28, 5-75.
- VIDAL, O. & GOFFÉ, B. (1991): Cookeite $\text{LiAl}(\text{Si}_3\text{Al})\text{O}_{10}(\text{OH})_8$: Experimental study and thermodynamical analysis of its compatibility relations in the $\text{Li}_2\text{O}-\text{Al}_2\text{O}_3-\text{SiO}_2-\text{H}_2\text{O}$ system. - Contrib. Mineral. Petrol., 108, 72-81.
- VIDAL, O., GOFFÉ, B. & THEYE, T. (1992): Experimental study of the stability of sudoite and magnesio-carpholite and calculation of a new petrogenetic grid for the system $\text{FeO}-\text{MgO}-\text{Al}_2\text{O}_3-\text{SiO}_2-\text{H}_2\text{O}$. - J. metamorphic Geol, 10, 603-614.
- VUICHARD, J. P. & BALLÈVRE, M. (1988): Garnet-chloritoid equilibria in eclogitic pelitic rocks from the Sesia zone (Western Alps): their bearing on phase relations in high pressure metapelites. - J. metamorphic Geol., 6, 135-157.

manuscript received: June 2004

manuscript accepted: July 2004

**EXPLANATORY NOTES TO THE MAP:
METAMORPHIC STRUCTURE OF THE ALPS
TRANSITION FROM THE WESTERN TO THE CENTRAL ALPS**

by

**Romain Bousquet¹, Martin Engi², Guido Gosso³, Roland Oberhänsli⁴, Alfons Berger²,
Maria Iole Spalla³, Michele Zucali³ & Bruno Goffè⁵**

¹Department of Earth Sciences

University of Basel, Bernoullistrasse 30, CH-4056 Basel, Switzerland

²Institute of Geological Sciences

University of Bern, Baltzersstrasse 1-3, CH-3012 Bern, Switzerland

³Dipartimento di Scienze della Terra

Università di Milano, Via Manggiagalli 34, I-20133 Milano, Italy

⁴Institut für Geowissenschaften

Universität Potsdam, Karl-Liebknecht-Str. 25, 14476 Potsdam-Golm, Germany

⁵Laboratoire de Géologie

UMR 8538, CNRS, Ecole Normale Supérieure, 24 rue Lhomond, 75005 Paris, France

The northern-western Alps, located between two major tectonic structures, the Simplon and the Aosta-Ranzolla faults, represent a "transition" zone where all paleogeographic domains involved within the alpine orogenic wedge are present and clearly distinguishable on a map (e.g. BIGI et al., 1990; SCHMID et al., 2004). The structural style and metamorphic record in the area linking the West and South-West Lepontine to the Western Alps has particular characteristics, which warrant this separate chapter. This concerns the Lepontine zone from just East of Valle d'Ossola to the western limit set by the continental Bernhard nappe system in the North-West, the ocean-derived Piedmont-Ligurian zone and its prolongation to the west (Préalps), as well continental units issued either from the Adriatic continent domain (Sesia and Dent-Blanche massifs) or from the European margin (Mt Blanc massif).

All units will be described after that from east to west following Figure 1, while structural relationship between different units is described in details in SCHMID et al. (2004).

Sesia zone

The Sesia Zone (SZ) of the western Austroalpine is a huge portion of Alpine continental crust widely recording alpine eclogite-facies assemblages. For the very first time it was possible to demonstrate that even granites were brought outside the stability field of plagioclase and recrystallized under eclogite facies conditions (DAL PIAZ et al., 1972; COMPAGNONI & MAF-FEO, 1976; COMPAGNONI et al., 1977; LARDEAUX et al., 1982; OBERHÄNSLI et al., 1982).

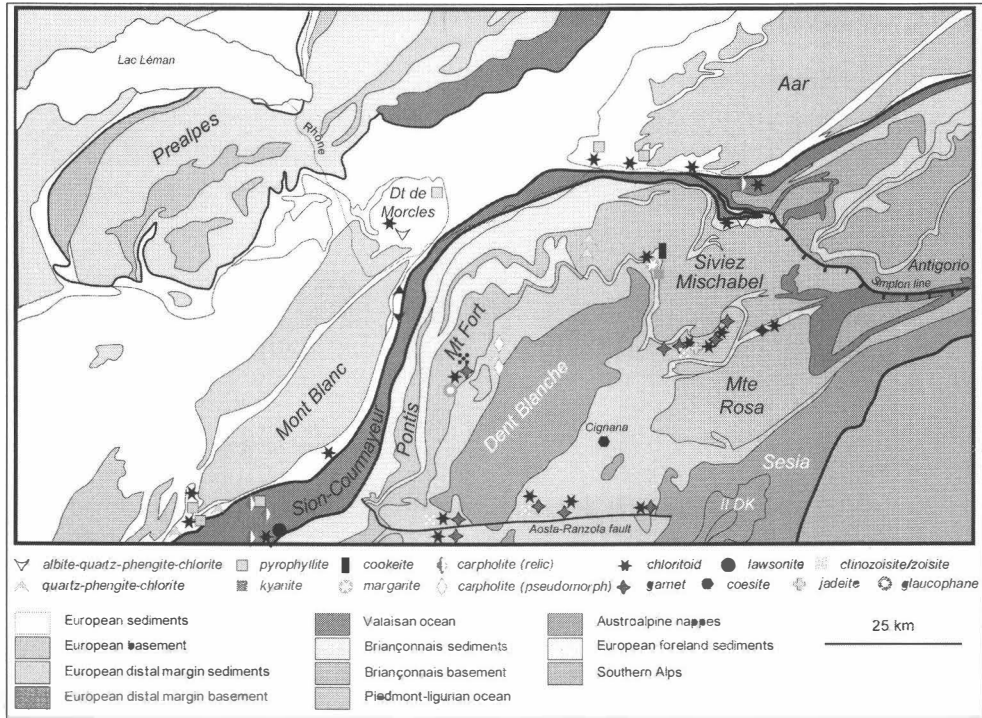


Figure 1

Structural map of the "transition" area between the Simplon line and the Aosta-Ranzola fault (after BIGI et al., 1990; SCHMID et al., 2004) displaying occurrences of metamorphic index mineral indicating greenschist, blueschist and eclogites metamorphic conditions observed in Mesozoic Alpine metasediments.

The Sesia Lanzo zone consists of an upper and a lower unit: the lower unit comprises the Gneiss Minuti Complex (GMC) and the Eclogitic Micaschists Complex (EMC), whereas the upper unit is constituted by the II Dioritic-Kinzigitic Zone (IIDK and Vasaro units; e.g. COMPAGNONI et al., 1977; POGNANTE et al., 1987). The upper unit is characterised by high-pressure blueschist mineral assemblages and its contact with the lower unit is marked by mylonitic belts, developed under eclogite or blueschist facies conditions (LARDEAUX et al., 1982; POGNANTE et al., 1987) and later overprinted by greenschist facies mylonites (RIDLEY, 1989; STÜNITZ, 1989). In the central and southern part of the lower unit, the alpine evolution is characterised by a LT eclogite imprint, following by a blueschist re-equilibration during the decompression (e.g. CASTELLI, 1991; POGNANTE, 1991 and references therein), and then by a low-pressure greenschist facies overprint (OBERHÄNSLI et al., 1985). Gneiss Minuti Complex and Eclogitic Micaschists Complex, both pervasively eclogitized, strongly differ in the volume percentage of greenschist retrogression. The Gneiss Minuti Complex, is widely re-equilibrated under greenschist facies conditions. This greenschist imprint is generally associated to mylonitic textures (STUENITZ, 1989; SPALLA et al., 1991). On the other hand, in the Eclogitic Micaschists Complex, which constitutes the innermost part of the Sesia Zone, the greenschist facies overprint is confined to discrete shear zones, more pervasively developed towards its inner boundary with the Southern Alps.

The Alpine structures are crosscutting by calc-alkaline and ultrapotassic dykes during Oligocene (DAL PIAZ et al., 1972, 1979). In the southernmost part of the massif, some thrust sheets, the metamorphic complex of Rocca Canavese thrust sheets, display mineral assemblages indicating blueschist facies conditions (POGNANTE, 1989a; 1989b). These thin tectonic slices are separated from each other by alpine blueschist mylonitic horizons. These differences in mineralogical occurrences could be interpreted either as an effect of the chemical composition of the rocks (RUBIE, 1986; RIDLEY, 1986) or by different metamorphic evolution. In this latter case, the coupling of EMC, GMC and RCT units is interpreted to have occurred in blueschist facies conditions, synchronous with the early exhumation stages of the Eclogitic Micaschists Complex (POGNANTE, 1989b). In the northern part of the Sesia zone SLZ, the lower unit display mineral assemblages indicating upper blueschist facies conditions similar to those of the upper (IIDK) unit.

The very low T/P ratio, characterising the SLZ Alpine metamorphic history, favours preservation of pre-Alpine relic assemblages in spite of several a strong greenschist overprint. This ancient granulite to amphibolite evolution could be interpreted as consequent to a lithospheric extension-related uplift of the pre-Alpine lower crust, during Permo-Triassic times (DAL PIAZ, 1993; LARDEAUX & SPALLA, 1991; REBAY & SPALLA, 2001).

Piedmont-Ligurian unit

The Piedmont-Ligurian zone in the north of the Western Alps is classically divided into two units, the Tsaté nappe (or Combinzone) and the Zermatt-Saas nappe (e.g SARTORI & THÉLIN, 1987; DAL PIAZ, 1999 and references therein), separated by a major extensional fault (BALLÈVRE & MERLE, 1993; REDDY et al., 2003). The distinction between both units was based both on lithostratigraphic (BEARTH, 1962; MARTHALER, 1984; MARTHALER & STAMPFLI, 1989) and on metamorphic differences (DAL PIAZ, 1965; KIENAST, 1973; CABY et al., 1978).

The lowermost unit, the Zermatt-Saas nappe, is composed mainly of mafic and ultramafic ophiolites, displaying an oceanic affinity. Since the famous BEARTH'S work, this nappe is well known for its high-pressure mineral assemblages (BEARTH, 1967; ERNST & DAL PIAZ, 1978; CHINNER & DIXON, 1973). The discovery of coesite inclusions within garnet in some Mn-bearing metasediments in Lago di Cignana suggests that some piece of the Piedmont-Ligurian were deeply subducted up to 28 kbar at 600°C (REINECKE, 1991). The most eclogites of the Zermatt-Saas nappe display high-pressure mineral assemblages formed by omphacite-garnet-chloritoid-talc-zoisite or omphacite-garnet-kyanite-clinozoisite ± talc (OBERHÄNSLI, 1980; BARNICOAT & FRY, 1986; GANGUIN, 1988). The eclogites are strongly retrogressed into epidote amphibolites ± garnet toward the contact with the uppermost unit in the West.

The uppermost unit, the Tsaté nappe, is an ophiolitic unit dominated by carbonate and terrigenous calcschists, alternating with tholeiitic metabasalts. The lack of eclogites and relics of sodic amphiboles in metabasites (DAL PIAZ & ERNST, 1978; AYRTON et al., 1982; SPERLICH, 1988) as well in Mn-rich quartzitic schists associated with Mn-rich garnets (DAL PIAZ, 1979b; CABY, 1981) have been led to consider the Tsaté nappe to have overall the same metamorphic evolution, both western and eastern of the Dent-Blanche. However the ground of metasediments shows a metamorphic gradient from west to east (Fig. 1).

Calcschists and other terrigenous sediments display pseudomorphs after carpholite (PFEIFFER et al., 1991) in the west and relics of garnet, Mg-rich chloritoid and phengite assemblages in strongly retrogressed albite-rich metapelites in the east at the contact with eclogites of the Zermatt-Saas nappe.

At the base of the Tsaté nappe occur discontinuous exotic sheets of continental origin (Cime Bianche and Frilhorn units) displaying jadeite-quartz-phengite mineral assemblages (SCHAUB, pers. com.).

The western end of the Lepontine dome and the Monte Rosa

The western culmination of the Lepontine Alps (i.e. the Toce dome) imparts a westerly axial plunge to the Pennine nappe stack. This results in successively higher thrust sheets being visible at today's erosional level, from the lowest Penninic gneiss units (e.g. Antigorio nappe) up to the Austroalpine Dent Blanche nappe appearing at the top, some 50 km further west. The nappe system is polydeformed and cut by the late orogenic (D4) Simplon fault, running to the NW from Valle d'Ossola to Simplon Pass. Tectonic unroofing by this major ductile/brittle normal fault (MANCKTELOW, 1985) brought the high grade Lepontine belt into a position opposite the greenschist facies Grand St-Bernard nappe system. The NW-part of the Simplon line marks the western limit of the Central Alpine amphibolite facies. In the Simplon area this Barrovian overprint has been dated at ~30 Ma (garnet growth in metaclastics, VANCE & O'NIONS, 1992). By contrast, in the area W and SW of Domodossola the Barrovian amphibolite facies/greenschist facies boundary crosscuts all major tectonic boundaries, and the medium pressure overprint is the sequel of an earlier (Eocene) HP-history. Decompression stages dated between 38 and 32 Ma in the western Monte Rosa nappe, but as young as 26 Ma in its eastern section (ENGI et al., 2001b), can be linked with the evolution in the Moncucco-Camughera unit, where KELLER (2004) showed the Barrovian reequilibration to be associated with D3 back-thrusting (top-WSW) and dextral shearing at amphibolite facies conditions. These are responsible for the sillimanite and staurolite zone boundaries shown in (Fig. 2); as in the eastern TAC units (NAGEL et al., 2002; ENGI et al., 2004) these Al-phases were formed at the expense of paragonite and phengite during decompression (at $P \sim 1.1-0.8$ MPa), but with no evidence of a heating spike (KELLER, 2004). In the upper parts of the Monte Rosa nappe and westerly adjacent units, the decompressional Barrovian overprint reached only greenschist facies, as shown already by BEARTH (1958) who mapped the albite/oligoclase isograd (Fig. 2).

The geometry of the metamorphic zone boundaries in the westernmost Lepontine and southerly adjacent nappes is remarkable, as it reflects (a) the rapid exhumation of the Pennine nappe stack of the Central Alps, and (b) the strong dextral transpression at their southern contacts. This led to a far more rapid thermal quench in the eastern part of the Central Alps (in ENGI et al., 2004), with closely spaced isotherms as compared to the western part, where they are more widely spaced. The successive transfer of heat from the Central Alpine block is also reflected in the succession of isograds extending to the south of the Centovalli line, a ductile-brittle fault running from Locarno to Valle d'Ossola (Fig. 1), which evidently served as a major truncation surface in the late-Alpine exhumation history of the Central Alps.

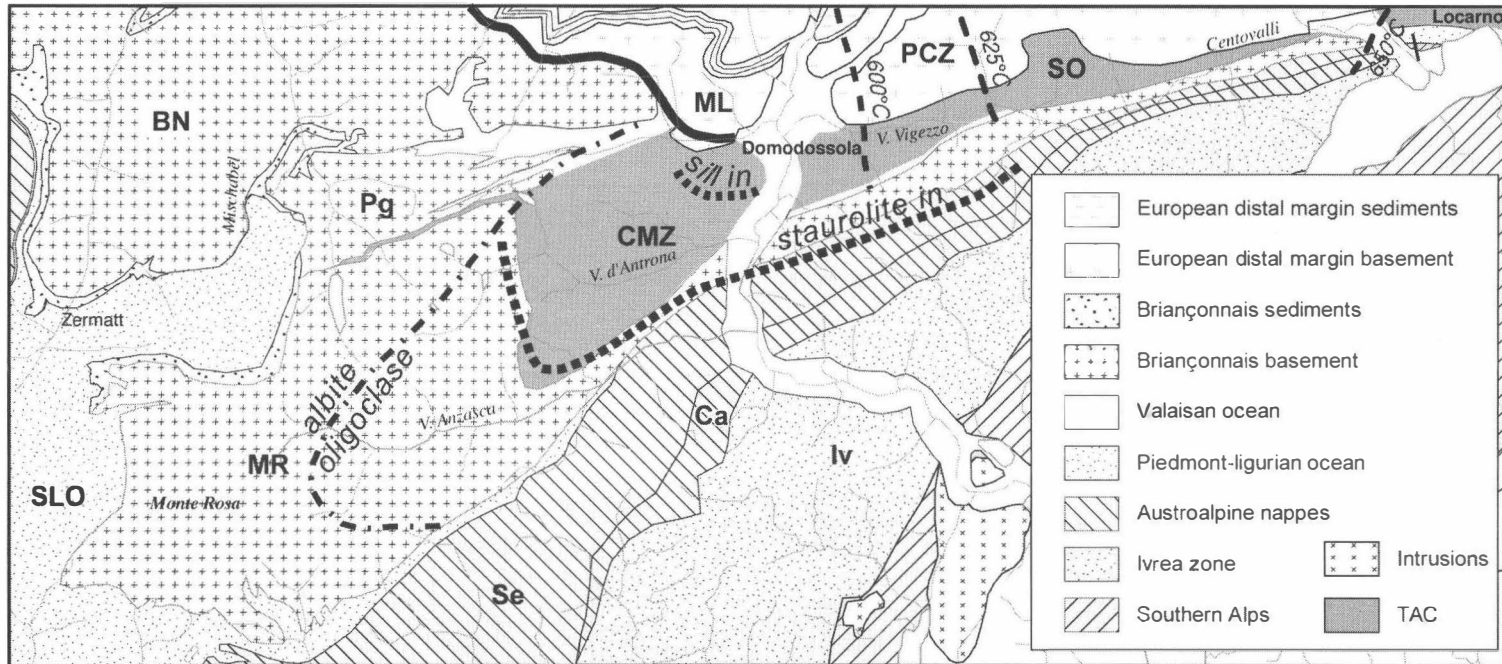


Fig. 2
 Metamorphic elements in the transition zone from the Central Alps to the Western Alps, updated from ENGI et al. (2001b) using data from KELLER (2004).
 Iv: Ivrea Zone, ML: Monte Leone nappe, MR: Monte Rosa nappe, Se: Sesia zone.

The Monte Rosa nappe and in its footwall neighbors (Camughera-Moncucco and Antrona unit) are tentatively considered to be part of the tectonic accretion channel (TAC, ENGI et al., 2001a). These TAC units reveal evidence of an earlier collisional HP phase which reached eclogite facies during D₁/D₂ decompressional deformation, with top to N or NW thrusting (KELLER, 2004). HP metamorphism has also been extensively documented from units further to the SW and W. Recent geochronological results, however, challenge the earlier views of a common eclogite stage for these two groups (e.g. discussion in HANDY et al., 2004). It appears now that the classic "Eoalpine" stage (DAL PIAZ et al., 1972; HUNZIKER, 1974), which is Late Cretaceous according to more recent data (reviewed by DAL PIAZ, 1999) is restricted to units such as the Sesia-Lanzo zone (as well as units of the Western Alps s.s.), whereas the Saas-Zermatt zone, Monte Rosa nappe, and underlying units reached eclogite facies during the Eocene (CHOPIN & MONIÉ, 1984 and summary in DAL PIAZ, 1999), with maximum pressures of 1.4-1.6 GPa at 500-550°C (BORGHI et al., 1996; ENGI et al., 2001b; KELLER, 2004). The last pre-Tertiary metamorphic imprint in the Monte Rosa nappe is not Cretaceous but Permian and yielded widespread low-P assemblages (BEARTH, 1952, PAWLIG & BAUMGARTNER, 2001).

Dent Blanche

The alpine metamorphic events in the Dent Blanche rocks are polyphase. The last major phase of metamorphism affecting all rocks of this unit produced mineral assemblages of the lower to upper greenschist facies. This greenschist facies event was preceded by subduction related high-pressure metamorphism. The rocks of the Dent Blanche nappe have been affected in various degrees by this event and the preservation of high-pressure indications is variable. Contrarily to the underlying eclogite facies rocks of the Zermatt-Saas Fee unit (BEARTH 1959, 1967), the Dent Blanche rocks only experienced epidote-blueschist facies or transitional alkali-amphibole greenschist facies conditions (BALLÈVRE & MERLE, 1993; CORTIANA et al., 1998). Sodic amphiboles were found in mylonites along the contacts of Permian Gabbros (STRØN, 1990) and in the northernmost part of the nappe (AYRTON et al., 1982). The gneisses of the Arolla series also contain relics of the Eo-alpine event. Thermobarometry with phengite+Kfs+biotite+chlorite yields P-T conditions of 0.10 to 0.12 GPa and 350-400°C (OBERHÄNSLI & BUCHER, 1987; BUCHER et al., 2004). The rocks of the Valpelline series contain chloritoid and kyanite replacing sillimanite as indicators of a high-pressure phase (KIENAST & NICOT, 1971; DE LEO et al., 1987; CANEPA et al., 1990; PENNACCHIONI & GUERMANI, 1993). An early Alpine assemblage of glaucophane-crossite and aegirine-augite coexisting with phengite yielded an age of 75 Ma in the Pillonet klippe (CORTIANA et al. 1998).

The Briançonnais domain

The Briançonnais microcontinent in this part of the Alps, classically called Grand St-Bernard nappe system (LUGEON & ARGAND, 1905), consists of several units (see details in ESCHER, 1988; GOUFFON, 1993) that display different metamorphic evolution (THÉLIN et al., 1994). The major part, of the called Grand St-Bernard nappe system, formed by the Houillère zone and the Siviez-Mischabel unit, displays a metamorphic evolution within greenschist facies conditions.

The Siviez-Mischabel unit is characterized by an augen-schist horizon with albite megaporphyroblasts that extends for hundred kilometres along the contact with the basement. Texture and mineralogy vary little in this horizon and indicate a synkinematic crystallization of albite porphyroblasts (SARTORI & THÉLIN, 1987).

In two units, one in the north (the Barrhorn series), one in the south (the Pontis unit), high-pressure greenschist mineralogy has been described. The Barrhorn series, located on the top of the Siviez-Mischabel unit, contains pockets of. The rock-forming minerals of the metabasites are phengite, Zn-staurolite, kyanite, margarite, chloritoid, diaspore, paragonite \pm cookeite (SARTORI, 1990; CHOPIN et al., 2003). Southward in the Pontis unit, pinched between the Houillère zone and the Siviez-Mischabel unit, micaschists contain neocrystallization of chloritoid \pm kyanite (OULIANOFF & TRÜMPY, 1958) parallel to the main foliation (GOUFFON & BURRI, 1997). Paradoxically this is the uppermost unit of the Grand St-Bernard nappe system, the Mont Fort unit that display the deepest evolution into high-pressure metamorphic conditions. The Alpine metamorphic evolution is characterized by extensive development of mineral assemblage of epidote-blueschist facies conditions: chloritoid, glaucophane, epidote, garnet, phengite (SCHAER, 1959; BEARTH, 1963).

The "external" units: Valaisan - Mt Blanc - Préalps

Pinched between two continental domains (the Briançonnais microcontinent and the European margin), metasediments of the Sion-Courmayeur zone represent a second oceanic domain, the Valaisan ocean, situated north to the Piedmont-Ligurian (FRISCH, 1979; STAMPFLI, 1993). Metamorphism of this area is characterized by high-pressure conditions (blueschist to eclogites, BOUSQUET et al., 2002; GOFFÉ et al., 2004).

The Mont Blanc massif is one of several Variscan "external crystalline massifs" of the European margin within western and central Alps. It is made of paragneisses, orthogneisses, migmatites and granites (BONIN et al., 1993). During the Tertiary, the Mont Blanc massif was affected by the Alpine orogeny and developed a non pervasive greenschist facies metamorphic assemblage that consists, in granites, of quartz, albite, muscovite, biotite, chlorite, epidote and stilpnomelane (VON RAUMER, 1974; BORGHI et al., 1987). The Mont Blanc Massif is also well known for its hydrothermal veins mainly filled by chlorite, quartz, muscovite, adularia and calcite (POTY et al., 1974). These veins have been dated at 13-18 Ma in the granite using K/Ar and Rb/Sr techniques on adularia and muscovite (LEUTWEIN et al., 1970) and are contemporaneous with shear zones containing biotite-muscovite-chlorite-epidote-quartz-albite assemblages.

The Préalps consist of cover nappes of Triassic to Eocene formations, derived from the Valais, Briançonnais and Piedmont-Ligurian domains. These nappes escaped of their original setting before that these later undergone in subduction. Thus the Préalps suffered only low metamorphic conditions. Occurrences of diaspore, pyrophyllite, paragonite, phengites and corrensite in the Préalps Médiannes (JABOYEDOFF & THÉLIN, 1996, and references therein) and of prehnite, pumpellyite, epidote, actinolite, sodic amphibole, stilpnomelane in gabbro and diabase of the Gêts nappes are the main indicator of the low metamorphic conditions (BERTRAND, 1970; BILL et al., 2001). This main metamorphic event affected the Préalps during their Penninic origin, and the process responsible for the metamorphism was progressive burial by thrust stacking, probably during late Eocene (JABOYEDOFF & THÉLIN, 1996).

References

- AYRTON, S., BUGNON, C., HAARPAINTER, T., WEIDNMANN, M. & FRANK, E. (1982): Géologie du front de la nappe de la Dent Blanche dans la région des Monts-Dolin. - *Ecolgae Geol. Helv.* 75, 269-286.
- BALLÈVRE, M. & MERLE, O. (1993): The Combin Fault: compressional reactivation of a Late Cretaceous-Early Tertiary detachment fault in the Western Alps. - *Schweiz. Mineral. Petrogr. Mitt.* 73, 205-227.
- BARNICOAT, A. C. & FRY, N. (1986): High-pressure metamorphism of the Zermatt-Saas ophiolite zone, Switzerland. - *J. Geol. Soc.* 143, 607.
- BEARTH, P. (1952): Geologie und Petrographie des Monte Rosa. - *Beitr. geol. Karte Schweiz.* - 96. Bern, of 94 pp.
- BEARTH, P. (1958): Ueber einen Wechsel der Mineralfazies in der Wurzelzone des Penninikums. - *Schweiz. Mineral. Petrogr. Mitt.* 38, 363-373.
- BEARTH, P. (1959): Ueber Eklogite, Glaukophanschiefer und metamorphe Pillowlaven. *Schweiz. Mineral. Petrogr. Mitt.* 39, 267-286.
- BEARTH, P. (1962): Versuch einer Gliederung alpinmetamorpher Serien der Westalpen. - *Schweiz. Mineral. Petrogr. Mitt.* 42, 127-137.
- BEARTH, P. (1963): Contribution à la subdivision tectonique et stratigraphique du cristallin de la nappe du Grand Saint-Bernard dans le Valais (Suisse). - In: DURAND DELGA, M. (ed.): *Livre à la mémoire du Professeur Fallot.* - 2. Mémoire de la Société géologique de France, Paris, 407-418.
- BEARTH, P. (1967): Die Ophiolite der Zone von Zermatt-Saas Fee. - *Beitr. geol. Karte Schweiz.* - 132. Bern, of 130 pp.
- BERTRAND, J. (1970): Etude pétrographique des ophiolites et des granites du flysch des Gêts (Haute-Savoie, France). - *Arch. Sci. (Genève)* 23, 279-342.
- BIGI, G., CASTELLARIN, A., COLI, M., DALPIAZ, G. V., SARTORI, R., SCANDONE, P. & VAI, G. B. (1990): Structural model of Italy 1:50'000, Sheet 1. In: (ed.)^(eds): *Progetto Geodinamica. SELCA, Firenze,*
- BILL, M., MASSON, H. & THÉLIN, P. (2001): Low-grade metamorphism of the Gets nappe (Western Alps). - *Schweiz. Mineral. Petrogr. Mitt.* 81/2, 229-238.
- BONIN, B., BRANDLEIN, P., BUSSY, F., DESMONS, J., EGGENBERGER, U., FINGER, F., GRAF, K., MARRO, C., MERCOLII, I., OBERHÄNSLI, R., PLOQUIN, A., VON QUADT, A., VON RAUMER, J. F., SCHALTEGGER, U., P. S. H., VISONI, D. & VIVIER, G. (1993): Late Variscan magmatic evolution of the Alpine basement. - In: VON RAUMER, J. F. & NEUBAUER, F. (ed.): *Pre-Mesozoic Geology in the Alps.* - Springer, Heidelberg, 171-201.
- BORGHI, A., GALLO, L. M. & PORRO, A. (1987): Osservazioni petrografiche nel settore francese del traforo del Monte Bianco. - *Bollettino del Museo Regionale di Scienze Naturali* 5, 69-96.
- BORGHI, A., COMPAGNONI, R. & SANDRONE, R. (1996): Composite P-T paths in the internal Penninic massifs of the western Alps: Petrological constraints to their thermo-mechanical evolution. - *Ecolgae Geol. Helv.* 89/1, 345-367
- BOUSQUET, R., GOFFÉ, B., VIDAL, O., OBERHÄNSLI, R. & PATRIAT, M. (2002): The tectono-metamorphic history of the Valaisan domain from the Western to the Central Alps: New constraints for the evolution of the Alps. - *Bulletin of the Geological Society of America* 114/2, 207-225.
- BUCHER, K., DALPIAZ, G. V., OBERHÄNSLI, R., GOUFFON, Y., MARTINOTTI, G. & POLINO, R. (2004): Blatt 1347 Matterhorn - 1:25000, Erläut. - *Geologisches Atlas der Schweiz* 107,
- CABY, R., KIENAST, J.-R. & SALIOT, P. (1978): Structure, métamorphisme et modèle d'évolution tectonique des Alpes Occidentales. - *Rev. Géogr. phys. Géol. dyn.* XX/4, 307-322.
- CABY, R. (1981): Le Mésozoïque de la zone du Combin en Val d'Aoste (Alpes Graies) : Imbrications tectoniques entre séries issues des domaines pennique, austroalpin et océanique. - *Géologie Alpine* 57, 5-13.

- CANEPA, M., CASTELLETTO, M., CESARE, B., MARTIN, S. & ZAGGIA, L. (1990): The Austroalpine Mont Mary nappe (Italian Western Alps). - *Mem. Sc. Geol.* 42, 1-17.
- CASTELLI, D. (1991): Eclogitic metamorphism in carbonate rocks: the example of impure marbles from the Sesia - Lanzo Zone, Italian Western Alps. - *J. Metamorph. Geol.* 9, 61-77.
- CHINNER, G. A. & DIXON, J. E. (1973): Some High-Pressure Parageneses of Allalin Gabbro, Valais, Switzerland. - *J. Petrology* 14/2, 185-202.
- CHOPIN, C. & MONIÉ, P. (1984): A unique magnesiochloritoid-bearing, high-pressure assemblage from the Monte Rosa, Western Alps: petrologic and ^{40}Ar - ^{39}Ar radiometric study. - *Contrib. Mineral. Petrol.* 87, 388-398.
- CHOPIN, C., GOFFÉ, B., UNGARETTI, L. & OBERTI, R. (2003): Magnesio-staurolite and zincostaurolite: mineral description with a petrogenetic and crystal-chemical update. - *Eur. J. of Mineral.* 15, 167-176.
- CORTIANA, G., DAL PIAZ, G. V., DEL MORO, A., HUNZIKER, J.-C. & MARTIN, S. (1998): ^{40}Ar - ^{39}Ar and Rb-Sr dating of the Pillonet klippe and Sesia-Lanzo basal slice in the Ayas valley and evolution of the Austroalpine-Piedmont nappe stack. - *Mem. Sc. Geol.* 50, 177-194.
- DAL PIAZ, G. V. (1965): La formation mesozoica dei calescisti con pietre verdi fra la Valsesia e la Valtourmanche ed i suoi rapporti strutturali con il recopimento Monte Rosa e con la Zona Sesia-Lanzo. - *Boll. Soc. Geol. It.* 84, 67-104.
- DALPIAZ, G. V., HUNZIKER, J. C. & MARTINOTTI, G. (1972): La Zona Sesia - Lanzo e l'evoluzione tettonico-metamorfica delle Alpi Nordoccidentali interne. - *Mem. Soc. Geol. It.* 11, 433-460.
- DAL PIAZ, G. V. & ERNST, W. G. (1978): Areal geology and petrology of eclogites and associated metabasites of the piemontese ophiolite nappe, Breuil-St. Jacques area, Italian Western Alps. - *Tectonophysics* 51, 99-136.
- DAL PIAZ, G. V., VENTURELLI, G. & SCOLARI, A. (1979): Calc-alkaline to ultrapotassic post-collisional volcanic activity in the internal northwestern Alps. - *Mem. Instit. Geol. Min. Univ. Padova* /32,
- DAL PIAZ, G. V., DI BATTISTINI, G., KIENAST, J.-R. & VENTURELLI, G. (1979): Manganiferous quartzitic schists of the Piemonte ophiolite nappe in the Valsesia-Valtourmanche area (Italian Western Alps). - *Mem. Sc. Geol.* 32, 4-24.
- DAL PIAZ, G. V. (1993): Evolution of Austroalpine and Upper Penninic basement in the Northwestern Alps from Variscan convergence to post-Variscan extension. - In: VON RAUMER, J. & NEUBAUER, F. (ed.): *Pre-Mesozoic geology in the Alps*. - Springer, 325-342.
- DAL PIAZ, G. V. (1999): The Austroalpine-Piedmont nappe stack and the puzzle of Alpine Tethys. - In: GOSSO, G., JADOUL, F., SELLA, M. & SPALLA, M. I. (ed.): *3rd Workshop on Alpine Geological Studies*. - 55. *Memorie di Scienze Geologiche*, Padova, 155-176.
- DE LEO, S., BIINO, G. & COMPAGNONI, R. (1987): Riequilibrazioni metamorfiche alpine nelle serie di Valpelline e di Arolla a nord di Bionaz (Valpelline, Aosta). - *Rend. Soc. It. Min. Petr.* 42, 181-182.
- ENGI, M., SCHERRER, N. C. & BURRI, T. (2001): Metamorphic evolution of pelitic rocks of the Monte Rosa nappe: Constraints from petrology and single grain monazite age data. - *Schweiz. Mineral. Petrogr. Mitt.* 81/3, 305-328.
- ENGI, M., BERGER, A. & ROSELLE, G. T. (2001): Role of the accretion channel in collisional orogeny. - *Geology* 29/12, 1143-1146.
- ENGI, M., BOUSQUET, R. & BERGER, A. (2004): Metamorphic Structure of the Alps: Central Alps. - *Mitt. Österr. Min. Ges.*, 149, 157-173.
- ERNST, W. G. & DAL PIAZ, G. V. (1978): Mineral parageneses of eclogitic rocks and related mafic schists of the Piemonte ophiolite nappe, Breuil-St Jacques area, Italian Western Alps. - *Am. Mineral.* 63, 621-640.
- ESCHER, A. (1998): Structure de la nappe du Grand Saint-Bernard entre le val de Bagnes et les Mischabel. - *Rapp. géol. Serv. hydrog. géol. nat.* - 7. Bern, of pp.

- FRISCH, W. (1979): Tectonic progradation and plate tectonics of the Alps. - *Tectonophysics* 60, 121-139.
- GANGUIN, J. (1988): Contribution à la caractérisation du métamorphisme polyphase de la zone de Zermatt-Saas Fee (Alpes valaisannes). - Unpubl. Ph. D, ETH, of 312 pp.
- GOFFÉ, B., SCHWARTZ, S., LARDEAUX, J. M. BOUSQUET, R. (2004): Metamorphic Structure of the Alps: Western and Ligurian Alps. - *Mitt.Österr.Min.Ges.*, 149, 125-144.
- GOUFFON, Y. (1993): Géologie de la "nappe" du Grand St-Bernard entre la Doire Baltée et la frontière suisse. - *Mémoires de Géologie.* - Lausanne, of pp.
- GOUFFON, Y. & BURRI, M. (1997): Les nappes des Pontis, de Siviez-Michabel et du Mont Fort dans les vallées de Bagnes, d'Entremont (Valais, Suisse) et d'Aoste (Italie). - *Eclogae Geol. Helv.* 90, 29-41.
- HANDY, M. R. & OBERHÄNSLI, R. (2004): Metamorphic Structure of the Alps: Age map of the metamorphic structure of the Alps – tectonic interpretation and outstanding problems. - *Mitt.Österr.Min.Ges.*, 149, 201-226.
- HUNZIKER, J. C. (1974): Rb-Sr and K-Ar age determination and the Alpine history of the Western Alps. - *Mem. Ist. Geol. Mineral. Univ. Padova* 31, 1-54.
- JABOYEDOFF, M. & THÉLIN, P. (1996): New data on low-grade metamorphism in the Briançonnais domain of the prealps, Western Switzerland. - *Eur. J. of Mineral.* 8, 577-592.
- KELLER, L. (2004): Relationships between metamorphism and deformation: Examples on the micro- to macro-scale from the Western Alps (Camughera-Moncucco unit and Monte Rosa nappe, N-Italy). - Unpubl. Ph.D., University of Basel, of 133 pp.
- KIENAST, J. R. & NICOT, E. (1971): Presence of a Disthene Paragenesis and Chloritoid Probably Alpine in Sillimanite Gneiss, Garnet and Cordierite of Valpelline (Val d'Aoste, Italy). - *C. R. Acad. Sci. Paris* 272/14, 1836-1840.
- KIENAST, J.-R. (1973): Sur l'existence de deux séries différentes au sein de l'ensemble des "Schistes Lustrés-ophiolites" du Val d'Aoste, quelques arguments fondés sur les roches métamorphiques. - *C. R. Acad. Sci. Paris* 276, 2621-2624.
- LARDEAUX, J.-M., GOSSO, G., KIENAST, J.-R. & LOMBARDO, B. (1982): Relations entre le métamorphisme et la déformation dans la zone Sésia-Lanzo (Alpes Occidentales) et le problème de l'éclogitisation de la croûte continentale. - *Bull. Soc. géol. Fr.* 24/4, 793-800.
- LARDEAUX, J. M. & SPALLA, M. I. (1991): From Granulites to Eclogites in the Sesia Zone (Italian Western Alps) - a Record of the Opening and Closure of the Piedmont Ocean. - *J. Metamorph. Geol.* 9/1, 35-59.
- LEUTWEIN, F., POTY, B., SONET, J. J. & ZIMMERMAN, J. L. (1970): Age des cavités à cristaux du granite du Mont Blanc. - *C. R. Acad. Sci. Paris* 271, 156-158.
- LUGEON, M. & ARGAND, E. (1905): Sur les grandes nappes de recouvrement de la zone du piémont. - *C. R. Acad. Sci. Paris* 140, 1364-1367.
- MANCKTELOW, N. S. (1985): The Simplon Line: a major displacement zone in the western Lepontine Alps. - *Eclogae Geol. Helv.* 78/1, 73-96.
- MARTHALER, M. (1984): Géologie des unités penniques entre le val d'Anniviers et le val de Tourtmagne. - *Eclogae Geol. Helv.* 77, 395-448.
- MARTHALER, M. & STAMPFLI, G. M. (1989): Les schistes lustrés à ophiolites de la nappe du Tsaté: un ancien prisme d'accrétion issu de la marge active apulienne? - *Schweiz. Mineral. Petrogr. Mitt.* 69, 211-216.
- NAGEL, T., DE CAPITANI, C. & FREY, M. (2002): Isograds and PT evolution in the eastern Lepontine Alps, Switzerland. - *J. Metamorph. Geol.* 20/3, 309-324.
- OBERHÄNSLI, R. (1980): P-T Bestimmungen anhand von Mineralanalysen in Eklogiten und Glaukophaniten der Ophiolite von Zermatt. - *Schweiz. Mineral. Petrogr. Mitt.* 60, 215-235.
- OBERHÄNSLI, R., HUNZIKER, J.-C., MARTINOTTI, G. & STERN, W. B. (1985): Geochemistry, geochronology and petrology of Monte Mucrone: an example of Eo-alpine eclogitization of pernian granitoids in

- the Sesia-Lanzo zone, Western Alps, Italy. - *Chem. Geol.* 52, 165-184.
- OBERHÄNSLI, R. & BUCHER, K. (1987): Tectonometamorphic evolution of the Dent Blanche nappe. - *Terra Cognita* 7/2-3, 95.
- OULIANOFF, N. & TRÜMPY, R. (1958): Grand Saint Bernard. In: (ed.)^(eds): Atlas géologique de la Suisse au 1:25'000. Commission géologique de la Suisse, Bern,
- PAWLIG, S. & BAUMGARTNER, L. P. (2001): Geochemistry of a talc-kyanite-chloritoid shear zone within the Monte Rosa granite, Val d'Ayas, Italy. - *Schweiz. Mineral. Petrogr. Mitt.* 81/3, 329-346.
- PENNACCHIONI, G. & GUERNANI, A. (1993): The mylonites of the Austroalpine Dent Blanche nappe along the northwestern side of the Valpelline valley (Italian Western Alps). - *Mem. Sc. Geol.* 45, 37-55.
- PFEIFFER, H. R., COLOMBI, A., GANGUIN, J., HUNZIKER, J.-C., OBERHÄNSLI, R. & SANTINI, L. (1991): Relics of high-pressure metamorphism in different lithologies of the Central Alps, an updated inventory. - *Schweiz. Mineral. Petrogr. Mitt.* 71, 441-451.
- POGNANTE, U. (1987): Incomplete blueschist re-crystallization in high grade metamorphics from the Sesia-Lanzo unit (Vasario - Sparone subunit, Western Alps ophiolites): a case history of metastability. - *Lithos* 21, 129-142.
- POGNANTE, U. (1989): Lawsonite, blueschist and eclogite formation in the southern Sesia Zone (Western Alps, Italy). - *Eur. J. of Mineral.* 1, 89-104.
- POGNANTE, U. (1989): Tectonic implications of lawsonite formation in the Sesia zone (Western Alps). - *Tectonophysics* 162, 219-227.
- POGNANTE, U. (1991): Petrological constraints on the eclogite- and blueschist-facies metamorphism and P-T-t paths in the Western Alps. - *J. Metamorph. Geol.* 9, 5-17.
- POTY, B., STADLER, H. A. & WEISBROD, A. M. (1974): Fluid inclusion studies in quartz from fissures of the Western and Central Alps. - *Schweiz. Mineral. Petrogr. Mitt.* 54, 717-752.
- REBAY, G. & SPALLA, M. I. (2001): Emplacement at granulite facies conditions of the Sesia-Lanzo metagabbros: an early record of Permian rifting? - *Lithos* 58, 85-104.
- REDDY, S., WHEELER, J., BUTLER, R. W. H., CLIFF, R. A., FREEMAN, S. R., INGER, S., PICKLES, C. & KELLEY, S. P. (2003): Kinematic reworking and exhumation within the convergent Alpine Orogen. - *Tectonophysics* 365, 77-102.
- REINECKE, T. (1991): Very-high-pressure metamorphism and uplift of coesite-bearing metasediments from the Zermatt-Saas zone, Western Alps. - *Eur. J. of Mineral.* 3, 7-17.
- RIDLEY, J. R. & THOMPSON, A. B. (1986): The Role of Mineral Kinetics in the Development of Metamorphic Microtextures. - In: WALTHER, J. V. & WOOD, B. J. (ed.): *Fluid-Rock Interactions during Metamorphism. Advances in Physical Geochemistry.* - 5. Springer, 154-193.
- RUBIE, D. C. (1986): The Catalysis of Mineral Reactions by Water and Restrictions on the Presence of Aqueous Fluid During Metamorphism. - *Min. Mag.* 50/357, 399-415.
- SARTORI, M. & THÉLIN, P. (1987): Les schistes œillés albitiques de Barneuzza (Nappe de Siviez-Michabel, Valais, Suisse). - *Schweiz. Mineral. Petrogr. Mitt.* 87/3, 229-256.
- SARTORI, M. (1990): L'unité du Barrhorn (zone pennique, Valais, Suisse). - *Mémoires de Géologie.* - 6. Lausanne, of 156 pp.
- SCHAER, J.-P. (1959): Géologie de la partie septentrionale de l'éventail de Bagnes (entre le Val d'Hérémence et le Vaal de Bagnes, Valais, Suisse). - *Arch. Sci. (Genève)* 12, 473-620.
- SPALLA, M. I., LARDEAUX, J.-M., DAL PIAZ, G. V. & GOSSO, G. (1991): Métamorphisme et tectonique à la marge externe de la zone Sesia-Lanzo (Alpes occidentales). - *Mem. Sc. Geol.* 43, 361-369.
- SPERLICH, R. (1988): The transition from crossite to actinolite in metabasites of the Combin unit in Vallée St. Barthélemy (Aosta, Italy). - *Schweiz. Mineral. Petrogr. Mitt.* 68, 215-224.

- STAMPFLI, G. M. (1993): Le Briançonnais, terrain exotique dans les Alpes? - *Eclogae Geol. Helv.* 86/1, 1-45.
- STRØM, E. (1990): Petrography, Deformation and Metamorphism of the Arolla Cross Section, SW-Switzerland. - Unpubl. Cand. Sci. Thesis, of pp.
- STÜNITZ, H. (1989): Partitioning of metamorphism and deformation in the boundary region of the "Seconda Zona Diorito-Kinzigitica", Sesia Zone, Western Alps. - Unpubl. Ph. D n°8817, ETH Zürich.
- THÉLIN, P., GOUFFON, Y. & ALLIMANN, M. (1994): Caractéristiques et métamorphisme des phyllosilicates dans la partie occidentale de la "super" nappe du Grand St-Bernard (Val d'Aoste, Valais). - *Bulletin de géologie, Lausanne* 327, 93-145.
- VANCE, D. & O'NIONS, R. K. (1992): Prograde and retrograde thermal histories from the Central Swiss Alps. - *Earth Planet. Sci. Lett.* 114, 113-129.
- VON RAUMER, J. (1974): Zur Metamorphose amphibolitischer Gesteine im Altkristallin des Mont Blanc- und Aiguilles-Rouges-Massivs. - *Schweiz. Mineral. Petrogr. Mitt.* 54, 471-488.

manuscript received: June 2004

manuscript accepted: July 2004

**EXPLANATORY NOTES TO THE MAP:
METAMORPHIC STRUCTURE OF THE ALPS
CENTRAL ALPS**

by

Martin Engi¹, Romain Bousquet² & Alfons Berger¹

¹Institute of Geological Sciences
University of Bern, Baltzersstrasse 1-3, CH-3012 Bern, Switzerland
²Department of Earth Sciences
University of Basel, Bernoullistrasse 30, CH-4056 Basel, Switzerland

The area of the Central Alps (Fig. 1) is delimited by the Subalpine Swiss Molasse to the north, the Austroalpine nappes in the Grisons and the Bergell in the east, and the Insubric Line to the south. The western limit is geologically less evident and is somewhat arbitrarily set in the Simplon area. Within the core portion of the Alpine orogen, some 72% of the (pre-Quaternary) units exposed have witnessed at least one pre-Alpine orogeny. Evidence of polymetamorphism is thus widespread in the basement; relics from the Variscan (Hercynian), Caledonian, and even Precambrian orogenies have been recognized. The intensity of the Alpine overprint is quite variable, and this had plagued early efforts of documenting regional metamorphic patterns (NIGGLI, 1974). Over the past thirty years it has become possible, despite the poly-orogenic metamorphic record, to decipher the Alpine cycle in considerable detail, by combining tectonic and seismic studies with petrology and geochronology.

The Central Alps comprise units attributed to four paleogeographic domains, from N to S:

<u>Domain</u>	<u>Original setting</u>
Helvetic shelf	Distal continental margin of the European craton
North-Pennine (= Valais)	Small oceanic basin (opening: Early Cretaceous)
Middle Penninic (= Briançonnais)	Microcontinental platform
South Pennine (= Piemont-Liguria)	Oceanic basin (opening: Middle Jurassic)

The Austroalpine orogenic lid has been entirely removed, by erosion and tectonic unroofing, in the area of the Central Alps. Whereas their external parts (Helvetic nappes and Penninic Prealps; Fig. 1) are almost entirely composed of post-Variscan shelf sediments, the imbricate thrust sheets in the Lepontine area are dominated by pre-Triassic crystalline cores. These basement units (of the European and Briançonnais domains) comprise largely supracrustal rock types, with abundant granitoid gneiss and clastic schist, subordinate amphibolite, and only minor other rock types. Relics of pre-Alpine orogenic reworking are more abundant in the External Massifs and in the northern parts of the Lepontine area, where the Alpine overprint is modest, but even in units which during the mid-Tertiary reached upper amphibolite facies, traces of a polycyclic history are not uncommon.

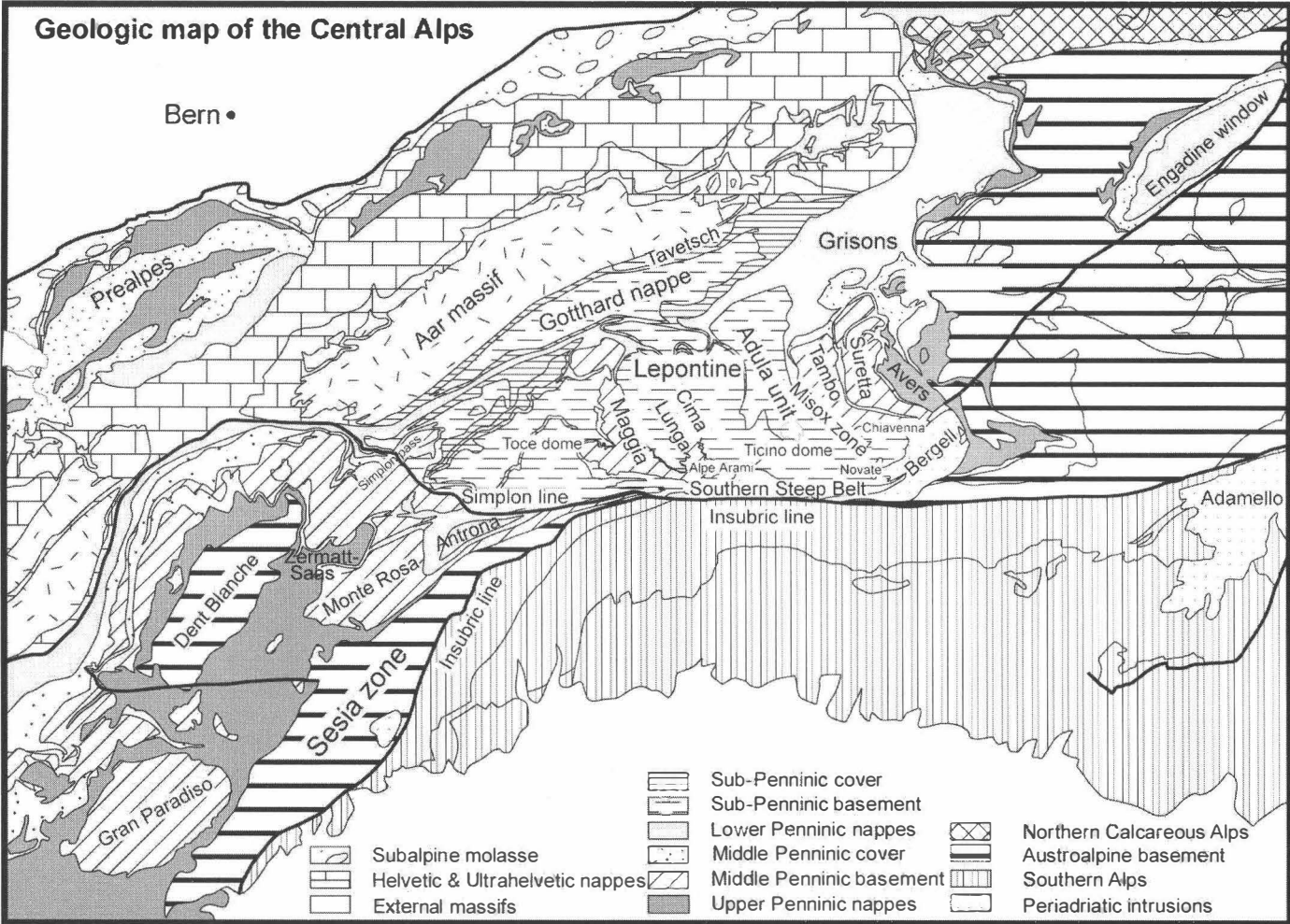


Fig. 1
Map showing locations and tectonic units to which the text refers.

This chapter presents the metamorphic evolution recognized in the Central Alps in chronological sequence, outlining the present state of understanding and indicating some of the limits. To keep the text concise, references to the essential primary data are far from exhaustive. Recent reviews are cited where available, and progress due to studies not treated in these is summarized in more detail. Still, it is not possible here to refer to all relevant studies produced in this classic orogen.

Pre-Alpine metamorphism in the Central Alps

At least two pre-Alpine cycles of orogenic metamorphism and deformation have been recognized in the External massifs and in the northernmost thrust sheets, all belonging to paleo-Europe. Following Proterozoic magmatism in a rift setting, Ordovician (Caledonian) high grade metamorphism and magmatism is well established, notably in the External Massifs, and the Permian (Variscan) magmatic and metamorphic imprint affected all of the basement units.

Caledonian orogeny: Case studies in the Central Alps (ABRECHT et al., 1991; ABRECHT & BIINO, 1994; BIINO, G., 1994; 1995; BIINO, G. G. et al., 1997) show eclogite facies and \pm coeval granulite facies conditions. In the Gotthard and Tavetsch nappes for example, lawsonite grew on the prograde path, and eclogite formation peaked at $P_{\max} \sim 2.4 \pm 0.3$ GPa and $T \sim 680 \pm 30^\circ\text{C}$; the subsequent granulite and migmatite stages occurred at $0.9\text{-}0.7$ and $0.7\text{-}0.5$ GPa, respectively, all at about the same temperature. This evolution reflects a collisional orogeny dated at $\sim 460\text{-}464$ Ma (OBERLI et al., 1994; GEBAUER et al., 1988). However, several stages of migmatite formation have been dated between 470 and 445 Ma, a period for which larger magmatic intrusions, both basic and granitic, are known from various units (as reviewed by SCHALTEGGER & GEBAUER, 1999). Amphibolite facies grade metamorphism and migmatites are widespread in the late Ordovician, as are large granitoid intrusives (MERCOLLI et al., 1994). To account for the tectono-metamorphic imprint during the Caledonian cycle, an active margin setting of a peri-Gondwana micro-continent has been invoked (VON RAUMER, 1998; VON RAUMER et al., 1999).

Variscan continent-continent collision: This cycle left its imprint both in the sedimentary record (Early Carboniferous synorogenic flysch: MATTE, 1986; FLÜGEL, 1990) and in widespread syn- and late-orogenic magmatism (360-320 Ma and 320-260 Ma, respectively). The metamorphic grade reached (low- to medium-P) amphibolite facies in the Central Alps. The overprint was thus less pronounced than in the Caledonian orogeny, but the effects of the two cycles are often difficult to distinguish. The spatial distribution of the Variscan phenomena suggests that continental terranes were accreted between the Silurian and the Devonian to the upper plate, now exposed e.g. in the External Massifs of the northern Central Alps. No such accretion is known from the (Variscan) lower plate, i.e. in Austroalpine and Southern Alpine units.

Alpine metamorphism in the Central Alps

Metamorphic assemblages in post-Variscan units, notably in post-Permian sedimentary sequences, are definitely attributable to the Tertiary Alpine cycles (NIGGLI, 1960). Yet even in such samples, evidence of a plurifacial Alpine metamorphism is fairly common in the Central Alps.

Similarly, this part of the Alpine orogen shows several generations of structural overprint (MILNES, 1974b; 1974a). Both the tectonic and metamorphic patterns in the Lepontine appear rather simple at first sight, concealing much of the complexity of their evolution. The nappe stack as a whole shows a central part which is relatively flat lying, despite two young, regional culminations (Ticino and Toce domes), whereas two steep belts delimit this central part both to the north and south. However, detailed studies of the structural evolution in several parts of the Lepontine nappe stack (e.g. northern Maggia-Lebendun: GRUJIC & MANCKTELOW, 1996; southern Simano-Adula: NAGEL et al., 2002b) indicate at least four phases of deformation, from early nappe-forming (D_1 and D_2 ; main schistosity and tight folds) to exhumation-related deformation, including the late-orogenic back-folding. Efforts to decipher the concomitant metamorphic evolution have recognized three discrete phases based on petrologic analysis and geochronology: (1) High-pressure assemblages of Eocene age are restricted to certain tectonic units; (2) a pervasive medium-pressure (Barrovian) overprint, connected with Oligocene nappe stacking, affected the Lepontine as a whole, postdates D_2 and either outlasted or was (locally) affected by D_3 ; (3) a far less pervasive, late-orogenic phase attained lower metamorphic grades, but was locally quite effective, notably related with hydrothermal fluids.

High-Pressure Relics in the Central Alps

a. Low- to medium-temperature HP rocks are found in several Middle- and South-Pennine units outside the Lepontine (amphibolite facies) belt, notably in the following:

- Several nappes, with different metamorphic patterns due to different tectonic histories, represent the Piemont-Ligurian domain in eastern part of the Central Alps. Regional metamorphic grade in these units was classically viewed (NABHOLZ, 1945) to increase from anchizonal conditions in the North (near Arosa, FERREIRO-MÄHLMANN, 1995) to biotite-greenschist facies to the south (Val Malenco, TROMMSDORFF & NIEVERGELT, 1983). However recent studies have recognized more complexity in the regional metamorphic distribution. In units mainly composed of mafic and ultramafic rocks (Arosa, Platta, Malenco), which have a thin Jurassic cover, overprinting under greenschist facies conditions only has been reported for the Alpine metamorphism dated between 70 and 100 Ma (PHILIPP, 1982; HANDY et al., 1996). On the other hand in the Avers unit, where the Piemont-Ligurian domain is mainly composed of Jurassic marbles and Cretaceous calcschists (equivalents to the Schistes Lustés in the Western Alps) with some MORB-type metabasalts, abundant evidence of HP metamorphism has been documented. Mineral assemblages such as Gln-Gt \pm Ctd in metabasalts (OBERHÄNSLI, 1978), Gln-phengite in marbles, and Gt-Ctd in calcschists (WIDERKEHR, pers. com.) indicate Tertiary metamorphic conditions around 12 kbar and 400°C (RING, 1992a; 1992b). A major shear zone (Turba mylonite zone) separates Avers Bündnerschiefer from the Platta nappe (NIEVERGELT et al., 1996).
- To the East of the Lepontine, the Briançonnais microcontinent is reduced to two basement units (Tambo and Suretta nappes) and a metasedimentary nappe (Schams). The Tambo and Suretta nappes comprise polycyclic gneisses (NUSSBAUM et al., 1998) with Permian intrusives (Truzzo granite, Roffna porphyry) and monocyclic metasediments (strongly deformed and reduced Mesozoic series) – show Alpine assemblages which range from HP-greenschist / blueschist facies (in the N) to high-P amphibolite facies (in the S). Mineral assemblage data of blueschist facies conditions are scarce.

Phengite barometry yields $P_{\max} \sim 10\text{-}13$ kbar (at $T \sim 400^\circ\text{C}$ in the N, $\sim 550^\circ\text{C}$ in the central part, BAUDIN & MARQUER, 1993; RING, 1992a) for the Tambo nappe, and 9-12 kbar (at $400\text{-}450^\circ\text{C}$, CHALLANDES, 1996; NUSSBAUM et al., 1998) for the Suretta nappe. However newly "rediscovered" occurrences of porphyroblasts of Ctd and Gt (STAUB, 1926, WIDERKEHR pers. com.) in Carbonifero-Permian cover of the Suretta nappe seem indicate that the previous estimates are only minimum conditions. In the Schams nappes, consisting mainly of limestones and breccias, the characteristic assemblage Phe-Chl-Qtz-Ab-Cal-Stp-Ep indicates lower greenschist facies metamorphism, with temperatures around $300\text{-}400^\circ\text{C}$ (SCHREURS, 1995). However, according to their structural position (SCHMID et al., 1996), the Schams is likely to have experienced metamorphic conditions similar to those of the Tambo and Suretta nappes, i.e. blueschist facies between 45 and 50 Ma (CHALLANDES et al., 2003).

- Valaisan units (North Pennine Bündnerschiefer) to the NE and NW of the central Lepontine belt: A large volume shaly-calcareous-terrigenous sediments, is outcropping in northern Graubünden, i.e. at the northeastern border of the Lepontine dome. Here the Bündnerschiefer can be separated into two nappes, the Grava nappe below and the Tomül nappe above (STEINMANN, 1994). The main body of Bündnerschiefer was deposited in Cretaceous times (STEINMANN & STILLE, 1999) until the late Eocene (BAGNOUD et al., 1998). Basaltic intercalations of MORB composition (DÜRR et al., 1993; STEINMANN & STILLE, 1999) within Bündnerschiefer metasediments indicate that the Valaisan is floored by oceanic crust (TRÜMPY, 1980).

Bündnerschiefer north and south of Thusis contain the typical mineral assemblage Ms + Pg + Na, K-mica + Chl + Qtz + Cal + organic matter \pm Alb \pm Dol (THUM & NABHOLZ, 1972). The same assemblage is also predominant in the Piz Aul area in front of the Adula nappe (KUPFERSCHMID, 1977) as well in Grava and Tomül nappes (STEINMANN, 1994; RAHN et al., 2002). Based on this, the metamorphic conditions experienced by Bündnerschiefer of northern Graubünden were generally interpreted as greenschist conditions. Rather than a metamorphic climax, these occurrences represent a strong retrograde overprint. Indeed, indications of an earlier high-pressure and low-temperature metamorphism have been found within the Bündnerschiefer as well within metabasaltic rocks. (Fe, Mg)-carpholite occurs as relic hair-like micro-fibres, included in quartz of quartz-carbonate segregations (GOFFÉ & OBERHÄNSLI, 1992) and chloritoid occurs within the rocks (OBERHÄNSLI et al., 1995). Glaucofanite occurrences in the ophiolites are well known (OBERHÄNSLI, 1978; HEIM & SCHMIDT, 1891; NABHOLZ, 1945), but in contrast to the Engadine window, the Na-amphibole (OBERHÄNSLI, 1986) is richer in Mg and Fe^{3+} (Vals valley).

For carpholite-bearing rocks devoid of chloritoid, calculated pressures range from 10 to 12 kbar and temperatures from 350 to 375°C , whereas for carpholite + chloritoid-bearing rocks, temperatures estimated from the Fe-Mg partitioning between chloritoid and chlorite range from 360 to 400°C , and pressures estimated range from 12 and 14 kbar (BOUSQUET et al., 2002). In the HP metamorphic unit, two types of P-T paths are observed. In the (Fe, Mg)-carpholite zone without chloritoid where the carpholite fibers are well preserved, maximum P-T conditions are $\sim 11\text{-}12$ kbar and 350°C (BOUSQUET et al., 1998). The preservation of carpholite and the absence of imply a decompression path that did not cross the equilibrium.

The retrograde P-T path must have been cold and fast enough to metastably preserve carpholite but not aragonite (GILLET & GOFFÉ, 1988). In addition, partially replaced carpholite occurs in association with chloritoid, implying a warmer decompressional P-T path. Associated with these blueschists, eclogite (with $P > 12$ kbar at $T \sim 510 \pm 50^\circ\text{C}$) is known from a single locality in the (southernmost) Misox Zone (OBERHÄNSLI, 1994).

These calculated P-T conditions confirm an increase in metamorphic grade from the northeast to the southwest, as reported by NABHOLZ (1945).

- Where these accretionary wedge sequences attained amphibolite facies conditions, i.e. in the central Lepontine area, HP-assemblages have not been found so far. However, such assemblages ((Fe, Mg)-carpholite – chloritoid) have recently been discovered both to the east (OBERHÄNSLI et al., 2004) and west of the Lepontine amphibolite facies region, hence it seems likely that these had existed also in the central portion prior to the strong Barrovian overprint.

b. Alpine eclogite facies remnants in the central Lepontine area appear to be restricted to tectonic mélange units. They are isolated occurrences in a belt that includes relics of variegated high grade metamorphism, from granulite facies to eclogite to (typically HP) amphibolite facies. Collectively these are thought to represent remnants of a tectonic accretion channel (TAC: ENGI et al., 2001), which had developed along the convergent plate boundary during Alpine subduction, collision, and extrusion. Classic eclogite (and garnet peridotite) localities (TROMMSDORFF, 1990) are in the Adula nappe (e.g. Trescolmen) and the Cima Lunga unit (e.g. Gagnone), but we have recently found eclogite relics in several additional units, including the Mergoscia-Arbedo zone and the Someo-Orselina zone. All of these TAC units (Fig. 2) constitute tectonic mélanges, i.e. highly deformed and imbricated slices of various gneiss types, trails of clastic metasediments with lenses of marble, sparse ultramafic rocks, and dismembered mafic rocks. The metamorphic grade varies greatly within and between the different TAC units, and the patterns are far from fully understood. For example, a regional PT-gradient (HEINRICH, 1986; MEYRE et al., 1997; 1999) is evident in the Adula nappe, with eclogite stage conditions increasing from the north (1.0-1.5 GPa at $500 \pm 50^\circ\text{C}$) to the south (3.0-3.6 GPa at 800 - 900°C). Although the Adula nappe is made up of an imbricated series of thin slices, at least the northern and central parts shows a consistent metamorphic field gradient of 20 ± 5 MPa/km and $9.6 \pm 2.0^\circ/\text{km}$ over the frontal 25 km of the nappe (DALE & HOLLAND, 2003). This field gradient links Eocene HP-assemblages formed within the TAC, which was dipping $\sim 45^\circ\text{S}$, and this terrane apparently behaved as a coherent tectonic unit along the exhumation path.

Metagabbroic kyanite eclogite and metabasaltic eclogite fragments occur in other TAC units as well, and PT-conditions show substantial variation among individual HP-fragments (Fig. 3), both in their P_{max} and the decompression-cooling paths they experienced (ENGI et al., 2001; BROUWER & ENGI, 2004). Internal mobility within the TAC during its extrusion is also evident in the southern parts of the Adula nappe, based on structural and petrological data (NAGEL et al., 2002b; DALE & HOLLAND, 2003). Most prominent among the HP-fragments are the classical localities of Cima di Gagnone and Alpe Arami which belong, respectively, to the Cima Lunga unit and the Mergoscia-Arbedo zone. Whereas metarodingites show a serpentinization stage prior to the HP-metamorphism for the former (EVANS & TROMMSDORFF, 1978; PFIFFNER & TROMMSDORFF, 1997), this is not the case for any of the HP-bodies known within the latter.

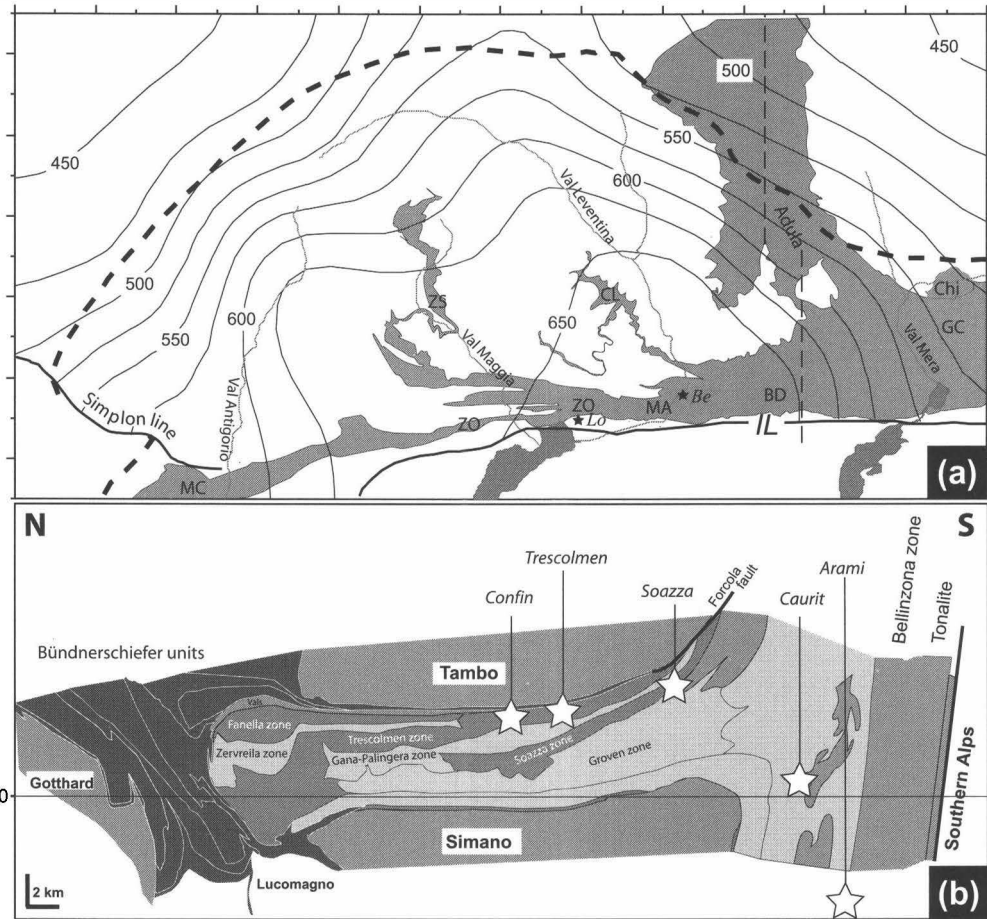
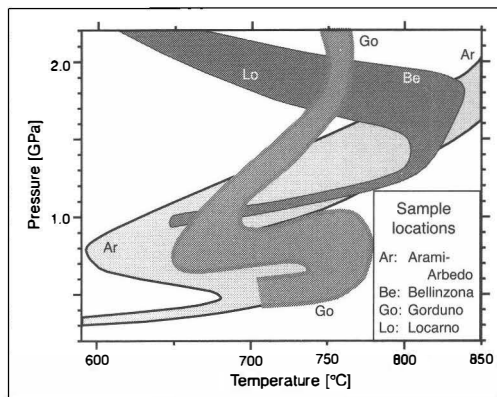


Fig. 2a
 Map of the tectonic mélangé belt in the Central Alps interpreted to represent a portion of the tectonic accretion channel (TAC). Labels refer to some of the more prominent subunits of this belt classically mapped as individual "zones" (BD: Bellinzona-Dascio zone, CL: Cima Lunga unit, CM: Camughera-Moncucco unit, GC: Gruf complex, Chi: Chiavenna ophiolite, MA: Mergoscia-Arbedo zone, ZS: Someo zone, ZO: Orselina zone; stars mark some towns; Be: Bellinzona; Lo: Locarno). Trace of synthetic profile for Fig. 2b and isotherms from Fig. 4b are also shown.

Fig. 2b
 Schematic Profile through the central Lepontine Alps. The classic Adula thrust sheet is a nappe-shaped body comprising a number of these zones (various shades of grey). Internal slices in the Adula nappe after JENNY et al. (1923), KÜNDIG (1926), and NAGEL et al. (2002). Occurrences of relic eclogites (stars indicate some of the localities) are restricted to the TAC. Its internal structure is outlined, with mapped zones representing slices of imbricated mélangé sheets, each comprising a distinct spectrum of rock types. Eclogite relics are missing in the basal part of the Adula nappe, which is thus tentatively separated from the TAC zones in the upper part. Bündnerschiefer units comprise several slices (after LÖW, 1987) of the Alpine accretionary prism.

Fig. 3

P-T paths documented for various lenses within the TAC (BROUWER, 2000; TÓTH et al., 2000; ENGI et al., 2001; GRANDJEAN, 2001; NIMIS & TROMMSDORFF, 2001; BROUWER & ENGI, 2004). The HP-route documented for each body may differ substantially from those of nearby lenses, but their P-T paths converge at mid-crustal levels, indicating a fairly uniform (coherent ?) exhumation of the TAC during its final emplacement.



Some authors have suggested UHP (ultra-high pressures) for the early evolution of garnet peridotite from Alpe Arami (DOBRZHINETSKAYA et al., 1996: > 300 km; BRENNER & BREY, 1997: > 5 GPa; BOZHILOV et al., 1999: > 8 GPa; OLKER et al., 2003: 5.9 GPa, 1180°C), whereas others derived conditions (e.g. NIMIS & TROMMSDORFF, 2001: 3.2 GPa, 840°C) much more in line with those found for other Alpine garnet lherzolite and associated eclogite lenses from the southern parts of the TAC (e.g. NIMIS et al., 1999: 3.0-3.2 GPa, 740-840°C). The controversy regarding the highest pressures is unresolved at this time. It is possible (but not clear) that the reported UHP conditions may document an early stage within the Mantle. Since comparable pressures have neither been reported for associated eclogites nor metapelites (and no coesite or diamond relics have been found to date), Arami may not be a relevant constraint to estimate the maximum depth reached by the TAC.

The central portion of the mélangé unit interpreted to represent an Alpine TAC (shown as a variegated facies unit on the Map of Alpine Metamorphism), is definitely delimited from the Pennine nappes adjacent to the north. Towards the eastern and western boundary of this belt, the separation is more tentative at this time. The TAC does not appear to extend beyond the Bergell intrusive sheet in the E, but the Gruf unit (with Alpine granulite facies relics) and Chiavenna ophiolite are interpreted as belonging to the TAC. Similarly, in the W the Monte Rosa nappe is a definite limit, but the Antrona and Moncucco-Camughera units are tentatively considered to be part of the TAC.

c. Age constraints for the HP-stage in the Central Alps show that Early Tertiary closure of the Piemont-Ligurian basin lead to accretion of a sedimentary wedge (South Pennine Bündnerschiefer) during the Paleocene, with subduction of the Briançonnais microcontinent following by early Eocene. The Tambo and Suretta terranes were welded to Apulia, and a coherent TAC formed in their footwall during the subsequent closure (50-47 Ma, SCHMID et al., 1996) of the Valais basin, where sedimentation continued into the Eocene (LIHOU, 1995; 1996). Eclogite formation (FROITZHEIM et al., 1996) in TAC units was initially dated between ~43-36 Ma for fragments from both Arami and Gagnone (BECKER, 1993; GEBAUER, 1996; 1999), but recent data for other fragments in the Central Alpine TAC indicates eclogite facies conditions in an age range from ~55 to 35 Ma (BROUWER et al., 2003a; 2003b). Exhumation from depths of >100 km to the Barrovian overprint (25-15 km) by 32 Ma implies a short time interval for the very rapid extrusion of parts of the TAC to mid-crustal levels.

The Oligo-/Micene Lepontine Belt

A relatively simple zonal pattern in the metamorphic field gradient (Fig. 4a) has long been recognized in the Lepontine Alps. Mineral zone boundaries and metamorphic reaction isograds (see recent review by FREY & FERREIRO MÄHLMANN, 1999) outline a classical Barrovian belt. Conditions range from anchimetamorphic – in the northern, most external parts of the orogen – to sillimanite-Kfsp / grade in the southern, most internal portion of the dome. Abundant late-orogenic migmatites occur within the Southern Steep Belt. Immediately to the South of this shear belt, the core part of the Alpine orogen is truncated by the Insubric Line, separating the Central Alps from the Southern Alps. The latter show but incipient Alpine metamorphism.

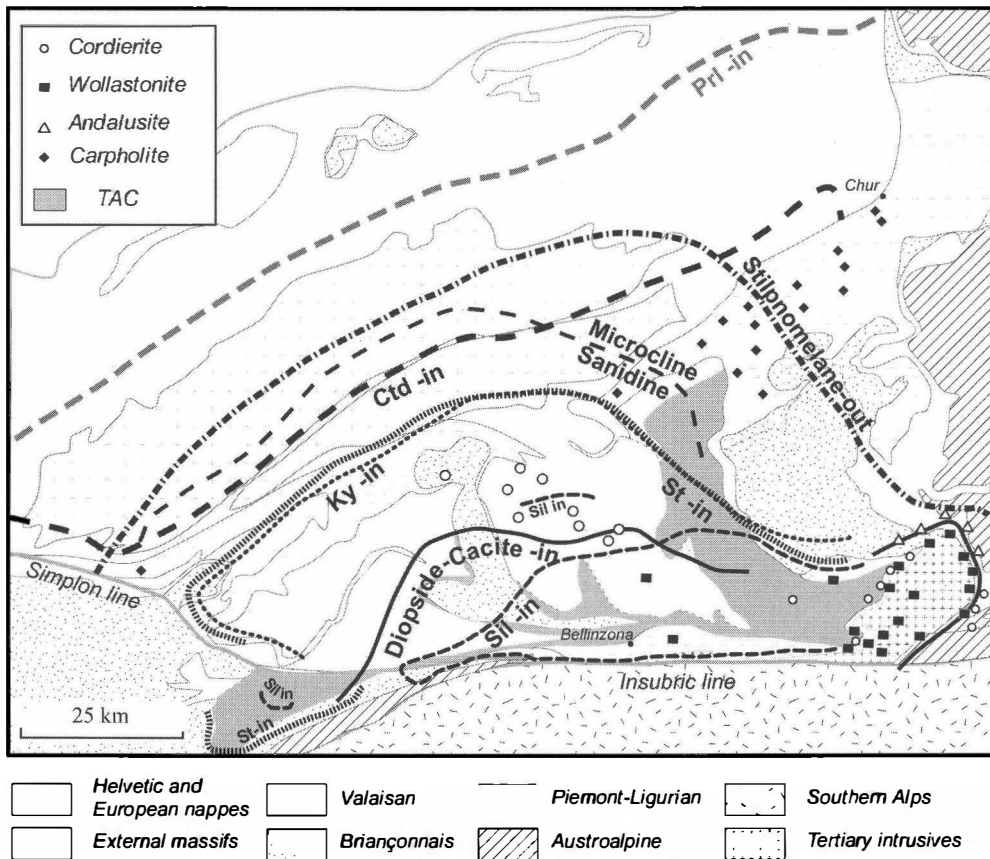


Fig. 4a

Select isograds (solid curves) and mineral zone boundaries (dashed curves) of Alpine metamorphism in the Central Alps. Updated from FREY & FERREIRO MÄHLMANN (1999), based on NIGGLI & NIGGLI (1965), TROMMS-DORFF (1980), BERNOTAT & BAMBAUER (1982), IROUSCHEK (1983) and FREY (1987); with additions from KELLER (2004) and data on Mg-Fe carpholite from GOFFÉ & OBERHÄNSLI (1992) and BOUSQUET (unpubl.). SF: Simplon fault, CF: Centovalli fault.

A wealth of detail has been established regarding the metamorphic overprint in the Central Alps, manifested by Barrovian mineral zones of stilpnomelane, chloritoid, staurolite and kyanite, as well as (fibrolitic) sillimanite (NIGGLI & NIGGLI, 1965; FREY & FERREIRO MÄHLMANN, 1999). It should be noted that the first appearance of any one of these aluminous phases does not reflect one specific irreversible reaction, and such a mineral zone boundary thus does not constitute a metamorphic isograd *sensu stricto*.

For example, in the Adula and Simano nappe, NAGEL et al. (2002a) showed that several paragonite breakdown reactions lead to the appearance of staurolite (as well as kyanite and sillimanite), whereas in the Lucomagno area, FREY (1974) found staurolite to grow at the expense of chloritoid. The former reactions took place during (\pm isothermal) decompression, the latter along a prograde burial path. Nevertheless, at least the medium and upper amphibolite facies, mineral zone boundaries for metapelites and ultramafic rocks (TROMMSDORFF & EVANS, 1969; 1974; NAGEL et al., 2002a) do outline a zonal pattern which corresponds rather closely to proper mineral (reaction) isograds, such as tremolite-calcite and diopside-calcite mapped for siliceous dolomite marbles by TROMMSDORFF (1966).

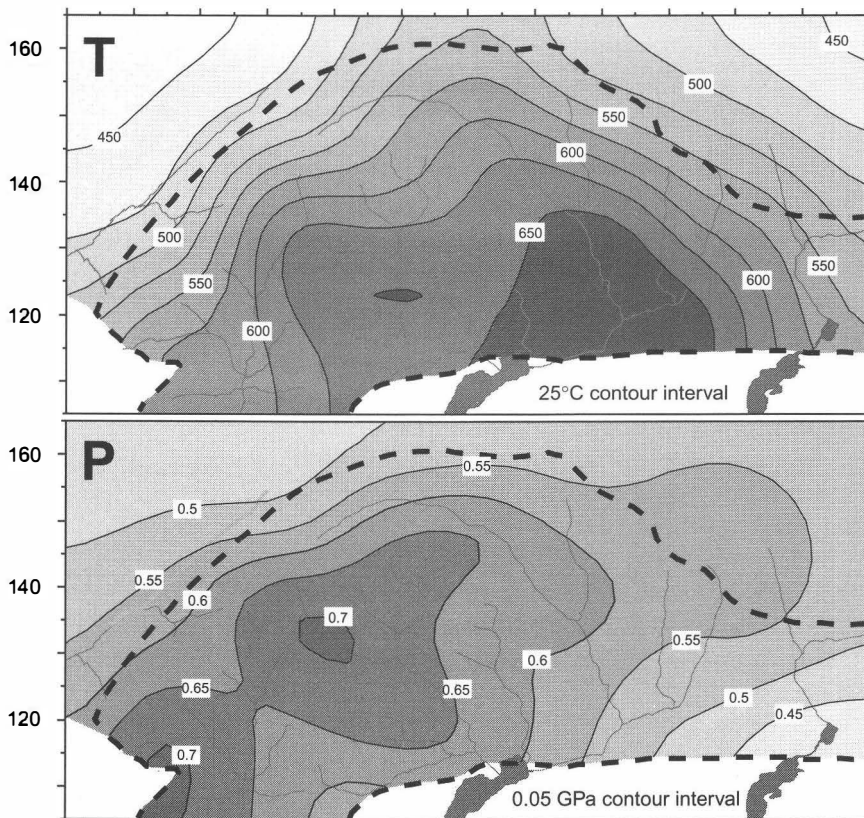


Fig. 4b/c

Map of isotherms and isobars for the Barrovian overprint in the Lepontine (updated from ENGI et al., 1995; TODD & ENGI, 1997), reflecting conditions near T_{max} and $P(T_{max})$.

The regional thermal and baric structure of the Lepontine belt (Fig. 4b/c), combined with recently determined PTt-paths from several tectonic units and mineral age data, indicate that the mid-Tertiary overprint which produced the Barrovian structure was diachronous by about 7 My. The thermal peak was first reached in the Southern Steep Belt, about 28 Ma ago, at pressures of 0.5-0.55 GPa only. During this late stage of decompression, fluid-assisted partial melting occurred (BURRI, 2004), producing up to ~30 vol-% leucosomes, which are variably deformed (by D₃ backfolding). Intrusive ages for the Novate stock, a small S-type granite that segregated late-stage partial melts, provide another age constraint for the migmatization (~24 Ma, LIATI et al., 2000). This magmatism is distinct from and clearly postdates the intrusion of the Bergell granodiorite and the associated tonalite sheet (VON BLANCKENBURG, 1992; OBERLI et al., 2004). In units further to the north, i.e. the central parts of the Lepontine, the thermal peak appears to have been reached at successively later times, between 26 and ~21 Ma ago, but here the thermal climax was reached at greater depths (P = 0.6-0.75 GPa). At the northern margin of the Lepontine amphibolite facies belt, T_{max} and P(at T_{max}) are lower (Fig. 2), but the age pattern remains unclear (HUNZIKER et al., 1992; ENGI et al., 1995). Ages between 42 and 16 Ma have been reported on the basis of different mineral chronometers, and it seems likely that these represent a mix of signals (and noise) recorded over 2-3 stages of evolution, i.e. the early HP phase (?), a prograde medium-pressure subduction phase, and the Barrovian overprint following emplacement of the TAC units and final exhumation of the nappe stack.

During this progressive exhumation process (NAGEL et al., 2002b) TAC-units with an earlier eclogite facies imprint were variably overprinted under amphibolite facies conditions (e.g. HEINRICH, 1982; MEYRE et al., 1999). The extent of this overprint was strongly dependent on the availability of hydrous fluids and localized deformation. Tectonic fragments now contained in the TAC-units in many cases show no early HP segment in their PT-paths, whereas nearby lenses differ strongly in the P_{max} and/or T(at P_{max}) they recorded (ENGI et al., 2001; NAGEL et al., 2002b), it is difficult to infer at what stage the accretion channel consolidated to a coherent tectonic unit. While much remains to be investigated, it certainly appears from the tectonic location and internal characteristics of this mélange unit that it played a crucial role in the tectono-metamorphic evolution of the Central Alps. Thermal modelling (ROSELLE et al., 2002) indicates that the relatively high temperatures reached during the regional Barrovian metamorphism can be explained by considering the dominantly upper crustal contents of the TAC, which in the Central Alps has an average heat production of 2.67 μW m⁻³. Recent reports (ÁBALOS et al., 2003; LÓPEZ SÁNCHEZ-VIZCAÍNO et al., 2003) indicate that tectonic elements of similar character as the Alpine TAC are important in other collisional belts as well.

In the section of Lepontine between Valle Mera and Locarno, the Southern Steep Belt of the Central Alps is terminated to the south by the Insubric Line, and TAC units, in part intruded by the Bergell tonalite sheet, form the limit to the Southern Alps. To the West of Locarno, however, the Insubric Line swings SW, whereas the Steep Belt continues in a westward direction, being cut in part by the Centovalli Line, an important late-orogenic E-W lineament with largely brittle character. In between the southernmost TAC-units and the Insubric Line two thrust sheets emerge, the Monte Rosa and the Sesia nappe, gaining in thickness towards the west. The Barrovian overprint in units south of the Centovalli Line rapidly decays, and the transition from greenschist facies to amphibolite facies runs nearly E-W.

However, in contrast to areas in the SSB east of Locarno the tectonic units lying immediately south of the TAC units do show Barrovian overprint. Quenching of the heat advected by the Central Alpine belt was directly against the Southern Alps in the eastern section, but against the Sesia and Ivrea bodies in the western section of the SSB. The spacing of isotherms (Fig. 4b) gets notably much wider in the west. This is likely to reflect the dextral transpressional exhumation, during which the southern block was successively heated by the hottest portion of the northern block and, as the transfer of heat from the hot Central Alpine block to the cool southern block was most effective initially, leading to rapid quenching in the eastern part of the Central Alps, whereas the thermal quench was less pronounced in their western portion. This topic is further elaborated in the chapter by BOUSQUET et al. (2004).

References

- ÁBALOS, B., PUELLES, P. & GIL IBARGUCHI, J. I. (2003): Structural assemblage of high-pressure mantle and crustal rocks in a subduction channel (Cabo Ortegal, NW Spain). - *Tectonics*, 22(2).
- ABRECHT, J. & BIINO, G. G. (1994): The metagabbros of the Kastelhorn area (Gotthard massif, Switzerland): their metamorphic history inferred from mineralogy and texture. - *Schweiz. Mineral. Petrogr. Mitt.*, 74(1), 53-68.
- ABRECHT, J., BIINO, G. G., MERCOLLI, I. & STILLE, P. (1991): Mafic-ultramafic rock associations in the Aar, Gotthard and Tavetsch massifs of the Helvetic domain in the Central Swiss Alps: markers of ophiolitic pre-Variscan sutures, reworked by polymetamorphic events? - *Schweiz. Mineral. Petrogr. Mitt.*, 71, 295-300.
- BAGNOUD, A., WERNLI, R. & SARTORI, M. (1998): Découverte de foraminifères planctoniques paléogènes dans la zone de Sion-Courmayeur à Sion (Valais, Suisse). - *Eclogae geol. Helv.*, 91, 421-429.
- BAUDIN, T. & MARQUER, D. (1993): Métamorphisme et déformation dans la nappe de Tambo (Alpes centrales suisses): évolution de la substitution phengitique au cours de la déformation alpine. - *Schweiz. Mineral. Petrogr. Mitt.*, 73, 285-299.
- BECKER, H. (1993): Garnet peridotite and eclogite Sm-Nd mineral ages from the Lepontine dome (Swiss Alps): New evidence for Eocene high-pressure metamorphism in the central Alps. - *Geology*, 21, 599-602.
- BIINO, G. (1994): The pre-Late Ordovician metamorphic evolution of the Gotthard-Tavetsch massifs (Central Alps): from lawsonite to kyanite eclogites to granulite retrogression. - *Schweiz. Mineral. Petrogr. Mitt.*, 74(1), 87-104.
- BIINO, G. (1995): Pre-Variscan evolution of the eclogitised mafic rocks from the Helvetic basement of the central Alps. - *Eur. J. Mineral.*, 7(1), 57-70.
- BIINO, G., MARQUER, D. & NUSSBAUM, C. (1997): Alpine and pre-Alpine subduction events in polycyclic basements of the Swiss Alps. - *Geology*, 25(8), 751-754.
- BOUSQUET, R., ENGI, M., GOSSO, G., OBERHÄNSLI, R., BERGER, A., SPALLA, I., ZUCALI, M. & GOFFÉ (2004): Metamorphic structure of the Alps: Transition from the Western to the Central Alps. - *Mitt. Öster. Min. Ges.*, 149, 145-156.
- BOUSQUET, R., GOFFÉ, B., VIDAL, O., OBERHÄNSLI, R. & PATRIAT, M. (2002): The tectono-metamorphic history of the Valaisan domain from the Western to the Central Alps: New constraints on the evolution of the Alps. - *GSA Bulletin*, 114(2), 201-225.
- BOUSQUET, R., OBERHÄNSLI, R., GOFFÉ, B., JOLIVET, L. & VIDAL, O. (1998): High pressure-low temperature metamorphism and deformation in the Bündnerschiefer" of the Engadine window (eastern Central Alps): Implications for regional evolution. - *J. metamorphic Geol.*, 16, 653-674.

- BOZHILOV, K. N., GREEN, H. W. I. & DOBRZHINETSAYA, L. (1999): Clinoenstatite in Alpe Arami peridotite; additional evidence of very high pressure. - *Science*, 284, 129-132.
- BRENKER, F. E. & BREY, G. P. (1997): Reconstruction of the exhumation path of the Alpe Arami garnet-peridotite body from depths exceeding 160 km. - *J. of metamorphic Geology*, 15, 581-592.
- BROUWER, F. M. (2000): Thermal evolution of high-pressure metamorphic rocks in the Alps. - Unpub. Ph.D. Thesis, Utrecht University, Utrecht.
- BROUWER, F. M., BURRI, T., BERGER, A. & ENGI, M. (2003a): Collision in the Central Alps: 2. Exhumation of high-pressure fragments. - In: EGS - AGU - EUG Joint Assembly, Nice.
- BROUWER, F. M. & ENGI, M. (2004): Staurolite and other high-alumina phases in Apline eclogite: Analysis of domain evolution. - *Can. Mineral.*, Carmichael volume, 25 p. (in print).
- BROUWER, F. M., ENGI, M., BERGER, A. & BURRI, T. (2003b): Towards complete PTt paths: Unravelling Alpine eclogite relics. - *Norsk Geol. Unders. Report*, 2003.055, 25-26.
- BURRI, T. (2004): From high pressure to migmatization: on the orogenic evolution of the southern Lepontine (Central Alps, Switzerland / Italy). - Unpub. Ph.D. Thesis, University of Bern, Bern.
- CHALLANDES, N. (1996): Déformation hétérogène et transfert de matière dans les zones de cisaillement des Roffna porphyres de la nappe de Suretta (Col du Splügen, Grisons). - Unpub. Diploma Thesis, Université de Neuchâtel.
- CHALLANDES, N., MARQUER, D. & VILLA, I.M. (2003): Dating the evolution of C-S microstructures: a combined $^{40}\text{Ar}/^{39}\text{Ar}$ step-heating and UV laserprobe analysis of the Alpine Roffna shear zone. - *Chem. Geol.*, 197(1-4), 3-19.
- DALE, J. & HOLLAND, T. J. B. (2003): Geothermobarometry, P-T paths and metamorphic field gradients of high-pressure rocks in the Adula Nappe, Central Alps. - *J. metamorphic Geol.*, 21, 813-829.
- DOBRZHINETSAYA, L., GREEN, H. W. & WANG, S. (1996): Alpe Arami: a peridotite massif from depths of more than 300 kilometers. - *Science*, 271, 1841-1845.
- DÜRR, S. B., RING, U. & FRISCH, W. (1993): Geochemistry and geodynamic significance of North Penninic ophiolites from the Central Alps. - *Schweiz. Mineral. Petrogr. Mitt.*, 73, 407-419.
- ENGI, M., BERGER, A. & ROSELLE, G. T. (2001): Role of the tectonic accretion channel in collisional orogeny. - *Geology*, 29(12), 1143-1146.
- ENGI, M., TODD, C. S. & SCHMATZ, D. R. (1995): Tertiary metamorphic conditions in the eastern Lepontine Alps. - *Schweiz. Mineral. Petrogr. Mitt.*, 75(3), 347-369.
- EVANS, B. W. & TROMMSDORFF, V. (1978): Petrogenesis of garnet lehrzolitite, Cima di Gagnone, Lepontine Alps. - *Earth. Planet. Sci. Lett.*, 40, 333-348.
- FERREIRO-MÄHLMANN, R. (1995): Das Diagenese-Metamorphose-Muster von Vitrinireflexion und Illit-"Kristallinität" in Mittelbünden und im Oberhalbstein. Teil I: Bezüge zur Stockwerktektonik. - *Schweiz. Mineral. Petrogr. Mitt.*, 75(1), 85-122.
- FLÜGEL, H. W. (1990): Das voralpine Basement im Alpin-Mediterranen Belt – Überblick und Problematik. - *Jb. Geol. Bundesanstalt*, 133, 181-222.
- FREY, M. (1974): Alpine metamorphism of pelitic and marly rocks in the Central Alps. - *Schweiz. Mineral. Petrogr. Mitt.*, 54, 489-506.
- FREY, M. & FERREIRO MÄHLMANN, R. (1999): Alpine metamorphism of the Central Alps. - *Schweiz. Mineral. Petrogr. Mitt.*, 79, 135-154.
- FROITZHEIM, N., SCHMID, S. M. & FREY, M. (1996): Mesozoic paleogeography and the timing of eclogite-facies metamorphism in the Alps: A working hypothesis. - *Eclogae geol. Helv.*, 89(1), 81.
- GEBAUER, D. (1996): A P-T-t-path for an (ultra?) high-pressure ultramafic/mafic rock association and its felsic country-rocks based on SHRIMP-dating of magmatic and metamorphic zircon domains. Example: Alpe

- Arami (Swiss Central Alps). - In: *Earth Processes: Reading the Isotopic Code*, pp. 309-328, American Geophysical Union.
- GEBAUER, D. (1999): Alpine geochronology of the Central and Western Alps: new constraints for a complex geodynamic evolution. - *Schweiz. Mineral. Petrogr. Mitt.*, 79, 191-208.
- GEBAUER, D., VON QUADT, A., COMPSTON, W. WILLIAMS, I. S. & GRÜNENFELDER, M. (1988): Archean zircons in a retrograded Caledonian eclogite of the Gotthard Massif (Central Alps, Switzerland). - *Schweiz. Mineral. Petrogr. Mitt.*, 68, 485-490.
- GILLET, P. & GOFFÉ, B. (1988): On the significance of aragonite occurrence in the Western Alps. - *Contrib. Mineral. Petrol.*, 99, 70-81.
- GOFFÉ, B. & OBERHÄNSLI, R. (1992): Ferro- and magnesiocarpholite in the "Bündnerschiefer" of the eastern Central Alps (Grisons and Engadine Window). - *Eur. J. Miner.*, 4, 835-838.
- GRANDJEAN, V. (2001): Petrographical evolution of mafic relics and their interpretation for the geodynamics of the Central Alps. - Unpub. Ph.D. Thesis, University of Bern.
- GRUJIC, D. & MANCKTELOW, N. S. (1996): Structure of the northern Maggia and Lebendun nappes, central Alps, Switzerland. - *Eclogae geol. Helv.*, 89(1), 461-504.
- HANDY, M. R., HERWEGH, M., KAMBER, B. S., TIETZ, R. & VILLA, I. M. (1996): Geochronologic, petrologic and kinematic constraints on the evolution of the Err-Platta boundary, part of a fossil continent-ocean suture in the Alps (Eastern Switzerland). - *Schweiz. Mineral. Petrogr. Mitt.*, 76(3), 453-474.
- HEIM, A. & SCHMIDT, C. (1891): *Geologie der Hochalpen zwischen Reuss und Rhein mit einem Anhang von petrographischen Beiträge von Carl Schmidt*. - *Beitr. Geol. Karte CH*, 25.
- HEINRICH, C. A. (1982): Kyanite-eclogite to amphibolite facies evolution of hydrous mafic and pelitic rocks, Adula nappe, Central Alps. - *Contrib. Mineral. Petrol.*, 81, 30-38.
- HEINRICH, C. A. (1986): Eclogite facies regional metamorphism of hydrous mafic rocks in the Central Alpine Adula nappe. - *J. Petrol.*, 27(123-154).
- HUNZIKER, J. C., DESMONS, J. & HURFORD, A. J. (1992): Thirty-two years of geochronological work in the Central and Western Alps; a review on seven maps. - *Mém. Géol. Lausanne*, 13.
- JENNY, H., FRISCHKNECHT, G. & KOPP, J. (1923): *Geologie der Adula*. - *Beitr. Geol. Karte CH*, NF 51.
- KÜNDIG, E., 1926. *Beiträge zur Geologie und Petrographie der Gebirgskette zwischen Val Calanca und Misox*. - *Schweiz. Mineral. Petrogr. Mitt.*, 4, 1-99.
- KUPFERSCHMID, C. (1977): *Geologie auf des Lugnezer Seite der Piz Aul-Gruppe*. - *Eclogae geol. Helv.*, 70, 1-58.
- LIATI, A., FANNING, M. & GEBAUER, D. (2000): U-Pb SHRIMP dating of co-magmatic and inherited zircons of the Novate granite (Bergell, Central Alps): implications for Oligocene-Miocene magmatism, Jurassic-Cretaceous continental rifting and opening of the Valais trough. - *Schweiz. Mineral. Petrogr. Mitt.*, 80(3).
- LIHOU, J. C. (1995): A new look at the Blattengrat unit of eastern Switzerland: Early Tertiary foreland basin sediments from the South Helvetic realm. - *Eclogae geol. Helv.*, 88, 91-114.
- LIHOU, J. C. (1996): Structure and deformational history of the infrahelvetic flysch units, Glarus Alps, eastern Switzerland. - *Eclogae geol. Helv.*, 89(1), 439.
- LÓPEZ SÁNCHEZ-VIZCAÍNO, V., GÓMEZ-PUGNAIRE, M.T., AZOR, A. & FERNÁNDEZ-SOLER, J. M. (2003): Phase diagram sections applied to amphibolites: a case study from the Ossa-Morena / Central Iberian Variscan suture (Southwest Iberian Massif). - *Lithos*, 68, 1-21.
- MATTE, P. (1986): Tectonic and plate tectonics model for the Variscan belt of Europe. - *Tectonophysics*, 126, 329-374.
- MERCOLLI, I., BIINO, G. G. & ABRECHT, J. (1994): The lithostratigraphy og the pre-Mesozoic basement of the Gotthard massif: a review. - *Schweiz. Mineral. Petrogr. Mitt.*, 74, 29-40.

- MEYRE, C., DE CAPITANI, C. & PARTZSCH, J. H. (1997): A ternary solid solution model for omphacite and its application to geothermobarometry of eclogites from the middle Adula Nappe (Central Alps, Switzerland). - *J. metamorphic Geol.*, 15(6), 687-700.
- MEYRE, C., DE CAPITANI, C., ZACK, T. & FREY, M. (1999): Petrology of high-pressure metapelites from the Adula nappe (Central Alps, Switzerland). - *J. Petrol.*, 40(1), 199-213.
- MILNES, A. G. (1974a): Post-nappe folding in the western Lepontine Alps. - *Eclogae geol. Helv.*, 67, 333-348.
- MILNES, A. G. (1974b): Structure of the Pennine Zone: a new working hypothesis. - *Geol. Soc. Am. Bull.*, 85, 1727-1732.
- NABHOLZ, W. (1945): Geologie der Bündnerschiefer zwischen Rheinwald, Valsler- und Safiental. - *Eclogae geol. Helv.*, 38, 1-119.
- NAGEL, T., DE CAPITANI, C. & FREY, M. (2002a): Isograd and P-T evolution in the eastern Lepontine Alps (Graubünden, Switzerland). - *J. metamorphic Geol.* 20, 309-324.
- NAGEL, T., DE CAPITANI, C., FREY, M., FROITZHEIM, N., STÜNITZ, H. & SCHMID, S. M., (2002b): Structural and metamorphic evolution during rapid exhumation in the Lepontine dome (southern Simano and Adula nappes, Central Alps, Switzerland). - *Eclogae geol. Helv.*, 95, 301-321.
- NIEVERGELT, P., LINIGER, M., FROITZHEIM, N. & FERREIRO-MÄHLMANN, R. (1996): Early to mid Tertiary crustal extension in the Central Alps: The Turba Mylonite Zone (Eastern Switzerland). - *Tectonics*, 15(2), 329-340.
- NIGGLI, E. (1960): Mineral-Zonen der alpinen Metamorphose in den Schweizer Alpen. - *Int. geol. Congr. Copenhagen, Rep. 21st Sess. Norden*, 13, 132-138.
- NIGGLI, E. (1974): Metamorphism and Tectonics of the Alps. - *Mem. Soc. geol. It.*, 13, 285-289.
- NIGGLI, E. & NIGGLI, C. (1965): Karten der Verbreitung einiger Mineralien der alpidischen Metamorphose in den Schweizer Alpen (Stilpnomelan, Alkali-Amphibol, Chloritoid, Staurolith, Disthen, Sillimanit). - *Eclogae geol. Helv.*, 58, 335-368.
- NIMIS, P. & TROMMSDORFF, V. (2001): Revised thermobarometry of Alpe Arami and other garnet peridotites from the Central Alps. - *J. Petrol.*, 42(1), 103-115.
- NIMIS, P., TROMMSDORFF, V. & RUSSO, U. (1999): Revised thermobarometry of grt-peridotites from the Cima Lunga - Adula nappe complex, Central Alps. - *Ofioliti*, 24(1a), 143-144.
- NUSSBAUM, C., MARQUER, D. & BIINO, G. G. (1998): Two subduction events in a polycyclic basement: Alpine and pre-Alpine high-pressure metamorphism in the Suretta nappe, Swiss Eastern Alps. - *J. metamorphic Geol.*, 16, 591-605.
- OBERHÄNSLI, R. (1978): Chemische Untersuchungen an Glaukophan-führenden basischen Gesteinen aus den Bündnerschiefern Graubündens. - *Schweiz. Mineral. Petrogr. Mitt.*, 58, 139-156.
- OBERHÄNSLI, R. (1986): Blue amphibole in metamorphosed Mesozoic mafic rocks from Central Alps. IN: *Blue-schists and Eclogites* (EVANS, B. W. & BROWN, E. H., EDS) - *Geol. Soc. Amer., Memoir*, 164, 239-247.
- OBERHÄNSLI, R. (1994): Subducted and obducted ophiolites of the Central Alps: Paleotectonic implications deduced by their distribution and metamorphism overprint. - *Lithos*, 33, 109-118.
- OBERHÄNSLI, R., BOUSQUET, R. & GOFFÉ, B. (2004): Comment to "Chloritoid composition and formation in the eastern Central Alps: a comparison between Penninic and Helvetic occurrences" - *Schweiz. Mineral. Petrogr. Mitt.*, in press.
- OBERHÄNSLI, R., GOFFE, B. & R. B. (1995): Record of a HP-LT metamorphic evolution in the Valais zone: Geodynamic implications. - *Boll. Mus. Reg. Sc. nat. Torino*, 13(2), 221-240.
- OBERLI, F., MEIER, M., BERGER, A., ROSENBERG, C. L. & GIERÉ, R. (2004): U-Th-Pb and ²³⁰Th/²³⁸U disequilibrium isotope systematics: precise accessory mineral chronology and melt evolution tracing in the Alpine Bergell intrusion. - *Geochim. Cosmochim. Acta*, 68(11), 2543-2560.

- OBERLI, F., MEIER, M. & BIINO, G. G. (1994): Time constraints on the pre-Variscan magmatic / metamorphic evolution of the Gotthard and Tavetsch units derived from single-zircon U-Pb results. - *Schweiz. Mineral. Petrogr. Mitt.*, 74, 483-488.
- OLKER, B., ALTHERR, R. & PAQUIN, J. (2003): Fast exhumation of the ultrahigh-pressure Alpe Arami garnet peridotite (Central Alps, Switzerland): constraints from geospeedometry and thermal modelling. - *J. metamorphic Geol.*, 21, 395-402.
- PIFFNER, M. & TROMMSDORFF, V. (1997): Evidence for high-pressure metamorphosed ophiocarbonate rocks, Cima di Gagnone, Central Alps. - *Terra Nova Abstract Supplement*, 1, 26.
- PHILIPP, R. (1982): Die Alkali amphibole der Platta-Decke zwischen Silsersee und Lunghinpass (Graubünden). - *Schweiz. Mineral. Petrogr. Mitt.*, 62, 437-455.
- RAHN, M., STEINMANN, M. & FREY, M. (2002): Chloritoid composition and formation in the eastern Central Alps: a comparison between Penninic and Helvetic occurrences. - *Schweiz. Mineral. Petrogr. Mitt.*, 82(2), 409-426.
- RING, U. (1992a): The Alpine geodynamic evolution of Penninic nappes in the eastern Central Alps: geothermobarometric and kinematic data. - *J. metamorphic Geol.*, 10, 33-53.
- RING, U. (1992b): The Kinematic History of the Penninic Nappes east of the Lepontine Dome: Implications for the Tectonic Evolution of the Central Alps. - *Tectonics*, 11(6), 1139-1158.
- ROSELLE, G. T., THÜRING, M. & ENGI, M. (2002): MELONPIT: A finite element code for simulating tectonic mass movement and heat flow within subduction zones. - *Am. J. Sci.*, 302, 381-409.
- SCHALTEGGER, U. & GEBAUER, D. (1999): Pre-Alpine geochronology of the Central, Western and Southern Alps. - *Schweiz. Mineral. Petrogr. Mitt.*, 79(1), 79-88.
- SCHMID, S. M., PFIFFNER, O. A., FROITZHEIM, N., SCHÖNBORN, G. & KISSLING, E. (1996): Geophysical-geological transect and tectonic evolution of the Swiss-Italian Alps. - *Tectonics*, 15(5), 1036-1064.
- SCHREURS, G. (1995): Geometry and kinematics of the Schams nappes and adjacent tectonic units. - *Beitr. Geol. Karte Ch, NF 167, Part II*.
- STAUB, R. (1926): Geologische Karte des Avers. - *Beitr. Geol. Karte CH, NF 97*.
- STEINMANN, M. (1994): Ein Beckenmodell für das Nordpenninikum der Ostschweiz. - *Jb. Geol. Bundesanstalt*, 137, 675-721.
- STEINMANN, M. & STILLE, P. (1999): Geochemical evidence for the nature of the crust beneath the eastern North Penninic basin of the Mesozoic Tethys ocean. - *Geol. Rundsch.*, 87(4), 633-643.
- THUM, I. & NABHOLZ, W. (1972): Zur Sedimentologie und Metamorphose der penninischen Flysch- und Schieferabfolgen im Gebiet Prättigau-Lenzerheide-Oberhalbstein. - *Beitr. Geol. Karte Ch, NF 144*.
- TODD, C. S. & ENGI, M. (1997): Metamorphic field gradients in the Central Alps. - *J. metamorphic Geol.*, 15, 513-530.
- TÓTH, M., GRANDJEAN, V. & ENGI, M. (2000): Polyphase evolution and reaction sequence of compositional domains in metabasalt: A model based on local chemical equilibrium and metamorphic differentiation. - *Geol. J.*, 35, 163-183.
- TROMMSDORFF, V. (1966): Progressive Metamorphose kiesiliger Karbonatgesteine in den Zentralalpen zwischen Bernina und Simplon. - *Schweiz. Mineral. Petrogr. Mitt.*, 46, 431-460.
- TROMMSDORFF, V. (1990): Metamorphism and tectonics in the Central Alps: The Alpine lithospheric mélange of Cima Lunga and Adula. - *Mem. Soc. Geol. It.*, 45, 39-49.
- TROMMSDORFF, V. & EVANS, B. W. (1969): The stable association enstatite-forsterite-chlorite in amphibolite facies ultramafics of the Lepontine Alps. - *Schweiz. Mineral. Petrogr. Mitt.*, 49(2), 325-332.
- TROMMSDORFF, V. & EVANS, B. W. (1974): Alpine Metamorphism of Peridotitic Rocks. - *Schweiz. Mineral. Petrogr. Mitt.*, 54, 333-352.

- TROMMSDORFF, V. & NIEVERGELT, P. (1983): The Bregaglia (Bergell) Iorio intrusive and its field relations. - Mem. Soc. Geol. It., 26, 55-68.
- TRÜMPY, R. (1980): Geology of Switzerland - a guide book. - Wepf & Co. Publishers, Basel, New York.
- VON BLANCKENBURG, F. (1992): Combined high-precision chronometry and geochemical tracing using accessory minerals: applied to the Central-Alpine Bergell intrusion (central Europe). - Chem. Geol., 100, 19-40.
- VON RAUMER, J. (1998): The Paleozoic evolution of the Alps: from Gondwana to Pangea. - Geol. Rundsch., 87, 407-435.
- VON RAUMER, J., ABRECHT, J., BUSSY, F., LOMBARDO, B., MÉNOT, J.-P. & SCHALTEGGER, U. (1999): The Paleozoic metamorphic evolution of the Alpine External Massifs. - Schweiz. Mineral. Petrogr. Mitt., 79(1), 5-22.

manuscript received: June 2004

manuscript accepted: July 2004

**EXPLANATORY NOTES TO THE MAP:
METAMORPHIC STRUCTURE OF THE ALPS
METAMORPHIC EVOLUTION OF THE EASTERN ALPS**

by

Ralf Schuster¹, Friedrich Koller², Volker Hoeck³, Georg Hoinkes⁴ & Romain Bousquet⁵

¹Geological Survey

Rasumofskygasse, A-1030 Vienna, Austria

²Institute of Geological Sciences

University of Vienna, Althanstrasse 14, A-1090 Vienna, Austria

³Institute of Geology and Paleontology

University of Salzburg, Hellbrunnerstrasse 23, A-5020 Salzburg, Austria

⁴Institute of Mineralogy and Petrology

University of Graz, Universitätsplatz 2, A-8010 Graz, Austria

⁵Department of Earth Sciences

University of Basel, Bernoullistrasse 30, CH-4056 Basel, Switzerland

1. Introduction

The Eastern Alps are the product of two orogenies, a Cretaceous orogeny followed by a Tertiary one (FROITZHEIM et al., 1996). The former is related to the closure of an embayment of the Neotethys ocean into Apulia (Meliata ocean), the latter is due to the closure of the Alpine Tethys oceans between Apulia and Europe.

The result of the orogenic movement is a complex nappe stack, which is built up from north to south and from bottom to the top by the following units (Plate 1 in SCHMID et al., 2004): The proximal parts of the Jurassic to Cretaceous European margin built up the northern Alpine foreland and the Helvetic nappes, whereas the distal margin is represented by the Subpenninic nappes. The Penninic nappes comprise the Piemont-Ligurian and Valais ocean (Alpine Tethys) and the Briançonnais Terrain. Apulia consists of the northern Austroalpine nappes and the Southern Alpine unit (STAMPFLI & MOSAR, 1999). Remnants of the Neotethys embayment occur as slices within the eastern part of the Austroalpine nappe stack. Both orogenic events are accompanied by regional metamorphism of variable extent and P-T conditions. The Cretaceous (Eo-Alpine) metamorphism affects mainly the Austroalpine Nappes, the Penninic domain by the Tertiary metamorphism, some units of the Lower Austroalpine Nappes show signs of both events.

2. Metamorphic evolution of the Eastern Alps

2.1. Geological Framework of the Eastern Alps

In the Eastern Alps (Plate 1 in SCHMID et al., 2004) the Jurassic to Cretaceous European margin is represented by the Helvetic and Ultrahelvetic Nappes composed of Mesozoic sedimentary series and by the Subpenninic nappes consisting of orthogneisses with remnants of roof pendants (Altes Dach), Paleozoic metasediments and a transgressive Mesozoic cover. The Helvetic and Ultrahelvetic Nappes built up the northern foothills of the orogen, whereas the Subpenninic Nappes occur in the Tauern Window in the south.

The Penninic nappes are present along the northern margin of the Alps and within the Lower Engadin Window, Tauern Window, and Rechnitz Window Group. Cretaceous ophiolitic fragments overlain by Cretaceous to Tertiary (Lower Engadin Window) calcareous schists as well as flysch sediments (Rhenodanubian flysch) of the Valais ocean form the Lower Penninic Nappes. The eastern offshoots of the Middle Penninic Nappes reach until the Lower Engadin Window. They consist of a continental basement with a Mesozoic cover. The Upper Penninic Nappes (Piemont-Ligurian ocean) are characterised by slices of subcontinental mantle and oceanic crust in connection with Jurassic radiolarites and Cretaceous to Tertiary calcareous schists.

The Austroalpine nappes are composed of crustal material with a complex Phanerozoic history. They can be subdivided in a Lower and an Upper Austroalpine unit. The former shows a remarkable reworking related to the opening and closure of the Piemont-Ligurian and Valais ocean, whereas the internal structure of the latter is due to the closure of the Tethys embayment. Coming from the north the Upper Austroalpine unit is built up by Mesozoic sedimentary sequences of the Northern Calcareous Alps, Paleozoic metasediments and metavolcanics of the Graywacke zone and the crystalline basement units with remnants of Paleozoic and Mesozoic metasediments. The crystalline basement can be subdivided into four parts: The lowermost Silvretta-Seckau nappe system is predominantly consisting of a deeply eroded Variscan metamorphic crust with a partly preserved Mesozoic cover (NEUBAUER et al., 1999a, NEUBAUER, 2002). The overlying Wölz-Koralpe nappe system is built up exclusively by pre-Mesozoic rocks and represents an extruding metamorphic wedge. Above this wedge the Ötztal-Bundschuh and the Gurktal-Drauzug nappe system are present. To the south of the Periadriatic lineament the Southern Alpine unit is located. The nappe systems above the wedge as well as the Southern Alpine unit are composed of crystalline basement, Paleozoic metasedimentary rocks and Permomesozoic cover sequences.

Nearly all nappe units contain metasedimentary sequences and/or metabasaltic rocks of Mesozoic age. During the Alpine tectonometamorphic events prograde assemblages formed in these rocks, defining the grade of the Alpine metamorphic imprints. However, large parts of the Austroalpine nappes, especially those of the Wölz-Koralpe nappe system lack prograde sequences, but show complex polyphase microstructures. It is not always easy to distinguish between several metamorphic events, which reach sometimes similar conditions. Therefore, due to missing geochronological data, different individual metamorphic events including the Variscan or Permian event, were sometimes mixed up in the older literature.

2.2. Pre-alpine metamorphic history of the Austroalpine Unit

In the Austroalpine unit two regional Palaeozoic metamorphic imprints are well documented. In the Penninic and Subpenninic unit of the Eastern Alps only one is known up to now and this one is restricted to the basement of the Tauern Window.

2.2.1. Variscan tectonometamorphic event

Pre-Alpine metamorphic basement units are exposed within different continental microplates of the Eastern Alps: the Subpenninic, Penninic, Austroalpine and Southalpine units. They show variable metamorphic imprints due to the variety of metamorphic facies and age of metamorphism. These imprints are interpreted to result from accretion of various units to the active Laurasian continental margin.

The Variscan metamorphic event was induced by the collision of Africa, Baltica, Laurentia and intervening microplates (TAIT et al., 1997). A collision related LT/HP imprint occurred prior to 350 Ma. The thermal metamorphic peak was reached at about 340 Ma at medium pressure conditions. Typical Variscan cooling ages are about 310 Ma (MILLER & THÖNI; 1995, NEUBAUER et al. 1999a; THÖNI, 1999).

The Subpenninic basement exposed within the Tauern Window is largely overprinted by Variscan migmatite-grade metamorphism associated with intrusions of Variscan granites. Rare eclogites of Silurian age predate migmatite formation. The Austroalpine basement units vary in metamorphic grade and timing of metamorphism ranging from greenschist to granulite facies conditions. Only a Variscan greenschist metamorphic overprint is recorded in the eastern part of the Southalpine unit.

2.2.2. Permo-Triassic tectono-thermal event

The Permo-Triassic imprint reflects lithospheric extension after the late Variscan orogenic collapse. It may be due to the anticlockwise rotation of Africa and the southern part of the Apulian microplate with respect to Eurasia and the northern part of the Apulian microplate and caused extension within the Austroalpine and South Alpine realm. Accompanied thinning of the lithosphere resulted in a high temperature metamorphic imprint (HT/LP) (SCHUSTER et al., 2001). The Permo-Triassic imprint is widespread in the Austroalpine unit (Fig. 1) and affects pre-Permian rocks of different metamorphic grade (HABLER & THÖNI, 2001; SCHUSTER et al., 2001). Well preserved Permo-Triassic metamorphic rocks occur in the Gurktal-Drauzug nappe system between the southern border of Alpine metamorphism (SAM, HOINKES et al. 1999) and the Periadriatic Lineament, as well as in the western part of the Silvretta-Seckau nappe system. Similar lithologies with an Eo-Alpine overprint of different grade are present in the Wölz-Koralpe nappe system.

Areas with well preserved Permo-Triassic HT/LP lithologies south of the SAM

Well preserved Permo-Triassic HT/LP assemblages occur within more or less complete sections of Permo-Triassic crustal fragments up to c. 15 km structural depth. They comprise of an upper and middle continental crust and their Permo-Triassic sedimentary cover sequences with intercalations of Lower Permian quartz-porphyrines. In the crust a continuous increase of the metamorphic grade up to high amphibolite facies lithologies with local anatexis can be identified by

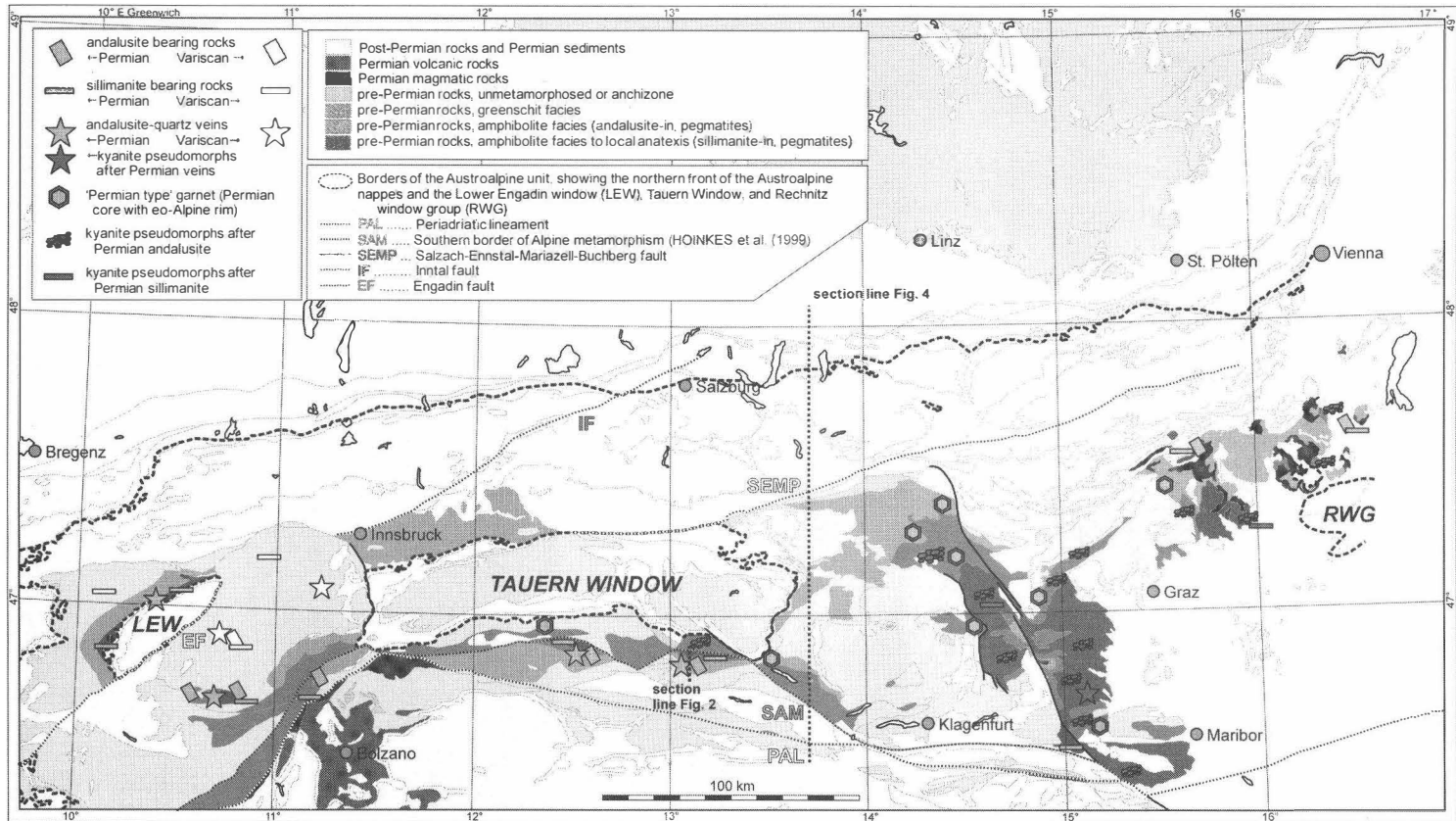


Fig. 1

Tectonic map of the Eastern Alps showing the distribution of the Permo-Triassic metamorphic imprint. Additionally the section lines of the transects in Fig. 2 and Fig. 4 are given.

decreasing cooling ages, different HT/LP assemblages and the occurrence of Permian magmatic rocks. The structurally deepest parts are outcropping along Tertiary structures, e.g. along the Deferegggen-Antholz-Vals fault, the Ragga-Teuchl fault or the thrust plane along the northwestern margin of the Lower Engadin Window.

One of the most complete sections is preserved in the Kreuzeck and Goldeck Mountains (Fig. 2). In this profile a Permo-Triassic event is overprinting Variscan metamorphic rock sequences of different metamorphic grade. In the tectonic higher units (south of the profile shown in Fig. 2), white mica Ar-Ar ages of ~310 Ma reflect post-Variscan cooling. The Variscan structures and assemblages are well preserved. In the upper part of the Strieden Complex post-deformation mica growth with respect to the Variscan structures can be observed, the white mica Ar-Ar ages range from 290 in the south to 260 Ma in the north. Below a zone with andalusite bearing lithologies occurs (HOKE, 1990). Andalusite, forming up to several centimetres large porphyroblasts, is frequently found within layers of Al-rich metapelites (24.9-26.9 wt% Al₂O₃) with a low X_{Mg} (0.19-0.23). Together with plagioclase and coarse-grained biotite flakes andalusite is overgrowing the Variscan microfabrics and porphyroblasts of staurolite and garnet. Andalusite is formed by the breakdown of chlorite (Chl + Ms ⇌ And + Bt + Qtz + H₂O) and paragonite (Pg + Qtz ⇌ Ab + And + H₂O). Furthermore, there are lithologies where staurolite is present only as small and dismembered inclusions with identical optical orientation within the andalusite porphyroblasts. In this case the andalusite growth is due to the breakdown of staurolite (St + Ms + Qtz ⇌ And + Bt + H₂O). Coarse-grained veins with mineral assemblages of Qtz + And + Ms ± Pl ± Ilm are crosscutting the Variscan foliation of the andalusite-bearing schists. Within these veins andalusite idioblasts up to 20 cm in length occur. Within deformation zones they are ductily deformed and fibrolitic sillimanite was growing within highly sheared areas. Ar-Ar muscovite ages of the andalusite-zone are in the range of 200-230 Ma.

In the lowermost part of the andalusite-zone isolated pegmatites appear, whereas pegmatites are frequent in the sillimanite-zone below. In metapelites sillimanite occurs within biotite-rich layers and as millimetre-sized patchy pseudomorphs, which often contain relics of garnet or staurolite covered by quartz. Locally plagioclase porphyroblasts up to 1 cm in size are growing. With structural depth the content of muscovite is decreasing. In the lowermost part anatectic mobilisates composed of Qtz + Pl + Kfsp ± Bt ± Sil are present. Obviously sillimanite is formed by the successive breakdown of paragonite (Pg + Qtz ⇌ Ab + Sil + H₂O), staurolite, garnet (Grt + Ms ⇌ Sil + Bt + Qtz + H₂O) and muscovite (Ms + Qtz ⇌ Sil + L). Together with the continuous change in the mineralogy a syn-metamorphic foliation becomes more prominent with structural depth. In the lowermost part the Variscan mineral assemblages and microstructures are nearly totally annealed. The pegmatites exhibit magmatic assemblages of Kfsp + Pl + Qtz + Ms + Turm ± Grt. Most of them are concordant or slightly discordant with a weak ductile deformation. Some are folded by the syn-metamorphic schistosity. Magmatic crystallisation ages of the pegmatites yielded 260-285 Ma. The pegmatites are obviously related to the HT/LP event, because they occur only in the lowermost andalusite-zone and within the sillimanite-zone. Additionally spodumene-bearing pegmatites are known. Typical Ar-Ar muscovite ages of the sillimanite zone are ~190 Ma.

In the NKFMAH grid (SPEAR, 1993) the following assemblages characterise the Permo-Triassic imprint (Fig. 3): And + Bt + Ms + Pl (500-570°C, <0.35 GPa), Sil + Bt + Ms + Pl (550-650°C, 0.3-0.45 GPa), Sil + Bt + Pl + melt (>650 °C, <0.45 GPa).

These assemblages define an elevated metamorphic gradient of $\sim 40^{\circ}\text{C}/\text{km}$. According to the age data on the synmetamorphic pegmatites the metamorphic peak occurred at ~ 270 Ma. After 270 Ma. the rock pile was not exhumed but cooled down to heat flow conditions of $\sim 25^{\circ}\text{C}/\text{km}$, which was reached at ~ 190 Ma (SCHUSTER et al., 2001).

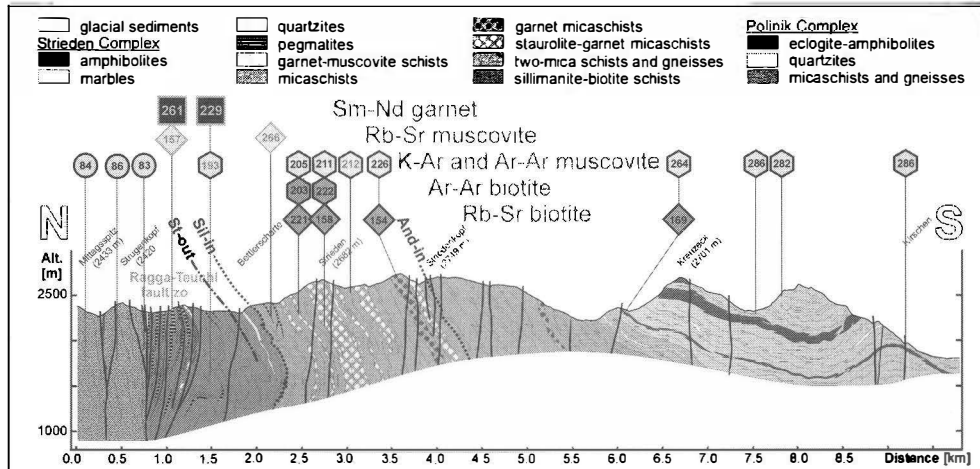


Fig. 2

Transsect through the Kreuzeck mountains (Carinthia/Austria). The Polinik Complex to the north of the Tertiary Ragga-Teuchl fault zone experienced an eclogite and high-amphibolite facies imprint during the Eo-Alpine thermal event. Typical K-Ar muscovite cooling ages are about 85 Ma. The Strieden Complex to the south of the fault zone is characterised by an anchizonal to lowermost greenschist facies Eo-Alpine imprint. Therefore the Permo-Triassic thermal imprint can be studied. In the structural lowermost part sillimanite is the typical aluminosilicate phase, whereas above andalusite can be found. Ar-Ar muscovite ages show increasing values towards the top.

Permo-Triassic HT/LP lithologies north of the SAM

In the western part of the Eastern Alps a Permian to middle Cretaceous diastathermal metamorphism has been reported. During Permian and lower Triassic times a high heat flow caused a near surface geothermal gradient of $\sim 70^{\circ}\text{C}/\text{km}$ and burial temperatures up to 300°C (FERREIRO-MÄHLMANN, 1995, 1996).

Within the Wölz-Koralpe Nappe system the units with the highest Eo-Alpine metamorphic grade also exhibit the most intense Permo-Triassic imprint. The latter can be identified by the occurrence of Permian garnet cores within polyphase garnet crystals, characteristic kyanite aggregates pseudomorphosed after andalusite and sillimanite, and by the occurrence of Permian magmatic rocks like pegmatites (SCHUSTER & FRANK, 2000; THÖNI & MILLER, 2000), gabbros (MILLER & THÖNI, 1997), and granites (MORAUF, 1980).

The Wölz Complex is mainly formed by garnet-micaschist with intercalations of amphibolites and marbles. In some areas garnet porphyroblasts with optically and chemically distinct cores and younger rims occur. The cores are idiomorphic, almandine-rich and poor in grossular ($\text{alm}_{0.73}\text{sps}_{0.08}\text{pyr}_{0.09}\text{grs}_{0.09}$). They have a pinkish colour and contain inclusions of margarite ($\text{ma}_{0.83}\text{pa}_{0.13}\text{ms}_{0.04}$), paragonite ($\text{pa}_{0.92}\text{ma}_{0.06}\text{ms}_{0.02}$), muscovite ($\text{ms}_{0.91}\text{pa}_{0.09}\text{ma}_{0.00}$), epidote, quartz and ilmenite.

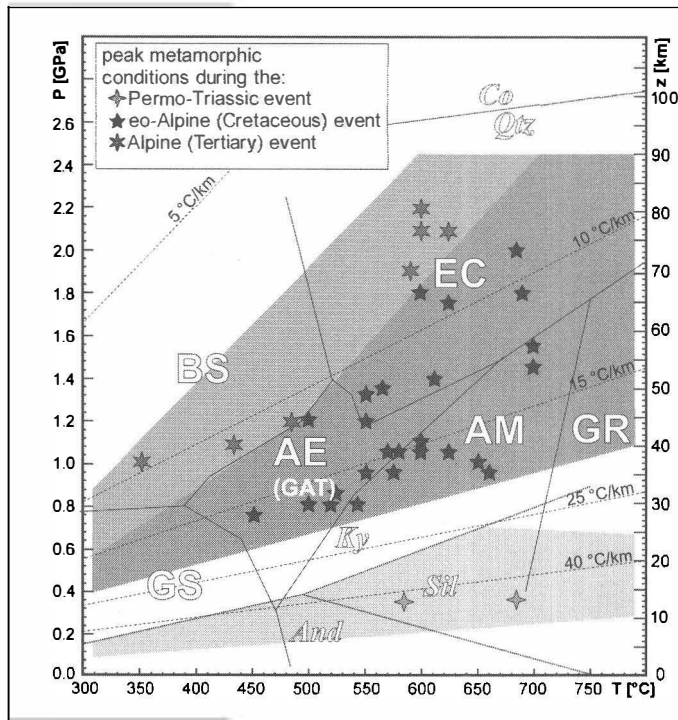


Fig. 3
Diagram showing the peak metamorphic P-T data referred in the text. The Permo-Triassic, Eo-Alpine and Alpine metamorphic event are characterised by different geothermal gradients during the metamorphic peak.

The core of one garnet yielded a well defined Sm-Nd crystallisation age of 269 ± 4 Ma and hence a Permian age of formation. Based on the coexistence of white mica phases during the growth of the garnet core, upper greenschist facies conditions at low pressures can be estimated (SCHUSTER & FRANK, 2000). Also from other units of the Wölz-Koralpe Nappe system garnet cores yielded Permian formation ages in the range of 265-285 Ma (THÖNI, 1999). They prove a metamorphic imprint of at least upper greenschist facies conditions for these areas.

In the Strallegg Complex the transformation of Permian andalusite and sillimanite-bearing assemblages into kyanite-bearing gneisses can be observed. This unit is composed of biotite-rich micaschists and migmatic gneisses, scarce amphibolites and intercalations of fine-grained granitic orthogneisses and pegmatites. Similar as in the Strieden Complex the andalusite and sillimanite-bearing lithologies contain relics of Variscan garnet and staurolite. They show mineral assemblages of $Sil + And + Kfs + Bt + Pl$ and also cordierite has been reported. Based on observations from TÖRÖK (1999) two sillimanite generations occur: the older developed by the breakdown of paragonitic mica by the reaction $Pg + Qtz \leftrightarrow Sil + Ab + H_2O$. This sillimanite is present as inclusions within andalusite. The latter formed by the reaction $St + Ms + Qtz \leftrightarrow And + Bt + H_2O$ at lower pressures (Fig. 3). A younger sillimanite generation occurs within extensional shear bands and between boudinaged andalusite porphyroblasts. Metamorphic peak conditions reached 640-710 °C at 0.22- 0.38 GPa (DRAGANITS, 1998; TÖRÖK, 1999). The granites and pegmatites represent syn-metamorphic intrusions with respect to the HT/LP event. They are crosscutting the schistosity defined by the HT/LP assemblages, but they are also deformed by syn-metamorphic structures. The age of the HT/LP imprint is defined by Sm-Nd garnet isochrone ages of metasedimentary and magmatic rocks in the range of 263-286 Ma.

The Eo-Alpine transformation of the aluminosilicate starts with the formation of distinct kyanite crystals along the edges and within cracks. Finally andalusite and sillimanite are totally replaced by fine-grained kyanite aggregates. These pseudomorphs are very typical even when they are affected by a strong deformation later on.

The Saualpe-Koralpe Complex consists of various kyanite-bearing micaschists and paragneisses with intercalated marbles, eclogites and amphibolites. Rocks of magmatic origin are (meta-)gabbros and frequent pegmatite gneisses. The present day metamorphic and structural behaviour is the result of the Eo-Alpine tectonothermal event, which reached eclogite and subsequent amphibolite facies conditions (see below). Relics of an amphibolite facies Permian HT/LP imprint are frequent kyanite pseudomorphs after andalusite and sillimanite, similar to those in the Strallegg Complex. Further Permian garnet cores and Permian pegmatites have been identified. The latter are interpreted as vein mobilisations from the host rocks (THÖNI & MILLER, 2000). Further gabbroic rocks yielded Permian crystallisation ages in the range of 240-285 Ma (MILLER & THÖNI, 1997; THÖNI, 1999). However, the most impressive relics of the HT/LP event are up to half a meter long kyanite pseudomorphs after chiastolithic andalusite from metapelites and idiomorphic kyanite pseudomorphs after andalusite within pre-existing andalusite-quartz veins. HÄBLER & THÖNI (2001) calculated metamorphic conditions of $590 \pm 20^\circ\text{C}$ at 0.38 ± 0.1 GPa for the HT/LP imprint. They used relic assemblages preserved within garnet cores from metapelites. A summary of the Permian imprint in the Austroalpine unit was published by SCHUSTER et al. (2001).

2.3. Alpine metamorphic history

In the Eastern Alps Alpine tectonometamorphism is triggered by two independent plate tectonic events:

- 1) **The Eo-Alpine (Cretaceous) metamorphic event** is widespread within the Austroalpine unit. It is related to the continental collision following the closure of an embayment of the Tethys ocean. The latter opened in Triassic to Jurassic times in the southeast of the Austroalpine unit (STAMPFLI & MOSAR, 1999) and was closed in Upper Jurassic to Cretaceous times. The geometry during the closure of this embayment is not well understood yet. However, recent investigations argue that the northern part of the Austroalpine unit formed the tectonic lower plate, whereas the southern parts and the north-eastern margin of the Southalpine unit acted as the tectonic upper plate during the continental collision following the disappearance of the oceanic embayment (SCHMID et al., 2004). The peak of the Eo-Alpine metamorphic event was reached at about 100 Ma, the youngest cooling ages reach 65 Ma (FRANK et al. 1987a; THÖNI, 1999).
- 2) **The Tertiary Alpine metamorphic event** is due to the closure of the Jurassic to early Tertiary Briançonnais and Valais oceans (Alpine Tethys). According to WAGREICH (2001) the re-arrangement of the Penninic-Austroalpine border zone from a passive to an active continental margin began at about 120 Ma. From that time on the oceanic lithosphere and slices from the northern margin of the Austroalpine unit (Lower Austroalpine units) were subducted towards the south below (Upper) Austroalpine units. The Tertiary event reached blueschist facies conditions in some Mesozoic parts of Penninic windows and some units of the Lower Austroalpine (Tarntal nappe). Eclogite facies conditions occur only in a narrow zone of the Tauern Window.

After the thermal peak at about 30 Ma (BLANKENBURG et al., 1989) uplift and cooling is recorded by K-Ar and Ar-Ar ages on white micas and fission track ages on zircon and apatite (LUKSCHWEITER & MORTEANI, 1980; GRUNDMANN & MORTEANI (1985); FÜGENSCHUH et al., 1998).

2.3.1. Eo-Alpine (Cretaceous) metamorphic event

In the Lower Austroalpine nappes the Eo-Alpine metamorphic imprint is expressed by a retrograde overprint on pre-Alpine metamorphic rock series and a prograde metamorphic imprint in Mesozoic cover sequences. During the retrogressive overprint the assemblage Chl + Ab + Ms + Qtz was stable in the basement rocks, indicating lower greenschist facies conditions. For the northern part of the Wechsel nappe MÜLLER et al. (1999) proposed temperatures of 350°C, whereas SLAPANSKY & FRANK (1987) estimated 350-400°C for the Radstadt nappe system.

In the Upper Austroalpine unit the Eo-Alpine metamorphic imprint shows a generally north-south orientated zonation, which is disrupted by Tertiary faults. Coming from the north the Eo-Alpine metamorphic conditions increase with structural depth from diagenetic up to greenschist facies conditions from the Northern Calcareous Alps down into the Silvretta-Seckau nappe system. Within the lower part of the overlying Wölz-Koralpe nappe system the metamorphic grade is increasing upwards from lower greenschist facies at the base to eclogite and high amphibolite facies in the central part. In the upper part it is decreasing upwards again to epidote-amphibolite or greenschist facies conditions at the top. The latter trend is continuing in the overlying Ötztal-Bundschuh and Drauzug-Gurktal nappe systems, where anchizonal or diagenetic conditions can be found in the tectonically uppermost units (Fig. 4). In the following chapter general outlines on this metamorphic zonation are given, whereas more detailed information on the metamorphic imprint of the individual units is given in HOINKES et al. (1999). Units, referred in here, are shown in a map by SCHUSTER et al. (2001, Fig. 1).

The metamorphic grades given for the Northern Calcareous Alps are based on illite-crystallinity data, coalification ranks and conodont alteration indices (CAI) (FERREIRO-MÄHLMANN, 1995; 1996; KRÁLIK & SCHRÁMM, 1994; GAWLIK et al. 1994). Palygorskite occurs within unmetamorphosed sediments, whereas paragonite, margarite, pyrophyllite and paragonite/muscovite mixed layer minerals were formed during the Eo-Alpine thermal imprint (KRÁLIK et al., 1987). There is an overall southward increase of the metamorphic grade, with diagenetic conditions in the Bajuvaric and northern Tirolic nappe system, to upper anchizonal conditions and lowermost greenschist facies in the southern part of the Tirolic nappe system. This seems to be more complicated by local trends. For example, in the western part of the Northern Calcareous Alps lowermost greenschist facies is reported from the tectonic uppermost Krabachjoch Nappe (KÜRMANN, 1993) and on the other hand, along the southeastern margin of the Northern Calcareous Alps the conditions are decreasing upwards from upper anchizonal conditions within the Permoscythian metasediments of the Tirolic nappes to diagenetic conditions in the uppermost Schneeberg nappe (Juvavic Nappe system). GAWLICK et al. (1994) reported the distribution of conodont alteration indices (CAI) for large parts of the Northern Calcareous Alps. Based on this data also a Jurassic thermal event can be recognised. The highest indices up to CAI 7 can be found in the Juvavic nappe system (FRISCH & GAWLICK, 2003).

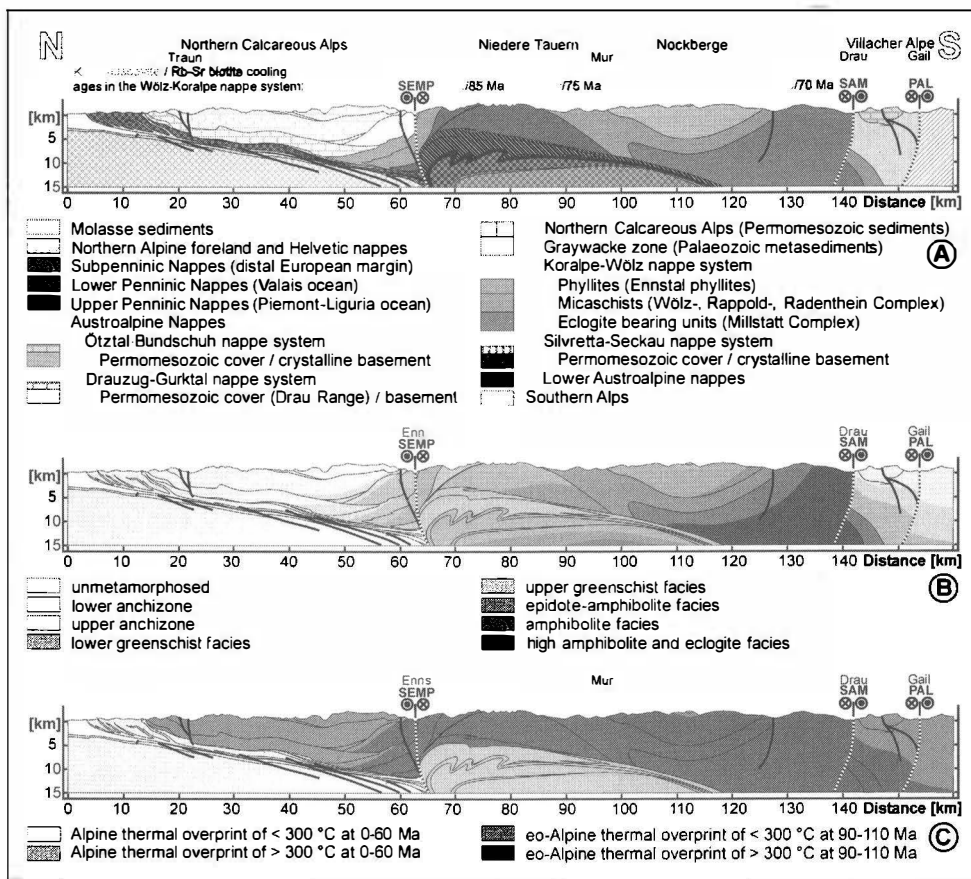


Fig. 4
Schematic transect through the eastern part of the Eastern Alps. The transects show the main tectonic units in (A), the metamorphic grade in (B) and the age distribution of the metamorphic imprint based on HANDY & OBERHÄNSLI (2004) in (C).

In the Noric, Silbersberg and Veitsch nappe of the Greywacke zone lower greenschist facies conditions are proved by illite crystallinity data, the grade of graphitisation and the occurrence of chloritoid. Only for some areas along the border to the Silvretta-Seckau nappe system temperatures of up to 500°C, indicating upper greenschist facies conditions, are reported. For these areas the local appearance of Eo-Alpine garnet is described by RATSCHBACHER & KLIMA (1985). In the Silvretta-Seckau nappe system high anchizonal to upper greenschist facies conditions have been reached along the northern margin. In the west, in the pre-Alpine amphibolite facies metamorphic rocks of the Silvretta Complex Variscan and Permo-Triassic K-Ar and Ar-Ar muscovite cooling ages are still preserved and even the Rb-Sr isotopic system in biotite is not totally reset. For this reason only anchizonal or lowermost greenschist facies conditions have been inferred as maximum conditions. On the other hand, in the Troiseck-Floning Komplex towards the east some biotite ages are totally reset and lower greenschist facies conditions are proved by the growth of Eo-Alpine biotite and chloritoid.

The highest conditions and an internal southward increase of the metamorphic grade are determined for the central part. In the north transgressive Permian metasediments on top of the Seckau Complex are characterised by the assemblage Ms + Ctd + Chl + Qtz, indicating upper greenschist facies conditions (500°C at 0.8 GPa). In this area Variscan Ar-Ar hornblende ages are still preserved. Towards the south epidote-amphibolite facies conditions of 550-600°C at 0.9-1.0 GPa and the total reset of the hornblende ages has been observed (FARYAD & HOINKES, 2001; 2003). In the northern, tectonically lower part of the Wölz-Koralpe nappe system, the metamorphic grade is increasing upwards. Assemblages of Ms/Pg + Chl + Qtz ± Bt ± Grt ± Ep (Ennstal Phyllites) are typical for the northernmost part. The Wölz Complex above is characterised by prograde assemblages of predominantly micaschist (Grt ± St ± Ky ± Ab + Ms/Pg + Bt + Qtz ± Chl) with intercalations of amphibolites and marbles. An internal gradient is indicated by the distribution of staurolite and the local breakdown of staurolite by the reaction $St + Qtz \leftrightarrow Ky + Grt + H_2O$. The amphibolites are variable and include massive amphibolites as well as mica-rich hornblende garben-schists (Ca-Amp + Grt + Ms/Pg + Pl + Chl ± Ep ± St ± Ky). Besides pure calcitic marbles also dolomitic marbles with assemblages of Cc + Dol + Qtz + Tr occur. According to FARYAD & HOINKES (2003) the metamorphic conditions in the uppermost parts of the unit reach 600-650°C at 1.0-1.1 GPa. From the same authors similar conditions have been reported for the overlying Rappold Complex. However the prograde breakdown of staurolite is very typical in the latter unit. For the Grobgness Complex in the eastern part of the Eastern Alps Eo-Alpine metamorphic upper greenschist facies and epidote amphibolite facies conditions of 550°C at 0.9 GPa have been determined (KOLLER et al., 2004). Somewhat higher conditions of ~560°C at 1.3 GPa were reported for the overlying Strallegg Complex (DRAGANITS, 1998; TÖRÖK 1999).

The central part of the Wölz-Koralpe nappe system is characterised by eclogite-bearing (Grt + Omp + Ca-Amp + Ep/Zoi + Ru + Qtz + Phe) units. Peak conditions for the easternmost Sieggraben Complex are 710°C at 1.5 GPa (NEUBAUER et al., 1999b; PUTIS et al., 2000). Variable results are reported for the Saualpe-Koralpe Complex (600°C at 1.8 GPa. (MILLER, 1990); 685°C at 2.0 GPa (MILLER & THÖNI, 1997); 700°C at 1.8 GPa (STÜWE & POWELL, 1995); 700°C at 1.6 GPa (GREGUREK et al., 1997); 690°C at 1.8 GPa (FARYAD & HOINKES, 2003). These widespread results may be due to the fact that the Saualpe-Koralpe complex consists of several subunits which might have reached different depths during the Eo-Alpine collisional event. Towards the west, conditions of c. 600°C at 1.1 GPa have been determined for the Millstatt and Polinik Complexes (HOINKES et al., 1999) whereas 550°C at 1.2 GPa were measured for the westernmost occurrence in the Texel mountains (HOINKES et al., 1991). All the eclogite-bearing units show a subsequent overprint at (high-)amphibolite facies conditions.

Decreasing metamorphic conditions are characteristic in the upper part of the Wölz-Koralpe nappe system: On top of the Saualpe-Koralpe Complex the metamorphic grade is decreasing from amphibolite facies conditions of 570°C at 1.05 GPa within the garnet-micaschists (Grt + Ky + St ± Ctd + Ms/Pg + Qtz ± Chl) of the Plankogel Complex (GREGUREK et al., 1997) to greenschist facies conditions in the micaschists above. Towards the west investigations yielded 600°C at 1.1 GPa for the Radenthein Complex (KOROKNAI et al., 1999) and 580°C at 1.05 GPa for the Schneeberg Complex (KONZETT & HOINKES, 1996), which are composed of lithologies very similar to those of the Wölz Complex.

In general the P-T-t paths in the lower part of the Wölz-Koralpe nappe system show a pronounced heating after the metamorphic peak, whereas those from the central and upper part are characterised by isothermal decompression.

In the Ötztal-Bundschuh and Gurktal-Drauzug nappe systems the upward decrease in the metamorphic grade is continuing. In the west the metamorphic grade is decreasing from epidote-amphibolite facies conditions along the southeastern margin of the Ötztal Complex to anchizonal conditions in the northwest. The same trend is visible in the transgressive Mesozoic cover. The epidote amphibolite facies is indicated by the occurrence of an Eo-Alpine garnet. Towards the north the occurrence of chloritoid defines the area of upper greenschist facies conditions. Further to the north the formation of stilpnomelane and a second generation of phengitic white mica within metagranitoides indicates a LT/HP imprint (< 300°C at c. 0.5 GPa). In the overlying Steinach Nappe high anchizonal conditions can be expected by coalification ranks.

The Bundschuh Complex is very similar to the Ötztal Complex. In its tectonic lowermost part amphibolite facies conditions of 600°C at 1.05 GPa were determined by KOROKNAI et al. (1999), whereas the conditions are decreasing to (lower)-greenschist facies conditions below and in the transgressive Mesozoic cover (SCHUSTER & FRANK, 2000). Assemblages of Ms + Chl ± Grt + Ab + Bt + Ep + Czoi + Cc + Dol suggest upper greenschist facies conditions in the Paleozoic sequences of the overlying Murau nappe. The pre-Alpine medium grade rocks of the Ackerl nappe and the Paleozoic metasediments of the uppermost Stolzalpen nappe show lower greenschist facies and anchizonal conditions. According to the fact that the latter unit experienced a similar metamorphic grade during the Variscan event, the detailed distribution of the Eo-Alpine anchizonal and lower greenschist facies imprint is not known (HOINKES et al., 1999). The late Carboniferous cover sequences of the Stolzalpen nappe show an anchizonal imprint, indicated by pyrophyllite, paragonite/muscovite mixed layer minerals and paragonite (SCHRAMM, 1982).

Within the Austroalpine units to the south of the SAM (HOINKES et al. 1999) (Fig. 1) the metamorphic grade is decreasing upwards. Greenschist facies conditions have been reached only in the northern part of the Goldeck mountains, whereas anchizonal conditions can be expected for the main part of the crystalline basement. This is mostly based on Rb-Sr biotite ages, which yield Eo-Alpine ages in the northern Goldeck mountains (DEUTSCH, 1988) and partial reset or unaffected pre-Alpine ages in the other areas. Based on illite-crystallinity and vitrinite reflection data anchizonal or diagenetic conditions occur within the Mesozoic cover sequences of the Drau Range (RANTITSCH, 2001; RANTITSCH & RAINER, 2003)

The observed Eo-alpine metamorphic zoning of the Austroalpine unit can be explained as follows: Based on a number of geochronological data (THÖNI, 1999) the pressure peak occurred at 100 ± 10 Ma. These data include Ar-Ar ages on fine fractions of white mica and whole rocks of low grade metamorphic rocks from tectonically high levels, as well as Sm-Nd garnet isochron ages on high-pressure rocks. Prior to 100 Ma shortening within the Austroalpine realm was compensated by W-NW directed (RATSCHBACHER, 1986) thrusting in the brittle tectonic wedge of the upper part and ductile deformation in the lower part of the crust. The northern part of the Austroalpine nappe stack, including the Northern Calcareous Alps, the Greywacke zone and the northern part of the Silvretta-Seckau nappe system, as well as the southern part of the Austroalpine unit comprising the Ötztal-Bundschuh and Gurktal-Drauzug nappe systems were substantially formed by this event. During the metamorphic peak their principal present day relations within the Austroalpine nappe stack were established. For this reason this units exhibit an upright metamorphic zoning.

After 100 Ma the deeply buried, highly metamorphosed and partly eclogite-bearing nappes of the Wölz-Koralpe nappe system were exhumed. In the area to the east of the Tauern Window their exhumation is due to NW-N directed thrusting (e.g. KROHE, 1987) in the lower part and by SE-directed normal faulting in the upper part of the nappe system. This post-peak metamorphic tectonic caused the inversion of the peak metamorphic grade in the lower part of the Wölz-Koralpe nappe system (Fig. 5). Therefore the Wölz-Koralpe nappe system has been defined as an extruding metamorphic wedge by SCHMID et al. (2004). Towards the west the eclogite-bearing units are outcropping in a back folding structure of the wedge. As only the upper limb of the back fold structure is visible, an upright metamorphic zoning can be observed in the field (Fig. 4). In general, the metamorphic cooling ages of the Eo-Alpine metamorphic event show an interference of two trends. Firstly, within the nappe piles formed prior to the metamorphic peak the oldest Eo-Alpine cooling ages are younger than the metamorphic peak (< 110 Ma) and decrease downward in the section. The second trend shows younger ages towards the south within the units of the metamorphic wedge (Wölz-Koralpe nappe system). In the northern, lower part of the wedge Ar-Ar muscovite ages and Rb-Sr biotite ages are c. 90 Ma and 85 Ma respectively. In the southern part and also in the back fold structure cooling ages of ~75 Ma (Ar-Ar muscovite) and ~70 Ma (Rb-Sr biotite ages) have been measured (Fig. 4A).

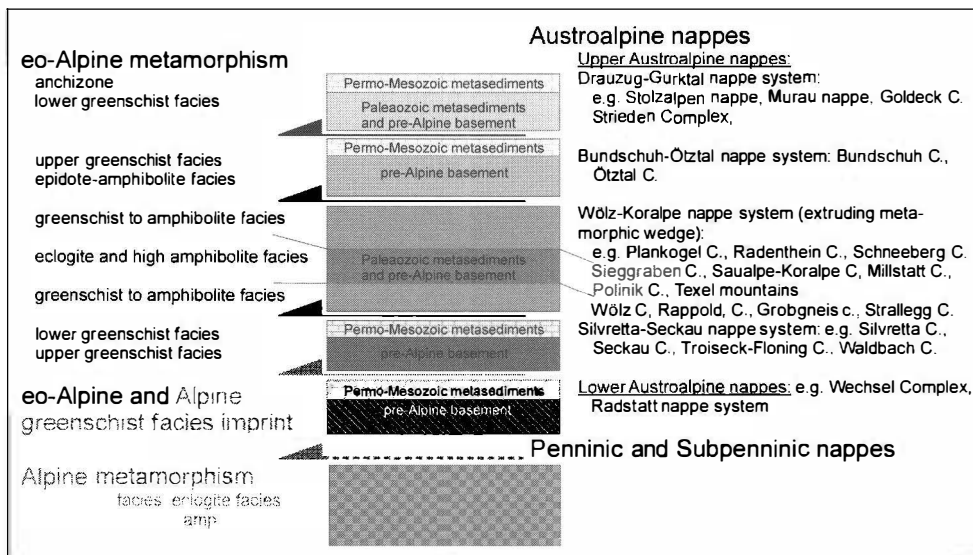


Fig. 5
Schematic nappe stack of the SE part of the Eastern Alps with the metamorphic evolution. Further the possible correlation to individual Austroalpine nappes from the western part of the Eastern Alps are show together with their metamorphic evolution.

2.3.2. The Tertiary Alpine metamorphic event

The Tertiary metamorphism is restricted to the Penninic Zone including the Suppenninic nappes and its immediate neighboring units, i.e. parts of the Lower Austroalpine unit (DINGELDEY et al., 1997, LIU et al., 2001) and the Austroalpine units just southwest of the Tauern Window (BORSI et al., 1978).

The Penninic nappes, widely distributed in the Western and Central Alps, can be followed along a series of windows across the whole range of the Eastern Alps. These are, from the W to the E the Lower Engadin Window (LEW), the Tauern Window (TW) and a group of small windows at the eastern margin of the Alps called the Rechnitz Window Group (RWG) (HÖCK & KOLLER, 1989; KOLLER & HÖCK, 1990). The Rhenodanubian Flyschzone is also ascribed to the Penninic realm (e.g. OBERHAUSER, 1995).

Stratigraphically, the metamorphics in the Penninic zone range from the Late Proterozoic(?) to the Paleogene. Pre-Mesozoic rocks are restricted to the TW and to small fragments at the basement of the Tasna nappe in the LEW (FLORINETH & FROITZHEIM, 1994). Mesozoic rocks, such as Triassic quartzites, marbles and dolomites as well as Jurassic and Cretaceous phyllites, micaschists, calcareous micaschists and other metasediments, ophiolites and non-ophiolitic volcanics occur throughout all Penninic windows. The upper stratigraphic boundary of the Mesozoic to Cenozoic sequences is still under discussion. Late Cretaceous and Paleogene sediments are proven from the LEW (OBERHAUSER, 1995), Early Cretaceous from the TW (REITZ et al., 1990) and the RWG (PAHR, 1980). The occurrence of Late Cretaceous and Tertiary sediments in the more easterly windows is questionable.

The Radstadt nappe system in the northeast of the Tauern Window is built up by slices of pre-Alpine amphibolite facies rocks and Mesozoic cover sequences. An Alpine lower greenschist metamorphic imprint is indicated by prograde assemblages in the Mesozoic rocks and retrogression within the basement.

2.3.2.1 Lower Engadine Window

Situated between the Eastern and Central Alps, the Lower Engadine Window forms an antiform trending NE-SW (KLÄY, 1957). It exposes a stack of Penninic nappes, overlain and framed by Austroalpine nappes. The Lower Engadine Window can be subdivided into several distinct units (CADISCH et al., 1968; TRÜMPY, 1975; OBERHAUSER, 1980); from top to base they are as follows.

The **Arosa zone** is a highly tectonized ophiolite-bearing unit (RING et al., 1990) with an ophiolite sequence mostly of serpentinites, gabbros and basalts (HÖCK & KOLLER, 1987) of the Piemont-Ligurian ocean. It is covered by a sequence of radiolarian cherts, pelagic limestones, black shales of Hauterivian-Aptian age (WEISSERT & BERNOULLI, 1985) and flysch. The Arosa zone in the eastern part of the Grisons continues southward into the Platta nappe with similar chemical and paleogeographic features (DIETRICH, 1976; FRISCH et al., 1994). It is likely to be correlative with the Matrei zone in the Tauern Window (FRISCH et al., 1987) that was interpreted as part of an imbricated thrust stack formed by the overriding of the Austroalpine units. According to Ring (1992) the Matrei zone can be compared to an accretionary prism.

The metamorphism of the ophiolites is twofold; an older HT oceanic metamorphism can be separated from a younger HP metamorphism. Evidence for the former comes from the replacement of gabbroic clinopyroxenes by amphiboles (pargasite, magnesio hornblende to actinolite) formed at relatively high temperatures. This together with some metasomatic changes of the bulk geochemistry (mainly Na enrichment) and some local strong oxidation argues for this hydrothermal event. Remnants of the E-W striking oceanic high temperature deformation planes in the gabbros show commonly formation of black amphibole in their vicinity indication of H₂O infiltration. The cores of these amphiboles in the altered gabbros contain still high Cl contents up to 4000 ppm.

In the hyaloclastites and pillow breccias the hydrothermal influence of the oceanic metamorphism causes locally ~E-W striking epidote-rich veins. The same event causes locally an intensive oxidation, defined by the dark red color of some hyaloclastite layers.

The Tertiary Alpine metamorphic grade of the Idalp ophiolite sequence belongs to the LT conditions at the transition between greenschist and blueschist facies with 0.7-0.9 GPa at ~350°C. The mineral assemblages are defined by pumpellyite + chlorite + albite. The pumpellyite of the metagabbro is Mg-rich, the green pumpellyite of the diabases with a $Fe_{tot}/(Fe_{tot}+Al)$ range between 0.11-0.15. Prograde replacement to epidote is rare. In the metabasite locally a high phengitic micas with an Si of 3.6 pfu were found.

The **Tasna nappe** is a continuous sedimentary sequence from the Permo-Triassic to the late Cretaceous, locally associated with slices of continental basement (WAIBEL & FRISCH, 1989). The Lias-Cretaceous sequence is composed mainly of turbidites with associated debris flows and pelagic limestones. However, recent studies in the Tasna nappe basement (FLORINETH & FROITZHEIM, 1994) revealed a preserved transition from the continental crust of the Briançonnais terrane to the oceanic crust of the Valais ocean. The metamorphic conditions belong to the lower greenschist facies.

The **Ramosch Zone** represents the transition between a continental unit (Briançonnais) and an oceanic (Valais) unit (FLORINETH & FROITZHEIM, 1994). The main unit is of a serpentinized peridotite-body associated with ophicarbonates and serpentinite breccias (VUICHARD, 1984). Metagabbros are lenticular within and adjacent to the serpentinite body. Directly underlying the serpentinite along an Alpine, top-north directed thrust fault, pillow basalts represent a part of the Valais ocean (FROITZHEIM et al., 1996). Further a huge mass of Bündnerschiefer, forming the deepest units of the Lower Engadine Window, with up to 10 km of calcschists interbedded with shales and quartzites (HITZ, 1995). It grades upward into flysch deposits that are lithologically very similar to the Bündnerschiefer and are dated as Late Cretaceous to Eocene (ZIEGLER, 1956). Some mafic bodies are intercalated within the schists particularly in the core of the window. These bodies are mainly composed of pillow basalts and hyaloclastites associated with metaradiolarites, where geochemical criteria suggest an oceanic basement (DÜRR et al., 1993). This unit is the remnant of the northern Penninic ocean, the Valais basin (FRISCH, 1976; TRÜMPY, 1980; STAMPFLI, 1993).

In Bündnerschiefer and associated metabasites of the LEW two units displaying distinct metamorphic have been reported by BOUSQUET et al. (1998, 2002). The structurally lower unit (Mundin unit) has a clear HP-LT history, whereas in the upper unit (Arina unit) no obvious HP-LT mineral assemblages were found.

In the Mundin unit blueschist metamorphic conditions are exclusively found in the central part of the window forming the core of a late anticline. These conditions are characterized by the occurrences of (Fe,Mg)-carpholite in metasediments (GOFFÉ & OBERHÄNSLI, 1992; OBERHÄNSLI et al., 1995). In the core of the Mundin unit antiform, carpholite appears as relicts. For the Mundin unit, P-T estimates range between 1.1-1.3 GPa for a temperature around 350-375°C (BOUSQUET et al., 2002). Indication of the LT-HP metamorphic assemblages in the metabasites are rare and occur mainly in samples which underwent prior an oceanic metamorphism. Glauco-phane (BOUSQUET et al., 1998) and Na-pyroxene were found in metabasites. The Na-pyroxene assemblages are partly replaced by riebeckite or Mg-riebeckite. Also aragonite was found as a relict in the Na-pyroxene bearing assemblages, partly or strongly replaced by calcite.

In the Arina unit, evidence for HP metamorphism is scarce. However, crossite and lawsonite occur in metabasites (LEIMSER & PURTSCHHELLER, 1980), and Mg-pumpellyite in association with chlorite, albite, and phengite occur in metapelites. The P-T conditions calculated by BOUSQUET et al. (1998) range around 0.6 GPa, 300°C.

2.3.2.2. Tauern Window

The oldest rocks in the TW are found in a volcano-sedimentary sequence comprising ophiolites, island arc volcanics and associated sediments of Late Proterozoic to Paleozoic age (Habach Group). A part of this sequence underwent pre-Mesozoic metamorphism, partly migmatitisation and was intruded by Variscan granitoids. According to the tectonic classification of SCHMID et al. (2004) the Paleozoic sequences belong to the Subpenninic nappes.

The post-Variscan sequences start with Permo-Triassic quartzites, middle Triassic limestones and dolomites and upper Triassic sandstones and shales. The Triassic rocks are overlain by shales, marls and shaly limestones of Jurassic to Early Cretaceous age (Bündnerschiefer Group). Locally, sandstones, breccias and arcoses occur. Associated with the sediments are ophiolites and other basic intrusions and volcanics. The youngest sediments proven so far are of Early Cretaceous age. Comparison with lithologically similar sediments in the LEW and the Penninic realm in the Western Alps suggests the occurrence of younger sediments.

Tectonically two nappes are generally delineated (FRISCH, 1976): the lower Venediger nappe (Subpenninic nappes according to SCHMID et al. (2004)) comprising most of the pre-Mesozoic rocks and relatively little Mesozoic sediments and volcanics and the higher Glockner nappe (Lower Penninic nappes according to SCHMID et al. (2004) including most of the Triassic rocks, the Bündnerschiefer and the ophiolites. Both nappes were later folded forming a huge anticline with an axis following approximately the main ridge of the Alps. Apart from the pre-Mesozoic metamorphism three episodes of metamorphic events were recognized: an eclogite event, a blueschist metamorphism, and the final greenschist to amphibolite facies metamorphism. The eclogitisation affects only a relatively small strip mainly at the southern escarpment of the TW, the blueschist metamorphism is more widely distributed but restricted to the ophiolites, their immediate cover and the areas tectonically below. The Tertiary greenschist to amphibolite facies metamorphism can be seen in all rocks of the TW.

Two metamorphic events are recognizable in all Penninic windows where the older is regarded as a HP/LT metamorphism and the younger as Barrovian type. Only in the TW an earlier eclogite metamorphism is recorded with a retrograde evolution path, entirely different from the rest of the Penninic metamorphics of the Eastern Alps.

The most conspicuous eclogite assemblages are found in metabasic rocks but some original basalt-sediment interfaces are still preserved. Consequently some metasediments exhibit high-pressure mineral assemblages (FRANK et al., 1987b; FRANZ & SPEAR, 1983). Inclusions in the eclogitic mineral assemblage in the metabasites indicate a greenschist to amphibolite facies event prior to the eclogitisation (MILLER, 1977; DACHS, 1986; DACHS et al., 1991).

The P-T conditions of the formation of eclogite are fairly well established within the analytical error and the errors of the different geobarometers used. The eclogitized metabasics and metasediments passed through a mantle/crust segment in a depth of 70 km (possibly 85 km according to STÖCKHERT et al., 1997). With T_{max} around 600- 630°C and $P \sim 1.9-2.2$ GPa (HOSCHEK, 2001) they formed at a very low geothermal gradient of 7-9°C/km, typical for subduction zones.

It should be noted here that only the structurally lowest part of the Mesozoic sediments and volcanics below the ophiolites underwent the eclogite metamorphism.

Whereas the P-T conditions are well constraint no dating of the eclogites is available yet. If the Ar-Ar age data of ZIMMERMANN et al. (1994) are valid for the blueschist event, the eclogites formed prior to the Eocene/Oligocene boundary. ZIMMERMANN et al. (1994) estimate the age of mica formation related to the eclogites between 40 and 50 Ma.

By contrast to the eclogite assemblages, which are well preserved, the minerals formed during the blueschist event survived only rarely. They can be traced by some individual mineral relicts and by pseudomorphs. The most conspicuous relicts from this stage are pseudomorphs after lawsonite. Some jadeite poor omphacites coexisting with albite rich plagioclase derived from the decomposition of a more jadeite rich omphacite also represents the blueschist facies. Occasionally blue amphiboles such as glaucophane and/or crossite are preserved and probably barroisitic amphiboles. Associated with this stage and possibly also with the eclogite event are high Si phengite with Si = 3.30-3.40 pfu. In extreme cases the Si content may reach 3.65 pfu (ZIMMERMANN et al., 1994). From that data FRANK et al. (1987a) estimated the conditions of blueschist formation as T = 400-450°C and P around 0.9 GPa. ZIMMERMANN et al. (1994) calculated 1.0 GPa at 400°C. The blueschist event is neither well constraint in respect to the P-T path, nor in respect to age dating. The data by ZIMMERMANN et al. (1994) suggest for the TW an age of late Eocene - early Oligocene for the formation of the blueschist assemblages. Again the low thermal gradient of 10-13°C/km suggests a subduction related environment.

At the southern rim of the TW the zone of Matrei (Upper Penninic nappes according to SCHMID et al., 2004) consists of various lithologies including serpentinites and metabasites. Below the serpentinites thin horizons of blueschist assemblages in basaltic to ophiocarbonate lithologies were found recently in several localities (KOLLER & PESTAL, 2003). This assemblage contains blue amphiboles or an older alkali pyroxene (up to 20% Jd), and stilpnomelane together with albite. In some cases a replacement to bluish-green amphiboles is common.

2.3.2.3. Rechnitz Window Group

At the eastern end of the Alps close to the Austrian-Hungarian border several small Penninic windows occur below the Lower Austroalpine nappes. All these windows comprise huge masses of Mesozoic metasediments and locally some ophiolites. The lithology consists of a several km thick sequence of metasediments with calcareous micaschists, quartz-phyllites, graphite phyllites, rare breccias and few horizons of rauhwackes. Within the ophiolitic section remnants of oceanic metamorphism occur together with various degrees of oxidation. This event can be traced in most of the metagabbros and ophiocarbonates, as well as in some metabasalts (KOLLER, 1985).

Blueschist facies event

Within the ophiolitic sequence remnants of a HP/LT event are widespread. Typical minerals are alkali pyroxenes, glaucophane or crossite, rare pseudomorphs of lawsonite, high-Si phengite, Mg-rich pumpellyite, stilpnomelane, hematite and rutile. At high Fe³⁺ contents in metabasites alkali pyroxene+hematite and rutile occur. No clear high pressure assemblage can be defined for the metabasalts containing only rare relicts of blue amphibole, stilpnomelane and pseudomorphs after lawsonite. High-Si phengite is also observable in metabasalts and common in metasediments. For the blueschist facies event KOLLER (1985) calculated temperatures of 330-370°C at a minimum pressure of 0.6-0.8 GPa.

Low-pressure greenschist event

The high-pressure event is followed by a common greenschist overprint forming the general assemblages (metabasalts, metasediments). From the north to the south, there is a slight increase in temperature observable, which can be defined by following mineral isogrades: (1) Disappearance of metastable stilpnomelane and Mg-pumpellyite in the northern part of the Rechnitz Window, (2) first appearance of green biotite in the northern part of the Bernstein Window, and (3) the first appearance of garnet in metapelites is restricted to the southernmost outcrops of the Penninic units.

No reliable age dating exists from the high pressure event. The greenschist event is dated by K-Ar ages of muscovite in the range of 22-19 Ma (FRANK in KOLLER, 1985). Fission-track ages were reported by DUNKL & DEMÉNY (1997) for zircon from 21.9-13.4 Ma and for apatite from 7.3-9.7 Ma. Furthermore the Penninic rocks of the RWG are overlain by non-metamorphosed sediments of Miocene and Pliocene age (PAHR, 1980).

2.3.2.4. Lower Austroalpine

2.3.2.4.1. Radstadt nappe system

The Lower Austroalpine nappes of the "Radstädter Tauern" form the NE rim of the Tauern Window (TOLLMANN, 1977; HÄUSLER, 1987). They contain the tectonically highest quartzphyllite nappes with an inverse layering and different Permo-Mesozoic sequences, as the Hochfeind, Lantschfeld, Pleisling and Kesselspitz nappes. Well defined modern P-T path investigations on the Alpidic metamorphic evolution are still missing.

In the basement the Alpidic metamorphic event defines a retrograde evolution. The first geochronological results obtained by SLAPANSKY & FRANK (1987) on white micas (K-Ar and Ar-Ar ages) revealed a decreasing age from the uppermost nappe (~100 Ma) to the base (~50 Ma). More recent studies by LIU et al. (2001) confirm the general trend, giving Cretaceous ages in the upper Radstadt nappes and Paleogene age in the lower Hochfeind nappe. Similar ages were obtained by DINGELDEY et al. (1997) from the Reckner nappe.

The metamorphic evolution of the Permo-Mesozoic sediment sequences can be defined by the assemblage of phengite + chlorite and without forming biotite. Only locally also chloritoid and kyanite were mentioned by VOLL (1977). Temperatures of 450°C and pressures of at least 0.3 GPa have been assumed by SLAPANSKY & FRANK (1987). In general there is an increase of metamorphic conditions towards to the south.

2.3.2.4.2. Tarntal Nappes

The Lower Austroalpine Nappes cover the Penninic rocks of the TW also at the NW (Tarntal mountains). According to TOLLMANN (1977) the tectonic succession consists in the NW of the Tauern Window of three individual nappes. From the base to the top they are the Innsbruck quartzphyllite nappe, the Hippold nappe and the Reckner nappe.

The Innsbruck quartzphyllite nappe consists of various phyllites with rare diabases and quartz-porphyrines, further carbonate (calcite, dolomite and magnesite) lenses. The top of this sequence is formed by Permo-Triassic sediments. By contrast, the Hippold and Reckner nappe are built up by a huge variety of partly fossil bearing Mesozoic sediment sequences ranging from Skyth to Malm ages (ENZENBERG, 1967; ENZENBERG-PRAEHAUSER, 1976). The top of the Reckner nappe is formed by the serpentinites and blueschists of the Reckner complex (DINGELDEY et al., 1997).

For both, the Reckner and the Hippold nappe a Tertiary HP/LT event in the range of ~350°C and ~1.0 GPa has been reported by DINGELDEY et al. (1997). Typical minerals of this event are alkalipyroxenes, Mg-rich pumpellyite, stilpnomelane and high Si phengite. The Penninic meta-sediments adjoining the Hippold nappe exhibit only intermediate pressure conditions (0.6-0.7 GPa).

This high pressure event was followed by a classical greenschist paragenesis with blue amphiboles replacing the alkalipyroxenes, low-Si muscovites, epidote, green biotite instead of stilpnomelane. Only a LP/LT event was found in the underlying Innsbruck Quartzphyllite nappe (~400 °C and < 0.4 GPa).

Ar-Ar-measurements on high-Si phengites from the Reckner nappe recorded ages around 50 Ma. In the underlying Hippold nappe and in the adjoining Penninic "Bünderschiefer" the high-Si phengites define ages between 44-37 Ma (DINGELDEY et al., 1997). Only rejuvenisation of Variscan micas and no clear Alpidic ⁴⁰Ar/³⁹Ar plateau ages were found in the Innsbruck Quartzphyllite nappe.

2.3.2.4. Correlation of the Penninic Windows of the Eastern Alps

The subsequent greenschist to amphibolite facies event has its lowest T_{max} with 350°C in the LEW. In the RWG a T_{max} of 450°C is recorded and in the TW between 500-550°C. T_{max} is combined with a pressure of 0.2-0.4 GPa in the LEW, 0.3-0.4 GPa in the RWG and 0.6-0.8 GPa, locally reaching up to 1.0 GPa in the TW approaching a geothermal gradient of 20-35°C/km, typical for a Barrovian type metamorphism. It is coeval with the total disappearance of the Penninic zone beneath the Austro-Alpine nappes. This metamorphic stage was reached shortly after 30 Ma and is further recorded by cooling ages down to 16 Ma. Similar cooling ages are reported from the RGW, the scarce data from the LEW record probably the onset of the low grade metamorphism. The cooling and exhumation in the TW and RWG can be followed through fission track studies of apatites down to 4 and 7 Ma respectively (FÜGENSCHUH et al., 1998).

3. Conclusions

The distribution of the metamorphic facies zones in the Eastern Alps is mainly controlled by the northwards transport of the Austroalpine nappes. They show a Cretaceous metamorphism and are thrust over the Penninic domains with Tertiary metamorphism (Fig. 4). The latter are exposed in the Eastern Alps only as tectonic windows.

The *Eo-Alpine (Cretaceous) metamorphic event* is widespread within and restricted to the Austroalpine unit. It is related to the continental collision following the closure of an embayment of the Tethys ocean during late Jurassic to Cretaceous times. Recent investigations indicate that the northern part of the Austroalpine unit forms the tectonic lower plate. The southern parts and the north-eastern margin of the Southalpine unit acted as the tectonic upper plate during the continental collision following the disappearance of the oceanic embayment (SCHMID et al., 2004). In the Austroalpine nappes the Eo-Alpine metamorphic event overprints Variscan and/or Permo-Triassic metamorphic rocks as well as Permo-Mesozoic sedimentary sequences. The peak of the Eo-Alpine metamorphic event was reached at about 100 Ma, the youngest cooling ages are recorded at 65 Ma (THÖNI, 1999).

The metamorphic conditions reached sub-greenschist and greenschist facies in the northern part of the Austroalpine. To the south, in the Wölz-Koralpe nappe system the conditions increase upwards up to eclogite facies in the middle part of the nappe system (Fig. 5). In its upper part of the Wölz-Koralpe nappe system and in the overlying units the metamorphic degree is decreasing again until sub-greenschist facies. This zoning indicates a transported metamorphism at least in the Wölz-Koralpe nappe system.

The *Tertiary Alpine metamorphic event* is due to the closure of the Jurassic to early Tertiary Briançonnais and Valais oceans (Alpine Tethys). According to WAGREICH (2001) the re-arrangement of the Penninic-Austroalpine border zone from a passive to an active continental margin starts at about 120 Ma. From that time on the oceanic lithosphere and slices from the northern margin of the Austroalpine unit (Lower Austroalpine units) were subducted towards the south below (Upper) Austroalpine units. The Tertiary event reaches blueschist facies conditions in some Mesozoic parts of Penninic windows and some units of the Lower Austroalpine (Tarntal nappe). Eclogite facies conditions followed by a blueschist event occur only in a narrow zone of the Tauern Window. The thermal peak ranges from greenschist to amphibolite facies, the latter was only reached in the central part of the Tauern Window. After the thermal peak at about 30 Ma (BLANKENBURG et al., 1989) uplift and cooling is recorded by K-Ar and Ar-Ar ages on white micas and fission track ages on zircon and apatite (LUKSCHWEITER & MORTEANI, 1980; GRUNDMANN, & MORTEANI, (1985); FÜGENSCHUH et al., 1998). In the lower nappes of the Lower Austroalpine units the Tertiary Alpine metamorphism overprints the Cretaceous metamorphic event.

References

- BLANKENBURG, F. v., VILLA, I. M., BAUR, H., MORTEANI, G. & STEIGER, R. H. (1989): Timecalibration of a PT-path from the Western Tauern Window, Eastern Alps: the problem of closure temperatures. - *Contrib. Mineral. Petrol.*, 101, 1-11.
- BORSI, S., DEL MORO, A., SASSI, F. P., ZANFERRARI, A. & ZIRPOLI, G. (1978): New geopetrologic and radiometric data on the Alpine History of the Austridic continental margin south of the Tauern Window (Eastern Alps). - *Mem. Ist. Geol. Mineral. Univ. Padova*, 32, 1-19.
- BOUSQUET, R., OBERHÄNSLI, R., GOFFE, B., JOLIVET, L. & VIDAL, O. (1998): High-pressure - low-temperature metamorphism and deformation in the Bündnerschisfer of the Engadin window: implications for the regional evolution of the Central Alps. - *J. Metam. Geol.*, 16, 657-674.
- BOUSQUET, R., GOFFÉ, B., VIDAL, O., OBERHÄNSLI, R. & PATRIAT, M. (2002): The tectono-metamorphic history of the Valaisan domain from the Western to the Central Alps: new constraints on the evolution of the Alps. - *Geol. Soc. Amer. Bull.*, 114, 207-225.
- CADISCH, J., EUGSTER, H. & WENK, E. (1968): *Geologischer Atlas der Schweiz 1:25.000, Blatt 44 Scoul, Schuls-Tarasp*. - *Schweiz. Geol. Komm. (mit Erläuterungen)*, Bern 1968.
- DACHS, E. (1986): High-pressure mineral assemblages and their breakdown-products in metasediments south of the Großvenediger, Tauern Window, Austria. - *Schweiz. mineral. petrogr. Mitt.*, 66, 145-161.
- DACHS, E., FRASL, G. & HOINKES, G. (1991): Mineralogisch-petrologische Exkursion ins Penninikum des Tauernfensters (Großglockner Hochalpenstraße/Südliches Großvenediger Gebiet) und in das Ötztal-kristallin (Timmelsjoch/Schneebergerzug). - *Europ. J. Mineralogy*, 3, Beiheft 2, 79-110.

- DEUTSCH, A. (1988): Die frühalpide Metamorphose in der Goldeck-Gruppe (Kärnten). - Nachweis anhand von Rb-Sr-Altersbestimmungen und Gefügebeobachtungen. - *Jb. Geol. B.-A.*, 131/4: 553-562.
- DINGELDEY, C., DALLMEYER, R. D., KOLLER, F. & MASSONNE, H.-J. (1997): P-T-t history of the Lower Austroalpine Nappe Complex in the "Tamtaler Berge" NW of the Tauern Window: implications for the geotectonic evolution of the central Eastern Alps. - *Contrib. Mineral. Petrol.*, 129, 1-19.
- DIETRICH, V. (1976): Plattentektonik in den Ostalpen. Eine Arbeitshypothese. - *Geotekt. Forsch.*, 50, 1-84.
- DRAGANITS, E. (1998): Seriengliederung im Kristallin des südlichen Ödenburger Gebirges (Burgenland) und deren Stellung zum Unterostalpin am Alpenostrand. - *Jb. Geol. B.-A.*, 141, 113-146, Wien.
- DUNKL, I. & DEMENY, A. (1997): Exhumation of the Rechnitz Window at the border of the Eastern Alps and Pannonian Basin during Neogene extension. - *Tectonophysics*, 272, 197-211.
- DÜRR S. B., RING, U. & FRISCH, W. (1993): Geochemistry and geodynamic significance of the north Penninic ophiolites from the Central Alps. - *Schweiz. Mineral. Petrogr. Mitt.*, 73, 407-419.
- ENZENBERG, M. (1967): Die Geologie der Tamtaler Berge (Wattener Lizum), Tirol. - *Mitt. Ges. Geol. Bergbaustud.*, 17, 5-50.
- ENZENBERG-PRAEHAUSER, M. (1976): Zur Geologie der Tamtaler Berge und ihrer Umgebung im Kamm Hippold-Kalkwand (Tuxer Voralpen, Tirol). - *Mitt. Ges. Geol. Bergbaustud.*, 23, 163-180
- FARYAD, S. W. & HOINKES, G. (2001): Alpine chloritoid and garnet from the Hochgrössen Massif. - *Mitt. Österr. Mineral. Ges.*, 146, 387-396.
- FARYAD, S. W. & HOINKES, G. (2003): P-T gradient of Eo-Alpine metamorphism within the Austroalpine basement units east of the Tauern Window (Austria). - *Mineralogy and Petrology*, 77, 129-159.
- FERREIRO-MÄHLMANN, R. (1995): Das Diagenese-Metamorphose-Muster von Vitrinireflexion und Illit-"Kristallinität" in Mittelgraubünden und im Oberalpin Teil 1: Bezüge zur Stockwerktektonik. - *Schweiz. Mineralog. Petrogr. Mitt.*, 75: 85-122.
- FERREIRO-MÄHLMANN, R. (1996): Das Diagenese-Metamorphose-Muster von Vitrinireflexion und Illit-"Kristallinität" in Mittelgraubünden und im Oberalpin Teil 2: Korrelation kohlenpetrographischer und mineralogischer Parameter. - *Schweiz. Mineralog. Petrogr. Mitt.*, 76: 23-46.
- FLORINETH, D. & FROITZHEIM, N. (1994): Transition from continental to oceanic basement in the Tasna nappe (Engadin window, Graubünden, Switzerland): evidence for Early Cretaceous opening of the Valais ocean. - *Schweiz. mineral. petrogr. Mitt.*, 74, 437-78.
- FRANK, W., HÖCK, V. & MILLER, C. (1987b): Metamorphic and tectonic history of the central Tauern Window. - In: FLÜGEL, H. W., FAUPL, P. (Eds): *Geodynamics of the Eastern Alps*. Deuticke: Wien, 34-54.
- FRANK, W., KRÁLIK, M., SCHARBERT, S. & THÖNI, M. (1987a): Geochronological Data from the Eastern Alps. - In: FLÜGEL, H. W., FAUPL, P. (Eds): *Geodynamics of the Eastern Alps*. Deuticke: Wien, 272-281.
- FRANZ, G. & SPEAR, F. S. (1983): High pressure metamorphism of siliceous dolomites from the central Tauern Window, Austria. - *Am. J. Sci.*, 283-A, 369-413.
- FRISCH, W. (1976): Ein Modell zur alpidischen Evolution und Orogenese des Tauernfensters. - *Geol. Rundsch.*, 65/2, 375-393.
- FRISCH, W., RING, U., DÜRR, S., BORCHERT, S. & BIEHLER, D. (1994): The Arosa Zone and Platta Nappe Ophiolites (Eastern Swiss Alps): Geochemical Characteristics and their meaning for the Evolution of the Penninic ocean. - *Jahrb. Geol. Bundesanst. Wien*, 137, 19-33.
- FRISCH, W. & GAWLICK, H.-J. (2003): The nappe structure of the central Northern Calcareous Alps and its disintegration during Miocene tectonic extrusion - a contribution to understanding the orogenic evolution of the Eastern Alps. - *Int. J. Earth Sci. (Geol. Rundschau)*, 92, 712-727.
- FROITZHEIM, N., SCHMID, S. M. & FREY, M. (1996): Mesozoic paleogeography and the timing of eclogite-facies metamorphism in the Alps: A working hypothesis. - *Eclogae geol. Helv.*, 89, 81-110, Basel.

- FÜGENSCHUH, B., SEWARD, D. & MANCKTELOW, N. (1998): Exhumation in a convergent orogene: the western Tauern window. - *Terra Nova*, 9, 213-217.
- GAWLICK, H.-J., KRYSZYN, L. & LEIN, R. (1994): Conodont colour alteration indices: Paleotemperatures and metamorphism in the Northern Calcareous Alps - a general view. - *Geol. Rundsch.*, 83, 660-664.
- GOFFÉ, B. & OBERHÄNSLI, R. (1992): Ferro- and magnesiocarpholite in the "Bündnerschiefer" of the eastern Central Alps (Grisons and Engadine Window). - *Eur. J. Mineral.*, 4, 835-838.
- GREGUREK, D., ABART, R. & HOINKES, G. (1997): Contrasting Eoalpine P-T evolution in the southern Koralpe, Eastern Alps. - *Mineralogy and Petrology*, 60, 61-80.
- GRUNDMANN, G. & MORTEANI, G. (1985): The Young Uplift and Thermal History of the Central Eastern Alps (Austria/Italy), Evidence from Apatite Fission Track Ages. - *Jb. Geol. Bundes-Anst. Wien*, 128, 197-216.
- HABLER, G. & THÖNI, M. (2001): Preservation of Permo-Triassic low-pressure assemblages in the Cretaceous high-pressure metamorphic Saualpe crystalline basement (Eastern Alps, Austria). *J. metamorphic Geol.*, 19, 679-697.
- HANDY, M. & OBERHÄNSLI, R. (2004): Metamorphic Structure of the Alps: Age map of the metamorphic structure of the Alps – tectonic interpretation and outstanding problems - *Mitt. Österr. Min. Ges.*, 149, 201-226.
- HÄUSLER, H. (1987): The northern Austroalpine margin during the Jurassic: breccias from the Radstädter-Tauern and the Tarntaler Berge. - In: Flügel, H. W. & Faupl, P. (eds.): *Geodynamic evolution of the Eastern Alps*. - 103-111, Deuticke (Wien).
- HITZ, L. (1995): The 3D crustal structure of the Alps of eastern Switzerland and western Austria interpreted from network of deep-seismic profiles. - *Tectonophysics*, 248, 71-96.
- HÖCK, V. & KOLLER, F. (1987): The Idalp Ophiolite (Lower Engadine Window, Eastern Alps): Petrology and Geochemistry. - *Ofioliti*, 12, 179-192.
- HÖCK, V. & KOLLER, F. (1989): Magmatic evolution of the Mesozoic ophiolites in Austria. - *Chemical Geology*, 77, 209-227
- HOINKES, G., KOLLER, F., RANTITSCH, G., DACHS, E., HÖCK, V., NEUBAUER, F. & SCHUSTER, R. (1999): Alpine metamorphism in the Eastern Alps. - *Schweiz. Mineral. Petrogr. Mitt.*, 79, 155-181.
- HOINKES, G., KOSTNER, A. & THÖNI, M. (1991): Petrologic Constraints for Eoalpine Eclogite Facies Metamorphism in the Austroalpine Ötztal Basement. - *Mineralogy and Petrology*, 43, 237-254.
- HOKE, L. (1990): The Altkristallin of the Kreuzeck Mountains, SE-Tauern Window, Eastern Alps - Basement Crust in a convergent plate Boundary Zone. - *Jb. Geol. B.-A.*, 133, 5-87, Wien.
- HOSCHEK, G. (2001): Thermobarometry of metasediments and metabasites from the Eclogite zone of the Hohe Tauern, Eastern Alps, Austria. - *Lithos*, 59, 127-150.
- KLÄY, L. (1957): *Geologie der Stammerspitze*. - *Ecol. Geol. Helv.*, 50, 323-467.
- KOLLER, F. (1985): *Petrologie und Geochemie des Penninikums am Alpenostrand*. - *Jb. Geol.-Bundes-Anst., Wien*, 128, 83-150.
- KOLLER, F. & HÖCK, V. (1990): Mesozoic ophiolites in the Eastern Alps. - In: MALPAS, J., MOORES, E. M., PANAYIOTOU, A., XENOPHONTOS, C. (Eds.): *Ophiolites, Oceanic Crustal Analogues, Proceedings of the Symposium "TROODOS 1987"*, 253-263.
- KOLLER, F., PUMHÖSL, H., THÖNI, M., FARYAD, S. W., SEIFERT-FALKNER, C., FRANK, W., SATIR & M., MILLER, C. (2004): Origin and evolution of Permian gabbroic intrusions within the Grobgneiss-Unit, Lower Austroalpine Unit (Eastern Alps). - Submitted to *Lithos*.
- KOLLER, F. & PESTAL, G. (2003): Die ligurischen Ophiolite der Tarntaler Berge und der Matreier Zone. - *Geol. Bundesanst. Arbeitstagung '03 Blatt 148 "Brenner"* (ISBN-3-85316-18-2), 65-76.
- KONZETT, J. & HOINKES, G. (1996): Paragonite-hornblende assemblages and their petrological significance: an example from the Austroalpine Schneeberg Complex, Southern Tyrol, Italy. - *J. metamorphic Geol.* 14, 85-101.

- KOROKNAI, B., NEUBAUER, F., GENSER, J. & TOPA, D. (1999): Metamorphic and tectonic evolution of Austroalpine units at the western margin of the Gurktal nappe complex, Eastern Alps. - *Schweiz. Mineral. Petrogr. Mitt.*, 79, 277-295.
- KRALIK, M., KRUMM, W. & SCHRAMM, J.-M. (1987): Low grade and very low grade metamorphism in the Northern Calcareous Alps and in the Greywacke Zone: illite crystallinity data and isotopic ages. - In: FLÜGEL, H. W. & FAUPL, P. (Hrsg.): *Geodynamics of the Eastern Alps*, 164-178, (Deuticke) Wien.
- KRALIK, M. & SCHRAMM, J. M. (1994): Illit- Wachstum: Übergang Diagenese - Metamorphose in Karbonat- und Tongesteinen der Nördlichen Kalkalpen: Mineralogie und Isotopengeologie (Rb-Sr, K-Ar und C-O). - *Jb. Geol. Bundes-Anst. Wien*, 137/1, 105-137, Wien.
- KROHE, A. (1987): Kinematics of Cretaceous nappe tectonics in the Austroalpine basement of the Koralpe region (eastern Austria). - *Tectonophysics*, 136, 171-196.
- KÜRSMANN, H. (1993): Zur Hochdiagenese und Anchimetamorphose in Permotria-Sedimenten des Austroalpins westlich der Tauern. - *Bochumer geol. U. geotech. Arb.*, 41, 1-328.
- LEIMSER, W. & PURTSCHELLER, F. (1980): Beiträge zur Metamorphose von Meta-vulkaniten im Pennin des Engadiner Fensters. - *Mitt. Österr. Geol. Ges.*, 71/72, 129-137.
- LUCKSCHEITER, B. & MORTEANI, G. (1980): Microthermometrical and chemical studies of fluid inclusions in minerals from Alpine veins from the penninic rocks of the central and western Tauern Window (Austria/Italy). - *Lithos*, 13, 61-77.
- LIU, Y., GENSER, J., HANDLER, R., FRIEDL, G. & NEUBAUER, F. (2001): $^{40}\text{Ar}/^{39}\text{Ar}$ muscovite ages from the Penninic-Austroalpine plate boundary, Eastern Alps. - *Tectonics*, 20, 526-547.
- MILLER, Ch. (1977): Über die polyphase alpinmetamorphe Entwicklung der Eklogite im Penninikum des Tauernfensters, Österreich. In: BÖGEL, H. (Ed.): - *Geodynamics and geotraverses around the Alps*, Salzburg 1977.
- MILLER, C. (1990): Petrology of the type locality eclogites from the Koralpe and Saualpe (Eastern Alps), Austria. - *Schweiz. Mineral. Petrogr. Mitt.*, 70, 287-300.
- MILLER, C. & THÖNI, M. (1995): Origin of eclogites from the Austroalpine Ötztal basement (Tirol, Austria): geochemistry and Sm-Nd vs. Rb-Sr isotope systematics. - *Chem. Geol. (Isotope Geoscience Section)*, 122, 199-225.
- MILLER, C. & THÖNI, M. (1997): Eo-Alpine eclogitisation of Permian MORB-type gabbros in the Koralpe (Eastern Alps, Austria): new geochronological, geochemical and petrological data. - *Chem. Geol.*, 137, 283-310, Amsterdam.
- MORAU, W. (1980): Die permische Differentiation und die alpidische Metamorphose des Granitgneises von Wolfsberg, Koralpe, SE-Ostalpen, mit Rb/Sr- und K/Ar-Isotopenbestimmungen. - *Tschernmaks Mineral. Petrogr. Mitt.* 27: 169-185, Wien.
- MÜLLER, W., DALLMEYER, R. D., NEUBAUER, F. & THÖNI, M. (1999): Deformation-induced resetting of Rb/Sr and $^{40}\text{Ar}/^{39}\text{Ar}$ mineral systems in a low-grade, polymetamorphic terrane (Eastern Alps, Austria). - *J. Geol. Soc.*, 156/3, 261-278.
- NEUBAUER, F. (2002): Evolution of late Neoproterozoic to early Palaeozoic tectonic elements in Central and Southeast European Alpine mountain belts: review and synthesis. - *Tectonophysics*, 352, 87-103.
- NEUBAUER, F., DALLMEYER, R. D. & TAKASU, A. (1999b): Conditions of eclogite formation and age of retrogression within the Siegraben unit, Eastern Alps: implications for Alpine-Carpathian tectonics. - *Schweiz. Mineral. Petrogr. Mitt.*, 79, 297-307.
- NEUBAUER, F., HOINKES, G., SASSI, F. P., HANDLER, R., HÖCK, V., KOLLER, F. & FRANK, W. (1999a): Pre-Alpine metamorphism in the Eastern Alps. - *Schweiz. Mineral. Petrogr. Mitt.*, 79, 41-62.

- OBERHAUSER, R. (1980): Das Unterengadiner Fenster. - In: OBERHAUSER, R. (Ed.): Der Geologische Aufbau Österreichs. - Springer-Verlag Wien-New York, 291 - 299.
- OBERHAUSER, R. (1995): Zur Kenntnis der Tektonik und der Paleogeographie des Ostalpenraumes zur Kreide-, Paleozän- und Eozänzeit. - Jb. Geol. Bundes-Anst. Wien, 138, 369-432.
- PAHR, A. (1980): Die Fenster von Rechnitz, Bernstein und Möltern. - In: OBERHAUSER, R. (Ed.): Der Aufbau Österreichs. - Springer-Verlag Wien-New York, 320-326.
- PUTIS, M., KORIKOVSKY, S. P. & PUSHKAREV, Y. D. (2000): Petrotectonics of an Austroalpine Eclogite-Bearing Complex (Sieggraben, Eastern Alps) and U-Pb Dating of Exhumation. - Jb. Geol. B.-A., 142: 73-93.
- RANTITSCH, G. (2001): Thermal history of the Drau Range (Eastern Alps). - Schweiz. Mineralog. Petrogr. Mitt., 81: 181-196.
- RANTITSCH, G. & RAINER, T. (2003): Thermal modeling of Carboniferous to Triassic sediments of the Karawanken Range (Southern Alps) as a tool for paleogeographic reconstructions in the Alpine-Dinaridic-Pannonian realm. - Int. J. Earth Sci. (Geol. Rundschau), 92, 195-209.
- RATSCHBACHER, L. (1986): Kinematics of Austro-Alpine cover nappes: changing translation path due to transpression. - Tectonophysics, 125, 335-356, Amsterdam.
- RATSCHBACHER, L. & KLIMA, K. (1985): Übersicht über Geologie und Mineralgehalt in einem Querprofil von Altkristallin zur Kalkalpenbasis (Triebener Tauernpaß - Flitzenschlucht, Paltental, Steiermark, Österreich). - Jb. Geol. Bundes-Anst. Wien, 128, 151-173.
- REITZ, E., HÖLL, R., HUPAK, W. & MEHLTRETTER, C. (1990): Palynologischer Nachweis von Unterkreide in der Jüngeren (Oberen) Schieferhülle des Tauernfensters (Ostalpen). - Jb. Geol. Bundes-Anst. Wien, 133, H.4, 611-618.
- RING, U. (1992): The Alpine geodynamic evolution of Penninic nappes in the eastern Central Alps: geothermobarometric and kinematic data. - J. Metam. Geol., 10, 33-53.
- RING, U., RATSCHBACHER, L., FRISCH, W., DÜRR, S. & BORCHERT, S. (1990): The internal structure of the Arosa Zone (Swiss-Austrian Alps). - Geol. Rundschau, 79, 725-739.
- SCHMID, S. M., FÜGENSCHUH, B., KISSLING, E. & SCHUSTER, R. (2004): Tectonic map and overall architecture of the Alpine orogen. - Eclog. Geol. Helv., 97, 93-117
- SCHRAMM, J. M. (1982): Zur Metamorphose des feinklastischen Permoskyth im Ostabschnitt der Nördlichen Kalkalpen (Ostösterreich). - Verh. Geol. B.-A., 1982/2: 63-72.
- SCHUSTER, R. & FRANK, W. (2000): Metamorphic evolution of the Austroalpine units east of the Tauern Window: indications for Jurassic strike slip tectonics. - Mitt. Ges. Geol. Bergbaustud. Österreich, 42 (1999), 37-58, Wien.
- SCHUSTER, R., SCHARBERT, S., ABART, R. & FRANK, W. (2001): Permo-Triassic extension and related HT/LP metamorphism in the Austroalpine - Southalpine realm. - Mitt. Geol. Bergbau Stud. Österr., 44, 111-141.
- SLAPANSKY, P. & FRANK, W. (1987): Structural Evolution and Geochronology of the Northern Margin of the Austroalpine in the Northwestern Schladming Crystalline (NE Radstädter Tauern). - In: FLÜGEL, H.W. & FAUPL, P. (Hrsg.): Geodynamics of the Eastern Alps., 244-262, (Deuticke) Wien.
- SPEAR, F. S. (1993): Metamorphic Phase Equilibria and Pressure-Temperature-Time Paths. - Mineralogical Society of America Monograph, Washington, 799 pp.
- STAMPFLI, G. M. (1993): Le Briançonnais, terrain exotique dans les Alps? - Eclog. Geol. Helv., 86, 1-45.
- STAMPFLI, G. M. & MOSAR, J. (1999): The making and becoming of Apulia. - Memorie di Scienze Geologiche, 51/1: 141-154, Padova.
- STÖCKHERT, B., MASSONNE, H.-J. & NOWLAN, E. U. (1997): Low differential stress during high-pressure metamorphism: The microstructural record of a metapelite from the Eclogite Zone, Tauern Window, Eastern Alps. - Lithos, 41, 103-118.

- STÜWE, K. & POWELL, R. (1995): PT Paths from modal properties: application to the Koralm Complex, Eastern Alps. - *Contr. Mineral. Petrol.*, 119, 83-93.
- TAIT, J. A., BACHRADSE, V., FRANKE, W. & SOFFEL, H. C. (1997): Geodynamic evolution of the European Variscan fold belt: Paleomagnetic and geological constraints. - *Geologische Rundschau*, 86, 585-598.
- TOLLMANN, A. (1977): *Geologie von Österreich, Band 1*. Wien: Deuticke, 766 pp.
- THÖNI, M. (1999): A review of geochronological data from the Eastern Alps. - *Schweiz. Mineral. Petrogr. Mitt.*, 79/1, 209-230, Zürich.
- THÖNI, M. & MILLER, C. (2000): Permo-Triassic pegmatites in the eo-Alpine eclogite-facies Koralpe complex, Austria: age and magma source constraints from mineral chemical, Rb-Sr and Sm-Nd isotopic data. - *Schweiz. Mineral. Petrogr. Mitt.*, 80, 169-186, Zürich.
- TÖRÖK, K. (1999): Pre-Alpine development of the andalusite-sillimanite-biotite-schist from the Sopron Mountains (Eastern Alps, Western Hungary). - *Acta Geol. Hung.*, 42/2: 127-160, Budapest.
- TRÜMPY, R. (1975): Penninic-Austroalpine boundary in the Swiss Alps: A presumed former continental margin and its problems. - *Amer. J. Science*, 275A, 209-238.
- TRÜMPY, R. (1980): *Geology of Switzerland, a guidebook*. - Wepf, Basel, 104pp.
- VOLL, G. (1977): Seriengliederung, Gefügeentwicklung und Metamorphose in den Nördlichen Radstädter Tauern zwischen Forstau- und Preunegg-Tal. In: BÖGEL, H. (ed.): *Geodynamic and geotraverses around the Alps*, Abstract 2, Salzburg.
- VUICHARD, D. (1984): The ophiolitic suite of the Alp Champatsch (Lower Engadine Window, Switzerland): the metamorphic and tectonic evolution of a small oceanic basin in the Penninic Realm? - *Ofioliti*, 9, 619-632.
- WAGREICH, M. (2001): A 400-km-long piggyback basin (Upper Aptian-Lower Cenomanian) in the Eastern Alps. - *Terra Nova*, 13, 401-406.
- WAIBEL, A. F. & FRISCH, W. (1989): The Lower Engadine Window: sediment deposition and a calcitretion in relation to the plate-tectonic evolution of the Eastern Alps. - *Tectonophysics*, 162, 229-241.
- WEISSERT, H. J. & BERNOULLI, D. (1985): A transform margin in the Mesozoic Thethys: evidence from the Swiss Alps. - *Geol. Rundschau*, 74, 665-679.
- ZIEGLER, W. H. (1956): *Geologische Studien in den Flyschgebieten des Oberhalbsteins (Graubünden)*. - *Eclog. Geol. Helv.*, 49, 1-78.
- ZIMMERMANN, R., HAMMERSCHMIDT, K. & FRANZ, G. (1994): Eocene high pressure metamorphism in the Penninic units of the Tauern Window (Eastern Alps): evidence from Ar/Ar dating and petrological investigations. - *Contrib. Mineral. Petrol.*, 117, 175-186.

manuscript received: June 2004

manuscript accepted: July 2004

**EXPLANATORY NOTES TO THE MAP:
METAMORPHIC STRUCTURE OF THE ALPS
AGE MAP OF THE METAMORPHIC STRUCTURE OF THE ALPS –
TECTONIC INTERPRETATION AND OUTSTANDING PROBLEMS**

by

M. R. Handy¹ & R. Oberhänsli²

¹Institut für Geologische Wissenschaften

Freie Universität Berlin, Malteserstrasse 74-100, 12249 Berlin, Germany

²Institut für Geowissenschaften

Universität Potsdam, Karl-Liebknecht-Str. 25, 14476 Potsdam-Golm, Germany

Abstract

The mapped distribution of post-Jurassic mineral isotopic ages in the Alps reveals two metamorphic cycles, each consisting of a pressure-dominated stage and a subsequent temperature-dominated stage: (1) a Late Cretaceous cycle in the Eastern Alps, indicated on the map by purple dots and green colours; and (2) a Late Cretaceous to Early- to Mid-Tertiary cycle in the Western and Central Alps, Corsica and the Tauern window, marked on the map with blue and red dots and yellow and orange colours.

The first cycle is attributed to the subduction of part of the Austroalpine passive margin following Jurassic closure of the Middle Triassic, Meliata-Hallstatt ocean basin. This involved nappe stacking, extensional exhumation and cooling.

The second cycle is related to the subduction of the Jurassic-Cretaceous, Liguro-Piemont and Valais ocean basins as well as distal parts of the European and Apulian continental margins. Subsequent exhumation and cooling of the Tertiary nappe pile occurred during oblique indentation of Europe by the Apulian margin in Oligo-Miocene time. Despite a wealth of geochronologic work in the Alps, there are still large areas where relevant data are lacking or where existing data yield conflicting interpretations. Most such conflicts reflect the difficulty of relating the behaviour of mineral isotopic systems to the formation of structures and to the stability of metamorphic mineral assemblages. The age map of metamorphic structure thus also points to areas of future research in the Alps.

Introduction

This map is a compilation of metamorphic ages in the Alps grouped according to tectonic episodes that have been recognized on the scale of the Alpine orogen. As such, it represents a departure from the more traditional approach of distinguishing pre-Alpine and Alpine ages or from depicting the age data in the most objective possible fashion, usually as a forest of sample location points and numbers. In fact, this map is rather more interpretative, because it is based on the correlation of metamorphic mineral assemblages with structures (faults, foliations, folds) that can be related to kinematically distinct tectonic events. It therefore sacrifices objectivity from the metamorphic and geochemical standpoints in favour of a synthetic approach that allows one to regard Alpine metamorphism in a broad geodynamic context. It is intended as an aid to the tectonic interpretation of the Map of the Metamorphic Structure of the Alps.

When referring to metamorphism as "Alpine", we mean metamorphism in the Alps that post-dates the deposition of marine sediments in Mesozoic ocean basins and adjacent continental margins of the Alps. These sediments range in age from Early Triassic to Early Tertiary, with syn-rift sedimentation being older in the Eastern Alps (Middle Triassic) than in the Central and Western Alps (Early to Middle Jurassic). The term "Alpine" is therefore used in both temporal and spatial senses. This dualistic convention is sometimes confusing to extra-Alpine colleagues! The ages of metamorphism in the Alps were recently reviewed in a series of excellent papers accompanying the 1999 version of the Metamorphic Map of the Alps. The reader is especially referred to DESMONS et al. (1999a-c) and FREY et al. (1999) for the Western and Central Alps, to HOINKES et al. (1999) and THÖNI (1999) for the Eastern Alps, and to COLOMBO & TUNESI (1999) for the Southern Alps. This paper is therefore intended as a supplement to, not a replacement of, this previous work. The breadth of these reviews allows us to restrict citations below to papers published since 1999 or to earlier articles in the Alpine literature that are essential to understanding this map. This paper should therefore be regarded as a guide to reading the map rather than as a full-fledged review. Accordingly, the reference list includes metamorphic literature used to construct the map and, where appropriate, some selected tectonic literature.

Following brief descriptions of the tectonic base map and the colour schemes used to distinguish metamorphic age patterns in the Alps, we discuss some of the problems in dating Alpine metamorphism and in assigning ages to mapped units. The next chapter is devoted to the tectonic interpretations proposed in recent years to account for the distribution of Alpine metamorphic ages. We conclude with some remarks on combining tectonic and metamorphic information in the Alps as a requisite for use of the Alps as a natural laboratory for studying crustal processes.

The tectonic base map

The base map for the metamorphic ages is a simplified and modified version of the recently compiled Tectonic Map of the Alps (SCHMID et al., 2004), itself based on sheets 1 and 2 of the Structural Model of Italy (BIGI et al., 1991). The black lines represent major tectonic boundaries and basement-sediment contacts. The tectonic boundaries include the contacts of main nappe units in both sedimentary and basement rocks. Other tectonic contacts in the map of SCHMID et al. (2004), all of them secondary in importance, were omitted because they are not related to the distribution of metamorphic ages on the map scale at hand.

Ophiolites marking sutures between the former continental margins in the Alps are not distinguished on the map. These sutures are shown in Figs. 1 and 2, and only partly coincide with the Late Cretaceous and Early Tertiary, pressure-dominated metamorphic events represented by variously coloured dots in the metamorphic structure map.

The reddish-purple lines represent the main segments of the Periadriatic Fault System (PFS). This fault system was active from about 35 Ma to 10-15 Ma and significantly modified the Tertiary Alpine edifice (SCHMID & KISSLING, 2000; HANDY et al., 2004). The Oligocene to Miocene activity of these faults is closely related to the areal distribution of Tertiary overprinting metamorphism in the Alps. This is especially true of mylonitic rocks along the Tonale and Canavese segments of the PFS and of low-angle normal faults flanking the Tauern and Lepontine metamorphic domes, as depicted in Fig. 1 and discussed below.

Topographic features in the map include the major lakes and rivers, as well as the largest cities. The drainage pattern of these lakes and rivers reflects Plio-Pleistocene glaciation and fluvial activity, which was itself channelled by many of the middle- to late Tertiary tectonic lineaments shown in reddish purple (e.g., FRISCH et al., 1998). This is potentially interesting to map users because some workers have argued that erosional denudation controlled exhumation and cooling of the metamorphic basement in the core of the Alps (SCHLUNEGGER & HINDERER, 2001; SCHLUNEGGER & WILLET, 2002).

The metamorphic age patterns

The colour patterns on the tectonic base map represent two broad categories of metamorphic ages related to the tectonic evolution of the Alps:

1) *Dotted areas* depict tectonic units that were subducted to depths corresponding to high-pressure greenschist-, blueschist-, and eclogite-facies conditions. These are the HPGS, BS, UBS, BET, ECL fields on the map of Metamorphic Structure of the Alps. The purple, blue and red colours of the dots indicate the three broad age ranges of subduction-related deformation and metamorphism, as discussed below. Solid dots represent relatively well constrained ages, whereas open dots indicate areas in which the available ages are sparse, controversial, or even contradictory, and have therefore been constrained by indirect lines of argument.

The age of high-pressure metamorphism is estimated with high-retentivity isotopic systems, including Sm-Nd and Hf-Lu on high-pressure assemblages. In part of the Western Alps, we also cited U-PB SHRIMP ages on zircons from leucosomes in eclogite. We purposely avoided using ages of high-pressure minerals and mineral assemblages that were obtained in the absence of detailed element analyses before about 1990. Many of these first-generation ages are controversial or even meaningless because they were derived from low-retentivity isotopic systems and were affected by partial resetting during temperature-dominated metamorphism or hydrothermal activity (e.g., K-Ar white mica, discussion in HAMMERSCHMIDT & FRANK, 1991).

2) *Solidly coloured areas* indicate rock units that underwent temperature-dominated metamorphism from sub-anchizonal to upper amphibolite facies conditions, including partial melting. This includes the DIA, SGS, LGS, UGS, GAT, AM and VT fields of the metamorphic structure map. Where pressure- and temperature-dominated metamorphism coincide in space in the Alps, the latter always overprints the former.

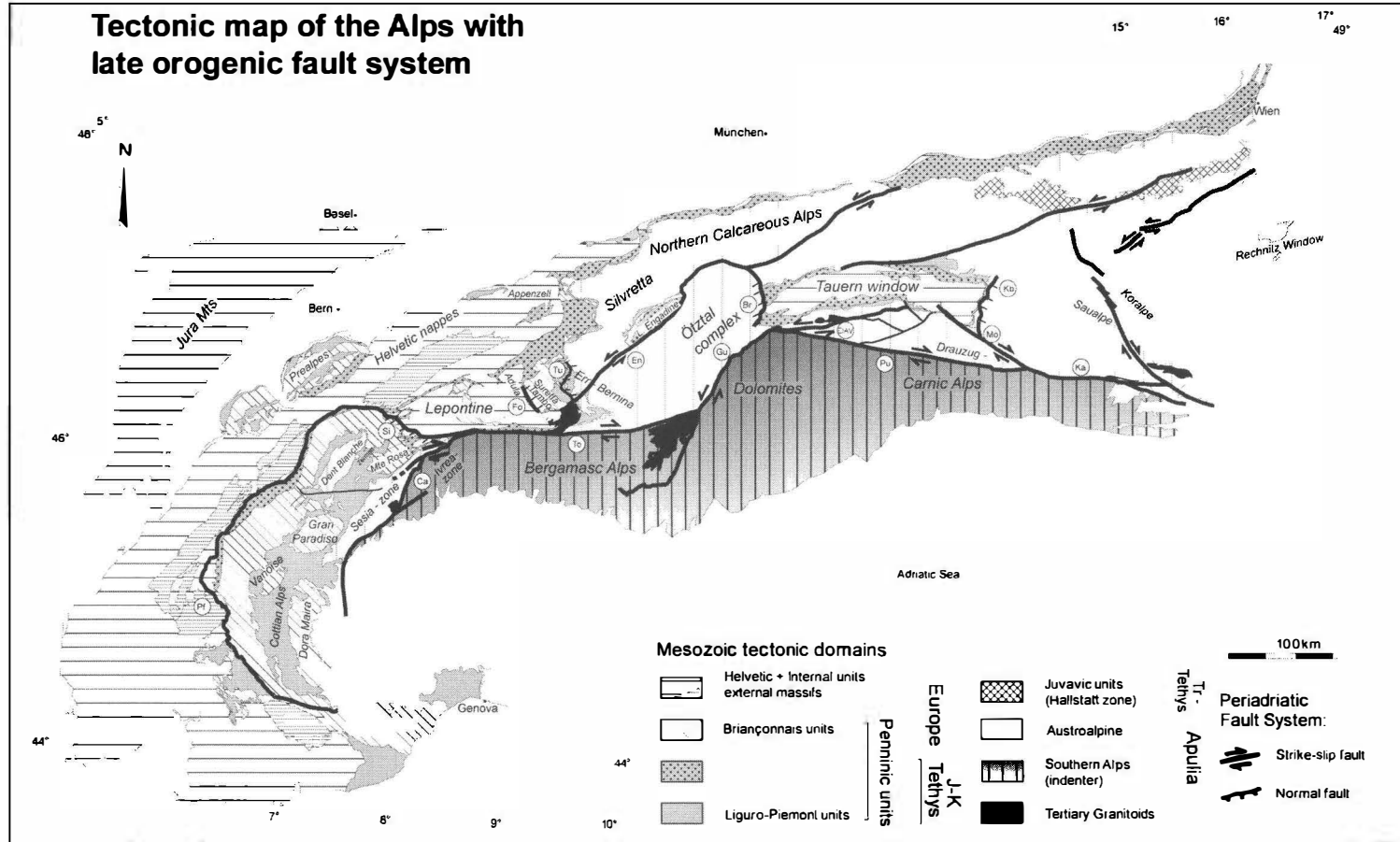


Figure 1

Tectonic map of the Alps after Handy et al. (2004) with names of tectonic units and segments of the late orogenic, Periadriatic fault system (thick lines) discussed in the text: Kb = Katschberg extensional fault, Ka = Karawanken fault, Mö = Mölltal fault, Pu = Pustertal fault, DAV = Defereggan-Antholz-Vals fault, Br = Brenner extensional fault, Gu = Giudicarie fault, En = Engadine fault, Tu = Turba extensional fault, To = Tonale segment of the Insubric mylonite belt, Fo = Forcola extensional fault, Ca = Canavese segment of the Insubric mylonite belt, Si = Simplon extensional fault, Pf = Penninic frontal thrust.

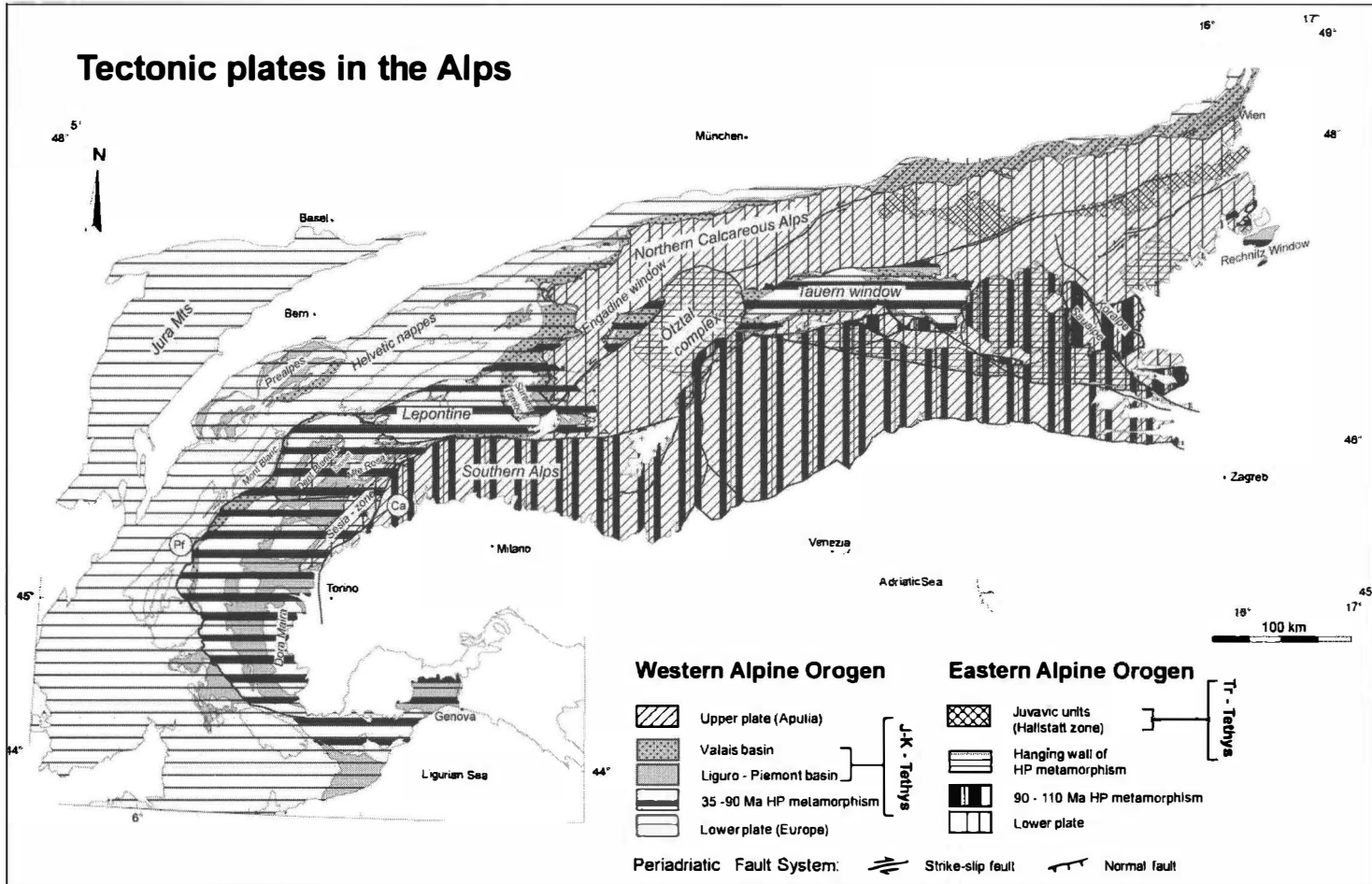


Figure 2
 Tectonic map of the Alps after Handy et al. (2004) showing boundaries of the upper and lower tectonic plates, oceanic sutures, and units of both plates affected by HP metamorphism. Base of upper plate in the Eastern Alps from Schuster (2003). See text for explanation.

The temperature-dominated metamorphism is divided into two age groups, 0-59 Ma and 60-110 Ma, depicted with yellow-orange and green shades of colour. These groups are related to the kinematically distinct, Late Cretaceous and Tertiary orogenic events in the Alps (SCHMID et al., 1996; STAMPLI et al., 1998). Each group is further divided into two colour subgroups (yellow and orange for the 0-59 Ma range, light green and dark green for the 60-110 Ma range) in order to distinguish areas that experienced maximum temperatures below 300°C from those where temperatures exceeded this value. This colour distinction based on temperature was both necessary and convenient; necessary because for the radiometric age systems used in dating (Rb-Sr, Ar-Ar and K-Ar biotite and white mica) 300°C represents the effective lower limit for intra-granular diffusion of radiogenic Ar and Rb, even in fine grained mica aggregates; convenient because 300°C marks the transition from fracture and frictional sliding to dislocation glide and creep in quartz deformed at geological strain rates (reviews in SNOKE & TULLIS, 1998; STÖCKHERT et al., 1999). Structural studies have shown that quartz aggregates usually govern the bulk strength of granitic rocks in the intermediate continental crust (e.g., HANDY et al., 1999). Thus, in rocks where 300°C was never attained, Rb-Sr, Ar-Ar and K-Ar biotite systems generally yield formational ages, indicating rocks where deformation at that time was brittle. In rocks above this temperature, the same mica systems yield cooling ages and show where deformation prior to and during that time involved viscous, mylonitic creep. Where age data from two systems whose closure temperatures straddle 300°C (e.g., mica ages and zircon fission track ages) are lacking, the trace of the 300°C isotherm on the tectonometamorphic age map was drawn parallel to the boundary between sub-greenschist and greenschist facies on the metamorphic map.

For areas with a sufficiently dense distribution of published radiometric ages, concordant Rb-Sr and K-Ar biotite cooling ages were contoured to show the cooling pattern of the thermal overprint (data compiled by HUNZIKER et al., 1992; MOST, 2003; SCHUSTER, personal communication and SCHUSTER et al., 2004, this volume). In areas where there are very few published data or where the ages vary, an approximate age or range of ages is printed on the map. Ticks on dashed contours delimit areas with mixed mica ages from those with primarily Alpine cooling ages. Mixed mica ages occur frequently in pre-Mesozoic basement rocks where weak Alpine metamorphism overprinted an older Paleozoic metamorphism (see inset to Metamorphic Map of the Alps, 1999 and review thereof in FREY et al. 1999).

The ages of low-grade and sub-greenschist facies metamorphism are difficult to constrain given the low temperatures and lack of dateable minerals under such conditions. In most cases, the metamorphic age is best constrained by the age of the youngest sediments affected by metamorphism (see HOINKES et al., 1999; DESMONS et al., 1999b, c). In this way, the broad ranges of Tertiary and Cretaceous ages were extrapolated over large volumes of sediment in the Alpine fore- and hinterlands. Unfortunately, the very limited number of published mica formational ages in such rocks precluded any age contouring of low-grade metamorphism.

Horizontal orange and thin green stripes in narrow parts of Austroalpine units just east and south-west of the Tauern window indicate overprinting of 60-110 Ma metamorphic ages during 0-59 Ma temperature-dominated metamorphism and deformation. These are the only areas in the Alps where metamorphism related to the Late Cretaceous cycle was overprinted by the Latest Cretaceous to predominantly Tertiary cycle.

Problems in dating Alpine metamorphism

Assigning unequivocal metamorphic ages to some parts of the Alps is difficult due to several circumstances: (1) Discrepancies in the metamorphic ages derived from different systems that have been applied to the same rocks, minerals or mineral assemblages; (2) Contradictions between radiometric and sedimentary ages; (3) A dearth or even lack of reliable ages.

Most of these problems concern the age of pressure-dominated metamorphism. This is not surprising given the relatively sluggish reaction kinetics at the temperatures of high-pressure conditions, the potentially high rates of exhumation of high-pressure rocks and the overprint of the pressure-dependent assemblages by temperature-dominated metamorphism. In addition, most of the ages on high-pressure (HP) assemblages must be interpreted as minimum ages, because geochronometers are strongly temperature-dependent and the thermal peak of metamorphism often followed the baric peak. Below, we consider these problems in some key areas, but hasten to add that our coverage of such problems is far from complete. As stated above, our citation of previous work is selective rather than all-inclusive.

Austroalpine units in the Western Alps

Varied ages are obtained for pressure-dominated metamorphism of Austroalpine units in the Western Alps: The structurally highest of these units, the Sesia Zone (Fig. 1), contains Late Cretaceous eclogites and blueschists (blue dots on the map). The age range is well established by 69 ± 2.7 Ma Hf-Lu ages on coexisting garnet and phengite (DUCHENE et al., 1997), ca. 65 Ma U-Pb SHRIMP ages on zircons from leucosome in eclogite (RUBATTO et al., 1999), and a plethora of Rb-Sr phengite ages ranging from 60 to 90 Ma (DAL PIAZ et al., 2001; OBER-HÄNSLI et al., 1985 and references in HUNZIKER et al., 1992; DESMONS et al., 1999c). The phengite ages also constrain the age of HP metamorphism due to the proximity of the 500°C closing temperature in the Rb-Sr phengite system to the maximum temperatures of 500-650°C reached at, or soon after, the baric peak of metamorphism (KOONS, 1986, TROPPER & ESSENE, 2002).

The Pillonet klippe is similarly situated at the top of the Western Alpine nappe pile and yields a 75 Ma $^{40}\text{Ar}/^{39}\text{Ar}$ phengite age from an eclogite (CORTIANA et al., 1998). Blueschist-facies assemblages in the Dent Blanche klippe (Fig. 1, AYRTON et al., 1982) have not been dated yet, but on the age map we assigned them a similar 60-90 Ma age range to the Sesia Zone (open blue dots) based on the structural continuity of this klippe with the Pillonet klippe and the Sesia Zone. The remaining Austroalpine units (Mont Emilius, Glacier-Raffay, Etirol-Levaz) are imbricated with the underlying, Early Tertiary nappe pile. Some of these units are so small as to be barely visible on the age map. All of them yield Early Tertiary, Rb-Sr phengite ages (DAL PIAZ et al., 2001): 40-49 Ma in the Mont Emilius klippe, and 45-47 Ma in the Glacier-Raffay and Etirol-Levaz outliers. A 92 Ma $^{40}\text{Ar}/^{39}\text{Ar}$ phengite age from the Glacier-Raffay outlier is interpreted to reflect Ar overpressure and therefore has no geological relevance. Taken together, these 40-50 Ma phengite ages are identical within error to ages from high-retentivity mineral isotopic systems in HP- and UHP-assemblages of the underlying Zermatt-Saas and Monte Rosa units (DAL PIAZ et al., 2001; LAPEN et al., 2004; and references in DESMONS et al., 1999c). As mentioned above, these varied HP metamorphic ages are attributed to Early Tertiary imbrication of a series of Jurassic extensional allochthons at the transition of the Liguro-Piemontese ocean and the Austroalpine continental margin (DAL PIAZ et al., 2001).

We note that previously produced Late Cretaceous Rb-Sr whole rock and mineral isochron (gacpx-plag) ages for eclogite-facies metagranites in the Sesia Zone (OBERHÄNSLI et al., 1985) are not geologically relevant, as they rest on very shaky analytical and methodological foundations (K. HAMMERSCHMIDT, pers. comm.): (1) No analytical error is listed for any of the samples; (2) Of the 12 sample points used to calculate the whole-rock isochron, only eight analyses are listed in the data table and none of them has the $^{87}\text{Rb}/^{86}\text{Sr}$ value of 3.5 at the righthand end of the isochron; (3) Of the samples plotted on the sample location map in their Fig. 1, two are not used for the isochron and only one is listed in the data table. Even if one disregards these problems, recalculation of the isochrons with the original data and the newest regression techniques (LUDWIG, 2000) yields a Rb-Sr whole rock age of 153 ± 75 Ma (Sr initial of 0.7130 ± 0.018) and a Rb-Sr gacpx-plag isochron of 114 ± 23 Ma (Sr initial of 0.7150 ± 0.00052). The errors calculated above are only minimal as they do not include the unknown analytical error. Even more importantly, both ages are entirely inconsistent with the HP metamorphic ages obtained in more recent studies, as well as with the regional geological context discussed below.

Schistes Lustrés and European basement units in the Western Alps

Conflicting ages of HP metamorphism are obtained with high-retentivity systems from ophiolitic units and Bündnerschiefer (Schistes Lustrés) in the Monviso area (Lago Superiore) near the Dora Maira basement unit (Fig. 1), as discussed by DESMONS et al. (1999c) and BRUNET et al. (2000): A Sm-Nd garnet-clinopyroxene isochron yields 60-62 Ma (CLIFF et al., 1998), whereas a Hf-Lu whole rock-garnet isochron yields 49 Ma (DUCHENE et al., 1997). These ages are certainly younger than the Cretaceous ages previously obtained with lower retentivity mica systems and systems prone to Ar overpressure (SCAILLET, 1996). The 10-15 Ma discrepancy in the high-retentivity ages is puzzling, especially because in other parts of the Alps, HP ages in the 60-90 Ma range are restricted to formerly subducted, Lower Austroalpine units.

A study of Sm-Nd systematics in the same samples analyzed by DUCHENE et al. (1997) revealed that the garnets contained submicroscopic inclusions with low Sm/Nd ratios (LUAIS et al., 2001). These ratios are indicative of crustal contamination processes, e.g., pulses of fluid, and lead LUAIS et al. (2001) to conclude that the 60-62 Ma isochron age cited above is apparent. Since then, AGARD et al. (2002) obtained $^{40}\text{Ar}/^{39}\text{Ar}$ phengite ages in the 55-60 Ma range for HP metamorphism along an east-west transect of the Schistes Lustrés in the Cottian Alps (Fig. 1). Phengites that grew during later deformation yield 45-51 and 35-40 Ma $^{40}\text{Ar}/^{39}\text{Ar}$ age clusters, with the latter cluster interpreted as the age range of retrograde, greenschist-facies metamorphism associated with extensional exhumation and cooling (AGARD et al., 2002). Similarly, MEFFAN-MAIN et al. (2004) recently obtained a 43 Ma Rb-Sr apatite-phengite isochron on HP assemblages of the Gran Paradiso basement (Fig. 1). Greenschist-facies overprinting in the same unit occurred in the interval of 34-36 Ma.

Further to these studies, two geologic arguments support an Early Tertiary age of HP metamorphism in all Liguro-Piemont and European (Briançonnais) units of the Western Alps: (1) the Liguro-Piemont units in the Western Alps are lithologically and tectonically continuous, so that the well-documented Eocene ages of HP- and UHP metamorphism in the vicinity of the Zermatt-Saas and Monte Rosa units (cited below) also pertain elsewhere in the same units; (2) the metamorphic ages cannot be older than the stratigraphic age of the youngest protolith sediments (Paleocene-Lower Eocene in the Briançonnais cover and Ligurian Alps, DEBELMAS

& DESMONS, 1997; DESMONS et al., 1999b; Upper Cretaceous in the Combin Zone, DEVILLE et al., 1992 and references therein, DESMONS et al., 1999b). In light of the results and arguments above, we extrapolated the 35-60 Ma age interval for pressure-dominated metamorphism all over the Western Alps to include areas where no data are currently available (open red dot pattern).

Corsica

The age of HP metamorphism on western (Alpine) Corsica is also controversial. A Sm-Nd whole rock-Grt-Gla-Cpx isochron age of 83.8 ± 4.9 Ma in an eclogitic lense intercalated with Schistes Lustrés (LAHONDRE & GUERROT, 1997) provides the only evidence of a Cretaceous HP event in the Schistes Lustrés. This is apparently consistent with the observation that Eocene sediments which lack HP assemblages rest unconformably on basement of western Corsica as well as on the Schistes Lustrés (DESMONS et al., 1999c). On the other hand, HP assemblages in the Inzecca units that are thrust onto sediments with reworked, late Lutetian nummulites seem to indicate that pressure-dominated metamorphism was younger than 41 Ma (references in DESMONS et al., 1999c). BRUNET et al. (2000) conducted $^{40}\text{Ar}/^{39}\text{Ar}$ studies using conventional and spot laser ablation and found two or more generations of white mica in rock samples. These white micas have a large, discordant spread of ages (35-65 Ma) with evidence of isotopic heterogeneities related to the presence of K-poor phyllosilicate. Therefore, the authors consider that only the minimum 35 Ma age is possible, consistent with 34-40 Ma $^{40}\text{Ar}/^{39}\text{Ar}$ phengite ages of MALUSKI (1977) and LAHONDERE (1991). $^{40}\text{Ar}/^{39}\text{Ar}$ ages in the 25-35 Ma range are interpreted to date greenschist-facies overprinting during extensional shearing (BRUNET et al., 2000).

The Tenda Massif is a large gneiss dome located to the west of the Schistes Lustrés, and represents part of the distal European margin. The presence of Bartonian nummulites in a metamorphic conglomerate containing blue amphiboles indicates that HP greenschist-facies metamorphism in the Tenda massif and Corté imbricates is less than 37 Ma (BÉZERT & CABY, 1988). This contradicts two early dating attempts: A crude, two-step discordant $^{40}\text{Ar}/^{39}\text{Ar}$ age spectra on glaucophane of about 90 Ma, interpreted as the age of the thermal peak (MALUSKI, 1977), and a Rb-Sr whole-rock age of 105 ± 8 Ma for the East Tenda extensional shear zone (COHEN et al., 1981). More recent $^{40}\text{Ar}/^{39}\text{Ar}$ ages of BRUNET et al. (2000) on coarse, high-Si phengites yield 34-45 Ma plateaus, which are interpreted as the age of the pressure-dominated metamorphism. Smaller phengites yield ca. 25 Ma, interpreted as the age of top-E extensional shearing in the East Tenda extensional shear zone (BRUNET et al., 2000). Fission track ages also point to Oligo-Miocene exhumation of this shear zone (JAKNI et al., 1998), which is believed to have exhumed HP rocks in its footwall (e.g., JOLIVET et al., 1991).

The recent isotopic evidence for an Early Tertiary age of HP metamorphism on Alpine Corsica is backed up by regional geological arguments as above in the Western Alps: The close lithological and tectonic affinity of the Schistes Lustrés and Tenda massif on Corsica, respectively, with the Schistes Lustrés and European basement units in the Western Alps strongly supports the idea that HP metamorphism on Alpine Corsica is also Early Tertiary age. This is consistent with paleogeographic reconstructions of STAMPFLI et al. (1998). The age map of Corsica is therefore filled with open red dots to reflect this expectation.

Central Alps

Age determinations on HP assemblages and stratigraphic age constraints in the Central Alps indicate Early Tertiary closure and subduction of the Liguro-Piemont basin including the formation of a Paleocene accretionary wedge at the boundary with the upper plate, Apulian continental margin (review and references of age data in FREY et al., 1999). This was followed by Late Eocene subduction of European (Briançonnais) basement between the previously sutured Liguro-Piemont basin to the southeast and the Valais basin to the northwest (SCHMID et al., 1996, 1997; STAMPFLI et al., 1998).

For example, the Tambo and Suretta nappes, two Briançonnais basement units at the eastern part of the Lepontine thermal dome (Fig. 1), were tectonically accreted to the Apulian upper plate some 47-50 Ma (SCHMID et al., 1996). In the Valais basin, sedimentation continued into Eocene time (LIHOU, 1995, 1996) when the basin finally closed and was subducted and accreted to the previously accreted European, Liguro-Piemontese and Apulian units making up the active margin (FROITZHEIM et al., 1996). This subduction involved HP metamorphism of crustal units as well as UHP metamorphism in upper mantle rocks (garnet-peridotites of Alpe Arami, Fig. 1 in ENGI et al., 2004; this vol.). Eclogite derived from oceanic crust of the Valais basin was initially dated at 36-43 Ma (localities at Alpe Arami and Gagnogne, BECKER, 1993, GEBAUER, 1996, 1999) but recent data from fragments in the VT unit on the main metamorphic structure map indicate a broader age range of about 35 to 55 Ma for this HP metamorphism (BROUWER et al., 2003a, b). These phase equilibria studies indicate that the rocks were exhumed rapidly from depths of more than 100 km to about 15-25 km, where they underwent Barrovian overprinting at 32 Ma. The exhumation of at least 75 km, possibly within a time as short as 3 Ma inferred from the minimum difference in ages between pressure- and temperature-dominated metamorphism in these units, was potentially very fast.

Engadin, Tauern and Rechnitz windows in the Eastern Alps

The Engadin, Tauern and Rechnitz windows expose folded and metamorphosed European, Valais and Liguro-Piemont units below a thrust contact with the overlying Austroalpine units. No attempts have been made so far to date HP metamorphism in the Engadin window. Certainly, this metamorphism is younger than the age of the youngest sediments (Late Cretaceous and Paleogene, OBERHAUSER, 1995). An Early Tertiary age is likely based on lateral correlation of the Valais and Liguro-Piemont units to the west.

Much more age data on metamorphism is available for the Tauern window, as reviewed in HOINKES et al. (1999) and, previous to that, in FRANK et al. (1987). Large parts of the European basement and its Paleozoic cover (Venediger nappe) as well as basal slices of the Tethyan ocean basin (Glockner nappe = Schistes Lustrés unit) experienced eclogite-facies metamorphism, overprinted by blueschist facies metamorphism. The baric peak was reached in Eocene time (ca. 45 Ma, CHRISTENSEN et al., 1994, ZIMMERMANN et al., 1994). In a detailed petrological and geochronological study of eclogitic garnets, CHRISTENSEN et al. (1994) determined that ages range from 35-55 Ma in the garnet cores to 30.5-32 Ma in their rims. The oldest reliable age for HP metamorphism in the Tauern window (62 Ma) was obtained by extrapolating back to the time of garnet nucleation with a calculated growth rate (CHRISTENSEN et al., 1994). Eocene/Oligocene (32-36 Ma) ages were obtained from $^{40}\text{Ar}/^{39}\text{Ar}$ studies of Si-rich phengites associated with blueschists in the Paleozoic cover (Lower Schieferhülle) of the European basement (ZIMMERMANN et al., 1994).

This places a minimum age on eclogitization, as the blueschist-facies metamorphism overprints the eclogites. DINGELDEY et al. (1997) reported 38-43 Ma $^{40}\text{Ar}/^{39}\text{Ar}$ ages for greenschist-facies phengites in the Valais unit (Upper Schieferhülle). Taken together, the data so far suggest that pressure-dominated metamorphism in the Tauern window occurred in Early Tertiary time, as expected from correlative lithotectonic units in the Central and Western Alps.

Temperatures during Tertiary, greenschist- to amphibolite-facies metamorphism peaked in Oligocene time (26-30 Ma, INGER & CLIFF, 1994; REDDY et al., 1993). The contoured Rb-Sr and K-Ar biotite cooling ages on the map delineate two thermal subdomes at each end of the Tauern window.

The contours in the western end are truncated by the overlying Brenner extensional fault, indicating that movement on this fault continued after cooling to below 300°C in the footwall (see also FÜGENSCHUH et al., 1997). Unfortunately, the temperatures achieved during this Tertiary overprinting metamorphism were insufficient to completely reset the Rb/Sr ages of pre-Tertiary white micas (REDDY et al., 1993), so that many of these ages may be mixed ages. In addition, the K-Ar system was affected to an unknown extent by excess Ar (CLIFF et al., 1985). The $^{40}\text{Ar}/^{39}\text{Ar}$ method would provide a means for controlling the amount of excess Ar, but investigations with this system are still rare in this area. The Rb-Sr and K-Ar mica ages reviewed in HOINKES et al. (1999) and FRANK et al. (1987) indicate that most of the cooling related to exhumation of the Tauern window occurred after 30 Ma in Oligocene to Miocene time. Muscovite ages (K-Ar, Rb-Sr) cluster at 21-30 Ma in the eastern Tauern window and at about 13 Ma and 15-24 Ma in western part. Rb-Sr and K-Ar biotite ages of 15-24 Ma occur in the eastern Tauern window.

The age map shows that the limit of Tertiary, temperature-dependent metamorphism corresponds to the Oligo-Miocene, DAV and Mölltal mylonitic faults (Fig. 1). The age map shows that the limit of Tertiary, temperature-dependent metamorphism corresponds to the Oligo-Miocene, DAV and Mölltal mylonitic faults (Fig. 1 and horizontal stripes at the southwest side of Tauern window on the age map). These strike-slip faults lie south of the southern boundary of the Tauern window as defined by the thrust contact between Austroalpine units and the underlying Penninic units. Recent structural studies (HANDY et al., 2004) have shown that in the Austroalpine crustal wedge between the Tauern window and the DAV fault, the main foliation was active during intrusion of the Rieserferner pluton (28-33 Ma, Rb-Sr white mica formational ages in MÜLLER et al., 2001) and overprints an earlier Alpine foliation of Early Tertiary (Müller et al. 2001) or Late Cretaceous age (BORSI et al., 1973; STÖCKHERT, 1984, discussion of dating methods in MANKTELOW et al., 2001). The DAV fault is therefore interpreted to have accommodated a significant exhumational component of N-side up motion, juxtaposing Alpine high-pressure, amphibolite facies assemblages in the north (STÖCKHERT, 1984) with Alpine-unmetamorphosed rocks in the south (SCHULZ, 1994) before becoming active as an Oligo-Miocene strike-slip fault (HANDY et al., 2004).

Exhumation of the Tertiary nappe pile in the Tauern window accelerated in Miocene time as manifested by T-t paths constructed with different mineral isotopic systems (Fig. 4 in DUNKL et al. 2003) and by sediment mass balance of the peri-Alpine basins (CLIFF et al., 1985; FRISCH et al., 1999). The distribution of zircon and apatite fission track (FT) ages suggest that exhumation of the eastern part of the Tauern window was slightly earlier (Zr ages: 16.3-21.5 Ma, DUNKL et al., 2003) than that of the western part (zircon mean age of 11.4 Ma, FÜGENSCHUH et al., 1997).

There are currently no reliable ages for the HP metamorphism in the Rechnitz window, although metamorphism was certainly younger than the youngest metamorphosed sediments (Lower Cretaceous) and no older than the youngest, unmetamorphosed sediments overlying the sequence (Miocene and Pliocene, PAHR, 1980). The overprinting greenschist-facies metamorphism is dated at 19-22 Ma by K-Ar muscovite (KOLLER, 1985). Zircon and apatite FT ages are, respectively, 13-22 Ma and 7-10 Ma (DUNKL & DEMENY, 1997). The average zircon FT age of 17.8 Ma is identical within error to the average age of 17.1 Ma in the eastern Tauern Window (DUNKL et al., 2003). These authors interpret the Tertiary exhumation of the Tauern and Rechnitz Windows to have been coeval. The poor exposure of the Rechnitz window has hampered efforts to find the structures associated with this exhumation and denudation.

Austroalpine units in the Eastern Alps

Recent isotopic age work in the Austroalpine nappes is reviewed in THÖNI (1999) and in SCHUSTER et al. (2004), so that only several points of contention are treated here. In the Silvretta-Seckau nappe system (Fig. 1), the line separating 60-110 Ma cooling mica ages from mixed, pre-Alpine and Alpine mica ages (ticked, dashed line in the age map) does not correspond everywhere with the metamorphic contact between sub-greenschist and greenschist facies. This reflects the resistance of the mica systems to resetting, even in parts of the nappe where temperatures in Late Cretaceous time approached 500°C. Similarly, Ar-Ar hornblende ages in the Seckau complex, part of the Silvretta-Seckau nappe system, are only reset where temperatures attained 500-600°C (FARYAD & HOINKES, 2003). Thus, some parts of the Silvretta-Seckau nappe system coloured light green in the age map may have experienced Late Cretaceous temperatures in excess of 300°C, at least for short times.

Late Cretaceous, sub-greenschist facies metamorphism in basement south of the Tauern window occurs in the lowest tectonic levels south of the large Tertiary faults marking the apparent southern limit of Alpine metamorphism (HOINKES et al., 1999). The light green colour of these units in the age map is based on the distribution of partially reset Rb-Sr biotite ages that indicate a mix between Late Cretaceous and pre-Alpine ages (DEUTSCH, 1988). The general weakening of metamorphism to anchizonal and diagenetic conditions with decreasing tectonic level in these basement units precludes an unequivocal determination of their metamorphic age. Similar problems are found in dating the low-grade metamorphism in the Northern Calcereous Alps.

Within parts of the Austroalpine basement that experienced HP-metamorphism, the pressure peak at about 100 ± 10 Ma (Sm-Nd garnet isochron ages, Ar-Ar white mica, review in THÖNI, 1999) was followed by overprinting under upper amphibolite-facies conditions at about 75 Ma (see cooling ages marked in blue on the age map). Tertiary metamorphism never attained 300°C in any of these units. In the Austroalpine basement southeast of the Tauern window, zircon FT ages increase away from the window from 30 Ma in the north to 160 Ma in the south (DUNKL et al., 2003). These authors attribute the trend to the superposition of Tertiary metamorphism onto an earlier thermal regime related to Jurassic (Tethyan) rifting. This weak Tertiary overprint decreases away from Tauern window. The lack of Neogene resetting of the FT ages is interpreted by DUNKL et al. (2003) to show that there was little or no exhumation associated with strike-slip motion during eastward lateral extrusion of the Austroalpine basement in Miocene time.

Southern Alps

Very low-grade metamorphism related to pervasive foliation and thrusting of the highest (Orobic) thrust sheet of the Bergamasc part of the Southern Alps (Fig. 1) is argued to be Late Cretaceous age, based on truncation of this thrust by the Early to Mid-Tertiary (29-43 Ma, DEL MORO et al., 1983) Adamello pluton (SCHMID et al., 1996). Another age constraint cited by COLOMBO & TUNESI (1999) is the occurrence of discordant 50-60 Ma dykes that truncate this foliation (K-Ar whole-rock ages, ZANCHI et al., 1990). For this reason, the southernmost limit of the light green colour in the age map of the Bergamasc Alps corresponds to the trace of the Orobic thrust. A later Alpine foliation in the basement and Mesozoic cover rocks seems to be younger than the Adamello granitoid intrusion (CARMINATI et al., 1997).

The extrapolation of this metamorphic age into the westernmost part of the Southern Alps (light green in the age map) is based on the correlation of S- and SE-directed thrusting and folding there with the structures in the Bergamasc Alps (SCHUMACHER et al., 1997). Although admittedly tenuous, this correlation is confirmed by the few available FT zircon ages in the Ivrea and Strona-Ceneri Zones (60-85 Ma, review in HURFORD et al., 1991). The occurrence of 15-30 Ma FT zircon and apatite ages adjacent to the Insubric mylonites along the Canavese fault (thin yellow domain in the age map, location in Fig. 1, HURFORD et al., 1991) is attributed to local reheating of the southern Alpine crust during Insubric backthrusting and exhumation in the retro-wedge of the Tertiary Alpine orogen.

Tectonic interpretations of the metamorphic age patterns

The most striking feature of the metamorphic age pattern is that Late Cretaceous ages (green shades) predominate in the Eastern Alps, whereas Tertiary ages (yellow-orange) are ubiquitous in the structurally deeper units of the Western Alps. Tertiary metamorphism in the Eastern Alps is restricted to the Lower Engadine Window, the Tauern Window and the smaller Rechnitz Window, between Vienna and Graz (Fig. 1). The separation of Late Cretaceous and Late Cretaceous-Tertiary metamorphism, respectively, in the Eastern and Western Alps, together with a similar pattern in space and time for flysch sedimentation (e.g., TRÜMPY, 1980) prompted SCHMID et al. (1996) to refer to the Alps as a composite mountain belt; a Jurassic-Late Cretaceous orogen in the east with the remains of a Triassic oceanic basin (Meliata-Halstatt) that rides "piggyback" on top of a Late Cretaceous to Tertiary orogen exposed in the west with the remains of two, Jurassic-Cretaceous oceanic basins (Valais and Liguro-Piemont). The remnants of the continental margins making up these orogens, as well as the basic rocks and marine metasediments marking the sutured ocean basins between them, are distinguished in Figure 2. From this figure, it is evident that in both orogens the limits of pressure-dependent metamorphism overlap with the lithotectonic boundaries between the upper and lower plates, and do not everywhere coincide with the oceanic sutures.

Pressure-dominated metamorphism

The 90-110 Ma ages of pressure-dominated metamorphism in the Eastern Alps (purple dots on the map) are interpreted to date east-southeastward subduction of a part of the Middle Triassic, Austroalpine passive margin beneath distal parts of the same margin to the east. Figure 2 shows that the pressure-dominated metamorphism is far from the nearest fragments of the Middle

Triassic, Meliata-Hallstatt ocean basin, exposed in mélanges within the Juvavic nappes of the Northern Calcereous Alps (MANDL & ONDREJICKI, 1991; KOZUR & MOSTLER, 1992). Prior to Late Cretaceous time, this ocean basin was located to the east, between the Austroalpine and Tisian continental margins (NEUBAUER, 1994; FROITZHEIM et al., 1996) and is best exposed in the northwestern Carpathians. Closure of a westward embayment of the Meliata-Hallstatt basin in the Eastern Alps is manifested by Late Jurassic thrusting in the Juvavic units (Hallstatt mélange of FRISCH & GAWLICK, 2003), earlier than 90-110 Ma subduction and HP-metamorphism of the Austroalpine units. This spatial and temporal discrepancy has fueled considerable debate, as recently discussed in FROITZHEIM et al. (1996) and MILLER & THÖNI (1996). Because the Mid-Triassic passive margin sequence in the NCA was originally situated north and/or east of the Austroalpine basement (e.g., FRISCH & GAWLICK, 2003), Jurassic to Cretaceous shortening that culminated in 90-110 Ma subduction must have migrated from east to west, away from the Meliata-Hallstatt suture and into the lower plate (FROITZHEIM et al., 1996). Thus, the Eastern Alps do not contain the upper plate to this suture and the boundary marked in Figure 2 is the base of the overthrust hangingwall to the HP rocks within the lower (Austroalpine) plate margin.

The anomalous position of 90-110 Ma HP- and even UHP-metamorphism within the formerly passive, Austroalpine margin (e.g., MILLER & THÖNI, 1996) may reflect the localization of subduction within a Late Paleozoic/Early Mesozoic rift system, manifested by the Permian age of gabbroic relics in Late Cretaceous eclogites (e.g., Koralpe eclogites, MILLER & THÖNI, 1997; THÖNI & MILLER, 2000). An alternative view that the 90-110 Ma eclogites mark the northern or western branch of another sutured ocean basin (e.g., the Vardar basin in the Dinarides, or a "southern Tethyan" ocean, KOZUR & MOSTLER, 1992) is considered less likely due to the lack of pelagic sediments associated with the high-pressure rocks.

Pressure-dominated metamorphism in the Western and Central Alps (35-90 Ma, red and blue dots in the age map) is younger than in the Eastern Alps and partly overprints the imbricated remnants of the Valais and Liguro-Piemont basins as well as their adjacent European and Apulian margins (Fig. 2). These oceanic basins were located west of the Meliata-Hallstatt suture (FROITZHEIM et al., 1996) and opened as the latter basin was closing in Jurassic to Cretaceous time. East-southeastward subduction of the Liguro-Piemont oceanic basin initiated at 100-120 Ma, as recorded by flysch and mélange with ophiolitic and high P/T detrital minerals (e.g., WINKLER, 1988; WAGREICH, 2001). Then, distal parts of the upper-plate continental margin were subducted, as evidenced by 60-90 Ma pressure-dominated metamorphism in the Lower Austroalpine units of the Eastern and Western Alps (blue dots on the age map). Subsequent migration of subduction into the footwall is indicated by 35-60 Ma HP- and UHP-metamorphism in the Liguro-Piemont and European units (red dots on the map). This NW migration of subduction (e.g., GEBAUER, 1999) is consistent with the younging of Tertiary flysch ages in progressively more external European units that escaped metamorphism (e.g., SCHMID et al., 1996 and references therein). The aforementioned occurrence of Late Cretaceous to Early Tertiary, pressure-dominated metamorphic ages in Austroalpine units of the Western Alps is attributed to progressive subduction and imbrication of extensional allochthons of the Apulian, upper plate margin that were situated in the southeastern part of the Liguro-Piemont ocean basin (DAL PIAZ et al., 2001). Exhumation of the HP metamorphic units also appears to have migrated to the NW behind the subduction zone (WHEELER et al. 2001), as manifested by spatial variation in mica cooling ages from 40-60 Ma in the Sesia Zone to 35-28 Ma in the more external Liguro-

Piemont and European basement units. Several mechanisms have been proposed for the exhumation of these HP rocks, including the extrusion of thin, basement nappes within the subduction channel (SCHMID et al., 1996; ESCHER & BEAUMONT, 1997). However, it is unlikely that all, or even most, of the exhumation involved extensional faulting in the hanging-wall of the subduction zone as proposed by WHEELER et al. (2001), because retrograde metamorphism in the footwall of extensional faults observed so far never exceeded upper greenschist-facies conditions. The mechanisms by which HP rocks were exhumed is the subject of ongoing work.

If pressure-dependent metamorphism is taken as a marker for Alpine subduction, then the boundaries of Alpine subduction in Figure 2 are neither easily defined nor everywhere clearly exposed in the field. This is due to the migration of subduction and collision, as well as to the overprinting of HP assemblages during temperature-dominated metamorphism and multistage exhumation. In the Eastern Alps, for example, both Late Cretaceous and Oligo-Miocene oblique-slip tectonics have severely segmented the Jurassic-Cretaceous, Austroalpine margin adjacent to the sutured Meliata-Hallstatt ocean (e.g., FRISCH & GAWLICK, 2003). The southern border of 90-110 Ma pressure-dominated metamorphism within this margin is the southern border of Tertiary, Alpine metamorphism marked by reactivated, Oligo-Miocene mylonitic faults (e.g., the DAV, Mölltal and Karawanken faults, Fig. 1). In the Western and Central Alps, it is difficult, if not actually impossible, even to consider Late Cretaceous to Tertiary subduction in terms of a channel. Part of the limit of 60-90 Ma, pressure-dominated metamorphism in the Apulian upper plate is truncated to the south by the Canavese segment of the Periadriatic fault system (Fig. 2). The northward extent of Late Cretaceous HP metamorphism in the footwall is overprinted by Eocene, pressure-dominated metamorphism in the Liguro-Piemont and European basement units. In turn, this Early Tertiary, HP-metamorphism is delimited to the north and west by the multiply folded contact of the European (Briançonnais) basement with the Valais oceanic unit. In the Western Alps, the lower limit of Eocene subduction for the Valais basin and adjacent European margin is truncated by the Miocene Penninic frontal thrust (Fig. 2), whereas in the Central Alps, it corresponds with the boundary of the ultrahelvetic metasediments (cover of the Gotthardmassif) lacking traces of HP metamorphism and the HP metamorphic Schistes Lustrées of the Valais basin. In the Lepontine thermal dome, a narrow unit marked VT on the main metamorphic structure map contains variegated continental and oceanic lithologies with HP and HT parageneses; these are interpreted as mélange relics within a tectonic accretionary channel (TAC of ENGI et al., 2001). This putative channel formed within a broader zone of subduction that included parts of the adjacent European margin.

Temperature-dominated metamorphism

Temperature-dominated metamorphism post-dated the stacking of most basement nappes in the Alps, as shown by the fact that basement nappe contacts are usually cut discordantly by metamorphic facies contacts and cooling age contours. This is most obvious for the Tertiary, temperature-dominated metamorphism of the Lepontine and Tauern thermal domes (red cooling age contours on the map). However, it also pertains to Late Cretaceous metamorphism of the Eastern Alps (blue cooling age contours on the map) as well as to Tertiary metamorphism of other internal basement units in the arc of the Western Alps. In fact, most basement thrusting and nappe stacking occurred during the accretion-subduction stages of Alpine metamorphism,

before the attainment of peak temperatures. Temperature-dominated metamorphism is therefore related to the syn- to late-collisional stages of the two Alpine tectonometamorphic cycles outlined above.

In the Koralpe and Saualpe basement units (Fig. 1), exhumation of 90-110 Ma HP units involved coeval top-N to -NW thrusting under upper amphibolite-facies conditions in the footwall and top-SE extensional faulting above (RATSCHBACHER et al., 1991, see ages in FRANK et al., 1983). The mica cooling ages in this area (70-80 Ma blue ages and contours in the age map) cut across the nappe contacts. SCHUSTER et al. (2004) attribute younger mica cooling ages (70-75 Ma, THÖNI, 1999) further to the south as the result of later backfolding in the retro-wedge of the Late Cretaceous orogen. In the Ötztal complex and Silvretta unit (Fig. 1), retrograde amphibolite-to-greenschist facies metamorphism at about 70-90 Ma is well exposed in the footwall of low-angle normal faults that accommodated top-E displacement of the hangingwall along reactivated, E-dipping nappe thrusts (RATSCHBACHER et al., 1989, e.g., the Schlinig fault in FROITZHEIM et al., 1997). This extensional deformation is interpreted to have exhumed and cooled the Austroalpine basement nappes to below 300°C some 70-90 Ma, i.e., within 30 Ma or less of W-directed thrusting at near-peak temperatures (see discussion on pp. 218-219 of THÖNI, 1999).

In the Lower Austroalpine Ent-Bernina complex (Fig. 1), extensional exhumation may have occurred simultaneously in the hangingwall of thrusting and subduction. Thrusting and accretion under HP-greenschist facies conditions at 76-88 Ma overlapped with extensional deformation under lower pressure, greenschist facies at 67-80 Ma, by which time subduction had migrated westwards into the Liguro-Piemont oceanic domain (HANDY et al., 1996). HANDY (1996) proposed extensional exhumation of the accreted Austroalpine, continental margin behind the westwardly retreating hinge of the Tethyan subduction zone.

Thrusting post-dated metamorphism in the thrust-and-fold belts of the Alpine fore- and hinterlands, where there are several well-documented examples of transported metamorphism in the hanging wall of thrust sheets (e.g., Glarus thrust in the Helvetic nappes, HUNZIKER et al., 1986; PFIFFNER, 1993; RAHN & GRASEMANN, 1999) that root in basement thrusts in their hinterlands (e.g., SCHMID et al., 1996; TRANSALP working group, 2002). Most of these examples of transported metamorphism are too small to depict on the Map of Metamorphic Structure in the Alps, the notable exceptions being Tertiary, low-grade metamorphism in thrust sheets of the Préalpes Romandes (Fig. 1, BOREL, 1991) and Late Cretaceous, sub-greenschist metamorphism in the hangingwall of the Orobic thrust in the Bergamasc part of the Southern Alps (SCHUMACHER et al., 1997).

The arcuate to concentric, Tertiary biotite cooling age contours in the Lepontine and Tauern thermal domes reflect exhumation of the Penninic basement nappes along various segments of the Periadriatic fault system (Fig. 1). This fault system and related post-nappe folds formed at about 35 Ma to 10-15 Ma, a period that ARGAND (1916) and many others since have referred to as the Insubric Phase. Insubric deformation substantially modified the Alpine orogenic edifice in response to tectonic indentation by the cold and therefore rigid, southern Alpine lithosphere. The map in Figure 1 shows the southern Alpine indenter and the Periadriatic fault system. Insubric deformation occurred under mostly mylonitic, retrograde amphibolite- to greenschist-facies conditions, but continued under brittle, sub-greenschist facies conditions in late Miocene time (SCHMID et al., 1996).

In the case of the Lepontine dome, exhumation involved a combination of S-directed thrusting and folding along the steeply N-dipping, Tonale segment of the Insubric mylonite belt (Fig. 1, SCHMID et al., 1989), and NE-SW directed, orogen-parallel extension along the Simplon, Forcola and Turba low-angle normal faults at either end of the dome (GRASEMANN & MANCK-TELOW, 1993, MEYRE et al., 1998). Similarly, exhumation of the Tauern dome initiated at its southern margin along the conjugate DAV and Mölltal mylonitic faults, and ended along the Brenner and Katschberg extensional faults (Fig. 1, HANDY et al., 2004). Faulting was broadly coeval with the development of large (km-amplitude), upright folds in the basement core of the domes (HANDY et al., 2004). These folds have a strong component of stretching parallel to their axes and deformed the cooling age contours for the Rb-Sr white mica and biotite systems in the Lepontine (STECK & HUNZIKER, 1994) and Tauern (CLIFF et al., 1985; REDDY et al., 1993) thermal domes, as shown in the age map. This suggests that folding continued to below 500°C and possibly to below 300°C, the temperatures commonly cited for the closure to diffusion of the Rb-Sr systems in white mica and biotite, respectively (von BLANKENBURG et al., 1989). In this context, it is interesting to note that Insubric exhumation and cooling of the Lepontine thermal dome in the core and retro-wedge of the Central and Western Alps was coeval with N- and NW-directed thrusting of the weakly metamorphosed Helvetic units towards the northern Alpine foreland (e.g., the Glarus thrust, SCHMID et al., 1996).

The Lepontine and Tauern thermal domes have been likened to metamorphic core complexes (e.g., FRISCH et al., 2000), but this comparison is somewhat misleading from a structural standpoint; unroofing of the basement rocks in the classical core complexes of North America involved low-angle normal faulting during regional extension (e.g. CRITTENDEN, 1980), whereas exhumation of the Lepontine and Tauern thermal domes was syn-orogenic in the retro-wedge of the Alpine orogen. It involved a combination of south-directed thrusting ("backthrusting", "Rücküberschiebung" or "retrocarriage" in Alpine parlance) and strike-slip faulting in addition to orogen-parallel, low-angle normal faulting.

We note that our division of Alpine metamorphic ages into two pressure- and temperature-dominated cycles does not completely correspond to TRÜMPY's (1980) well-known division of Alpine orogenic history into Eo-Alpine, Meso-Alpine and Neo-Alpine phases. These phases were based largely on age relationships between deformation and sedimentation. Although the 90-110 Ma HP-metamorphism in the Eastern Alps indeed coincides with the Eo-Alpine phase in the sense of TRÜMPY, 35-60 Ma and 60-90 Ma HP-metamorphism in the Western Alps was not regionally recognized when TRÜMPY proposed his orogenic phases. Early Tertiary, pressure-dominated metamorphism overlaps in time with his Meso-Alpine phase which is centered in the Penninic domain. TRÜMPY's Neo-Alpine phase involved Miocene to Pliocene folding and thrusting, together with intracrustal subduction along the southern border of the External basement massifs. Since the 1970s, however, structural work has shown that the External massifs were not the site of subduction, and were uplifted to their present altitude in Miocene to Pliocene time (BURCKHARD, 1988, LE LOUP et al., 2004), i.e., at about the same time as folding and thrusting in the unmetamorphosed Jura mountains.

Final remarks

The new map of the age and structure of Alpine metamorphism comes close to realizing an old idea of Hans Stille, recently revived by HSU (1995), of integrating tectonic and metamorphic information in a tectonometamorphic facies map for an entire orogen. Such a map is useful from a geodynamic standpoint because it combines information about P-T-X conditions in the orogenic crust with information about the structure and timing of orogenic deformation. The map therefore serves as a basis for reconstructing the tectonic and dynamic evolution of an orogen, especially when combined with geological maps on the same scale.

As the example of the Alps shows, structures and metamorphism are closely linked in a positive feedback loop: Metamorphic phase transformations enhance strain localization by changing the rheology of the crust. The heterogeneous structure resulting from strain localization in turn affects the distribution of metamorphism and the susceptibility of the crust to further deformation. Strain-induced heterogeneities associated with Mesozoic rifting and with subsequent subduction were the structural template on which the architecture of the Alpine orogen formed. Modifications to this structure occurred during exhumation, especially when the Periadriatic fault system segmented large tracts of metamorphosed crust. This fault system also accommodated the upward advective flow of fluids and granitic melts. Boundaries between first-order tectonic units like lithospheric plates therefore rarely coincide exactly with the boundaries between metamorphic facies domains. Rather, the distribution of these domains is usually related to the fabric developed during orogenic deformation.

Finally, a map like this is useful not only because it summarizes what we think we understand about crustal evolution, but also because it indicates where data are lacking or insufficient to draw firm conclusions. Use of the Alps as a natural laboratory to test ideas on crustal processes, for example, the causes of seismicity, or on the effect of climate on tectonics, will continue to depend on obtaining a dense distribution of radiometric ages. Future research will undoubtedly focus on the application of high-resolution, in-situ dating techniques to obtain ages of minerals within a well-established structural and petrological framework.

Acknowledgements

We thank all members of the CCGM commission for fruitful collaboration. Among these, Friedrich Koller and Ralf Schuster were especially helpful in providing newest information on the age of metamorphism in the Eastern Alps. Romain Bousquet ensured that the age pattern corresponded with the final version of the metamorphic map. Konrad Hammerschmidt helped us to understand analytical problems in geochronology and their effect on the interpretation of radiometric ages. In addition, we benefited from discussions with Lukas Baumgartner (Lausanne), Niko Froitzheim (Bonn), Jochen Babist, Matthias Konrad, and Claudio Rosenberg (all in Berlin), Manfred Linner and Martin Thöni (Vienna) and Stefan Schmid (Basel). In drafting many versions of this map, M. Grundmann (Berlin) made valuable suggestions for the map presentation. Some of the age data presented here were generated as part of projects Ha 2403/3 (TRANSALP) and Ha 2403/5 funded by the Deutsche Forschungsgemeinschaft (DFG).

References

- AGARD, P., MONIÉ, P., JOLIVET, L. & GOFFÉ, B. (2002): Exhumation of the Schistes Lustrés complex: in-situ laser probe $^{40}\text{Ar}/^{39}\text{Ar}$ constraints and implications for the Western Alps. - *J. metamorphic Geol.*, 20, 1-19.
- ARGAND, E. (1916): Sur l'arc des Alpes Occidentales. - *Ecolgae geol. Helv.*, 14, 145-191.
- AYRTON, S., BUGNON, C., HAARPAINTNER, T., WEIDMANN, M. & FRANK, E. (1982): Géologie du front de la nappe de la Dent-Blanche dans la région des Monts-Dolins, Valais. - *Ecolgae geol. Helv.* 75/2, 269-286.
- BECKER, H. (1993): Garnet peridotite and eclogite Sm-Nd mineral ages from the Lepontine dome (Swiss Alps): New evidence for Eocene high-pressure metamorphism in the central Alps. - *Geology*, 21, 599-602.
- BÉZERT, P. & CABY, R. (1988): Sur l'âge post-bartonien des événements tectono-métamorphiques alpin en bordure orientale de la Corse cristalline (Nord de Corté). - *Bull. Soc. Géol. Fr.*, 6, 965-971.
- BIGI, G., CASTELLARIN, A., CATALANO, R., COLI, M., COSENTINO, D., DAL PIAZ, G. V., LENTINI, F., PAROTTO, M., PATACCA, E., PRATURLON, A., SALVINI, F., SARTORI, R., SCANDONE, P. & VAI, G. B., (1989): Synthetic structural-kinematic map of Italy. - C.N.R., Progetto Finalizzato Geodinamica, SELCA Firenze.
- BLANCKENBURG, F.v., VILLA, I. M., BAUR, H., MORTEANI, G. & STEIGER, R. H. (1989): Time calibration of a PT-path from the Western Tauern Window, Eastern Alps: the problem of closure temperatures. - *Contrib. Mineral. Petrol.*, 101, 1-11.
- BOREL, G. (1991): Études Géologiques et Mineralogiques de la Region du Widdersgrind (Préalpes-Romandes). - Ph.D. thesis, Université de Neuchatel.
- BORSI, S., DEL MORO, A. & SASSI, F. P. (1973): Metamorphic evolution of the Austridic rocks to the south of the Tauern Window (Eastern Alps): radiometric and geopetrological data. - *Mem. Soc. Geo. It.*, 12, 549-571.
- BORSI, S., DEL MORO, A., SASSI, F. P., ZANFERRARI, A. & ZIRPOLI, G. (1978): New geopetrologic and radiometric data on the Alpine History of the Austridic continental margin south of the Tauern Window (Eastern Alps). - *Mem. Ist. Geol. Mineral. Univ. Padova*, 32, 1-19.
- BROUWER, F. M., BURRI, T., BERGER, A. & ENGI, M. (2003a): Collision in the Central Alps: 2. Exhumation of high-pressure fragments. - In: EGS - AGU - EUG Joint Assembly, Nice.
- BROUWER, F. M., ENGI, M., BERGER, A. & BURRI, T. (2003): Towards complete PTt paths: Unravelling Alpine eclogite relics. - *Norsk Geol. Unders. Report*, 2003.055, 25-26.
- BRUNET, C., MONIÉ, P., JOLIVET, L. & CADET, J.-P. (2000): Migration of compression and extension in the Tyrrhenian Sea, insights from $^{40}\text{Ar}/^{39}\text{Ar}$ ages on micas along a transect from Corsica to Tuscany. - *Tectonophysics*, 321, 127-155.
- BURCKHARD, M. (1988): L'Helvétique de la bordure occidentale du massif de l'Aar (évolution tectonique et métamorphique). - *Ecolgae geol. Helv.*, 81, 1, 63-114.
- CARMINATI, E., SILETTO, G. B. & BATTAGLIA, D. (1997): Thrust kinematics and internal deformation in the basement involved fold and thrust belts: The eastern Orobic Alps case (Central Southern Alps, northern Italy). - *Tectonics*, 16, 2, 259-271.
- CHRISTENSEN, J. N., SELVERSTONE, J., ROSENFELD, J. L. & DePAOLO, D. J. (1994): Correlation by Rb-Sr geochronology of garnet growth histories from different structural levels within the Tauern Window, Eastern Alps. - *Contrib. Mineral. Petrol.*, 118, 1-12.
- CLIFF, R. A., DROOP, G. T. R. & REX, D. C. (1985): Alpine metamorphism in the south-east Tauern Window, Austria: 2. Rates of heating, cooling and uplift. - *J. metamorphic Geol.*, 3, 403-415.
- CLIFF, R. A., BARNICOAT, A. C. & INGER, S. (1998): Early Tertiary eclogite facies metamorphism in the Montviso Ophiolite. - *J. metamorphic Geol.*, 16, 447-455.

- COHEN, C. R., SCHWEICKERT, R. A. & ODOM, A. L. (1981): Age of emplacement of the Schistes Lustrés nappe, Alpine Corsica. - *Tectonophysics*, 72, 267-284.
- COLOMBO, A. & TUNESI, A. (1999): Alpine metamorphism of the Southern Alps. IN: The new metamorphic map of the Alps, FREY, M., DESMONS, J., NEUBAUER, F. (eds). - *Schweiz. Mineral. Petrogr. Mitt.*, 79, 1, 23-40.
- CORTIANA, G., DAL PIAZ, G. V., DEL MORO, A., HUNZIKER, J. C. & MARTIN, S. (1998): ⁴⁰Ar-³⁹Ar and Rb-Sr dating of the Pillonet klippe and Sesia-Lanzo basal slice in the Ayas valley and evolution of the Austroalpine-Piedmont nappe stack. - *Mem. Sci. geol. (Padova)* 50, 177-194.
- CRITTENDEN, M. D. (1980): Metamorphic core complexes of the North American Cordillera: Summary. IN: Cordilleran Metamorphic Core Complexes. CRITTENDEN, M. D., CONEY, P. J. & DAVIS, G. H. (Eds). - *Geol. Soc. Amer. Mem.*, 153, 485-590.
- DAL PIAZ, G. V., CORTIANA, G., DEL MORO, A., MARTIN, S., PENNACCHIONI, G. & TARTAROTTI, P. (2001): Tertiary age and paleostructural inferences of the eclogitic imprint in the Austroalpine outliers and Zermatt-Saas ophiolite, western Alps. - *Intern. J. Earth Sci.*, 90, 668-684.
- DEBELMAS, J & DESMONS, J. (1997): Géologie de la Vanoise. - Documents du BRGM, 266, 187 pp.
- DEL MORO, A., PARDINI, G., QUERCIOLI, C., VILLA, I. M. & CALLEGARI, E. (1983): Rb-Sr and K-Ar chronology of Adamello granitoids. - *Mem. Soc. Geol. It.*, 26, 285-299.
- DEVILLE, E., FUDRAL, S., LAGABRIELLE, Y., MARTHALER, M. & SARTORI, M. (1992): From oceanic closure to continental collision: a synthesis of the "Schistes lustrés" metamorphic complex of the Western Alps. - *Geol. Soc. Amer. Bull.*, 104, 127-139.
- DESMONS, J., COMPAGNONI, R., CORTESOGNO, L., FREY, M. & GAGGERO, L. (1999a): Pre-Alpine metamorphism of the Internal zones of the Western Alps. IN: The new metamorphic map of the Alps, FREY, M., DESMONS, J. & NEUBAUER, F. (eds). - *Schweiz. Mineral. Petrogr. Mitt.*, 79, 1, 23-40.
- DESMONS, J., APRAHAMIAN, J., COMPAGNONI, R., CORTESOGNO, L. & FREY, M. with the collaboration of GAGGERO, L., DALLAGIOVANNA, G. & SENO, S. (1999b): Alpine metamorphism of the Western Alps: I. Middle to high T/P metamorphism. IN: The new metamorphic map of the Alps. FREY, M., DESMONS, J. & NEUBAUER, F. (eds): - *Schweiz. Mineral. Petrogr. Mitt.*, 79, 1, 89-110.
- DESMONS, J., COMPAGNONI, R. & CORTESOGNO, L. with the collaboration of FREY, M., GAGGERO, L., DALLAGIOVANNA, G., SENO, S. & RADELLI, L. (1999c): Alpine metamorphism of the Western Alps: I. High P/T and related pre-greenschist facies metamorphism. IN: The new metamorphic map of the Alps. FREY, M., DESMONS, J. & NEUBAUER, F. (eds). - *Schweiz. Mineral. Petrogr. Mitt.*, 79, 1, 111-134.
- DEUTSCH, A. (1988): Die frühalpide Metamorphose in der Goldeck-Gruppe (Kärnten). - Nachweis anhand von Rb-Sr-Altersbestimmungen und Gefügebeobachtungen. - *Jb. Geol. B.-A.*, 131/4: 553-562.
- DINGELDEY, C., DALLMEYER, R. D., KOLLER, F. & MASSONNE, H. J. (1997): P-T-t history of the Lower Austroalpine Nappe Complex in the "Tarntaler Berge" NW of the Tauern Window: implications for the geotectonic evolution of the central Eastern Alps. - *Contrib. Mineral. Petrol.*, 129, 1-19.
- DUCHENE, S., BLICHERT-TOFT, J., LUIS, B., TÉLOUK, P., LARDEAUX, J.-M. & ALBARÈDE, F. (1997): The Lu-Hf dating of garnets and the ages of the Alpine high-pressure metamorphism. - *Nature*, 387, 586-588.
- DUNKL, I. & DEMÉNY, A. (1997): Exhumation of the Rechnitz window at the border of the Eastern Alps and Pannonian basin during Neogene extension. - *Tectonophysics*, 272, 197-211.
- DUNKL, I., FRISCH, W. & GRUNDMANN, G. (2003): Zircon fission track thermochronology of the southeastern part of the Tauern Window and the adjacent Austroalpine margin, Eastern Alps. - *Eclogae geol. Helv.*, 96, 209-217.
- ENGI, M., BERGER, A. & ROSELLE, G. T. 2001. Role of the tectonic accretion channel in collisional orogeny. - *Geology*, 29, 1143-1146.

- ENGI, M., BOUSQUET, R. & BERGER, A. (2004): Metamorphic Structure of the Alps: Central Alps, IN: Explanatory notes to the Map of Metamorphic Structures of the Alps. OBERHÄNSLI, R. (ed). - Mitt. Öster. Min. Ges., 149, 157-173.
- ESCHER, A. & BEAUMONT, C. (1997): Formation, burial and exhumation of basement nappes at crustal scale: a geometric model based on the Western Swiss-Italian Alps. - *J. Structural Geology*, 19, 7, 955-974.
- FARYAD, S. W. & HOINKES, G. (2003): P-T gradient of Eo-Alpine metamorphism within the Austroalpine basement units east of the Tauern Window (Austria). - *Mineral. Petrol.*, 77: 129-159.
- FRANK, W., ESTERLUS, M., FREY, I., JUNG, G., KROHE, A. & WEBER, J. (1983): Die Entwicklungsgeschichte von Stub- und Koralpenkristallin und die Beziehung zum Grazer Paläozoikum. - *Jahresbericht Hochschulschwerpunkt S15 (Vienna)* 4, 263-293.
- FRANK, W., KRALK, M., SCHARBERT, S. & THÖNI, M. (1987): Geochronological data from the Eastern Alps. IN: *Geodynamics of the Eastern Alps*. FLÜGEL, H. W. & FAUPL, P. (Eds). - Deuticke, Wien, 272-281.
- FREY, M., DESMOND, J. & NEUBAUER, F. (Eds.) with contributions of J. APHAHA-MIAN, S. BOGDANOFF, A. BORIANI, G. G. BIINO, C. CHOPIN, A. COLOMBO, R. COMPAGNONI, L. CORTESOGNO, G. V. DAL PIAZ, M. ENGI, R. FERREIRO-MÄHLMANN, W. FRANK, D. GEBAUER, B. GOFFÉ, G. GOSSO, A. GREGNANIN, R. HÄNNY, V. HÖCK, G. HOINKES, J. C. HUNZIKER, R. KIENAST, F. KOLLER, V. KÖPPEL, L. LATOUCHE, B. LOMBARDO, M. MAGGETTI, G. MARTINOTTI, H. MASSON, R. P. MÉNOT, B. MESSIGA, A. MONTRASIO, A. MOTTANA, J. MULLIS, P. NIEVERGELT, A. PÊCHER, H. R. PFEIFFER, G. B. PICCARDO, U. POGNATE †, R. POLINO, R. POTENZA, F. PURTSCHELLER, J. VON RAUMER, R. SACCHI, R. SANDRONE, F. P. SASSI, J. M. SCHRAMM, A. STECK, R. STEIGER, M. THÖNI, V. TROMMSDORFF, A. TUNESI, M. VANOSSI & G. VIVIER (1999): Metamorphic Map of the Eastern Alps. - *Beilage zu Schweiz. Mineral. Petrogr. Mitt.*, 79/1.
- FREY, M., DESMONS, J. & NEUBAUER, F. (1999): The new metamorphic map of the Alps: Introduction. - *Schweiz. Mineral. Petrogr. Mitt.*, 79, 1-4.
- FRISCH, W., BRÜGEL, A., DUNKL, I., KUHLEMANN, J. & SATIR, M. (1999): Post-Collisional Large-Scale Extension and Mountain Uplift in the Eastern Alps. - *Mem. Sci. Geol.*, 51, 1, 3-23.
- FRISCH, W., DUNKL, I. & KUHLEMANN, J. (2000): Post-collisional large-scale extension in the Eastern Alps. - *Tectonophysics*, 327, 239-265.
- FRISCH, W. & GRAWLICK, H.-J. (2003): The nappe structure of the central Northern Calcereous Alps and its disintegration during Miocene tectonic extrusion – a contribution to understanding the orogenic evolution of the Eastern Alps. - *Intern. J. Earth Sci.*, 92, 5, 712-727.
- FRISCH, W., KUHLEMANN, J., DUNKL, I. & BRÜGEL, A. (1998): Palinspastic reconstruction and topographic evolution of the Eastern Alps during late Tertiary tectonic extrusion. - *Tectonophysics*, 297, 1-15.
- FROITZHEIM, N., SCHMID, S. M. & FREY, M. (1996): Mesozoic paleogeography and the timing of eclogite-facies metamorphism in the Alps: A working hypothesis. - *Eclogae Geol. Helv.*, 89(1), 81.
- FROITZHEIM, N., CONTI, P. & VAN DAALLEN, M. (1997): Late Cretaceous, synorogenic, low-angle faulting along the Schlinig fault (Switzerland, Italy, Austria) and its significance for the tectonics of the Eastern Alps. - *Tectonophysics*, 280, 267-293.
- FÜGENSCHUH, B., SEWARD, D. & MANCKTELOW, N. (1997): Exhumation in a convergent orogen: the western Tauern window. - *Terra Nova*, 9, 213-217.
- GEBAUER, D. (1996): A P-T-t-path for an (ultra?) high-pressure ultramafic/mafic rock association and its felsic country-rocks based on SHRIMP-dating of magmatic and metamorphic zircon domains. Example: Alpe Arami (Swiss Central Alps). - IN: *Earth Processes: Reading the Isotopic Code*, pp. 309-328, Amer. Geophys. Union.

- GEBAUER, D. (1999): Alpine geochronology of the Central and Western Alps: new constraints for a complex geodynamic evolution. - *Schweiz. Mineral. Petrogr. Mitt.*, 79, 191-208.
- GRASEMANN, B. & MANCKTELOW, N. (1993): Two-dimensional thermal modelling of normal faulting: the Simplon Fault Zone, Central Alps, Switzerland. - *Tectonophysics*, 225, 155-165.
- HAMMERSCHMIDT, K. & FRANK, E. (1991): Relics of high pressure metamorphism in the Lepontine Alps (Switzerland) - $^{40}\text{Ar}/^{39}\text{Ar}$ and microprobe analyses on white K-micas. - *Schweiz. Mineral. Petrogr. Mitt.*, 71, 261-275.
- HANDY, M. R. (1996): The Transition from Passive to Active Margin Tectonics: A Case Study from the Zone of Samedan (eastern Switzerland). - *Intern. J. Earth Sci.*, 85, 4, 832-851.
- HANDY, M. R., WISSING, S. B. & STREIT, J. E. (1999): Frictional-viscous flow in mylonite with varied biminerale composition and its effect on lithospheric strength. - *Tectonophysics*, 303, 175-191.
- HANDY, M. R., HERWEGH, M., KAMBER, B., TIETZ, R. & VILLA, I. (1996): Geochronologic, petrologic and kinematic constraints on the evolution of the Err-Platta boundary, part of a fossil continent-ocean suture in the Alps (eastern Switzerland). - *Schweiz. Mineral. Petrogr. Mitt.*, 76, 3, 453-474.
- HANDY, M. R., BABIST, J., ROSENBERG, C. L., WAGNER, R. & KONRAD, M. (2004): Decoupling and its relation to strain partitioning in continental lithosphere – Insight from the Periadriatic fault system (European Alps). IN: *Deformation mechanisms, Rheology and Tectonics*. J. P. BRUN, P. R. COBBOLD, & D. GAPAIS (eds). - *Geol. Soc. London, Spec. Publ.* (in press).
- HOINKES, G., KOLLER, F., RANTITSCH, G., DACHS, E., HÖCK, V., NEUBAUER, F. & SCHUSTER, R. (1999): Alpine metamorphism in the Eastern Alps. - *Schweiz. Mineral. Petrogr. Mitt.*, 79, 155-181.
- HUNZIKER, J. C., FREY, M., CLAUER, N., DALLMEYER, R. D., FRIEDRICHSEN, H., FLEHMING, W., HOCHSTRASSER, K., ROGGWILLER, P. & SCHWANDER, H. (1986): The evolution of illite to muscovite mineralogical and isotopic data from the Glarus Alps, Switzerland. - *Contrib. Mineral. Petrol.*, 92, 157-180.
- HUNZIKER, J. C., DESMONS, J. & HURFORD, A. J. (1992): Thirty-two years of geochronological work in the Central and Western Alps: a review on seven maps. - *Mém. Géol. Lausanne*, 13, 1-59.
- HURFORD, A. J., HUNZIKER, J. C. & STÖCKERT, B. (1991): Constraints on the late thermotectonic evolution of the western Alps: Evidence for episodic rapid uplift. - *Tectonics*, 10, 4, 758-769.
- HSU, K. (1995): *The Geology of Switzerland: An Introduction to tectonic Facies*. - Princeton University Press, Princeton, New Jersey, 249 pp.
- INGER, S. & CLIFF, R. A. (1994): Timing of metamorphism in the Tauern Window, Eastern Alps: Rb-Sr ages and fabric formation. - *J. metamorphic Geol.*, 12, 695-707
- JAKNI, B., DUBOIS, R., FOURNIER, M., GOFFÉ, B., MICHARD, A. & JOURDAN, C. (1998): Thermochronologie par trace de fission des marges ligures (Maures Tanneron Corse). - *RST 17, Soc. Géol. Fr., Brest*.
- JOLIVET, L., DANIEL, J.-M. & FOURNIER, M. (1991): Geometry and kinematics of extension in Alpine Corsica. - *Earth Planet. Sci. Lett.*, 104, 278-291.
- KOLLER, F. (1985): Petrologie und Geochemie des Penninikums am Alpenostrand. - *Jb. Geol. B.-A. Wien*, 128, 83-150.
- KOONS, P. O. (1986): Relative geobarometry from high-pressure rocks of quartzofeldspathic composition from the Sesia Zone, Western Alps, Italy. - *Contrib. Mineral. Petrol.* 93: 322-334
- KOZUR, H. & MOSTLER, H. (1992): Erster paläontologischer Nachweis von *Meliaticum* und *Süd-Rudabányaicum* in den Nördlichen Kalkalpen (Österreich und ihre Beziehung zu den Abfolgen in den Westkarpathen. - *Geol. Paläontol. Mitt. Innsbruck*, 18, 87-129.
- LAHONDERE, D. (1991): Les schistes bleus et les éclogites à lawsonite des unités continentales et océaniques de la Corse alpine: Nouvelles données pétrologique et structurales. - Thèse de 3ème cycle, Université de Montpellier II, France.

- LAHONDRE, D. & GUERROT, C. (1997): Datation Sm-Nd du métamorphisme écolitique en Corse alpine: un argument pour l'existence au Crétacé supérieure d'une zone de subduction active localisées sous le bloc corso-sarde. - *Géol. France*, 3, 3-11.
- LAPEN, T. J., JOHNSON, C. M., BAUMGARTNER, L. P., MAHLEN, N. J., BEARD, B. L. & AMATO, J. M. (2004): Burial rates during prograde metamorphism of an ultrahigh pressure terrane: An example from Lago di Cignaga, western Alps, Italy. - Submitted to *Earth Planet. Sci. Lett.*
- LE LOUP, P. H., ARNAUD, N., SOBEL, E. R. & LACASSIN, R. (2004): Insight to the structural evolution of the external Alps from the timing and mode of exhumation of the highest Alpine range: the Mont-Blanc massif. - *Tectonics* (in review).
- LIHOU, J. C. (1995): A new look at the Blattengrat unit of eastern Switzerland: Early Tertiary foreland basin sediments from the South Helvetic realm. - *Eclogae geol. Helv.*, 88, 91-114.
- LIHOU, J. C. (1996): Structure and deformational history of the infrahelvetica flysch units, Glarus Alps, eastern Switzerland. - *Eclogae geol. Helv.*, 89(1), 439.
- LUAIS, B., DUCHENE, S., DE SIGOYER, J. (2001): Sm-Nd disequilibrium in high-pressure, low-temperature Himalayan and Alpine rocks. - *Tectonophysics*, 342, 1-22.
- LUDWIG, K. R. (2000): User's Manual for Isoplot/Ex: A geochronological toolkit for Microsoft Excel. - Berkeley Geochronological Center, Spec. Publ., 1a, 55 pp.
- MALUSKI, H. (1977): Application de la méthode $^{40}\text{Ar}/^{39}\text{Ar}$ aux minéraux des roches cristallines perturbées par les événements thermiques et tectoniques en Corse. - *Bull. Soc. Géol. France*, 19, 4, 849-855.
- MANCKTELOW, N. S., STÖCKLI, D. F., GROLLIMUND, B., MÜLLER, W., FÜGENSCHUH, B., VIOLA, G., SEWARD, D. & VILLA, I. M. (2001): The DAV and Periadriatic fault systems in the Eastern Alps south of the Tauern window. IN: *Developments in Alpine Geodynamics*. FRISCH, W. & MANCKTELOW, N. S. (eds). - *Intern. J. Earth Sci.*, 90, 3, 593-622.
- MANDL, G. W., ONDREJICKI, A. (1991): Über eine triadische Tiefwasserfazies (Radiolarite, Tonschiefer) in den Nördlichen Kalkalpen – ein Vorbericht. - *Jb Geol. B-A, Wien*, 134, 309-318.
- MEFFAN-MAIN, S., CLIFF, R. A., BARNICOAT, A. C., LOMBARDO, B., COMPAGNONI, R. (2004): A Tertiary age for Alpine high-pressure metamorphism in the Gran Paradiso massif, Western Alps: a Rb-Sr microsampling study. - *J. metamorphic Geol.*, 22, 4, 267.
- MEYRE, C., MARQUER, D., SCHMID, S. M. & CIANCALEONI, L. (1998): Syn-orogenic extension along the Forcola fault: Correlation of Alpine deformations in the Tambo and Adula nappes (Eastern Penninic Alps). - *Eclogae geol. Helv.*, 91, 409-420.
- MILLER, C. & THÖNI, M. (1996): Garnet Sm-Nd data from the Saualpe and the Koralpe (Eastern Alps, Austria): Eo-Alpine eclogitisation of Permian MORB-type gabbros in the Koralpe (Eastern Alps, Austria): new geochronological, geochemical and petrological data. - *Chem. Geol.*, 137, 283-310.
- MILLER, C. & THÖNI, M. (1997): Eo-Alpine eclogitisation of Permian MORB-type gabbros in the Koralpe (Eastern Alps, Austria): new geochronological, geochemical and petrological data. - *Chem. Geol.*, 137: 283-310, Amsterdam.
- MOST, P. (2003): Late Alpine cooling histories of tectonic blocks along the central part of the TRANSALP traverse (Inntal-Gardatal): constraints from geochronology. - Ph.D. thesis, Universität Tübingen, 97 pp. 2003.
- MÜLLER, W., PROSSER, G., MANCKTELOW, N. S., VILLA, I. M., KELLEY, S. P., VIOLA, G. & OBERLI, F. (2001): Geochronological constraints on the evolution of the Periadriatic Fault System (Alps). In: *FRISCH, W. & MANCKTELOW, N. S. (eds) Developments in Alpine Geodynamics*. - *Intern. J. Earth Sci.*, 90, 3, 623-653.
- NEUBAUER, F. (1994): Kontinentkollision in den Ostalpen. - *Geowissenschaften*, 12, 136-140.

- OBERHÄNSLI, R., HUNZIKER, J. C., MARTINOTTI, G. & STERN, W. (1985): Geochemistry, geochronology and petrology of Monte Mucrone: an example of Eo-Alpine eclogitization of Permian granitoids in the Sesia-Lanzo Zone, Western Alps, Italy. - *Chem. Geol.* 52: 165-184
- OBERHAUSER, R. (1995): Zur Kenntnis der Tektonik und der Paleogeographie des Ostalpenraumes zur Kreide-, Paleozän- und Eozänzeit. - *Jb. Geol. B.-A.*, 138, 369-432.
- PAHR, A. (1980): Die Fenster von Rechnitz, Bernstein und Möltern. - In: OBERHAUSER, R. (Ed.): *Der Geologische Aufbau Österreichs*. - Springer-Verlag Wien-New York, 320-326.
- PIFFNER, O. A. (1993): The structure of the Helvetic nappes and its relation to the mechanical stratigraphy. - *J. Structural Geology*, 15, 3-5, 511-521.
- RAHN, M. K. & GASEMANN, B. (1999): Fission track and numerical thermal modeling of differential exhumation of the Glarus thrust plane (Switzerland). - *Earth Planet. Sci. Lett.*, 169, 245-259.
- RATSCHBACHER, L., NEUBAUER, F., SCHMID, S. M. & NEUGEBAUER, J. (1989): Extension in compressional orogenic belts: the Eastern Alps. - *Geology*, 17, 404-407.
- RATSCHBACHER, L., WENK, H.-R. & SINTUBIN, M. (1991): Calcite texture: examples from nappes with strain-partitioning. - *J. Structural Geology*, 13, 369-384.
- REDDY, S. M., CLIFF, R. A. & EAST, R. (1993): Thermal history of the Sonnblick Dome, south-east Tauern Window, Austria: Implications for heterogeneous uplift within the Pennine basement. - *Geol. Rundschau*, 82, 667-665.
- RUFFET, G., GRUAU, G., BALLÈVRE, M., FÉRAUD, G. & PHILLIPOT, P. (1997): Rb-Sr and $^{40}\text{Ar}/^{39}\text{Ar}$ laser probe dating of high-pressure phengites from the Sesia Zone (Western Alps): underscoring of excess argon and new age constraints on the high-pressure metamorphism. - *Chem. Geol.*, 141, 1-18.
- RUBATTO, D., GEBAUER, D. & COMPAGNONI, R. (1999): Dating of eclogite-facies zircons: the age of Alpine metamorphism in the Sesia-Lanzo Zone (Western Alps). - *Earth Planet. Sci. Lett.*, 167, 141-158.
- SCAILLET, S. (1996): Excess ^{40}Ar transport scale and mechanism in high-pressure phengites: A case study from an eclogitized metabasite of the Dora-Maira nappe, western Alps. - *Geochim. Cosmochim. Acta*, 60, 6, 1075-1090.
- SCHLUNEGGER, F. & HINDERER, M. (2001): Crustal Uplift in the Alps: Why the drainage pattern matters. - *Terra Nova*, 13, 425-432.
- SCHLUNEGGER, F. & WILLET, S. (2002): Spatial and temporal variations in exhumation of the central Swiss Alps and implications for exhumation mechanisms. In: RING, U., BRANDON, M. T., LISTER, G. S. & WILLET, S. D. (Eds) *Exhumation Processes: Normal Faulting, Ductile Flow and Erosion*. - *Geol. Soc. Spec. Publ.*, 154, 157-179.
- SCHMID, S. M., AEBLI, H. R., HELLER, F. & ZINGG, A. (1989): The role of the Periadriatic Line in the tectonic evolution of the Alps. In: *Alpine Tectonics*. COWARD, M. P., DIETRICH, D. & PARK, R. (eds). - *Geol. Soc. Spec. Publ.*, 45, 153-171.
- SCHMID, S. M., PFIFFNER, O. A., FROITZHEIM, N., SCHÖNBORN, G. & KISSLING, E. (1996): Geophysical-geological transect and tectonic evolution of the Swiss-Italian Alps. - *Tectonics*, 15(5), 1036-1064.
- SCHMID, S. M., PFIFFNER, O. A. & SCHREUERS, G. (1997): Rifting and collision in the Penninic domain. In: *Deep Structure of the Alps: Results of NFP20*. PFIFFNER, O. A., LEHNER, P., HEITZMANN, P., MUELLER, ST. & STECK, A. (eds). - Birkhäuserverlag, Basel, Switzerland, 380 p.
- SCHMID, S. M. & KISSLING, E. (2000): The arc of the western Alps in the light of geophysical data on deep crustal structure. - *Tectonics*, 19, 1, 62-85.
- SCHMID, S. M., FÜGENSCHUH, B., KISSLING, E. & SCHUSTER, R. (2004): Tectonic map and overall architecture of the Alpine orogen. - *Eclogae geol. Helv.*, in press.

- SCHULZ, B. (1994): Geologische Kartierung des Altkristallins östlich des Tauferer Tals (Südtirol). Erlanger Geologische Abhandlungen, C, 124, 1-28.
- SCHUMACHER, M. E., SCHÖNBORN, G., BERNOULLI, D. & LAUBSCHER, H. P. (1997): Rifting and collision in the Southern Alps. IN: Deep Structure of the Alps: Results of NFP20. PFIFFNER, O. A., LEHNER, P., HEITZMANN, P., MUELLER, S. T. & STECK, A. (eds). - Birkhäuserverlag, Basel, Switzerland, 380 p.
- SCHUSTER, R. (2003): Das eo-Alpine Ereignis in den Ostalpen: Plattentektonische Situation und interne Struktur des Ostalpinen Kristallins. - Geologische Bundesanstalt Arbeitstagung 2003 Blatt 148 Brenner, 2003: 141-159.
- SCHUSTER, R., KOLLER, F., HOECK, V., HOINKES, G. & BOUSQUET, R. (2004): Metamorphic Structure of the Alps: Eastern Alps. IN: Explanatory notes to the Map of Metamorphic Structures of the Alps. OBERHÄNSLI, R. (ED). - Mitt. Öster. Min. Ges., 149, 175-199.
- SNOKE, A. W. & TULLIS, J. (1998): An overview of fault rocks. pp. 3-18 IN: Fault-related rocks: A photographic atlas. SNOKE, A. W., TULLIS, J. & TODD, V. (eds), Princeton University Press, Princeton, New Jersey, USA, 617 p.
- STAMPFLI, G. M., MOSAR, J., MARQUER, D., MARCHANT, R., BAUDIN, T. & BOREL, G. (1998): Subduction and obduction processes in the Swiss Alps. - Tectonophysics, 296, 159-204.
- STECK, A. & HUNZIKER, J. (1994): The Tertiary structural and thermal evolution of the Central Alps - Compressional and extensional structures in an orogenic belt. - Tectonophysics, 238, 229-254.
- STÖCKHERT, B. (1984): K-Ar determinations on muscovites and phengites from deformed pegmatites, and the minimum age of Old Alpine deformation in the Austric basement to the South of the western Tauern Window (Ahrn valley, Southern Tyrol, Eastern Alps). - N. Jb. Miner. Abh., 150, 2, 103-120.
- STÖCKHERT, B., BRIX, M. R., KLEINSCHRODT, R., HURFORD, A. J. & WIRTH, R. (1999): Thermochronometry and microstructures of quartz - a comparison with experimental flow laws and predictions on the temperature of the brittle-plastic transition. - J. Structural Geology, 21, 351-369.
- TRANSALP Working Group. (2002): First deep seismic reflection images of the Eastern Alps reveal giant crustal wedges and transcrustal ramps. - Geophys. Res. Lett., 29, 10, 1029/2002GL014911.
- TROPPER, P. & ESSENE, E. J. (2002) Thermobarometry in eclogites with multiple stages of mineral growth: an example from the Sesia-Lanzo Zone (Western Alps, Italy). - Schweiz. Mineral. Petrogr. Mitt., 82 (3): 487-514 2002
- THÖNI, M. (1999): A review of geochronological data from the Eastern Alps. IN: The new metamorphic map of the Alps. FREY, M., DESMONS, J. & NEUBAUER, F. (eds). - Schweiz. Mineral. Petrogr. Mitt., 79, 1, 209-230.
- THÖNI, M. & MILLER, C. (2000): Permo-Triassic pegmatites in the Eo-Alpine eclogite-facies Koralpe complex, Austria: age and magma source constraints from mineral chemical, Rb-Sr and Sm-Nd isotopic data. - Schweiz. Mineral. Petrogr. Mitt., 80: 169-186, Zürich.
- TRÜMPY, R. (1980): Geology of Switzerland: A guide book. Part A: An Outline of the Geology of Switzerland. - Edited by the Schweizerische Geologische Kommission, Wepf & Co. Publ., Basel, New York.
- WAGREICH, M. (2001): A 400-km-long piggyback basin (Upper Aptian-Lower Cenomanian) in the Eastern Alps. - Terra Nova, 13, 401-406.
- WHEELER, J., REDDY, S. M. & CLIFF, R. A. (2001): Kinematic linkage between internal zone extension and shortening in more external units in the NW Alps. - J. Geol. Soc. London, 158, 439-443.
- WINKLER, W. (1988): Mid-to Early Late Cretaceous Flysch and Melange Formations in the Western Part of the Eastern Alps: Paleotectonic Implications. - Jahrb. Geol. Bund., Wien, 131, 2, 341-389.
- ZANCHI, A., CHIESA, S. & GILLOT, P. Y. (1990): Tectonic evolution of the Southern Alps in the Orobic chain: structural and geochronological indications for pre-Tertiary compressive tectonics. - Mem. Soc. Geol. It., 45, 77-82.

ZIMMERMANN, R., HAMMERSCHMIDT, K. & FRANZ, G. (1994): Eocene high-pressure metamorphism in the Pennine units of the Tauern window (Eastern Alps): Evidence from $^{40}\text{Ar}/^{39}\text{Ar}$ dating and petrological investigations. - *Contrib. Mineral. Petrol.*, 117, 175-186.

manuscript received: June 2004

manuscript accepted: July 2004

Metamorphic structure of the Alps

Scale 1:1.000.000

Commission for the Geological Map of the World/Commission de la Carte Géologique Mondial

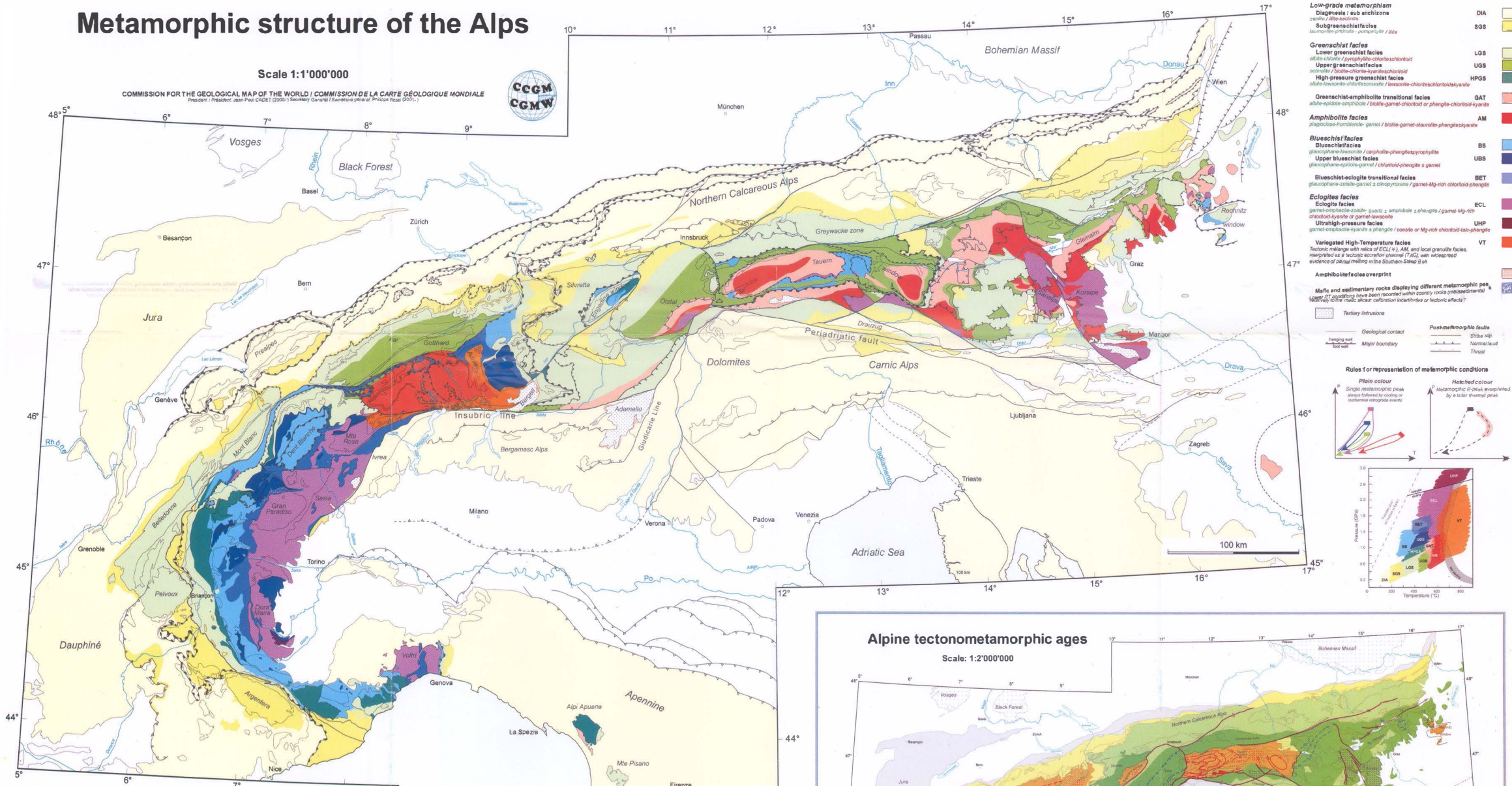
Edited by Roland Oberhänsli (Coordinator, Universität Potsdam), Romain Bousquet (Universität Basel), Martin Engi (Universität Bern), Bruno Goffé (ENS Paris-CNRS), Guido Gosso (Università di Milano), Mark Handy (Freie Universität Berlin), Volker Höck (Universität Salzburg), Friedrich Koller (Universität Wien), Jean-Marc Lardeaux (Université de Nice), Riccardo Polino (IGG-CNR Torino), Philippe Rossi (BRGM, Paris), Ralf Schuster (Geologische Bundesanstalt Wien), Stéphane Schwartz (Université de Grenoble), Iole Spalla (Università di Milano)

Advisory board R. Caby (Université de Montpellier), Ch. Chopin (ENS Paris-CNRS), R. Compagnoni (Università di Torino), G. V. Dal Piaz (Università di Padova), R. Ferreira Mählmann (Technische Universität Darmstadt), Ch. Miller (Universität Innsbruck), St. Schmid (Universität Basel)

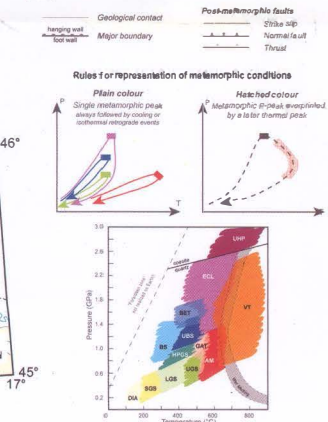
with contributions from Ph. Agard (Université Paris VI), J. Babist (Freie Universität Berlin), A. Berger (Universität Bern), R.J. Bertle (Universität Vienna), St. Bucher (Universität Basel), T. Burri (Universität Bern), P. Heitzmann (BWG Bern), G. Hoinkes (Universität Graz), L. Jolivet (Université Paris VI), L. Keller (Universität Basel), M. Linner (Geologische Bundesanstalt Wien), B. Lombardo (IGG-CNR Torino), G. Martinotti (Università di Torino), A. Michard (ENS Paris), G. Pestal (Geologische Bundesanstalt Wien), A. Proyer (Universität Graz), G. Rantisch (Universität Leoben), C. Rosenberg (Freie Universität Berlin), J.M. Schramm (Universität Salzburg), H. Soelva (Universität Wien), M. Thoeni (Universität Wien), M. Zucali (Università di Milano)

Computer graphics: R. Bousquet, J. Tensi, M. Grundmann

Metamorphic structure of the Alps



Low-grade metamorphism Diagenesis / sub anchizone schists / siltstones Subgreenschistfacies Kaukasiten/Protinitid / Amphibolite / Zeile	DIA
Greenschist facies Lower greenschist facies albite-chlorite / pyrophyllite-chlorite-schistoid Upper greenschist facies actinolite / biotite-chlorite-glaucophane-schistoid High-pressure greenschist facies Albite-nauseonite-chlorite-crocoisite / Naeseonite-chlorite-schistoid/kyanite	LOS UGS HPGS
Greenschist-amphibolite transitional facies Albite-garnet-amphibolite / biotite-garnet-chloritoid or phengite-chloritoid-kyanite	GAT
Amphibolite facies Biotite-hornblende-garnet / biotite-garnet-staurolite-phengite/kyanite	AM
Blueschist facies Lower blueschist facies glaucophane-lawsonite / carpholite-phengite/psilophyllite Upper blueschist facies glaucophane-epidote-garnet / chloritoid-phengite + garnet	BS UBS
Blueschist-eclogite transitional facies glaucophane-zoisite-garnet + clinopyroxene / garnet-Mg-rich chloritoid-phengite	BET
Eclogite facies Eclogite facies garnet-cordierite-zoisite-quartz + amphibole + phengite / garnet-Mg-rich chloritoid-kyanite or garnet-lawsonite	ECL
Ultrahigh-pressure facies garnet-cordierite-sillimanite / coesite or Mg-rich chloritoid-feldspar	UHP
Variegated High-Temperature facies Facies mixture with relics of ECU + AM and local granulite facies. Interpreted as a tectonic accretion channel (TAC) with widespread evidence of partial melting in the Southern Alps Belt	VT
Amphibolite facies overprint Mafic and sedimentary rocks displaying different metamorphic peak. Layer 1) secondary have been reported within country rocks (pre-metamorphic). Layer 2) mafic dykes collection uncertainties or tectonic effects?	

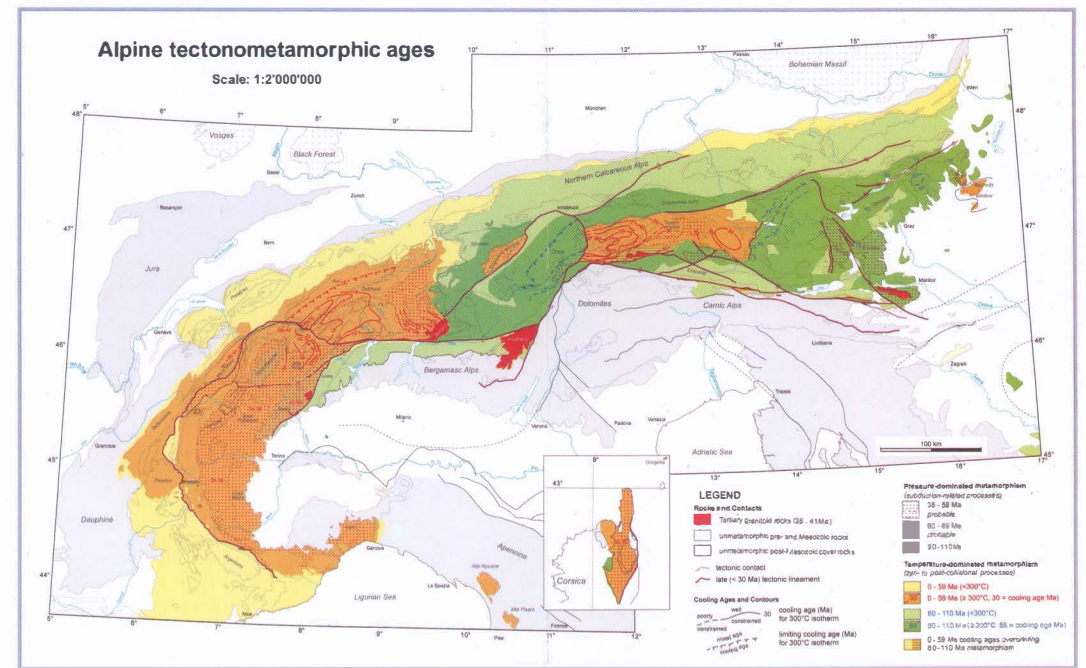


Edited by Roland Oberhänsli (Coordinator, *Universität Potsdam*), Romain Bousquet (*Universität Basel*), Martin Engi (*Universität Bern*), Bruno Goffé (*ENS Paris-CNRS*), Guido Gosso (*Università di Milano*), Mark Handy (*Freie Universität Berlin*), Volker Höck (*Universität Salzburg*), Friedrich Koller (*Universität Wien*), Jean-Marc Lardeaux (*Université de Nice*), Riccardo Polino (*IGG-CNR Torino*), Philippe Rossi (*BRGM, Paris*), Ralf Schuster (*Geologische Bundesanstalt Wien*), Stéphane Schwartz (*Université de Grenoble*), Iole Spalla (*Università di Milano*)

Advisory board R. Caby (*Université de Montpellier*), Ch. Chopin (*ENS Paris-CNRS*), R. Compagnoni (*Università di Torino*), G. V. Dal Piaz (*Università di Padova*), R. Ferreira Mählmann (*Technische Universität Darmstadt*), Ch. Miller (*Universität Innsbruck*), St. Schmid (*Universität Basel*)

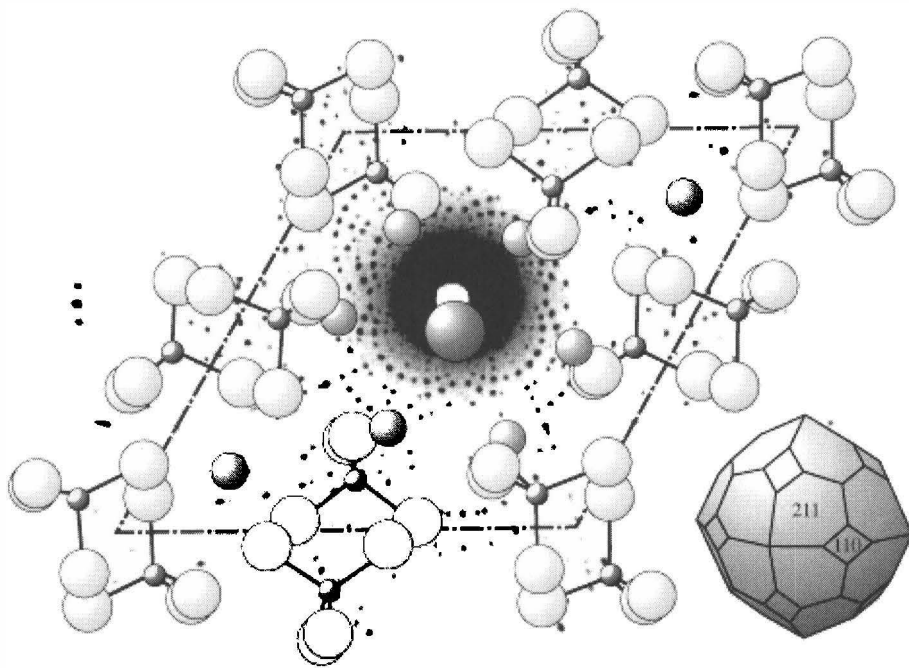
with contributions from Ph. Agard (*Université Paris VI*), J. Babat (*Freie Universität Berlin*), A. Berger (*Universität Bern*), R.J. Bertle (*Universität Vienna*), St. Bucher (*Universität Basel*), T. Burri (*Universität Bern*), P. Heitzmann (*BIWG Bern*), G. Hoinkes (*Universität Graz*), L. Jolivet (*Université Paris VI*), L. Keller (*Universität Basel*), M. Linner (*Geologische Bundesanstalt Wien*), B. Lombardo (*IGG-CNR Torino*), G. Mattioli (*Università di Torino*), A. Michard (*ENS Paris*), G. Pesta (*Geologische Bundesanstalt Wien*), A. Proyer (*Universität Graz*), G. Rantsch (*Universität Leoben*), C. Rosenberg (*Freie Universität Berlin*), J.M. Schramm (*Universität Salzburg*), H. Soelva (*Universität Wien*), M. Thoeni (*Universität Wien*), M. Zucali (*Università di Milano*)

Computer graphics: R. Bousquet, J. Tenal, M. Grundmann



Rock and Contacts	Pressure-dominated metamorphism Isoclinal-to-rotational prograde
Tertiary dykes (ca. 4-13 Ma)	35 - 50 Ma predictable
Ultramylonitic pre- and Mesozoic rocks	60 - 65 Ma (pre-40 Ma)
Ultramylonitic post- and Mesozoic cover rocks	90 - 110 Ma
LEGEND	Temperature-dominated metamorphism (due to post-collisional processes)
tectonic contact	0 - 50 Ma (<300°C)
late (< 30 Ma) tectonic truncation	50 - 110 Ma (<300°C)
Cooling Ages and Contours	90 - 110 Ma (<300°C)
cooling age (Ma) for 300°C isotherm	30 - 110 Ma (>200°C, 30 = cooling age Ma)
limiting cooling age (Ma) for 300°C isotherm	0 - 50 Ma cooling ages overprinting 00-110 Ma metamorphism

ORIGINALARBEITEN



**ERICH SCHROLL, EIN WEGBEREITER FÜR DIE
GEOCHEMISCHE FORSCHUNG IN ÖSTERREICH.
ZUM 80. GEBURTSTAG
(MIT EINEM SCHRIFTENVERZEICHNIS)**

von

Katalin Augustin-Gyurits¹ & Franz Pertlik²

¹Hauptstraße 59, A-2801 Katzelsdorf, Niederösterreich

²Institut für Mineralogie und Kristallographie
Universität Wien, Geozentrum, Althanstrasse 14, A-1090 Wien

*wer sleht den lewen? wer sleht den risen?
wer überwindet jenen und disen?
daz tuot einer der sich selber twinget.
Walther von der Vogelweide, L. 81,7.*

Einleitung

Der Doyen der geochemischen Forschung in Österreich, Erich (Robert) Schroll, vollendete 2003 sein 80. Lebensjahr (* 8.12.1923). Dieses Jubiläum sei zum Anlass genommen, einen kurzen Überblick sowohl ganz allgemein über sein Leben, als auch im Speziellen über seine berufliche Laufbahn, sein Wirken in Lehre und Forschung, sowie sein wissenschaftliches Werk zu geben.

Wohl kein anderer Ausspruch als jener, der einleitend angeführt und dem Lyriker WALTHER VON DER VOGELWEIDE (um 1220) zugeschrieben wird, kann die Person Erich Schroll besser charakterisieren. Bereits anlässlich des 60. Geburtstages des Jubilars stellte CERNY (1983) eine Laudatio zusammen, in der diese Selbstüberwindung in einem kurzen Satz angedeutet wurde (wörtlich):

Von Jugend an nicht ganz schwindelfrei, hört man Erich Schroll leise vor sich hinsagen – "Erich ganz ruhig" – sei es auf Steigbäumen, in alten Gruben oder auf schroffen Karen stehend; seine Begeisterung für die Wissenschaft ist ihm die Selbstüberwindung wert."

Im Anhang an diese Laudatio findet sich des Weiteren auch eine Zusammenstellung aller bis zu diesem Zeitpunkt von Schroll veröffentlichten wissenschaftlichen Arbeiten (HAGENGUTH, 1983). Zu erwähnen ist auch eine kurze Würdigung des Lebenswerkes des Jubilars durch WEBER (2003).

Elternhaus, Jugend und Ausbildung

Eine Ahnentafel dreier Generationen der Familie Schroll ist in Tabelle 1 wiedergegeben. Als einleitender Bericht über Jugendjahre, Schule und Studium des Jubilars erscheint ein in seiner Dissertation veröffentlichter, selbstverfasster Lebenslauf am besten geeignet. Dieser sei hier wörtlich wiedergegeben:

Alois Jakob Schroll * 18.7.1898, Wiener Neustadt † 1959, Wiener Neustadt	Hedwig Therese Baumgarth * 17.9.1901, Pistau bei Igllau † 9.8.1982, Wiener Neustadt	Josef Flegel * 22.5.1890, Weisenfels, Krain † 22.8.1957, Wiener Neustadt	Anna Krautwurst * 20.12.1881, Feistritz, Wechsel † 5.12.1970, Wiener Neustadt
∞ 25.2.1922, Igllau		∞ 2.7.1921, Wiener Neustadt	
Erich Robert Schroll * 8.12.1923, Wiener Neustadt		Karoline Anna Maria Flegel * 1.8.1922, Wiener Neustadt	
∞ 17.11.1962, Wiener Neustadt			
Gerhard Robert Schroll * 28.1.1967, Wien			

Tabelle 1

Ahnentafel des Jubilars mit persönlichen Daten.

Curriculum vitae

Ich wurde am 8.Dez.1923 als einziges Kind meiner Eltern Alois und Hedwig S c h r o l l, geb. Baumgarth, zu Wiener-Neustadt in Nieder-Österreich geboren. Mein Vater war Beamter der Österreichischen Bundesbahnen. In Wr. Neustadt bin ich aufgewachsen, dort habe ich eine vierklassige Volksschule (Übungsschule der dortigen Lehrerbildungsanstalt) und im Anschluß daran die acht Klassen eines humanistischen Gymnasiums absolviert.

Nach meiner Matura im Jahre 1942 wurde ich sofort zur Wehrmacht eingezogen. Mit drei Verwundungen entging ich als gewöhnlicher Infantrist der Hölle dreier Kriegsjahre. Noch im Frühjahr 1945 wurde Haus und Wohnung meiner Eltern bei einem der letzten Bombenangriffe auf Wr. Neustadt zur Gänze zerstört.

So begann ich im Herbst 1945 meine Studien an der Universität Wien. Geldliche Schwierigkeiten, die durch den Bruch der Ehe meiner Eltern auf mir laste[te]n, zwangen mich gleichzeitig, durch Stundengeben einem ständigen Nebenverdienst nachzugehen.

Schon in der Oberstufe des Gymnasiums hatte die Neigung zu den Naturwissenschaften die Oberhand über die anfänglich bevorzugten philologischen Fächer gewonnen. In den ersten vier Semestern, zum Teil noch unschlüssig, hatte ich reichlich die Gelegenheit benützt, chemische Vorlesungen und Übungen zu besuchen und mathematisch-physikalische Kenntnisse zu erwerben. Im dritten Semester habe ich dann mein Studienziel der Mineralogie zugewandt, wobei vom Beginn an das Spezialgebiet der Geochemie und Lagerstättenlehre meine gesamte Aufmerksamkeit auf sich gezogen hat. Als Dissertationsthema habe ich mir denn auch eine Arbeit über genetische und geochemische Probleme der Blei-Zink-Lagerstätte Bleiberg-Kreuth in Kärnten erwählt. Ich habe den Wunsch und die Absicht, in dieser Fachrichtung weiter zu arbeiten.

Bereits im Jahre 1949, noch als Student am Institut für Mineralogie, vollendete Schroll seine erste wissenschaftliche Arbeit über Wulfenite aus Nordtirol und Kärnten (SCHROLL, 1949). Während des Studiums und der Abfassung seiner Dissertation wurde er in Vorlesungen und Übungen, gehalten von Herbert Haberlandt (1904–1970), Dozent am Institut für Mineralogie, erstmals mit dem Fach Geochemie konfrontiert (SCHROLL & PERTLIK, 2001).

Diese ersten Kontakte mit diesem Wissensgebiet prägten ganz entscheidend seine weiteren wissenschaftlichen Arbeiten, wie nachfolgend ausführlicher beschrieben wird.

Mit 11.5.1950 reichte er seine Dissertation ein (SCHROLL, 1950), welche den Professoren Felix Karl Ludwig Machatschki (1895–1970) und Hans Leitmeier (1885–1967) zur Begutachtung vorgelegt wurde. Nach Ablegung der vorgeschriebenen strengen Prüfungen promovierte Schroll am 15.7.1950 zum Doktor der Philosophie (Hauptfach Mineralogie und Petrographie, Nebenfach Geologie). Die Venia Legendi für das Fach "Mineralogie mit besonderer Berücksichtigung der Geochemie" an der Universität Wien wurde ihm nach Vorlage der aus drei Teilpublikationen bestehenden Habilitationsschrift (SCHROLL, 1953; 1954; 1956) und nachfolgender Examinations mit 19.7.1956 verliehen (Erlass des Bundesministeriums für Unterricht, Zl. 1704-5-56). Zu diesem Zeitpunkt wirkte er bereits an der ehemaligen Bundesversuchs- und Forschungsanstalt Arsenal in leitender Position. Einer Entschließung des Bundespräsidenten entsprechend, wird mit 28.6.1963 der Berufstitel "Außerordentlicher Universitätsprofessor" an Schroll verliehen.

Berufliche Etablierung

Nach Abschluss seines Studiums war Schroll in den Jahren 1951 und 1952 als wissenschaftliche Hilfskraft am Mineralogischen Institut der Universität Wien beschäftigt (Direktor: Felix Karl Ludwig Machatschki). Im darauf folgenden Jahr trat er kurzfristig in die Dienste der Bleiberger Bergwerksunion (BBU) ein. Als "Zimmermann I. Klasse" angestellt, bestand seine Aufgabe in der Beprobung und Ermittlung der Haldenvorräte an Blei, Zink und Molybdän in Bleiberg. Außerdem legte er einen Bericht über Germanium- und Thalliumgehalte in Erzkonzentraten vor.

Mit 1.3.1953 wurde Schroll als Vertragsbediensteter des Bundes (VB Ia) an der Bundesversuchs- und Forschungsanstalt Arsenal (BVFA) in den Bundesdienst aufgenommen, wobei seine erste Aufgabe in der Errichtung eines spektrographischen und chemischen Laboratoriums bestand. Für die Zeit vom 1.10.1961 bis 28.2.1963 wurde Schroll provisorisch mit der Leitung der Geschäfte der Wärme-, Kälte- und Strömungstechnik (WKS) betraut, zu welcher auch die chemischen Laboratorien gehörten. Mit der Reorganisation der Forschungsanstalt erfolgte am 17.3.1964 seine Ernennung zum definitiven Leiter des neu gegründeten Grundlageninstitutes unter Zusammenschluss der chemischen Laboratorien (Analytische Chemie, Brennstoffchemie, Silikatchemie und Röntgenanalytik) mit der Isotopenabteilung. Mit 1.5.1967 zum Oberbaurat und mit 1.2.1972 zum "Wirklichen Hofrat" ernannt, wurde ihm am 1.1.1974 die Leitung des – aus obgenanntem Grundlageninstitut hervorgegangenen, umbenannten und vergrößerten – Geotechnischen Institutes der BVFA mit den Gruppen Geochemie, Geophysik und Straßenwesen übertragen. Am 28.10.1988 erfolgte seine Ernennung zum Vizedirektor der BVFA.

Ende des Jahres 1988 trat Schroll in den Ruhestand und hinterließ die bestausgerüstete außeruniversitäre erdwissenschaftliche Forschungsstätte Österreichs mit sechzig Mitarbeitern in den folgenden Abteilungen: Analytische Geochemie, Umweltgeologie, Umweltchemie, Isotopengeophysik, Angewandte Mineralogie & Gesteinskunde, Hydrogeologie & Angewandte Geophysik, Bodenmechanik, Straßenbautechnik, sowie einer Abteilung "IDS" (Internationale Dokumentation Straße).

Eine Vorstellung der Aktivitäten sämtlicher Institute der BVFA erfolgte in einer ausführlichen Dokumentation (ARSENAL 2000). Neben einer zentralen Verwaltung war die BVFA in drei große Einheiten (Institute) unterteilt: Maschinenbau (MTI) – Elektrotechnik (ETI) – Geotechnik (GTI). Zur Charakterisierung und Stellung dieser Institute im wissenschaftlichen Leben seien einige Geleitworte des für die BVFA zuständigen Bundesministers BUSEK (1990) wiedergegeben:



Abbildung 1

Erich Schroll (Porträt aufgenommen im Jahre 2003 von Foto Tschank G.m.b.H., Wiener Neustadt).

Zum Geleit

Vorwort des Bundesministers für Wissenschaft und Forschung

Die BUNDESVERSUCHS- und FORSCHUNGSANSTALT ARSENAL hat sich zur größten technisch-wissenschaftlichen Anstalt des Bundes in Österreich entwickelt.

Sie ist nicht auf der grünen Wiese geplant und gebaut worden, sondern ist organisch auf dem Gelände einer vom Krieg zerstörten Waffenfabrik unter Ausnutzung einer vorgegebenen Infrastruktur gewachsen.

In den vierzig Jahren ihres Bestehens sind Leistungen für Wirtschaft und Staat erbracht worden, die nationale und internationale Beachtung und Anerkennung gefunden haben.

Bescheidenheit ist heute keine Zier. Es ist deshalb zu begrüßen, daß in dem vorliegenden Buch sowohl Leistungen aus vergangenen Tagen als auch das derzeitige Leistungspotential mit all seinen Zukunftsperspektiven festgehalten werden.

Wer weiß beispielsweise, daß im Wiener Arsenal wesentliche technische Impulse für den Bau der Hochgeschwindigkeitsbahnen Europas und für den Komfort im Reisezugsverkehr gegeben werden und wurden? Bahnfahrzeuge aus der ganzen Welt treffen einander in Wien in der dortigen Fahrzeugsversuchsanlage.

Im Fernheizwerk wurde die erste Wärme-Kraft-Kupplung Österreichs erprobt und damit die Voraussetzung geschaffen, mit dieser ökotechnisch beispielhaften Lösung ganze Stadtteile Wiens mit Wärme zu versorgen. Dies sind nur zwei markante Beispiele aus dem reichen und bunten Leistungsbuket[1] der Bundesversuchs- und Forschungsanstalt Arsenal.

Vieles ist vorausschauend geschaffen worden und trägt zum stetigen Erfolg und Ansehen der BVFA-Arsenal bei. Auch in Zukunft wird sie mit ihren Großeinrichtungen ein wichtiges, im Hinblick auf den europäischen Binnenmarkt sogar unentbehrliches Zentrum der technischen Forschung und des österreichischen Prüfwesens sein.

Die weiter zunehmende Bedeutung der Natur- und Technikwissenschaften für die Wirtschaft und unsere Umwelt verlangt nach Forschungszentren, die mit den Universitäten, außeruniversitären Einrichtungen und der Wirtschaft national und international vernetzte Systeme bilden, in sich hohe fachliche Spezialisierungen entwickeln, und nach außen kommunikativ und kooperativ wirksam werden.

Der internationale wirtschaftlich-technische Wettbewerb und die natürlichen und technogenen Probleme lassen Forschungsbereitschaft und Einsatz jedes innovativ orientierten Landes weiter steigen.

Die ausgewogene Förderung der Universitäten und der außeruniversitären Einrichtungen ist eine unaufschiebbare politische Aufgabe.

Am Einsatzwillen, dem Fleiß und der Kreativität aller Mitarbeiterinnen und Mitarbeiter der BVFA-Arsenal wird es liegen, daß permanente Impulse zur Weiterentwicklung der Anstalt führen. In diesem Sinne wünsche ich auch im Interesse der Republik Österreich der BVFA-Arsenal einen erfolgreichen Aufbruch ins 3. Jahrtausend!

Wien, im Oktober 1990

Dr. Erhard Busek

Bundesminister für Wissenschaft und Forschung.

Als erfahrener Politiker mit Kompetenz und Weitblick hatte Busek die Bedeutung dieser bundeseigenen Einrichtung sowohl als Prüfstelle als auch als Forschungsstätte erkannt und ihre Förderung als maßgebliche politische Aufgabe angesehen.

In den Folgejahren wurde über die Ausgliederung von außeruniversitären staatlichen Forschungsanstalten und daraus resultierenden Kosten eine rege Diskussion entfacht. Sowohl die BVFA im Allgemeinen als auch das Geotechnische Institut waren davon betroffen. Damals wurde eine schon lange andiskutierte Einbindung in die Geologische Bundesanstalt in Erwägung gezogen. Durch den Erlass des die gesamte BVFA betreffenden "Arsenalgesetzes" wurde jedoch jede Diskussion hinfällig, da die BVFA in eine Gesellschaft mit beschränkter Haftung übergeführt wurde. Der §1 dieses Bundesgesetzes sei hier wörtlich wiedergegeben:

15. Bundesgesetz über das Österreichische Forschungs- und Prüfzentrum Arsenal Gesellschaft mit beschränkter Haftung. Ausgegeben am 10. Jänner 1997.

Der Nationalrat hat beschlossen:

Errichtung

§1. (1) Zur Wahrnehmung des bisher von der betriebsähnlichen Einrichtung des Bundes Bundesforschungs- und Prüfzentrum Arsenal wahrgenommenen Aufgaben wird eine Gesellschaft mit beschränkter Haftung errichtet. Diese Gesellschaft führt die Firma "Österreichisches Forschungs- und Prüfzentrum Arsenal Gesellschaft m.b.H." (im folgenden: die Gesellschaft) und steht zu 100 % im Eigentum des Bundes. Die Gesellschaft entsteht unter Ausschluß des § 2 Abs. 1 GmbH-Gesetz mit Inkrafttreten dieses Bundesgesetzes. Im übrigen ist, soweit dieses Gesetz keine abweichenden Vorschriften enthält, das Gesetz über die Gesellschaften mit beschränkter Haftung, RGBl. Nr. 58/1906, anzuwenden.

Im Rahmen der neu definierten Geschäftsordnung wurden zum Teil einschneidende Strukturänderungen vorgenommen. Aus den drei Instituten Elektrotechnik (ETI), Geotechnik (GTI) und Maschinenbau (MTI) entstanden vier neue Bereiche: Verkehr, Energie, Bauen und Geotechnik, wobei sich der Bereich Bauen aus den Abteilungen: Straßenbautechnik, Bodenmechanik (beide vormals GTI), Lärm & Schwingung und Kältetechnik (beide vormals MTI) zusammensetzte. Im Zuge der Vollziehung obgenannten Bundesgesetzes wurde somit auch das Geotechnische Institut in Verkenning der Bedeutung der Erdwissenschaften irreversibel organisatorisch zerschlagen. Neben der angeführten Umstrukturierung und weitgehenden Auslagerung der technisch orientierten Abteilungen Straßenbautechnik und Bodenmechanik wurden die höchst spezialisierten Abteilungen für anorganische und organische Analytik praktisch aufgelöst. Mit 16.3.1998 wurden einige Abteilungen des Geotechnischen Institutes zum Bereich "Umwelt" zusammengefasst. Unter Hinweis auf eine angebliche Bedeutungslosigkeit der Geowissenschaften erfolgten auch die Umbenennungen von Instituts- und Abteilungsbezeichnungen unter bewusster Ausschaltung des Begriffes "Geo"

Zweifellos und auch dokumentiert war das Geotechnische Institut der BVFA in seiner erdwissenschaftlichen Orientierung eine international anerkannte Institution. Seit 1953 wurde von dieser Institution in verschiedenen angewandten Disziplinen der Erdwissenschaften allgemein anerkannte Pionierarbeit geleistet, die in zahlreichen Berichten, Veröffentlichungen und Fachtagungen ihre Dokumentation fand.

Es war grundsätzlich sicherlich wünschenswert und zweckmäßig, die in Österreich vorhandenen außeruniversitären Forschungseinrichtungen aus Gründen größerer Effizienz und der Vermeidung von Doppelgleisigkeiten zusammenzulegen. Als optimale Lösung hätte sich die Einbindung der erdwissenschaftlichen Einrichtungen der BVFA in die Geologische Bundesanstalt geradezu angeboten. Dies nicht zuletzt auch deshalb, weil der sorgfältige und verantwortungsbewusste Umgang mit den natürlichen Ressourcen wie Rohstoffen, Energie und Wasser ebenso wie der Schutz der Umwelt vor industrieller Verunreinigung eine verpflichtende Aufgabe der öffentlichen Hand darstellt. Leider wurde dieses Lösungsmodell nicht realisiert. Im letzten Jahrzehnt des 20. Jahrhunderts wurden somit die Institute und Abteilungen der BVFA ausgelagert bzw. großteils aufgelöst. Damit war eine in ihrer Art beispielhafte und effiziente Institution, der quasi Behördencharakter zukam, dem "Management" der öffentlichen Hand zum Opfer gefallen.

Erich Schroll hat dieses unrühmliche Ende der BVFA und im Speziellen des Geotechnischen Institutes, dessen Aufbau ein Teil seines Lebenswerkes darstellte, stets auf das Schärfste verurteilt, da eine Forschungsstätte von internationaler Bedeutung ohne ersichtlichen Grund aufgelöst wurde, ohne dass ihre Aufgabenbereiche von einer anderen adäquaten Institution übernommen worden wären.

Erich Schroll als akademischer Lehrer

Seine erste Vorlesung in Eigenverantwortlichkeit an der Universität Wien kündigte Schroll im Wintersemester 1956/57 an:

Einführung in die Emissionsspektrographie (mit Demonstrationen), 2 st., n. Ü.; Mineralog. Inst.

Universität Wien

Assareh, Abdol Rahman, * 16.10.1938, Ramhormoz, Kuzistan, Iran.

Beitrag zur Geochemie der Tongesteine.

Ein.: 9.12.1969. Prom.: 26.6.1970.

Ref. 1: Schroll. Ref. 2: Wieseneder.

Caglayan, Hidir, * 28.7.1947, Terzan/Erzincan, Türkei.

Die Vererzung der fluorit-molybdänglanz-führenden Blei-Zink-Lagerstätten von Keban-Elazig im Südost-Taurus (Türkei).

Ein.: 8.6.1984.

Ref. 1: Schroll. Ref. 2: Richter.

Cardich-Loarte, Lucio Adolfo, * 9.5.1941, Huanuco, Peru.

Beitrag zur Geochemie des Strontiums in der Blei-Zinklagerstätte Bleiberg/Kreuth.

Ein.: 22.4.1971. Prom.: 20.12.1971.

Ref. 1: Zemann. Ref. 2: Schroll.

Dolezel, Peter, * 19.3.1936, Brünn.

Zur Geochemie der ostalpinen Sideriterze.

Ein.: 27.4.1976. Prom.: 1.2.1978.

Ref. 1: Schroll. Ref. 2: Zemann.

Hagenguth, Gerd, * 24.7.1955, Köln.

Geochemische und fazielle Untersuchungen an den Maxerbänken im Pb-Zn-Bergbau von Bleiberg-Kreuth / Kärnten.

Ein.: 17.5.1983. Prom.: 6.7.1983.

Ref. 1: Tollmann. Ref. 2: Schroll.

Hauk, Peter, * Wien.

Beitrag zur Mineralchemie und instrumentellen Mineralanalyse "komplexer Niob-Tantal-Erze"

Ein.: 7.7.1965. Prom.: 21.12.1965.

Ref. 1: Schroll. Ref. 2: Wieseneder.

Huber, Ingeborg, nat. Schausberger, * 3.5.1938, Warnsdorf, Tschechien.

Zur Geochemie der Fluszsparite.

Ein.: 22.6.1965. Prom.: 1.4.1966.

Ref. 1: Schroll. Ref. 2: Wieseneder.

Khomami, Jussef, * 31.10.1939, Resht, Iran.

Beitrag zur Geochemie der Andesite.

Ein.: 17.2.1971. Prom.: 20.12.1971.

Ref. 1: Schroll. Ref. 2: Wieseneder.

Nawaratne, Sirinagha Wimaladharm, * 13.8.1950, Kirindigala, Balangoda, Sri Lanka.

Geochemical, petrological and isotope studies related to the genesis of antimony deposits in the Eastern Alps with special reference to the deposit of Schlaining, Burgenland, Austria.

Ein.: 6.6.1989.

Ref. 1: Schroll. Ref. 2: Richter.

Pholiadis, Dimitrios, * 7.9.1948, Athen.

Beitrag zur Geochemie der Bleiberger Fazies der Carditaschiefer.

Ein.: 13.11.1984.

Ref. 1: Schroll. Ref. 2: Richter.

Reden, Günther, * 3.2.1955, Wien.

Beiträge zur Geologie, Geophysik und Geochemie der Gesteine und Mineralisationen im Gebiet der Goldvorkommen in den Hohen Tauern (Badgastein – Kolm Saigurn - Heiligenblut) mit besonderer Berücksichtigung der Gangmineralisationen.

Ein.: 16.7.1991.

Ref. 1: Schroll. Ref. 2: Richter.

Reinold, Paul, * 6.12.1933, Wien.

Beitrag zur Geochemie und Mineralogie der ostalpinen Salzlagerstätten.

Ein.: 25.6.1965. Prom.: 1.4.1966.

Ref. 1: Schroll. Ref. 2: Wieseneder.

Sauer, Dieter, * 5.1.1935, Wien.

Ein Beitrag zur Geochemie der Bauxite.

Ein.: 25.6.1965. Prom.: 1.4.1966.

Ref. 1: Schroll. Ref. 2: Wieseneder.

Technische Universität Wien

Pimminger, Michael

In situ Spuren- und Isotopenanalyse mit der Sekundärmassenspektrometrie.

Ref. 1: Grasserbauer. Ref. 2: Schroll.

Montanuniversität Leoben

Malekgasemi, Ferhard

Sulfidzerparagenesen in Eisenkarbonaten der Nördlichen Kalkalpen.

Ref. 1: Holzer. Ref. 2: Schroll.

Tabelle 2

Unter der Anleitung Schrolls verfasste Dissertationen, in denen Schroll auch namentlich als Referent angeführt wird (in alphabetischer Ordnung).

Ein.: Datum, an welchem die Dissertation zur Begutachtung eingereicht wurde. Prom.: Promotionsdatum. Ref. 1: / Ref. 2: Referenten (Begutachter) der jeweiligen Dissertation.

Universität Wien

Agiorgitis, Georgios, * 6.8.1941, Argos, Griechenland.

Beitrag zur Geochemie der Basalte.

Ein.: 31.5.1966. Prom.: 23.11.1966.

Ref. 1: Machatschki. Ref. 2: Wieseneder.

Grohmann, Helmut, * 28.6.1938, Prag.

Beitrag zur Geochemie granitoider Gesteine Österreichs.

Ein.: 21.5.1964. Prom.: 22.12.1964.

Ref. 1: Machatschki. Ref. 2: Wieseneder.

Janda, Ingeborg, * 11.3.1934, Wien.

Beitrag zur Geochemie des Graphites.

Ein.: 13.4.1959. Prom.: 19.12.1959.

Ref. 1: Machatschki. Ref. 2: Wieseneder.

Khalili, Hedayatollah Djahromi, * 27.11.1941, Djahrom, Iran.

Zur Geochemie der Pegmatite des Kärntner Altkristallins.

Ein.: 15.6.1967. Prom.: 2.2.1968.

Ref. 1: Machatschki. Ref. 2: Wieseneder.

Nazmy, Azer Ibrahim, * 14.8.1924, Kairo.

Beitrag zur geochemischen Analyse Ostalpiner Fahlerze.

Ein.: 27.9.1955. Prom.: 30.11.1955.

Ref. 1: Machatschki. Ref. 2: Leitmeier.

Rockenbauer, Wilfried, * 4.12.1928, Wien.

Spektrochemische Bestimmungen von Selen in ostalpinen Erzen. (Ein Beitrag zur Geochemie des Selen).

Ein.: 15.6.1956. Prom.: 20.12.1956.

Ref. 1: Machatschki. Ref. 2: Leitmeier.

Weninger, Manfred, * 9.4.1940, Liebing, Burgenland.

Beiträge zur Geochemie der Graphitlagerstätten der Grauwackenzone mit besonderer Berücksichtigung der Vorkommen von Kaisersberg und Sunk/Steiermark.

Ein.: 30.3.1966. Prom.: 30.6.1966.

Ref. 1: Machatschki. Ref. 2: Wieseneder.

Tabelle 3

Unter der Anleitung Schrolls verfasste Dissertationen, in denen Schroll nicht namentlich als Referent angeführt wird (in alphabetischer Ordnung). Legende wie in Tabelle 2.

Seit diesem Zeitpunkt kündigt er regelmäßig – bis zu jüngsten Zeitpunkt – einschlägige Lehrveranstaltungen an der Universität Wien an. Ein Beispiel aus dem Wintersemester 2001/02:

Technische Mineralogie und Petrographie I (LA-B+WL(alt); VO.; n.Ü., Inst. f. Mineralogie u. Kristallographie, UZA II-Geozentrum.

Neben seinen Lehrverpflichtungen (Lehraufträge unter anderem für Lagerstättenkunde, Geochemie und Erzmikroskopie) an der Universität Wien vertrat Schroll in den Jahren von 1977 bis 1998 in regelmäßigen Lehrveranstaltungen das Fach "Geochemie" auch an der Montanuniversität Leoben. Vom Studienjahr 1977/78 an war Schroll Mitglied der II. Diplomprüfungskommission für Montangeologie an dieser Universität. Mit dem Ersatz dieses Studium durch jenes der "Angewandten Geowissenschaften" ab dem Studienjahr 1993/94 schied er aus dieser Kommission aus. Zu erwähnen sind ferner Gastprofessuren am National Research Center in Kairo in den Jahren 1960 und 1962, sowie an der Universität von Assuan (Ägypten) im Jahre 1972.

Während seiner Tätigkeit als akademischer Lehrer betreute Schroll zweiundzwanzig Studentinnen und Studenten an der Universität Wien, der Technischen Universität Wien und der Montanuniversität Leoben bei der Ausarbeitung ihrer Dissertationen. In den Tabellen 2 und 3 sind diese Dissertantinnen und Dissertanten mit einigen persönlichen Daten unter Angabe von Titel und Begutachter der jeweiligen Dissertation wiedergegeben.

Erwähnenswert und hier angeführt sei noch die Ablehnung einer Berufung Schrolls nach Berlin.

Im Jahre 1977 wurde er im Zusammenhang mit der Ausschreibung des Postens eines Leiters des Institutes für Geochemische Lagerstättenforschung, betrieben von der Freien Universität Berlin in Zusammenarbeit mit dem Hahn-Meitner-Institut, zu einem Vortrag eingeladen, in dem er seine Vorstellungen über die geochemischen Parameter von hydrothermalen Lagerstätten darlegte. Im Rahmen eines Auswahlverfahrens wurde Schroll an erste Stelle gereiht und eine Berufung auf eine Professorenstelle (C4) ausgesprochen. Aufgrund einer Schlechterstellung, nicht nur bezüglich der Arbeitsmöglichkeiten, sondern auch in finanzieller Hinsicht, lehnte Schroll, zu diesem Zeitpunkt bereits Hofrat und Leiter des Geotechnischen Institutes, diese Berufung ab.

Das wissenschaftliche Werk

Bei einer Besprechung der einzelnen Veröffentlichungen Schrolls ist an erster Stelle die Verfassung eines ersten deutschsprachigen Lehrbuches "Analytische Geochemie" (in zwei Bänden) anzuführen, da dieses Werk die Entwicklung des Wissenschaftszweiges Geochemie vor allem in Österreich wesentlich beeinflusst hat (SCHROLL, 1975; 1976). Die Wertschätzung dieses Werkes kann am besten durch die Kommentare zweier Fachkollegen in Buchbesprechungen belegt werden.

WIEDEN (1975) wörtlich zu Band I (auszugsweise):

Wichtig erscheinen alle die praktischen Hinweise, die sich aus einer jahrzehntelangen Erfahrung des Autors, sowohl auf dem Gebiet der instrumentellen Untersuchung, als auch aus den durch die Forschungstätigkeit auf dem Gebiet der Geochemie erworbenen Erkenntnissen ergeben. Der rasche Fortschritt und vor allem die rasche Entwicklung der Untersuchungstechnik auf dem Gebiet der Erdwissenschaften setzen immer bessere Kenntnisse der physikalisch-chemischen Grundlagen voraus. So kann das Buch jedem auf dem Gebiet der Erdwissenschaften Arbeitenden, vor allem auch dem Studierenden mit Nachdruck empfohlen werden. Es stellt eine Bereicherung der Literatur auf dem Methodischen Gebiet dar, schließt eine Lücke, die sonst zwischen allgemeiner Chemie und geochemischer Methodik entstehen könnte.

ZEMANN (1976) wörtlich zu Band II (auszugsweise):

Im Abschnitt I findet man nach Ansicht des Referenten gelegentlich eine etwas unklare Ausdrucksweise, wobei man jedoch dem Autor zubilligen muß, daß eine präzise und leicht verständliche Präsentation des umfangreichen Stoffes auf dem knappen Raum sicher nicht leicht ist. Stärker beeindruckt ist der Referent vom Abschnitt II. Hier bringt der Autor eine erstaunliche Fülle an Material und erleichtert mit (geschätzt) ca. 1300 Zitaten sehr den Zugang zur weit verstreuten Originalliteratur.

Als Lehrbuch für Anfänger ist das vorliegende Werk wahrscheinlich weniger geeignet. Vorgeschnittene Studenten der Geochemie und Forscher auf dem Gebiet der Erdwissenschaften können jedoch daraus viele sehr interessante Informationen entnehmen; damit hat E. SCHROLL für seine Kollegen nützliche Arbeit geleistet.

In zeitlicher Reihung sei die Mitarbeit von Schroll bei dem von einer Arbeitsgemeinschaft – VOEST-ALPINE / Bundesversuchs- und Forschungsanstalt Arsenal / Geologische Bundesanstalt - erstellten Werkes "Geochemischer Atlas der Republik Österreich" anzuführen, in dem er als verantwortlicher Autor mitgewirkt hat (THALMANN et al. 1989).

Ferner sei erwähnt, dass im "Handbuch der Lagerstätten der Erze, Industriemineralien und Energierohstoffe" (1997) Schroll u. a. den Abschnitt V: Geochemische und geochronologische Daten und Erläuterungen, sowie Beiträge zur Beschreibung von siebzehn Erzbezirken, vom Rechnitzer Fenster bis zum Evaporitbezirk Montafon, verfasst hat.

Das Arbeitspensum fand seinen Niederschlag in 244 Veröffentlichungen, von denen etwa ein Drittel von Schroll als Einzelautor verfasst worden sind. An dieser Stelle sei vermerkt, dass der Jubilar nur in jenen Arbeiten als Autor aufscheint, zu welchen er auch einen erheblichen Teil zum Gelingen beigetragen hat. Der heutzutage praktizierten arroganten Gepflogenheit von leitenden Wissenschaftlern, dass in allen von den Mitarbeitern in ihren Abteilungen erarbeiteten Veröffentlichungen auch ihr Name unter den Autoren angeführt werden muss, ohne dass sie einen Beitrag geleistet haben, stand Schroll stets ablehnend gegenüber.

Ein Resümee: Schrolls langfristige Forschungsziele und daraus resultierende Veröffentlichungen können rückblickend, mehr oder weniger willkürlich, neun Wissensgebieten zugeordnet werden, die ihrerseits unter den übergeordneten Begriff "Geochemie" fallen. Auch die zahlreichen Beiträge zur chemischen Analytik betrafen vornehmlich geologisches Material.

1. Allgemeine Themen:

Geochemische Charakterisierung hydrothermaler Lagerstätten

Geochemische Charakterisierung von Mineralen und Erzen

Geochemie "Seltene Elemente"

Isotopengeochemie und Lithochemie

Sedimentäre Mineralbildungen

2. Spezielle Themen:

Metallogenese der Ostalpen

Geochemische Untersuchungen zur Lagerstätte Bleiberg-Kreuth in Kärnten

Buntmetallagerstätten in der alpinen Trias

3. Chemische Analytik:

Atomemissions-Spektralanalytik und Multielementanalytik.

Darüber hinaus veröffentlichte Schroll zahlreiche Arbeiten, die einem weit gespannten Themenkreis zuzuordnen sind. Hervorzuheben sind vor allem Beiträge zur angewandten Geochemie, die von der Archäometrie bis zur Umweltgeochemie und Geomedizin reichen. Umweltrelevante geochemische Arbeiten gaben Anstöße zur Untersuchung von Stäuben, Niederschlägen und Wässern, wie eine Studie der Umweltbelastung in der Großstadt Wien im Vergleich zur ländlichen Umgebung oder die erste geochemische Untersuchung des Donauwassers in Österreich.

Die wissenschaftliche Laufbahn Schrolls begann zu einer Zeit, als sich bereits der Wandel der geologischen Wissenschaft von dogmatischer Aussage zur Anwendung exakter Methodik und Denkweise abzeichnete. Schroll erkannte diese Zeichen und versuchte stets, das geologische Erscheinungsbild durch geochemische Daten zu ergänzen, um auf diese Weise zu einer der Natur entsprechenden Deutung beizutragen. Eine Zusammenstellung seiner wissenschaftlichen Veröffentlichungen ist in einem Anhang unter "Schriftenverzeichnis von Erich Schroll" zu finden.

Mitgliedschaften bei in- und ausländischen Vereinigungen

Die eigene Weiterbildung aber auch das Vermitteln von selbst erarbeiteten neuen Erkenntnissen sah und sieht Schroll als eine der Hauptaufgaben eines Universitätslehrers und Wissenschafters an. Aus diesem Grund war er auch stets um internationale Kontakte bemüht. Ein Spiegelbild dieser Bestrebungen ist die große Anzahl von Vereinigungen, deren Mitglied er ist. In willkürlicher Reihung seien diese Vereinigungen im Folgenden aufgezählt:

Österreichische Mineralogische Gesellschaft
Österreichische Geologische Gesellschaft
Gesellschaft Österreichischer Chemiker
Bergmännische Vereinigung
Naturwissenschaftlicher Verein für die Steiermark
Naturwissenschaftlicher Verein für Kärnten
Deutsche Mineralogische Gesellschaft (einschl. Sektion Geochemie und Archäometrie)
Schweizerische Mineralogische und Petrographische Gesellschaft
Society for Geology Applied to Mineral Deposits (SGA)
Society of Economic Geologists (SEG)
International Association on the Genesis of Ore Deposits (JAGOD)
The Geochemical Society
Academia Scientiarum et Artium Europea
Vorstandsmitglied und wissenschaftlicher Beirat der Geoschule Payerbach.

Mitgliedschaft bei der Österreichischen Mineralogischen Gesellschaft

Erich Schroll wurde am 13.11.1948 als studentisches Mitglied in diesen Verein aufgenommen. Teile seiner Dissertation, an der philosophischen Fakultät der Universität Wien am 11.5.1950 eingereicht, sowie Teile seiner Habilitationsschrift wurden in der Folge als Sonderhefte (im Eigenverlag des Vereines) den Mitgliedern vorgestellt:

Dissertation: *Über die Minerale und Spurenelemente, Vererzung und Entstehung der Blei-Zink-Lagerstätte Bleiberg-Kreuth / Kärnten in Österreich. (Sonderheft 2, 1953).*

Habilitation: *Ein Beitrag zur geochemischen Analyse ostalpiner Blei-Zink-Erze. (Sonderheft 3, 1954).*

In den Vereinsjahren von 1961 bis 1992 war Schroll im Vorstand des Vereines tätig und bekleidete von 1965 bis 1968 das Amt des Vorsitzenden (Präsidenten), 1974 jenes des zweiten Vorsitzenden. In der Hauptversammlung vom 12.1.2004 wurde ihm der Titel eines Ehrenmitgliedes verliehen. Antragsteller waren die Vereinsmitglieder Franz Pertlik und Ekkehart Tillmanns.

Auszeichnungen und Ehrungen

Die Forschung und die Lehre, im Zusammenwirken mit den Hohen Schulen in Leoben und Wien, sowie das Engagement beim Auf- und Ausbau des Geotechnischen Institutes der Bundesversuchs- und Forschungsanstalt Arsenal fand und findet Anerkennung in einer Reihe von Ehrungen für Erich Schroll. Es sind dies folgende (in chronologischer Reihenfolge):

- 1960 *Förderpreis der Theodor Körner Stiftung.*
 1975 *Großes Ehrenzeichen für Verdienste um die Republik Österreich (23.4.1975).*
 1985 *Korrespondierendes Mitglied der Geologischen Bundesanstalt (25.11.1985).*
 1986 *Ehrenpräsident der Austrian Cooperative Research (ACR), deren Geschäftsführer er in den vorangegangenen Jahren war (2.12.1986).*
 1990 *Ehrenkreuz für Wissenschaft und Kunst I. Klasse (5.10.1990).*
 2000 *Erneuerung des Doktordiploms der Universität Wien (2.5.2000).*
 2004 *Ehrenmitglied der Österreichischen Mineralogischen Gesellschaft (12.1.2004).*

Glückwünsche

Wenn daher im Jahre 2003 dem von seinen Kollegen und Mitarbeitern hochgeschätzten Wirklichen Hofrat und Universitätsprofessor Erich Schroll zur Vollendung seines achtzigsten Lebensjahres die aufrichtigsten und herzlichsten Glückwünsche überbracht wurden, so geschah dies nicht nur aus reiner Höflichkeit. Es geschah vielmehr aus Hochachtung, da die Erdwissenschaften, und hier im Speziellen die Geochemie, durch seine herausragenden Arbeiten auf diesem Gebiet eine ganz besondere Förderung und Bereicherung erfahren haben.

Seine Kollegen und Mitarbeiter hoffen und wünschen, dass sich der großen Anzahl seiner wissenschaftlichen Arbeiten noch viele weitere anschließen mögen, nicht nur zur Förderung der Wissenschaft, sondern – auf Grund seiner ungebrochenen Freude an wissenschaftlicher Arbeit – auch zur eigenen persönlichen Erbauung des Jubilars. Er möge aus den vorstehenden kurzen Ausführungen entnehmen, welche große Wertschätzung sein bisheriges Wirken gefunden hat.

Dank

Für die Hilfe bei der Erfassung von Fakten und Daten erlauben sich die Autoren folgenden Personen ihren herzlichsten Dank auszusprechen: DDr. Dieter Sauer (Wien) und Univ. Prof. MR Dr. Leopold Weber (Wien), sowie den Professoren der Universität Wien Dr. Friedrich Koller, Dr. Hermann Reichert und Dr. Josef Zemann. Besonders aber sei dem Jubilar selbst für die Überlassung persönlicher Fakten und Daten gedankt.

Literatur und Quellenverzeichnis

- ARSENAL 2000. Bundesversuchs- und Forschungsanstalt Arsenal. Anlässlich des 40-Jahr-Jubiläums. Hrsg.: Erich Schroll. © 1990 Metrica Fachverlag, Ing. Werner H. Bartak, Wien.
- BUSEK, E. (1990): Zum Geleit. Vorwort des Bundesministers für Wissenschaft und Forschung. - In: Arsenal 2000. Bundesversuchs- und Forschungsanstalt Arsenal. Anlässlich des 40-Jahr-Jubiläums. - Hrsg.: Erich Schroll. © 1990 Metrica Fachverlag, Ing. Werner H. Bartak, Wien.
- CERNY, I. (1983): Herm Prof. Dr. Erich Schroll zum 60. Geburtstag. - Mitt. Ges. Geol. Bergbaustud. Österr. 29, V-VI.
- HAGENGUTH, G. (1983): Verzeichnis der wissenschaftlichen Arbeiten von E. Schroll. - Mitt. Ges. Geol. Bergbaustud. Österr. 29, IX-XVIII.

- Handbuch der Lagerstätten der Erze, Industriemineralien und Energierohstoffe Österreichs (1997). - Hrsg. Leopold Weber. Archiv für Lagerstättenforschung 19, Geologische Bundesanstalt Wien, im Eigenverlag.
- SCHROLL, E. (1949): Wulfenite von Nassereith/Dirsentritt (Tirol) und Bleiberg (Kärnten). - *Tschermaks Min. Petr. Mitt.* 1, 325-341.
- SCHROLL, E. (1950): Beiträge zur Geochemie und Genesis der Blei- und Zinklagerstätte Bleiberg - Kreuth/Kärnten. - Diss. phil. Fak. Universität Wien.
- SCHROLL, E. (1953): Über Minerale und Spurenelemente, Vererzung und Entstehung der Blei-Zink-Lagerstätte Bleiberg-Kreuth/Kärnten in Österreich. - *Mitt. Österr. Miner. Ges., Sonderheft 2.*
- SCHROLL, E. (1954): Ein Beitrag zur geochemischen Analyse ostalpiner Blei-Zink-Erze. Teil 1. - *Mitt. Österr. Miner. Ges., Sonderheft 3.*
- SCHROLL, E. (1955): Über das Vorkommen einiger Spurenmetalle in Blei-Zink-Erzen der ostalpinen Metallprovinz. - *Tschermaks Min. Petr. Mitt.* 5, 183-208.
- SCHROLL, E. (1975): Analytische Geochemie, Band I: Methodik. - Mit 96 Abb. u. 56 Tab., 292 S. Stuttgart: Ferdinand Enke Verlag.
- SCHROLL, E. (1976): Analytische Geochemie, Band II: Grundlagen und Anwendungen. - Mit 126 Abb. u. 79 Tab., 374 S. Stuttgart: Ferdinand Enke Verlag.
- SCHROLL, E. & PERTLIK, F. (2001): Herbert Eduard Haberlandt: Ein Pionier der Geochemie in Österreich. (* 3.6.1904 Mödling † 9.6.1970 Wien). (Eine Biographie mit Schriftenverzeichnis). - *Mitt. Österr. Miner. Ges.* 146, 435-447.
- WALTHER VON DER VOGELWEIDE: Der Bogener-Ton. - In: Die politischen Lieder Walthers von der Vogelweide (Hrsg.: F. Maurer) 100-102. Max Niemeyer Verlag Tübingen 1972.
- WEBER, L. (2003): Würdigung, Erich Schroll 80 Jahre. - *Berg- u. Hüttenm. Mh., Jg.* 2003, 511.
- THALMANN, F., SCHERMANN, O., SCHROLL, E. & HAUSBERGER, G. (1989): Geochemischer Atlas der Republik Österreich. Böhmisches Mass und Zentralzone der Ostalpen. Textteil. - Geologische Bundesanstalt Wien, im Eigenverlag.
- WIEDEN, P. (1975): In "Buchbesprechungen" *Mitt. Österr. Geol. Ges.* 68, 236.
- ZEMANN, J. (1976): In "Buchbesprechungen" *Mitt. Österr. Geol. Ges.* 69, 387.

Schriftenverzeichnis von Erich Schroll

1949

- Wulfenite von Nassereith/Dirsentritt (Tirol) und Bleiberg (Kärnten). - *Tschermaks Min. Petr. Mitt.* 1, 325-341.
- Über die Anreicherung von Mo und V in der Hutzone der Pb-Zn-Lagerstätte Bleiberg-Kreuth in Kärnten. - *Verh. Geol. B.-A., Jg.* 1949, 138-157.

1950

- Spurenelementparagenese (Mikroparagenese) ostalpiner Zinkblenden. - *Österr. Akad. Wiss., Math.-naturwiss. Kl., Anzeiger* 87, 21-25.
- Beiträge zur Geochemie und Genesis der Blei- und Zinklagerstätte Bleiberg-Kreuth/ Kärnten. - Diss. phil. Fak. Univ. Wien.
- H. Haberlandt & E. Schroll: Färbung und Fluoreszenz des Wulfenits im Zusammenhang mit dem Gehalt an Chrom und anderen Spurenelementen. - *Experientia* 6, 89-91.
- H. Haberlandt & E. Schroll: Lumineszierende Anwachszone in der Zinkblende von Bleiberg-Kreuth (Kärnten, Österreich). - *Experientia* 6, 91-92.

1951

Spurenelementparagenese (Mikroparagenese) ostalpiner Bleiglanze. - Österr. Akad. Wiss., Math.-naturwiss. Kl., Anzeiger 88, 6-12.

1953

Über Unterschiede im Spurengehalt bei Wurtziten, Schalenblenden und Zinkblenden. - Sitzungsber. Österr. Akad. Wiss. Wien, Math.-naturwiss. Kl., 162, 305-332.

Über Minerale und Spurenelemente, Vererzung und Entstehung der Blei-Zink-Lagerstätte Bleiberg-Kreuth/Kärnten in Österreich. - Mitt. Österr. Miner. Ges. Sonderheft 2.

Mineralparagenese und Mineralisation der Bleiberg-Kreuther Blei-Zink-Lagerstätte. - Carinthia II 143/63. (Gesteine, Erze- und Minerallagerstätten Kärntens). 47-55.

1954

Bemerkungen zur "alpinen Metallogene" der kalkalpinen Blei-Zink-Lagerstätten. - Tschermaks Min. Petr. Mitt. 5, 96-98.

Ein Beitrag zur geochemischen Analyse ostalpiner Blei-Zink-Erze. Teil 1. - Mitt. Österr. Miner. Ges. Sonderheft 3. H. Haberlandt & E. Schroll: Über den Wert oder Unwert der Spurenelement-Analyse für die Lagerstättenforschung, Mineralogenese und Petrogenese. - Tschermaks Min. Petr. Mitt. 5, 110-122.

1955

Über das Vorkommen einiger Spurenmetalle in Blei-Zink-Erzen der ostalpinen Metallprovinz. - Tschermaks Min. Petr. Mitt. 5, 183-208.

W. Rockenbauer & E. Schroll: Ein empfindlicher spektrochemischer Nachweis von Selen in Erzen. - Österr. Akad. Wiss., Math.-naturwiss. Kl., Anzeiger 92, 192-196.

1956

Aufgaben und Bedeutung der Geochemie. - Praschu (Praktische Schule), Z. naturwiss. Experimentalunterricht 32, 33-35 und 53-55 (München).

W. Rockenbauer & E. Schroll: Spektrochemische Selenbestimmung in Kieserzen. - Coll. Spectr. Int. VI (Amsterdam), 338-341.

1958

Über das Barytvorkommen von Oberzeiring (Steiermark). - Österr. Akad. Wiss., Math.-naturwiss. Kl., Anzeiger 95, 30-31.

Ein neuer Fund von Beryll im Waldviertel. - Kultur Nachrichten aus NÖ 11, 86.

Die ostalpine Vererzung im Lichte der geochemischen Forschung. - Tschermaks Min. Petr. Mitt. 6, 409-411.

Das Aufsuchen von Erzlagerstätten mit Hilfe geochemischer Methoden. - Tschermaks Min. Petr. Mitt. 6, 429-432.

M. Brandenstein & E. Schroll: Spektralanalytische Untersuchungen von Bleifunden aus Kärntner Ausgrabungen. - Archaeologica Austriaca 1958, 116-120.

E. Schroll & I. Janda: Emissionsspektrographische Nachweismethode leichtflüchtiger Spurenelemente in Graphit- und Kohlengesteinen. - Österr. Akad. Wiss., Math.-naturwiss. Kl., Anzeiger 95, 19-22.

1959

Germanium in mineralogischen Rohstoffen Österreichs (Forschungsbericht 1. - Das Vorkommen seltener Grundstoffe in Österreich). - Montan-Rundschau 7, 23-26.

Zur Geochemie und Genese der Wässer des Neusiedler Seegebietes. - Wiss. Arbeiten a. d. Burgenland 23, 55-64. Geochemical Activities in Austria. - Geochemical News 1959, 3.

I. Janda & E. Schroll: Über Quecksilberspuren in Graphiten. - Experientia, 15, 125-126.

E. Schroll & N. Azer Ibrahim: Beitrag zur Kenntnis ostalpiner Fahlerze. - Tschermaks Min. Petr. Mitt. 7, 70-105.

I. Janda & E. Schroll: Über Borgehalte in einigen ostalpinen Kohlen und anderen Biolithen. - Tschermaks Min. Petr. Mitt. 7, 118-129.

I. Janda & E. Schroll: Emissionsspektrographische Doppelbogenanalyse leichtflüchtiger Spurenelemente in Graphiten. - Mikrochimica Acta 1959, 389-401.

E. Schroll, M. Brandenstein & I. Janda: Spektralanalytische Bestimmung des Bors als leichtflüchtiges Element in Graphiten. - Österr. Akad. Wiss., Math.-naturwiss. Kl., Anzeiger 96, 60-64.

M. R. Zaki & E. Schroll: Spektrochemische Spurenanalyse auf Seltene Erden in Schwerspäten. - Österr. Akad. Wiss., Math.-naturwiss. Kl., Anzeiger 96, 162-165.

E. Schroll, M. Brandenstein, I. Janda & W. Rockenbauer: Emissionsspektrographische Spurenanalyse mit der Doppelbogenmethode. - Coll. Spect. Int. VIII, 145-149.

1960

Strontianit aus Bleiberg (Kärnten). - Carinthia II 150./70. 39-42.

M. Brandenstein & E. Schroll: Borgehalte in Magnesiten. - Radex-Rundschau 1960, 150-158.

M. Brandenstein, I. Janda & E. Schroll: Emissionsspektrographische Methode zur Bestimmung geringster Borgehalte in Reaktorgraphiten. - Mikrochimica Acta 1960, 935-945.

M. Brandenstein, I. Janda & E. Schroll: Seltene Elemente in österreichischen Kohlen- und Bitumengesteinen. - Tscherma's Min. Petr. Mitt. 7, 260-285.

E. Schroll & P. Wieden: Eine rezente Bildung von Dolomit im Schlamm des Neusiedler Sees. - Tscherma's Min. Petr. Mitt. 7, 286-289.

I. Janda & E. Schroll: Geochemische Untersuchungen an Graphitgesteinen. - Geochem. Cycles, Internat. Geol. Congress 40-53 (Copenhagen).

W. Rockenbauer & E. Schroll: Das Vorkommen von Selen in österreichischen Erzen. - Montan-Rundschau 1960, 48-52.

1961

Kieserzlagertstätten auf Chalkidike, Kassandra und Eisenmanganerzlagertstätten bei Kavalla. - Tscherma's Min. Petr. Mitt. 7, 483-484.

Seltene Elemente in biogenen Sedimenten. - Tscherma's Min. Petr. Mitt. 7, 488-490.

Gallium im Erdöl. - Österr. Akad. Wiss., Math.-naturwiss. Kl., Anzeiger 98, 105-106.

Über das Vorkommen von Magnesit in alpinen Salzlagertstätten. - Radex-Rundschau 1961, 704-707.

Das Chemische Laboratorium der Bundesversuchs- und Forschungsanstalt Arsenal Wien als Forschungsstelle für angewandte Geochemie und Mineralogie. - Montan-Rundschau 9, 281-283.

N. Grögler, M. Grünfelder & E. Schroll: Bleiisotopenhäufigkeiten in Bleiglanzen der Ostalpen. - Österr. Akad. Wiss., Math.-naturwiss. Kl., Anzeiger 98, 106-111.

1962

P. Reinold & E. Schroll: Spektrographischer Nachweis von Jod im Kohlebogen. - Z. analyt. Chemie 190, 410-413.

Spektrochemische und mineralogische Untersuchung von Farben römischer Fresken aus Carnuntum. - Carnuntum Jb., 1961/62, 22-24. Böhlau: Graz-Köln.

1963

Geochemie der Wässer des Neusiedlerseegebietes. - Tscherma's Min. Petr. Mitt. 8, 631-632.

Über die Anwendung thermochemischer Reaktionen in der emissions-spektrographischen Spurenanalyse und ihre Bedeutung für den Carriereffekt. - Z. analyt. Chemie 198, 40-55.

I. Janda, I. Schausberger & E. Schroll: Beitrag zur emissionspektrographischen Spurenanalyse in Uranoxyd. - Mikrochimica Acta 1963, 122-130.

E. Schroll, I. Janda, I. Schausberger & H. Spatzek: Eine Methode zur Spurenanalyse von Titan und Vanadin in graphitischen Materialien. - Mikrochimica Acta 1963, 1126-1131.

E. Schroll, E. Skol & E. Stepan: Zur Röntgenfluoreszenzanalyse schwerer Spurenelemente in leichter Matrix unter Verwendung der Röhrenhauptlinien als internen Standard. - Österr. Akad. Wiss., Math.-naturwiss. Kl., Anzeiger 100, 149-153.

1964

Advanced studies on single binary and ternary systems of oxides with halogenides (fluorides, chlorides etc.) sulfates, carbonates, nitrates in respect to the formation of refractory compounds and volatile phases and to the application in spectrochemical distillation-methods. - Final Technical Report, US Research Bureau, Contract No 91-591-EUC-2830, 01-360464-B.

E. Schroll & H. Grohmann: Seltene Elemente in granitoiden Gesteinen des Waldviertels und der Ostalpen. - Fortschr. Miner. 41, 183.

E. Schroll & P. Hauk: Eine emissionsspektrographische Methode zur Bestimmung der inneren Oberfläche und von Korngrößen an pulverigen Substanzen hoher Temperaturbeständigkeit. - Mikrochimica Acta 1964, 731-739.

E. Schroll & D. Sauer: Beitrag zur Geochemie der Bauxite. - Symposium sur les bauxites, oxydes et hydroxydes d'aluminium, Teil 1, 201-225 (Zagreb).

E. Schroll & E. Stepan: Eine Methode zur Bestimmung des Wassergehaltes auf röntgenfluoreszenzanalytischem Wege. - Österr. Akad. Wiss., Math.-naturwiss. Kl., Anzeiger 101, 226-227.

1965

Die analytischen Möglichkeiten der Anwendung thermochemischer Reaktionen in der emissionsspektrographischen Bogenmethode. - Rozprawy narod. techn. musea v. praze Emisni spektralni analyze III, 15, 7-14 (Praha).

Zur Geochemie der Halogene in Wässern des Neusiedlerseegebietes und anderer mineralisierter Wässer des Burgenlandes (Ein Zwischenbericht). - Wiss. Arbeiten a. d. Burgenland 30, 109-124.

Anomalous composition of lead isotopes in the lead-zinc deposits of calcareous alps sediments. - Rudarsko-Metalurski Zbornik 2, 139-154 (Ljubljana).

E. Jäger, M. Grünenfelder, N. Grögler & E. Schroll: Mineralalter granitischer Gesteine aus dem österreichischen Moldanubikum (Weinsberger und Mauthausner Granit). - Tschermaks Min. Petr. Mitt. 10, 528-534.

I. Janda, E. Schroll & M. Sedlazeck: Zum Problem der geochemischen Unterscheidung von Para- und Orthoamphiboliten am Beispiel einiger Vorkommen des Waldviertels und der Ostalpen. - Tschermaks Min. Petr. Mitt. 10, 552-572.

E. Schroll, E. Stepan, W. Geymayer & H. Horn: Der "Protocalcit" von Gumpoldskirchen (Niederösterreich). - Tschermaks Min. Petr. Mitt. 10, 573-585.

N. Grögler, M. Grünenfelder & E. Schroll: Ein Hinweis auf Jungpräkambrium und Altpaläozoikum im Altkristallin Kärntens. - Tschermaks Min. Petr. Mitt. 10, 586-594.

E. Schroll & H. Grohmann: Beitrag zur Kenntnis des K/Rb-Verhältnisses in magmatischen Gesteinen. - Geol. Rundschau 55, 261-274.

E. Schroll, A. F. Tauber & P. Wieden: Nördliches und mittleres Burgenland (Exkursion A/II). - Fortschr. Miner. 42, 119-131.

E. Schroll & M. Weninger: Eine empfindliche spektrochemische Analysenmethode zur Bestimmung von Germanium und Zinn unter Verwendung sulfidierender thermochemischer Reagenzien. - Mikrochimica Acta 1965, 378-385.

1966

Zur Geochemie der seltenen Elemente in granitoiden Gesteinen. - Tschermaks Min. Petr. Mitt. 11, 317-347.

H. Grohmann & E. Schroll: Zur Frage der Abhängigkeit der Konzentrationen seltener Elemente von der Altersfolge der granitoiden Gesteine der südlichen Böhmisches Masse. - Tschermaks Min. Petr. Mitt. 11, 348-357.

E. Schroll & D. Sauer: Use of large graphite beakers in double-arc analysis. - Applied Spectroscopy 20, 404-407.

1967

Die Entstehung der chemischen Elemente und ihre geochemischen Verteilungsgesetzmäßigkeiten. - Schrift. d. Ver. z. Verbreit. Naturwiss. Kenntnisse Wien 107, 41-78.

Über die Bedeutung und Anwendung thermochemischer Reaktionen bei der spektrochemischen Bogenanalyse. - Coll. Spectr. Int. XIV (Debrecen), 397-434.

- Spektrochemische Analyse mit Riesenelektroden. - Coll. Spectr. Int. XIV (Debrecen) 911-915.
- Über den Wert geochemischer Analysen bei stratigraphischen und lithologischen Untersuchungen von Sediment-Gesteinen am Beispiel ausgewählter Profile der ostalpinen Trias. - Geol. Sbornik 18, 315-330.
- I. Huber-Schausberger & E. Schroll: UV-Lumineszenz und Seltenerdgehalte in Flussspaten. - Geochim. Cosmochim. Acta 31, 1333-1341.
- V. Rajner, E. Schroll & E. Stepan: Tritiummessungen von heißen Wässern am Strand der Insel Vulcano (Liparische Inseln). - Österr. Akad. Wiss., Math.-naturwiss. Kl., Anzeiger 104, 58-60.
- E. Schroll & P. Hauk: Zinnstein aus dem Pegmatit vom Lieserrain bei Spittal an der Drau, Kärnten. - Miner. Mitt. Joanneum 1967, 99-103.
- E. Schroll, V. Rajner & O. Zellhofer: Über radiophysikalische Altersdatierung des Grundwassers. - Österr. Wasserwirtschaft (Wien) 19, 8-15.
- E. Schroll & E. Stepan: Bestimmung des Massenschwächungskoeffizienten in der Fluoreszenz- und Diffraktionsanalyse. - Österr. Akad. Wiss., Math.-naturwiss. Kl., Anzeiger 104, 60-63.
- E. Schroll & E. Stepan: Zur quantitativen Röntgenfluoreszenzanalyse schwerer Mikroelemente in variabler-leichter Matrix. - Acta Geol. Geogr. Univ. Comenia 15, 267-277.
- Das Grundlageninstitut der Bundesversuchs- und Forschungsanstalt Arsenal. – Maschinenwelt-Elektrotechnik 9, 279.
- 1968**
- Zur radiophysikalischen Altersbestimmung des Grundwassers. - Gas/Wasser/Wärme 22, 211-215.
- Abundances of the chemical elements in the main rock types of the lithosphere in relation to a system of correlations. - In: Origin and distribution of the elements (L. H. Ahrens ed.). 599-617. Pergamon Press: Oxford-New York.
- E. Schroll, I. Huber-Schausberger, I. Janda & H. Spatzek: Extreme spektrochemische Spurenanalyse von Reinstgraphit auf Titan und Vanadin. - Mikrochimica Acta 1968, 649-659.
- E. Schroll & D. Sauer: Beitrag zur Geochemie von Titan, Chrom, Nickel, Cobalt, Vanadin und Molybdän in bauxitischen Gesteinen und das Problem der stofflichen Herkunft des Aluminiums - Travaux du Comité Inter. pour l'étude des Bauxites, des Oxydes et des Hydroxydes d'Aluminium, Acad. Yougoslave Sc. Arts 5, 83-96 (Zagreb).
- E. Schroll & E. Stepan: Beitrag zur quantitativen Analyse von Mineralphasen mittels Röntgendiffraktion. - Tschermarks Min. Petr. Mitt. 12, 392-402.
- 1969**
- E. Schroll & E. Stepan: Zur Röntgenfluoreszenzanalyse geologischer Materials. - Tschermarks Min. Petr. Mitt. 13, 131-147.
- Exkursion in die Wüste Ägyptens. - Tschermarks Min. Petr. Mitt. 13, 308-310.
- Altersbestimmung an Wässern. - Tschermarks Min. Petr. Mitt. 13, 345-346.
- Anwendung der Röntgenfluoreszenzanalyse auf die Bestimmung geringer Konzentrationen in geologischem Material. - Symposium o Metódach Stanovenia Nizkych Koncentracii Prvkov v Nerastnych Surovinach, Smolenice 1969, 235-252.
- P. Wieden & E. Schroll: Untersuchungen von Referenzproben mineralischer Rohstoffe im Rahmen eines Programms der OECD-Mineralforschung. - Montan-Rundschau 1969, 88-89.
- 1970**
- I. Huber-Schausberger, I. Janda, P. Dolezel & E. Schroll: Chemische und spektrochemische Analyse internationaler Referenzgesteinsproben. - Tschermarks Min. Petr. Mitt. 14, 195-211.
- G. Agiorgitis, E. Schroll & E. Stepan: K/Rb-, Ca/Sr- und K/Ti-Verhältnisse in basaltoiden Gesteinen der Ostalpen und benachbarter Gebiete. - Tschermarks Min. Petr. Mitt. 14, 285-309.
- E. Schroll & H. Krachsberger: Untersuchungen zur Geochemie der Verunreinigungen in atmosphärischen Niederschlägen im Stadtgebiet von Wien. - Radex-Rundschau 1970, 331-341.
- E. Stepan & E. Schroll: Memorial to Felix Machatschki. - Geol. Soc. Amer. Ass. 7, Tulsa.

Bericht über Aktivitäten des Grundlageninstitutes der Bundesversuchs- und Forschungsanstalt Arseal in Wien im Arbeitsbereich Steine und Erden in den Jahren 1968 und 1969. - Montan-Rundschau 1970, 91-93.

1971

Beitrag zur Geochemie des Bariums in Carbonatgesteinen und klastischen Sedimenten der ostalpinen Trias. - Tschermaks Min. Petr. Mitt. 15, 258-278.

E. Schroll & P. Dolezel: Über den Berylliumgehalt in Staubniederschlägen der Wiener Stadtatmosphäre. - Österr. Akad. Wiss., Math.-naturwiss. Kl., Anzeiger 108, 148-149.

Jahresbericht des Grundlageninstitutes 1970. - Montan-Rundschau 1971, 154-157.

1972

L. A. Cardich-Loarte & E. Schroll: Zur Geochemie des Strontiums in den Blei-Zink-Erzmineralisationen vom Typ Bleiberg-Kreuth und die Beziehung zur Erzgenese. - 2nd Inter. Sym. Miner. Dep. of the Alps, Geologija 15, 337-342 (Ljubljana).

P. Dolezel & E. Schroll: Zur Geochemie der ostalpinen Siderite. - 2nd Inter. Symp. Miner. Dep. of the Alps, Geologija 15, 343-359 (Ljubljana).

I. Janda & E. Schroll: Zur spektrochemischen Spurenanalyse von Bleimetall im Gleichstromabreißbogen. - Mikrochimica Acta 1972, 902-907.

E. Schroll & K. H. Wedepohl: Schwefelisotopenuntersuchungen an einigen Sulfid- und Sulfatmineralen der Blei-Zink-Erzlagerstätte Bleiberg / Kreuth, Kärnten. - Tschermaks Min. Petr. Mitt. 17, 286-290.

Jahresbericht des Grundlageninstitutes 1971. - Montan-Rundschau 1972, 330-333.

1973

L. Cardich-Loarte & E. Schroll: Die Verteilung und Korrelation einiger Elemente in einem Erzalkalprofil der Bleiberger Fazies (Bleiberg/Kärnten - Rudolfschacht). - Tschermaks Min. Petr. Mitt. 20, 59-70.

Beitrag zur Hydrogeochemie des Donauwassers in Österreich - Tschermaks Min. Petr. Mitt. 20, 240-246.

H. Puchelt, H. H. Schock & E. Schroll: Rezente marine Eisenerze auf Santorin, Griechenland; I. Geochemie, Entstehung, Mineralogie. - Geol. Rundschau 62, 786-803.

Jahresbericht des Grundlageninstitutes 1972. - Montan-Rundschau 1973, 368-370.

Das Geotechnische Institut der Bundesversuchs- und Forschungsanstalt Arseal. - Österr. Ingenieur Zeitschrift 402-408.

1974

Seltenelementpegmatite in Nuristan/Afghanistan. - Mitt. Österr. Miner. Ges. 124, 3-5.

M. Rasmay & E. Schroll: Indium und Gallium in Zinkerzen aus Bleiberg-Kreuth. - Österr. Akad. Wiss., Math.-naturwiss. Kl., Anzeiger 111, 153-157.

1975

Analytische Geochemie, Bd. 1: Methodik. - Ferdinand Enke Verlag: Stuttgart.

Angewandte Geochemie. - Österr. Ingenieur Zeitschrift 429-431.

E. Z. Basta, A. M. El Kamar & E. Schroll: Rare earth elements distribution in some Egyptian phosphorites. - Rep. 2nd Anal. Conf. Miner. Resources, Cairo 1975.

E. Schroll, H. Krachsberger & P. Dolezel: Hydrogeochemische Untersuchung des Donauwassers in Österreich in den Jahren 1971 und 1972. - Arch. Hydrobiol./Suppl. (Donauforschung 5) 44, 492-514.

1976

Analytische Geochemie, Bd. 2: Grundlagen und Anwendungen.- Ferdinand Enke Verlag: Stuttgart.

E. Schroll & E. Pak: Die Schwefelisotopenzusammensetzung in Schwerspäten aus Lagerstätten im Grazer Paläozoikum als Beitrag zu deren Altersstellung. - Österr. Akad. Wiss., Math.-naturwiss. Kl., Anzeiger 113, 1-4.

E. Schroll & I. Janda: Über das Vorkommen von Wolfram in Gesteinen der Ostalpen und der Böhmisches Masse. - Österr. Akad. Wiss., Math.-naturwiss. Kl., Anzeiger 113, 4-10.

1977

Fortschritte der optischen Emissionsspektroskopie auf dem Gebiete der Analyse geologischen Materials. - Fortschr. Miner. 54, 167-191.

Umweltbelastung durch natürliche Schadstoffe. - Z. angew. Bäder- u. Klimaheilkunde 24, 240-244.

E. Schroll & I. Janda: Das Vorkommen von Molybdän in Gesteinen der Ostalpen und der Böhmisches Masse. - Österr. Akad. Wiss., Math.-naturwiss. Kl., Anzeiger 114, 203-209.

L. Brigo, L. Kostelka, P. Omenetto, H. J. Schneider, E. Schroll, O. Schulz & I. Štruel: Comparative reflections on four alpine Pb-Zn deposits. - In: Time- and Strata-Bound Ore Deposits (D. D. Klemm and H. J. Schneider eds.), 273-293. Springer: Berlin-Heidelberg-New York.

E. Schroll & H. Krachsberger: Beitrag zur Kenntnis des Chemismus der Porenwässer des Neusiedlerseeschlammes. - Biol. Forsch. Anst. Bgld., 24, 35-62 (Illmitz).

O. Schulz & E. Schroll: Die Pb-Zn-Lagerstätte Bleiberg-Kreuth. Stand der geowissenschaftlichen Forschung 1976, Projekte 2437, 2776 S. - Verh. Geol. B.-A., Jg. 1977, 375-386.

1978

Zur Korrelation geochemischer Charakteristika der Blei-Zink-Lagerstätte Bleiberg-Kreuth mit anderen schichtgebundenen Vererzungen in Karbonatgesteinen. - In: Ergebnisse der österreichischen Projekte des Internationalen Geologischen Korrelationsprogramms (IGCP) bis 1976 (H. Zapfe ed.). Österr. Akad. Wiss., Schriftenreihe Erdwiss. Kommiss. 3, Springer: Wien - New York.

Contribution to the mineralogy of the iron-rich mud sediments of Santorini, Greece. - In: Thera and the Aegean World I (G. Dumas ed.). 2nd Inter. Sc. Congress 333-342 (London).

E. Schroll & U. Eicher: Sauerstoff- und Kohlenstoffisotopenbestimmungen an einigen Kalksteinen und Kalziten aus der Blei-Zink-Lagerstätte Bleiberg-Kreuth/Kärnten. - Österr. Akad. Wiss., Math.-naturwiss. Kl., Anzeiger 115, 159-161.

1979

Trace elements in kaolinites and bauxites in relation to their genesis. - Travaux du Comité Inter. pour l'étude des Bauxites, de l'Alumine et de l'Aluminium, CMS-ICSOBA Conf., Kingston 1977, Acad. Yougoslave Sc. Arts, 15, 35-41 (Zagreb).

Beitrag der Geochemie zur Kenntnis der Lagerstätten der Ostalpen. - Verh. Geol. B.-A., Jg. 1978, 461-470.

Progress in the knowledge of indicator elements. - In: Origin and Distribution of the Elements (L. H. Ahrens ed.), 213-216. Pergamon Press: Oxford-New York.

Electron microscopic investigations of the mud sediments. - In: Neusiedlersee. The Limnology of a Shallow Lake in Central Europe (H. Löffler ed.), 145-149. Monographiae Biologiae: Boston- London.

Geochemical diagnostic features of lead-zinc ore deposits in carbonatic rocks. - JUGS-IGCP-Program No. 6, Alger 1979. Vortragsmanuskript: Bundesversuchs- und Forschungsanstalt Arsenal Wien.

P. Dolezel & E. Schroll: Beitrag zur Geochemie der Siderite in den Ostalpen. - Verh. Geol. B.-A., Jg. 1978, 293-299.

V. Köppel & E. Schroll: Bleiisotopenzusammensetzung von Bleierzten aus dem Mesozoikum der Ostalpen. - Verh. Geol. B.-A., Jg. 1978, 403-409.

D. Rank & E. Schroll: Test for the applicability of combined nuclear and geochemical methods in relation to the water balance of Lake Neusiedl, Austria. - In: Isotopes in Lake Studies 121-130. Inter. Atomic Energy Agency (Wien).

1980

I. Cerny, L. Kostelka, E. Schroll & O. Schulz: Buntmetalle in triassischen Sedimenten der Ostalpen. - Almanach '80 der österr. Forsch., 208-213 (Verb. wiss. Ges. Österreichs).

G. Niedermayr & E. Schroll: Beryllium in den Hohen Tauern. - Almanach '80 der österr. Forsch., 214-218. (Verb. wiss. Ges. Österreichs).

E. Pak, E. Schroll & L. Weber: Schwefelisotopenzusammensetzung der Pb-Zn-Vererzung des Grazer Paläozoikums

(Ostalpen). - Mineralium Deposita 15, 315-325.

E. Schroll & E. Pak: Schwefelisotopenzusammensetzung von Baryten aus den Ost- und Südalpen. - Tschermaks Min. Petr. Mitt. 27, 79-91.

1981

REM-Untersuchungen an Schalenblenden: Ein Beitrag zur As- und TI-Führung von Sphaleriten. - Fortschr. Miner. 59, 178-179.

E. Pak, E. Schroll & O. Schulz: Zur Schwefelisotopenzusammensetzung des Antimonits von Schlaining/Burgenland. - Österr. Akad. Wiss., Math.-naturwiss. Kl., Anzeiger 118, 21-23.

I. Cerny, E. Pak & E. Schroll: Schwefelisotopenzusammensetzung von Antimoniten und anderen Erzen aus Lagerstätten der Kreuzeckgruppe. - Österr. Akad. Wiss., Math.-naturwiss. Kl., Anzeiger 118, 161-163.

1982

I. Cerny, J. Scherer & E. Schroll: Blei-Zink-Verteilungsmodell in stillliegenden Blei-Zink-Revieren der Karawanken. - Arch. f. Lagerst.forsch. Geol. B.-A. 2, 15-22.

F. Kappel & E. Schroll: Ablauf und Bildungstemperatur der Blei-Zink-Vererzung von Bleiberg-Kreuth/Kärnten. - Carinthia II 172./92. 49-62.

D. Sauer & E. Schroll: Anwendung spektralchemischer Methoden bei der Großserienmultielementanalyse geologischen und verwandten Materials. - VII CANAS, Sopron 1982.

1983

Geochemical characterization of the Bleiberg type and other carbonate-hosted lead-zinc mineralizations. - In: Mineral Deposits of the Alps and of the Alpine Epoch in Europe (J. H. Schneider ed.). 189-197. Springer: Berlin.

E. Schroll & E. Pak: Sulfur isotope investigations of ore mineralizations of the Eastern Alps. - In: Mineral Deposits of the Alps and of the Alpine Epoch in Europe (J. H. Schneider ed.). 169-175. Springer: Berlin, Heidelberg.

G. Niedermayr & E. Schroll: The tungsten distribution in rocks of the western Hohe Tauern. - In: Mineral Deposits of the Alps and of the Alpine Epoch in Europe (J. H. Schneider ed.). 240-248. Springer: Berlin, Heidelberg.

E. Schroll, O. Schulz & E. Pak: Sulphur isotope distribution in the Pb-Zn-deposit Bleiberg (Carinthia, Austria). - Mineralium Deposita 18, 17-25.

V. Köppel & E. Schroll: Bleiisotope und Remobilisation von Erzlagerstätten. - Schriftenreihe der Erdwissenschaftl. Kommission, Österr. Akad. Wiss. 6, 39-51.

Nachruf für Prof. Dr. Norbert Grögler. - Mitt. Öster. Miner. Ges. 129, 25.

M. Pimminger, M. Grasserbauer, E. Schroll & I. Cerny: Multielement Spurenanalyse in Mikrobereichen von geologischen Proben mit SIMS. - Fres. Zeitschr. Analyt. Chem. 316, 293.

1984

Geochemical indicator parameters of lead-zinc ore deposits in carbonate rocks. - In: Syngeneses and Epigenesis on the Formation of Mineral Deposits (A. Wauschkuhn et al. eds.). 294-205. Springer: Berlin-Heidelberg.

M. Pimminger, M. Grasserbauer, E. Schroll & I. Cerny: Sulfur isotopic microanalyses in galena by secondary ion mass spectrometry. - Analytical Chemistry 56, 407-411.

Mineralisation der Blei-Zink-Lagerstätte Bleiberg-Kreuth (Kärnten). - Aufschluß 35, 339-350.

E. Schroll & D. Sauer: Kombinierte Anwendung spektrochemischer Analysemethoden bei der Multielementanalyse geologischer Materialien in Großserien. - Symp. instrumenteller Multielementanalytik. KFA Jülich 1984, Abstrakt 98.

E. Schroll & H. Spatzek: Dickit und eine Mikroerzmineralisation aus dem Graphitbergbau Kaisersberg, Steiermark. - Mitt. Abt. Miner. Landesmuseum Joanneum 52, 23-25.

1985

E. Schroll & E. Pak: Sulphur isotopes in the Lake Neusiedel water. - IAEA, Advisory group meeting on isotope hydrology and geochemistry of sulphur. Abstract 1, 95.

- Blei-Zink-Lagerstätten in Sedimenten. - Arch. f. Lagerst.forsch. Geol. B.-A. 6, 157-165.
- Geochemische Parameter der Blei-Zink-Vererzung in Karbonatgesteinen und anderen Sedimenten. - Arch. f. Lagerst.forsch. Geol. B.-A. 6, 167-178.
- M. Pimminger, M. Grasserbauer, E. Schroll & I. Cerny: Anwendung der Ionenstrahlmikroanalyse zur geochemischen Charakterisierung von Zinkblenden. - Arch. f. Lagerst.forsch. Geol. B.-A. 6, 209-214.
- V. Köppel & E. Schroll: Herkunft des Pb der triassischen Pb-Zn-Vererzungen in den Ost- und Südalpen. Resultate bleiisotopengeochemischer Untersuchungen. - Arch. f. Lagerst.forsch. Geol. B.-A. 6, 215-222.
- M. Pimminger, M. Grasserbauer, E. Schroll & I. Cerny: Trace element distribution in sphalerites from Pb-Zn-ore occurrences of the Eastern Alps. - *Tschermaks Min. Petr. Mitt.* 34, 131-141.
- Die Minerale Österreichs. - *Mitt. Österr. Miner. Ges.* 130, 33-44.
- E. Schroll & D. Sauer: Kombinierte Anwendung spektrochemischer Analysemethoden bei der Multielementanalyse geologischen Materials. - In: *Instrumentelle Multielementanalyse* (B. Samsoni ed.). 677-691, VCH-Verlagsges.: Weinheim.
- Geochemical characterization of ore deposits: From the guide element to the geochemical classification. - *Monograph Series on Mineral Deposits* 25, 1-14. Gebrüder Bornträger: Berlin-Stuttgart.
- W. Papesch & E. Schroll: Kohlenstoff- und Sauerstoffisotope in Eisenkarbonaten der Ostalpen und einigen ausseralpinen Vorkommen. - *Österr. Akad. Wiss., Math.-naturwiss. Kl., Anzeiger* 122, 73-75.
- 1986**
- E. Schroll, W. Papesch & P. Dolezel: Beitrag der C- und O- Isotopenanalyse zur Genese ostalpiner Sideritvorkommen. - *Mitt. Österr. Geol. Ges.* 78, 181-191.
- Spurenelemente in heimischen Rohstoffen für Hochtechnologien. - *Berg- u. Hüttenmänn. Monatshefte* 131, 110-115.
- E. Schroll, W. Siegl & W. Papesch: Kohlenstoff- und Sauerstoffisotopenverteilung in einigen Magnesiten. - *Österr. Akad. Wiss., math-naturw. Kl., Anzeiger* 123, 1-4.
- Schwefelisotope in Wässern des Neusiedlersee- Gebiets. - *BFB-Bericht* 58, 73-75 (Illmitz).
- O. Schulz, E. Schroll, K. Dieber & H. Fuchs: Zur Frage der Sideritgenese der Lagerstätten um Hüttenberg in Kärnten. - *Carinthia* II 176./96. 479- 512.
- E. Schroll & M. Caglayan: The Pb-Zn-deposits of Keban (SE-Taurus Mountains) and its position in the Aegean-Tauriden Metallogenic Province. - *Schriftenreihe Erdwiss. Kommission. Öst. Akad. Wiss., Bd. 8*, 75-85.
- L. Kostelka, I. Cerny & E. Schroll: Coordination of diagnostic features in ore occurrences of base metals in dolomites and limestones. - *Schriftenreihe Erdwiss. Kommission. Öst. Akad. Wiss., Bd. 8*, 283-298.
- Geochemie und Humanmedizin. - *Mitt. Österr. Geol. Ges.* 79, 359-372.
- Geochemistry of stream sediments of their relations to the Clark value of the continental Earth's crust. - *International South European symposium on Exploration Geochemistry, Abstract 98* (Athen).
- 1987**
- G. Hausberger, O. Schermann, E. Schroll & F. Thalmann: Geochemical prospection activity in Austria by the Geological Survey and VOEST- Alpine AG. - *12th Internat. Geochemical Exploration Symposium (4th Symposium on Methods of Geochemical Prospecting). Abstract 164* (BRGM, Orleans).
- E. Schroll & E. Pak: Sulphur isotope in the water of Lake Neusiedl, Austria. *Studies on sulphur isotope variations in nature. - Proceeding of the Advisory Group Meeting on Sulphur Isotope Variations in Nature, IAEA (Vienna).*
- Metallogeny of the Eastern Alps in the light of geochemical and isotopic data. - *MFGS, Abstract, 79*, (Dubrovnik).
- 1988**
- V. Köppel, M. Boni & E. Schroll: Metal sources of Alpine and Sardiic Pb-Zn deposits: Results of isotopic investigations of ore and rock leads. - *ENSMP : Colloque International. Mobilité et concentration des metaux de base dans les couvertures sedimentaires, Abstract 19* (BRGM, Orleans).
- V. Köppel & E. Schroll: Pb-isotope evidence for the origin of lead in strata-bound Pb-Zn deposits in triassic car-

bonates of the Eastern and Southern Alps. - *Mineralium Deposita* 23, 96-103.

J. Raith, W. Papesch & E. Schroll: Kohlenstoff- und Sauerstoffisotope scheelitfreier und scheelitführender Karbonatgesteine aus den Ostalpen. - *Österr. Akad. Wiss., Math.-naturwiss. Kl., Anzeiger* 125, 59-64.

R. B. Carl, R. Höll & E. Schroll: Ein Metadioritvorkommen in der Habachformation westlich der Achselalm/Hollersbachtal (Hohe Tauern, Österreich). - *Mitt. Österr. Geol. Ges.* 81, 123 -132.

1989

F. Thalmann, O. Schermann, E. Schroll & G. Hausberger: Geochemischer Atlas der Republik Österreich. Böhmisches Masse und Zentralzone der Ostalpen. - *Geologische Bundesanstalt* 1-141, Wien.

Recent formation of magnesite in evaporitic environment. The example of the Coorong Lagoon (South Australia). - In: *Magnesite Formation*. (P. Möller ed.). *Monograph Series of Mineral Deposits* 28, 29-34.

M. Kralik, P. Ahron, E. Schroll & V. Zachmann: Carbon and oxygen isotope systematics of magnesites. - In: *Magnesite Formation*. (P. Möller ed.). *Monograph Series of Mineral Deposits* 28, 197-224.

E. Schroll, W. Siegl & E. Pak: Sulfur isotopes of minerals of Austrian magnesites occurrences. - In: *Magnesite Formation*. (P. Möller ed.). *Monograph Series of Mineral Deposits* 28, 233-236.

1990

Die Metallprovinz der Ostalpen im Lichte der Geochemie. - *Geol. Rundschau* 79, 479-493.

E. Schroll, V. Köppel & M. Kralik: Nachweis von "Benzinblei" in der Wiener Umwelt. - 2. Arbeitstagung "Erdwissenschaftliche Aspekte des Umweltschutzes" Geotechnisches Institut BVFA-Arsenal Wien.

Arsenal 2000. Bundesversuchs- und Forschungsanstalt Arsenal. Anlässlich des 40-Jahr-Jubiläums. - Hrsg.: Erich Schroll. © 1990 Metrica Fachverlag, Ing. Werner H. Bartak, Wien.

1992

K. Augustin-Gyurits & E. Schroll: Beitrag zur geochemischen Charakterisierung österreichischer Kohlen. - *Mitt. Ges. Geol. Bergbaustud. Österr.* 38, 195-211.

1993

H. Kürzl, E. Schroll & O. Weinzirl: Geochemistry of carbonate hosted Pb-Zn-deposits in respect to classification by multivariate data. - *Workshop MVT Proceeding, Campus Jussieu. Soc. Geol. de France*, 121-124 (Paris).

Conceptual model of the origin of the Alpidic carbonate hosted lead zinc mineralizations based on geological aspects in relation to geochemical data. - *Workshop MVT Proceeding, Campus Jussieu. Soc. Geol. de France*, 175-182 (Paris).

V. Köppel, F. Neubauer & E. Schroll: Pre-Alpidic ore deposits in the Central, Eastern and Southern Alps (Europe). - In: *Pre-Mesozoic Geology in the Alps*. (J.F. Raumer and F. Neubauer eds.), 145-162, Springer: Berlin.

1994

E. Schroll, H. Kürzl & O. Weinzirl: Geochemometrical studies applied to the Pb-Zn-deposit Bleiberg/Austria. - In: *Sediment-hosted Zn-Pb ores* (L. Fontebote and M. Boni eds.). 228-245. Springer: Berlin.

I. Cerny & E. Schroll: Blei-Zink-Rohstoffe sowie die mit diesen assoziierten Nebenelemente (Spezialmetalle) in Österreich. - In: *Rohstoffe für neue Technologien* (G. Sterk ed.). *Österr. Akad. Wiss., Schriftenreihe d. Erdwissenschaftlichen Kommissionen* 11, 65-70.

ACR. Austrian Cooperative Research. 40 Jahre Kooperative Forschungsinstitute der österreichischen Wirtschaft. - (E. Schroll ed.), COMO Werbe & PR GmbH., 4020 Linz.

1995

The Triassic carbonate-hosted lead-zinc ore mineralization in the Alps (Europe). - *Int. Field Conference on carbonate hosted lead-zinc deposits. Ext. Abstr.* 271-273 (St. Louis).

I. Cerny & E. Schroll: Heimische Vorräte an Spezialmetallen (Ga, In, Tl, Ge, Se, Te und Cd) in Blei-Zink- und anderen Erzen. - *Arch. f. Lagerst.forsch. Geol. B.-A.* 18, 5-33.

G. Rantitsch, R. F. Sachsenhofer & E. Schroll: Anorganische Geochemie mesozoischer Kohlen der Ostalpen (Österreich). - *Arch. f. Lagerst.forsch. Geol. B.-A.* 18, 121-133.

1996

E. Schroll, H. Kürzl & O. Weinzirl: Geochemometrische Charakterisierung sedimentgebundener Blei-Zink-Vererzungen mittels multivariater Techniken. - Berg- u. Hüttenm. Monatshefte 141, 158-164.

E. Schroll, V. Köppel, I. Cerny, P. Spindler & A. von Quadt: Geochemische Charakterisierung der "Schwellen- und Lagunenfazies" in Bleiberg, Josefscholle: Ein Versuch zur Anwendung der Multivariatetechnik. - Mitt. Österr. Miner. Ges. 141, 209-210.

The Triassic carbonate hosted Pb-Zn mineralizations in the Alps (Europe). - In: Carbonate hosted lead – zinc deposits. (D. F. Sangster ed.). 182-194 (Littleton).

1997

G. Rantitsch, B. Russenegger, R. F. Sachsenhofer, J. Jochum & E. Schroll: Hydrocarbon-bearing fluid inclusions in the Drau Range (Eastern Alps, Austria: implications for the genesis of the Bleiberg Pb-Zn-deposit. - In: Mineral deposits (H. Papunen ed.). 567-569. Balkema: Rotterdam.

Geochemische und geochronologische Daten und Erläuterungen. - In: Handbuch der Lagerstätten der Erze, Industriemineralien und Energierohstoffe Österreichs (L. Weber, ed.). Arch. f. Lagerst.forsch. Geol. B.-A. 19/IV, 395-542.

I. Cerny, E. Schroll & L. Weber: Rechnitzer Fenstergruppe. - In: Handbuch der Lagerstätten der Erze, Industriemineralien und Energierohstoffe Österreichs (L. Weber, ed.). Arch. f. Lagerst.forsch. Geol. B.-A. 19/IV/2.3.2.3, 287-290.

O. Schulz & E. Schroll: Sideritbezirk Hüttenberg. - In: Handbuch der Lagerstätten der Erze, Industriemineralien und Energierohstoffe Österreichs (L. Weber, ed.). Arch. f. Lagerst.forsch. Geol. B.-A. 19/IV/2.4.1.1.2, 291-293.

L. Weber & E. Schroll: Chromit-Asbest-Magnetitbezirk Kraubath-Hochgrössen. - In: Handbuch der Lagerstätten der Erze, Industriemineralien und Energierohstoffe Österreichs (L. Weber, ed.). Arch. f. Lagerst.forsch. Geol. B.-A. 19/IV/2.4.1.1.7, 296-297.

E. Schroll, E. Tufar & L. Weber: Polymetallischer Erzbezirk Mittelkärntner Altkristallin. - In: Handbuch der Lagerstätten der Erze, Industriemineralien und Energierohstoffe Österreichs (L. Weber, ed.). Arch. f. Lagerst.forsch. Geol. B.-A. 19/IV/2.4.1.2.6, 301-302.

E. Schroll & L. Weber: Polymetallischer Erzbezirk Wölzer Tauern. - In: Handbuch der Lagerstätten der Erze, Industriemineralien und Energierohstoffe Österreichs (L. Weber, ed.). Arch. f. Lagerst.forsch. Geol. B.-A. 19/IV/2.4.1.2.8, 304.

Quarz-Feldspatpegmatitbezirk Liesergneissserie. - In: Handbuch der Lagerstätten der Erze, Industriemineralien und Energierohstoffe Österreichs (L. Weber, ed.). Arch. f. Lagerst.forsch. Geol. B.-A. 19/IV/2.4.1.5.1, 316-317.

L. Weber & E. Schroll: Kieserzlagstätte Walchen/Öblam. - In: Handbuch der Lagerstätten der Erze, Industriemineralien und Energierohstoffe Österreichs (L. Weber, ed.). Arch. f. Lagerst.forsch. Geol. B.-A. 19/IV/2.4.2.4, 325.

F. Vavtar, O. Schulz & E. Schroll: Magnetitbezirk Hochfilzen (Hohe-Salve-Einheit). - In: Handbuch der Lagerstätten der Erze, Industriemineralien und Energierohstoffe Österreichs (L. Weber, ed.). Arch. f. Lagerst.forsch. Geol. B.-A. 19/IV/2.4.2.6.1.3.2., 334-335.

L. Weber & E. Schroll: Magnetit-(Talk-) Bezirk Veitscher Decke. - In: Handbuch der Lagerstätten der Erze, Industriemineralien und Energierohstoffe Österreichs (L. Weber, ed.). Arch. f. Lagerst.forsch. Geol. B.-A. 19/IV/2.4.2.6.2.4.1, 339-340.

E. Schroll & L. Weber: Kupfererzbezirk postvariszische Transgressionsserien Montafon und Arlberg. - In: Handbuch der Lagerstätten der Erze, Industriemineralien und Energierohstoffe Österreichs (L. Weber, ed.). Arch. f. Lagerst.forsch. Geol. B.-A. 19/IV/2.4.3.1.2.1, 354.

O. Schulz & E. Schroll: Pb-Zn-(Fahlerz-) Erzbezirk Anis Nordtiroler Kalkalpen. - In: Handbuch der Lagerstätten der Erze, Industriemineralien und Energierohstoffe Österreichs (L. Weber, ed.). Arch. f. Lagerst.forsch. Geol. B.-A. 19/IV/2.4.3.1.2.2, 355-358.

O. Schulz & E. Schroll: Pb-Zn-Erzbezirk Karn (Wettersteinkalk, -dolomit) Nordtiroler Kalkalpen. - In: Handbuch der Lagerstätten der Erze, Industriemineralien und Energierohstoffe Österreichs (L. Weber, ed.). Arch. f. Lagerst.forsch.

Geol. B.-A. 19/IV/2.4.3.1.2.3, 358-359.

L. Weber & E. Schroll: Evaporitbezirk Montafon. - In: Handbuch der Lagerstätten der Erze, Industriemineralien und Energierohstoffe Österreichs (L. Weber, ed.). Arch. f. Lagerst.forsch. Geol. B.-A. 19/IV/2.4.3.1.4.4, 367-368.

I. Cerny & E. Schroll: Pb-Zn-Erzbezirk Anis Drauzugmesozoikum. - In: Handbuch der Lagerstätten der Erze, Industriemineralien und Energierohstoffe Österreichs (L. Weber, ed.). Arch. f. Lagerst.forsch. Geol. B.-A. 19/IV/2.4.3.2.1.1, 371.

I. Cerny & E. Schroll: Pb-Zn-Erzbezirk Karn Drauzugmesozoikum. - In: Handbuch der Lagerstätten der Erze, Industriemineralien und Energierohstoffe Österreichs (L. Weber, ed.). Arch. f. Lagerst.forsch. Geol. B.-A. 19/IV/2.4.3.2.1.2, 372-379.

Bauxitbezirk Nördliche Kalkalpen. - In: Handbuch der Lagerstätten der Erze, Industriemineralien und Energierohstoffe Österreichs (L. Weber, ed.). Arch. f. Lagerst.forsch. Geol. B.-A. 19/IV/2.4.3.4.1.1, 389.

R. F. Sachsenhofer & E. Schroll: Glanzbraunkohlenbezirk Grünbach. - In: Handbuch der Lagerstätten der Erze, Industriemineralien und Energierohstoffe Österreichs (L. Weber, ed.). Arch. f. Lagerst.forsch. Geol. B.-A. 19/IV/2.4.3.4.2.1, 390.

I. Cerny & E. Schroll: Südalpen - In: Handbuch der Lagerstätten der Erze, Industriemineralien und Energierohstoffe Österreichs (L. Weber, ed.). Arch. f. Lagerst.forsch. Geol. B.-A. 19/IV/4.0, 392-394.

1998

E. Schroll, P. Andráš & M. Chovan: Comparison of antimony ore deposits of the Eastern Alps and the Western Carpathians using geochemical data. - Carpathian-Balkan Geological Assoc. XVI Congress, Abstract 41 (Vienna). Geochemical contributions to the metallogenic map of Austria. - Carpathian-Balkan Geological Assoc. XVI Congress, Abstract 538 (Vienna).

1999

P. Andráš, M. Chovan & E. Schroll: A first attempt to geochemically compare ore deposits of the Western Carpathians and the Eastern Alps. - *Geologica Carpathica* 50, Special Issue, 192-194 (Bratislava).

G. Rantitsch, J. Jochum, R. F. Sachsenhofer, B. Russegger, E. Schroll & B. Horsfield: Hydrocarbon-bearing fluids in the Drau range (Eastern Alps, Austria) : implications for the genesis of Bleiberg-type Pb-Zn deposits. - *Mineralogy and Petrology* 65, 141-159.

Gallium: Element and geochemistry. - In: *Encyclopedia of Geochemistry* (C. P. Marshall and R. W. Fairbridge eds.), 257-259, Kluwer Academic Publ.: Dordrecht-Boston-London.

Germanium: Element and geochemistry. - In: *Encyclopedia of Geochemistry* (C. P. Marshall and R. W. Fairbridge eds.), 307-308, Kluwer Academic Publ.: Dordrecht-Boston-London.

Indium: Element and geochemistry. - In: *Encyclopedia of Geochemistry* (C. P. Marshall and R. W. Fairbridge eds.), 339-340, Kluwer Academic Publ.: Dordrecht-Boston-London.

2000

M. Kling, R. Höll & E. Schroll: Literaturstudie über Germanium in Gesteinen, Mineralen, Erzen und Lagerstätten. - *Berichte zur Lagerstätten- und Rohstoffforschung* (Hannover), 59, 1-117.

2001

H. Kucha, E. Schroll & E. F. Stumpff: Direct evidence for bacterial sulphur reduction in Bleiberg-type deposits. - In: *Mineral deposits at the beginning of the 21st century* (A. Piestrzynski et al. eds.), 149-152, Swetz & Zeitlinger Publ.:Lisse.

H. Kucha, E. Schroll & E. F. Stumpff: Banded ZnS from Bleiberg deposits and concepts of formation. - In: *Mineral deposits at the beginning of the 21st century* (A. Piestrzynski et al. eds.), 157-160, Swetz & Zeitlinger Publ.: Lisse.

H. Kucha, E. Schroll & E. F. Stumpff: Bacteriogenic ore formation in Bleiberg-type deposits. - *Mitt. Österr. Miner. Ges.* 146, 160-162.

Zur geochemischen Charakterisierung von Lagerstätten. - Mitt. Österr. Miner. Ges. 146, 266-268.

E. Schroll & F. Pertlik: Herbert Eduard Haberlandt: Ein Pionier der Geochemie in Österreich (*3.6.1904 Mödling †9.6.1970 Wien). (Eine Biographie mit Schriftenverzeichnis). - Mitt. Österr. Miner. Ges. 146, 435-447.

2002

M. Chovan, P. Andráš, E. Schroll, F. Ebner, J. Kotulová, R. Mali & W. Prochaska: Stibnite mineralization of Western Carpathians and Eastern Alps: Geological, mineralogical, and geochemical features. - *Geologica Carpathica* 53, 91-96. Proceed. XVIIth Congress of CBGA (Bratislava).

M. Chovan, P. Andráš, E. Schroll, F. Ebner, J. Kotulová, R. Mali & W. Prochaska: Sb-Mineralizations of the Eastern Alps and of the Western Carpathians – a comparison. - *Pangea Austria*. Abstract 32 (Salzburg).

Zur Genese von Bleiberg und anderer Pb-Zn-Vererzungen der alpinen Mitteltrias. - *Pangea Austria*. Abstract 163 (Salzburg).

H. Kucha, E. Schroll & E. F. Stumpfl: Bacteriogenic lead zinc mineralization in the Bleiberg deposit, Austria. - *Geochim. Cosmochim. Acta*, Sec. Supl. Abstracts of the 12th Annual V. M. Goldschmidt Conference, A 688.

E. Schroll & G. Rantitsch: Sulfur isotope distribution at Bleiberg lead-zinc deposit (Austria) and its genetic implication. - 4th Austrian Workshop on Stable Isotopes in Environmental and Earth Sciences. Abstract 29 (Graz).

Genesis of magnesite deposits in the view of isotope geochemistry. - *IGCP 443 Magnesite and Talc. Newsletter No 2. Boletim Paranaense de Ciências, Special Issue 50, 59-68 (Curitiba, Brazil).*

2003

P. Andráš, M. Chovan, E. Schroll, A. M. Neiva, P. Král & N. Zachariáš: Western Carpathian and selected European Sb-mineralizations; Pb-isotope study. - *Acta Mineralogica-Petrographica*, Abstract Ser.1, 4 (Szeged).

Lead-zinc deposits hosted by sedimentary rocks in the Alps in the view of lead isotopes. - *Mitt. Österr. Miner. Ges.* 148, 280-282.

F. Pertlik & E. Schroll: Arthur Marchet (18.9.1892-30.5.1980). Ordentlicher Professor und Dekan der philosophischen Fakultät der Universität Wien. Sein wissenschaftliches Werk. - *Mitt. Österr. Miner. Ges.* 148, 373-385.

G. Piccotini, E. F. Schroll & P. Spindler: Ein römerzeitlicher Bleibarren vom Magdalensberg. - *Rudolfinum, Jahrbuch des Landesmuseums Kärnten 2002*, 153-161 (Klagenfurt).

E. Schroll & G. Rantitsch: Isotope pattern in the Bleiberg deposit (Eastern Alps) and its implication for genetically affiliated Pb-Zn deposits. - In: *Mineral exploration and sustainable development 2*, (Eliopoulos et al. eds.), 1023-1026. Millpress: Amsterdam.

Die Geschichte vom Wulfenit. - 4. Symposium "Geschichte der Erdwissenschaften in Österreich", Klagenfurt. *Ber. Geol. Bundesanst.* 64, Anhang 69-70.

E. Schroll, E. Stumpfl, H. Kucha & G. Rantitsch: Wann und wie entstand die Pb-Zn Lagerstätte Bleiberg? - *Int. Symp. Österr. Akad. Wiss., Kommission für Grundlagen der Mineralstoffforschung (Wien).*

bei der Redaktion eingegangen: 3. März 2004

Manuskript angenommen: 7. März 2004

**GEOMETRISCHE STUDIEN ZU DEN PENTAGONALEN UND DEKAGONALEN
DREIDIMENSIONALEN PUNKTGRUPPEN**

von

Robert Krickl

Institut für Mineralogie und Kristallographie
Universität Wien, Geozentrum, Althanstrasse 14, A-1090 Wien

Summary

Geometrical studies on the pentagonal and decagonal 3-dimensional point groups. Stereograms of symmetry elements and poles of general equivalent faces of each of the seven pentagonal and five decagonal point groups are given. Descriptions of the faces with special and general forms are further topics of this article.

Zusammenfassung

Stereographische Projektionen der Symmetrieelemente und der Pole der allgemeinen Flächenformen von jeder der sieben pentagonalen und fünf dekadalen Punktgruppen werden vorgestellt. Die Charakterisierung der Flächen der speziellen und allgemeinen Formen ist ein weiterer Teil dieses Artikels.

Einleitung

Wie Johann Friedrich Hessel (*1796, †1872) als Erster zeigen konnte, gibt es, resultierend aus der Kombination von makroskopischen Symmetrieelementen, nur 32 unterschiedliche dreidimensionale kristallographische Punktgruppen (HESSEL, 1830; vgl. auch SOHNCKE, 1891 und HESS, 1896). Als mögliche einfache, makroskopische Symmetrieelemente treten neben Inversionszentrum und Symmetrieebene(n), nur Drehachsen mit den Zähligkeiten (1), 2, 3, 4 und 6 (auch Mono-, Di-, Tri-, Tetra- und Hexagyre genannt) in der klassischen Kristallographie auf. Jene mit einer Zähligkeit von 5 (Pentagyre) ist hingegen nicht verwirklichtbar. Der Grund für dieses Verbot liegt in der Unvereinbarkeit der fünfzähligen Symmetrie mit der translatorischen Wiederholung identer Baueinheiten - den Elementarzellen - durch die ein Kristall charakterisiert ist. Gleiches gilt auch für die n-zählige Symmetrie mit $n > 6$, wie zum Beispiel die zehnzählige, auf die hier auch des Weiteren eingegangen werden soll. Die durch Pentagyren und Dekagyren erzeugten Punktanordnungen erfüllen nicht die Bedingung für Netzebenen, die entlang von Gittergeraden eine Identität und gleich bleibenden Translationsabstand aufweisen müssen.

Eine anschauliche geometrische Erklärung für den zweidimensionalen Fall sieht so aus, dass man eine Ebene zwar in gleichseitige Drei-, Vier- und Sechsecke lückenlos translatorisch unterteilen kann, eine derartige lückenlose Unterteilung in gleichseitige Fünfecke, sowie auch in Polygone mit mehr als sechs Ecken, aber nicht möglich ist (Abb. 1).

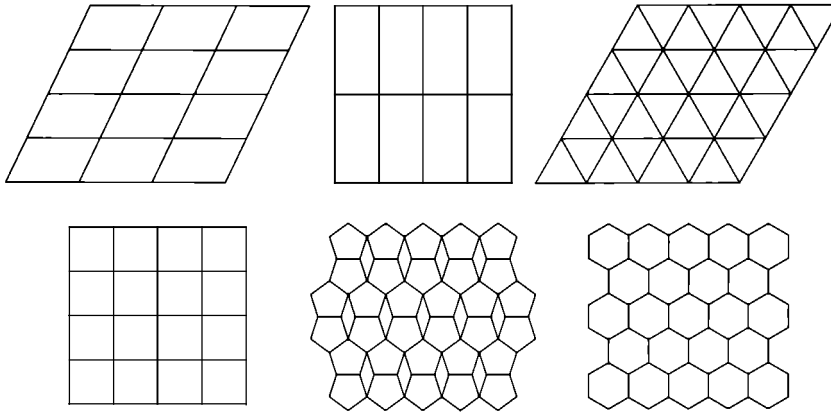


Abb. 1

Die Unterteilung einer Ebene ist nur mit Rechtecken, Parallelogrammen, gleichseitigen Drei-, Vier- und Sechsecken möglich, hingegen nicht mit gleichseitigen Fünfecken.

Obwohl demnach eine pentagonale Symmetrie für einen gesamten (Translations-)Kristall nicht in Frage kommt, ist die Beschreibung lokaler Symmetrien durch dreidimensionale pentagonale Punktgruppen möglich und durchaus sinnvoll (KOSTOV & KOSTOV, 1988). Im Folgenden sollen daher neben diesen Punktgruppen auch deren mögliche Flächenformen vorgestellt werden, durch die eine Beschreibung von Koordinationspolyedern und auch ganz allgemein von pentagonalen Körpern ermöglicht wird.

Analog zu Überschneidungen und Ähnlichkeiten zwischen den trigonalen und hexagonalen Punktgruppen werden zusätzlich zu den pentagonalen auch die dekalagonalen Punktgruppen behandelt.

Phänomenologie der Pentagyre

Die Ableitung der dreidimensionalen pentagonalen Punktgruppen und die Zuordnung von internationalen Symbolen durch KOSTOV & KOSTOV (1988) basiert auf der Analogie zu den trigonalen Punktgruppen. Diese Autoren wollten gleichsam eine Lücke in der Zahlenreihe der dreidimensionalen Punktgruppen schließen, um eine Beschreibung lokaler Symmetrien zu erleichtern.

Ausgehend von der mathematischen Realisierbarkeit von Achsenkombinationen, sei auf die von Leonhard Euler (*1707, †1783) abgeleitete Formel

$$\cos (A \wedge B) = \frac{\cos (\gamma / 2) + \cos (\alpha / 2) \cos (\beta / 2)}{\sin (\alpha / 2) \sin (\beta / 2)}$$

verwiesen, wobei $A \wedge B$ den Winkel zwischen den beiden Drehachsen A und B, α den Drehwinkel um A, β den Drehwinkel um B und γ die Ersatzdrehung um eine Achse C bezeichnet. Hieraus ergibt sich, dass lediglich die Kombination einer fünfzähligen oder zehnzähligen Achse mit zweizähligen Achsen eine endliche Wiederholung ermöglicht. Die Kombinationsmöglichkeiten der Symmetrieelemente sind in Tabelle 1 dargestellt und führen zu den sieben achsialen pentagonalen und fünf dekagonalen Punktgruppen.

Daneben existieren noch Punktgruppen, die mehr als eine fünfzählige Achse besitzen: Die Ikosaedergruppen $235 (I)$ und $2/m\bar{3}5 (I_h)$, auf die hier nicht näher eingegangen wird.

Punktgruppe	Symbol nach		Symmetrieelemente				
	Hermann-Mauguin	Schoenflies	Hauptachse	m parallel	m senkrecht	2 senkrecht	Inversionszentrum
Pentagonal Pyramidal	5	C_5	5p	-	-	-	-
Pentagonal Streptoedrisch	$\bar{5}$	C_{5i} $\equiv S_{10}$	$\bar{5}$	-	-	-	Z
Pentagonal Trapezoedrisch	52	D_5	5	-	-	52p	-
Dipentagonal Pyramidal	5m	C_{5v}	5p	5m	-	-	-
Dipentagonal Skalenoedrisch	$\bar{5} 2/m$ ($\bar{5} m$)	D_{5d}	$\bar{5}$	5m	-	52	Z
Pentagonal Dipyramidal	$5/m$ $\equiv \bar{10}$	C_{5h}	5	-	1m	-	-
Dipentagonal Dipyramidal	$5/m\bar{m}2$ $\equiv \bar{10}m2$	D_{5h}	5	5m	1m	52p	-
Dekagonal Pyramidal	10	C_{10}	10p	-	-	-	-
Dekagonal Dipyramidal	10/m	C_{10h}	10	-	1m	-	Z
Dekagonal Trapezoedrisch	1022	D_{10}	10	-	-	102	-
Didekagonal Pyramidal	10mm	C_{10v}	10p	10m	-	-	-
Didekagonal Dipyramidal	$10/m\bar{2}/m\bar{2}/m$ ($10/m\bar{m}m$)	D_{10h}	10	10m	1m	102	Z

Tabelle 1

Die Symmetrieelemente der sieben pentagonalen und fünf dekagonalen dreidimensionalen Punktgruppen.

Die Angaben parallel und senkrecht beziehen sich auf die Lage zur Hauptachse (p: polare Achse).

Diskussion

Die pentagonalen und dekagonalen Punktgruppen und ihre Flächenformen (Tabelle 2) korrespondieren mit den entsprechenden trigonalen und hexagonalen Punktgruppen. Zur Beschreibung der Flächenformen der nichtkristallographischen Punktgruppen können jedoch keine rationalen Millerschen Indizes verwendet werden. Der Unterschied der Millerschen Indizes in den mathematischen Punktgruppen liegt darin, dass sie aufgrund der fehlenden Translation nicht ganzzahlig sein können, wie es in den kristallographischen Punktgruppen der Fall ist. Stereographische Projektionen der allgemeinen Formen sind in Abb. 2 wiedergegeben.

Anzahl der Flächen	Name der Form	Punktgruppen											
		5	$\bar{5}$	52	5m	$\bar{5} 2/m$ ($\bar{5} m$)	$5/m$ $\equiv \bar{10}$	$5/mm2$ $\equiv \bar{10} m2$	10	10/m	1022	10mm	10/m2/m2/m (10/mmm)
1 ; o	Pedion	+			+				+			+	
2 ; o	Pinakoid		+	+		+	+	+		+			+
5 ; o	Pentagonales Prisma	+		+	+		+	+					
5 ; o	Pentagonale Pyramide	+			+								
10 ; o	Dipentagonales Prisma			+	+			+					
10 ; o	Dekagonales Prisma		+	+	+	+		+	+	+	+	+	+
10 ; o	Dipentagonale Pyramide				+								
10 ; o	Dekagonale Pyramide				+				+			+	
10 ; g	Pentagonale Dipyramide			+			+	+					
10 ; g	Pentagonales Streptoeder		+	+		+							
10 ; g	Pentagonales Trapezoeder			+									
20 ; o	Didekagonales Prisma					+				+		+	+
20 ; o	Didekagonale Pyramide										+		
20 ; g	Dipentagonale Dipyramide							+					
20 ; g	Dekagonale Dipyramide					+		+	+	+			+
20 ; g	Dipentagonales Skalenoeder					+							
20 ; g	Dekagonales Trapezoeder									+			
40 ; g	Didekagonale Dipyramide												+

Tabelle 2

Die speziellen und allgemeinen (möglichen) idealisierten Flächenformen der sieben pentagonalen und fünf dekadagonalen dreidimensionalen Punktgruppen (o: offene Form, g: geschlossene Form).

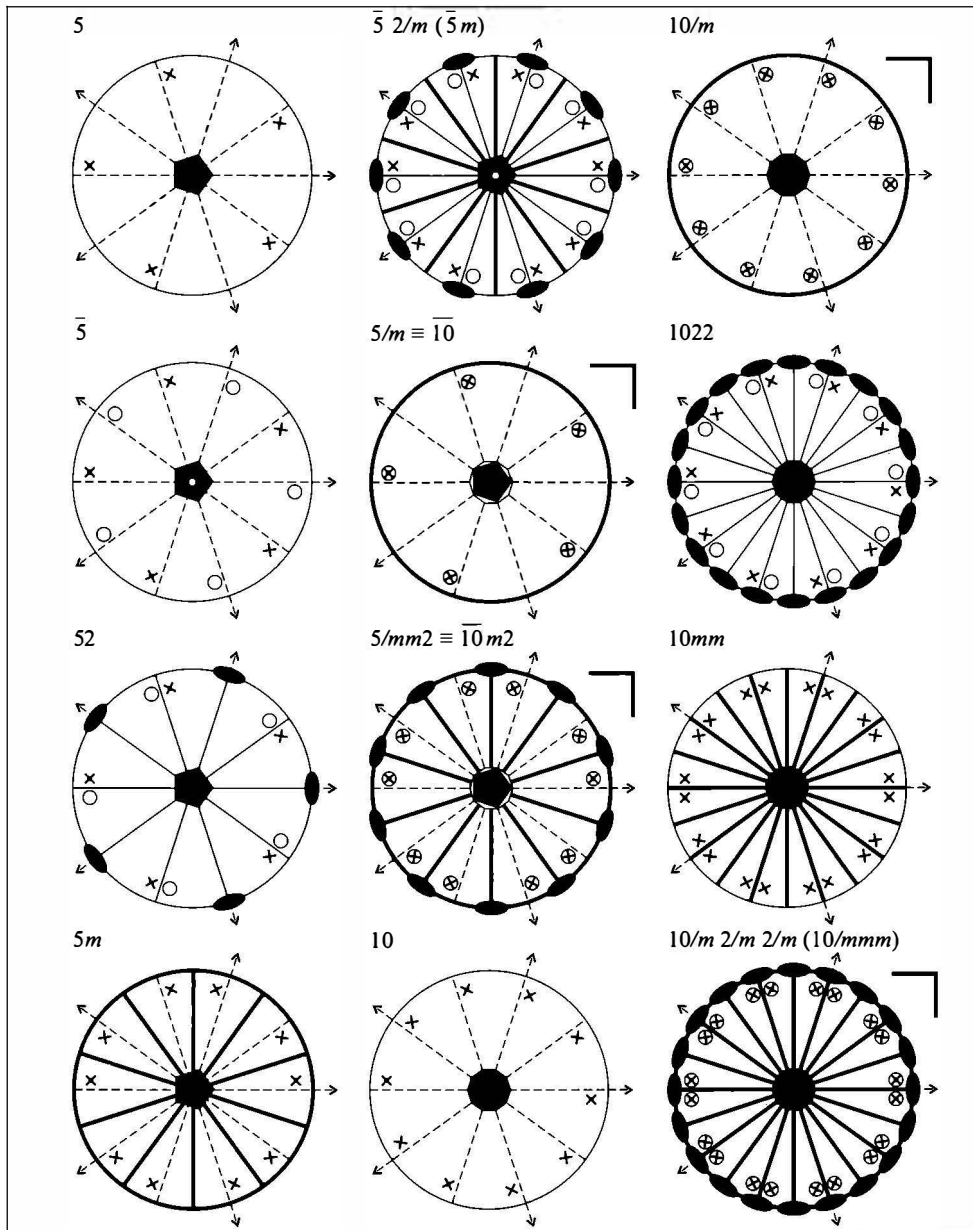


Abb. 2

Die sieben pentagonalen und fünf dekagonalen dreidimensionalen Punktgruppen: Symmetrieelemente und Pole der Flächen allgemeiner Lage in stereographischen Projektionen. Die fünfzählige oder zehnzählige Achse steht jeweils normal auf die Zeichenebene.

- Hilfslinien zur Verdeutlichung der pentagonalen und dekagonalen Symmetrie
- Symmetrieebenen normal zur Zeichenebene
- zweizählige Achsen parallel zur Zeichenebene
- × Flächenpole allgemeiner Lage oberhalb der Zeichenebene
- ⊔ Symmetrieebene parallel zur Zeichenebene
- Flächenpole allgemeiner Lage unterhalb der Zeichenebene

Zu den trigonalen Punktgruppen werden üblicherweise auch jene zwei Gruppen gezählt, die als Charakteristikum eine dreizählige Achse normal auf eine Symmetrieebene aufweisen, wobei $3/m$ ident mit $\bar{6}$ ist (CORRENS, 1968). Zu bemerken ist, dass die Gruppen mit einer sechszähligen Inversionsachse und den internationalen Symbolen $\bar{6}$ und $\bar{6}m2$, in der Literatur unterschiedlich, auch zum hexagonalen Kristallsystem gezählt werden. In Analogie zu den von Correns angegebenen Kristallographischen Tabellen werden in vorliegender Arbeit jedoch die Klassen $\bar{10}$ ($\cong 5/m$) und $\bar{10}m2$ ($\cong 5/m2$) zu den pentagonalen Gruppen gestellt.

Die Punktgruppe $\bar{5}$ steht in Analogie zur trigonal rhomboedrischen Punktgruppe $\bar{3}$. Das Rhomboeder ist allerdings ein definierter, von sechs kongruenten Rhomben begrenzter Körper des trigonalen Systems. Für das pentagonale Pendant wurde die Bezeichnung "Streptoeder" (= "Gedrehtflächner") gewählt (NIGGLI, 1941) und daher die Punktgruppe auch "pentagonal streptoedrisch" genannt.

Dank

Die vorliegende Arbeit wurde im Rahmen der im Sommersemester 2003 an der Universität Wien von Herrn Prof. Dr. Franz Pertlik angebotenen Lehrveranstaltung "Mineralmorphologie" erarbeitet. Für die Anregung zu diesem Artikel, sowie für weiterführende Diskussionen erlaubt sich der Autor neben dem Leiter dieser Lehrveranstaltung auch Frau Prof. Dr. Herta Effenberger und Herrn Prof. Dr. Manfred Wildner seinen Dank auszusprechen.

Literatur

- CORRENS, C. W. (1968): Einführung in die Mineralogie. - Springer-Verlag Berlin Heidelberg New York.
- HESS, E. (1896): J. F. C. Hessel. Zur Säcularfeier seines Geburtstages (27. April 1796). - Neues Jb. Miner., Geol. u. Palaeont., II, Jg. 1896, 107-122.
- HESSEL, J. F. (1830): Krystall. - In: Gehlers Physikalisches Wörterbuch II, Band 5, 1023-1340.
- KOSTOV, R. I. & KOSTOV, I. (1988): On the fivefold cluster symmetry. - Cryst. Res. Technol. 23, 973-977.
- NIGGLI, P. (1941): Lehrbuch der Mineralogie und Kristallchemie. - Verlag von Gebrüder Borntraeger Berlin-Zehlendorf.
- SOHNCKE, L. (1891): Die Entdeckung des Eintheilungsprincips der Krystalle durch J. F. Hessel. Eine historische Studie. - Z. Kristallogr. 18, 486-498.

bei der Redaktion eingegangen: 3. März 2004

Manuskript angenommen: 7. März 2004

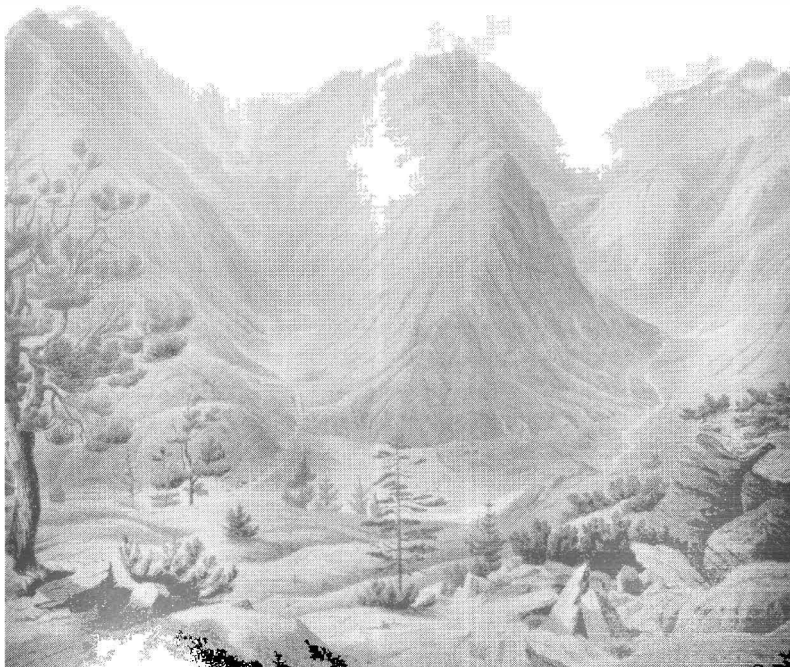
MINPET 2003

15. – 21. SEPTEMBER 2003

NEUKIRCHEN AM GROSSVENEDIGER/SALZBURG

ABSTRACTS

NACHTRAG



**BULK MODULI AND PHASE TRANSITIONS OF CARBIDONITRIDOSILICATES
AND OXONITRIDOSILICATES AT HIGH PRESSURES UP TO 36 GPa**

**A. Friedrich¹, K. Knorr², A. Lieb³, St. Rath², H. A. Höppe³, B. Winkler¹,
W. Schnick³ & M. Hanfland⁴**

¹Institut für Mineralogie, Abteilung Kristallographie
Johann Wolfgang Goethe-Univ., Senckenberganlage 30, D-60054 Frankfurt a. M., Germany

²Institut für Geowissenschaften

Christian-Albrechts-Universität, Olsenhausenstrasse 40, D-24098 Kiel, Germany

³Department Chemie

Ludwig-Maximilians-Universität, Butenandtstrasse 5-13/D, D-81377 München, Germany

⁴European Synchrotron Radiation Facility (ESRF)

B.P. 220, F-38043 Grenoble, France

A new exciting field in material science was opened by the systematic investigation of nitridosilicates [1-3]. Nitridosilicates and oxonitridosilicates can be formally derived from oxosilicates by a total or partial exchange of nitrogen for oxygen. All of them are synthesised by high-temperature reactions and mainly form condensed three-dimensional networks. The exceptional thermal and chemical stability combined with high performance mechanical properties (hardness and strength) make these compounds very interesting for the materials science community. The replacement of oxygen by the more covalently behaving nitrogen extends the structural possibilities significantly. New structural features appear which are not known in oxosilicate chemistry. For example, nitridosilicates with star-like units $[\text{N}^{(4)}(\text{SiN}_3^{(2)})_4]$ of four SiN_4 -tetrahedra, which share a common corner, were recently found for the first time [4-6]. A further extension of the nitridosilicates can be found by a formal exchange of the central nitrogen of the $[\text{N}^{(4)}(\text{SiN}_3^{(2)})_4]$ unit by carbon in carbidonitridosilicates [7]. Nitridosilicates allow a long range of cation- and anion-substitution mechanisms leading to a variation of their physical properties. We have begun to study the influence of substitution effects on the properties of these materials by in situ high-pressure X-ray diffraction as well as ab initio computations.

In situ high-pressure powder diffraction experiments up to pressures of 36 GPa were performed at beamline ID09 of the ESRF. The samples were loaded into diamond anvil cells using liquid neon as a pressure-transmitting medium. Pressures were determined by means of the laser-induced ruby fluorescence method. Full powder diffraction rings were recorded on a MAR345 image plate system using a wavelength of 0.4138 Å. The images were processed and integrated with FIT2D [8]. LeBail refinements were carried out with GSAS [9].

Carbidonitridosilicates: $Ln^{III}_2[Si_4N_6C]$ ($Ln = Ho, Er$)

In the $Ln_2[Si_4N_6C]$ compounds [7], the carbon atom is negatively polarised. It connects four Si tetrahedra-centres to form a star-like unit $[C^{4-}(SiN_3^{2+})_4]$. $Ho_2[Si_4N_6C]$ [$P2_1/c$, $a = 5.931(1)$, $b = 9.900(1)$, $c = 11.877(3)$ Å, $\beta = 119.69(1)^\circ$, $V = 605.74(5)$ Å³] and isotypic $Er_2[Si_4N_6C]$ [$V = 602.70(5)$ Å³] were both investigated up to pressures of 36 and 21 GPa, respectively.

Both compounds show a similar compressional behaviour. Hence, the substitution of lanthanides, such as Ho and Er, seems to have no significant influence on the high-pressure properties. A third-order Birch-Murnaghan equation of state was fitted to the P-V data of $Ho_2[Si_4N_6C]$ between 0.0001 and 36 GPa. The values obtained for the isothermal bulk modulus and its pressure derivative are $B_0 = 159(3)$ GPa and $B' = 5.6(2)$. The bulk modulus is higher if compared to the computed bulk moduli of other nitridosilicates, such as $SrSiAl_2O_3N_2$ with $B_0 = 131.9(3)$ GPa, and $Ce_4[Si_4O_4N_6]O$ with $B_0 = 131(2)$ GPa and $B' = 5.0(2)$ [10]. The more covalent character of the Si-C bond compared with the Si-N bond might have an influence on the improved hardness and structural high-pressure stability of these compounds. The axial compressibilities show anisotropic behaviour with the b axis being most compressible. Quantum-mechanical DFT-based computations of the high-pressure properties of $Y_2[Si_4N_6C]$ are on-going and will be compared to the experimental results, allowing a further evaluation of the influence of lanthanide substitution.

Oxonitridosilicates (Sions):

With $Ce_4[Si_4O_4N_6]O$ (space group $P2_13$) a novel layer structure type was found [11]. The topology of the layer is hyperbolically corrugated, which can explain the unprecedented cubic symmetry for a layer silicate. The layer is built up by three-membered rings of corner-sharing $SiON_3$ tetrahedra, cross-linked through additional $SiON_3$ tetrahedra. While such small rings are not favoured in oxosilicates due to the electrostatic repulsion of SiO_4 tetrahedra, they are frequently found in less ionic nitridosilicates. Quantum-mechanical DFT-based computations at high pressures revealed a bulk modulus of $B_0 = 131(2)$ GPa for $Ce_4[Si_4O_4N_6]O$ [10]. However, when calculating the elastic constants of $Ce_4[Si_4O_4N_6]O$ by imposing finite strains, very large errors for the bulk modulus [$B_0 = 155(23)$ GPa] indicated structural instabilities and a possible phase transition at high pressures up to 18 GPa. Our experiments up to 28 GPa confirmed the proposed instability of this structure type. We detected a first-order phase transition occurring in a range between 8 and 10 GPa. This phase transition is reversible and shows a slight hysteresis. The space group symmetry is reduced to $P2_12_12_1$ following a group-subgroup relationship, which indicates a displacive structural mechanism.

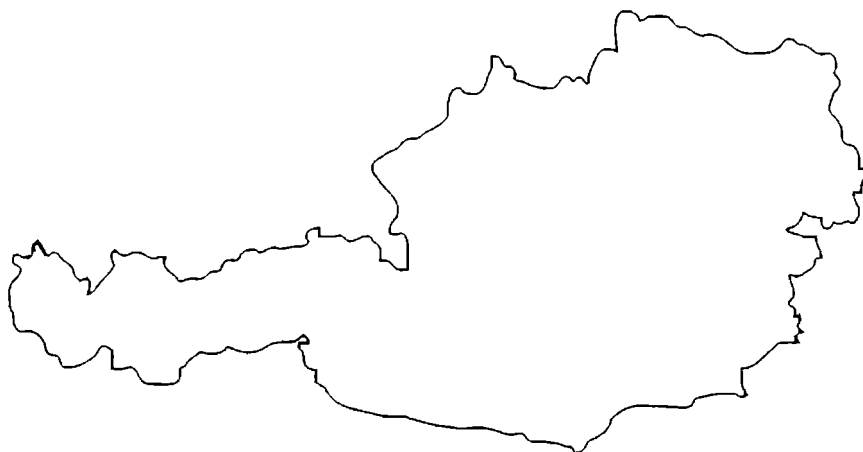
The authors gratefully acknowledge financial support from the Deutsche Forschungsgemeinschaft (DFG) through a Research Fellowship (WI 1232/17-1) within the project SPP-1136. Thanks are due to the ESRF for synchrotron beam time.

Literature

- [1] SCHNICK, W. & HUPPERTZ, H. (1997): Nitridosilicates - a Significant Extension of Silicate Chemistry. - Chem. Eur. J., 3, 679-683.

- [2] SCHNICK, W., HUPPERTZ, H. & LAUTERBACH, R. (1999): High-Temperature Syntheses of Novel Nitrido- and Oxonitridosilicates and Sialons Using RF Furnaces. - *J. Mater. Chem.*, 9, 289-296.
- [3] SCHNICK, W. (2001): Nitridosilicates, Oxonitridosilicates (Sions), and Oxonitridoaluminosilicates (Sialons) – New Materials with Promising Properties. - *Int. J. Inorg. Mater.*, 3, 1267.
- [4] HUPPERTZ, H. & SCHNICK, W. (1996): BaYbSi₄N₇ - überraschende strukturelle Möglichkeiten in Nitridosilicaten. - *Angew. Chem.*, 108, 2115; *Angew. Chem. Int. Ed. Engl.*, 35, 1983.
- [5] HUPPERTZ, H. & SCHNICK, W. (1997): Synthese, Kristallstruktur und Eigenschaften der Nitridosilicate SrYbSi₄N₇ und BaYbSi₄N₇. - *Z. Anorg. Allg. Chem.*, 623, 212.
- [6] HUPPERTZ, H. & SCHNICK, W. (1997): Eu₂Si₅N₈ and EuYbSi₄N₇ - The First Nitridosilicates with a divalent Rare Earth. - *Acta Crystallogr. Sect. C*, 53, 1751.
- [7] HÖPPE, H. A., KOTZYBA, G., PÖTTGEN, R. & SCHNICK, W. (2001): High-temperature synthesis, crystal structure, optical properties, and magnetism of the carbidonitridosilicates Ho₂[Si₄N₆C] and Tb₂[Si₄N₆C]. - *J. Mater. Chem.*, 11, 3300-3306.
- [8] HAMMERSLEY, A. (1998): FIT2D, Version 10.27, Reference Manual, ESRF, Grenoble, France.
- [9] LARSON, A. C. & VON DREELE, R. B. (1994): Los Alamos National Laboratory Report LAUR, 86-748.
- [10] WINKLER, B., HYTHA, M., HANTSCH, U. & MILMAN, V. (2001): Theoretical study of the structures and properties of SrSiAl₂O₃N₂ and Ce₄[Si₄O₄N₆]O. - *Chemical Physics Letters*, 343, 622-626.
- [11] IRRAN, E., KÖLLISCH, K., LEONI, S., NESPER, R., HENRY, P. F., WELLER, M. T. & SCHNICK, W. (2000): Ce₄[Si₄O₄N₆]O – a Hyperbolically Layered Oxonitridosilicate Oxide with an Ordered Distribution of Oxygen and Nitrogen. - *Chem. Eur. J.*, 6, 2714-2720.

**DIPLOMARBEITEN UND DISSERTATIONEN
ÖSTERREICHISCHER UNIVERSITÄTEN
(AUSZÜGE)**



**SHOCK PETROGRAPHY AND GEOCHEMICAL STUDIES OF ROCKS FROM THE
WOODLEIGH (AUSTRALIA), CHESAPEAKE BAY (USA), EL'GYGTYN (RUSSIA)
IMPACT STRUCTURES AND VARIATION IN CHEMICAL COMPOSITION IN
AUSTRALASIAN TEKTITES FROM DIFFERENT LOCALITIES OF VIETNAM**

by

Kassa Amare

Dissertation zur Erlangung des Doktorgrades an der
Formal- und Naturwissenschaftlichen Fakultät der Universität Wien

Institut für Geologische Wissenschaften
Wien, Juni 2004

Abstract

This thesis presents the results of shock petrographic studies of rocks from the Woodleigh (Australia), Chesapeake Bay (USA), and the El'gygtygn (Russia) impact structures. Also included are the results of a comparative study of chemical compositions of Australasian tektites from different localities of Vietnam.

Petrographic studies of 11 thin sections from the Woodleigh impact structure, obtained from the Woodleigh 1 drill core between 194.5 to 272 m, depth have provided for the identification of planar deformation features (PDFs). The purpose of this study is to provide supportive evidence for the shock pressure involved, by measuring crystallographic orientation of PDFs with universal stage (U-stage). Shock metamorphosed effects in the Woodleigh structure include multiple sets of (PDFs), diaplectic glass (in quartz and feldspar), and kink bands in biotite. All thin sections examined display the PDF deformation phenomenon. Abundant PDFs in quartz, in addition to diaplectic glass and isotropization, are the main shock deformation effects observed in this study. The measurements of the crystallographic orientation of PDFs showed the occurrence of the shock characteristic rational crystallographic planes, {10-13}, {10-12}, {11-22} and {10-11} with a dominance of the {10-13}, and {10-12} orientations. These features provide conclusive evidence that rocks and minerals at Woodleigh structure have undergone shock metamorphism; which are generally taken to indicate average shock pressure on the order of 15 to 25 GPa. Moreover, the abundance of diaplectic quartz and/or feldspar glass displayed by some samples requires shock pressure around 30 to 35 GPa.

Shock petrographic studies were conducted on impact rocks from the Chesapeake Bay impact crater from four different drill cores. These cores were taken from Exmore, Windmill Point,

Kiptopke, and Newport News; these have penetrated into the Exmore breccia. More than 50 thin sections collected from 4 drill cores of the Chesapeake Bay crater were examined for the presence of distinct mineral deformation features. The numbers of the shocked fragments found in the thin section is relatively variable in each sample suite, where a limited number of shocked grains was identified from all the analyzed samples of this study. Shock metamorphism in Chesapeake Bay samples is manifested by a number of quartz grains with single and occasionally with multiple sets of PDFs. Up to to three sets of PDFs with characteristic crystallographic orientation were found in quartz and feldspar grains. The PDFs in the shocked quartz were found to occur in intersecting sets of planes corresponding to specific crystallographic orientation with {10-13}, {10-12}, {10-11} and {21-31}. These planes are indicative of moderate shock pressures.

The 18 km diameter El'gygytgyn impact crater, Chukotka (Russia), is the only currently known impact structure formed in siliceous volcanic, including tuffs. Shock metamorphism of siliceous volcanic rocks were studied by investigations of the progressive shock-induced changes in quartz and feldspar phenocrysts and clasts of porphyritic volcanic rocks and tuffs. The stages of shock metamorphism of volcanic rocks and tuffs observed range from weakly shocked rocks to partially and completely melted rocks.

One hundred thirteen tektite samples collected from different localities of Vietnam (Hanoi, Vinh, Dalat and Saigon), were studied for their major and trace element composition using instrument neutron activation analysis and electron microprobe analysis. The main objective of the study was to determine the variation in chemical composition, and to compare their chemical variation with other Australasian tektites. The results were statistically treated for significance in the element abundances and their variation with each other and with other Australasian tektites. The tektites of this study are classified in to two groups based on their appearance and chemical variation: Splash-form and Muong Nong-type. The splash-form are usually spherical, tear-drop, dumbbell, and disc shaped with pitted or grooved surface and slightly lower silica contents from 69.7 to 76 wt.%, whereas Muong Nong-type tektites are considerably larger than splash-form and are blocky and chunky appearance with higher silica contents in the range 74 to 80.85 wt.%. The major elements of all samples show an inverse correlation with the SiO₂. Correlation coefficient have been calculated for each tektite group of this study. Many chemical similarities are noted between Hanoi and Vinh tektites, from the North of Vietnam and between Dalat and Saigon tektites. Tektites found in the North Vietnam (Hanoi and Vinh) are recognized by higher contents of Na₂O, K₂O and CaO, where as tektites found in the South Vietnam (Dalat and Saigon) are rich in MgO, FeO, Cr and Ni. The major elements of the tektites from Hanoi, Vinh, Dalat and Saigon are almost similar in composition with the average splash-form of indochinites. Similarly the average major element composition of the Muong Nong-type of this study closely resembles those of Muong Nong-type indochinites, indicating that they were derived from rocks of similar composition. However, the high-Mg tektites, high-Ca philippinites and high-Ca australites from data of CHAPMAN & SCHEIBER (1969) are distinctly different from the Vietnam tektites (this study) being higher in MgO and CaO, respectively compared to the tektites of this study. The trace element ratios Ba/Rb, Th/Sm, Th/Sc and the rare earth element (REE) contents of tektites of this study are similar to the average upper continental crust.

**ZUR GEOLOGIE DES PIZ MUNDIN-GEBIETES
(ENGADINER FENSTER, ÖSTERREICH-SCHWEIZ):
STRATIGRAPHIE, GEOCHRONOLOGIE, STRUKTUREN**

von

Rufus J. Bertle

Dissertation zur Erlangung des Doktorgrades an der
Naturwissenschaftlichen Fakultät der Universität Wien

Institut für Geologische Wissenschaften
Wien, März 2004

This thesis represents a completely new investigation of the region between Samnaun und Reschenpass at the Austrian – Swiss border. The whole region was mapped in a scale of 1 : 10.000. This thesis presents the first mapping of this region since HAMMER (1923). Mapping was combined with detailed petrological-geochronological and micropaleontological investigations of the outcropping rocks.

The working area can be divided into two main units: the penninic units of the Engadine Window and the frame consisting of the Austroalpine nappes. The frame is made up by the Silvretta nappe, which reduces its thickness from W to E. The Ötztal nappe overthrusts the Silvretta nappe along the Schlinig fault. W-directed overthrusting took place during the Cretaceous. Later the fault was reactivated as a east-directed normal fault. Thrusting along the Schlinig fault resulted in ductile carbonate mylonites in mesozoic sediments of the Engadiner Dolomiten just below the thrust. In this mylonites calcite is deformed in a ductile way whereas dolomite reacts brittle. Therefore the mylonite consists of a ductile calcite-matrix in which brittle deformed dolomite clasts are embedded. The exact trace of the Schlinig fault was unknown in the region of Piz Lad until now. New mapping showed that the mesozoic sequence of Piz Lad rests above biotite-paragneisses (type Plamort).

Thrusting of the Ötztal nappe over the Silvretta nappe resulted in diaphoreses of the basement rocks of the Silvretta nappe: feldspar and biotite break down to chlorite and growth of white mica in the sediments of the Engadiner Dolomiten is observed. The age of thrusting and related metamorphism in the Austroalpine nappes is Cretaceous in age, proofed by geochronological dating. The Silvretta nappe itself is thrust upon the Engadine Window along a highly ductile calcmylonite.

The Engadine window of the working area consists of the Middle Penninic Tasna nappe and the deeper Zone of Pfunds of North Penninic (Valais) origin. Structural imprint of the penninic units is much younger than that of the Austroalpine nappes as indicated by fossils and geochronological data from the penninic units.

The Tasna nappe shows a reduced sequence compared to its type locality further in the W. It is built up of a basement which crops out as a crust-mantle-boundary. This contact can be studied very well near Mot and Plattamala:

Ultramafics of lherzolitic composition (with preserved olivine, clinopyroxene and orthopyroxene) are overlain by small discontinuous lenses of gabbro. A few outcrops also show small basaltic dikes within the ultramafics. Along a transitional contact banded amphibolites border the ultramafics and gabbros. The amphibolites grade into the acid and less deformed Tasna granite. Sometimes schlieren-type to intrusive contacts of gabbroic rocks to granites can be observed. A metamorphic overprint of the ultramafics is indicated by the occurrence of older paragonitic hornblende (Al_2O_3 up to 14 %) and later actinolitic-tremolitic amphiboles which are found in joints. Within the ultramafics retrograde garnet peridotites can be found. The retrograde peridotites are characterized by symplectites of green spinell and pyroxene, indicating that the rock was probably a garnet peridotite, that was metamorphosed at about 900°C and 16 kbar. Discordant basaltic dikes and small gabbro lenses within the ultramafic body of Nauders show within-plate signatures in the geochemical characteristics. A very special ultramafic rock in the core of the occurrence shows the paragenesis of large hercynite (up to more than 1 cm size) rimmed by epidote?, pyroxene, kaersutite, phlogopite and an unidentifiable symplectite.

The sedimentary cover of the Tasna nappe is very reduced in the working area. Relics of Steinsberg limestone (crinoid-belemnite-limestone of lower liassic age) rest directly on ultramafics, in some parts also Tristelformation and Gault formation (lower Cretaceous) can be found.

The imprint of regional metamorphism in the Tasna nappe is difficult to assess. Green amphiboles in joints of the serpentinites, breakdown of feldspar of the Tasna granite (feldspar reacts to chlorite, albite, epidote, tremolite and questionable pumpellyite) as well as growth of stilpnomelane in the latter indicate lower greenschist-facies overprint during alpine time. In joints of diorite type rocks blue amphibole was observed.

Until now a detailed stratigraphic sequence of the undifferentiated Graue Bündnerschiefer of the Zone of Pfunds was missing. During the mapping campaigns of this thesis 6 formations could be distinguished:

The oldest sediments that crop out are radiolarites of upper Jurassic to lower Cretaceous age, which can always be found in stratigraphic contacts to the blueschist-facies basalts of Piz Mundin. In most cases however the basalts are overlain by the tuffitic transition member which itself grades into the Neokomschiefer. This transition is given by reduction of the chlorite content of the sediment from bottom to top and increasing carbonate content of the rock at the same time. The Neokomschiefer grade into the Tristelformation which is of Barremian to Aptian age as indicated by foraminifera and dasycladales. *Neotrocholina fribourgensis*, orbitolinids and *Quinqueloculina* sp. are found at the Saderer Joch, dasycladales and *Quinqueloculina* sp. as well as questionable *Orbitolina* sp. at Piz Mundin. Both indicate a lower Cretaceous age of the sediment. Decreasing carbonate content and simultaneous increase of the amount of quartz clasts are typical for the gradational part of the Tristelformation to the stratigraphically higher Gault formation. The Gault formation is a turbiditic sequence characterized by the rhythmic change of quartz sandstones layers and dark phyllite layers. At the base of the Gault formation single layers of Tristelkalk are intercalated.

The Gault formation is overlain by the Fuorcla d'Alp formation which represents black shales of probable Albian age (max. age R. *appeninica* zone). The age of the black shales is defined by lithostratigraphic comparison with the nonmetamorphic and fossiliferous sequence of the helvetic units of Vorarlberg. The youngest part of the stratigraphic column at Piz Mundin is represented by the Malmurainza sequence. It is a turbiditic sequence of upper Cretaceous to lower Tertiary age. The sandstones show highly variable composition: pure calc sandstones can change with pure quartz sandstones as well as with sandstones containing blonde dolomite clasts and gneissic clasts. Parts of the Malmurainza sequence which show strong input of detrital mica may correspond to the Reiselsberg sandstone (Cenomanian to Turonian) of the Rhenodanubic realm. Taking this comparison in consideration the paleogeographic position of the Rhenodanubic realm would be in between the Piz Mundin ophiolite in the north and the Tasna nappe in the south. The Roz breccia may represent the youngest parts of the Malmurainza sequence and is of upper most Cretaceous age as indicated by reworked *Orbitoides* sp. and *Globotruncana* arca. In the field where no difference between the formations was visible due to unfavourable intersection of schistosity and topography only Graue or Bunte Bündnerschiefer were mapped.

The rocks of the Zone of Pfunds suffered HP-LT-metamorphism, the retrograde path was reconstructed using petrological methods:

Bündnerschiefer in the region of Piz Mundin are characterized by the HP-paragenesis of carpholite – phengite. Overprint of greenschist facies grade resulted in the break down of carpholite to chlorite and in the growth of a phengitic rim with lower Si-content around phengite I. Radiolites contain the HP-paragenesis jadeitic pyroxene – blue amphibole.

Basalts and ophicarbonates are characterized by the following HP-paragenesis:

Jadeitic clinopyroxene – aragonite – blue amphibole – stilpnomelane.

The following greenschist facies overprint is defined by actinolite – epidote/clinozoisite – chlorite and pumpellyite (partly these minerals were also produced during oceanic metamorphism before the HP-event).

Geothermobarometric calculations resulted in:

P_{\min}	=	ca. 10 kbar and $T = 350^{\circ}\text{C}$ (Jadeite)
P	=	13 kbar and $T = 375^{\circ}\text{C}$ (Carpholite)
P	=	7.5 kbar and $T = 375^{\circ}\text{C}$ (Aragonite)
T_{\max}	=	ca. 400°C (Stilpnomelane)
T_{\max}	=	380°C (Carpholite)

The cross cutting veins of the basalts are characterized by quartz, calcite, feldspar and axinite which is missing in veins in the Bündnerschiefer. Axinite was only visible at Piz Mundin. Fluid inclusion investigations in quartz helped us to define the low grade evolution of the metamorphic path. The fluid inclusions (FI) investigations resultet in:

Vein quartz from the Piz Mundin was suprisingly rich in FI. At the base of the vein quartz at the contact to the host rock (blueschist) epidote-clinozoisite cristalls are visible. Futhermore amphibole is visible. It is common at the base of the vein quartz and decreases towards the middle of the vein. FI occure as H_2O -rich FI indicating high pressure of trapping.

Quartz from the upper most part of the Zone of Pfunds from S of Zebblasjoch (W of Samnaun Dorf) shows two main groups of primary FI could be differentiated at room temperature: homogenous FI and such with a bubble. All FI were frozen at max. temperatures of ca. -56°C . Bigger FI show cracking due to crystallisation pressure (build up of wings), the cracks however closed again during heating, so that the FI remained closed. Initial melting started between -20°C (first recrystallisation signs) and -9°C , final melting was observable at -1°C to 0°C . Then the FI was a.) homogenous or b.) showed a bubble. Homogenisation Temp. of the inclusions with bubble were in the range of 70 to 100°C , most of them between 70 and 80°C . The data indicate a more or less pure H_2O -system for the FI under high pressure. Assuming a crystallisation temperature of the crystals of about 200 to 250°C and a density of the FI between 0.97 and 1.0 g/cm^3 pressures of 2.5 to 4.5 kbar are indicated for the time of trapping of the fluids.

The same P-T-conditions (same chemistry and melting & homog. Temp.) could be derived from FI in quartz from the Salaaser Kopf (Idalpe) for the late metamorphic evolution of the Fimber unit.

The reconstructed metamorphic evolution of the Piz Mundin area shows all signs of a very cool pressure-dominated subduction-related metamorphism. The reconstructed P-T path is similar to the well known ones of Crete and the San Franciscan complex.

The metamorphic overprint of the penninic units was dated using different geochronological methods: It was tried to date carpholite using the Sm-Nd-method. Unfortunately the spread of the mineral concentrate was too low to calculate a reasonable age.

The blue amphiboles were dated using the Ar-Ar-methode. However dating resulted in Ar-excess-ages of no geological significance. Ar-ages range within ca. 30 and ca. 47 Ma within the Zone of Pfunds and show a complex pattern of regional distribution. It is interestingly to note, that all age spectras with plateau ages show older ages in the high-temperature-steps of the Ar-release diagram. Ar-plateau age of amphibole from the crust-mantle-boundary at Mot is ca. 185 Ma .

Rb-Sr dating of white mica from the Bündnerschiefer and the tuffitic transition member resulted in ages between 26 and 37 Ma . The metamorphic ages gained from the micas of the tuffitic transition member may be correlated with the HP-event. Whole rock thin slab investigations of blueschists with the Rb-Sr-method did not allow to calculate age as spread of the different lithologies was too small.

Fission track dating gives us some information about the late exhumation and cooling stages of the penninic units. One sample from Piz Malmurainza resulted in 48 Ma for zircon, one sample from Nauders also in 48 Ma for zircon. Thus the FT-ages of zircon are older than micas dated with Ar-Ar from nearby localities. It can be concluded, that subduction and exhumation of the schistes lustrés was very fast.

In the presented paleogeographic reconstruction the Zone of Pfunds is located in the North penninic realm (Valais). The Briançonnais (Tasna nappe) is located south of the Zone of Pfunds. Based on stratigraphic and sedimentological arguments the Rhenodanubic realm is located N of the Zone of Pfunds. Its detrital input mainly originates from the W and N. Because of stratigraphic, sedimentological and tectonic arguments the Glocker nappe of the Tauern window is also located within the North penninic realm and correlated to the Zone of Pfunds. A Middle penninic realm (Briançonnais) does not outcrop or did not exist in the Tauern realm. The paleogeographic position of the Rhenodanubic realm in the Tauern section is not clear at the moment.

**NATÜRLICHE GESTEINE ALS SENSORMATERIALIEN ZUR ERFASSUNG VON
UMWELTEINFLÜSSEN AUF BAUDENKMÄLER**

von

Thomas Bidner

Dissertation zur Erlangung des Doktorgrades an der
Naturwissenschaftlichen Fakultät der Universität Innsbruck

Institut für Mineralogie und Petrographie
Innsbruck, Dezember 2003

Die Erhaltung historischer Denkmäler als Zeugen unseres kulturellen Erbes ist eine Aufgabe, die in ihrer Komplexität nur in der Zusammenarbeit verschiedener Fachdisziplinen zu bewältigen ist. In den kommenden Jahren wird der sorgsame Umgang mit den verfügbaren finanziellen Reserven einen stetig steigenden, zentralen Stellenwert innerhalb der Aktivitäten zum Schutz und zur Erhaltung historischer Denkmäler einnehmen. Dies bedeutet, daß neben der weiterführenden Arbeit zur Entwicklung verbesserter Methoden zur Konservierung und Restaurierung kultureller Güter, die auf dem wachsenden Verständnis grundlegender Prinzipien und Mechanismen der Materialzerstörung beruhen muß, die Dokumentation und das Management der Kulturgütererhaltung verstärkte Aufmerksamkeit erhalten müssen. Prioritätenlisten, basierend auf interdisziplinärer wissenschaftlicher Dokumentation, sollen die Verantwortlichen für die Erhaltung von Kulturgütern in ihrer Entscheidung unterstützen, wo, wann und wie konservierende und / oder restaurierende Eingriffe an Denkmälern zu setzen sind. Die sorgfältige Beobachtung von Umwelteinflüssen und der daraus resultierenden Schadensentwicklung ist ein essentieller Teil einer vorausschauenden Erhaltungsstrategie, eine Anforderung die häufig aufgrund der damit im Allgemeinen verbundenen hohen Kosten nicht realisierbar ist.

Das "in-situ Monitoring" mittels Sensormaterialien stellt den Versuch einer neuen Annäherung an diese Forderung dar. Für Metall und Glas sind entsprechende Monitoring-Systeme bereits etabliert. Auch für den Einsatz von Natursteinen liegt bereits eine VDI-Richtlinie vor (VDI-Richtlinie 3955, Blatt 3) in der Anwendungsempfehlungen für den Einsatz von Baumberger Sandstein als Schadstoffdetektor zusammengefaßt sind. In Ergänzung zu bestehenden Ansätzen, die von der Reaktion der Materialien auf belastende Einflüsse ausgehen und den Zustand der Materialien als grundlegende Bewertungskategorie erfassen, und in Anlehnung an die angeführten Richtlinien, versteht sich der vorliegende Ansatz als Versuch, den Dokumentationsanspruch über die Beobachtung (Monitoring) exogener Faktoren zu erweitern.

Sensoren aus natürlichen Materialien detektieren im Gegensatz zu den apparativen Meßsystemen Umwelteinflüsse in Summe. Diese Einflüsse verändern die Eigenschaften des Materials und sind über die Bestimmung bestimmter Parameter summarisch zu erfassen.

Die analytische Behandlung ist vergleichsweise einfach, die Anwendung kostengünstig und die Sensoren sind an verschiedenen Stellen eines Bauwerkes zu befestigen. Die große Schwierigkeit besteht darin jene Parameter festzulegen, die am Besten geeignet sind, die Umwelteinflüsse zu charakterisieren. Freilandexperimente an verschiedenen Standorten unter möglichst gut definierbaren, aber jeweils unterschiedlichen, Umweltbedingungen stellen einen möglichen Ansatz dar, um eine Unterscheidung zwischen zumindest einigen der relevanten Parameter oder zumindest Parametergruppen zu erreichen. Diesem Ansatz folgen auch die im Rahmen der gegenständlichen Dissertation durchgeführten Untersuchungen.

In Anlehnung an bereits erfolgte Vorarbeiten (FIMMEL, 1996) wurde für die Exposition der Proben von Laaser und Sterzinger Marmor, sowie Baumberger und Obernkirchner Sandstein, eine Ausbringung auf Mank'schen Karussellen gewählt.

Auf den Trägergerüsten können die Proben auf frei drehbar aufgesetzten Karussellen sowohl nass, also dem Regen ausgesetzt, wie auch trocken, das heißt vor direkter Beregnung geschützt, exponiert werden. Pro Auslageposition (nass / trocken) können jeweils 4 Karusselle mit je 9 Proben so bestückt werden, dass eine möglichst freie, durch die übrigen Proben möglichst wenig behinderte Bewitterung aller exponierten Proben möglich ist.

Aus einheitlichen Blöcken der vier verwendeten Gesteine wurden Plättchen mit den Maßen 5 x 5 x 1 cm geschnitten, im Ultraschallbad gereinigt und bei 105°C bis zur Massekonstanz getrocknet. Ein Teil der Plättchen wurde als Nullprobe zurückbehalten, die übrigen wurden auf den Stationen exponiert. Von jeder Gesteinsart wurden pro Station und Auslage (naß / trocken) jeweils 9 Proben ausgebracht. Daraus ergibt sich eine Gesamtzahl von 216 Proben. Die Exposition startete im September 1997, nach 9 und 22 Monaten wurden die Proben für Untersuchungen in das Labor gebracht. Nach der ersten Expositionsreihe von 9 Monaten wurden an allen Proben Massebestimmungen und Ultraschalluntersuchungen vorgenommen, an allen Marmorproben Messungen der Oberflächenfarbe und von allen Gesteinen von jeder Station und Auslage wurden jeweils 2 Proben für weiterführende Untersuchungen im Labor behalten (Ionenchromatographie, Sorptionsisothermen), die verbliebenen Plättchen wurden wieder exponiert. Nach 22 Monaten wurden alle Proben in das Labor geholt und nach den Untersuchungen als Rückstellproben verwahrt.

Der Auswahl der Standorte lag die Überlegung zugrunde, möglichst große Unterschiede im Hinblick auf die Umweltparameter, sowohl betreffend den klimatischen Einfluss wie auch die anthropogen induzierten Schadstoffe, zu erreichen.

In Anlehnung an die bereits zitierten Vorarbeiten (FIMMEL, 1996) wurden auch für die vorliegende Studie die Stationen in Obergurgl, als relative Reinluftstation, sowie die stärker mit Schadstoffen belasteten urbanen Standorte Innsbruck-Fallmerayerstraße und am Dach des Universitätsgebäudes in Innsbruck, Bruno-Sander-Haus, Innrain 52, genutzt.

Die Ergebnisse der Studie zeigen, dass eine Kombination von feinkörnigen Marmoren (wie z.B. dem Laaser Marmor) und verwitterungsempfindlichen karbonatisch gebundenen Sandsteinen (Baumberger) geeignet ist, über die Masseänderung an trocken und nass exponierten Proben die Umweltbedingungen sowohl an stark als auch an gering mit Schadstoffen belasteten Standorten integral zu erfassen.

Die Untersuchungen zum Aufnahmeverhalten hinsichtlich der vorrangig interessanten Schwefel- und Stickstoffverbindungen haben gezeigt, dass der Baumberger Sandstein die jeweils höchsten Sulfat- und Nitratgehalte aufweist. Außerdem war es möglich, mit diesem Gestein auch einen signifikanten Anstieg der Chloridgehalte nachzuweisen.

Die vorliegenden Daten zeigen, dass es möglich ist, die drei unterschiedlichen Standorte im Vergleich der Sulfatgehalte zu unterscheiden. Bei gleichzeitiger Anwendung eines karbonatisch gebundenen Sandsteines (Baumberger) und eines quarzitisches gebundenen (Obernkirchener), ist es weiterhin möglich zwischen exogen eingetragenen Sulfat und an der Rezeptoroberfläche karbonatischer Materialien durch Reaktion mit den S-Verbindungen entstandenes Sulfat zu unterscheiden.

Für den Nitratgehalt, als Indikator für den Eintrag von Stickstoffverbindungen über die Luft, ist mittels des Baumberger Sandsteines eine klare Unterscheidung zwischen stärker (urbaner Zentralbereich Innsbruck) und schwächer (alpiner Bereich in Obergurgl) belasteten Standorten möglich.

Die durchgeführten Untersuchungen konnten zeigen, dass insbesondere die Kombination eine sensibel auf Umweltbelastungen reagierenden Kalksandsteines mit einem vergleichsweise widerstandsfähigen quarzitisches gebundenen Sandstein eine gute Erfassung und Auftrennung der Belastung unterschiedlicher Standorte mit Schwefel-, Stickstoff und Chlorverbindungen möglich ist und damit eine Methode zur Überwachung sensibler Baudenkmäler zur Verfügung steht.

FIMMEL, R. (1996): Verwitterungsverhalten der alpinen Marmore von Laas und Sterzing. – Dissertation am Institut für Mineralogie und Petrographie der Universität Innsbruck, 116 Seiten, 7 Anlagen.

VDI-Richtlinie 3955, Blatt 3 (2000): Bestimmung der korrosiven Wirkung komplexer Umgebungsbedingungen auf Werkstoffe. Exposition von Naturstein-Plättchen (Manksches Karussell) – Kommission Reinhaltung der Luft (KRdL) im VDI und DIN-Normenausschuss, Fachbereich Umweltqualität, Ausschuss Wirkung auf Werkstoffe, VDI/DIN-Handbuch Reinhaltung der Luft, Band 1 a, 24 Seiten

**HYDROGEOLOGISCHE, SEDIMENTPETROGRAPHISCHE UND HYDROGEOCHEMISCHE
UNTERSUCHUNGEN IM RAUM VON STERZING/ITALIEN**

von

Achim Constantin

Diplomarbeit zur Erlangung des Magisterrgrades an der
Formal- und Naturwissenschaftlichen Fakultät der Universität Wien

Institut für Geologische Wissenschaften
Wien, Februar 2004

Kurzfassung

Im Sterzinger Becken und im unteren Ridnauntal wurden in zwei Beprobungsreihen hydrogeochemische Untersuchungen an Quell-, Fließ- und Grundwässern durchgeführt. Aufgrund des Chemismus konnten so Aussagen über die geologischen Einzugsgebiete der Quellen und Bäche getroffen werden. Oberflächennahe Hangwasserquellen konnten dadurch in der Regel von Grundwäseraustritten mit größeren bzw. tieferen Einzugsgebieten getrennt werden. Daran angeschlossen isotopenchemische Untersuchungen an Quellwässern mit auffällig hoher Mineralisation ergaben Verweilzeiten von wenigen Monaten bzw. Jahren.

Im Bereich landwirtschaftlich genutzter Flächen konnten erhöhte Kaliumgehalte aus dem Düngemiteleinsatz in Quell- und Bachwässern nachgewiesen werden. Analysen auf Nitrat und Nitrit ergaben vereinzelte Überschreitungen der Grenzwerte- im allgemeinen zeichnete sich aber keine größere Kontaminationsproblematik durch Stickstoffverbindungen ab.

An ausgewählten Quell- und Grundwasserproben wurden desweiteren Analysen aus Schwermetalle und insbesondere Arsen durchgeführt. Trotz möglicher geogener und antropogener Kontamitations-Quellen, konnten an diesen Proben keine erhöhten Konzentrationen festgestellt werden. Die hydrologischen Rahmenbedingungen, mit hohen Niederschlägen und geringer Verdunstungsrate, in diesem Gebiet dürften zum raschen Abtransport bzw. Verdünnung von Kontaminationen beigetragen haben. Neben der Auswertung von bestehenden Bohrprofilen wurden geoelektrische Bodensondierungen im Projektgebiet durchgeführt, um Informationen über die Sedimentausbildung der Talfüllungen zu erhalten. Auf dieser Basis wurde ein hydrogeologisches Modell entwickelt, aus dem die Lage von potenziellen Trinkwasserspeichern, aber auch die Mächtigkeit des Abdeckhorizontes hervor geht. Die Erkenntnisse zur hydrostratigraphischen Gliederung des Taluntergrundes konnte auch das Auftreten von artesisch gespannten Grundwässern in diesem Bereich erklären.

Erkundungen zu Altlasten bzw. Verdachtsflächen, sowie potentiellen Gefahrenquellen für das Grundwasser durch den ehemaligen Bergbau am Schneeberg, die landwirtschaftliche Nutzung oder die industrielle Erschließung des Gebietes, liefern darüber hinaus einen Beitrag zum Gewässerschutz.

**KONTAMINATION ODER NATÜRLICHE LÖSUNGERSCHEINUNGEN:
UNTERSUCHUNGEN AN WÄSSERN UND SEDIMENTEN
M NORDOSTEN DER LANDSEER BUCHT, BURGENLAND**

von

Fanko Daniel Humer

Diplomarbeit zur Erlangung des Magisterrgrades an der
Formal- und Naturwissenschaftlichen Fakultät der Universität Wien

Institut für Geologische Wissenschaften
Wien, 2004

Zusammenfassung

Im Zuge der Studie "Grundwasserhöflichkeit im Mittleren Burgenland" (SCHROFFENEGGER, RAKASEDER & KURZWEIL, 1999) wurden im Nordosten des damaligen Untersuchungsgebietes, dem Oberpullendorfer Becken, ungewöhnlich hohe Ionenkonzentrationen in den Oberflächenwässern und oberflächennahen Grundwässern festgestellt. Zusammenhänge mit dort auftretenden Mineralwässern bzw. höher mineralisierten Grundwässern konnten nur lokal ausgewiesen werden, sodass Beeinflussungen der Wässer durch intensive agrarische Nutzung des Gebietes vermutet wurden. Da im Verlauf dieser Studie diese Vermutungen nicht verifiziert werden konnten, war es nun die Aufgabe der hier vorliegenden Arbeit dieser Kontaminationsproblematik nachzugehen und mögliche Kontaminationsquellen aufzuzeigen und zu bestätigen.

Die Untersuchungen basierten im wesentlichen auf Probenahmen aus der Anlage maschinell hergestellter Schürfe, die bis zum ersten Grundwasserhorizont gegraben wurden. Damit sollten einerseits die vorhandenen hydrochemischen Daten verifiziert werden, andererseits sollte durch gezielte Probenahme aus jeder geologisch unterscheidbaren Tiefenstufe des Bodens die Qualität des Abdeckhorizontes und dessen Auslaugungsverhalten geprüft werden.

Die entnommenen Bodenproben wurden hinsichtlich Kornaufbau, sowie Mineralogie untersucht und Eluate angefertigt, mit deren Hilfe es möglich war, physikalische und chemische Eigenschaften des Bodens unter besonderer Berücksichtigung allfälliger mobilisierbarer Schadstoffgehalte bis zum obersten Grundwasserhorizont zu verfolgen. Die erhöhten Ionenkonzentrationen konnten sowohl in den Oberflächenwässern wie auch in den oberflächennahen Grundwässern sehr gut reproduziert werden. Durch Granulometrie und Eluatanalytik konnte zudem sehr anschaulich die Qualität des Abdeckhorizontes nachgewiesen werden.

Schließlich konnte auch anhand von Ionenbewertungen der Einfluss höher mineralisierter Tiefenwässer auf die Chemismen von Grund- und Oberflächenwässern weitestgehend ausgeschlossen werden. Die erhöhten Ionenkonzentrationen sind somit eindeutig auf anthropogenen Einfluss, wahrscheinlich auf die Ausbringung von Düngemitteln, zurückzuführen.

**PETROGRAPHY AND GEOCHEMISTRY OF METASEDIMENTARY, IMPACTOCLASTIC
AND GRANITOID ROCKS FROM DIVERSE GEOLOGICAL SETTINGS**

by

Crispin Katongo

Dissertation zur Erlangung des Doktorgrades an der
Formal- und Naturwissenschaftlichen Fakultät der Universität Wien

Institut für Geologische Wissenschaften
Wien, 2004

Abstract

This thesis presents results of petrographic and geochemical studies on rocks from diverse geological settings. The rocks studied range from impactoclastic, metasedimentary and granitoid rocks. Several spectroscopic analytical techniques were used to obtain whole-rock chemical compositions, including instrumental neutron activation analysis (INAA), X-ray fluorescence spectrometry (XRF), and atomic absorption spectrometry (AAS), whereas mineral compositions were determined by electron microprobe analysis (EMPA). Age determination by the U- Pb zircon method was achieved by thermal ionization mass spectrometry (TIMS) and secondary ionization mass spectrometry (SIMS). The operating principles of each of these analytical methods are described. Because most of the thesis is concerned with various aspects of meteoritic impact cratering and shock metamorphism, an outline of impact cratering processes is also presented. Because of the diversity of the geological problems addressed in this thesis, objectives, results and conclusions of each study are presented separately.

1) The Lukanga Swamp, in central Zambia, was previously proposed as the site of a large (52 km diameter) impact structure on the basis of alleged observation of shock-diagnostic planar deformation features (PDFs). The main objective of this study was to confirm or discount the meteoritic impact origin of the Lukanga Swamp. Petrographic studies showed that the alleged planar features in quartz were not PDFs, but widely spaced, randomly oriented, subparallel, non-planar fluid inclusion trails. Siderophile element abundances such as Cr, Ni, and Co in rocks around the swamp that may indicate extraterrestrial contamination of target rocks were normal for quartz-rich crustal rocks. Similarly, neither aeromagnetic nor seismic data indicated an impact origin of the swamp. Regional structural data synthesis suggested that the Swamp may be of tectonic origin due to reactivation of movements along the major dislocation zones such as the Nyama and Kapiri-Mposhi Dislocation Zones.

2) The Crow Creek Member of the Upper Cretaceous Pierre Shale Formation of eastern South Dakota and northeastern Nebraska contains shock-metamorphosed minerals from the 74-Ma Manson impact structure (MIS). The study was aimed at evaluating the variation of ejecta thickness with distance from the MIS, estimating shock pressures from planar deformation features in shocked quartz, determining meteoritic contamination, if any, in the layer and tracing the source of the ejecta material through the mineralogy and bulk-chemistry of the ejecta. Samples from the Gregory 84-21 core, Iroquois core and Wakonda lime quarry were studied. Contents of siderophile elements could not unambiguously confirm an extraterrestrial component in the Crow Creek Member. PDF measurements on shocked quartz grains recovered mainly from the basal-unit samples of the Gregory 84-21 core indicated shock pressures of at least 15 Gpa. Results of major and trace element abundances and elemental ratios critical to provenance studies coupled with accessory mineral compositions, suggested that the source rocks of the Crow Creek Member were of mixed provenance, ranging from quartzose, intermediate and mafic compositions derived in part from the MIS region. The expected ejecta thicknesses at the sampled locations (409 to 219 km from Manson) were calculated to range from ca. 1.9 to 12.2cm (for the present-day crater radius of Manson), or 0.4 to 2.4 cm (for the estimated transient cavity radius). The trend agreed with the observed thicknesses of the basal unit of the Crow Creek Member, but the actually observed thicknesses are larger than the calculated ones, indicating that not the entire basal unit comprises impact ejecta.

3) There are several pre-orogenic Neoproterozoic granitoid and metavolcanic rocks in the Lufilian-Zambesi belt in Zambia and Zimbabwe that are interpreted to have been emplaced in a continental rift setting that is associated with the break-up of Rodinia Supercontinent. Petrographic and whole-rock chemical analyses of Nchanga granite, Lusaka granite, Ngoma gneiss, metarhyodacites, Munali hills granite and Mpande gneiss, from the Zambian part of the belt were conducted in order to evaluate their chemical characteristics, and tectonic emplacement settings. The geological setting, mineralogical and geochemical features (calcalkaline and peraluminous-metaluminous compositions) indicated that these rocks are not true continental rift granitoids as previously suggested, but exhibit inherited source characteristics of calcalkaline granitic precursor rocks previously emplaced in a continental arc setting. A U-Pb zircon age of 1116.3 ± 1.7 Ma of the Munali hills granite was also obtained, which indicated that some supracrustal rocks in the Zambesi belt of Zambia, which were previously thought to be Neoproterozoic in age, could well be Mesoproterozoic in age or older and places new constraints on regional correlations and tectono-thermal activity in the Lufilian-Zambesi belt.

4) Scapolite is a notable aspect of metamorphism in the Lufilian-Zambesi belt. metamorphism in the belt generally ranged from greenschist facies to amphibolite facies, but locally reached up to eclogite facies. Scapolite is widespread in calc-silicates, marbles, amphibolites and metagabbros and rare granitoid that are metamorphosed at low metamorphic grades. Scapolite was observed in the Munali hills granite gneiss. Both field petrographic studies of the granite gneiss, and associated rocks from the Munali hills area indicated that scapolization was due to metasomatic processes. The scapolite occurs as a pervasive replacement of plagioclase in mineral assemblages that are indicative of amphibolite facies metamorphism. Results of mineral analyses showed that all the scapolites have calcian-marialite compositions, which range from 27-47 Me% and Cl varying from 0.37-0.50 a.p.f.u.

The composition of scapolite is similar to that of the Copperbelt region where there is evidence of evaporite horizons. Moderate to high NaCl salinity, which range from 0.2 – 0.5 moles, and high contents of Cl in scapolite indicate that metamorphism in the belt was accompanied by NaCl-rich fluids, which were derived from evaporite horizons that existed in the metasedimentary succession in the area.

DER REHOVE-OPHIOLITH IM SÜDLICHEN ALBANIEN

von

Elisabeth Katharina Kneringer

Diplomarbeit zur Erlangung des Magistergrades an der
Fakultät für Naturwissenschaften und Mathematik der Universität Wien

Institut für Geologische Wissenschaften
Wien, April 2004

Zusammenfassung

Der Rehove-Ophiolith ist Teil des mesozoisch-thetischen Ophiolithgürtels, der sich in einen Ost- und einen Westtyp unterteilen lässt (OHNENSTETTER, 1995). Im Balkan erstreckt sich der Ost-Ophiolithgürtel an der Grenze zum Serbo-Makedonischen Massiv, das von Zentralserbien über die Vardar-Zone nach Nordgriechenland verläuft (z.B. SMITH & SPRAY, 1984). Die albanischen Ophiolithe sind Teil des West-Ophiolithgürtels, der von Kroatien, Nordbosnien über Montenegro und Albanien nach Griechenland reicht und allgemein als MORB-Ophiolith bezeichnet wird. Dieser West-Ophiolithgürtel kann in Albanien nochmals in einen östlichen und einen westlichen Ophiolithgürtel unterteilt werden, wobei der westliche albanische Ophiolithgürtel einen MORB-Ophiolith darstellt und der östliche allgemein als SSZ-Ophiolith bezeichnet wird (z.B. SHALLO, 1992, 1994; BECCALUVA et al., 1994a, b; ROBERTSON & SHALLO, 2000; BEBIEN et al., 2000). Diese beiden albanischen Gürtel wurden in Nordalbanien schon mehrfach untersucht. Die Untersuchungsergebnisse wurden z.B. von SHALLO 1992, 1994; BECCALUVA et al., 1994a, b publiziert. Die Diplomarbeit beschäftigt sich nun mit der geologischen und petrologischen Situation in Südalbanien, worüber noch wenig veröffentlicht wurde.

Der Rehove-Ophiolith sowie seine Nachbar-Ophiolithe Voskopoja und Morava befinden sich nach den Ergebnissen der Diplomarbeit über der tektonisch überlagernden Melange. Die Manteltektonitsequenz des Rehove-Ophiolithes beinhaltet Lherzolithe, innerhalb derer es häufig zum Auftreten von Harzburgiten, sowie selten zum Auftreten von Duniten kommt. Möglicherweise befindet sich unter den Manteltektoniten eine Einheit von Amphiboliten (PULAJ, 2000) als "metamorphic sole" (wie das unter der oberen Manteltektonitsequenz der Nachbarophiolithe, (Voskopoja und Morava) die zwei Manteltektonitsequenzen aufweisen, der Fall ist.) Darüber treten die Kumulate auf, die hauptsächlich aus Plagiklas-Wehrlithen, Wehrlithen, Troktoolithen, Kumulat-Olvingabbros, sowie aus Melagabbros aufgebaut sind. Über den ultramafischen und mafischen Kumulaten kommt es zum Auftreten von isotropen Gabbros. Geringmächtige massive Basalte und Basaltgänge in den Gabbros definieren die Vulkanite.

Der Großteil des basaltischen Materials findet sich jedoch in Form von Brekzien. Sheeted Dykes und Pillowlaven kommen nur innerhalb der Brekzien als große Komponenten, die ein Volumen von einigen Kubikmetern bis zu mehreren hundert Kubikmetern aufweisen, vor. Die basaltischen Brekzien gehen in ihrer Abfolge in Sandsteinlagen über, die in einigen Fällen auch von Radio-lariten und weiteren Brekzienabfolgen überlagert werden.

Die Brekzien sind folgendermaßen zu beschreiben:

Diese sind in der unteren Einheit monomikt und weisen eckige Komponenten auf; in der oberen Einheit bestehen diese jedoch aus vielen verschiedenen kantengerundeten bis angerundeten Komponenten. Daher können die Brekzien in 4 verschiedene Gruppen eingeteilt werden:

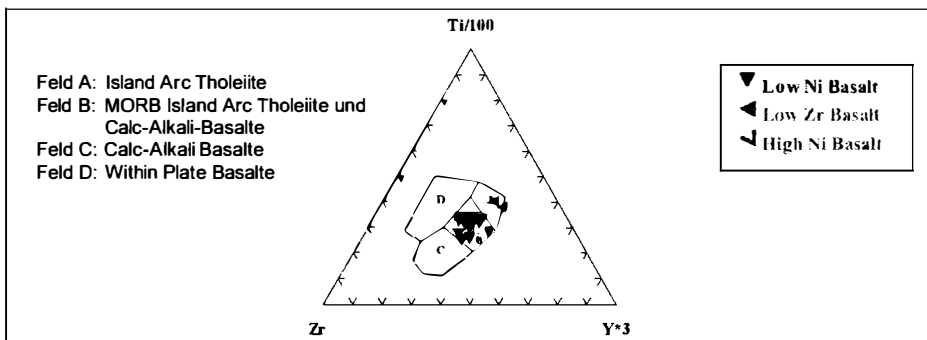
- 1.) Monomikte Brekzien, die nur aus einem Gesteinstyp (meist Basalt) bestehen, keine Matrix enthalten und nur sehr eckige Komponenten aufweisen (Brekzien der unteren Einheit)
- 2.) Brekzien, die aus verschiedenen Basalten und Diabasen bestehen
- 3.) Polymikte Brekzien, die unterschiedliches magmatischen Material (Basalte, Gabbros, Reste von Kumulaten) aufweisen und deren Komponenten eckig bis leicht kantengerundet sind.
- 4.) Polymikte Brekzien, die magmatisches Material und Sedimente aufweisen und kantengerundet bis angerundet sind (Brekzien der oberen Einheit).

Der Großteil der Brekzien gehört zu den Gruppen 1 und 4.

Die Basalte sind folgendermaßen einzuteilen:

Die Basalte weisen im Ti/1000 vs. V Diagramm (nach SHERVAIS, 1982) die gesamte Breite der MORB-Zusammensetzung auf, die von der Grenze zu den Arc Basalten über die der normalen MORB Basalte bis zur Grenze zu den Intra Plate Basalten reicht.

In den klassischen Diskriminierungsdiagrammen (z.B. dem Ti/100-Zr-Y*3 Dreieck, PEARCE & CANN, 1973) befinden sich die meisten Basalte MORB-Feld; eine kleine Gruppe fällt im Diagramm jedoch in das Feld der Volcanic Arc Basalte. Im Zr/Y vs. Zr Diagramm (PEARCE & NOVY, 1979) fällt der Hauptteil der Proben entweder in den überlappenden Teil von Island Arc Basalten und Mittelozeanischen Rücken-Basalten oder an die Grenze der Within Plate Basalte zu den Mittelozeanischen Rücken-Basalten; eine kleine Gruppe mit einem sehr niedrigen Zr/Y zu Zr-Verhältnis (unter 2) weist jedoch eine klare Volcanic Arc Signatur auf.



Ti-Zr-Y Diskriminierungsdiagramm für Basalte nach Pearce & Cann (1973).

Diese Diagramme zusammen ergeben eine Unterscheidung von mindestens zwei Gruppen für den Rehove-Ophiolith:

- a) eine große Gruppe mit intermediärem Ti und Zr Gehalt
- c) eine kleine Gruppe mit niedrigem (bis intermediärem) Ti und Zr Gehalt

Im Nachbar-Ophiolith Voskopoja gibt es auch noch eine Gruppe

- b) mit einem hohem Ti und Zr Gehalt (HOECK et al. 2002).

Wird Ni (ppm) gegen MgO (Gew.%) geplottet, sind zwei Trends innerhalb der gesamten Reichweite der MgO-Zusammensetzung von 6-12 % erkennbar.

Ein Trend zeigt eine starke Anreicherung von Ni (bis zu 400 ppm) bei hohem Mg; der andere Trend zeigt auch bei hohem Mg nur eine kleine Anreicherung von Ni (höchstens 125 ppm). Bemerkbar ist, dass die intermediäre Ti-Zr-Gruppe diese Trends unterteilt. Die Werte von TiO₂, P₂O₅, Y, Sc und V zeigen bei ansteigenden Ni-Gehalt eine fallende Tendenz.

Wenn man nun diese Einteilung mit der Einteilung in die Basalte kombiniert, so erhält man schließlich mindestens drei Gruppen für den Rehove-Ophiolith:

Gruppe 1 weist einen intermediäre Ti- und Zr- mit niedrigem Ni- Gehalt auf (Low Ni Group).

Gruppe 2 stellt Basalte mit intermediären Ti- und Zr- mit hohem Ni- Gehalt dar (High Ni Group).

Gruppe 4 hat niedrige Ti- und Zr- Gehalte (mit hohem Ni Gehalt) (low Ti Group) (Im Voskopoja-Massiv (Nachbarmassiv) gibt es nach HOECK et al. (2002) auch noch eine Gruppe 3.) mit einem hohem Ti und Zr- Wert (high Ti Group)).

Gruppe 4 tendiert in Richtung SSZ-Basalte, die Ähnlichkeiten mit den Basalten des nordalbanischen Ostgürtels aufweisen. Aus diesem Grund ist nach HOECK et al. (2002) anzunehmen, dass sich der Rehove-Ophiolith, sowie seine Nachbar-Ophiolithe Voskopoja und Morava an einem Übergangsbereich, von MORB zu SSZ-Environment gebildet hat.

Bei einem Vergleich der ultramafisch bis mafischen Kumulate sowie der basaltischen Vulkaniten des Rehove-Massives (sowie seiner Nachbarmassive Voskopoja und Morava) mit den Massiven des westlichen Ophiolithgürtels in Nordalbanien sowie der Gegenüberstellung mit dem Pindos-Ophiolith zeigt sich eine systematische Variation in Petrographie und Geochemie von Nord nach Süd im Westgürtel mit einer ansteigenden SSZ Signatur Richtung Süden. Somit zeigen die albanischen Ophiolithe des Westgürtels hinsichtlich ihrer petrologischen und geochemischen Daten insgesamt eine systematische Variation von Nord nach Süd mit einer ansteigender SSZ-Signatur Richtung Süden.

Geochemisch gesehen stellen also die Basalte einen Übergang von einem MORB zu einem SSZ-Environment dar. Dies ist auf folgende mögliche Arten zu erklären:

1a) Eine intraozeanischen Subduktionszone stört einen asthenosphärischen Mantelplume unter einem Mittelozeanischen Rücken (BEBIEN et al., 2000; INSERGUEIX-FILIPPI et al. 2000). Das könnte durch enge räumliche und zeitliche Verknüpfungen zwischen einem noch produzierenden asthenosphärischen Mantel, der noch MORB-Schmelzen erzeugt, und einer von der Subduktionszone beeinflussten Mantelsektion verursacht werden. Durch das Wasser der Subduktionszone kann es zur Bildung von low-Ti und very-low-Ti (boninitische) Magmen kommen (BEBIEN et al., 2000; INSERGUEIX-FILIPPI et al. 2000).

1b) Von JONES & ROBERTSON (1991), ROBERTSON & SHALLO (2000) und ROBERTSON (2002) werden ähnliche Prozesse vorgeschlagen, die ein gemeinsames Auftreten von MOR- zu SSZ- Basalten erklärt. Der Unterschied besteht darin, dass das Modell von INSERGUEIX-FILIPPI et al. (2000) eine gleichzeitige Eruption beider Laventypen erlaubt, während das Modell von ROBERTSON und Coautoren eine sukzessive Erzeugung von MORB zu SSZ-Basalten bevorzugt.

2) Ein alternatives Modell dazu könnte die Situation des dreieckig geformten Laue-Beckens sein. Hier ist die Spreading-Zone eines Back Arc-Basins in separate Spreading Center unterteilt (PEARCE, 1999; PEARCE & PARKINSON, 1993). Während sich die Subduktionszone im Süden, wo das Becken enger wird, in der Tiefe der überlagernden Spreadingzone annähert, beeinflusst die Subduktionszone steigend das Magma durch die Beimengung von Wasser und anderer mobiler Elemente wie K, Ba oder Rb. Dort wo die Spreading-Zone weiter entfernt ist, entstehen Magmen, die dem MORB ähnlich sind.

Dieses Modell könnte besonders gut auf die albanischen Ophiolithe zutreffen, weil es die Variabilität der Zusammensetzung der basaltischen Laven entlang des Streichens der West-ophiolithe von stärkeren MOR Basalten im Norden zu stärkeren SSZ-Basalten im Süden erklärt. Es gibt jedoch keine überzeugenden Beweise für eine Back-Arc Interpretation der West-Ophiolithe.

Aufgrund der Struktur des Ophiolithes mit seinen extrem starken Auftreten von verschiedenen Arten von Brekzien und einem Vergleich anderer Massive, die eine solche Entstehungsgeschichte erfahren haben (z.B. das Masirah-Massiv nach z.B. MEYER et al., 1997), ist anzunehmen, dass sich der Rehove-Ophiolith an einer Transform-Fault gebildet haben muss. Diese könnte z. B. nahezu vertikal zu dem Spreading, das sich innerhalb der Übergangszone von MORB zu SSZ stattfindet, verlaufen sein.

Literatur

- BEBIEN, J., DIMO-LAHITTE, A., VERGELI, P., INSERGUEIX-FILIPPI, D. & DUPEYRAT, L. (2000): Albanian ophiolites. I. Magmatic and metamorphic processes associated with the initiation of a subduction. - *Ophioliti* 25(1), 39-45.
- BECCALUVA, L., COLTORTI, M., DEDA, T., GJATA, K., HOXHA, L., KODRA, A., PIRDENI, A., PREMTI, I., SACCANI, E., SELIMI, R., SHALLO, M., SIENA, F., TASHKO, A., TERSHANA, A., TURKU, I. & VRANAI, A. (1994a): A cross section through western and eastern ophiolitic belts of Albania (Working Group meeting of IGCP Project no. 256 - Field trip A). - *Ophioliti*, 19 (1), 3-26.
- BECCALUVA, L., COLTORTI, M., PREMTI, I., SACCANI, E., SIENA, F. & ZEDA, O. (1994b): Mid-ocean ridge and suprasubduction affinities in the ophiolitic belts of Albania. - *Ophioliti*, 19 (1), 77-96.
- HOECK, V., KOLLER, F., MEISEL, T., ONUZI, K. & KNERINGER, E. (2002): The Jurassic South Albanian ophiolites: MOR- vs. SSZ-type ophiolites. - *Lithos* 65, 143-164.
- INSERGUEIX-FILIPPI, D., DUPEYRAT, L., DIMO-LAHITTE, A., VEGRELY, P. & BEBIEN, J. (2000): Albanian ophiolites. II.- Model of subduction zone infancy at a Mid Ocean Ridge. - *Ophioliti* 25(1), 47-53.
- ISPGJ-FGJM-IGJN, 1983. Harta gjeologjike e Shqipërisë. Scale 1:200 000, Tirana.
- JONES, G. & ROBERTSON, A. H. F. (1991): Tectono-stratigraphy and evolution of the Mesozoic Pindos ophiolite and related units, northwestern Greece. - *J. Geol. Soc.* 148, 267- 288.

- MEYER, J., MERCOLLI, A. & IMMENHAUSER, A. (1997): Off-ridge magmatism and seamount volcanoes in the Masirah island ophiolite. - *Oman. Tectonophysics* 267, 187-208.
- OHNENSTETTER, M. (1995): Introduction, In: Workshop on Albanian ophiolites and related mineralization. - IUGS/UNESCO Modeling Programme, Papers and Abstracts, Field guidebook, 10. - 17. October, 1995, 3-5. Editions BRGM.
- PEARCE, J. A. (1999): Western Pacific analogues of Eastern Mediterranean ophiolites. - *EUG 10, Strasbourg. Conf. Abstr.* 4, 406-407.
- PEARCE, J. A. & CANN, J. R. (1973): Tectonic setting of basic volcanic rocks determined using trace element analyses. - *EPSL*, 19, 290-300.
- PEARCE, J. A. & NORRY, M. J. (1979): Petrogenetic implications of Ti, Zr, Y and Nb variations in volcanic rocks. - *Contrib. Mineral. Petrol.* 69, 33-47.
- PEARCE, J. A. & PARKINSON, I. J. (1993): Trace element models for mantle melting: application to volcanic arc petrogenesis. - In: PRICHARD, H. M., ALABASTER, T., HARRIS, N. B. W. & NEARY, C. R. (eds), 1993, *Magmatic Processes and Plate Tectonics. Geol. Soc. Spec. Publ.* 76, 373-403.
- PULAJ, H. (2000): Hartografim gjeologjik ne shkalle 1:25000 i planshetit 83 Erseka.
- ROBERTSON, A. H. F. (2002): Overview of the genesis and emplacement of Mesozoic ophiolites in the Eastern Mediterranean Tethyan region. - *Lithos* 65, 1-67.
- ROBERTSON, A. H. F. & SHALLO, M. (2000): Mesozoic-Tertiary tectonic evolution of Albania in its regional Eastern Mediterranean context. - *Tectonophysics*, 316, 197-254.
- SHALLO, M. (1992): Geological evolution of the Albanian ophiolites and their platform periphery. - *Geol. Rdsch.*, 81, 3, 681-694, Stuttgart.
- SHALLO, M. (1994): Outline of the Albanian ophiolites. - *Ofioliti*, 19 (1), 57-75.
- SHERVAIS, J. W. (1982): Ti-V plots and the petrogenesis of modern and ophiolitic lavas. - *Earth & Planetary Sci. Lett.* 59, 101-118.
- SMITH, A. G. & SPRAY, J. G. (1984): A half ridge transform model for the Hellenic-Dinaric ophiolites. - In: Dixon, J. E. & Robertson, A. H. F. (eds.): *The geological evolution of the Eastern Mediterranean.* - *Geol. Soc. Spec. Publ.* 17, 1984, 629 – 644.

**ZUR PETROLOGIE UND AUSGEWÄHLTEN TECHNOLOGISCHEN EIGENSCHAFTEN
DER INSCRIFTENTAFELN DES RÖMISCHEN TEMPELBEZIRKES
AUF DEM PFAFFENBERG BEI CARNUNTUM**

von

Nina Mayr

Diplomarbeit zur Erlangung des Magistergrades an der
Fakultät für Naturwissenschaften und Mathematik der Universität Wien

Institut für Geologische Wissenschaften
Wien, 2003

Zusammenfassende Beurteilung der Untersuchungsergebnisse

Nachfolgend sind die Ergebnisse der durchgeführten Untersuchungen in den Tabellen 12 und 13 zusammenfassend dargestellt. Grundlegendes Ziel dieser Arbeit war es, die Inschriftenfragmente in makroskopisch unterscheidbare Gesteinsarten einzuteilen, sie mit sedimentpetrographischen und technischen Methoden hinsichtlich ihrer Qualität zu beurteilen und soweit wie möglich auf die Herkunft der verwendeten Gesteinstypen zu schließen.

Es konnten fünf Gesteinstypen festgestellt werden, im Wesentlichen handelt es sich dabei um Leithakalke in unterschiedlichen Ausbildungsarten. Die Ergebnisse der sedimentpetrographischen und röntgenanalytischen Untersuchungen zeigen generell Kalksandsteine bzw. Kalke, welche sich durch Calcit als Hauptkomponente, daneben Quarz, Feldspat und Glimmer als Nebengemengteile bzw. akzessorisch und stellenweisem Auftreten von Dolomit auszeichnen.

Mittels mikrofazieller Analyse konnten die Gesteinsarten den Fazieszonen 6, 7 und 8 (WILSON, 1975) zugeteilt werden, womit eine Entstehung im flachen Schelfmeer gegeben ist. Die genaue Herkunft der verwendeten Gesteinsarten konnte nicht eindeutig geklärt werden, sie wird aber in der näheren Umgebung von Carnuntum vermutet, insbesondere in den Hainburger Bergen und um Wolfsthal. Die erfassten gesteintechnischen Parameter geben einen allgemeinen Überblick über die Qualität der Gesteine und lassen vorsichtige Schlüsse auf selektive Nutzung oder Verwitterungsverhalten zu.

An vergleichbarem Material wurden außerdem ergänzende Untersuchungen zur Druckfestigkeit und der Abriebfestigkeit durchgeführt. Die Ergebnisse dieser Messungen korrelieren mit den anderen technischen Daten im Allgemeinen gut.

Die zur Herstellung von Inschriftentafeln verwendeten Gesteinsarten werden so als hauptsächlich poröse, weiche Kalke bzw. Kalksandsteine aus der näheren Umgebung von Carnuntum bewertet. Nachteilig auf die Beständigkeit der Gesteine wirken sich manche für die Bearbeitung vorteilhafte Eigenschaften aus, wie geringe Festigkeiten oder hohe Porosität.

Der Nutzen dieser Arbeit für die Denkmalpflege sollte im Wissen um spezifische Eigenschaften der verwendeten Gesteine bestehen. So können die gewonnenen Daten Restauratoren vor anfallenden Konservierungsmaßnahmen dieser Gesteine konkret, z.B. bei der Bestimmung geeigneter Festigungsmittel oder von Ausbesserungsmaterialien, hilfreich sein.

**FABRICATION OF BRICKS USING FLY ASH FROM
MAE MOH POWER PLANT (THAILAND)**

by

Kedsarin Pimraksa

Dissertation zur Erlangung des Doktorgrades an der
Formal- und Naturwissenschaftlichen Fakultät der Universität Wien

Institut für Geologische Wissenschaften
Wien, 2002

Kurzfassung

Das Ziel dieser Arbeit war die Herstellung von Ziegeln ausgehend von Flugasche des Kraftwerks Mae Moh in Thailand. Das Kraftwerk Mae Moh ist der größte Stromerzeuger in Thailand, und die Stromerzeugung basiert auf der Verbrennung von Lignite (Braunkohle). Jährlich fallen bei dieser Produktion 2 Millionen Tonnen Flugasche an.

Dies ist ein neuer Versuch zur Verwertung der Braunkohleflugasche. Derzeit werden ca. 50 % dieser Flugasche auf Deponien verbracht.

Die Möglichkeit diese Flugasche als Baustoff zu Verwenden wurde untersucht. In dieser Arbeit wurde die Herstellung von gebrannten und ungebrannten Ziegeln aus unbehandelter und bearbeiteter Flugasche untersucht. Gebrannte und ungebrannte Ziegeln aus Braunkohleflugasche wurden nach einem speziellen Trockenpressverfahren (stiff-mud Prozess) hergestellt. Die Eigenschaften dieser Proben wurden mit konventionellen Ziegeln verglichen.

In einem ersten Schritt wurde ein feuchtes Granulat hergestellt, welches anschließend mit 26 MPa in einem einachsigen Pressverfahren verdichtet wurde. Diese Formkörper wurden anschließend 4 Stunden bei 110°C getrocknet und anschließend bei 900, 950, 1000 und 1050°C eine Stunde gesintert, wobei die Aufheizrate bis zur Sintertemperatur 3°C/min betrug. Das Rohmaterial der gebrannten Ziegeln besteht aus 100 % Braunkohleflugasche. Versuche wurden mit der unbehandelten Flugasche und speziellen Siebfraktionen sowie mit gemahlener Flugasche durchgeführt. Die Verfestigung der Ziegeln während des Brennprozesses basiert auf Flüssigphasensinterung.

Nichtgebrannte Ziegeln wurden aus 90 % Flugasche und 10 % Calciumhydroxid (Ca(OH)₂) hergestellt. Das feuchte Granulat welches aus dieser Mischung hergestellt wurde, wurde mit 26 MPa in einer einachsigen Presse geformt, bei Raumtemperatur in einer Feuchtkammer (> 99%

rel. Feuchte) 40 Stunden gelagert und anschließend mit Dampf bei 120-130°C bei 1.4 bar, 4 Stunden behandelt. Unterschiedliche Siebfraktionen der Flugasche wurden in diesem Prozess untersucht. Die nichtgebrannten Ziegeln werden durch puzzolanische Reaktionen verfestigt. Glasphasen die in der Flugasche existieren reagieren zusammen mit Calciumhydroxid und Wasser. Dieses System wird durch Dampfbehandlung aktiviert. Dies wird als hydrothermaler Prozess bezeichnet.

Die untersuchten Produkte – gebrannte und ungebrannte Ziegeln aus Flugasche – wurden mit normalen Ziegeln verglichen, wobei zum Testen internationale Standards herangezogen wurden. Diese Forschungsprodukte erfüllen alle Anforderungen für Standard Ziegeln entsprechend JIS (Japanese Industrial Standard) und ASTM (American Standard Testing Material). Zusätzlich wurde die Qualität der Forschungsprodukte mit anderen Methoden überprüft, wie dem Frost-Tau Test und einem Säurebeständigkeitstest. Weiters wurde das Laugungsverhalten der gebrannten und ungebrannten Ziegeln untersucht.

Die Umweltauswirkungen beider Produktionsprozesse wurden untersucht und diskutiert.

**HYDROGEOLOGISCHE, SEDIMENTPETROGRAPHISCHE UND HYDROGEOCHEMISCHE
UNTERSUCHUNGEN IM OBEREN VINSCHGAU, BEREICH SULDENTAL-PRAD/ITALIEN**

von

Hans Schroll

Diplomarbeit zur Erlangung des Magistergrades an der
Fakultät für Naturwissenschaften und Mathematik der Universität Wien

Institut für Geologische Wissenschaften
Wien, 2004

Kurzfassung

Den inhaltlichen Schwerpunkt der Untersuchungen im oberen Vinschgau (Bereich Laas bis Prad und Suldental) stellten hydrogeochemische Analysen an Quellwässern, Fließgewässern und Porengrundwässern dar. Nach jeweils zwei zeitlich getrennten Beprobungsreihen, erfolgte die Bestimmung der Haupt- und Nebeninhaltsstoffe, sowie einiger umweltrelevanter Spurenelemente und Schwermetalle, wobei besonderes Augenmerk auf das Arsen gelegt wurde.

Bedingt durch ihr geologisches Einzugsgebiet weisen die Wässer unterschiedliche Chemismen auf. Von permomesozischen, karbonatischen Sedimentgesteinen beeinflusste Wässer besitzen einen höheren Mineralisierungsgrad als jene mit rein kristallinen Einzugsgebieten. Anthropogen bedingte Kontaminationen bedenklichen Ausmaßes konnten nicht festgestellt werden, die Haupt- und Nebeninhaltsstoffe betreffend, überschritt keiner der untersuchten Parameter die betreffenden Grenzwerte.

Anders stellt sich die Situation bei den Spurenelementen und Schwermetallen dar. im Zuge der flächendeckenden Arsenanalytik wurden in den Quellgewässern, in den Fließgewässern und in den Porengrundgewässern Überschreitungen des Grenzwertes für Arsen (= 10 µg/l) um bis zu mehr als ein Zehnfaches registriert.

Als Ursprung des Arsens ist das Suldental anzusehen. Dort treten die höchsten Konzentrationen in Nachbarschaft mit einer tektonischen Störung auf, in deren Umfeld hydrothermale Vererzungen bekannt sind. Anhand unterschiedlicher Analysemethoden konnte der, in derartigen Vererzungen häufig als Geleitmineral auftretender Pyrit, als eine Quelle des Arsens identifiziert werden.

Die Verteilung der Arsenkonzentration in den Porengrundwässern des Haupttales wird in erster Linie durch den sedimentpetrologischen Aufbau des Untergrundes bestimmt.

Geoelektrische Tiefensondierungen im Bereich des Suldenbach-Schwemmfächers ergaben einen Abschnittsweise grobkörnigen Sedimentaufbau der Talfüllungen in diesem Bereich. Als Folge der daraus resultierenden guten Durchlässigkeit wird einerseits arsenhaltiges Wasser aus dem Suldental relativ rasch weitertransportiert, und andererseits werden, bedingt durch die kurze Verweildauer des Wasser, Lösungsprozesse an etwaigen arsenhaltigen Sedimenten unterbunden. Die Porengrundwässer in diesem Bereich weisen daher, im Vergleich zu weiter östlich gelegenen, niedrigere Arsenwerte auf.

Der Arseneintrag norwestlich des Suldenbaches ist aufgrund von Referenzmessungen als gering einzustufen. Der Haupteintrag in das Etschtal erfolgt aus dem Suldental, an dessen Ausgang bei Prad der Schwemmfächer des Suldenbaches eine Art Verteilerfunktion einnimmt.

**HYDROGEOLOGISCHE, SEDIMENTPETROGRAPHISCHE UND HYDROGEOCHEMISCHE
UNTERSUCHUNGEN IM OBEREN VINSCHGAU, BEREICH SULDENTAL-LAAS/ITALIEN**

von

Astrid Tomberger

Diplomarbeit zur Erlangung des Magistergrades an der
Fakultät für Naturwissenschaften und Mathematik der Universität Wien

Institut für Geologische Wissenschaften
Wien, 2004

Kurzfassung

Das Arbeitsgebiet Suldental –Laas befindet sich im Oberen Vinschgau und erstreckt sich dort längs des Etschtales, von der Ortschaft Laas bis nach Prad am Stilfserjoch, und weiter südlich bis ins Suldental. Um eine möglichst detaillierte Vorstellung der hydrologisch–hydrogeologischen und sedimentpetrographischen Verhältnisse des Untersuchungsgebietes zu bekommen, wurden nach vorbereitenden Geländebegehungen, in einer Sommer- und Winterkampagne zunächst Wasserproben, sowohl aus Kluft-, Poren-, als auch aus Oberflächengewässern gezogen.

Durch die nachfolgenden hydrogeochemischen Untersuchungen in den Labors des Institutes für Geowissenschaften der Universität Wien konnten damit grundsätzliche Aussagen über das geologisch-lithologische Einzugsgebiet und die hier verteilten Wassertypen gemacht werden.

Vorrangiges Ziel der Arbeit war es jedoch lokal in den Wässern auftretende Arsen-Konzentrationen im Hinblick auf Herkunft und generelle Transportmechanismen zu untersuchen und die vorhandenen Kenntnisse zur Verteilung von Arsen im Untersuchungsgebiet zu erweitern bzw. zu begründen.

Die Herkunft der mit Arsen kontaminierten Wässern konnte durch gezielte Sedimentanalysen geklärt und das Liefergebiet eingegrenzt werden. Aufgrund von Schwermineralanalysen mittels Elektronenstrahl-Mikrosonde konnte nachgewiesen werden, dass die im Suldental an Quellen und Oberflächengewässern auftretenden Arsenkontaminationen an hydrothermale Vererzungen entlang einer W-E streichenden Störungszone, der Zumpanell-Linie, gebunden sind.

Arsen wird dort durch Verwitterungsprozesse mobilisiert und gelangt in den ober- und unterirdischen Abfluss.

Zur Beurteilung, ob Strukturen und variierender Kornaufbau in den Sedimenten der Talfüllung im Etschtal mit daran gebundenen, spezifischen Wegigkeitsentwicklungen zu lokalen Konzentrationsunterschieden von Arsen im Grundwasser beitragen, wurden geoelektrische Boden-sondierungen durchgeführt. Die mit Hilfe dieser Sondierungen ermittelten, sehr niederohmigen Sedimentpakete westlich von Laas, welche durch den Stau effekt des Gatria- Murschuttkegels entstanden sind, führen dort zu einer verstärkten Anreicherung von Arsen im Untergrund und sind als Ursache für die erhöhten Arsenwerte in den Tiefbrunnen vor Ort anzusehen.

Die weiters aus Sicht des Grundwasserschutzes durchgeführten Untersuchungen aus Nitrit, Nitrat und Ammonium ergaben keine Grenzwertüberschreitenden Konzentrationen.

VEREINSMITTEILUNGEN

TÄTIGKEITSBERICHT ÜBER DAS VEREINSJAHR 2003

1. Im Vereinsjahr 2003 fanden folgende Vorträge und Veranstaltungen statt:

Veranstaltungsort: Wien

- 13.01.03. G. Kurat (Naturhistorisches Museum, Wien)
"Meteorite wollen uns ihre Geschichte erzählen, aber niemand hört hin"
- 20.01.03. H. Fink (Gratkorn)
"Extremstrahlen in der Rauris"
- 12.03.03. R. Ramdohr (Schweiz)
"Neue Saphirvorkommen auf Madagaskar"
- 24.03.03. F. Langenhorst (Universität Bayreuth)
"Nanostrukturen in ultrahochdruckmetamorphem Coesit und Diamant: ein genetischer Fingerabdruck"
- 07.04.03. O. Appel (Geological Survey, Kopenhagen)
"Exploring Earth's oldest geological record in West Greenland"
- 30.04.03. M. Wild (Kirschweiler bei Idar Oberstein)
"Prunkgefäße aus Bergkristall – Steinbearbeitung aus 2 Jahrtausenden"
- 19.05.03. R. Oberhänsli (Universität Potsdam)
"Niedriggradige Hochdruckmetamorphose in der Westtürkei"
- 02.06.03. G. Fischer (Salzburg)
"Mineralfundstellen rund um Salzburg"
- 16.06.03. W. Pohl (Technische Universität Braunschweig)
"Metamorphogene Lagerstätten: Modelle und offene Fragen"
- 20.10.03. A. Strasser (Salzburg)
"Ein mineralogischer Querschnitt durch das Bundesland Salzburg"
- 10.11.03. V. Kahlenberg (Universität Innsbruck)
"Aspekte angewandter Kristallstrukturforschung"

- 17.11.03 B. Goffeé (CNRS, ENS-Paris)
 “Metasediment petrology in greenschist and blueschist metamorphic conditions: geodynamics and implications for the Western Alps”
- 24.11.03. S. Demidova (Vernadsky Institut, Moskau)
 “Mineralogy of the Polar Ural region”
- 01.12.03. G. Garuti (Univ. Modena)
 “The historical copper mines of the Northern Appennine ophiolites”

Ein Teil der Vorträge wurde gemeinsam mit der Österreichischen Gemmologischen Gesellschaft und dem Verein der Freunde des Naturhistorischen Museums in Wien veranstaltet.

Veranstaltungsort: Graz

- 25.03.03 F. Langenhorst (Universität Bayreuth)
 “Nanostrukturen in ultrahochdruckmetamorphem Coesit und Diamant: ein genetischer Fingerabdruck”
- 08.04.03. O. Appel (Geological Survey, Kopenhagen)
 “Exploring Earth’s oldest geological record in West Greenland”
- 17.06.03. W. Pohl (Technische Universität Braunschweig)
 “Metamorphogene Lagerstätten: Modelle und offene Fragen”
- 14.10.03. K. Reichmann (Universität Graz)
 “Spinelle und Perowskite in elektrokeramischen Anwendungen”
- 11.11.03. V. Kahlenberg (Universität Innsbruck)
 “Aspekte angewandter Kristallstrukturforschung”
- 18.11.03 B. Goffeé (CNRS, ENS-Paris)
 “Metasediment petrology in greenschist and blueschist metamorphic conditions: geodynamics and implications for the Western Alps”
- 02.12.03. G. Garuti (Univ. Modena)
 “The historical copper mines of the Northern Appennine ophiolites”

Die Vorträge wurden gemeinsam mit dem Naturwissenschaftlichen Verein für Steiermark und dem Joanneum-Verein veranstaltet.

Veranstaltungsort: Leoben

- 09.04.03. O. Appel (Geological Survey, Kopenhagen)
“Exploring Earth’s oldest geological record in West Greenland”
- 18.06.03. W. Pohl (Technische Universität Braunschweig)
Metamorphogene Lagerstätten: Modelle und offene Fragen”
- 12.11.03. V. Kahlenberg (Universität Innsbruck)
“Aspekte angewandter Kristallstrukturforschung”

Veranstaltungsort: Salzburg

- 12.03.03. J. Sureda (Univ. Salta, Argentinien)
“Zur Metallogene NW-Argentinien”
- 26.03.03. T. Berthold (Siemens AG, München)
“Untersuchung von Reaktionen in Multifilamentbändern von Cuprat-Supraleitern”
- 02.04.03. B. Lehmann (Universität Clausthal)
“Metallogene an einem aktiven Kontinentalrand: Die Zentralen Anden”
- 04.06.03. E. Libowitzky (Universität Wien)
“Wasserstoff in Mineralen”
- 05.11.03. V. Kahlenberg (Universität Innsbruck)
“Aspekte angewandter Kristallstrukturforschung”
- 19.11.03 B. Goffeé (CNRS, ENS-Paris)
“Metasediment petrology in greenschist and blueschist metamorphic conditions: geodynamics and implications for the Western Alps”

Veranstaltungsort: Innsbruck

- 09.01.03 E. Zechner (Universität Basel)
“Prinzip und Anwendungen der Georadar-Methode”
- 23.01.03. A. Pfiffner (Universität Bern)
“Bau und Entwicklung der Schweizer Alpen: Deckenbau und Morphogenese”

- 30.01.03. J. Reitner (Geologische Bundesanstalt, Wien)
 “Fazies und Stratigraphie der pleistozänen Sedimente im Raum Kitzbühel - St. Johann - Hopfgarten”
- 03.03.03. bis 04.03.03.
 Berufungsvorträge “Angewandte Mineralogie”
- 13.03.03. J. Nebelsick (Universität Tübingen)
 “Fressen und gefressen werden – die Paläontologie als Predation”
- 20.03.03. K. Koinig (Universität Innsbruck)
 “Spuren holozäner Klimaschwankungen in alpinen Seesedimenten”
- 27.03.03 F. Langenhorst (Universität Bayreuth)
 “Nanostrukturen in ultrahochdruckmetamorphen Coesit und Diamant: ein genetischer Fingerabdruck”
- 03.04.03. C. Weidenthaler (MPI für Kohlenforschung, Mülheim an der Ruhr)
 “Analytik als Bindeglied zwischen Mineralogie und Chemie”
- 08.05.03. G. Stirling (ETH Zürich)
 “Corals and climate change”
- 15.05.03. R. Oberhänsli (Universität Potsdam)
 “Vulkanische Relikte aus der Ultra-High-Pressure Region des Dabie Shan, China”
- 22.05.03. A. Mogessie (Universität Graz)
 “Platinum Group Minerals in the Yubdo mafic-ultramafic rocks and the petrology of the intruded Pan-African Basement, Western Ethiopia”
- 30.10.03. M. Meyer (Universität Wien)
 “Glazialgeologie und Paläoseismologie in E-Lunana (Bhutan, Himalaya)”
- 06.11.03. R. Kaindl (Universität Graz)
 “Raman-Spektroskopie – vom Blau des Mittelmeeres zum Nanodiamanten”
- 13.11.03.. V. Mair (Landesamt für Geologie und Baustoffprüfung, Bozen)
 “Neueste geologisch-petrologische Ergebnisse aus dem Ortler-Gebiet”
- 20.11.03 B. Goffeé (CNRS, ENS-Paris)
 “Metasediment petrology in greenschist and blueschist metamorphic conditions: geodynamics and implications for the Western Alps”
- 27.11.03. A. Borsato (Museo Tridentino Scienze Naturali, Trento)
 “Quaternary evolution of the Adige and Sarca valleys: new results from CARG mapping, seismic profiles and radiocarbon data”

- 04.12.03. M. Goebbels (Universität Erlangen)
“Modeme Angewandte Mineralogie – vom Leuchtstoff zum keramischen Schaum ?”
- 18.12.03. M. Fiebig (Bayerisches Geologisches Landesamt, München)
“Eiszeitengliederung in den Alpen – eine Standpunktsache ?”

Alle Veranstaltungen wurden im Rahmen des Geokolloquiums gemeinsam mit der Österreichischen Geologischen Gesellschaft abgehalten.

2. Tagung “Minpet 2003”

Anlässlich "100 Jahre Tauernfenster" wurde in Neukirchen am Großvenediger vom 15.-21. September 2003 die Tagung "Minpet 2003" veranstaltet. Das wissenschaftliche Programm der im Tauriska-Kammerlanderstall abgehaltenen Tagung umfasste eingeladene Vorträge, Kurzreferate, Posterpräsentationen sowie einen öffentlichen Abendvortrag.

3. Exkursionen

Im Rahmen der Tagung "MinPet 2003" wurden insgesamt fünf eintägige Exkursionen (Wolf-rambergbau Felbertal/Mittersill, Zentralgneise, Alpine Metamorphose im Südlichen Großvenedigergebiet, Klastische Sedimente am Nordrand des Tauernfensters, Smaragdbergbau Habachtal) durchgeführt.

4. Vorstandssitzungen und Jahreshauptversammlung

Die Abwicklung der geschäftlichen Angelegenheiten erfolgte in drei Vorstandssitzungen (13.1.2003, 6.6.2003 und 16.9.2003).

Die ordentliche Jahreshauptversammlung fand am 13. Jänner 2003 statt.

5. Vereinsvorstand für 2002

Präsident:	Prof. Dr. Friedrich Koller, Wien
Vize-Präsident:	Prof. Dr. Mirwald, Innsbruck
Kassier:	Prof. Dr. Herta Effenberger, Wien
Schriftführung:	Dr. Franz Brandstätter, Wien

Vorstandsmitglieder: Prof. Dr. Georg Amthauer, Salzburg; Prof. Dr. Larryn Diamond, Bern; Mag. Dorothea Grolig, Wien; Prof. Dr. Volker Höck, Salzburg; Prof. Mag. Dr. Eugen Libowitzky, Wien; Prof. Dr. Aberra Mogessi, Graz; Dr. Bernd Moser, Graz; Dr. Gerhard Niedermayr, Wien; Prof. Dr. Konstantin Petrakakis, Wien; Prof. Dr. Eugen F. Stumpfl, Leoben; Dr. Peter Tropper, Innsbruck.

Beirat: Dr. Rainer Abart, Graz; Prof. Dr. Franz Walter, Graz

6. Band 148 der "Mitteilungen der Österreichischen Mineralogischen Gesellschaft" wurde fertiggestellt und im September 2002 den Mitgliedern zugesandt.

7. Mitgliederbewegung

Mitgliederstand vom 31. 12. 2002: 297

Mitgliederstand vom 31. 12. 2003: 286

Ehrenpräsident:

Prof. Dr. J. Zemann / Wien

Ehrenmitglieder:

Prof. Dr. H. Heritsch / Graz

Prof. Dr. E. Jäger / Meikirch, CH

Prof. Dr. G. Kurat / Wien

Dr. G. Niedermayr / Wien

Prof. Dr. E. Niggli / Bern

Prof. Dr. A. Preisinger / Wien

Prof. Dr. H. Strunz / Unterwössen, D

Prof. Dr. E. F. Stumpfl / Graz

Prof. Dr. J. Zemann / Wien

Träger der Friedrich Becke-Medaille:

Prof. Dr. P. Cerny / Winnipeg, CA

Prof. Dr. W. Engelhardt / Tübingen, D

Prof. Dr. D. P. Grigoriew / St. Petersburg, RU

Prof. Dr. H. Jagodzinski / München, D

Prof. Dr. K. Langer / Berlin, D

Prof. Dr. W. Schreyer / Bochum, D

Prof. Dr. F. Seifert / Bayreuth, D

Prof. Dr. V. Trommsdorff / Zürich, CH

Prof. Dr. H. Waenke / Mainz, D

Prof. Dr. H. Wondratschek / Karlsruhe, D

Felix-Machatschki-Preis:

Mag. Dr. R. Miletich / Heidelberg

Mag. Dr. R. Abart / Basel

Mitglieder auf Lebenszeit:

W. Hollender / Wien

Dr. F. Marsch / Wien

Schriftentausch:

Bundesanstalt für Geowissenschaften & Rohstoffe, Bibliothek, Hannover

Sächsisches Landesamt für Umwelt & Geologie, Bibliothek, Freiberg

Der Dank für Spenden ergeht an folgende Mitglieder:

Prof. Dr. Rainer Altherr (Heidelberg), Prof. Dr. Anton Beran (Wien), Prof. Dr. Herta Effenberger (Wien), Dr. Karl Ettinger (Graz), Prof. Mag. Dr. Gerald Giester (Wien), Dr. Michael Götzinger (Wien), Prof. Dr. Volker Höck (Salzburg), Mag. Dr. Robert Holsteiner (Wien), Prof. Emilie Jäger Meikirch, Schweiz), Helmut Kuhn (Baden), Dr. Christian Lengauer (Wien), Mag. Hermine Lenitz (Wien), Prof. Mag. Dr. Eugen Libowitzky (Wien), Dr. Gerhard Niedermayr (Wien), Prof. Dr. Franz Pertlik (Wien), Dr. Richard Tessadri (Innsbruck), Prof. Dr. Ekkehart Tillmanns (Wien), Prof. Dr. Volkmar Trommsdorff (Zürich), Prof. Mag. Dr. Manfred Wildner (Wien), Prof. Dr. Josef Zemann (Wien)

Wien, 27. 2. 2004

F. Brandstätter
(Schriftführung)

Autorenhinweise für die

MITTEILUNGEN DER ÖSTERREICHISCHEN
MINERALOGISCHEN GESELLSCHAFT

Manuskripte müssen in zweifacher Ausfertigung als Laserausdruck/DINA4-Format bei der Redaktion eingereicht werden. Abbildungen (S/W-Strichzeichnungen, Tabellen, Fotos) sind gesondert beizufügen (bitte zur Beachtung: Verkleinerung auf bis 50 % berücksichtigen, keine Farben, sondern Signaturen bei Diagrammen verwenden, nur sehr kontrastreiche Fotos verwenden).

Nach dem Review müssen angenommene Manuskripte auf Diskette, CD oder via E-mail (als attachments) übersandt werden. Texte, Abbildungen und Tabellen müssen dabei getrennt gespeichert sein (Texte ausschließlich als WORD.DOC oder im RTF-Format, einfache Formatierung (linksbündig/Flattersatz) genügt, bevorzugter Font: Times 12 Punkt, Abbildungen und Tabellen ausschließlich als hochaufgelöste JPG-, EPS-, TIFF- oder PDF-Dateien !!!).

Manuskripte sollten möglichst nicht länger als zwanzig/dreiig Seiten inklusive Abbildungen umfassen. Abstracts zu Tagungen und Diplomarbeiten/Dissertationen sollten nicht mehr als ein/zwei Seiten umfassen.

Zitierungen von Autoren im Text (Beispiel):

„.....(ALEKSANDROV et al., 1985).....“

Zitierungen von Autoren bei der Literaturzusammenstellung (Beispiel):

ALEKSANDROV, I. V., KRASOV, A. M. & KOCHNOVA, L. N. (1985): The effects of potassium, sodium and fluorine on rock-forming mineral assemblages and the formation of tantaloniobate mineralization in rare-metal granite pegmatites. - *Geochem. Int.*, 22, 85-94.

Abgabetermin für alle eingereichten Arbeiten ist Ende März des jeweiligen Jahres.

Bei eingereichten Arbeiten in den Kategorien Originalarbeiten - Vorträge - Exkursionen werden generell 50 Sonderdrucke kostenlos hergestellt. Andere oder zusätzliche Sonderdrucke von Arbeiten, sowie Abbildungen in Farbe sind explizit zu bestellen und werden in Rechnung gestellt.

Die Zeitschrift erscheint einmal jährlich mit Ausgabe September/Oktober.

Alle Einzelarbeiten in den Kategorien Originalarbeiten - Vorträge - Exkursionen sind ab Band 142 (1997) auch als PDFs veröffentlicht.

ÖMG-Homepage: <http://www.univie.ac.at/Mineralogie/Oemg.htm>

(<http://www.earthsciences.uibk.ac.at>)

Zusendung von Manuskripten an: Friedrich Koller, Institut für Petrologie, Universität Wien, Geozentrum, Althanstraße 14, A-1090 Wien (E-Mail Adresse: Friedrich.Koller@univie.ac.at).

Zusendung von neu angenommenen Manuskripten via E-Mail an: Richard.Tessadri@uibk.ac.at